

**MODELLING CLIMATE VARIABILITY AND CLIMATE CHANGE AND
THEIR ASSOCIATED EFFECTS ON HIGHLAND COOKING BANANA
PRODUCTION IN UGANDA**

By

Sabiiti Geoffrey

I80/80585/2010

**A thesis submitted in fulfillment of the requirements for the degree of
Doctor of Philosophy in Meteorology, University of Nairobi, Kenya**

2016

DECLARATION

I declare that this thesis is my original work and has not been submitted elsewhere for examination and award of a degree or publication. Where other people's work or my own work has been used, this has properly been acknowledged and referenced in accordance with the University of Nairobi's requirements.

Signature:

Date:

Sabiiti Geoffrey

I80/80585/2010

Supervisors:

This thesis has been submitted for examination with our approval as University supervisors:

Signature:

Date:

Prof. L. A. Ogallo

Signature:

Date:

Prof. J. M. Ininda

Department of Meteorology

University of Nairobi

P. O. Box 30197-00100

Nairobi, Kenya

www.uonbi.ac.ke

DEDICATION

This work is dedicated to my supportive family and trustworthy friends.

ACKNOWLEDGEMENT

First, I thank the Almighty God for His mercies and blessings. Glory and Honour be unto His Holy Name.

My sincere appreciation and special thanks go to my dear supervisors; Prof. L. A. Ogallo and Prof. J. M. Ininda for their guidance on all aspects of this thesis. This work has been possible by the financial support of Makerere University, UK Meteorological Office (UKMO) and IGAD Climate Prediction and Applications Centre (ICPAC) to whom I am very grateful and indebted. In this connection, I am indebted to Prof. C. P. K. Basalirwa (Mak), Prof. L. A. Ogallo (ICPAC), Prof. J. M. Ininda and Dr. Richard Graham (UKMO) for their kind hearted considerations of funding this research.

I wish to thank the staff of the Department of Meteorology, University of Nairobi and those of the IGAD Climate Prediction and Applications Centre (ICPAC) who provided an enabling environment for conducting this research work. I also appreciate ICPAC for providing the computational resources that made this research a success.

My special appreciations go to the staff at the UKMO; Dr. Wilfram Moufouma Okia, Dr. Richard Graham, Manager David Hein Griggs and Mr. Simon Tucker for their overwhelming scientific and technical support in running the climate experiments and acquiring other climate model data for the study. I wish to appreciate in a special way my colleagues G. Kabaka, J. Kariyanjahi, V. Ongoma, J. Ouma, G. Otieno, E. Koech, M. Nduva, A. Musili, O. Kipkogei and H. Misiani for their readiness to help in all forms with selfless hearts. God bless all.

I wish to acknowledge, the staff of the Ministry of Agriculture, Animal Industry and Fisheries (MAAIF) especially Madam Hakuza Annunciata and Mr. Sunday for their assistance in obtaining the data on banana production for analysis in this study.

Lastly, the golden medals go to the members of my family especially Precious, Leticia and Junior for having endured an absentee daddy for all the time I was away in pursuit of this PhD.

ABSTRACT

Climate extremes associated with climate variability and change are on the rise both in time and space. These extremes have far reaching impacts on socio-economic sectors particularly for countries like Uganda that rely heavily on rain-fed agriculture. The highland cooking banana (*Musa* genome group AAA-EA) is a major food crop in Uganda. Its continuous cycles of harvests makes it an important crop for enhancing food security and farmers' incomes. Studies have, however, observed continuous decline in banana productivity due to biological and environmental factors including climate extremes.

This study is aimed at investigating the extent of climate variability and climate change and their associated effects on banana production over Uganda. The study used historical observed climate data (1931 to 2013), banana yields (1971 to 2009) and model simulated climate data (1991 to 2100). Climate data analysed consisted mainly of rainfall and temperature. The Providing Regional Climates for Impacts Studies (PRECIS) Regional Climate Model (RCM) was used to simulate high resolution climate projections based on the Special Report on Emission Scenarios (SRES) A1B and A2 scenarios. The study also analysed climate projection data based on the full range of the Inter-governmental Panel on Climate Change (IPCC) Fifth Assessment Report (AR5) Representative Concentration Pathways (RCPs) as policy scenarios.

In order to detect climate variability and change signals, the observed seasonal climate data were subjected to empirical analyses. This involved determination of the first upto fourth moments. The shift in the first moment constituted the trend whose significance was evaluated using the Mann-Kendall test. The moments of both standardized climate data and banana yields were determined and used to identify linkages between current climate variability and banana yields. The Crop Water Assessment Tool (CROPWAT) was used to determine banana water requirements, moisture deficits and yield reductions for the current period. The Pearson's product-moment correlation coefficient, Refined Wilmott Index and Root Mean Square Errors (RMSE) were used to assess climate model performance. Empirical Orthogonal Functions (EOFs) were used to characterize modes of climate variability in both observed and model seasonal rainfall. Comparative graphical analysis based on geo-spatial mapping techniques was used to analyse and map climate variability and change patterns from the high resolution future climate projection information for rainfall, temperature and soil moisture content based on different scenarios. The response of banana growth to expected changes in temperature under

A1B and A2 scenarios was assessed using a banana-temperature growth regression model. The FAO Eco-crop tool was used to estimate suitable climate conditions for optimal banana growth. The mapping of future suitability of banana during the period (2041-2080) was undertaken using ARCGIS.

The results showed that inter annual seasonal rainfall and temperature trends varied between - 0.18 to 0.26 mm per year and 0.05 to 0.63 °C per year respectively across the seasons. While there are significant increasing trends in temperature for all seasons at most stations of Uganda, the trends in seasonal rainfall were significant only in a few stations. Further analysis observed significant linkages in variations of current banana yields and climate variability especially with respect to temperature trends. The effect of climate on yields was observed to vary from region to region. This was attributable to variations in other non-climatic factors such as soil fertility and composition, pests and diseases and crop management practices across regions.

Results on climate model performance indicated a good match between PRECIS model outputs with observations over most parts of Uganda particularly during October-December. This is mainly attributable to the good representation of the large scale oceanic and atmospheric circulation systems that drive Uganda's short rains. Results based on Taylor diagrams observed high inter-model variability across different seasons and sub-regions especially during the long (March to May) rain season. Strong coherence in models was evident during the short (October to December) rains. Empirical orthogonal functions analysis also revealed that during October to December, the first mode explained 74.6% and 76.8% of observed and model simulated rainfall variability respectively.

The results of climate projections revealed that enhanced rainfall over Uganda is expected under the A1B scenario with depressed rainfall expected under the A2 scenario. In addition, the A1B scenario is projected to exhibit relatively cooler temperatures while the A2 scenario is projected to exhibit relatively warmer temperatures. Consequently, higher soil moisture stresses to banana production are expected under the A2 scenario. Climate extremes that may cause floods and droughts are expected under both scenarios. Comparatively, RCP 2.6 indicated cooler and drier seasonal temperature and rainfall respectively than current observations. Seasonal temperature and rainfall simulation of RCP 4.5 are slightly warmer and wetter than RCP 2.6 simulations. The projected seasonal rainfall is more enhanced in RCP 6.0

compared with projections in all other scenarios while RCP 8.5 is associated with highest temperatures for most parts of Uganda.

The results of the study further observed that the growth patterns and production of bananas are highly likely to be affected by projected rainfall extremes, increasing temperature and the resultant soil moisture variations across all scenarios and regions. The study observed a larger (smaller) area suitable for banana production under RCP 2.6 and RCP 6.0 (RCP 4.5 and RCP 8.5) for the intermediate period 2041-2060 over Uganda. Due to projected temperature increases across all scenarios, the areas suitable for banana production is likely to reduce under all the four RCP scenarios in the period 2061-2080 relative to the period 2041-2060. It is also expected that the projected temperature changes under the A1B scenario will enhance banana growth. In contrast, banana growth rate under the A2 scenario is expected to decline due to projected warmer temperatures and depressed rainfall under this scenario.

The study provides critical science-based evidence of climate variability and climate change over Uganda. It contributes to the understanding of the linkages between banana productivity and observed climate patterns and provides information on the future suitability of the banana crop production under different climate change scenarios. The results from the study are, therefore, pointers for the development of coping and adaptation strategies to expected climate extremes to improve banana productivity, promote the incomes of farmers and enhance food security for sustainable development of Uganda and neighboring countries.

TABLE OF CONTENTS

DECLARATION	2
DEDICATION	3
ACKNOWLEDGEMENT	4
ABSTRACT	5
TABLE OF CONTENTS	8
LIST OF TABLES	12
LIST OF FIGURES	15
LIST OF ACRONYMS AND ABBREVIATIONS	28
OPERATIONAL DEFINITION OF TERMS	31

CHAPTER ONE

INTRODUCTION	1
1.0 Background to the Study	1
1.0.1 History of Banana Production in Uganda	5
1.0.2 Banana Varieties	8
1.0.3 Pests and Diseases in Uganda’s Banana Sub-sector	8
1.0.3.1 Black Singatoka.....	11
1.0.3.2 Banana Streak Virus Disease.....	11
1.0.3.3 Banana Wilt Disease.....	12
1.0.4 Soil Fertility and Banana Production	12
1.1 Statement of the Problem	13
1.2 Objectives of the Study.....	14
1.3 Justification of the Study	15
1.4 Study Area	16
1.4.1 The Agricultural Systems in Uganda	17

CHAPTER TWO

LITERATURE REVIEW	20
2.1 The Agricultural Sector and Banana Sub-sector in Uganda.....	20
2.1.1 Banana Production Constraints in Uganda	22
2.2 Impacts of Climate on Agriculture	28
2.3 Climate Variability and Climate Change.....	31
2.3.1 Climate Variability and Change over Eastern Africa	33
2.4 Climate Modeling and Future Climate Change Scenarios	35

2.5	The Conceptual Framework of the Study	43
2.5.1	Introduction	43
2.5.2	Illustration of the Conceptual Framework	44

CHAPTER THREE

DATA AND METHODS	47	
3.1	Materials	47
3.1.1	Gridded Climate Observations and Model Outputs	50
3.1.1.1	Climate Research Unit Gridded Observations	50
3.1.1.2	University of Delaware Gridded Observations	51
3.1.1.3	ERA-Interim Dataset	52
3.1.2	Regional Climate Model Outputs.....	53
3.2	Methods	54
3.2.1	Estimation of Missing Data and Homogeneity Test	54
3.2.2	Establish the Linkages between Banana Productivity and Observed Climate Variability	55
3.2.2.1	Empirical Methods based on Changes in the Mean, Variance, Skewness and Kurtosis Coefficient	58
3.2.2.2	Correlation and Regression Analyses.....	62
3.2.2.3	FAO Crop Water Assessment Tool.....	65
3.2.3	Determination of the Performance of PRECIS RCM in Simulating Observed Climate Patterns	65
3.2.3.1	Climatological Regional Climate Model Evaluation Experiments.....	65
3.2.3.1.1	Climate Model Experimental Design.....	66
3.2.3.2	Correlation Analysis	69
3.2.3.3	Error Analysis.....	70
3.2.3.4	Refined Wilmott Index	70
3.2.3.5	Inter-model Performance Comparison	71
3.2.3.6	Principal Component Analysis	72
3.2.4	Establish the Extent of Expected Future Climate Change over Uganda.....	74
3.2.4.1	Regional Climate Model Experiments for Climate Projections.....	75
3.2.5	Determination of Potential Effects of Future Climate Change on Banana Production over Uganda.....	76

CHAPTER FOUR

RESULTS AND DISCUSSION	80
4.1 Results on Data Homogeneity Test and Quality Control	80
4.1.1 Monthly Rainfall, Minimum and Maximum Temperature Double Mass Curves	80
4.2.1 Ground Truthing of CRU Gridded Rainfall and Temperature Data over Uganda	83
4.2 Results on the Linkages between Current Banana Yields and Observed Climate Variability	88
4.2.1 Empirical Approaches	89
4.2.1.1 Drought Characteristics over Uganda	96
4.2.2 Observed Rainfall Trends	100
4.2.2.1 Rainfall Trend Results from Mann Kendall Statistics.....	109
4.2.3 Results from Changes in Skewness and Kurtosis Coefficients for Seasonal Rainfall Series	110
4.2.4 Trends of Surface Temperatures	111
4.2.5 Results on Banana Varieties and Production Patterns	121
4.2.6 Linkages between Observed Banana Productivity and Climate Variability based on Moments of Climate and Banana Series.....	127
4.2.7 Results from Correlation and Regression Analysis	129
4.2.8 Results on Multiple Regression Analysis	134
4.2.9 Results on FAO CROPWAT Simulation of Banana Crop Water Requirements	136
4.3 Results on the Performance of Regional Climate Models Outputs	144
4.3.1 Spatial Patterns of Observed and Simulated Mean Rainfall	144
4.3.2 Simulated and Observed Coefficient of Variation of Seasonal Rainfall.....	149
4.3.3 Results based on Empirical Orthogonal Functions	152
4.3.4 Seasonal 850 mb Wind Circulation Patterns.....	156
4.3.5 Results of Simulated and Observed Rainfall Seasonality	159
4.3.6 Interannual Rainfall Variability	161
4.3.7 Results of Model Performance based on Statistical Tests.	163
4.3.8 Inter-comparison of RCMs Performance	169
4.4 Results on Simulated Climate Projections.....	172
4.4.1 IPCC SRES A1B and A2 Climate Change Projections	172
4.4.1.1 Spatial Patterns of Projected Rainfall.....	173

4.4.2	Spatial Patterns of Projected Average Temperature	182
4.4.3	Spatial Patterns of Projected Soil Moisture Content at root zone	192
4.4.4	Projected Seasonality of Rainfall, Average Temperature and Soil Moisture Content for Sub-regions	200
4.4.5	Projected Trends in Seasonal and Annual Rainfall.....	206
4.4.6	Projected Trends in Seasonal and Annual Average Temperature.....	207
4.4.7	Projected Trends in Seasonal and Annual Soil Moisture Content	209
4.4.8	Relationship between Projected Rainfall, Temperature and Soil Moisture Content	211
4.4.9	Climate Projections under IPCC RCPs 4.5 and 8.5	213
4.4.9.1	Projected Spatial Patterns of IPCC RCPs Seasonal Rainfall and Temperature	213
4.4.9.2	Results on the Spatial Patterns of the Projected Bio-climatic Variables.....	217
4.5	Results on the Effects of the Future Climate Change on Bananas Production.....	228
4.5.1	Projected Suitable Areas for Banana Production under the RCP Climate Scenario on rainfall and temperature changes	229
4.6.2	Likely Effects of IPCC SRES A1B & A2 Projected Temperatures on Banana Growth.....	232

CHAPTER FIVE

SUMMARY, CONCLUSIONS AND RECOMMENDATIONS.....	240
5.1 Summary.....	240
5.2 Conclusions	241
5.3 Recommendations	244
5.3.1 National Meteorological and Hydrological Services, Training Institutions, and Government of Uganda	244
5.3.2 The Agricultural Sector and Banana Farmers.....	245
5.3.3 Other Users of Climate Information	245
5.3.4 Further Research	246
References.....	247

LIST OF TABLES

Table 1.1: Number of plots and size for main food crops in Uganda	7
Table 1.2: Common banana species and their purpose in Uganda	8
Table 2.1: Uganda’s GDP by agricultural subsector and other economic activity at current market prices, percentage share and calendar years.....	21
Table 2.2: Performance of agriculture in the Uganda’s economy (1990-2014, 1USD = UShs 3050)	22
Table 2.3: Contrast between the different technological and socio-economic drivers considered under the A1B and A2 scenarios (Source, Nakicenovic and Swart, 2000 and IPCC, 2007)	39
Table 2.4: Contrast of the different properties across the different RCPs (2.6, 4.5, 6.0 and 8.5) scenarios by the year 2100.	41
Table 3.1: Representative observation stations (also Figure 3.1a) over Uganda	48
Table 3.2: Analysis regions (also Figure 3.1b) over Uganda.....	48
Table 3.3: Effects of temperature thresholds on banana growth patterns (Samson, 1980 and German <i>et al.</i> , 2015).....	56
Table 3.4: Reference evapotranspiration (ET_o -FAO Penman-Monteith method), crop evapotranspiration (ET_c) and daily banana water consumption (WC) thresholds for banana growth (Samson, 1980).....	57
Table 3.5: Characteristics of Regional Climate Models used in the study	67
Table 3.6: Main features considered in MOSES 1 and MOSES 2.2.....	68
Table 3.7: Climate thresholds for GIS based Banana Production Suitability Mapping.....	78
Table 4.1: Values of Root Mean Square Error (RMSE) and Correlation Coefficient (CORR) for seasonal rainfall (a), minimum temperature (b) and maximum temperature (c).....	84
Table 4.2: Trend test statistics for MAM, JJA and OND seasonal rainfall	109
Table 4.3: Changes in the skewness coefficient of seasonal rainfall series between the periods 1961-1990 and 1991-2013 over Uganda.....	110
Table 4.4: Changes in the kurtosis coefficients of seasonal rainfall series between the periods 1961-1990 and 1991-2013 over Uganda.....	111
Table 4.5: Mann Kendall trend test statistics for seasonal surface minimum temperature.....	116
Table 4.6: Mann Kendall trend test statistics for seasonal surface maximum temperature	117
Table 4.7: Changes in the mean ($^{\circ}$ C) of seasonal maximum surface temperature series between the periods 1961-1990 and 1991-2013 over Uganda	118

Table 4.8: Changes in the variability (standard deviation, °C) of seasonal maximum surface temperature series between the periods 1961-1990 and 1991-2013 over Uganda.....	118
Table 4.9: Changes in the skewness coefficient of seasonal maximum surface temperature series between the periods 1961-1990 and 1991-2013 over Uganda.....	119
Table 4.10: Changes in the kurtosis coefficients of seasonal maximum surface temperature series between the periods 1961-1990 and 1991-2013 over Uganda.....	119
Table 4.11: Comparison of time series moments of normalized rainfall, maximum, minimum surface temperatures and banana yields (highlighted values indicate agreement on the direction) over western Uganda	128
Table 4.12: Comparison of time series moments of normalized rainfall, maximum, minimum surface temperatures and banana yields (highlighted values indicate strong linkages) over central Uganda	128
Table 4.13: Correlation coefficients (coefficient of determination, R^2) between climatic variables and banana yields for western and central regions of Uganda.	129
Table 4.14: Multiple regression statistics between banana yields and climate variables	135
Table 4.15: Banana crop water statistics and yield reductions (YR) from the CROPWAT model for two crop cycles (highlighted values indicate cases of high yield losses)....	143
Table 4.16: The Pearson's product-moment correlations coefficient for different model configurations with respect to CRU rainfall observations over different regions of Uganda. Values in green are significant at 95% confidence level.....	166
Table 4.17: The computed Root Mean Square Errors for different model configurations with respect to CRU rainfall observations over different regions of Uganda. Values in green show cases of low errors.	167
Table 4.18: The computed refined wilmott indices for different model configurations with respect to CRU rainfall observations over different regions of Uganda. Values in green show significant agreement.....	168
Table 4.19: IPCC SRES A1B scenario projected mean rainfall, standard deviation (SD) and change (mm/day) over different regions of Uganda.	181
Table 4.20: IPCC SRES A2 scenario projected mean rainfall, standard deviation (SD) and change (mm/day) over different regions of Uganda.	182
Table 4.21: IPCC SRES A1B projected average temperature (2011-2040 & 2061-2090) mean, standard deviation and change.	190

Table 4.22: IPCC SRES A2 projected average temperature (2011-2040 & 2061-2090) mean, standard deviation and change over sub-regions of Uganda.....	191
Table 4.23: PRECIS projected soil moisture content [mm/day] (2011-2040 & 2061-2090) mean, standard deviation and changes for A1B scenario.	198
Table 4.24: PRECIS projected soil moisture content [mm/day] (2011-2040 & 2061-2090) mean, standard deviation and changes for A2 scenario.	199
Table 4.25: Coefficient of variation (%) of projected rainfall and average temperature and soil moisture content for different scenarios and region of Uganda.	205

LIST OF FIGURES

Figure 1.1: Trends of global surface mean temperature based on observed (black), the AR5 RCPs (red) and AR4 SRES (blue) emissions scenarios together with the uncertainty estimates (shades) (Source: IPCC, 2014).....	2
Figure 1.2 (a-f): Observed and projected surface temperature anomalies (trends) over land for different continents, a - North America, b - Europe, c - Asia, d - South America, e - Africa and f - Australia (Source: IPCC, 2007).....	3
Figure 1.3: Drought occurrences for every 10 years in Uganda (1911-2000) (Source: NAPA, 2007).	5
Figure 1.4: Means of banana propagation (a) sword sucker, (b) maiden sucker and (c) tissue culture plantlet (Tushemereirwe <i>et al.</i> , 2001).	6
Figure 1.5: The relationship between weevil corm damage and altitude (a) and the impacts of weevil corm damage on banana bunch weight (b) (Wairegi <i>et al.</i> , 2010).	10
Figure 1.6: Agro-climatic zones and agricultural systems of Uganda (Adopted from Mwebaze, 1999).	16
Figure 1.7: Map showing administrative zones and districts of Uganda (UBOS, 2013).....	18
Figure 1.8: Average annual rainfall (mm/year) in Uganda. (Source: USAID, 2013).	18
Figure 1.9: Mean rainfall (mm) annual cycle for 1961-2013 for selected stations in Uganda. .	19
Figure 2.1 (a-f): Patterns of soil properties and composition levels based on the Harmonised World Soil Data (HWSD) over Uganda.....	26
Figure 2.2: The major components of a climate system (IPCC, 2014).....	35
Figure 2.3: AR5 (RCPs), AR4 (SRES) and IS92a emission scenarios pathways. (Source: IPCC, 2014).	38
Figure 2.4: A conceptual framework showing key variables and their linkages, experiments and methods used to study the relationships. Dotted arrows indicate factors that require experimental studies not considered but reviewed based on previous studies.....	45
Figure 3.1 (a-b): Representative observational stations for different homogeneous zones (a) and 0.5° model grid boxes, districts and seven analysis regions (b) over Uganda.	49
Figure 3.2: Comparison of changes in a timeseries based on (a) mean, (b) variability and (c) symmetry (IPCC, 2012).	62
Figure 3.3: Schematic representation of banana growth-temperature relationship. Source (Sastry, 1988).	64
Figure 3.4: PRECIS RCM optimal domain for the Eastern Africa region.....	66

Figure 3.5: Schematic representation of Taylor diagram. Source (Taylor 2012).	72
Figure 3.6: Climate requirements for banana growth under the FAO ECOCROP tool.....	77
Figure 4.1: Rainfall (a), minimum temperature (b) and maximum temperature (c) mass curves for Mbarara and Kabale.	81
Figure 4.2: Rainfall (a), minimum temperature (b) and maximum temperature (c) mass curves for Namulonge and Jinja.	82
Figure 4.3 (a-d): Comparison between insitu station observed rainfall (mm, orange) and CRU rainfall (mm, blue) during the June-August (JJA) season for Gulu, Kasese, Namulonge and Tororo stations for the period 1961-2009. Values for the root mean square errors (RMSE) and correlation coefficients (COR) have been indicated for each station.	85
Figure 4.4 (a-d): Comparison between insitu station observed rainfall (mm, orange) and CRU rainfall (mm, blue) during the October-December (OND) season for Gulu, Kasese, Namulonge and Tororo stations for the period 1961-2009. Values for the root mean square errors (RMSE) and correlation coefficients (COR) have been indicated for each station.	86
Figure 4.5 (a-d): Agreement between insitu station observed minimum surface temperature (°C) and CRU minimum surface temperature (°C) during the March-May (MAM, a, c) and the October-December (OND, b, d) seasons for Kasese (a, c) and Tororo (c, d) stations for the period 1961-2009. Values for the root mean square errors (RMSE) and correlation coefficients (COR) have been indicated for each station.	87
Figure 4.6 (a-d): Agreement between insitu station observed maximum surface temperature (°C) and CRU maximum surface temperature (°C) during the March-May (MAM, a, c) and the October-December (OND, b, d) seasons for Kasese (a, b) and Tororo (c, d) stations for the period 1961-2009. Values for the root mean square errors (RMSE) and correlation coefficients (COR) have been indicated for each station.	88
Figure 4.7 (a-i): Contribution of seasonal rainfall (%) to the total annual rainfall during March-May (MAM, a-c), June-August (JJA, d-f) and October-December (OND, g-i) for climatological periods 1931-1960 (a, d, g), 1961-1990 (b, e, h) and 1991-2013 (c, f, i) over Uganda.	90
Figure 4.8 (a-l): Spatial patterns of CRU seasonal rainfall mean (mm/day) for the periods 1931-2013 (a, e, i), 1931-1961 (b, f, g), 1961-1990 (c, g, k) and 1991-2013 (d, h, l) during March-May (MAM, a-d), June-August (JJA, e-h) and October-December (OND, i-l) over Uganda.	91

Figure 4.9 (a-f): Observed changes in CRU mean seasonal rainfall (mm/day) for the historical periods 1931-1960 (a, c, e) and 1961-1990 (b, d, f) for March-May (MAM, a-b), June-August (JJA, c-d) and October-December (OND, e-f) relative to the current period 1991-2013.	92
Figure 4.10 (a-l): Spatial patterns of CRU seasonal rainfall variability (mm/day) for the periods 1931-2013 (a, e, i), 1931-1961 (b, f, j), 1961-1990 (c, g, k) and 1991-2013 (d, h, l) during March-May (MAM, a-d), June-August (JJA, e-h) and October-December (OND, i-l) over Uganda.	94
Figure 4.11 (a-f): Observed changes in seasonal rainfall variability (standard deviation) (mm/day) during current period 1991-2013 relative to two historical periods; 1931-1960 (a, c, e) and 1961-1990 (b, d, f) for March-May (MAM, a-b), June-August (JJA, c-d) and October-December (OND, e-f) over Uganda.....	95
Figure 4.12 (a-c): Standardized precipitation indices (SPI) over Namulonge (a), Soroti (b) and Tororo (c). Blue indicated extremely wet periods while red indicated extremely dry (drought) periods during 1961-2013.	97
Figure 4.13 (a-c): Standardized precipitation indices (SPI) for Jinja (a), Kabale (b) and Mbarara (c). Blue indicated extremely wet periods while red indicated extremely dry (drought) periods during 1961-2013.	98
Figure 4.14 (a-c): Standardized precipitation indices (SPI) for Gulu (a), Arua (b) and Masindi (c). Blue indicated extremely wet periods while red indicated extremely dry (drought) periods during 1961-2013.	99
Figure 4.15: Inter-annual variability in annual rainfall totals (January-December) (mm) over Namulonge station during the period 1961-2013.....	101
Figure 4.16 (a-d): Inter-annual variability in seasonal rainfall totals (mm) during December-February (DJF, a), March-May (MAM, b), June-July (JJA, c) and October-December (OND, d) over Namulonge station during the period 1961-2013.	102
Figure 4.17: Inter-annual variability in annual rainfall totals (January-December) (mm) over Soroti station during the period 1961-2013.	103
Figure 4.18 (a-d): Inter-annual variability in seasonal rainfall totals (mm) during December-February (DJF, a), March-May (MAM, b), June-July (JJA, c) and October-December (OND, d) over Soroti station during the period 1961-2013.....	104
Figure 4.19: Inter-annual variability in annual rainfall totals (January-December, mm) over Tororo station during the period 1961-2013.	105

Figure 4.20 (a-d): Inter-annual variability in seasonal rainfall totals (mm) during December-February (DJF, a), March-May (MAM, b), June-July (JJA, c) and October-December (OND, d) over Tororo station during the period 1961-2013.....	106
Figure 4.21: Inter-annual variability in annual rainfall totals (January-December, mm) over Mbarara station during the period 1961-2013.....	107
Figure 4.22 (a-d): Inter-annual variability in seasonal rainfall totals (mm) during December-February (DJF, a), March-May (MAM, b), June-July (JJA, c) and October-December (OND, d) over Mbarara station during the period 1961-2013.	108
Figure 4.23: Inter-annual variability of annual minimum surface temperature anomalies over Tororo station during 1961-2013.	112
Figure 4.24 (a-d): Inter-annual variability of seasonal minimum surface temperature anomalies for December-February (DJF, a), March-May (MAM, b), July-August (JJA, c) and October-December (OND, d) over Tororo station during 1961-2013.	113
Figure 4.25: Inter-annual variability of annual maximum surface temperature anomalies over Tororo station during 1961-2013.	114
Figure 4.26 (a-d): Inter-annual variability of seasonal maximum surface temperature anomalies for December-February (DJF, a), March-May (MAM, b), July-August (JJA, c) and October-December (OND, d) over Tororo station during 1961-2013.	115
Figure 4.27 (a-c): Production (MT, a), area planted (Ha, b) and Yields (MT/Ha/yr, c) of different banana varieties in Uganda.....	122
Figure 4.28: FAO estimated trends in Uganda’s standardized Banana Area Harvested (AH, blue bars), Production (P, orange bars), and Banana Yields (BY, black line) during the period 1971-2009.	123
Figure 4.29: Annual banana production (% , blue) and area harvested (% , orange) for Central, Eastern, Western and Northern regions of Uganda.....	124
Figure 4.30 (a-b): Banana production (metric tonnes, a) and Banana yields (metric tonnes per Hactare per year, b) per district for 2008/2009 Uganda Census of Agriculture in Uganda (UBOS, 2010).	125
Figure 4.31 (a-c): Spatial patterns of banana area harvested (Ha, a), production (MT, b) and yields (MT/Ha, c) for 2008/2009 over Uganda.....	126
Figure 4.32: Relationship between banana yields (MT/Ha) and minimum surface temperature (°C) for the western region of Uganda.	130

Figure 4.33: Relationship between banana yields (MT/Ha) and maximum surface temperature (°C) for western region of Uganda.....	131
Figure 4.34: Relationship between banana yields (MT/Ha) and rainfall (mm) for western region.....	131
Figure 4.35: Relationship between banana yields (MT/Ha) and minimum surface temperature (°C) for central region of Uganda.....	132
Figure 4.36: Relationship between banana yields (MT) and maximum temperature for central region.....	133
Figure 4.37: Relationship between banana yields (MT/Ha) and rainfall (mm) for central region of Uganda.....	133
Figure 4.38: Regression model for banana yields over Western Uganda.....	135
Figure 4.39: Regression model for banana yields over Central Uganda.....	136
Figure 4.40 (a-c): Variation of monthly actual and effective mean rainfall for Kabale (a), Mbarara (b) and Kasese (c) stations. Numbers in the boxes indicate annual totals of actual and effective rainfall respectively.....	138
Figure 4.41 (a-c): Variation of monthly actual and effective mean rainfall for Jinja (a), Namulonge (b) and Mubende (c) stations. Numbers in the boxes indicate annual totals of actual and effective rainfall respectively.....	139
Figure 4.42 (a-c): Variation of monthly actual and effective mean rainfall for Soroti (a), Tororo (b) and Mbale (c) stations. Numbers in the boxes indicate annual totals of actual and effective rainfall respectively.....	142
Figure 4.43 (a-i): Spatial patterns of gridded observed (a-c) and regional climate model (PRECIS configurations, d-f and HadGEM3ra, g-h) simulated March-May (MAM) season mean (1991-2008) rainfall (mm/day) over Uganda. Multi-model ensemble (MME, i) shows the mean of five model configurations (d-h).....	147
Figure 4.44 (a-i): Spatial patterns of gridded observed (a-c) and regional climate model (PRECIS configurations, d-f and HadGEM3ra, g-h) simulated June-August (JJA) season mean (1991-2008) rainfall (mm/day) over Uganda. Multi-model ensemble (MME, i) shows the mean of five models configurations (d-h).....	148
Figure 4.45 (a-i): Spatial patterns of gridded observed (a-c) and regional climate model (PRECIS configurations, d-f and HadGEM3ra, g-h) simulated October-December (OND) season mean (1991-2008) rainfall (mm/day) over Uganda. Multi-model ensemble (MME, i) shows the mean of five model configurations (d-h).....	149

Figure 4.46 (a-i): Spatial patterns of gridded observed (a-c) and regional climate model (PRECIS configurations, d-f and HadGEM3ra, g-h) simulated March-May (MAM) season rainfall coefficient of variation (CV, x100%, 1991-2008) over Uganda. Multi-model ensemble (MME, i) shows the mean of five models configurations (d-h)..... 150

Figure 4.47 (a-i): Spatial patterns of gridded observed (a-c) and regional climate model (PRECIS configurations, d-f and HadGEM3ra, g-h) simulated June-August (JJA) season rainfall coefficient of variation (CV, x100%, 1991-2008) over Uganda. Multi-model ensemble (MME, i) shows the mean of five model configurations (d-h). 151

Figure 4.48 (a-i): Spatial patterns of gridded observed (a-c) and regional climate model (PRECIS configurations, d-f and HadGEM3ra, g-h) simulated October-December (OND) season rainfall coefficient of variation (CV, x100%, 1991-2008) over Uganda. Multi-model ensemble (MME, i) shows the mean of five model configurations (d-h).152

Figure 4.49 (a-d): Observed (a-b) and PRECIS RCM (c-d) spatial patterns of the first (a, c) and second (b, d) dominant modes of rainfall variability from Empirical Orthogonal Functions (EOFs) during March-May (MAM, 1991-2008) over Uganda. 153

Figure 4.50 (a-d): Observed (a-b) and PRECIS RCM (c-d) temporal patterns of the first (a, c) and second (b, d) dominant modes of rainfall variability from Empirical Orthogonal Functions (EOFs) during March-May (MAM, 1991-2008) over Uganda. 154

Figure 4.51 (a-d): Observed (a-b) and PRECIS RCM (c-d) spatial patterns of the first (a, c) and second (b, d) dominant modes of rainfall variability from Empirical Orthogonal Functions (EOFs) during October-December (OND, 1991-2008) over Uganda. 155

Figure 4.52 (a-d): Observed (a-b) and PRECIS RCM (c-d) temporal patterns of the first (a, c) and second (b, d) dominant modes of rainfall variability from Empirical Orthogonal Functions (EOFs) during October-December (OND, 1991-2008) over Uganda. 156

Figure 4.53 (a-c): ERA-Interim mean wind (ms^{-1}) patterns (1991-2008) at 850 mb for March-May (MAM, a), June-August (JJA, b) and October-December (OND, c) over Eastern Africa region. Shade colours represent wind speeds (m/s) while arrows represent direction..... 158

Figure 4.54 (a-c): PRECIS Simulated mean wind (ms^{-1}) patterns (1991-2008) at 850 mb for March-May (MAM, a), June-August (JJA, b) and October-December (OND, c) over Eastern Africa region. Shade colours represent wind speeds (m/s) while arrows represent direction..... 159

Figure 4.55 (a-d): Observed and simulated averaged (1991-2008) rainfall seasonality (annual cycles) over western (a), northwestern (b), central (c) and northeastern (d) regions of Uganda.	160
Figure 4.56 (a-b): Observed and simulated averaged (1991-2008) rainfall seasonality over eastern (a) and southwestern (b) regions of Uganda.	161
Figure 4.57: Observed and simulated interannual rainfall anomalies for MAM (a, c) and OND (b, d) over western (a-b) and central (c-d) regions of Uganda.	162
Figure 4.58: Inter model comparisons based on Taylor diagrams (summary of three model performance indices) for March-May (MAM) seasonal rainfall simulation during the period 1991-2008 over Uganda.	170
Figure 4.59: Inter model comparisons based on Taylor diagrams (summary of three model performance indices) for June-August (JJA) seasonal rainfall simulation during the period 1991-2008 over Uganda.	170
Figure 4.60: Inter model comparisons based on Taylor diagrams (summary of three model performance indices) for October-December (OND) seasonal rainfall simulation during the period 1991-2008 over Uganda.	171
Figure 4.61 (a-f): PRECIS simulated seasonal mean rainfall (mm/day) projections for the periods 2011-2040 (a-c) and 2061-2090 (d-f) during March-May (MAM a, d), June-August (JJA b, e) and October-December (OND c, f) seasons for SRES A1B scenario over Uganda.	174
Figure 4.62 (a-f): PRECIS simulated seasonal mean rainfall (mm/day) projections for the periods 2011-2040 (a-c) and 2061-2090 (d-f) during March-May (MAM a, d), June-August (JJA b, e) and October-December (OND c, f) seasons for SRES A2 scenario over Uganda.	175
Figure 4.63 (a-f): PRECIS simulated seasonal rainfall (mm/day) variability projections for the periods 2011-2040 (a-c) and 2061-2090 (d-f) during March-May (MAM a, d), June-August (JJA b, e) and October-December (OND c, f) seasons for SRES A1B scenario over Uganda.	176
Figure 4.64 (a-f): PRECIS simulated seasonal rainfall (mm/day) variability projections for the periods 2011-2040 (a-c) and 2061-2090 (d-f) during March-May (MAM a, d), June-August (JJA b, e) and October-December (OND c, f) seasons for SRES A2 scenario over Uganda.	177

Figure 4.65 (a-f): PRECIS simulated seasonal rainfall coefficient of variation (CV, %) projections for the periods 2011-2040 (a-c) and 2061-2090 (d-f) during March-May (MAM a, d), June-August (JJA b, e) and October-December (OND c, f) seasons for SRES A1B scenario over Uganda.....	178
Figure 4.66 (a-f): PRECIS simulated seasonal rainfall coefficient of variation (CV, %) projections for the periods 2011-2040 (a-c) and 2061-2090 (d-f) during March-May (MAM a, d), June-August (JJA b, e) and October-December (OND c, f) seasons for SRES A2 scenario over Uganda.	178
Figure 4.67 (a-f): PRECIS simulated seasonal rainfall (mm/day) changes for the periods 2011-2040 (a-c) and 2061-2090 (d-f) during March-May (MAM a, d), June-August (JJA b, e) and October-December (OND c, f) seasons for SRES A1B scenario over Uganda. ...	179
Figure 4.68 (a-f): PRECIS simulated seasonal rainfall (mm/day) changes for the periods 2011-2040 (a-c) and 2061-2090 (d-f) during March-May (MAM a, d), June-August (JJA b, e) and October-December (OND c, f) seasons for SRES A2 scenario over Uganda.....	180
Figure 4.69 (a-f): PRECIS simulated seasonal mean surface temperature (°C) projections for the periods 2011-2040 (a-c) and 2061-2090 (d-f) during March-May (MAM a, d), June-August (JJA b, e) and October-December (OND c, f) seasons for SRES A1B scenario over Uganda.	183
Figure 4.70 (a-f): PRECIS simulated seasonal mean surface temperature (°C) projections for the periods 2011-2040 (a-c) and 2061-2090 (d-f) during March-May (MAM a, d), June-August (JJA b, e) and October-December (OND c, f) seasons for SRES A2 scenario over Uganda.	183
Figure 4.71 (a-f): PRECIS simulated seasonal surface temperature (°C) variability (standard deviation) projections for the periods 2011-2040 (a-c) and 2061-2090 (d-f) during March-May (MAM a, d), June-August (JJA b, e) and October-December (OND c, f) seasons for SRES A1B scenario over Uganda.	184
Figure 4.72 (a-f): PRECIS simulated seasonal surface temperature (°C) variability (standard deviation) projections for the periods 2011-2040 (a-c) and 2061-2090 (d-f) during March-May (MAM a, d), June-August (JJA b, e) and October-December (OND c, f) seasons for SRES A2 scenario over Uganda.....	185
Figure 4.73 (a-f): PRECIS simulated seasonal surface temperature coefficient of variation (CV, %) projections for the periods 2011-2040 (a-c) and 2061-2090 (d-f) during March-May	

(MAM a, d), June-August (JJA b, e) and October-December (OND c, f) seasons for SRES A1B scenario over Uganda.....	186
Figure 4.74 (a-f): PRECIS simulated seasonal surface temperature coefficient of variation (CV, %) projections for the periods 2011-2040 (a-c) and 2061-2090 (d-f) during March-May (MAM a, d), June-August (JJA b, e) and October-December (OND c, f) seasons for SRES A2 scenario over Uganda.	186
Figure 4.75 (a-f): PRECIS simulated seasonal surface temperature changes ($^{\circ}$ C) for the periods 2011-2040 (a-c) and 2061-2090 (d-f) during March-May (MAM a, d), June-August (JJA b, e) and October-December (OND c, f) seasons for SRES A1B scenario over Uganda.	187
Figure 4.76 (a-f): PRECIS simulated seasonal surface temperature changes ($^{\circ}$ C) for the periods 2011-2040 (a-c) and 2061-2090 (d-f) during March-May (MAM a, d), June-August (JJA b, e) and October-December (OND c, f) seasons for SRES A2 scenario over Uganda.	188
Figure 4.77 (a-f): PRECIS simulated seasonal mean soil moisture content (mm/day) projections for the periods 2011-2040 (a-c) and 2061-2090 (d-f) during March-May (MAM a, d), June-August (JJA b, e) and October-December (OND c, f) seasons for SRES A1B scenario over Uganda.....	192
Figure 4.78 (a-f): PRECIS simulated seasonal mean soil moisture content (mm/day) projections for the periods 2011-2040 (a-c) and 2061-2090 (d-f) during March-May (MAM a, d), June-August (JJA b, e) and October-December (OND c, f) seasons for SRES A2 scenario over Uganda.	193
Figure 4.79 (a-f): PRECIS simulated seasonal variability (standard deviation) of soil moisture content (mm/day) projections for the periods 2011-2040 (a-c) and 2061-2090 (d-f) during March-May (MAM a, d), June-August (JJA b, e) and October-December (OND c, f) seasons for SRES A1B scenario over Uganda.	194
Figure 4.80 (a-f): PRECIS simulated seasonal variability (standard deviation) of soil moisture content (mm/day) projections for the periods 2011-2040 (a-c) and 2061-2090 (d-f) during March-May (MAM a, d), June-August (JJA b, e) and October-December (OND c, f) seasons for SRES A2 scenario over Uganda.	194
Figure 4.81 (a-f): PRECIS simulated seasonal coefficient of variation (CV, %) of soil moisture content projections for the periods 2011-2040 (a-c) and 2061-2090 (d-f) during March-	

May (MAM a, d), June-August (JJA b, e) and October-December (OND c, f) seasons for SRES A1B scenario over Uganda.	195
Figure 4.82 (a-f): PRECIS simulated seasonal coefficient of variation (CV, %) of soil moisture content projections for the periods 2011-2040 (a-c) and 2061-2090 (d-f) during March- May (MAM a, d), June-August (JJA b, e) and October-December (OND c, f) seasons for SRES A2 scenario over Uganda.	196
Figure 4.83 (a-f): Changes in PRECIS seasonal soil moisture content for SRES A1B (a-c) and A2 (d-f) scenarios during March-May (MAM a, d), June-August (JJA b, e) and October-December (OND c, f) seasons over Uganda.	197
Figure 4.84 (a-i): PRECIS projected variations of rainfall (a-c), temperature (d-f) and soil moisture content (g-i) for mean (a, d, g), standard deviation (b, e, h) and coefficient of variation (c, f, i) for both SRES A1B and A2 (see legend) over Western region of Uganda.	202
Figure 4.85 (a-i): PRECIS projected variations of rainfall (a-c), temperature (d-f) and soil moisture content (g-i) for mean (a, d, g), standard deviation (b, e, h) and coefficient of variation (c, f, i) for both SRES A1B and A2 (see legend) over Central region of Uganda.	203
Figure 4.86 (a-i): PRECIS projected variations of rainfall (a-c), temperature (d-f) and soil moisture content (g-i) for mean (a, d, g), standard deviation (b, e, h) and coefficient of variation (c, f, i) for both SRES A1B and A2 (see legend) over Eastern region of Uganda.	204
Figure 4.87 (a-b): A1B (a) and A2 (b) PRECIS projected seasonal and annual rainfall trends (2001-2095) over the Western region of Uganda.	206
Figure 4.88 (a-b): A1B (a) and A2 (b) PRECIS projected seasonal and annual rainfall trends (2001-2095) over the Central region of Uganda.	207
Figure 4.89 (a-b): A1B (a) and A2 (b) PRECIS projected seasonal and annual rainfall trends (2001-2095) over the Eastern region of Uganda.	207
Figure 4.90 (a-b): A1B (a) and A2 (b) PRECIS projected seasonal and annual average temperature trends (2001-2095) over the Western region of Uganda.	208
Figure 4.91 (a-b): A1B (a) and A2 (b) PRECIS projected seasonal and annual average temperature trends (2001-2095) over the Central region of Uganda.	208
Figure 4.92 (a-b): A1B (a) and A2 (b) PRECIS projected seasonal and annual average temperature trends (2001-2095) over the Eastern region of Uganda.	209

Figure 4.93 (a-b): A1B (a) and A2 (b) PRECIS projected seasonal and annual soil moisture content trends (2001-2095) over the Western region of Uganda.	210
Figure 4.94 (a-b): A1B (a) and A2 (b) PRECIS projected seasonal and annual soil moisture content trends (2001-2095) over the Central region of Uganda.	210
Figure 4.95 (a-b): A1B (a) and A2 (b) PRECIS projected seasonal and annual soil moisture content trends (2001-2095) over the Eastern region of Uganda.	211
Figure 4.96 (a-f): PRECIS projected annual soil moisture content (mm/day) and rainfall-temperature ratio (%) for SRES A1B (a-c) and A2 (d-f) scenarios (2011-2040).	212
Figure 4.97 (a-f): PRECIS projected annual soil moisture content (mm/day) and rainfall-temperature ratio (%) for SRES A1B (a-c) and A2 (d-f) scenarios (2061-2090).	213
Figure 4.98 (a-l): The RCP 4.5 (a, b, e, f, i, j) and RCP 8.5 (c, d, g, h, k, l) projected mean rainfall (2011-2040 & 2061-2090) during MAM (a-d), JJA (e-h) and OND (i-l) over Uganda.	214
Figure 4.99 (a-l): The RCP 4.5 (a, b, e, f, i, j) and RCP 8.5 (c, d, g, h, k, l) projected coefficient of variability of rainfall (2011-2040 & 2061-2090) during MAM (a-d), JJA (e-h) and OND (i-l) over Uganda.	215
Figure 4.100 (a-l): The RCP 4.5 (a, b, e, f, i, j) and RCP 8.5 (c, d, g, h, k, l) projected seasonal mean surface temperature (°C) (2011-2040 & 2061-2090) during MAM (a-d), JJA (e-h) and OND (i-l) over Uganda.....	216
Figure 4.101 (a-f): Spatial patterns of projected changes in seasonal surface temperature (°C) for RCP 4.5 (a, c, e) and RCP 8.5 (b, d, f) between the periods 2061-2090 and 2011-2040 over Uganda.	217
Figure 4.102 (a-d): Observed annual mean surface temperature (a), mean temperature of coldest quarter (b), annual mean rainfall (c) and mean rainfall of driest quarter (d) over Uganda.	219
Figure 4.103 (a-d): Projected annual mean surface temperature (a), mean temperature of coldest quarter (b), annual mean rainfall (c) and mean rainfall of driest quarter (d) for RCP 2.6 (2041-2060) over Uganda.....	220
Figure 4.104 (a-d): Projected annual mean surface temperature (a), mean temperature of coldest quarter (b), annual mean rainfall (c) and mean rainfall of driest quarter (d) for RCP 2.6 (2061-2080) over Uganda.....	221

Figure 4.105 (a-d): Projected annual mean surface temperature (a), mean temperature of coldest quarter (b), annual mean rainfall (c) and mean rainfall of driest quarter (d) for RCP 4.5 (2041-2060) over Uganda.....	222
Figure 4.106 (a-d): Projected annual mean surface temperature (a), mean temperature of coldest quarter (b), annual mean rainfall (c) and mean rainfall of driest quarter (d) for RCP 4.5 (2061-2080) over Uganda.....	223
Figure 4.107 (a-d): Projected annual mean surface temperature (a), mean temperature of coldest quarter (b), annual mean rainfall (c) and mean rainfall of driest quarter (d) for RCP 6.0 (2041-2060) over Uganda.....	224
Figure 4.108 (a-d): Projected annual mean surface temperature (a), mean temperature of coldest quarter (b), annual mean rainfall (c) and mean rainfall of driest quarter (d) for RCP 6.0 (2061-2080) over Uganda.....	225
Figure 4.109 (a-d): Projected annual mean surface temperature (a), mean temperature of coldest quarter (b), annual mean rainfall (c) and mean rainfall of driest quarter (d) for RCP 8.5 (2041-2060) over Uganda.....	226
Figure 4.110 (a-d): Projected annual mean surface temperature (a), mean temperature of coldest quarter (b), annual mean rainfall (c) and mean rainfall of driest quarter (d) for RCP 8.5 (2061-2080) over Uganda.....	227
Figure 4.111 (a-b): Projected future suitability of banana growth under RCP 2.6 for the period 2041-2060 (a) and 2061-2080 (b) over Uganda.....	229
Figure 4.112 (a-b): Projected future suitability of banana growth under RCP 4.5 for the period 2041-2060 (a) and 2061-2080 (b) over Uganda.....	230
Figure 4.113 (a-b): Projected future suitability of banana growth under RCP 6.0 for the period 2041-2060 (a) and 2061-2080 (b) over Uganda.....	231
Figure 4.114 (a-b): Projected future suitability of banana growth under RCP 8.5 for the period 2041-2060 (a) and 2061-2080 (b) over Uganda.....	231
Figure 4.115 (a-d): Projected effects of MAM surface temperature changes on banana growth under A1B and A2 scenarios for northwestern (a-b) and eastern (c-d) regions. Orange bars indicate frequency of SRES A1B temperature, blue bars indicate frequency of SRES A2 temperature, green curve indicate temperature-banana growth.....	233
Figure 4.116 (a-d): Projected effects of MAM surface temperature changes on banana growth under A1B & A2 scenarios for central (a-b) and western (c-d) regions. Orange bars	

	indicate frequency of SRES A1B temperature, blue bars indicate frequency of SRES A2 temperature, green curve indicate temperature-banana growth.	234
Figure 4.117 (a-d):	Projected effects of MAM surface temperature changes on banana growth under A1B & A2 scenarios for southwestern (a-b) and Uganda (c-d) regions. Orange bars indicate frequency of SRES A1B temperature, blue bars indicate frequency of SRES A2 temperature, green curve indicate temperature-banana growth.....	235
Figure 4.118 (a-d):	Projected effects of JJA surface temperature changes on banana growth under A1B & A2 scenarios for northwestern (a-b) and eastern (c-d) regions. Orange bars indicate frequency of SRES A1B temperature, blue bars indicate frequency of SRES A2 temperature, green curve indicate temperature-banana growth.....	236
Figure 4.119 (a-d):	Projected effects of JJA surface temperature changes on banana growth under A1B & A2 scenarios for central (top-panel) and western (c-d) regions. Orange bars indicate frequency of SRES A1B temperature, blue bars indicate frequency of SRES A2 temperature, green curve indicate temperature-banana growth.....	237
Figure 4.120 (a-d):	Projected effects of JJA surface temperature changes on banana growth under A1B & A2 scenarios for southwestern (a-b) and Uganda (c-d) regions. Orange bars indicate frequency of SRES A1B temperature, blue bars indicate frequency of SRES A2 temperature, green curve indicate temperature-banana growth.....	238

LIST OF ACRONYMS AND ABBREVIATIONS

ADW	Angular Distance Weighted
AGCM	Atmospheric General Circulation Model
AIM	Asia-Pacific Integrated Model
ANOVA	Analysis of Variance
AOGCM	Atmosphere Ocean Global Circulation Model
AR4	Assessment Report Four
AR5	Assessment Report Five
AVHRR	Advanced Very High Resolution Radiometer
AWS	Automated Weather Stations
CAI	Climatologically Aided Interpolation
CDD	Correlation-Decay Distance
CMIP3	Coupled Model Inter-comparison Project phase 3
CMIP5	Coupled Model Inter-comparison Project phase 5
CORDEX	Coordinated Regional Downscaling Experiments
CRF ₁₂	Cumulative Rainfall 12 months before harvest
CROPWAT	Crop Water Assessment Tool
CRU	Climate Research Unit
DfID	Department for International Development (UK Government)
DSSAT	Decision Support System for Agro-technology Transfer
ECHAM	European Centre-Hamburg Model
ECMWF	European Centre for Medium range Weather Forecasting
ECOCROP	Ecology of Crop species
EMU	External Monitoring Unit
ENSO	El Niño Southern Oscillation
EOFs	Empirical Orthogonal Functions
ERA	European Center for Medium Range Weather Forecasting (ECMWF) Re-Analysis
ESRI	Environment System Research Institute
FAO	Food and Agricultural Organization
FEWS NET	Famine Early Warning System Network
GCAM	Global Change Assessment Model
GCMs	General Circulation Models

GDP	Gross Domestic Product
GHA	Greater Horn of Africa
GHCN's	Global Historical Climatology Network's
GIS	Geographical Information Systems
GPCP	Global Precipitation Climatology Project
GPCP	Global Precipitation Climatology Project
GSOD	Global Surface Summary of the Day
HadAM3P	Hadley Centre Atmospheric Model version 3P
HadCM3	Hadley Centre Coupled Model version 3
HadGEM3-RA	Hadley Centre Global Environmental Model version 3 - Regional
HWSD	Harmonised World Soil Data
ICRA	Integrated Climate Risk Assessment
ICTP	International Centre for Theoretical Physics
IMAGE	Integrated Model to Assess the Global Environment
IOD	Indian Ocean dipole
IPCC	Inter-Governmental Panel on Climate Change
IS92	IPCC Scenarios of 1992
ITCZ	Inter-Tropical Convergence Zone
JJA	June, July, August
LDCs	Least Developed Countries
LER	Leaf Expansion Rate
MAAIF	Ministry of Agriculture, Animal Industry and Fisheries of Uganda
MAM	March, April, May
MDGs	Millennium Development Goals
MESSAGE	Model for Energy Supply Strategy Alternatives and their General Environmental Impact
MOSES	Met Office Surface Exchange Scheme
MPI	Max Plank Institute
MSLP	Mean Sea Level Pressure
NAPA	National Adaptation Plan for Action
NAR	Net Assimilation Rate
NARO	National Agricultural Research Organization
NCEP	National Centers for Environmental Prediction

OND	October, November, December
PCA	Principal Component Analysis
PRECIS	Providing Regional Climates for Impacts Studies
RCMs	Regional Climate Models
RCPs	Representative Concentration Pathways
RF	Radiative Forcing
RMSE	Root Mean Square Error
RSS	Residual Sum of Squares
SDGs	Sustainable Development Goals
SMC	Soil Moisture Content
SOM	Soil Organic Matter
SPI	Standardized Precipitation Index
SRES	Special Report on Emission Scenarios
SREX	Special Report on Extremes
SSE	Sum of Squared Errors
SSTs	Sea Surface Temperatures
SWAT	Soil and Water Assessment Tool
TAR	Third Assessment Report
UBOS	Uganda Bureau of Statistics
UCA	Uganda Census of Agriculture
UDel	University of Delaware
UEA	University of East Anglia
UKCIP	United Kingdom Climate Inter-comparison Project
UKMO	United Kingdom Meteorological Office
UNEP	United Nations Environmental Programme
UNFCCC	United Nations Framework Convention on Climate Change
UNHS	Uganda National Household Survey
UNMA	Uganda National Meteorological Authority
USAID	United States Agency for International Development
WMO	World Meteorological Organization
WWF	World Wildlife Fund

OPERATIONAL DEFINITION OF TERMS

Adaptation: This is the process whereby human systems adjust to actual or expected climate and its effects in order to minimize adverse effects or maximize beneficial effects.

Agricultural inputs: These refer to either physical or biological or chemical or inorganic compounds used in the production of agricultural products.

Climate change: This refers to a permanent shift in the state of climate that can be detected by use of statistical methods as changes in the mean and/or variability and persisting for decades or longer periods.

Climate extremes: This refers to the occurrence of a value of weather or climate variable beyond a given threshold in the range of observed values of the variable.

Climate scenarios: These refer to a set of simplified yet plausible description of how the future may evolve based on rational and internally consistent set of assumptions about key driving forces and relationships within a climate system.

Climate variability: This refers to the short term shifts in the mean state of climate and other statistics beyond the individual weather events at all spatial and temporal scales.

CROPWAT: This is a decision support system developed by the Land and Water Development Division of FAO for planning and management of irrigation. CROPWAT is meant as a practical tool to carry out standard calculations for reference evapotranspiration, crop water requirements and crop irrigation requirements, and more specifically the design and management of irrigation schemes. It allows the development of recommendations for improved irrigation practices, the planning of irrigation schedules under varying water supply conditions, and the assessment of production under rainfed conditions or deficit irrigation.

Drought: This refers to an extended period, either a season, year or longer characterized by deficiency of precipitation compared to statistical average over the same period over the region thus yielding to water shortage for both flora and fauna livelihoods.

Effective rainfall: This is the part of rainfall which is available to be used by the crop after rainfall lost due to surface run-off and deep percolation has been accounted for. The effective rainfall is ultimately used to determine soil moisture deficits under rainfed Agriculture.

El Niño/Southern Oscillation (ENSO): The interaction between the atmosphere and ocean in the tropical Pacific that results in a somewhat periodic variation between below-normal and above-normal sea surface temperatures and dry and wet conditions over the course of a few years. While the tropical ocean affects the atmosphere above it, so too does the atmosphere influence the ocean below it.

Emissivity: Emissivity is defined as the ratio of the energy radiated from a material's surface to that radiated from a blackbody (a perfect emitter) at the same temperature and wavelength and under the same viewing conditions.

Food security: This refers to a situation when all people, at all times, have physical, social and economic access to sufficient, safe and nutritious food which meets their dietary needs and food preferences for an active and healthy life.

General Circulation Model (GCM): This refers to a global, three-dimensional computer model of the climate system that can be used to simulate human-induced climate change. GCMs represent the effects of such factors as reflective and absorptive properties of atmospheric water vapor, greenhouse gas concentrations, clouds, annual and daily solar heating, ocean temperatures, and ice boundaries.

Global warming: This refers to intensifying greenhouse effect resulting from anthropogenic actions, where the consequence is an increase in the concentration of greenhouse gases, aerosols or their predecessors in the atmosphere, which absorb part of the infrared radiation emitted by the Earth's surface, thus increasing the average temperature on the planet and causing adverse climatic phenomena.

Greenhouse gases: These are gaseous constituents of the atmosphere, both natural and anthropogenic that absorb and re-emit infrared radiation causing global warming.

Grid cell: A rectangular area that represents a portion of the Earth's surface.

HadGEM3-RA: The HadGEM3-RA (Hadley Centre Global Environmental Model version 3 - Regional) is a relatively new United Kingdom Meteorological Office (UKMO) regional climate model that can provide climate simulations at variable resolution over a limited area on the globe.

Indian Ocean Dipole (IOD): It is an atmosphere-ocean coupled phenomenon in the tropical Indian Ocean characterised by a difference in western and eastern sea-surface temperatures. A positive IOD is associated with cooler than normal sea-surface temperatures in the eastern equatorial Indian Ocean and warmer than normal sea-surface temperatures in the western tropical Indian Ocean. The opposite phenomenon is called a negative IOD, and is characterised by warmer than normal SSTs in the eastern equatorial Indian Ocean and cooler than normal SSTs in the western tropical Indian Ocean.

Interannual variability: Year to year change in the mean state of the climate that is caused by a variety of factors and interactions within the climate system. One important example of interannual variability is the quasi-periodic change of atmospheric and oceanic circulation

patterns in the Tropical Pacific region, collectively known as El Niño-Southern Oscillation (ENSO).

Linkages: This refers to the nature and degree of the relationship between dependent (banana yields) and independent variables (rainfall and temperature) in the study.

Livelihood: This comprises the capabilities, assets (including both material and social resources) and activities for a means of living. A livelihood is sustainable when it can cope with and recover from climate and other stresses and shocks, maintain or enhance its capabilities and assets, while not undermining the natural resource base.

National Adaptation Programme of Action (NAPA): These provide a process for the Least Developed Countries (LDCs) to identify priority activities that respond to their urgent and immediate needs with regard to adaptation to climate change. Further delay could increase vulnerability or lead to increased costs at a later stage. The rationale for NAPAs rests on the limited ability of the LDCs to adapt to the adverse effects of climate change.

Providing Regional Climates for Impacts Studies (PRECIS): This is a regional climate modelling system with high resolution that can be run over a limited area of the globe. The PRECIS system can be set up and run using a relatively fast personal computer to provide current and future regional climate information for climate change vulnerability and impacts studies.

Rainfall Season: This measures the number of months between the onset and cessation of the rainfall in a particular region.

Regional Climate Model (RCM): High-resolution (typically 50 kilometers) computer model that represents local features. It is constructed for limited areas, run for periods of ~20 years, and driven by large-scale data.

Resilience: This is the ability of a system to adapt to climate change, whether by taking advantage of the opportunities or by dealing with the consequences.

Spatial downscaling: Refers to the methods used to derive climate information at finer spatial resolution from coarser spatial resolution GCM output. The fundamental basis of spatial downscaling is the assumption that significant relationships exist between local and large-scale climate.

Spatial resolution: In climate, spatial resolution refers to the size of a grid cell in which 10-80 km and 200 - 500 km are considered to be fine and coarse resolution respectively.

Sustainable development: This refers to development which meets the needs of the present without compromising the ability of future generations to meet their own needs.

Turkana Jet stream: This is a strong southeasterly low-level jet in the Turkana Channel which separates the Ethiopian highlands and the East African highlands. The jet exists throughout the year, with speeds exceeding 30 m s^{-1} on a number of occasions and sometimes exceeding 50 m s^{-1} . During February and March, the mean monthly winds of the jet stream based on the morning observations exceed 25 m s^{-1} .

Uncertainty: An expression of the degree to which a value (e.g., the future state of the climate system) is unknown. Uncertainty can result from lack of information or from disagreement about what is known or even knowable. Uncertainty can be represented by quantitative measures (a range of values calculated by various models), or by qualitative statements, reflecting the judgment of a team of experts.

Vulnerability: This refers to the degree of susceptibility or inability to protect oneself from the negative effects of climate change, a function of the type, magnitude and frequency of the climate events to which a system is exposed, in addition to its sensitivity to and capacity for adaptation

CHAPTER ONE

INTRODUCTION

1.0 Background to the Study

Extremes and fluctuations in climate patterns affect most socio-economic sectors including agriculture and food security, water, settlement, transport, and energy (Easterling *et al.*, 2000; Ogallo *et al.*, 2002; Pandey *et al.*, 2003; Parry *et al.*, 2004; FAO, 2008; IPCC, 2012 and Otieno *et al.*, 2015). IPCC (2012) Special Report on Extremes (SREX) observed that changes in frequency and severity of droughts, rainfall intensity and duration, erratic rainfall, floods and heat waves include some of the climate related hazards that are being experienced in many regions. Changes in the frequency, intensity, spatial extent, duration, and timing of climate extreme events continue to cause economic losses characterized with high spatial and inter-annual variability (IPCC, 2012). In addition, climate change is projected to cause more frequent and intense El Niño Southern Oscillation (ENSO) events, leading to widespread drought in some areas and widespread flooding in others (Wara *et al.*, 2005; McHugh, 2006; Riddle and Cook, 2008; Patricola and Cook, 2011; IPCC, 2014; Mwangi *et al.*, 2014; Ngaina *et al.*, 2014 and Otieno *et al.*, 2015). The recurrent droughts and floods among other climate extremes have had dramatic impacts on food security, migrations of people, livestock and wild life, resources based conflicts, water shortages, among many other socio-economic impacts in many parts of Africa (Easterling *et al.*, 2000; Ingram and Dawson, 2005; Funk *et al.*, 2008 and Egeru *et al.*, 2014).

The Greater Horn of Africa (GHA) including Uganda has in the recent past experienced an increased number of climate extremes (Ogallo *et al.*, 2002; Hastenrath and Polzin, 2004; Gitau, 2005; Barasa *et al.*, 2013; Mwangi *et al.*, 2014; Ngaina *et al.*, 2014 and Otieno *et al.*, 2015) that pose a challenge to the region's socio-economic development (Stern, 1996; Thornton *et al.*, 2009 and Egeru *et al.*, 2014). Climate extremes have contributed to poor performance of the agriculture sector (Stern, 1996 and Stern *et al.*, 2006). Recent economic assessment report and studies (Surendran *et al.*, 2014 and Ampaire *et al.*, 2015) showed that no sustainable development can be attained in the region without effective regional systems for climate risk reduction including climate change adaptation. Increases in the frequency and intensity of

these climate extremes are subjects of many recent studies and assessments (Easterling *et al.*, 2000 and IPCC, 2012; 2014).

The working groups of the Inter-Governmental Panel on Climate Change (IPCC) have produced a series of reports based on climate variability and climate change studies and associated impacts addressing several issues on global and regional climate variability and change (IPCC, 2001; 2007; 2012; 2014). The IPCC reports have provided an account of the climate science basis, trends in observed climate records, future climate scenarios and projected future climate patterns of different parts of the world using Global Climate Models (GCMs) with relatively low spatial resolution. Figure 1.1 gives an example of the global temperature trends between 1860 and 2010 for both observations and climate model projections based on the Coupled Model Inter-comparison Projects phases 3 and 5 (CMIP3 and CMIP5) (IPCC, 2014). There are however, variations in continental and regional surface temperature trends (IPCC, 2014) in both climate observations and projections across the different continents for the period 1900-2050 as depicted in Figure 1.2.

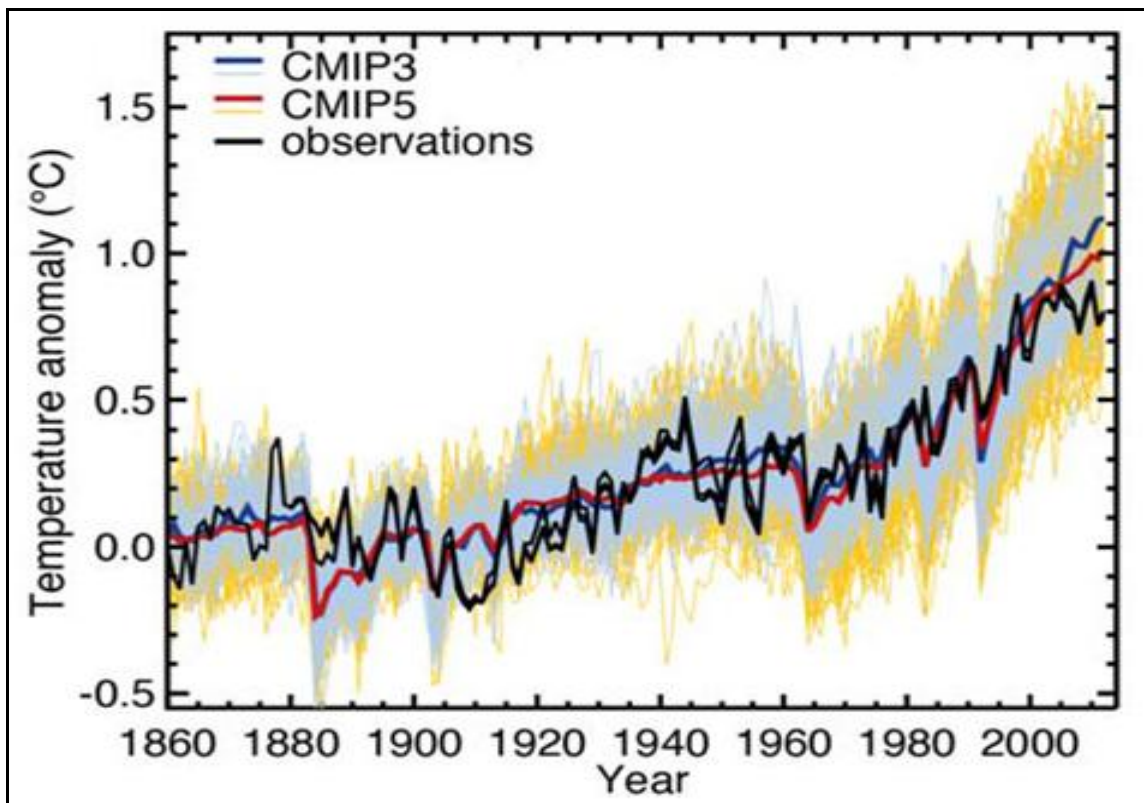


Figure 1.1: Trends of global surface mean temperature based on observed (black), the AR5 RCPs (red) and AR4 SRES (blue) emissions scenarios together with the uncertainty estimates (shades) (Source: IPCC, 2014).

Most of agriculture and food security and many other economic activities in Uganda rely directly on rainfall (Funk *et al.*, 2008 and Egeru, 2012). The variations in Uganda's Gross Domestic Product and food security have been linked to impacts of climate variability and change majorly due to over-reliance on rain-fed agriculture (Cooper *et al.*, 2011). Heavy reliance of agricultural activities on climate makes food security and economic viability of Uganda's agricultural sector highly vulnerable to extreme climatic conditions. Failure or underperformance in the agricultural sector particularly crop farming resulting from climate related impacts, not only leads to food insecurity but also to loss of incomes by farmers and loss of foreign exchange. This is due to the reduced exportable agricultural produce and raw materials and an increased need for importation of food into the Country. Previous studies (Funk *et al.*, 2008; FEWS NET, 2011 and Shongwe *et al.*, 2011) have observed that this region has already witnessed dire consequences of erratic climate conditions that are likely to be associated with regional climate changes.

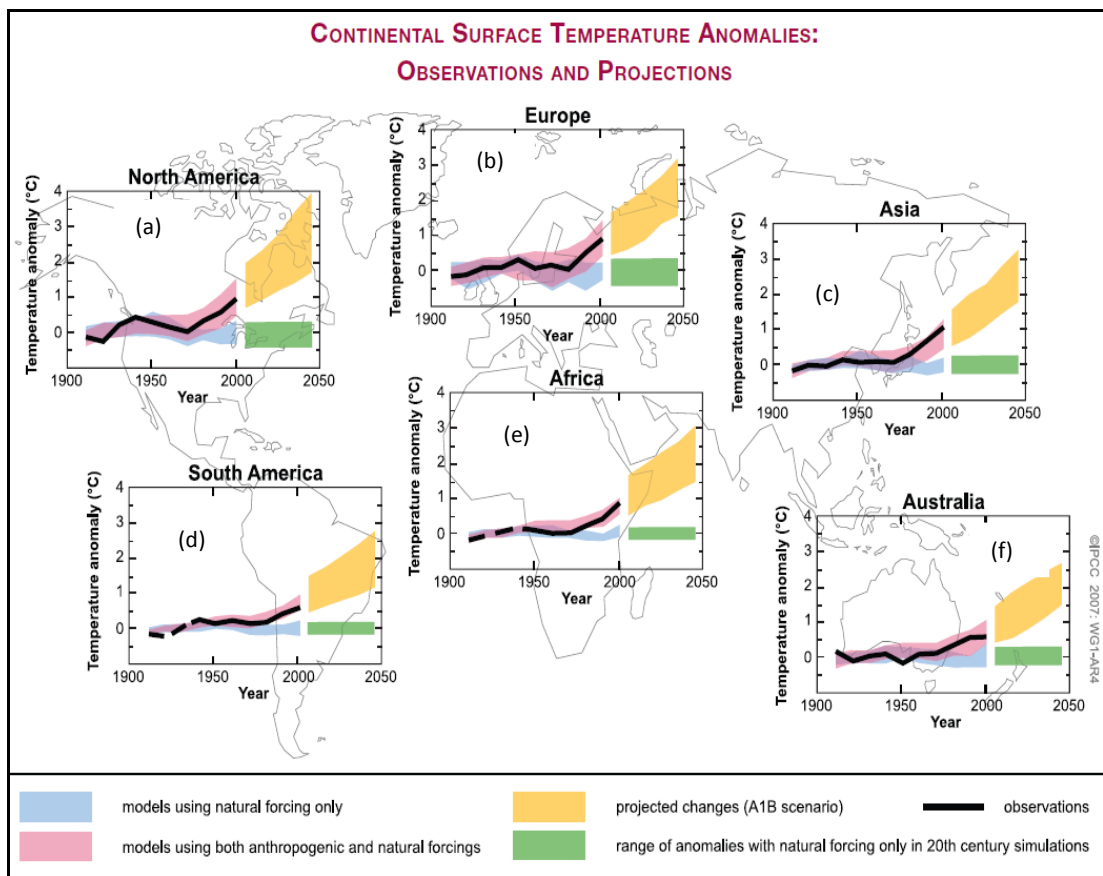


Figure 1.2 (a-f): Observed and projected surface temperature anomalies (trends) over land for different continents, a - North America, b - Europe, c - Asia, d - South America, e - Africa and f - Australia (Source: IPCC, 2007).

In the Lake Victoria region of Uganda particularly the central and western parts of the Country, banana is one of the most important crops and the staple food to many homes (Barekye *et al.*, 2013). Many smallholder and large scale commercial farmers significantly derive both income and food from the banana crop due to the crop's ability to produce mature banana fruits in continuous cycles throughout the year (Bagamba, 2007 and Barekye *et al.*, 2013).

Despite the socio-economic importance of the banana crop, recent studies (Wairegi *et al.*, 2010 and Van Asten *et al.*, 2011) have observed that actual production per hectare (yield) is far below the potential yield levels and banana yields have continued to decrease with time. These studies observed that the banana production is affected by both climatic and non-climatic factors. The climatic factors include extreme weather conditions such as droughts, floods and hail stones. The non-climatic factors include deteriorating soil fertility, availability of market, outbreak of crop pests and diseases and farm crop management practices (Tushemereirwe *et al.*, 2004). It should be noted that some non-climatic factors such as pests and disease incidences are, to some degree, often associated with certain weather conditions. The net impact of climate variability and change are likely to worsen the situation in the future as variation in rainfall, temperatures, relative humidity and soil moisture imbalances are critical to the productivity of the banana crop.

Other crops grown in Uganda include coffee, cotton, tea, sugarcane, maize, potatoes, groundnuts, beans, peas, millet and cassava. The productivity levels from a variety of such crops play a significant role in the agricultural sector and Uganda's economy at large. The diversity in crops in the sector not only enhances food security and promotes farmers' incomes, but also promotes other sectors of the economy through provision of raw materials to the industrial sector and hence creating employment in both the industrial and services sectors.

The role of the agricultural sector, the persistent poor crop harvests and increased cost and demand for farm inputs such as pesticides, fertilizers and water for irrigation in most agricultural seasons make planning in the sector inevitable. In Uganda, for example, the frequency of droughts was observed to be on the increase with seven droughts experienced in 1991-2000 in the different parts of the Country (NAPA, 2007) (Figure 1.3). The worst drought in the Eastern region occurred in 2011 and caused significant misery and disruption of socio-economic activities particularly agriculture (Barasa *et al.*, 2013 and Egeru *et al.*, 2014). Van Asten *et al.* (2011) and Washington and Pearce (2012) observed that many areas have

experienced recurrence of floods and/or droughts which have severely affected farming activities in the Country leading to reduction in crop productivity. Understanding the interaction between climate variations and crop productivity is therefore of paramount importance.

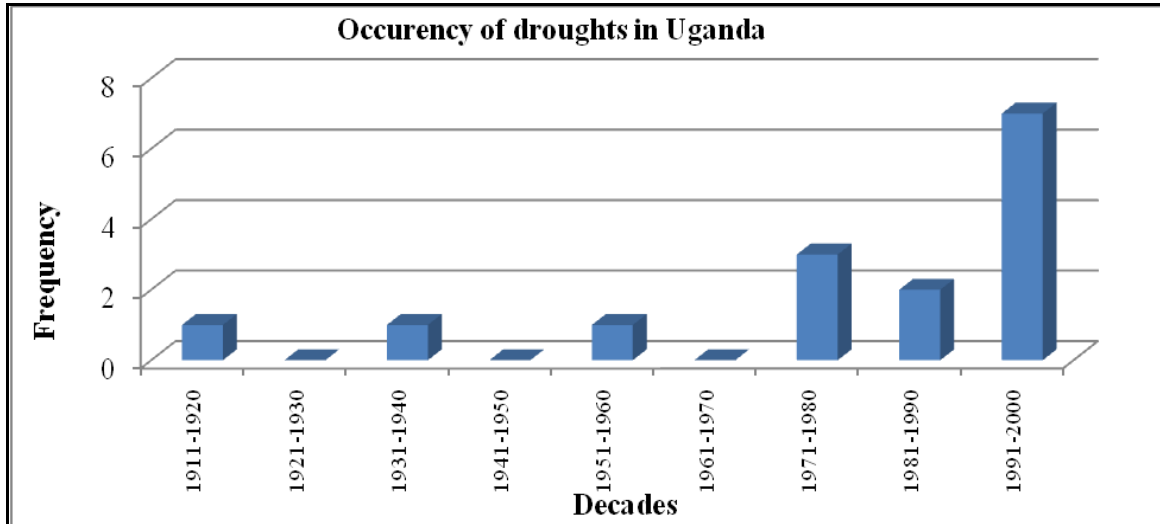


Figure 1.3: Drought occurrences for every 10 years in Uganda (1911-2000) (Source: NAPA, 2007).

1.0.1 History of Banana Production in Uganda

Banana (*Musa acuminata*) is one of the most important and oldest crops in Uganda with more than 7 million people, or 26% of the population depending on the plant as a source of food and income. Bananas are estimated to occupy about 1.5 million hectares of the total arable land, which is more than 38% of the cultivated land in the Country (Rubaihayo, 1991, Rubaihayo and Gold, 1993 and Wairegi *et al.*, 2010). Bananas propagate through seedlings or suckers. According to Tushemereirwe *et al.* (2001), the recommended sucker types include sword suckers, maiden suckers and tissue culture plantlets (Figure 1.4).

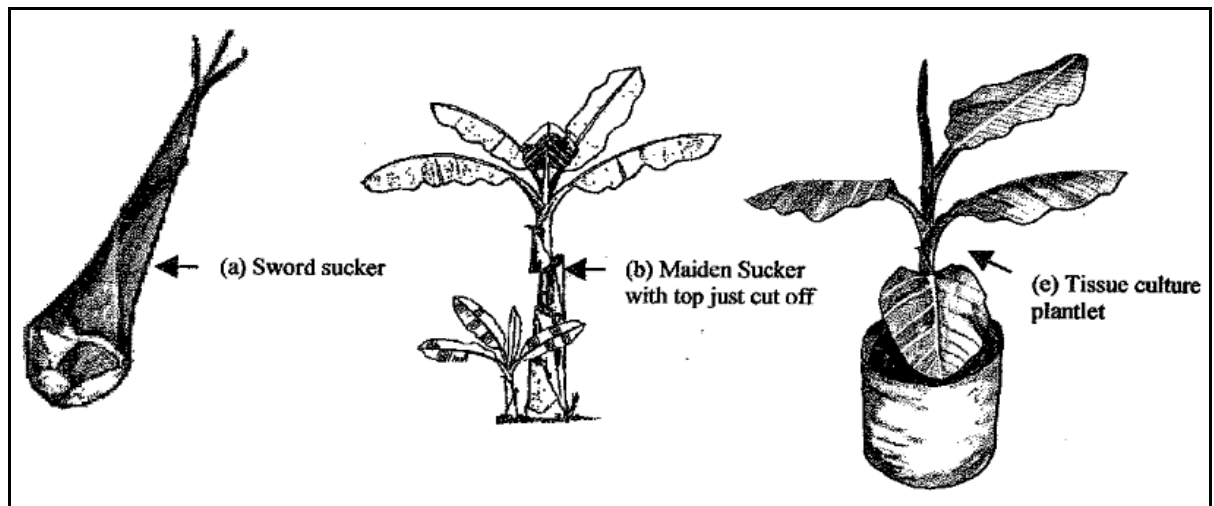


Figure 1.4: Means of banana propagation (a) sword sucker, (b) maiden sucker and (c) tissue culture plantlet (Tushemereirwe *et al.*, 2001).

The plant is grown primarily as a subsistence crop in rural areas, although consumption is not limited to rural areas as approximately 65% of urban consumers in Uganda have a meal of the cooking variety of banana at least once a day. Worldwide, Ugandans have the highest per capita consumption of cooking banana (Clarke, 2003). FAO (2004) observed that Ugandans consume 185 kg of cooking banana per capita per year comprising one-third of the caloric intake from starchy staples.

The highland cooking banana (*Musa* genome group AAA-EA) is the most important staple crop in East African Great lakes region comprising Uganda, Tanzania, Rwanda, Kenya, Burundi and Eastern Zaire. In Uganda, the crop has traditional roots in the Country's central region, where the Baganda consider it as their main dish. Between 1900 and 1930, banana cultivation moved further to non-traditional growing areas in the east and southwest of the Country. During the last 20 to 50 years, banana replaced millet as the key staple food in much of southwestern Uganda (Gold *et al.*, 1999 and Clarke, 2003).

During the same time, a decline in highland cooking banana production favored some other banana cultivars (mainly of the beer types ABB and AB) and annual food crops (cassava, sweet potatoes and maize) in central region. The decline was mainly attributed to low levels of Nitrogen (N) and Potassium (K) in soils and poor plantation management practices. The low levels of N and K most likely resulted from reductions in mulching or use of organic amendments and from discontinuation of soil conservation practices (Bagamba, 2007). Farmers attributed the decline in plantation management, productivity and stand size to a

number of socio-economic factors, ranging from resource availability (declining farm sizes, outward labour flow, declining household incomes) to infrastructure and institutional factors.

Following a combination of several factors, Rutherford and Gower (2003) classified Uganda banana production regions into three zones as follows: (a) Eastern and Central region, which is experiencing severe decline in production due to disease, pests, and poor soils (in these regions farmers are also diversifying their investments) (b) Southern region, where there is moderate production and noticeable decline as well and (c) Western region, where there is currently abundant production, though with a decline. Due to better returns on income and food security, there has been an increase in the number of small scale farmers intercropping coffee with bananas (Jassogne *et al.*, 2012; 2013).

Traditionally, farmers derived their income from coffee and cotton, growing bananas mainly for home consumption. Farmers in central Uganda depended on cheap migrant labour from the southwest of the Country. The 1970s were characterized by decline in coffee and cotton prices, deterioration in the marketing infrastructure that crippled farmers' income and capacity to pay for hired labour and agricultural inputs. Because of the limited labor required for banana production, banana became an ideal crop for many farmers in the region replacing coffee and cotton in many areas.

Table 1.1: Number of plots and size for main food crops in Uganda

Crop	Number of plots (x 1000)	Plot area (ha)	Area (x 1000 ha)	Yield (MT/ha)	Production (x 1000 MT)
Bananas	2,695	0.24	646.8	14.6	9443
Maize	1,001	0.26	260.3	1.4	364
Finger millet	856	0.27	231.1	0.6	139
Sorghum	805	0.27	217.4	0.7	152
Cassava	1,790	0.19	340.1	8.1	2755
Sweet potato	2,078	0.14	290.9	10.3	2990
Potatoes	183	0.14	25.6	8.0	204
Beans	1,360	0.17	231.2	0.9	199
Groundnuts	795	0.20	159.0	0.6	94

Source: Statistical Abstract, Uganda Bureau of Statistics (UBOS, 2010)

Uganda still remains one of the largest producers of cooking bananas in the world, being second only to India (Nyombi, 2013). Cooking banana production is approximated at 29.5% of the world banana production while production of dessert bananas is estimated to be 0.85% of

world production. Production is mainly by smallholder farmers with total number of plots up to 2,695,000 averaging 0.24 ha, making it the most widely cultivated crop (Table 1.1).

The Uganda National Household Survey (UNHS) report (1995-96) observed that the national average yield for bananas was at 14.9 tonnes per hectare, well above that observed by the National Bureau of Statistics (UBOS). Yields are known to be highest in Western Uganda, estimated at 26.4 tonnes per hectare and lowest in Central region where it is estimated at 5.5 tonnes per hectare.

1.0.2 Banana Varieties

Four groups of varieties of bananas are recognized and differentiated according to their use (Rubaihayo, 1991). These are: (i) cooking bananas (matooke) whose fruits are harvested, peeled, steamed and mashed before eating, (ii) beer bananas whose mature fruits are ripened and squeezed to extract juice that is fermented with sorghum to produce banana wine, (iii) dessert bananas that are eaten when ripe, (iv) roasting bananas whose fruits are ripened and roasted for eating. The genome, purpose and examples of different varieties are given in Table 1.2.

Table 1.2: Common banana species and their purpose in Uganda

Genome	Purpose	Examples
AAA	Dessert/cooking/juice	Gros-Michel/Carvendish/Matooke/Mbidde
AAB	Roasting/cooking/dessert	Plantains /Sukali Ndizi
ABB	Cooking/juice/beer	Bluggoe /Pisang awak (Kayinja)
AA	Dessert/beer	Pisang lillin
AB	Juice	Kisubi

1.0.3 Pests and Diseases in Uganda's Banana Sub-sector

Banana production per unit area (yield) in Uganda has shown a steady decline during recent years (Rubaihayo and Gold, 1993; Van Asten *et al.*, 2011 and Wairegi *et al.*, 2010). Pests and diseases are one of the major banana yield loss factors observed by many farmers and have attracted a lot of research attention (Speijer *et al.*, 1999b; Speijer and Kajumba, 2000 and Tushemereirwe *et al.*, 2004). Some of the pests and diseases are sensitive to both elevation and climatic factors. The effect of pests and diseases is stronger in bananas plantations in elevations of 890 to 2400 MSL (Speijer *et al.*, 1994).

Major pests in Uganda's banana plantations include the parasitic nematodes (Bridge, 1988; Speijer and Kajumba, 2000) and the banana weevils (Gold *et al.*, 1999). The most important

and wide spread plant parasitic nematode species in Uganda are; *Radolpholus similis*, *Pratylenchus goodeyi* and *Helicotylenchus muticinatus*. The distributions of these nematodes are influenced by altitude (temperature), with *R. similis* being dominant at low altitudes (<1400 MSL) associated with high temperatures and *P. goodeyi* being dominant at higher altitudes (>1400 MSL) associated with slightly lower temperatures. *Helicotylenchus muticinatus* and *Meloidogyne* species are found at all altitudes although there may be higher population densities of these nematodes at lower altitudes (Bridge, 1988; Elsen *et al.*, 1998 and Speijer *et al.*, 1994).

The banana growing regions of Uganda are at varying altitudes (Namulonge 1150 MSL, Mbarara 1330 MSL and Ntungamo 1450 MSL) and therefore offer different conditions for multiplication of the nematode densities. *Radolpholus similis* is most abundant in Namulonge (central Uganda), *Pratylenchus goodeyi* is a predominant species in Ntungamo (southwestern) and *Radolpholus similis* and *Pratylenchus goodeyi* occur together in Mbarara areas.

According to Gold *et al.* (1999), *Cosmopolites sordidus* is the main species of parasitic banana weevils, which is common in the central part of Uganda. Wairegi (2010) ascertained that average corm damage caused by these weevils was significantly more severe in central compared with south and southwestern regions. In this study, Wairegi (2010) concluded that pest constraints (nematodes and weevils) are particularly a problem in the central region. A previous study, Smithson *et al.* (2001) also showed that root necrosis is 12% and 24% in western and central Uganda while the southern region recorded 0.5%. Similarly, the corn damage from weevils is higher in the central region (5.3-18.6%) than the southern part (1%). According to Speijer *et al.* (1993), banana weevils have devastating impacts up to 1400 MSL while altitudes of above 1500 MSL do not contain the weevils (Figure 1.5 a). Corm damage and yield losses due to nematodes are recorded at altitudes between 1300-1750 MSL (Figure 1.5 a). Bunch weight losses due to corm damage are high, varying between 5-30 kg as depicted in Figure 1.5 (b).

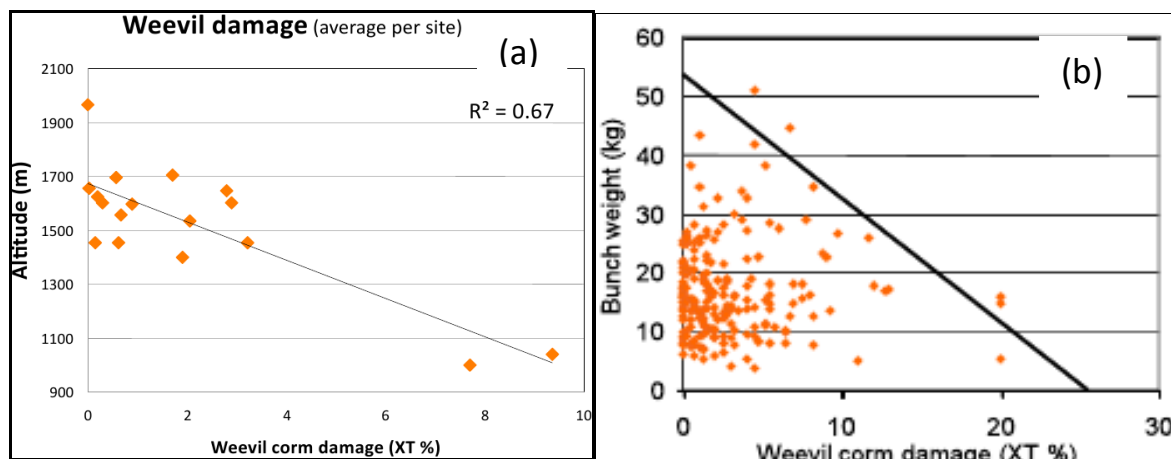


Figure 1.5: The relationship between weevil corm damage and altitude (a) and the impacts of weevil corm damage on banana bunch weight (b) (Wairegi *et al.*, 2010).

Nematode damage in bananas is associated with reduction in bunch weight (Figure 1.5 b), loss of bunches due to plant toppling, increase in crop cycle duration and decrease in plantation longevity (Gowen and Queneherve, 1990). Nematode related yield losses in East African highland bananas may range from 30% (Speijer *et al.*, 1999a) to 50% (Speijer and Kajumba, 1996).

Talwana *et al.* (2000) also identified the nematodes as the main pests, which degrade the roots of the bananas especially in Uganda. According to this study, the nematodes mainly affect the production of three Uganda's common species of bananas namely Nabusa, Sukali ndizi and Pisang awak. Critical analysis of the rate of root necrosis caused by the pests showed that Nematode densities were equal in all root types, which ranges from primary roots, secondary roots, and root tips. Statistically, nematode damage (root necrosis) tended to be higher close to the corm than further along the primary roots, a pattern that is consistent in all banana cultivars.

Wairegi *et al.* (2010) observed that besides nematodes, banana weevils have also contributed to the low production of the crop in most parts of the Country. Whereas nematodes cause about 10% loss, the weevils reduce the production rate by 6% (Wairegi *et al.*, 2010). The larvae of the weevils usually bore tunnels into the corm thus inflicting damages to the crop. Characteristically, the sheaths of the leaves splits, there is visible snapping of the affected corms and pseudo stem and detrimental impacts like the toppling over of the bananas. In addition according to Abera *et al.* (2000) plants affected by either weevils die prematurely or become stunted leading to delayed fruit maturation. Occasionally, the production is poor,

bunches are small while the suckers are low in number, which occurs due to reduced vigor, thus, leading to total crop failure (Mitchel, 1980 and Sengooba, 1986). Banana productivity in Uganda is also affected by diseases caused by disease pathogens in banana plantations (Tushemereirwe *et al.*, 2004). Main diseases that have been identified to cause high yield losses include the Black Singatoka, Banana Streak Virus and Banana Wilt (Tushemereirwe and Waller, 1993 and Tushemereirwe, 2006). These banana diseases are discussed briefly in the subsequent sub-sections.

1.0.3.1 Black Singatoka

The Black Singatoka is a windborne fungal disease in bananas caused by *Mycosphaerella fijensis*. It was first discovered in Fiji in early 1960s (Rhodes, 1964) and is considered to have originated in Papua New Guinea/Solomon island region (Stover, 1978). Black Singatoka was first observed in Uganda in 1989 (Tushemereirwe and Waller, 1993). During that time, it made an economically important impact on banana productivity after causing incomplete fruit filling leading to poor yields. Black Singatoka is considered a key constraint to banana productivity worldwide and is sensitive to variations in altitude and temperature (Tushemereirwe, 1996). Diagnostic survey results showed Black Singatoka was absent at elevation about 1450 MSL, where mean minimum temperature does not exceed 15 °C. Although Black Singatoka is a serious disease on bananas and plantains, it is possible to control it through breeding of banana varieties (Barekye, 2009).

Barekye *et al.* (2013) further observed that although the disease does not usually kill the plant, it causes heavy defoliation, which severely suppresses finger filling, leading to reduced bunch weight. The disease is responsible for attacking the leaves, resulting in pre-mature ripening of the fruit (Barekye *et al.*, 2013). Research on disease vulnerability in Uganda by Tushemereirwe *et al.* (2004) showed that nearly all triploids (AAA) are susceptible to this disease. A trial conducted in mid-elevation; Kawanda, 1250 MSL, banana systems of Eastern Africa (Uganda) revealed a loss of 37% in bunch weight in first ratoons (Tushemereirwe, 1996).

1.0.3.2 Banana Streak Virus Disease

Lockhart and Olszewski (1993) observed that the banana streak virus disease is believed to be affecting many banana growing areas in the world. The disease has been around for many years but it has never caused wide spread epidemics in many regions (Frison and Sharrock, 1998). However, the disease has caused significant yield loss in localized places causing some

fields to be knocked out of production in southern Uganda especially Rakai district (Tushemereirwe, 1996).

1.0.3.3 Banana Wilt Disease

The banana wilt disease has been observed only in Uganda where there is a trace back to about 1955. Tushemereirwe and Ploetz (1993) observed that highland bananas (AAA) that were known to be resistant to *Fusarium* wilt were observed to succumb to this wilt disease in areas above 1,330 MSL in western Uganda.

1.0.4 Soil Fertility and Banana Production

Soil fertility has been identified as one of the major constraints to banana productivity in Uganda (Zake *et al.*, 2000). This has caused reduction in bunch weight, lengthened the maturity period and shortened the longevity of banana plantations. In the 1960s, soils from 62 sites distributed over the whole of Uganda were sampled to determine soil nutrient concentrations (Foster, 1981), and were re-sampled during the Land Management Study (1999-2002). Results showed that soil pH, extractable phosphorus (P), calcium (Ca), and potassium (K) were often below critical concentrations for most crops.

The amount of soil organic matter (SOM), however, had not changed significantly (Ssali, 2002). In some cases, concentrations of available P, Ca and K in the top soil had declined by 20-70% compared with the 1960s. Nyombi (2013) observed that soil fertility seems poor in general to sustain good yields and nutrients need to be added through use of manure and artificial fertilizers to improve banana yields. Increased agricultural productivity is envisaged as key to alleviating poverty and ensuring food security in rural parts of Uganda. The African Green Revolution efforts supported by large donors are also calling for agricultural intensification through the use of fertilizer inputs.

Uganda's official mineral fertilizer recommendation for highland bananas is a single blanket rate of 100N-30P-100K-25Mg kilogram per hectare per year (Ssali *et al.*, 2003), irrespective of the inherent soil fertility status. The blanket fertilizer recommendation, however, fails to address variability in soil quality (chemical and physical properties) on banana farms. Van Asten *et al.* (2005) observed a range of nutrient deficiencies after application of 71N-8P-32K kilogram per hectare per year in banana demonstration plots in districts in southwest, south Uganda and around Mount Elgon. There is a need to develop site-specific fertilizer

recommendations that take into account the variability in soil chemical properties. Replenishment of soil fertility is recommended as a vital process towards improving crop productivity particularly bananas over Uganda.

1.1 Statement of the Problem

The socioeconomic performance and productivity of weather-dependent sectors particularly agriculture and food security is substantially affected by climate extremes and fluctuations (Ogallo *et al.*, 2002; Kurukulasuriya *et al.*, 2006 and Funk *et al.*, 2008). Previous studies observed that climate change has altered the frequency, intensity, spatial extent and duration of climate extreme events in many regions, especially Africa (Sachs *et al.*, 1999; Antle, 2010 and IPCC, 2014). High variability of seasonal rainfall over East Africa has made it less predictable (Schreck and Semazzi, 2004; Bowden and Semazzi, 2007 Patricola and Cook, 2011 and Nicholson, 2014). Shifts in the onset and cessation of rainfall have also been observed (Nimusiima *et al.*, 2013 and USAID, 2013) in some parts of Uganda.

While it is acknowledged that there is climate variability and change due to increasing global warming (Easterling *et al.*, 2000 and IPCC, 2012; 2014), there is inadequate information on how this translates into regional changes of surface temperature, rainfall seasonality (onset, intensity and cessation) and soil moisture patterns. Downscaling Global Climate Model (GCM) outputs using high-resolution regional climate models (RCMs) is necessary to improve representation of the meso- and local-scale detail that is lacking in the GCM outputs (Hudson *et al.*, 2004; Wang *et al.*, 2004 and Otieno *et al.*, 2015) over Uganda.

The agricultural sector in Uganda is particularly vulnerable to the impacts of climate extremes due to high dependence on rain-fed agriculture (Funk *et al.*, 2008; Cooper *et al.*, 2011; Egeru, 2012 and Mubiru *et al.*, 2012). The impacts including (1) changes in temperature and rainfall intensity and duration, (2) frequent and prolonged droughts and (3) floods have far reaching implications on the productivity of many crops including the banana crop that is a focus of this study.

Uganda has experienced significant losses in yields of major crops such as bananas in the recent years. For example, EMU (2007) observed that between 1999 and 2006 there was a decline in the yields of main crops include banana, coffee, beans, maize, among others. There was, however, an increase in yields of some crops like simsim, cassava and millet. Many farms

in Uganda have already been exposed to declining soil fertility (Zake *et al.*, 2000), increased infestation of banana diseases (Tushemereirwe, 2006; Nyombi, 2010 and Tushemereirwe *et al.*, 2004), nematodes and weevils (Bridge, 1988 and Harper *et al.*, 2004) and variation in climatic events (Nyombi, 2010) as major threats to banana production in the Country. Likely adverse effects from climate change may only worsen the situation.

Despite the socio-economic role of the banana crop and evidence of climate extremes associated with El Niño Southern Oscillation (ENSO) events in Uganda, the likely changes in the growth patterns and linkages of the crop to current climate variability as well as future climate change is not well understood. If the Country has to ensure food security through sustainable banana productivity, there is need to understand the likely linkages of current and future climate on banana productivity in Uganda.

This study aimed to answer the following research questions:

- (a) What is the nature of observable linkages between banana productivity and current climate variability in Uganda?
- (b) How accurate is the present day climate information from regional climate models particularly the UKMO PRECIS RCM over Uganda?
- (c) What is the extent of future regional climate change expected over Uganda?
- (d) How will the current areas suitable for banana production shift under different climate change scenarios over Uganda?

1.2 Objectives of the Study

The overall objective of this study was to determine the extent of climate variability and change and the associated effects on the banana farming in Uganda.

This was achieved through the following specific objectives;

- (i) Establish the linkages between banana productivity and current climate variability over Uganda.
- (ii) Determine the performance of the PRECIS RCM in simulating observed climate patterns over Uganda.
- (iii) Establish the extent of expected future climate change over Uganda.
- (iv) Determine potential effects of future climate change on banana production over Uganda.

1.3 Justification of the Study

Over Uganda and neighboring countries, agriculture still remains a major source of livelihood in terms of food, employment and foreign exchange earnings. Most communities in Uganda practice traditional subsistence farming by use of hand hoe and their livelihoods are highly dependent on variations in weather and climate. Most farmers hardly practice irrigation even during the known dry seasons (June-August, JJA and December to February, DJF) of the crop calendar.

Impacts of climate variability and change therefore remain a major threat to the production of major crops such as banana, coffee and maize (Laderach *et al.*, 2011; Kumar *et al.*, 2011; Hansen *et al.*, 2011 and Laderach and Van Asten, 2012) among others in the Sub-Saharan Africa regions particularly Uganda. Many parts of Uganda have experienced a number of adverse climatic events that have been significantly destructive, disruptive or of distress to farmers, particularly in banana growing communities.

Understanding potential effects of climate variability and future climate change on banana productivity provides useful information on the occurrence of these effects and how their impacts on banana productivity in time and space can be mitigated in Uganda. Timely access to detailed information on climate variability and change effects for both the present and future can guide the coping and adaptation mechanisms for various socio-economic sectors in the Country. This is particularly vital for Uganda to recover from the declining productivity of banana and other crops which can aid to strengthen the Country's agricultural sector. Enhancing the production of banana not only leads to food security in the region but also enhances farmers' incomes and contributes to poverty reduction in the region.

This study also provides the climate change information required by agricultural policy makers and analysts on the improvements of overall crop productivity in the region. The generated climate information can readily be used as inputs to sector specific impacts models such as Food and Agricultural Organization (FAO); Crop Water Assessment Tool (CROPWAT), Decision Support System for Agro-technology Transfer (DSSAT) and Soil and Water Analysis Tool (SWAT) among many others for effects and vulnerability assessment of climate change on the different sectors.

Reliable regional and national climate change information based on IPCC scenarios from RCMs is necessary to assess vulnerability, impacts and adaptation in among other sectors, agriculture and food security, water resources, energy, transport and health sectors for sustainable development of this region.

1.4 Study Area

This study was conducted over Uganda, a landlocked Country that lies astride the Equator, between latitudes 4° 12' N and 1° 29' S and longitudes 29° 34' E, and 35° 0' E (Figure 1.6). More than two-thirds of the Country is a plateau, lying between 1,000 and 2,500 meters above mean sea level (MSL). It shares borders with Kenya (East), Tanzania (South), Rwanda (South west), Democratic Republic of Congo (West) and South Sudan (North). The neighbouring countries provide an opportunity for ready demand and market for the agricultural products, which promotes farming activities and incomes of farmers.

Uganda has a total land area of 241,038 km² (93,072 sq. mi.). Lakes, swamps and protected areas constitute 25% of the total land area leaving about 75% of the Country available for cultivation, pasture, urban development and settlement. Inland water bodies of the Country include part of L. Victoria, L. Kyoga, L. George, L. Albert, L. Katwe, L. Edward. Major rivers include R. Nile, R. Katonga, R. Achwa, R. Kafu and R. Semliki. The Country is divided into 9 agro climatic zones (Figure 1.6) which also determine and influence the agricultural systems in the Country outlined in Section 1.4.1.

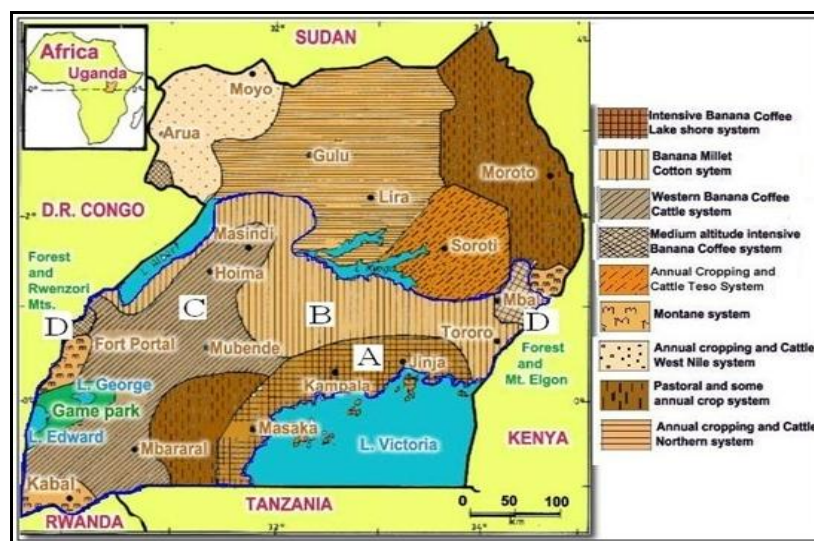


Figure 1.6: Agro-climatic zones and agricultural systems of Uganda (Adopted from Mwebaze, 1999).

The economy of Uganda relies heavily on agriculture with about 75% of its population depending on agriculture either directly or indirectly. Some of the major crops grown in Uganda include but are not limited to bananas, coffee, maize, beans, millet, sugarcane and cotton. The area to be covered is marked/outlined using blue covering zones labeled A, B, C and D that represent the regions in Uganda where bananas are grown as a mono crop or intercropped with other crops mainly coffee and legumes.

Figure 1.7 shows the administrative boundaries (districts and regions) of Uganda. Bananas are mainly grown in the western, southwestern, central and Eastern districts of Uganda. Limited banana production is found in the northwestern region particularly in Arua district. Although the study investigates the potential for banana production for the entire Country, the main focus is on two regions that are observed to grow bananas. These include the western and central regions that produce about 90% of the Country's banana yield per year (UBOS, 2010).

1.4.1 The Agricultural Systems in Uganda

A number of agricultural systems exist in Uganda (Figure 1.6). The agricultural systems are determined by a number of factors but most importantly are the culture and climate. These systems include: intensive banana-coffee lake shore, banana-millet-cotton, western banana-cattle, medium altitude intensive banana-coffee, annual cropping and cattle, montane, annual cropping and cattle in West Nile, pastoral and annual cropping, and annual cropping and cattle Northern. A shift of production zones for certain crops has been witnessed in many areas of the Country due to changes in soil fertility, variability in climate and cultural values attached to certain crops. This study focused on the banana production zones (A, B, C and D) that are observed in Figure 1.6. Subsequent sections review the history of banana production, banana varieties and the constraints of banana production.

Most of the Country experiences an equatorial type of climate with some parts in the northern and northeastern regions experiencing relatively dry conditions particularly during La Niña years. Average temperatures are in the range of 15 to 30 °C. The country receives annual rainfall varying from 750 mm in Karamoja (Northeast) to 1,500 mm in the high rainfall areas on the shores of Lake Victoria, in the highlands around Mt. Elgon (in the east) and the Ruwenzori Mountains (in the south-west, Figure 1.8).

Rainfall is fairly reliable, with most parts of the Country experiencing a bimodal rainfall regime with March to May (MAM) as the “long rain” season and October to December (OND) as the “short rain” season (Figure 1.9). There are, however, some stations particularly in northern Uganda that experience uni-model rainfall regime.



Figure 1.7: Map showing administrative zones and districts of Uganda (UBOS, 2013).

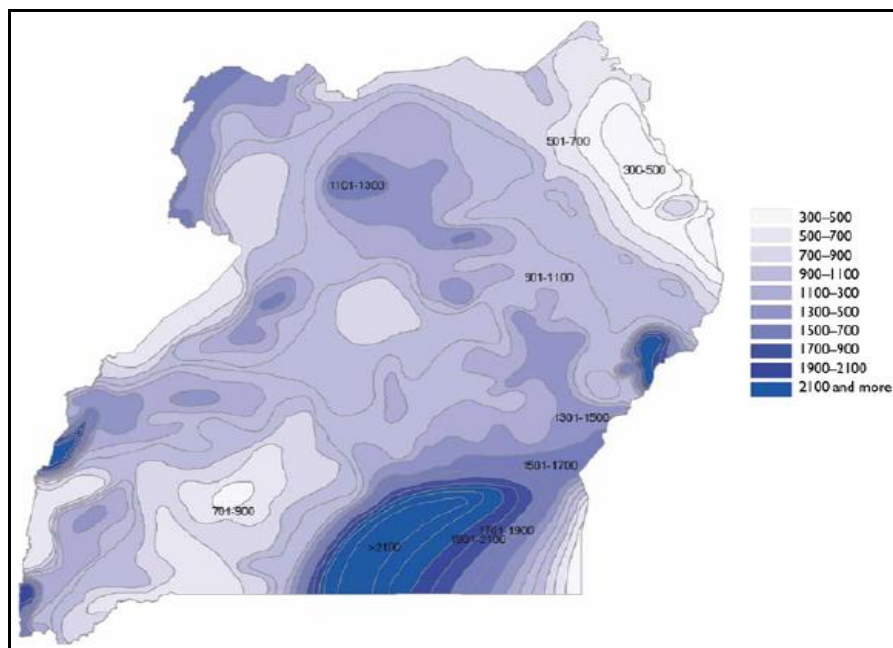


Figure 1.8: Average annual rainfall (mm/year) in Uganda. (Source: USAID, 2013).

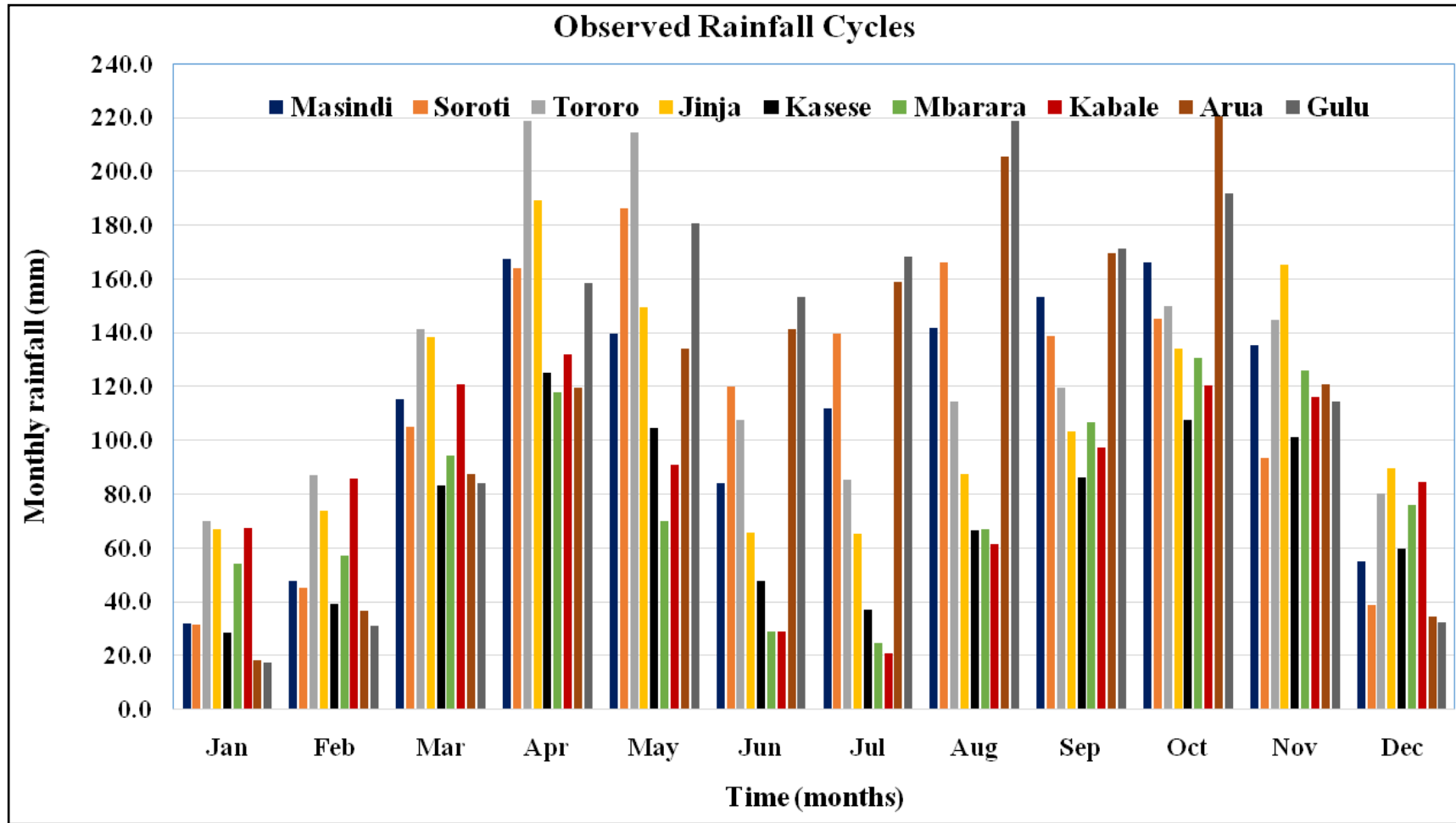


Figure 1.9: Mean rainfall (mm) annual cycle for 1961-2013 for selected stations in Uganda.

CHAPTER TWO

LITERATURE REVIEW

This chapter reviews previous studies on the Uganda's agricultural sector and banana sub-sector, constraints to banana production, climate variability and change, climate modeling, and the impacts of climate on agriculture.

2.1 The Agricultural Sector and Banana Sub-sector in Uganda

According to FAO (2003a), agriculture accounts for about 24% of the world's economic output, and occupies 40% of world's land area. Uganda's economy relies heavily on rain-fed agriculture (Egeru, 2012). The agricultural sector mainly contributes to the Country's economy in terms of foreign exchange and employment (UBOS, 2010). The sector is divided into the crop and livestock sub-sectors. In particular, the crop sub-sector is highly sensitive to climate extremes due to limited access to irrigation facilities and dominancy of traditional farming methods widely practiced by many small holder farmers and growing of traditional crops that are not resistant to changing climatic factors (Woomer *et al.*, 1998). Efforts are underway to modify the seeds of many crops in Uganda to produce 'improved' crops varieties including banana varieties that are resistant to droughts and other climate extremes. These new varieties have showed some success in the short run but the sustainability in the long run is not certain. Moreover, the improved varieties are less preferred by consumers than the traditional crop varieties in terms of quality, nutrient value and taste.

Despite effects from climate extremes and other constraints, Uganda's agricultural sector remains vital in terms of employment, GDP and food security. For example, the sector employed 72% (2012/2013) of the labor force (UBOS, 2015) and accounted for 25.4% (2010), 24.2% (2011), 23.6% (2012), 23.4% (2013) and 23% (2014) of the Country's total GDP (Table 2.1). Agricultural products also accounted for 47% of the Country's total exports in 2007 and 22% in 2012. It is also observed that most of Uganda's industrial sector is agro-based. Even though its share in the Country's Gross Domestic Product (GDP) has been declining (Table 2.2), agriculture remains important because it provides a basis for growth in other sectors such as manufacturing (through provision of raw materials and surplus labour) and transport service sectors.

Occurrences of climate extremes and high vulnerability of the agricultural sector to these extremes makes the farmer population particularly the poor in Africa vulnerable due to high human dependence on rain-fed agricultural livelihoods. Consequently, agriculture has become a focus of those modeling the impact of climate change on poverty in Africa. Benin *et al.* (2007), demonstrated that if agriculture in Uganda grew at an average rate of 2.8% per year as opposed to the average of 2.3% per year experienced in the previous years (1990 and 2000), the poverty rate would be reduced from 31.1% in 2005/06 to 26.5% by 2015. Therefore, improvements in the agricultural sector are necessary in achieving particularly the first and second Sustainable Development Goals (SDGs) that aim at ending poverty and hunger respectively.

Table 2.1: Uganda’s GDP by agricultural subsector and other economic activity at current market prices, percentage share and calendar years.

Years	2010	2011	2012	2013	2014
Agriculture, forestry and fishing	25.4	24.2	23.6	23.4	23
Cash Crops	1.7	1.8	1.7	1.8	1.7
Food crops	14.0	13.1	12.4	12.2	12.0
Livestock	4.4	4.2	4.2	4.1	4
Forestry	3.9	3.8	4.0	4.2	4.1
Fishing	1.4	1.3	1.3	1.2	1.2
Industry	17.8	18.5	18.2	18.2	18.4
Services	49.5	49.7	50.2	50.4	50.3

Source: Statistical Abstract, Uganda Bureau of Statistics (UBOS, 2015)

The East African Highland banana is one of the major banana clones in Uganda and neighboring regions (Nyombi *et al.*, 2009 and Nalumansi *et al.*, 2014) that serves as both a staple food and cash crop (Bagamba, 2007). Bananas were introduced into Africa as a tropical crop (Purseglove, 1988) from Southeast Asia during the 1st to 6th century AD, probably via trade (Simmonds and Shepherd, 1955). The banana crop is a multi-cycle crop of significant social and economic importance in Uganda’s crop agricultural sub-sector. The multi stage cycle of the crop leads to continuous crop production throughout the year. Banana production is therefore, ideal for promoting farmers’ income and food security in the region (Woomer *et al.*, 1998 and Tushemereirwe *et al.*, 2001). Nalumansi *et al.* (2014) has identified alternative importance of the banana crop as medicine for healing contractility of an isolated perfused rabbit heart.

Table 2.2: Performance of agriculture in the Uganda's economy (1990-2014, 1USD = UShs 3050)

Year	Total GDP (Ug.shs Billion)	Agricultural GDP (Ug.shs Billion)	Agricultural Share of GDP
1990	1,985	1,061	53%
1991	2,088	1,086	52%
1992	2,182	1,116	51%
1993	2,320	1,170	50%
1994	2,555	1,246	49%
1995	2,768	1,291	47%
1996	2,906	1,299	45%
1997	6,594	2,727	41%
1998	7,186	3,005	42%
1999	7,666	3,184	42%
2000	8,038	3,302	41%
2001	8,528	3,461	41%
2002	8,977	3,571	40%
2003	13,972	3,329	24%
2004	15,271	3,520	23%
2005	17,878	4,284	24%
2006	20,166	4,553	23%
2007	23,351	4,825	21%
2008	28,346	6,083	21%
2009	34,904	7,908	23%
2010	39,086	8,114	21%
2011	49,849	10,514	21%
2012	54,699	11,789	22%
2013	54,275	11,587	21%
2014	53,964	11,485	21%

Source: MAAIF (2008) and UBOS (2015).

Bananas can be planted as a mono-crop but most farmers in Uganda intercrop them with perennial crops especially coffee (Ssenyonga *et al.*, 1999). Bananas are perceived to provide shade in plantations when intercropped with coffee which helps to moderate micro-climate in the plantation fields. The sum total of inter cropped crop yields has been observed to be high compared to mono cropping. Intercropping, however, requires high levels of soil fertility and moisture content as opposed to mono cropping.

2.1.1 Banana Production Constraints in Uganda

Several studies have investigated the productivity of bananas in many parts of the world including Uganda. Reports on banana yield decline in Uganda dates back to the 1940s and 1950s (Masfield, 1949 and McMaster, 1962). Gold *et al.* (1999b) observed that yield decline

accelerated in the 1970s and 1980s. Wairegi *et al.* (2010) have also observed that banana productivity (production per hectare or yield) has been declining in the recent years. Lack of reliable and accurate banana production figures, however, makes it difficult to quantify yield decline and the importance of different yield loss factors.

The 1965 Agricultural Census observed that the total area under bananas in Uganda was 464,185 hectares with an estimated yield of 7 to 10 tonnes per hectare per year (Stover and Simmonds, 1987). While the acreage under banana has increased to about 1.5 million hectares of land, the banana productivity (yield) has decreased to an estimate of 4.8 tonnes per hectare per year according to Rubaihayo (1991) especially in central parts of Uganda.

Uganda Bureau of Statistics (UBOS, 2010) statistical abstract, estimated the total area under banana production at 1,682,000 hectares with production estimated at 9,512,000 tonnes. This put banana yields at 5.65 tonnes per hectare per year. There is, however, a wide variation in estimates of yield decline in the literature, the best estimate is that average yields in central Uganda declined from 9 tonnes per hectare per year before 1970 to 6 to 7 tonnes per hectare per year in 2005. Tushemereirwe *et al.* (2001) also observed a variation in banana yields in Masaka, Bushenyi and Ntungamo districts of Uganda. This study observed that banana yield are around 17 tonnes per hectare per year in the Masaka district and increase to 30 tonnes per hectare per year or more moving southwest to the Bushenyi and Ntungamo districts.

Beside a possible decline in the banana productivity, several experimental studies, for example, Smithson *et al.* (2001) and Tushemereirwe *et al.* (2001) indicate that there exists a huge disparity between actual yields of 5 to 30 tonnes per hectare per year and on-farm and on-station trials attainable yields of 60 to 70 tonnes per hectare per year. Van Asten *et al.* (2004) also observed that actual banana yields in Uganda are low (5 to 30 tonnes per hectare per year) compared to potential yields (70 tonnes per hectare per year).

Wairegi *et al.* (2010) observed that the decline in banana yields is attributed to a number of both biological and non-biological yield loss factors. The study observed that drought stress was the primary yield constraint in a quarter of studied farmer fields in southwest Uganda.

As observed earlier, a number of yield loss factors have been studied by several authors. These studies have investigated the loss in banana productivity associated with deteriorating soil fertility (Bekunda and Woome, 1996; Zake *et al.*, 2000; Gold *et al.*, 1999a; Nyombi, 2013 and

Umesh *et al.*, 2015), and drought occurrences (Okech *et al.*, 2004; Van Asten *et al.*, 2011; Nyombi, 2010 and Umesh *et al.*, 2015), banana weevils mainly *Cosmopolites Sordidus* (Gold *et al.*, 1999), banana parasitic nematodes including *Radolpholus Similis* and *Helicotylenchus Multicintus* (Speijer *et al.*, 1999b; Speijer and Kajumba, 2000 and Harper *et al.*, 2004), and banana plant diseases like Black Singatoka, Banana Streak Virus and Banana Wilt (Tushemereirwe, 2006).

Nyombi (2013) observed that bananas require considerable amounts of mineral nutrients, good management and control of crop pest and diseases through high crop hygiene, and good supply for soil moisture which is well distributed throughout the year with dry seasons shorter than three months to maintain high yields. Different thresholds of temperature ranges have been identified for different stages of banana growth. These thresholds indicated that banana requires mean monthly temperatures of about 25 to 27 °C for optimal growth.

Historically, fertile soils in addition to favorable climate (rainfall and temperature) promoted the growth of bananas in most parts of the Lake Victoria region including Uganda. According to Zake *et al.* (2000), bananas in Uganda grow on different soils. This study observed that although bananas can be grown on a wide range of soils, deep well drained retentive loam soils with high humus content are the best.

Bekunda *et al.* (2002) observed the diversity in soils in banana growing regions that range from ferralsols, nitisols and acrisols around L. Victoria regions to fluvisols and plinthosols in areas like Tororo and Pallisa in Eastern Uganda. Nitrogen, Potassium, and Phosphorus are the major nutrients required by bananas in bulk quantities and can be supplied by fertile soils or by commercial fertilizers. The representation of various composition and characteristics of soils in Uganda based on Harmonised World Soil Data (HWSD) set is depicted in Figure 2.1. Variations in the composition of soil affect crop growth patterns particularly bananas across Uganda.

Deterioration of soil fertility is one of the major causes of declining crop yields particularly bananas in most parts of Uganda. The hypothesis that the decline in soil fertility has contributed to the low banana yields in the region was first identified by Masefield (1949) and McMaster (1962) and has been repeated in subsequent studies (Bekunda and Woomer, 1996 and Sseguya *et al.*, 1999).

In addition, Gold *et al.* (1999) cites that the yield decline rate is higher in the central region of Uganda than in the western and southwestern regions due to a combination of factors. The high rate of yield decline has been attributed to the high incidence of pests and diseases in low land areas (high temperatures) in central region than in highland area (low temperature) of western and southwestern Uganda.

Nyombi (2010), studied association between banana production and rainfall in the Albertine rift and concluded that high rainfall of 1400 mm per annum was directly proportional to high banana productivity. The study observed that rainfall is a crucial factor in banana production because the ability of the plant to take up nutrients is related to the soil moisture content that is mainly supplied through rainfall for most of Uganda's agriculture. This study further observed that diseases and pests incidences in banana plantations are sensitive to variations in climatic parameters such as temperature, relative humidity and soil moisture content.

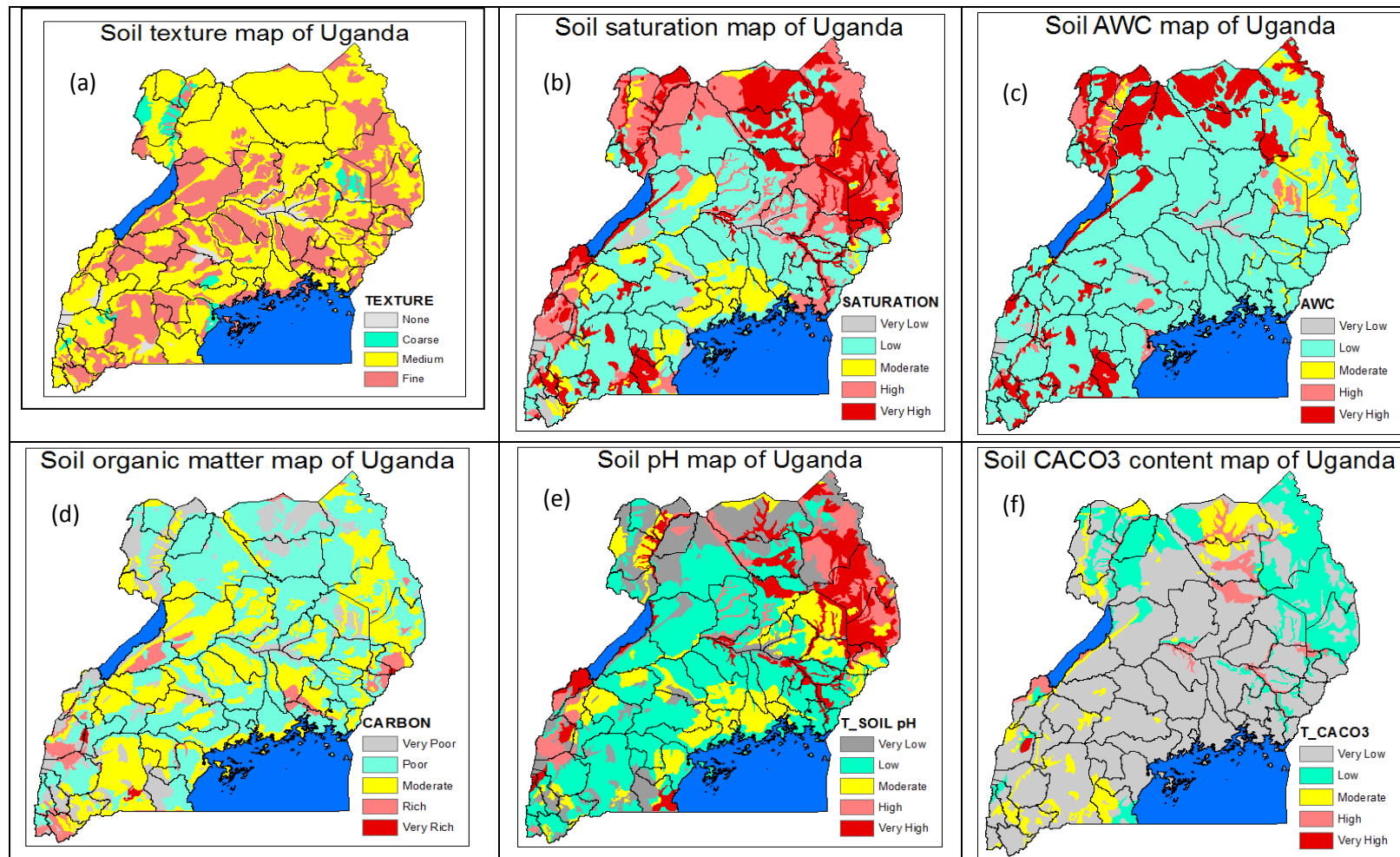


Figure 2.1 (a-f): Patterns of soil properties and composition levels based on the Harmonised World Soil Data (HWSD) over Uganda.

Van Asten *et al.* (2011) pointed out that farmers cite pests, soil fertility, diseases and drought as the major aspects contributing to poor productivity levels. In another study, Van Asten *et al.* (2011) examined the effect of drought on banana yield in three regions of Uganda. The trials were installed in research farms in Mbarara and Ntungamo in Southwest Uganda, and Kawanda in Central Uganda. The study examined variation in bunch weight and cumulative rainfall for 12 months before harvesting (CRF_{12}). The study observed that average bunch weight ranged from 8.0 to 21.9 kg between trials and cycles and was 8-28% less in drier ($CRF_{12} \leq 905$ mm) than in normal ($905 < CRF_{12} \leq 1365$ mm) rainfall periods. The study observed linear relations between CRF_{12} and maximum bunch weight over the whole range of observed CRF_{12} (500 to 1750 mm), whereby every 100 mm decline in rainfall caused maximum bunch weight losses of 1.5 to 3.1 kg or 8 to 10%. The study observed that optimum annual rainfall for East African highland bananas production is in the range of 1200-1300 mm per year. The study further observed that relative drought-induced yield losses were independent of soil fertility.

Bouwmeester *et al.* (2009) found that farmers in Rwanda, Burundi and eastern DRC also identified drought stress as the second most important constraint to production following declining soil fertility. Okech *et al.* (2004) observed that low annual rainfall (678 mm) reduced yields by about 50% in southwest Uganda.

Two main reasons were advanced to explain the high amount of water required for high production of bananas. For example, earlier study (Robinson, 1996 and Robinson and Alberts, 1989) attribute high moisture content requirement in banana fields to the enormous plant fresh biomass and broad leaves. In addition, Kashaija *et al.* (2004) observed that the root system of banana plants mostly concentrates within 30 cm below the soil surface rendering the plant low efficacy to extract water from the deeper surrounding soils and highly sensitive to drought conditions.

Climate variability and change is likely to expose many regions of Uganda to climate extremes that may favor or retard banana growth and yields. Changes in the growth patterns of major crops in many countries are likely to occur due to expected future changes in climate. Climate variability and change is also expected to affect rainfall distribution patterns and possibly result in more intense dry spells in East Africa (Hulme *et al.*, 2001 and Gitau *et al.*, 2011). This may further increase the impact of drought stress on banana production in some areas of Uganda.

2.2 Impacts of Climate on Agriculture

Low resolution (~250 km) climate information from coarse Global Climate Models (GCMs) has been used together with impacts models to assess and evaluate global changes in the agricultural output that would result from changes in climatic parameters. The Intergovernmental Panel on Climate Change Report (IPCC, 2007), for example, used climate information from multiple GCMs and agricultural models and has predicted a decrease in world food production of 5-11% by 2020 and 11-46% by 2050. The shortfall in the world's staple foods supply is estimated at 400 to 600 million tonnes by the 2080s and would increase hunger and poverty, particularly in the poor countries such as Uganda.

Kurukulasuriya and Rosenthal (2003) identified four ways in which climate affects agriculture. These include: (1) changes in temperature and rainfall directly affect crop production and can even alter the distribution of agro-ecological zones, (2) increased CO₂ is expected to have a positive effect on agricultural production due to greater water-use efficiency and higher rates of plant photosynthesis, (3) runoff or water availability is critical in determining the impact of climate change on crop production, especially in Africa and (4) agricultural losses can result from climate variability and the increased frequency of changes in temperatures and rainfall (including droughts and floods).

A large body of literature has been developed to analyze these effects in both developed and developing countries, although the impact of climate on agriculture became of interest only in the 1990s. The interest was spurred by the expectation that accumulation of CO₂ and other greenhouse gases will lead to global warming and other significant climate changes (Kabubo and Karanja, 2006). The study observed that although there are a large number of studies on the effects of climate change in global warming, on agriculture in developed countries, there is a paucity of such studies in developing countries, especially those in Africa. However, there is growing interest in studying these effects and making regional comparisons.

Two methods have been used in literature to study the impact of climate change on agriculture. The traditional approach uses a production function method which relies on functions to evaluate the impacts (Mendelsohn *et al.*, 1994). This study used the Ricardian technique to estimate the value of climate in US agriculture using cross-sectional data for about 300 counties in the United States. The study observed that climate has complicated effects on agriculture which can be highly non-linear and vary by season and location.

A number of other studies that employed the Ricardian approach have supported the findings by Mendelsohn *et al.* (1994) of an adverse impact of climate change on agriculture. For example, Mendelsohn and Dinah (2003) used the same approach to analyze the relationship between climate and rural income for two US states and municipality from Brazil. The study observed that favorable climate increases agricultural net revenues and thus per capita incomes. They conclude that climate is an important determinant of household welfare and therefore providing new technology and capital may be an ineffective strategy for increasing rural incomes in hostile climate regions.

Several other studies that have assessed the impact of climate change on agriculture include Mendelsohn *et al.* (2000); Seo *et al.* (2005); Kumar and Parikh (1998); Molua (2002); Parry *et al.* (2004); Sivakumar *et al.* (2005); Van den Bergh *et al.* (2012); Washington and Pearce (2012) and Bashaasha *et al.* (2013) among others. Most of these studies agree that the net impact of climate change on agriculture will reduce crop productivity in most regions leading to future food insecurity threats both globally and across regions.

Fischer *et al.* (2005) projected that global cereal production could continue to increase up to 3.7 to 4.8 billion tonnes by 2080 without climate change. When it is factored in, global cereal production could be within 2% of reference scenarios, but with potentially large regional variations. In general, decreases are expected in low latitudes and developing countries, reflecting both declining potential land available for crop cultivation observed above and changes in productivity. Sub-regional variations are masked by these figures, with some short term increases possible in areas of overall decrease (e.g. Africa). For example, in tropical highlands where current low temperatures prevent planting of certain crops, new land could become suitable for agriculture.

At high degrees of warming ($> 5\text{ }^{\circ}\text{C}$) some models project price increases of up to 30% on average, though most projections are generally more modest, and in the short and medium term, real prices could fall owing to higher outputs from slight temperature increases. Fischer *et al.* (2002) also observed that the impacts of climate change on agricultural GDP until 2080 are likely to be small at global level, and range between -1.5 to +2.6%, depending on the scenario, but with decreases in most developing regions.

DfID (2004) examined the implications of climate change on the agricultural sector of Africa and observed that on average, countries whose economies rely heavily on one or two

agricultural cash crops are vulnerable to climate variability and change. The study observed that an increase in average temperature of about 2 °C would drastically reduce the area suitable for growing Robusta coffee in Uganda, where it is a major export crop and limit growth to the highlands only.

Arnell *et al.* (2002), pointed out that, even with a stabilization of CO₂ concentration, cereal crop yields in Africa will still decrease by 2.5 to 5 percent by the 2080s. This was illustrated at the national level using models such as DSSAT to assess the impacts of climate change on crop yields. Most of these assessments used the IPCC IS92 emissions scenarios.

Gregory and Ingram (2000) and Davidson *et al.* (2003) observed that following IPCC SRES scenarios (Nakicenovic and Swart, 2000) and climate projections, food security threat posed by climate change is great for Africa, where agricultural yields and per capita food production have been steadily declining, and where population growth will double the demand for food, water and forage in the next 30 years.

In 1996, a report by the Food and Agricultural Organization observed that Africa's food supply would need to quadruple by 2050 to meet people's basic caloric needs, even under the lowest and most optimistic population projections (FAO, 2008). Parry *et al.* (1999) and Fischer *et al.* (2002) revealed that the total additional people at risk of hunger due to climate change would increase with Africa accounting for the majority by the 2080s.

Desanker *et al.* (2001) stressed that in Africa, the vulnerability of other socio-economic sectors such as health to the impacts of climate variability and change is also high. This vulnerability is a function of climatic as well as many other non-climatic factors such as poverty, conflicts and population displacement, access and availability and management of health services, in addition to other factors related to drug sensitivity of the pathogens, awareness and attitude towards preventive measures.

Van den Bergh *et al.* (2012) investigated the impacts of projected climate averages and variability under SRES A2 scenario on banana productivity based on the FAO ECOCROP tool over the tropics and subtropics. Their findings showed that based on current temperature and rainfall data, overall suitability for banana production in the subtropics is much lower than in the tropics. Moreover, within the subtropics, suitability varied greatly. This study further observed that rainfall is the most limiting factor to banana productivity within the tropics.

Another study (Washington and Pearce, 2012) investigated the climate of East Africa and assessed the implications of climate change on Agriculture over East Africa using a number of key crops in the region. The study projected a warmer future climate with wetting trends in some areas mainly during the short rains. In addition, the study observed that current crop distributions may be more affected by temperature changes in the future than by rainfall changes.

The current study used high resolution climate information from RCMs to investigate current and future climate projections and evaluated future effects of climate change on banana production in Uganda. The climate projections of IPCC SRES A1B and A2 scenarios (Nakicenovic and Swart, 2000) are considered alongside the full range of the AR5 RCPs (RCP 2.6, RCP 4.5, RCP 6.0 and RCP 8.5). This study focused on investigating patterns in climate variability and change and their associated effects on banana yields over Uganda. A detailed account of climate variability and change is provided in Section 2.3.

2.3 Climate Variability and Climate Change

Climate in many parts of the world especially the tropics is mainly characterized by the temporal and spatial variations of rainfall and temperature. Several studies have observed changes and variations in rainfall and temperature over many parts of the world. For example, IPCC (2014) has predicted an increase of 0.6 °C in global average surface temperature and observed that the period 1990 -1999 appears to have been the warmest ten years since instrumental records began in 1727. In addition, annual precipitation over land has been predicted to increase by between 0.5 and 1.0% per decade in the middle and high latitudes of Northern Hemisphere. Over the subtropics, rainfall has been predicted to decline by about 0.3% (IPCC, 2014).

Eriksen *et al.* (2008) observed that Africa has experienced a 0.5 °C rise in temperature over the course of the 20th century, with some areas warming faster than others. Boko *et al.* (2007) predicted that annual 5-year running mean surface temperatures are expected to increase by between 3 °C and 4 °C by 2099. Boko *et al.* (2007), further observed that Africa's vulnerability to climate change is highest due to the continent's complex climate system, high dependence on agriculture and socio-economic challenges, such as endemic poverty, poor governance, and limited access to capital and global markets that may all undermine communities' ability to adapt to climate change.

Caminade and Terray (2006) have observed that increased greenhouse gases and atmospheric aerosols concentration in the atmosphere have a strong effect on diurnal temperatures. With respect to rainfall, the variability of seasonal rainfall will increase, droughts may lengthen, with some regions becoming increasingly susceptible to drought and flooding (WWF, 2006; Mwangi *et al.*, 2014 and Ngaina *et al.*, 2014).

Rainfall over most parts of East Africa has been observed to exhibit spatial and temporal variability with great inter-annual rainfall variability (Ogallo, 1979; Nicholson, 2000; Hulme *et al.*, 2005 and Omondi, 2010). In some years, extreme events lead to too much (floods) or too little surface water (drought) with far reaching physical, environmental and socio-economic impacts (Ogallo, 2009 and Mwangi *et al.*, 2014).

Studies such as Conway (2005) have shown that within the Nile basin, there is a high confidence that temperature will rise. Hulme *et al.* (2001) also observed that the temperature rise will lead to greater water loss through evaporation placing additional stress on water resources (Lucinda, 2008) regardless of changes in rainfall. Other results from nine recent climate scenarios showed decreases in Nile flows from zero to approximately 40 percent by 2025 (Strzepek *et al.*, 2001).

In the East Africa region, snow cover on mountains such as Mount Kilimanjaro and Mount Kenya has been disappearing and has decreased by about 50% since 1960 due to land surface temperature increases (Molg *et al.*, 2009 and IPCC, 2014). This has serious implications for the rivers that depend on ice melt for their flow. Several rivers are already drying up in many regions due to depletion of the melt water, and recent projections suggest that if the recession continues at its present rate, the ice cap might disappear completely within 15 years (Molg *et al.*, 2009). Other glacial water reservoirs such as Ruwenzori in Uganda are facing similar threats (Desanker, 2002).

Findings of the Special Report on Extremes (SREX; IPCC, 2012) have showed that under the SRES A1B and A2 emissions scenarios, extremes events are likely. Foreexample, it has been observed that a 1-in-20 year hottest day become a 1-in-2 year event by the end of the 21st century in many regions. In the high latitudes especially in the Northern Hemisphere, however, it is likely to become a 1-in-5 year event. The regional details of climate change patterns over Uganda associated with these two SRES sceanrios over Uganda are provided in this study.

IPCC (2012) has also observed that there has been observed reduction in surface warming trend over the recent period 1998 to 2012 as compared to the period 1951 to 2012. According to the report, the reduction in surface warming has been attributed to a reduced trend in radiative forcing and a cooling contribution from natural internal variability, which includes a possible redistribution of heat within the ocean with medium level confidence. The reduced trend in radiative forcing has been primarily attributed to volcanic eruptions and the timing of the downward phase of the 11-year solar cycle (IPCC, 2012). Previous studies on climate extremes associated with climate variability and change over East Africa have been reviewed in section 2.3.1.

2.3.1 Climate Variability and Change over Eastern Africa

Monthly, seasonal and annual rainfall over East Africa has been observed to exhibit high spatial and temporal variability. Studies by Ogallo (1993), Mutai and Ward (2000), Washington and Pearce (2012) and Endris *et al.* (2015) among others have observed that the inter-annual rainfall variability over the East Africa arises from a complex interactions of oceanic and atmospheric systems. Major systems include Sea Surface Temperatures (SSTs) anomalies, large scale atmospheric patterns, synoptic scale weather disturbances, tropical cyclones and subtropical anticyclones, extra tropical weather systems, wave perturbations and free atmosphere variations (Washington and Pearce, 2012 and Endris *et al.*, 2015). Relative to the long rains, the short rains tend to have stronger inter-annual variability, greater spatial coherence across a large area and more significant associations with El Niño Southern Oscillation (ENSO). Warm El Niño events are associated with increased rain with negative anomalies occurring during La Niña events (Mutai and Ward, 2000 and Endris *et al.*, 2015) in most parts of eastern Africa.

McHugh (2006) identified a statistically significant (at the 98% level) relationship between El Niño events with the seasonal rainfall over East Africa. The study observed that the relationship exhibits a negative correlation with the long rains that occur in March-May (MAM) over East Africa. McHugh (2006) demonstrated that during El Niño events, moist South Atlantic westerly wind flows are increased over East Africa. In addition, during El Niño episodes the anomalous westerlies tend to prevent the inflow of thermally stable subsiding airmasses from the Indian Ocean. This increases low level moisture convergence, decreases

lower troposphere stability and increases cloudiness and precipitable water anomalies during the short rains during October-December (OND) rainy season (McHugh 2006).

Other important modes of climate variability that have a significant impact on East Africa inter-annual rainfall variability, particularly during the OND rains, are the Indian Ocean dipole (IOD) and Southern Indian Ocean Dipole (SIOD). Details of the relationship between the rainfall and IOD and SIOD can be found in several studies over the region (Schreck and Semazzi, 2004; Behera *et al.*, 2005; Song *et al.*, 2007 and Riddle and Cook, 2008).

Recent studies (Moise and Hudson, 2008 and Shongwe *et al.*, 2011) have undertaken an assessment of a subset of 12 CMIP3 GCMs outputs over Eastern Africa. The results from these studies suggested that by the end of the 21st Century, there will be a wetter climate with more intense wet seasons and less severe droughts during MAM and OND. These results project a reversal of historical trend in these seasons over the region (Riddle and Cook, 2008; Funk *et al.*, 2008 and Williams and Funk, 2011).

The spatial patterns of temperature over the region particularly Uganda is highly associated with the elevation (between 870 to 2,200 meters above sea level). Unlike the diurnal variations in temperature that is influenced by earth's outgoing longwave radiation, daily-monthly-seasonal-annual temperature variations at constant elevation are nearly uniform throughout the year. Low land areas are associated with high temperatures while high land areas are associated with low temperatures (Nsubuga *et al.*, 2014). The Country's mean temperatures in western, central and eastern regions support favorable growth of bananas. Warm temperatures are, however, associated with the high population densities of banana nematodes and weevils especially in the central region that tend to affect banana productivity (Bridge, 1988; Speijer *et al.*, 1993; Speijer and Kajumba, 1996 and Talwana *et al.*, 2000).

Christy *et al.* (2009) analysed 20 stations temperature over Kenya and Tanzania and concluded that from 1946-2004, trends in maximum temperature are near zero, whereas minimum temperature shows a significant positive trend over the same period. This shows a decrease in the diurnal temperature range, with respect to the 14th century which over Sudan and Ethiopia has decreased by between 0.5 °C and 1 °C since the 1950s (Caminade and Terray 2006).

2.4 Climate Modeling and Future Climate Change Scenarios

Several climate models have been developed and currently used to simulate the behavior of the climate system (Figure 2.2). The ultimate objective is to understand the key physical, chemical and biological processes which govern the climate systems. Through understanding the climate system, it is possible to obtain a clearer picture of past climates and associated processes by comparison with empirical observation, and predict future climate change based on some key assumptions. Models can be used to simulate climate on a variety of spatial and temporal scales. Henderson-Sellers and Robinson (1986) and Schneider (1992) provide detailed introductory discussions of the methods and techniques involved in climate modeling.

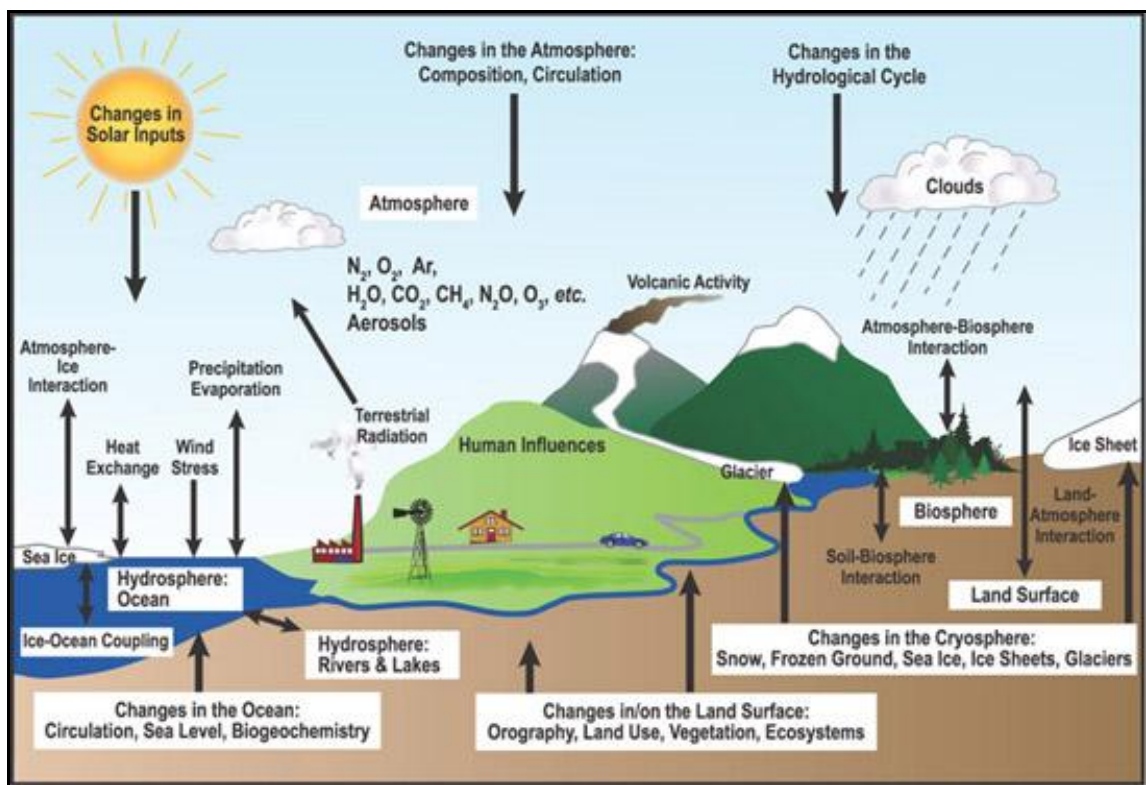


Figure 2.2: The major components of a climate system (IPCC, 2014).

According to Mearns *et al.* (2001), three major processes need to be considered when constructing a climate model: First, is the radiative process that refers the transfer of radiation through the climate system (reflection and absorption), second is the dynamical process that represents the horizontal and vertical transfer of energy (convection, advection, diffusion) and thirdly is the surface process as an inclusion of processes involving land/ocean/ice, and the effects of albedo, emissivity and surface-atmosphere energy exchanges.

The basic laws and other relationships necessary to model the climate system are expressed as a series of equations (Holton, 2004). These equations may be empirical in derivation based on relationships observed in the real world, they may be primitive equations which represent theoretical relationships between variables, or they may be a combination of the two. Solving the equations is usually achieved by finite difference methods. It is therefore important to consider the model resolution in both time and space that represents the time step of the model and the horizontal/vertical scales (Holton, 2004).

On the synoptic scale, present GCMs succeed to adequately simulate the main characteristics of the atmospheric circulation (Engelbrecht, 2000; Wang *et al.*, 2004; Holton, 2004; Otieno and Anyah, 2013; Otieno *et al.*, 2014 and Endris *et al.*, 2015). However, most GCMs employed for climate variability and climate change studies still have coarse resolutions. This is due to computational requirements for simulating finer scale (McGregor, 1993). Finer grid resolution requires smaller time steps that lead to more numerical equations to solve for a specific simulation to be completed. For this reason, most GCMs do not adequately represent detailed processes associated with regional to local climate variability that are required for regional and national climate change assessment (Denis *et al.*, 2002; Wang *et al.*, 2004; Sabiiti, 2008 and Giorgi *et al.*, 2009).

As an alternative, Regional Climate Models (RCMs) were introduced to provide more detailed climate simulations for various regions on the globe. RCMs dynamically downscale GCM output to scales more suitable to end user needs (Sun *et al.*, 2006) and are useful for understanding climate variability and change particularly in regions with complex topographical detail such as Uganda. These models are nested within global models and are fed across lateral boundaries by information produced by the GCMs or observational fields. It should be, however, emphasized that RCMs are not formulated to replace GCMs but rather to supplement GCMs by adding fine-scale detail to their coarser resolution simulations (Hudson *et al.*, 2004).

Globally, there has been increase in RCMs simulations (IPCC, 2007), yet, very few RCM studies have been performed over the East Africa region (Sun *et al.*, 1999a; Indeje *et al.*, 2000; Anyah, 2005; Anyah *et al.*, 2006; Anyah and Semazi, 2007; Sabiiti, 2008; Omondi, 2010; Endris *et al.*, 2013 and Endris *et al.*, 2015).

Future climate projections are based on a number of possible alternative future paths called scenarios. UKCIP (2003) defines climate change scenario as a coherent and internally consistent description of the change in climate by a certain time in the future. When developing climate scenarios, a specific modeling technique is used under specific assumptions about the levels of greenhouse gases and other emissions and other factors that may influence climate in the future such as development, technological progress, population growth, urbanization among other factors.

In 1996, the IPCC began the development of a new set of emission scenarios, effectively to update and replace the previously used IS92a scenarios. Four different narrative storylines were developed to describe the relationship between emission driving forces and their evolution and to add context for the scenario quantification as obtained from the WG1 (IPCC TAR, 2001). According to Mearns *et al.* (2001), these scenarios were mainly considered under main story lines, which include A1, A2, B1 and B2. A1 SRES scenario is further sub-divided into A1FI that represent a storyline along A1 that is fossil intensive (FI) and A1B representing a story line along A1 that employs a balance (B) between efficient technology (less fossil intensive) and less efficient technology (fossil intensive). This study evaluated future climate projections based on the high emission SRES A2 (also referred to as the “Business As Usual” scenario) and relatively low emission A1B scenario. A contrast between these two IPCC SRES scenarios (SRES A1B and SRES A2) used in this study is given in Table 2.3.

The fifth assessment report (AR5), IPCC, 2014 has developed new scenarios that relate concentrations to radiative forcing and named them Representative Concentration Pathways (RCP) scenarios (Moss *et al.*, 2010 and IPCC, 2014). The four RCP scenarios include one mitigation scenario leading to a very low forcing level (RCP 2.6), two stabilization scenarios (RCP 4.5 and RCP 6.0), and one scenario with very high greenhouse gas emissions (RCP 8.5) also referred to as the “no mitigation” scenario.

This set of scenarios is not directly based on socio-economic storylines and represent a range of 21st century climate policies, as compared with the no-climate policy of the Special Report on Emissions Scenarios (SRES, Nakicenovic and Swart, 2000; Morita and Robinson, 2001 and Mearns *et al.*, 2001) previously used in the third and fourth assessment reports. The RCP scenarios are based on a sequential approach and include more consistent short-lived gases and land use changes. The AR5 RCP scenarios are not necessarily more capable of representing

future climate patterns than the AR4 SRES scenarios but rather more leaned toward policy that can support climate change adaptation and mitigation.

These RCP climate scenarios have been extensively documented in published literature (Fujino *et al.*, 2006; Riahi *et al.*, 2007; van Vuuren *et al.*, 2007 and Wise *et al.*, 2009) and used within CMIP5 (Riahi *et al.*, 2011; Masui *et al.*, 2011 and Thomson *et al.*, 2011) and CORDEX climate simulations. Figure 2.3 shows the trajectories and the levels of radiative forcing associated with each scenario under both AR4 (IPCC, 2007) SRES and AR5 RCPs (van Vuuren *et al.*, 2011 and IPCC, 2014).

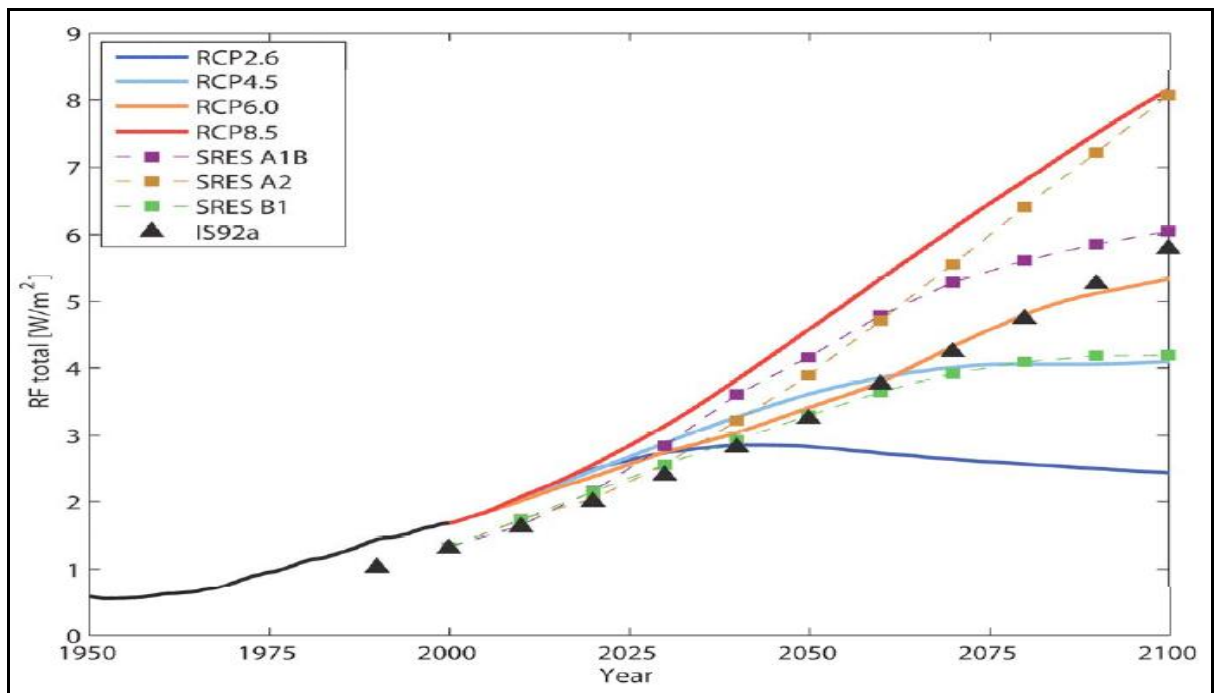


Figure 2.3: AR5 (RCPs), AR4 (SRES) and IS92a emission scenarios pathways. (Source: IPCC, 2014).

Table 2.3: Contrast between the different technological and socio-economic drivers considered under the A1B and A2 scenarios (Source, Nakicenovic and Swart, 2000 and IPCC, 2007)

Scenario	Baseline	SRES A1B			SRES A2		
Year	1990	2020	2050	2100	2020	2050	2100
Population (billion)	5.3	7.4 (7.4-7.6)	8.7	7.1 (7.0-7.1)	8.2	11.3	15.1
World GDP (10 ¹² , 1990, US\$/yr)	21	56 (52-61)	181 (164-181)	529	41	82	243
Per capita income ratio	16.1	6.4 (5.2-7.5)	2.8 (2.4-2.8)	16(15-17)	9.4 (9.4-9.5)	6.6	4.2
Final energy intensity (106J/US\$)	16.7	9.4 (8.7-12.0)	5.5 (5.0-7.2)	3.3 (2.7-3.3)	12.1 (11.3-12.1)	9.5 (9.2-9.5)	5.9 (5.5-5.9)
Primary energy (1018J/yr)	351	711 (589-875)	1347 (1113-1611)	2226 (1002-2683)	595 (595-610)	971 (971-1014)	1717 (1717-1921)
Share of coal in primary energy (%)	24	23 (8-26)	14 (3-42)	4 (4-41)	22 (20-22)	30 (27-30)	53 (45-53)
Share of zero carbon in primary energy (%)	18	16 (9-26)	36 (23-40)	65 (39-75)	8 (8-16)	18 (18-29)	28 (28-37)
CO ₂ from fossil fuels (GtC/yr)	6.0	12.1 (8.7-14.3)	16.0 (12.7-25.7)	13.1 (13.1-17.9)	11.0 (10.3-11.0)	16.5 (15.1-16.5)	28.9 (28.2-28.9)
CO ₂ from land use (GtC/yr)	1.1	0.5 (0.3-1.6)	0.4 (0.0-1.0)	0.4 (-2.0-2.2)	1.2 (1.1-1.2)	0.9 (0.8-0.9)	

Table 2.3 continued (Source, IPCC, 2007)

	Baseline	SRES A1B			SRES A2		
Year	1990	2020	2050	2100	2020	2050	2100
Cumulative CO ₂ from fossil fuels (GtC) for 1990-2100				1437 (1220-1989)			1773 (1651-1773)
Cumulative CO ₂ from land use (GtC) for 1990-2100				62 (31-84)			89 (81-89)
Cumulative CO ₂ , total (GtC) for 1990-2100				1499 (1301-2073)			1862 (1732-1862)
Sulfur dioxide (MtS/yr)	70.9	100 (62-117)	64 (47-64)	28 (28-47)	100 (80-100)	105 (104-105)	60 (60-69)
Methane (MtCH ₄ /yr)	310	421 (406-444)	452 (452-636)	289 (289-535)	424 (418-424)	598 (598-671)	889 (889-1069)
Nitrous oxide (MtN/yr)	6.7	7.2 (6.1-9.6)	7.4 (6.3-13.8)	7.0 (5.8-15.6)	9.6 (6.3-9.6)	12.0 (6.8-12.0)	16.5 (8.1-16.5)
CFC/HFC/HCFC (MtC equiv./yr)	1672	337	566	614	292	312	753

Under RCP 6.0 and RCP 8.5, radiative forcing does not peak by year 2100; radiative forcing peaks and declines for RCP 2.6 by the year 2100 while for RCP 4.5 it stabilizes by 2100. Each of these scenarios represents a different possible path in terms of economic growth, population growth, technology, environmental concerns and emission levels (Table 2.4) among others.

Table 2.4: Contrast of the different properties across the different RCPs (2.6, 4.5, 6.0 and 8.5) scenarios by the year 2100.

Scenario/feature	RCP 2.6	RCP 4.5	RCP 6.0	RCP 8.5
Integrated Assessment Model	IMAGE	GCAM (MiniCAM)	AIM	MESSAGE
Radiative forcing by 2100	2.6 W/m ²	4.5 W/m ²	6 W/m ²	8.5 W/m ²
CO ₂ concentration by 2100 (ppm)	490 ppm	650 ppm	850 ppm	1370 ppm
Pathway to stabilization	Peak around 3 W/m ² mid-century and decline to 2.6 W/m ² by 2100	Stabilization without overshooting	Stable rise without overshooting	Steady rise of radiative forcing

Otieno and Anyah (2013) assessed the skill of the CMIP5 models in simulating seasonal rainfall over the GHA region. The study showed that the correct location of rainfall was well simulated in most models. However, the moisture from the Congo basin, lakes and highland (Ethiopian highlands) was not properly simulated. This was attributed to the coarse resolution of most GCMs and the physical inconsistencies and poorly controlled evolution of the large scales. The current study uses high resolution climate model outputs and also evaluates the sensitivity of model rainfall simulations to variation resolution.

On the regional scale, GCMs are not adequate for climate modeling and impacts assessment. RCM have therefore been developed and extensively used over the past decade to offer an effective downscaling methodology for studying regional and local-scale climates associated with the interactions between local forcing and the prevailing circulation systems (Wang *et al.*, 2004). Regional climate modeling has been shown in several studies to improve simulations of the detailed regional scale climate (Dickinson *et al.*, 1989; Giorgi and Bates, 1989; Denis *et al.*, 2002; Sabiiti, 2008; Lucinda, 2008 and Omondi, 2010).

Hudson *et al.* (2004) and Wang *et al.* (2004) observed that Regional Climate Models (RCMs) make it possible to access finer spatial scales that are required for regional climate change impacts, vulnerability, coping and adaptation studies. RCMs such as PRECIS RCM (used in this study, Simon *et al.*, 2012) are available for downscaling studies and have been used

collectively in the Coordinated Regional Downscaling Experiments (CORDEX) programme for Africa (Nikulin *et al.*, 2012).

While the RCMs are used in simulating of regional climates, they still exhibit a great range of inaccuracies. Denis *et al.* (2002) identified nine potential sources of errors that sometimes cause the RCM outputs to significantly deviate from historical climate observations. These include: (i) numerical nesting methodology (mathematical nesting and strategy), (ii) spatial resolution difference between driving data and the nested regional climate model, (iii) spin up period, (iv) update frequency of lateral boundary conditions, (v) physical parameterization consistencies, (vi) horizontal and vertical interpolation errors, (vii) domain sizes, (viii) quality of driving data and (ix) climate drift or systematic error. Hein (2008) also reviews the implications of these sources of error for application of RCMs to simulate climatic parameters such as rainfall using a number of case studies for different regions.

Sabiiti (2008) used the PRECIS regional climate system to simulate the climate scenarios over the Lake Victoria basin. The study observed improvement of regional rainfall and temperature representation in the RCM simulation compared with the GCM outputs. However, a significant disparity was observed between the RCM simulation and the gridded observational dataset from Climate Research Unit (CRU). Studies by Sabiiti, 2008; Omondi, 2010; Nandozi *et al.*, 2012 and Otieno *et al.*, 2014 have, however, observed existence of uncertainties in the CRU gridded rainfall over East Africa region mainly due to the sparse network in the gauge observations in the region. The validation of RCM outputs therefore need to be extended to other observational gridded datasets of rainfall and temperature over the region.

Mutemi (2003) applied an updated version of ECHAM AGCM (ECHAM4.5) to study the variability of East Africa climate. The model reproduced the climatological mean pattern such as the bimodal seasonality of rainfall associated with the north-south migration of the ITCZ and monsoonal flow, except the correct amplitudes of the inter-annual variability linked to extreme El-Niño episodes such as the 1982 and 1997 were not well reproduced.

Opijah (2000) carried out numerical simulation of the impact of urbanization on the microclimate over Nairobi area. He found that one of the major factors influencing weather/microclimate in cosmopolitan Nairobi province is topography. Although comparatively smaller than the forcing through topography, the impacts of the land use/land

cover changes like the urban built up area and forests are substantial in spite of the relatively small areas currently occupied by forests.

Endris *et al.* (2013) evaluated the performance of 10 CORDEX regional climate models forced by ERA-Interim using a set of model performance metrics over the Eastern Africa region. The study observed improvements in model performance despite inter-modal variability among the models across the region. The study concluded that the use of Multi Model Ensemble (MME) greatly improves the representation of model simulated mean rainfall across the region. However, in many instances the information on extreme rainfall events is not adequately represented in the Multi Model Ensemble (MME).

In a further study, Endris *et al.* (2015) investigated teleconnection responses in multi-GCM driven CORDEX RCMs over Eastern Africa. This assessment observed that the MPI-ESM-LR driven RCMs better reproduce the large-scale signals such as the El Niño Southern Oscillation (ENSO) and the Indian Ocean Dipole (IOD) in the historical period over the eastern Africa region than RCMs run driven by the other GCMs.

2.5 The Conceptual Framework of the Study

This section presents the conceptual framework of the study (Figure 2.4). The framework highlights the data collected and generated through climate experiments. In this section, the linkages or relationship between methods, factors and outputs are demonstrated. In addition, the dependent, independent and intervening variables are shown and discussed. The section also provides the rationale for selection of the study, its contribution to research and the anticipated major study outcomes.

2.5.1 Introduction

This study sought to determine linkages between banana productivity and climate variability and change including extremes in the past and future periods. The study identified banana yield as the dependent variable that was related to banana growth and production. The independent variables included climatic and non-climatic variables. Climatic variables included rainfall, minimum and maximum temperatures while the non-climatic variables that have been reported to affect banana yields are soil fertility, pests and diseases, crop management practices, cultural values, market, political stability among others. The dotted arrows indicate variables that could not be studied in detail due to challenges in access long series of quality data records.

Previous field studies have extensively investigated the linkages between banana production and the non-climatic factors as discussed in previous sections. Despite reported changes in climate including recurrence of extremes over most parts of Uganda, very few studies have investigated the linkages of climatic factors to banana yields at national and sub national levels. Recent studies (Van den Bergh *et al.*, 2012 and German *et al.*, 2015) have assessed the impacts of future climate change on future banana production and suitability conditions across large global banana growing regions including the tropics and subtropics. Literature also showed that there is limited information on process based banana crop models to simulate the effects of changes in climate on banana growth stages and yields in the study region.

2.5.2 Illustration of the Conceptual Framework

The conceptual framework presents and discusses the key variables, their linkages and methods used to study the relationships. The study focused on understanding how changes in climatic factors affect banana yields mainly in two regions i.e western and central Uganda. Despite existence of different varieties of bananas, the study investigated patterns in yields of cooking bananas due to lack of good and consistent historical records, their high resistance to changes in climatic conditions and the limited scales of production of the other varieties of bananas.

In addition the cooking banana are the key staple food crop in most of Uganda and has the potential to promote food security in the region. Using empirical methods and CROPWAT, the study sought to determine the linkages between banana yields and current climate variability. Climate thresholds for banana production over Uganda were identified. Analysis of year to year patterns in climate was used to determine periods when certain threshold were achieved or not achieve was indicative of climate stress on bananas. Both high and low climate extremes had to be determined and linked to variability and changes in banana production. A review of several other previous related studies in this chapter have have been used to guide the materials and methods, presentation and discussion of the study results.

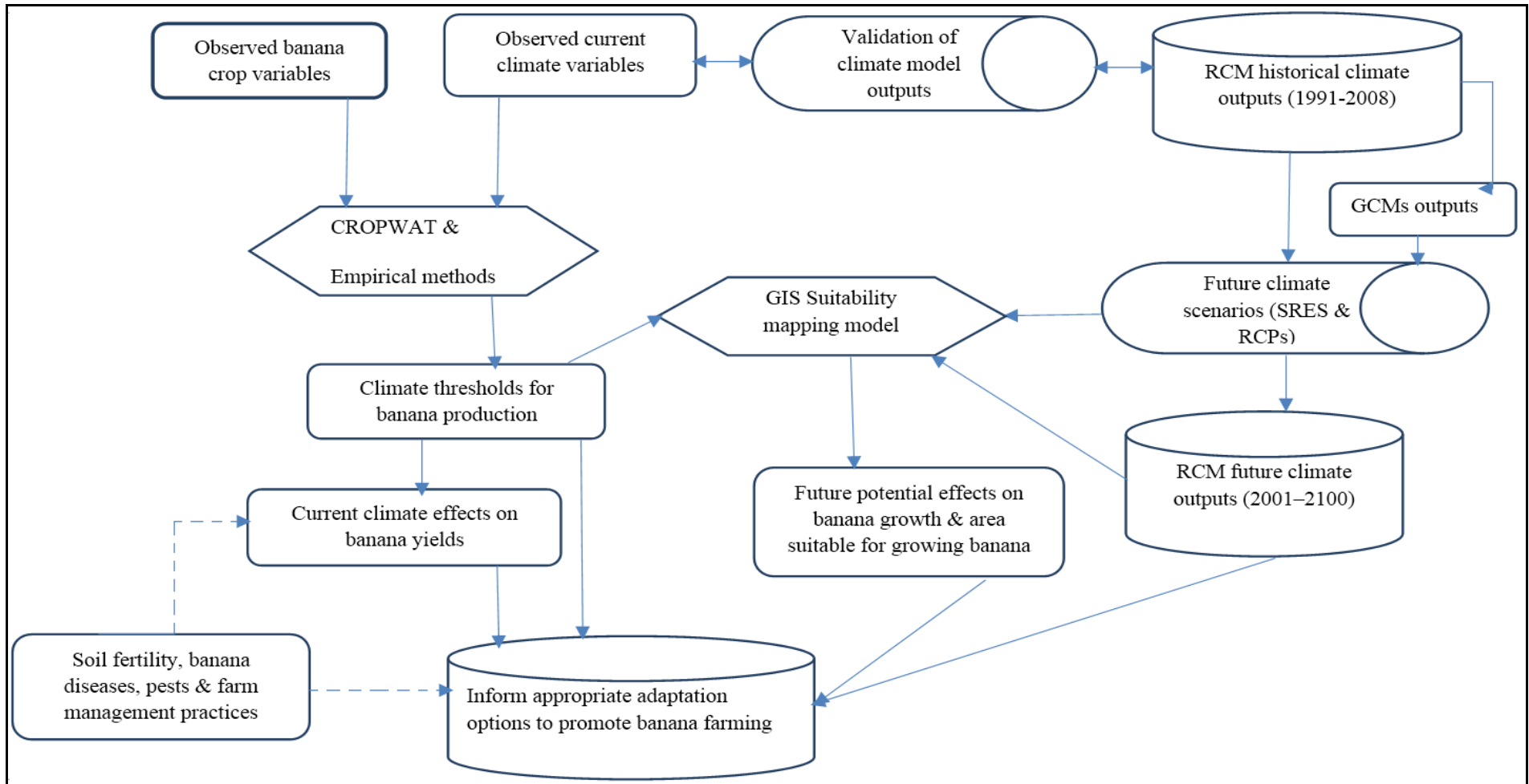


Figure 2.4: A conceptual framework showing key variables and their linkages, experiments and methods used to study the relationships. Dotted arrows indicate factors that require experimental studies not considered but reviewed based on previous studies.

The second part of the study aimed at determining the best regional climate model or group of models that would provide a more realistic climate change projection for Uganda. Validation of regional climate model outputs using different model performance metrics was therefore undertaken.

As a third step, the study generated relatively high (50 km) and also obtained very high (1 km) resolution future climate projections under different future scenarios over Uganda. Analysis aimed at understanding future climate patterns and extremes over Uganda under different scenarios. Future climate scenarios were purposively selected to represent a range of possible future climate outcomes from low temperature changes to very high temperature changes with varying levels of rainfall changes across Uganda.

Lastly, the suitability patterns in banana production, banana growth and yield response patterns were mapped under a changing climate for different scenarios over Uganda. The analysis in this part of the study would inform adaptation strategies required for sustainable future banana production and ensuring food security in Uganda and neighboring regions.

Specific details on research design including sampling techniques, variables, materials (data, tools and climate models) selected and analysis methods adopted to achieve the specific objectives have been presented in Chapter three under materials and methods.

CHAPTER THREE

DATA AND METHODS

This chapter describes in detail the materials used, regional climate experiments used for generating historical (performance of the RCM in simulating observed climate patterns over Uganda) and future climate change and the methods used to achieve the overall study objective through the specific objectives of the study. The materials used in the study are, however, discussed first.

3.1 Materials

The materials (data) used in the study included banana yields and climate data. Banana data included cross sectional banana production, area planted and yield data recorded in the Uganda Census of Agriculture (UCA, 2008/09) at district level. Additional data consisted of historical annual records of banana production, area of banana harvested and banana yields for national and district level for the period 1971 to 2009. The banana data were obtained from the Uganda Ministry of Agriculture, Animal Industry and Fisheries (MAAIF), and other information relevant including reports and abstracts on banana farming in Uganda were obtained from Uganda Bureau Of Statistics (UBOS). The banana yield was estimated as total production divided by total area harvested.

The banana data was collected and processed based on purposive and cluster sampling by taking districts that have high banana production and area harvested based on the percentile approach. The districts were selected from central and western regions of Uganda based on ecological zones discussed in chapter one (Figure 1.6). The districts were clustered following classified banana production regions of Uganda (Rutherford and Gowen, 2003).

Climate data consisted of both observed (insitu and gridded observations) and regional climate model simulated data for rainfall, temperature and soil moisture content for both historical and future climate patterns over Uganda. The insitu climate data was obtained from Uganda National Meteorology Authority (UNMA) and IGAD Climate Prediction and Applications Centre (ICPAC). The observed climate data considered representative stations (Figure 3.1 a) from each of the rainfall homogeneous zones following purposive sampling technique (Ogallo, 1980; Basalirwa, 1991; Indeje *et al.*, 2000 and Komutunga, 2006). The areal averages of

gridded observations and model outputs were extracted over subregions 1-7 (Figure 3.1 b and Tables 3.1-3.2).

Table 3.1: Representative observation stations (also Figure 3.1a) over Uganda

WMO Code	Station	Latitude	Longitude	Altitude (m)
86300000	Arua	3.05	30.917	1280
87320000	Gulu	2.783	32.283	1105
86320000	Kitgum	3.3	32.883	940
86340020	Kotido	3.017	34.1	1260
88330060	Soroti	1.717	33.617	1132
88310030	Masindi	1.683	31.717	1147
89320670	Namulonge	0.533	32.617	1130
90300030	Mbarara	-0.6	30.683	1420
89300630	Kasese	0.183	30.1	691
89330430	Jinja	0.45	33.183	1175
91290000	Kabale	-1.25	29.983	1869

Table 3.2: Analysis regions (also Figure 3.1b) over Uganda

Region	Latitude Interval	Longitude Interval	Region Description
REGION 1	1.5S-0	29.5E-31.0E	Southwestern
REGION 2	0-1.5N	30.0E-31.5E	Western
REGION 3	0-1.5N	32.0E-33.5E	Central
REGION 4	0.5N-2N	33.5E-35.0E	Eastern
REGION 5	2.0N-3.5N	31.0E-32.5E	Northwestern
REGION 6	2.5N-4.0N	33.0E-34.5E	Northeastern
REGION 7	1.5S-4N	30.0E-35.0E	Uganda

Gridded observations used in the study included Climate Research Unit (CRU), University of Delaware (UDel) and ERA-Interim datasets. The gridded observations were obtained from the archives of the United Kingdom Meteorological Office (UKMO) and the European Centre for Medium Range Weather Forecasting (ECMWF). The ERA-Interim data was used to drive the RCM experiments for a historical period (1989 to 2008). This study, however, acknowledged existence of an updated version of ERA-Interim dataset (1979 to 2011) which was not available during the time of the study experiment runs.

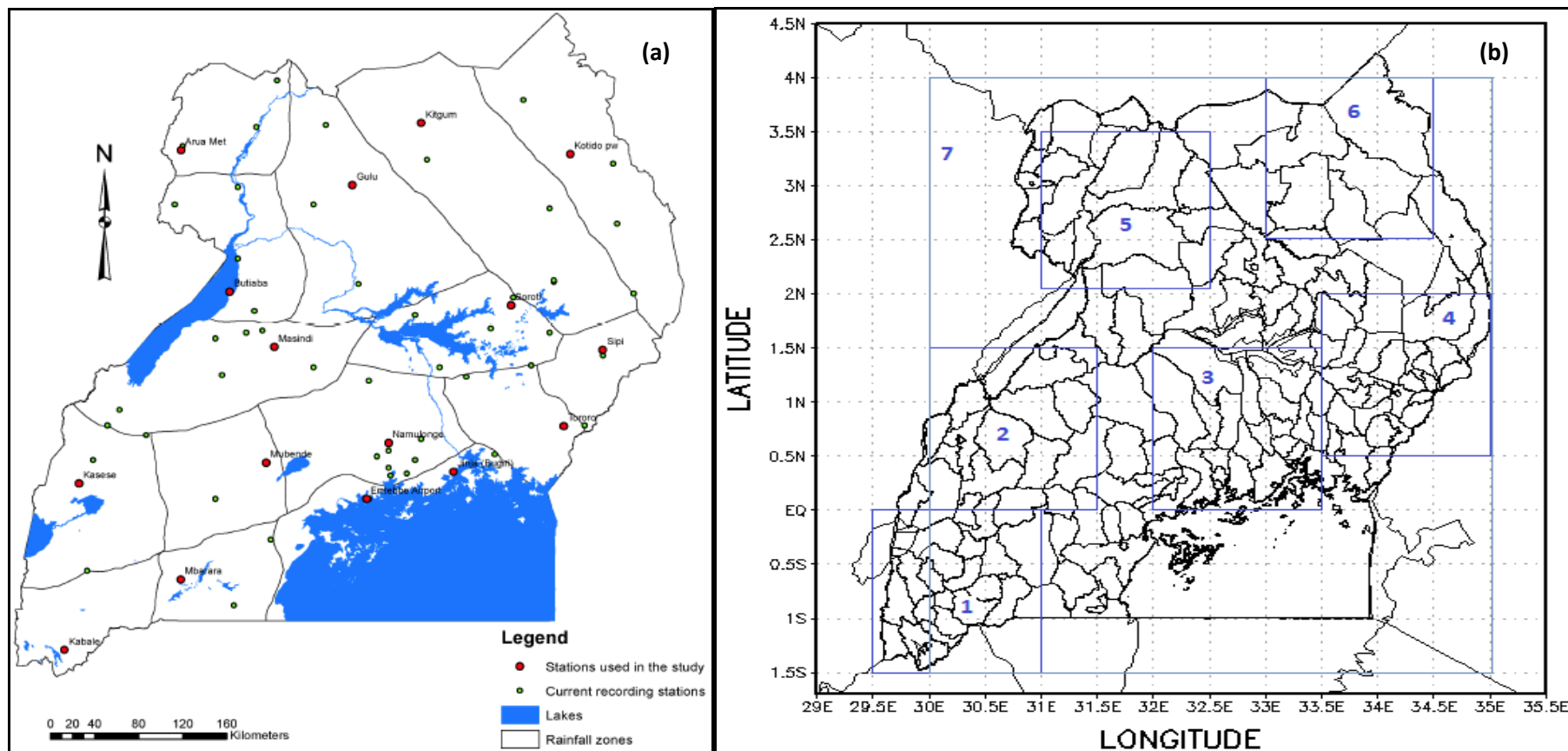


Figure 3.1 (a-b): Representative observational stations for different homogeneous zones (a) and 0.5° model grid boxes, districts and seven analysis regions (b) over Uganda.

The period of the study experiment was consistent with that of the historical CORDEX runs over Africa to aid comparisons in model performance. The gridded climate observations were considered for the periods 1931 to 2013 (for studying observed climate variability including trends) and 1991 to 2008 (for model validation, similar to the period of historical regional climate model runs to aid model validation). The gridded datasets used are described in sub-sections 3.1.1.

3.1.1 Gridded Climate Observations and Model Outputs

The CRU and UDel land-surface rainfall datasets provide gridded observed climate information based on different spatial interpolation methods and different sets of rain gauge records. This leads to some differences in the representation of rainfall over many regions in the two data sets. The interpolation methods and schemes used in both datasets are briefly discussed in sub-sections 3.1.1.1 and 3.1.1.2 respectively.

3.1.1.1 Climate Research Unit Gridded Observations

Climate Research Unit (CRU) gridded observations provide a land-only surface representation of key gridded climate surface fields interpolated from a subset of available observed climate station data. The CRU data set is prepared by the Climate Research Unit (CRU) at the University of East Anglia (UEA) and provides a gridded monthly time series from 1900 to date of key climate variables covering the entire globe. For this study, only a subset of CRU data has been used. The study examined the reliability of this dataset before analyzing the data to determine the extent of observed climate variability and evaluation of regional climate outputs over Uganda.

The CRU data is based on an interpolation method that bears conceptual similarity to the Shepard (1968) and Willmott *et al.* (1985) approaches. For each grid-node estimate, the ADW method weights each of the eight rain gauge and temperature station observations that are nearest to the grid node by taking into account the distance from the grid point using a Correlation-Decay Distance (CDD) and the directional angular isolation for each station. Interpolated fields are forced to the climatology mean value at grid points where there is no station within the CDD (New *et al.*, 2000 and Mitchell and Jones, 2005). For the case of Uganda, Table (3.1a) shows the stations that are used in CRU gridded data set. Cross validation was used to determine the level of accuracy of the CRU data.

There are two recently updated versions of CRU datasets, CRUTS 3.20 and CRUTS 3.21. CRU TS 3.20 uses the Global Historical Climatology Network's (GHCN's) method (Easterling and Peterson, 1995; Easterling and Peterson, 1992) to identify heterogeneity. This method uses the Residual Sum of Squares (RSS) applied at monthly time scale. A correction value is obtained for each month in case heterogeneity is identified (Mitchell and Jones, 2005). The CRUTS 3.21 dataset is produced in a similar way, though no homogenization is performed.

Several studies (Sabiiti, 2008; Omondi, 2010; Nandozi *et al.*, 2012; Otieno *et al.*, 2014 and Otieno *et al.*, 2015) have used this dataset to represent patterns and trends in key surface climate variables particularly rainfall over Eastern Africa. The studies observed a good representation of rainfall in relation of station observations over the region except over a few areas. This study has further undertaken analysis to understand the agreement between insitu and CRU rainfall and temperature observations for selected stations in Uganda.

3.1.1.2 University of Delaware Gridded Observations

The University of Delaware (UDel) dataset (Version 1.01) is based on the Willmott *et al.* (1985) traditional-interpolation method as well as on Climatologically Aided Interpolation (CAI; Willmott and Robeson, 1995 and Matsuura and Willmott, 2009). The method employed a spatially high-resolution climatology to obtain monthly rainfall differences at each station. These station differences are then spatially interpolated to obtain a gridded field using a version of Shepard's traditional algorithm (Willmott *et al.*, 1985). Each gridded monthly difference field is finally added back onto the corresponding monthly climatology field to obtain monthly land-surface rainfall (Matsuura and Willmott, 2009).

The UDel dataset also contains records from the Global Surface Summary of the Day (GSOD) archive which improves the station-network coverage of the land surface, especially during the recent past and over the more severe (drier and rugged) regions of the land surface. It follows that improved representation of the drier regions would reduce. It is also true, that the GSOD archive contains a variety of very extreme values, including long strings of zeros and a limited number of very high values. Although Matsuura and Willmott (2009) attempted to filter out only the truly unrealistic daily and monthly rainfall values from the GSOD station records, any erroneous zero that is missed or an incorrectly removed maximum value would tend to produce an underestimate.

3.1.1.3 ERA-Interim Dataset

ERA-Interim data set (Berrisford *et al.*, 2009 and Dee *et al.*, 2011) provides the latest global atmospheric reanalysis. This dataset is prepared by the ECMWF. ERA-Interim spans from 1979 to current. For the experiment runs, the study used the available data that covered a period from 1 January 1989 to 31 December 2008. The ERA-Interim gridded data fields include a large variety of 3-hourly surface parameters, describing weather as well as ocean-wave and land-surface conditions, and 6-hourly upper-parameters covering the troposphere and stratosphere.

The ERA-Interim was prepared to replace the ERA-40 data for climate and atmospheric circulation and address data assimilation problems encountered during the production of ERA-40. These are mainly related to the representation of the hydrological cycle, the quality of the stratospheric circulation, and the consistency in time of reanalyzed geophysical fields. A second objective was to improve on various technical aspects of reanalysis such as data selection, quality control, bias correction, and performance monitoring, each of which can have a major impact on the quality of the reanalysis products.

The ERA-Interim reanalysis is produced with a sequential data assimilation scheme, advancing forward in time using 12-hourly analysis cycles. In each cycle, available observations are combined with prior information from a forecast model to estimate the evolving state of the global atmosphere and its underlying surface. This involves computing a variation analysis of the basic upper-atmospheric fields such as (temperature, wind, humidity, ozone and surface pressure), followed by separate analyses of near surface parameters (2 m temperature and 2 m humidity), soil moisture at root zone and soil temperature, snow, and ocean waves. The analyses are then used to initialize a short-range model forecast, which provides the prior state estimates needed for the next analysis cycle.

The ERA-Interim archive currently contains 6-hourly gridded estimates of three-dimensional (3D) meteorological variables, 3-hourly estimates of a large number of surface parameters and other two-dimensional (2D) fields, for all dates from 1 January 1979. The complete contents of this archive are described in Berrisford *et al.* (2009). The ERA-Interim reanalysis is produced with the ECMWF IFS, which incorporates a forecast model with three fully coupled components for the atmosphere, land surface, and ocean waves.

The dynamical core of the atmospheric model is based on a spectral representation for the basic dynamical variables, a hybrid sigma-pressure vertical coordinate, and a semi-Lagrangian semi-implicit time stepping scheme. The ERA-Interim configuration uses a 30 minute time step and has a spectral T255 horizontal resolution (compared to T159 for ERA-40), which corresponds to approximately 79 km spacing on a reduced gaussian grid (125 km for ERA-40). The vertical resolution is unchanged, using 60 model layers with the top of the atmosphere located at 0.1 Pa. Several modifications to the model physics were introduced with potentially significant impact on the representation of the hydrological cycle (Dee *et al.*, 2011). This data was used in this study to provide the initial and boundary conditions to run historical climate experiments (PRECIS and CORDEX regional climate models) for evaluation of the performance of the region climate models over the study area.

3.1.2 Regional Climate Model Outputs

The PRECIS Regional Climate Model (RCM) was used to simulate climate data for both the historical and future periods for analysis in this study. Historical climate simulations were used for model validation and also understand regional trends and patterns based on regional climate model outputs (1989 to 2008) over Uganda. Regional climate model outputs of rainfall, minimum and maximum temperatures and soil moisture at root zone were simulated through a number of PRECIS RCM experiments over Uganda. Other models outputs from HadGEM3-RA, the UKMO's newly developed RCM (Diallo *et al.*, 2014 and Moufouma-Okia and Jones, 2014) and a number of RCM outputs under the Africa CORDEX climate runs were also used to provide analysis data for the study. Hadgem3-RA is a relatively new RCM of the UKMO.

The experiments of the Hadgem3-RA follow a one way nesting described by Davies (2013). The performance of this RCM has been evaluated and the study observed that the RCM has capability in capturing some aspects of observed rainfall patterns over West Africa (Diallo *et al.*, 2014) and different sub regions of Africa (Moufouma-Okia and Jones, 2014). Model outputs of monthly rainfall were aggregated into seasonal rainfall that were required for evaluating of RCM performance on seasonal time scales over Uganda.

Future climate simulations were used for examining climate change projections (2001-2100) on seasonal time scales over Uganda. One set of climate change experiments was based on downscaling of ECHAM GCM outputs under the IPCC SRES A1B and A2 scenarios. The RCM output for future climate were simulated at a relatively high resolution of 0.5°. Other

climate projection data sets used include the high resolution (30 seconds or 1km) projections based on the HadGEM-ES model that are based on the new RCPs (RCP 2.6, RCP 4.5, RCP 6.0 and RCP 8.5) climate change scenarios. This high resolution climate projection data is available for the period 2041-2080 and provides averaged monthly climate projections of mean rainfall, minimum temperature and maximum temperature for different climate models (http://www.worldclim.org/cmip5_30s, Hijmans *et al.*, 2005).

3.2 Methods

The main objective of this study was to determine the extent of climate variability as well as change and their associated effects on the banana farming in Uganda. This was achieved through the determination of linkages between banana productivity and current climate variability; performance of the PRECIS RCM in simulating observed climate patterns; extent of future climate changes over Uganda, and the potential effects of future climate change on banana production over Uganda. This section provides brief highlights of the various methods that were used to address the specific objectives of the study. The method for data quality control including estimation of missing data and homogeneity test is however presented first.

3.2.1 Estimation of Missing Data and Homogeneity Test

The study observed that in many cases, long-term meteorological data series particularly in Uganda that span from years to decades have a number of gaps during periods when data was not recorded (Komutunga, 2006 and Sabiiti, 2008). Several data series also contain inconsistencies caused by change of observers, relocation of stations, changes in the vicinity of the stations (urbanization), changes in instruments and observation practices (Aguilar *et al.*, 2003).

Meaningful climate data analysis therefore requires investigation of the time series for missing data and any heterogeneity. Homogeneity test ensures that the variations in the data series are solely caused by variations in weather and climate (Conrad and Pollak, 1950 and Gitau, 2011) as opposed to other causes. Another important requirement for climatology analyses is the quality of the individual values. Observed climate data series should be free from errors and that missing values are estimated (Vicente-Serrano *et al.*, 2010).

This study has undertaken data homogeneity check to ascertain data quality before their use for analysis. Numerous techniques and methods have been developed and applied to approximate

the missing climate records and to detect and correct for artificial shifts in a data series (Reeves *et al.*, 2007; Venema *et al.*, 2012). The methods for estimating missing records include the correlation and regression, distance weighted (inverse distance and Shepard), Schafer method, Thiessen polygon and Krigging. These methods have been discussed and used in several previous studies (Ogallo, 1982; Basalirwa, 1991; Schafer, 1991; Lynch and Schulze, 1995 and Gitau, 2011).

Missing data in this study were estimated using the correlation and regression method. In this method, the station that was highly correlated with the one having missing climate data was initially identified. The regression equation was derived for the two stations for the period during which both stations have the data. The established regression was later used to estimate the missing records. The study observed that World Meteorological Organization (WMO) recommends that a climate dataset more than 10% missing records is not good for analysis. It is worthy to mention that less than 4% (rainfall) and 9% (minimum and maximum temperature) of the data was estimated for the study period. After filling in the missing data, the quality of the data was assessed before any analysis was undertaken.

The single and double mass curves analysis was used to test the consistency of the climate records at different stations. The double mass curve method involved the plotting of the accumulated seasonal climate records at a station to be corrected with that of the accumulated seasonal climate records of the nearby station whose records are homogeneous. For homogeneous records, the double mass curve should be a straight line. It was observed that in most cases, the quality of observations used in the study was good and gave straight lines for mass curves.

3.2.2 Establish the Linkages between Banana Productivity and Observed Climate Variability

Weather and climate have direct and indirect effects on all ecosystems including the banana crop. The climate parameters that would impact on banana crop growth and yields in different ways in Uganda include too much/little rainfall resulting into floods/droughts, hailstorms, very hot surface temperatures that is associated with heat waves and excessive evapotranspiration among other factors. Their effects on banana crop growth and yields depends on the stage of growth of the crop at the time of occurrence of climate extremes, as well as overall cumulative

effects depending on the duration and frequency of the extreme climate events within a given crop cycle.

Banana is a multi-cycle crop and has a life cycle of 15-18 months from planting to harvesting. Examining of climate effects on banana yields would therefore require climate and banana data for a series of banana cycles in different locations. Field experimental studies have already demonstrated some observed linkages between banana growth and variations in temperature (direct effects) shown in Table 3.3 while Table 3.4 shows evapotranspiration (rainfall) thresholds for the banana crop at different growth stages. The banana crop parameters and processes that directly respond to temperature changes include leaf chlorophyll, dry matter assimilation, leaf area size, leaf expansion rate (LER), net assimilation rate (NAR) and closing or opening of the stomata.

Van Asten *et al.* (2005) also observed that the growth and productivity of bananas over Uganda is also affected by other factors such as soil fertility, pests and diseases, crop management among other factors which were not considered in this study. Indirect effects of temperature on banana production and growth patterns may be linked to the increase in banana pests and diseases out breaks and infestation as temperature increases.

Table 3.3: Effects of temperature thresholds on banana growth patterns (Samson, 1980 and German *et al.*, 2015)

Temperature Range (°C)	Critical level (°C)	Effect of Temperature
0-5	0	Frost damage, leaves die. Avoid planting bananas.
5-10	6	Leaf chlorophyll destruction. Leaves turn yellow depending on temperature drop below 6 °C and duration
10-15	14	Minimum mean temperature for growth (dry matter assimilation)
15-20	16	Minimum mean temperature for development (leaf area increases and LER)
20-25	22	Optimum mean temperature for NAR but LER reduced. Optimum for flower initiation
25-30	27	Over all optimum for productivity (optimum balance between NAR and LER)
30-35	31	Optimal mean temperature for LER but NAR reduced. Stomata open (no heat stress)
35-40	36	Physiological heat stress possible in afternoon
35-40	38	Growth stops, heat stress occurs. Stomata close (wilt)
40-45	40	Leaf temperature could approach thermal danger point
45-50	47	Thermal danger point for leaf temperature. Dries out in patches and burns avoid planting bananas

This objective of the study employed existing thresholds of temperature (Table 3.3) and rainfall (evapotranspiration, Table 3.4) for banana growth patterns based on previous field experimental studies (Samson, 1980). The frequency and extent to which these thresholds are being exceeded in the current climate records were analysed to provide an indication of climate risk to banana production in Uganda.

Table 3.4: Reference evapotranspiration (ET_o-FAO Penman-Monteith method), crop evapotranspiration (ET_c) and daily banana water consumption (WC) thresholds for banana growth (Samson, 1980)

Growing Season (days after planting-dap)	Days	ET_o(PM-FAO) (mm)	ET_c (mm)	WC (mm)
Planting to end of first harvest	434	1816	1698	3.9
End of first harvest to end of second harvest	213	827	861	4.0
End of second harvest to end of third harvest	317	1307	948	3.0

The first objective sought to determine the nature the linkages between changes in banana yields and climate variability and change over the western and central regions of Uganda. Observed monthly climate data were available in most banana growing areas while there was only annual banana yields data for these regions. This made it very difficult to quantify direct and indirect linkages amongst the changes in the past and present banana yields with past and current climate extremes on shorter intra annual timescales like monthly and seasonal ones. Examination of such linkages requires among others field experimental data.

Van Asten *et al.* (2011) conducted field experiments and analyzed the effect of drought on banana yields in three locations of Uganda including Kawanda, Mbarara and Ntungamo based on monthly time scales. The scope of this study was limited to the analysis of historical observations to determine the linkages between variations in banana yields and observed variations in surface temperature and rainfall patterns. This part of the study, therefore, focused on investigating the inter-annual patterns of both climate parameters and banana yields over the two highest banana producing regions of Uganda.

Climate and banana yields data on annual time scales were all standardized to enable desired comparisons to be made. Several studies by Ogallo and Nasib (1984), Ininda (1995), Kabanda and Jury (1999), Sabiiti (2008), Omondi (2010) and Otieno *et al.* (2014) have used

standardized indices of variables to investigate relationships and linkages. The standardized indices (Z) for the individual variables x_i s were expressed obtained using Equation 3.1a as;

$$Z = \frac{x_i - \bar{x}}{\sigma_x} \quad (3.1a)$$

In Equation (3.1a), x_i is the i^{th} observation of any given variable and n is number of observations.

The study also employed the Standardized Precipitation Index (SPI) based on rainfall anomalies to characterize extremely dry, normal and extremely wet events over different regions of Uganda. Details of the construction and application of the SPI are discussed in Kumar *et al.* (2009) and WMO (2012).

3.2.2.1 Empirical Methods based on Changes in the Mean, Variance, Skewness and Kurtosis Coefficients

In order to compare linkages between inter annual climate and banana production changes in this study, empirical approaches have been adopted. The empirical approaches examine and compare changes in the year to year variability of banana productivity and climate anomalies. Empirical parameters were derived from the first, second, third, and fourth moments of the specific time series represented by the mean, variance, skewness (extremes distributions), and kurtosis (shape or peakedness) respectively. For the first moment, the inter-annual trends of the individual banana yields and climate time series were examined. Parameters examined under the second moment also included recurrences of large positive/ negative climate extremes.

The first moment of a time series is represented using the mean (\bar{x}) of a variable which is the averaged of all observations with respect to time.

$$\bar{x} = \frac{1}{n} \sum_{i=1}^n x_i \quad (3.1b)$$

Under this method, the study period was sub divided into two parts; 1971-1990 and 1991-2009. Means for standardized data were then computed and compared for climate and banana yield data. This method was also used to assess the spatial patterns of seasonal climatology of rainfall during March to May, June to August and October to December for the past and

current periods over Uganda. Analysis of variations in climate patterns, however, considered a longer period (1931-2013) to provide a broader understanding of observed climate variability and change over Uganda.

Another method adopted in this study focused on trend analysis based on analysis of the interannual patterns of the first moment (mean). Trend analysis involved investigating of smoothed and unsmoothed standardized banana, rainfall and temperature anomalies. A regression is then fitted to these time series and statistical significance of regression coefficients examined. The autoregression is expressed as;

$$x_t = a_o + b x_{t-1} + \mathcal{E}_t \quad (3.2a)$$

In auto regressive Equation (3.2a), a_o and b are the intercept and slope respectively, x_t and x_{t-1} is the value of the variable at time t and $t-1$ respectively. The term \mathcal{E}_t represents the white noise. Trend of the time series is significant if the slope b is significant.

A test of the adequacy of the model is done by computing R^2 (the multiple coefficient of determination) given by $R^2 = 1 - \frac{SSE}{\sum_{i=1}^n (Y - \bar{Y})^2}$ (3.2b)

Trend detection was further conducted using the **non-parametric Mann-Kendall (MK)** test that takes care of all the distribution of the data set. Past regional studies by Kampata *et al.* (2008); Kizza *et al.* (2009); Longobardi and Villani (2010); Ngongondo *et al.* (2011); Nsubuga *et al.* (2011) and Ngaina and Mutai (2013) have used the non-parametric Mann-Kendall statistical test to characterize trends in climate records. This non-parametric test was used for detecting trends in observed climate time series for stations in Uganda. The Mann-Kendall test is described in the subsequent section.

The Mann-Kendall statistic S for any time series is given as;

$$S = \sum_{i=1}^{n-1} \sum_{j=i+1}^n \text{sgn}(x_j - x_i) \quad (3.3a)$$

The application of trend test is done to a time series x_i that is ranked from $i = 1, 2, \dots, n - 1$ and x_j , which is ranked from $j = i + 1, 2, \dots, n$. Each data point x_i is taken as a reference point which is compared with the rest of the data points x_j so that,

$$\text{Sgn}(x_j - x_i) = \begin{cases} +1, (x_j - x_i) > 0 \\ 0, (x_j - x_i) = 0 \\ -1, (x_j - x_i) < 0 \end{cases} \quad (3.3b)$$

When $n \geq 8$, the statistic is approximately normally distributed with the mean given by $E(S) = 0$

The variance statistic is given as

$$\text{Var}(S) = \frac{n(n-1)(2n+5) - \sum_{i=1}^m t_i(i-1)(2i+5)}{18} \quad (3.3c)$$

In Equation (3.3c), t_i is considered as the number of ties up to sample i .

$$\text{The test statistic } Z_c \text{ is computed as } Z_c = \begin{cases} \frac{S-1}{\sqrt{\text{Var}(S)}}, S > 0 \\ 0, S = 0 \\ \frac{S+1}{\sqrt{\text{Var}(S)}}, S < 0 \end{cases} \quad (3.3d)$$

Z_c in Equation (3.3d) follows a standard normal distribution. A positive (negative) value of Z signifies an upward (downward) trend. A significance level α is also utilized for testing either an upward or downward monotonic trend (a two tailed test). If Z_c appears greater than $Z_{\alpha/2}$ where α depicts the significance level, then the trend is considered as significant.

The second moment of a time series is represented by the variance or its square root which is the standard deviation. The variability was computed using the square root of variance (standard deviation) given as σ_x ;

$$\sigma_x = \sqrt{\frac{1}{n} \sum_1^n (x_i - \bar{x})^2} \quad (3.4)$$

The first empirical approach adopted for the second moment involved examining change in standard deviation of climate records as well as banana yields for two common sub periods namely 1971-1990 and 1991-2009.

In addition, spatial patterns and long-term rainfall change in both the mean (first moment) and variability (second moment) has been examined using the Climate Research Unit (CRU) data from 1931-2013. The data was divided into three time periods namely 1931-1960, 1961-1990 and 1991-2013. The changes in the spatial patterns of rainfall have been computed based on

the difference in the moments for the current period 1991-2013 and two historical periods (1931-1960 and 1961-1990). The analysis has used the rainfall rate (mm/day) in all the considerations and comparisons for the different seasons.

Examining the changes in **the 3rd moment** also involved computing skewness coefficients α_3 that is presented in Equation 3.5. The Karl Pearson measure of skewness coefficient deobserved α_3 can be expressed as;

$$\alpha_3 = \frac{\frac{1}{n} \sum_{i=1}^n (x_i - \bar{x})^3}{\left[\sum_{i=1}^n (x_i - \bar{x})^2 \right]^{\frac{3}{2}}} \quad (3.5)$$

Under the same principle, the **4th moment** represented by **Kurtosis (K)** was also computed for the two sub periods. K may be expressed as given by Equation 3.6;

$$K = \frac{\sum_{i=1}^n (x_i - \bar{x})^4}{(n-1)\sigma^4} \quad (3.6)$$

In Equations (3.4) to (3.6), x_i is the i^{th} observation of any given variable and n is number of observations.

Note that Kurtosis coefficient is expressed as K-3 (deviation of 3 from Kurtosis) and has been used in the computations of this study. If $K > 3$, the Kurtosis coefficient is positive (leptokurtic) implying concentration of data around the mean, if $K = 3$, Kurtosis coefficient is zero (mesokurtic) and $K < 3$ implies that Kurtosis coefficient is negative (platykurtic) and the spread of data away from the mean.

The usefulness of the moments of time series in data analysis and comparing different series has been demonstrated graphically in the IPCC (2012) on determining changes in extremes and changes in symmetry in climate variables (Figure 3.2). This approach was employed in this part of the study.

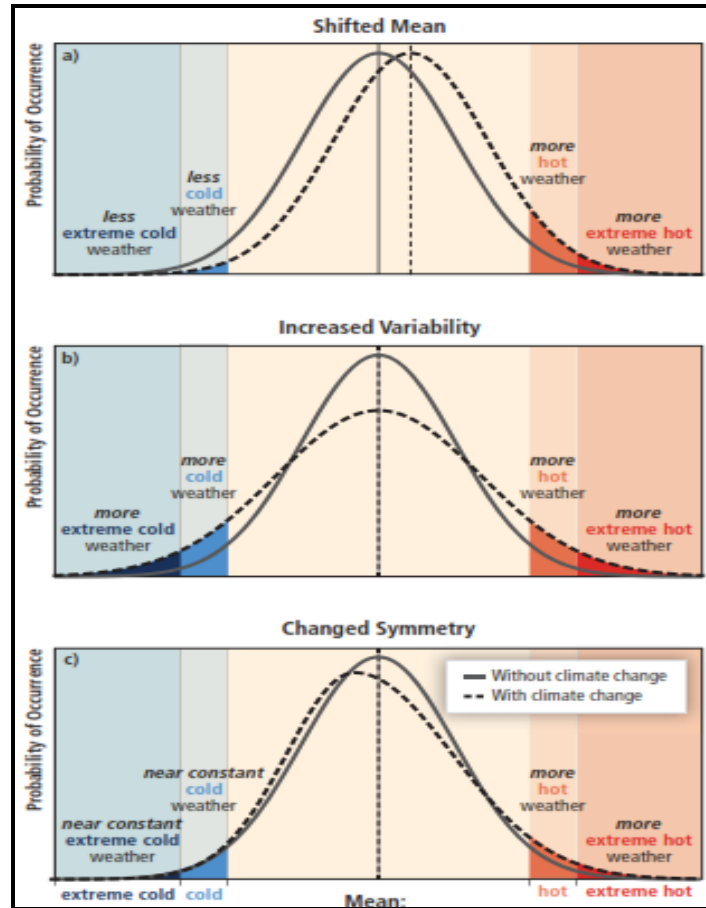


Figure 3.2: Comparison of changes in a timeseries based on (a) mean, (b) variability and (c) symmetry (IPCC, 2012).

3.2.2.2 Correlation and Regression Analyses

Other methods used to further examine the existing linkages between banana yields and climate variability included correlation and regression. Brief details of these methods are provided below.

Under correlation analysis, Pearson's product-moment correlation coefficient (ρ_{XY}) was used as a measure of the degree of agreement between variables. The correlation coefficients were computed (Equations 3.6) between standardized climate variables (X) and banana yields (Y) and the values were tested for significance (Equation 3.7).

$$\text{The correlation coefficient, } \rho_{XY} = \frac{\text{cov}(X, Y)}{\sigma_X \sigma_Y} \quad (3.6)$$

$$-1 \leq \rho_{XY} \leq 1$$

The significance of the correlation coefficients was tested using the statistical t-test. The test statistic t is given by the expression:

$$t_{n-2} = \rho_{XY} \sqrt{\frac{n-2}{1-\rho_{XY}^2}}$$

$$= \sqrt{\frac{\rho_{XY}^2(n-2)}{1-\rho_{XY}^2}} \quad (3.7)$$

In Equation (3.7), n is number of observations.

Under correlation method, it was assumed that cumulative annual climate stress has significant effects on annual banana yields and allows correlating annual climate and banana yield. The method of correlation analysis has been used by many authors, for example, Shukla and Paolino (1983); Ininda (1994); Sabiiti (2008); Omondi (2010) and Otieno *et al.* (2014) to investigate relationships between variables.

Regression analysis was undertaken for cases where correlation coefficients were significant. The study fitted a degree 2 polynomial regression model between banana yields and climate variables (rainfall, minimum temperature and maximum temperature). The choice of the degree 2 polynomial was based on the fact that it is desirable to determine the threshold values of the climatic (independent) variables that would give optimal banana yield (dependent) levels under different/contrasting non-climatic factors. The degree 2 polynomial regression equation is given as;

$$Y_i = a_o + \sum_{i=1}^2 b_i x_i^i + e_i \quad (3.8)$$

In Equation (3.8), Y_i represents the dependent variable, a_o and b_i are the intercept and slope of the regression equation respectively and X_i s are the independent climate variables.

The variance of the error term e_i , in this case is $S^2 = \frac{SSE}{n-(k+1)}$ (3.9)

A test of the adequacy of the model is done by computing R^2 (the multiple coefficient of determination) given by $R^2 = 1 - \frac{SSE}{\sum_{i=1}^n (Y - \bar{Y})^2}$ (3.10)

For $R^2 = 0$, it implies lack of fit, while $R^2 = 1$ implies perfect fit. The adjusted R^2 has been recommended as a better measure of variance explained and has been used in interpretation of results. The F-test based on the Analysis of Variance (ANOVA) was used to test for the significance of the coefficients of the polynomial regressions. This approach adopted is based on the banana growth-temperature curve (Figure 3.3).

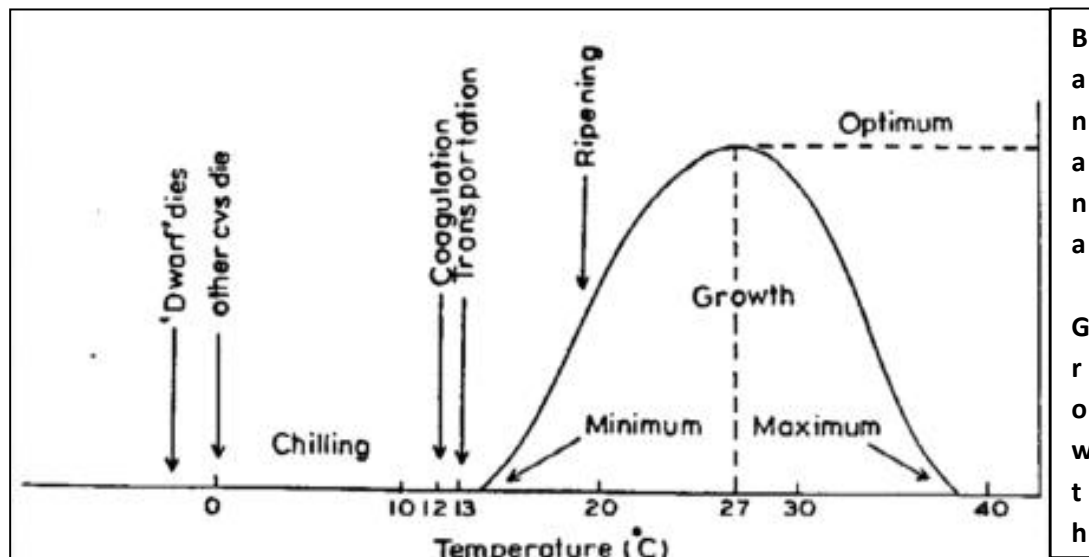


Figure 3.3: Schematic representation of banana growth-temperature relationship. Source (Sastry, 1988).

In addition, to understand the combined effect of climate variables on banana yields, the multiple linear regression was fitted between banana yields and climate variables. The climate variables used as independent variables in the regression model included; total annual rainfall, rainfall of the driest quarter, average annual temperature, and temperature of the coldest quarter.

The values of the regression coefficients represent the change in the yield (in standard deviations) associated with a change of one standard deviation in a particular climatic variable holding the values on the other independent variable constant. The value of R^2 (coefficient of determination) was used to account for the variance in yields explained by climate variability. The value $(1-R^2)$ accounted for the variance in yields explained by other non-climatic factors. The relationships and climatic variables developed in this part of the study were further used to map future banana suitability patterns for different climate change scenarios over Uganda.

3.2.2.3 FAO Crop Water Assessment Tool

Apart from using the empirical methods to compare linkages between interannual changes in climate and banana yields, the FAO Crop Water Assessment Tool (FAO-CROPWAT, Smith, 1992 and Clarke *et al.*, 2001) was also used to evaluate the current water stress (moisture deficits) and yield losses resulting from observed rainfall variability over different parts of Uganda. Based on the FAO CROPWAT, the study used the FAO Penman-Montieth method to calculate reference evapotranspiration (ET_o), banana crop water requirement (ET_m), moisture deficit at harvest (MDH) and yield losses (reductions) for various locations.

Assessment of the impact on yield of various levels of water supply could then be simulated by setting the dates and the application depths of water from rainfall or irrigation. Since banana production in Uganda is predominantly rain-fed, the CROPWAT model was run under rain-fed conditions (Clarke *et al.*, 2001). Using the soil moisture content at root zone and evapotranspiration rates, the model determined soil water balance on daily basis (Smith, 1992; Clarke *et al.*, 2001; FAO, 2003b and Karanja, 2006). The output tables were then used for the assessment of the resultant effects of water constraint on yield reductions and efficiencies in water supply for two banana crop cycles across the Country. This method was also used by Karanja (2006) to analyse crop water use in six districts of Kenya.

3.2.3 Determination of the Performance of PRECIS RCM in Simulating Observed Climate Patterns

The second objective was undertaken to determine the best regional climate model (or group of models) that would provide a more realistic simulation of observed climate patterns over Uganda. The different aspects considered included model dynamics (the formulation and solution of the model equations) and model physics (parameterization schemes, spatial resolution and domain size). The performance of different regional climate models with emphasis on the UKMO PRECIS regional climate system (Simon *et al.*, 2012) in simulating observed spatial and temporal rainfall patterns under different aspects outlined above has therefore being evaluated.

3.2.3.1 Climatological Regional Climate Model Evaluation Experiments

Regional climate experiments spanning a period 1989 to 2008 were set up and run using PRECIS RCM system. The experiments were forced (constrained at their boundaries) using

European Centre for Medium Range Weather Forecasting (ECMWF); the ERA-Interim data set (Dee *et al.*, 2011) to provide the initial conditions for model integration. For boundary forcing, sea ice and Reynolds SSTs were used. The integration of the RCM was performed over the Eastern Africa domain (Figure 3.4) for the period 1989 to 2008. This period was based on the availability and the length of the driving data at the time of running the experiments. As observed earlier, the study acknowledged the existence of a longer and updated ERA-Interim dataset (1979 to present). The characteristics of experiments used and other climate model outputs are shown in Table 3.5.

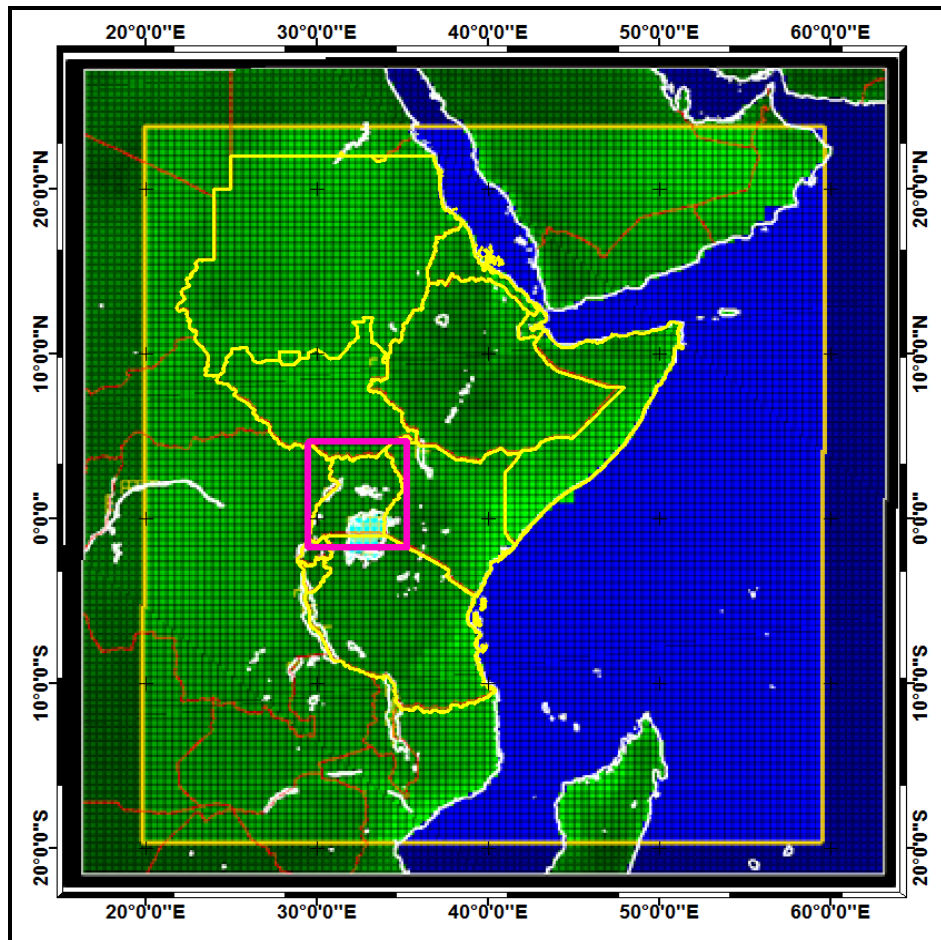


Figure 3.4: PRECIS RCM optimal domain for the Eastern Africa region

3.2.3.1.1 Climate Model Experimental Design

In this part of the study, climate experiments were designed for historical and current climate simulation over the study region. The design of the experiments was based on a number of factors including the physical formulation of the model, the spatial resolution, size of model domain and parametrization schemes. The characteristics of different experimental designs are shown in the Tables 3.5 and 3.6.

Table 3.5: Characteristics of Regional Climate Models used in the study

RCM		Institution	Horizontal Resolution	Parametrization Scheme	Period	Model Domain
1.	PRECISM1	UKMO	0.44°	MOSES1	1991-2008	CORDEX Africa
2.	PRECISM2	UKMO	0.44°	MOSES2	1991-2008	CORDEX Africa
3.	PRECISM2E A	UKMO	0.44°	MOSES2	1991-2008	Eastern Africa
4.	HadGEM3Ra 50	UKMO	0.44°	JULES	1991-2008	CORDEX Africa
5.	HadGEM3Ra 25	UKMO	0.22°	JULES	1991-2008	CORDEX Africa
CORDEX Models						
6.	CCLM	PIK	0.44°		1991-2008	CORDEX Africa
7.	RegCM3	ICTP, Italy	0.44°		1991-2008	CORDEX Africa
8.	WRF	UC, Spain	0.44°		1991-2008	CORDEX Africa
9.	MPIREMO	MPI, Germany	0.44°		1991-2008	CORDEX Africa

The two parametrization schemes available in PRECIS RCM (MOSES1 and MOSES2.2, Table 3.6) have been used to run PRECIS experiments at a resolution of 50 km x 50 km. This set of experiments aided the comparison in model performance between the two parametrization schemes.

Other regional climate model outputs used include the rainfall simulations from the HadGEM3-RA (Davies, 2013; Diallo *et al.*, 2014 and Moufouma-Okia and Jones, 2014), which is the new regional version of the Hadley Centre Global Environment Model version 3. This model was run at two resolutions (50 km x 50 km and 25 km x 25 km). The experiments enabled the study to evaluate the improvement in model performance over Uganda that would result from increasing (doubling) the model spatial resolution. The performance of selected CORDEX RCMs including; COSMO Climate Local Model (CCLM), the International Centre for Theoretical Physics (ICTP), Regional Climate Model version 3 (RegCM3), and Weather Research and Forecasting (WRF) shown in Table 3.5 have also been determined to provide a wide range of different model configurations and inter-model comparison.

Table 3.6: Main features considered in MOSES 1 and MOSES 2.2

Main features EATURES	MOSES 1	MOSES 2.2
Land surface representation	Grid homogeneity (Smith <i>et al.</i> , 2006)	Grid heterogeneity (tiled / mosaic schemes) (Smith <i>et al.</i> , 2006)
Land cover types	Advanced Very High Resolution Radiometer (AVHRR) 1km resolution land cover not applied	Nine (9); Five vegetative and four non-vegetative. Can also use 14 land cover types from AVHRR (Best, 2005)
Earth-Atmosphere Fluxes	Water, heat and carbon dioxide (Cox <i>et al.</i> , 1999)	Water, heat and carbon dioxide (Best, 2005; Essery <i>et al.</i> , 2003 and Smith <i>et al.</i> , 2006)
Moisture sources	Evaporation from canopy and bare soil, transpiration and sublimation of snow (Cox <i>et al.</i> , 1999)	Snow, canopy, soil, saturated places e.g. lake, calculate as potential evaporation (Essery <i>et al.</i> , 2003)
Surface energy balance	No difference between temperatures of different surface/hydrological regimes in the grid box (Cox <i>et al.</i> , 1999)	Surface enegery calculated explicitly for each unique sub-grid (Essery <i>et al.</i> , 2003)
Parameter for calculation of surface energy budget	Net radiation (Best, 2005)	Net shortwave radiation on tiles (Best, 2005)
Albedo	Four band single albedo for each grid box (Essery <i>et al.</i> , 2003)	Multiple albedos based on visible and near infrared for each tile (Essery <i>et al.</i> , 2003)
Soil depth	Four soil layers at 0.1, 0.25, 0.65 and 2.0 m, to a 3 m depth (Cox <i>et al.</i> , 1999)	Four soil layers at 0.1, 0.25, 0.65 and 2.0 m, to a 3 m depth (Essery <i>et al.</i> , 2003)
Soil numeric	Explicit solutions of sub-soil temperature and moisture (Cox <i>et al.</i> , 1999)	Implicit solutions of sub-soil temperature and moisture (Essery <i>et al.</i> , 2003). Calculations are accurate and stable at longer time-steps; and higher vertical resolutions
Super saturation of soil	Excess moisture drained downwards (Essery <i>et al.</i> , 2003)	Excess moisture removed by lateral flow hence fast run-off (Essery <i>et al.</i> , 2003)
Soil thermodynamics (Subsurface temperatures)	Thermal features represented by water phase changes-latent heat (Cox <i>et al.</i> , 1999) Hence soil temperature is a function of the moisture (liquid water and ice) content	Thermal features represented by water phase changes-latent heat (Best, 2005) Hence soil temperature is a function of the moisture (liquid water and ice) content

For any successful climate model experiment, the choice of the domain size, choice of Lateral Boundary Conditions (LBCs) and grid resolution are important aspects of dynamical downscaling (Xue *et al.*, 2007). The details of the extent and domain size together with the formulation of the PRECIS RCM system have been discussed in previous studies (Sabiiti, 2008; Davis *et al.*, 2009 and Omondi, 2010).

The spatial patterns of the outputs of regional models were validated against gridded observed rainfall data of CRU, UDel, GPCP and ERA-Interim. The comparison of the time evolution of patterns in climate model outputs and observations has however been restricted to CRU data set as it has been widely used over the region. The validation exercise considered a time span of 1991 to 2008. The study analysis focused mainly on testing the ability of different regional climate models in reproducing the observed rainfall climatology including observed rainfall spatial patterns (mean and variability), annual cycles for different sub-regions and inter-annual rainfall patterns on seasonal time scales. Different measures of agreement between observations and model outputs used include; Pearson moment correlation coefficient, Root Mean Square Error (RMSE) and the Refined Willmott Index (Willmott *et al.*, 2012). Brief details of these measures of agreement are described in the following sections.

3.2.3.2 Correlation Analysis

The Pearson's product-moment **correlation coefficient** was used to determine the correlation coefficients between the model-predicted (P) and observed (O) rainfall data. These correlation coefficients aided comparison of observed data and model outputs to determine the strength of the relationship between model rainfall outputs and observed rainfall on seasonal timescales over Uganda.

The Pearson's product-moment correlation coefficient (ρ_{PO}) was computed as follows;

$$\rho_{PO} = \frac{\text{cov}(P, O)}{\sigma_P \sigma_O} \quad (3.11)$$

$$-1 \leq \rho_{PO} \leq 1$$

The significance of the correlation coefficients was tested using the statistical t-test. The test statistic t is given by the expression:

$$t_{n-2} = \rho_{PO} \sqrt{\frac{n-2}{1-\rho_{PO}^2}}$$

$$= \sqrt{\frac{\rho_{PO}^2 (n-2)}{1 - \rho_{PO}^2}} \quad (3.12)$$

In Equation (3.12), n is number of observations and ρ_{PO} is the value of the coefficient.

The correlation technique is however limited as it does not give the magnitude of the error in model outputs. Therefore, the study employed the error analysis method to understand the systematic errors in the model rainfall against observations.

3.2.3.3 Error Analysis

The Root Mean Square Error (RMSE) was used to quantify the errors between the model outputs and observations. Errors were computed from Equation (3.13).

$$\text{Root Mean Square Error (RMSE)} = \left[\frac{1}{n} \sum_{i=1}^n (P_i - O_i)^2 \right]^{\frac{1}{2}} \quad (3.13)$$

Where P_i and O_i are the model simulated and observed values respectively.

3.2.3.4 Refined Willmott Index

The Refined Willmott Index (RWI) (Willmott *et al.*, 2012) was used as a measure of model performance. The index represents the sum of the magnitudes of the differences between the model-predicted (P) and observed (O) deviations about the observed mean relative to the sum of the magnitudes of the perfect-model ($P_i = O_i$, for all i) and observed deviations about the observed mean.

The index is denoted by d_r and expressed as follows;

$$d_r = \begin{cases} 1 - \frac{\sum_{i=1}^n |P_i - O_i|}{2 \sum_{i=1}^n |O_i - \bar{O}|}, & \text{when } \sum_{i=1}^n |P_i - O_i| \leq 2 \sum_{i=1}^n |O_i - \bar{O}| \\ \frac{2 \sum_{i=1}^n |O_i - \bar{O}|}{\sum_{i=1}^n |P_i - O_i|} - 1, & \text{when } \sum_{i=1}^n |P_i - O_i| > 2 \sum_{i=1}^n |O_i - \bar{O}| \end{cases} \quad (3.14)$$

With $-1 \leq d_r \leq 1$

In Equation (3.14), when $d_r = 0.5$, the sum of the error-magnitudes is one half of the sum of the perfect-model-deviation and observed-deviation magnitudes. When $d_r = 0$, it signifies that the sum of the magnitudes of the errors and the sum of the perfect-model-deviation and observed-deviation magnitudes are equivalent. When $d_r = -0.5$, the sum of the error-magnitudes is twice the sum of the perfect-model-deviation and observed-deviation magnitudes. Values of $d_r = -1$ can mean that the model-estimated deviations about O are poor estimates of the observed deviations; but, can also imply that there is simply little observed variability. $d_r = 1$, indicated a perfect model.

3.2.3.5 Inter-model Performance Comparison

In this study, inter-model performance comparison was based on Taylor diagrams (Figure 3.5) to provide a more concise statistical summary of how well patterns under consideration match each other (Taylor, 2012). The Taylor diagram compares model performance in terms of their correlation coefficients, mean square difference and standard deviations. This approach also helps to track changes in performance of a model (Taylor, 2012) across seasons and sub regions. The statistical significance of relative differences and the degree to which observational errors and inherent variability in a model limits the expected agreement between model-simulated and observed behaviors can also be evaluated in the Taylor diagram (Taylor, 2012). The position of each letter appearing on the plot quantifies how closely the model simulations are with the observations. In this study, Taylor diagrams were used to characterize the statistical relationship between observed and model rainfall outputs on seasonal timescales. The diagrams were also employed to aid in model performance inter-comparison (variations in model performance in relation to changing model dynamics and physics). Figure 3.5 shows an example of a Taylor diagram summarizing mean square difference, standard deviation and correlation coefficients. The mean square difference (E), standard deviation (σ), and correlation coefficient (ρ_{po}) are related through the Equation 3.15.

$$E^2 = \sigma_p^2 + \sigma_o^2 - 2\sigma_p\sigma_o\rho_{po} \quad (3.15)$$

In Equation 3.15, E is the mean square difference, σ_p is the standard deviation for model simulated and σ_o is the standard deviation for observed value and ρ_{po} is the correlation between predicted and observed values. This method has also been used by Endris *et al.* (2013) and Moufouma-Okia and Jones (2014) to evaluate the performance of regional climate models for sub regions over Africa.

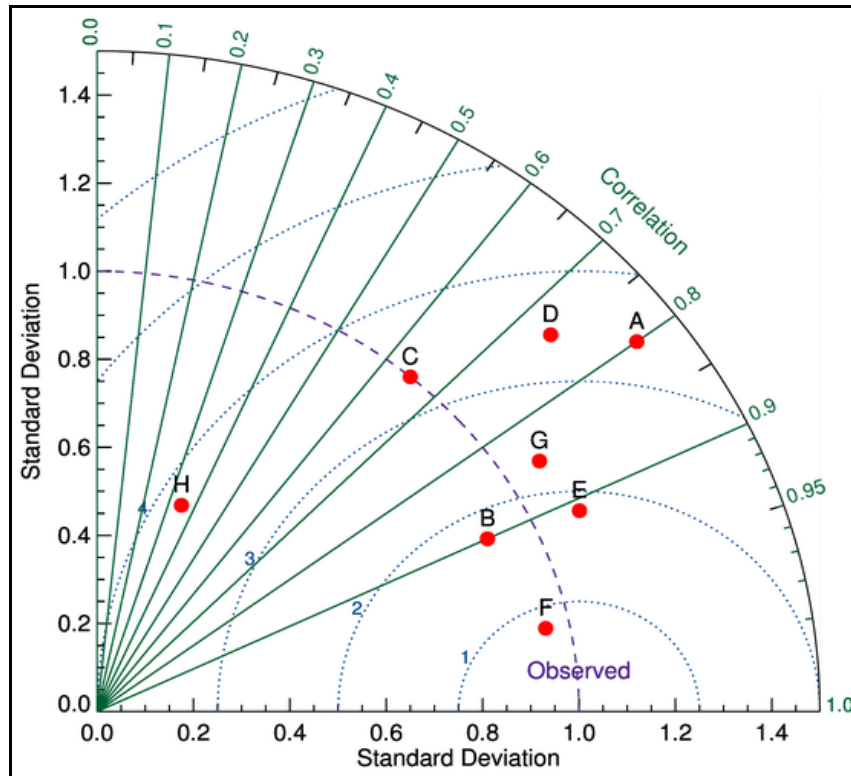


Figure 3.5: Schematic representation of Taylor diagram. Source (Taylor 2012).

3.2.3.6 Principal Component Analysis

The Empirical Orthogonal Functions (EOFs) based on the Principal Component Analysis (PCA) were also used to characterize the spatial and temporal patterns of the dominant modes of seasonal rainfall variability over Uganda. The PCA begins with an adjusted data matrix, X , which consists of n observations (rows) on p variables (columns). The adjustment is made by subtracting the variable's mean from each value. This adjustment is made since PCA deals with the covariances among the original variables. The new variables are constructed as weighted averages of the original variables. These new variables are called the factors (latent variables or principal components). Their specific values on a specific row are referred to as the factor scores (the component scores, or the scores).

The matrix of scores Y , is given by the basic equation of PCA in matrix notation as:

$$Y = W' X \quad (3.16)$$

In computational terms the principal components are found by calculating the eigenvectors and eigenvalues of the data covariance matrix. This equation may be thought of as a set of p linear equations that form the factors out of the original variables. Thus;

$$y_{ij} = w_{1i} x_{1j} + w_{2i} x_{2j} + \dots + w_{pi} x_{pj} \quad (3.17)$$

The weights, W , are constructed so that the variance of y_1 , $Var(y_1)$, is maximized. Also, so that $Var(y_2)$ is maximized and that the correlation between y_1 and y_2 is zero. The remaining y_i 's are calculated so that their variances are maximized, subject to the constraint that the covariance between y_i and y_j , for all i and j (i not equal to j), is zero.

The matrix of weights, W , is calculated from the variance-covariance matrix, S . This matrix is calculated using the formula;

$$s_{ij} = \frac{\sum_{k=1}^n (x_{ik} - \bar{x}_i)(x_{jk} - \bar{x}_j)}{n-1} \quad (3.18)$$

The singular value decomposition of S provides the solution to the PCA problem. This may be defined as;

$$U' S U = L \quad (3.19)$$

In Equation (3.19), L is the diagonal matrix of eigenvalues of S .

W is calculated from L and U as follows;

$$W = U L^{-\frac{1}{2}} \quad (3.20)$$

In Equation (3.20), W is simply the eigenvector matrix U , scaled so that the variance of each factor, y_i , is one. The correlation between the i^{th} factor and the j^{th} original variable may be computed using the formula;

$$r_{ij} = \frac{u_{ji} \sqrt{l_i}}{s_{jj}} \quad (3.21)$$

In Equation (3.21), u_{ji} is an element of U , l_i is a diagonal element of L , and s_{jj} is a diagonal element of S . The correlations are called the factor loadings. When the correlation matrix, R , is used instead of the covariance matrix, S , the Equation for Y must be modified. The new Equation is:

$$Y = W' D^{-\frac{1}{2}} X \quad (3.22)$$

In Equation (3.22), D is a diagonal matrix made up of the diagonal elements of S . In this case, the correlation formula may be simplified since s_{jj} are equal to one.

Several studies have discussed criteria for determining and dropping factors in PCA. Kaiser (1960) proposed dropping factors whose eigenvalues are less than one, since these provide less information than is provided by a single variable. The study suggests use of a cut off on the eigenvalues of 0.7 when correlation matrices are analyzed. Other studies observed that if the largest eigenvalue is close to one, then holding to a cutoff of one may cause useful factors to be dropped. However, if the largest factors are several times larger than one, then those near one may be reasonably dropped. PCA has been used in several studies (Ogallo, 1980; Ouma, 2000; Okoola and Camberlin, 2003; Schreck and Semazzi 2004; Komutunga, 2006 and Omondi, 2010) to investigate dominant modes of variability and relationships among variables particularly rainfall. The study approach is one similar to a previous study by Schreck and Semazzi (2004) that investigated the modes of rainfall variability in East Africa. This method has been used to understand the dominant modes of rainfall variability in both models and observed seasonal rainfall over Uganda.

3.2.4 Establish the Extent of Expected Future Climate Change over Uganda

The third objective assessed the downscaled future climate change projections over Uganda based on IPCC SRES scenarios (A1B and A2) (Morita and Robinson, 2001) and RCP 4.5 and RCP 8.5 (Moss *et al.*, 2010). The PRECIS regional climate system was used to downscale coarse resolution climate projections (SRES A1B and A2) produced by the European Centre Hamberg Model (ECHAM) over the GHA region (RCM domain shown in Figure 3.4). The new RCP climate scenarios (RCP 4.5 and RCP 8.5) were run under the CORDEX projections using the Africa-CORDEX domain have also been analysed. The detailed description of climate scenarios used is already given in Tables 2.3 and 2.4. Further analysis in this part of the study investigated changes in four bioclimatic variables (extreme climate analysis) for a full range of RCPs (RCP 2.6, RCP 4.5, RCP 6.0 and RCP 8.5) over Uganda. The bioclimatic

variables included spatial patterns in annual rainfall, rainfall of the driest quarter, annual temperature and temperature of the coldest quarter. A brief description of the methods used to generate climate change projections is however presented first.

3.2.4.1 Regional Climate Model Experiments for Climate Projections

In this part of the study, regional climate change experiments over Eastern Africa domain (Omondi, 2010), also Figure 3.4 were run to provide downscaled future climate projections for two SRES A1B and A2 scenarios over the region. In these experiments, PRECIS RCM system was used to downscale coarse climate projections of ECHAM GCM (Roeckner *et al.*, 1996; Roeckner *et al.*, 2003 and Roeckner *et al.*, 2006) for two IPCC SRES A1B and A2 scenarios. These experimental runs spanned the period 2001 to 2100. These experiments aimed at providing fairly high resolution (50 km x 50 km) future climate change information particularly for Uganda on current and future patterns of rainfall, surface temperature and soil moisture content at root zone among other parameters. This information was further used to assess the effects of future climate change under two climate change scenarios on the future production of bananas over Uganda.

The study also used climate change projections based on the new IPCC RCPs (van Vuuren *et al.*, 2011 and IPCC, 2014). Climate data from the downscaled CMIP5 climate projections under CORDEX Africa (Giorgi *et al.*, 2009, Jones *et al.*, 2011 and Hewitson *et al.*, 2012) experiments over Africa have also been used in this study to investigate climate projections over Uganda for the four new policy based climate scenarios. The new scenarios include; RCP 2.6, RCP 4.5, RCP 6.0, and RCP 8.5. Suitable very high resolution climate projection data (Hijmans *et al.*, 2005) was obtained on bioclimatic variables (www.worldclim.org) for mapping banana production suitability. Future climate projections across both the RCPs and SRES scenarios have therefore been assessed over Uganda in this study.

This part of the study employed time series analysis (Box *et al.*, 1994), trend analysis and graphical method to characterize climate change in both space and time. The 30 year seasonal rainfall composites (Equation 3.1b) have been analysed for different periods (2020s and 2070s) and changes in climate fields (rainfall, surface temperature and soil moisture content at root zone) have been evaluated for two climate scenarios over Uganda. The variability of rainfall has also been analysed based on the coefficient of variability (CV) for two future periods. The CV was computed as standard deviation (Equation 3.4) divided by the mean (Equation 3.1b).

Changes in the different climate fields between two periods relative to baseline climate observations (except soil moisture content) have been determined. The model projections were subjected to trend and cyclical analysis to examine future climate temporal patterns for seven sub-domains (described in Table 3.1b) over Uganda. Trends in seasonal climate projections were computed and plotted based on the cumulative sum of standardized anomalies in Equation (3.1a) for different climate fields.

The study also evaluated the spatial patterns of bioclimatic variables based on new RCPs scenarios over Uganda. The variables considered included; total annual rainfall, total rainfall of the driest quarter, annual surface temperature, and surface temperature of the coldest quarter. These bioclimatic variables were also used as a basis to map suitability conditions for banana production over Uganda under a changing climate.

The study analysed the future effects of changes in rainfall and temperature on soil moisture content for two SRES climate scenarios over sub regions of Uganda. The ratios of projected rainfall to surface temperatures expressed as a percentage were plotted against soil moisture content. This analysis aimed at estimating variations in soil moisture content resulting from changes in rainfall and surface temperature for different seasons over different locations of Uganda. This was undertaken to determine the resultant impact of climate change on future soil moisture content.

3.2.5 Determination of Potential Effects of Future Climate Change on Banana Production over Uganda

The fourth objective of the study determined the potential effects of projected future climate on banana production in Uganda. The climate scenarios based on AR4 SRES and AR5 RCPs have been used in the projection of future climate change scenarios over Uganda. The climate change projections were used to examine the potential effects of such climate changes on growth patterns and changes in suitability of bananas production across Uganda. The climate change information based on AR5 RCPs climate scenarios were used for the periods 2040 to 2080. The AR4 SRES (A1B and A2) climate change projections were based on the periods 2011 to 2040 and 2061 to 2090 provided regional climate change information that was used as indicators for future banana growth and productivity over Uganda. Detailed assumptions of the AR4 SRES and AR5 RCPs scenarios have been provided in Table 2.3 and Table 2.4

respectively while the different trajectories for the different scenarios under AR4 SRES scenarios and AR5 RCPs scenarios are shown in Figure 2.5 under Chapter Two.

Apart from comparing the projected climate change scenarios with the specific climate thresholds for banana growth (Table 3.6), the FAO ECO-Crop tool was also used to determine and map future suitability of banana growth in Uganda. The FAO ECO-Crop tool (Figure 3.6) was used to provide additional information on the thresholds of climate conditions for the banana crop over Uganda. The ECO-Crop tool was originally developed by Hijmans *et al.* (2001) and further improved, providing calibration and evaluation procedures (Ramirez-Villegas *et al.*, 2011b). The suitability mapping was based on projected climatic conditions under the different scenarios over Uganda.

The spatial patterns and trends in monthly rainfall, minimum and maximum surface temperatures have been used to identify variations in suitability of the banana growing regions of Uganda. The ARCGIS based suitability model was developed and used to determine future banana growth patterns and quantify the response of banana growth patterns to projected future climate patterns for different areas.

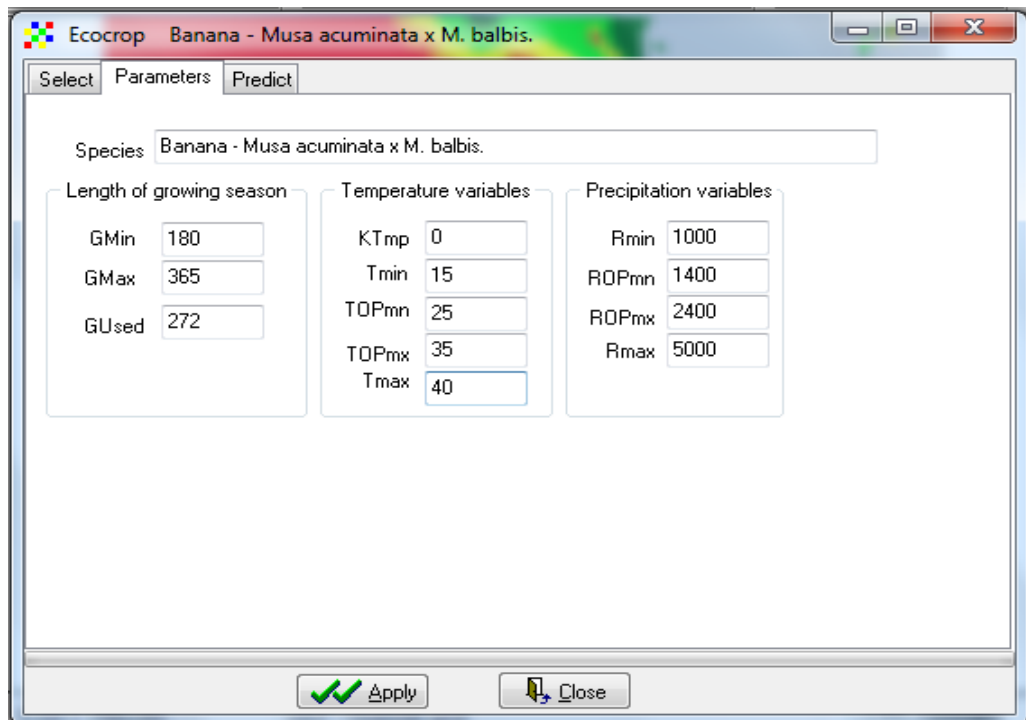


Figure 3.6: Climate requirements for banana growth under the FAO ECOCROP tool.

The suitability mapping delineated regions of varying future banana growth conditions as (1) excellent (86-100%), (2) very suitable (71-85%), (3) suitable (56-70%), (4) marginal (41-

55%), (5) very marginal (26-40%) and (6) unsuited (less than 25%). The construction of the banana suitability GIS based model was based on the classes and the climatic parameters in Table 3.7.

The suitability patterns was constructed in two periods (2041 to 2060 and 2061 to 2080) and also across a full range of AR5 RCPs that included RCP 2.6, RCP 4.5, RCP 6.0, and RCP 8.5 (Hijmans *et al.*, 2005; Moss *et al.*, 2010 and IPCC, 2014). Best case and worst case scenarios of future banana production resulting from a combination of projected temperature and rainfall were determined in this part of the study. German *et al.* (2015) adopted a similar approach to assess global banana production and suitability under climate change scenarios based on SRES A2 scenario with specific reference on the tropics and subtropics.

Table 3.7: Climate thresholds for GIS based Banana Production Suitability Mapping

Suitability Classes	Annual average temperature (°C)	Temperature of the coldest quarter (°C)	Annual Rainfall (mm)	Rainfall of driest quarter (mm)
1 (Excellent)	3 (24.1-25)	4 (23.1-24)	6 (>1800)	6 (>320)
2 (Very Suitable)	1 (<23)	2 (21.1-22)	5 (1601-1800)	5 (271-320)
3 (Suitable)	2 (23.1-24)	1 (<21)	4 (1401-1600)	4 (221-270)
4 (Marginal)	4 (25.1-26)	3 (22.1-23)	3 (1201-1400)	3 (121-220)
5 (Very Marginal)	5 (26.1-27)	5 (24.1-25)	2 (1001-1200)	2 (71-120)
6 (Not Suited)	6 (>27)	6 (>25)	1 (<1000)	1 (<70)

The study also utilized the banana-temperature non-linear regression model (Turner and Lahav, 1983 and Sastry, 1988) to assess the impact of future changes in temperature on banana growth. Increase in banana growth translates into increase bunch size (high banana productivity) and also shorter banana harvest cycles. The temperature-constrained banana growth was given by Equation 3.23.

$$V_t = 75.35 * e^{-0.0.5*(t-26.3)^2} \quad (3.23)$$

In Equation (3.23), V_t is the percentage growth rate of banana crop at a given temperature t (degrees Celsius), $t = 26.3$ °C was identified and used as the optimal surface temperature for banana growth over Uganda (similar to Figure 3.3). The projected temperatures for different

climate scenarios were super-imposed on the banana growth-temperature curve for the two periods which provided an indication of the anticipated growth from projections of temperature.

CHAPTER FOUR

RESULTS AND DISCUSSION

This chapter presents the results obtained from the various data analysis methods (discussed in Chapter Three) to achieve the overall and specific objectives of the study. The results from data homogeneity test and quality control are presented first and followed by other results in the order of specific objectives.

4.1 Results on Data Homogeneity Test and Quality Control

The double mass curve has been used to test for the homogeneity of the rainfall, minimum and maximum temperature observations for the period 1961-2013 for selected stations in this study. Results were obtained based on the methods described in Section 3.2.1 and are presented in Sub-section 4.1.1.

4.1.1 Monthly Rainfall, Minimum and Maximum Temperature Double Mass Curves

Figure 4.1 shows the double mass curves for mean monthly rainfall (a), minimum (b) and maximum (c) temperature for Mbarara and Kabale weather stations in southwestern Uganda. Figure 4.2 (a-c) present similar results but for Namulonge and Jinja for central Uganda. Despite there being some missing data for some stations that were filled using the described method (Section 3.2.1), the straight lines fitted indicate that the data was homogeneous and hence of good quality for analysis to give reasonable results for the study objectives.

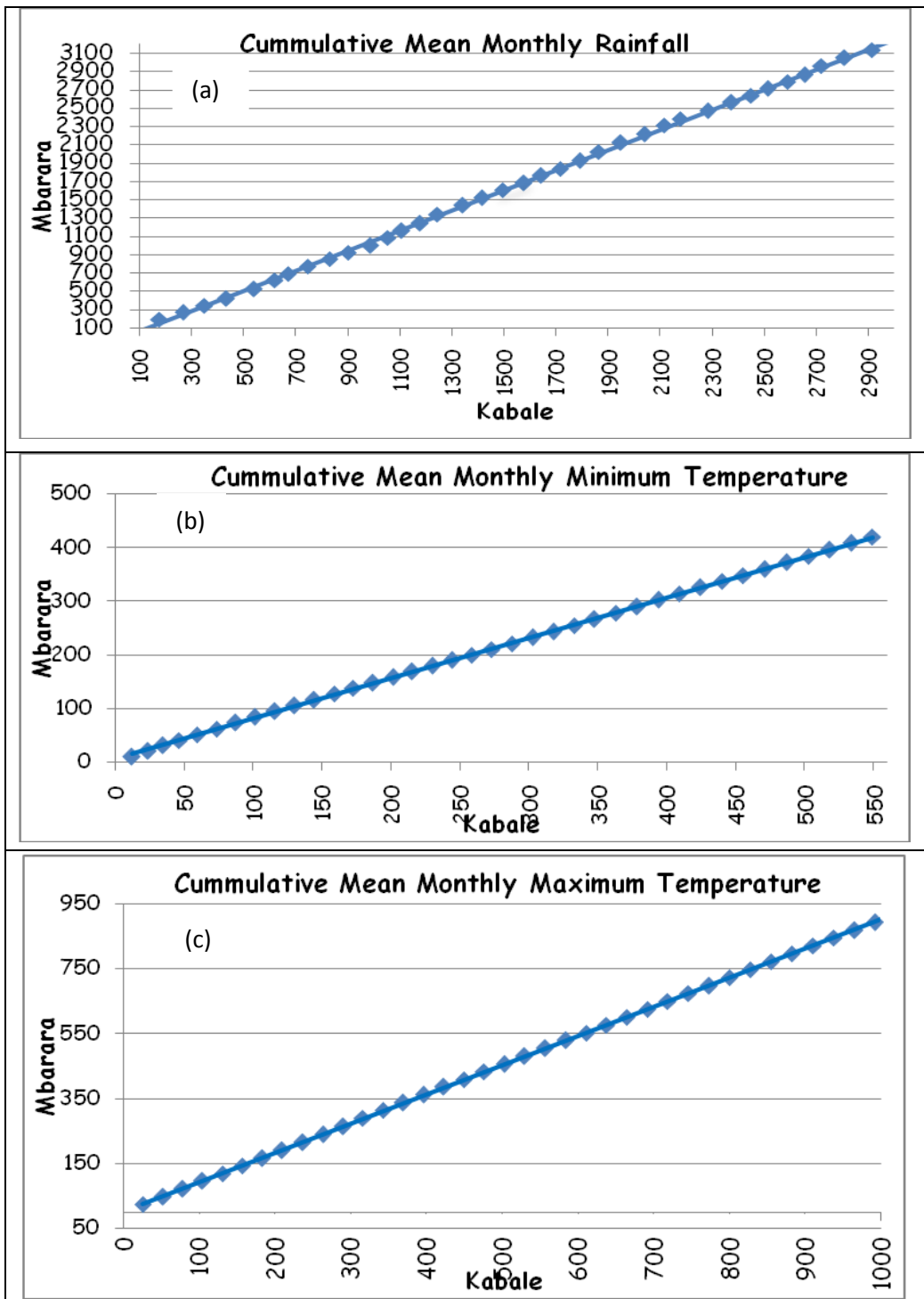


Figure 4.1: Rainfall (a), minimum temperature (b) and maximum temperature (c) mass curves for Mbarara and Kabale.

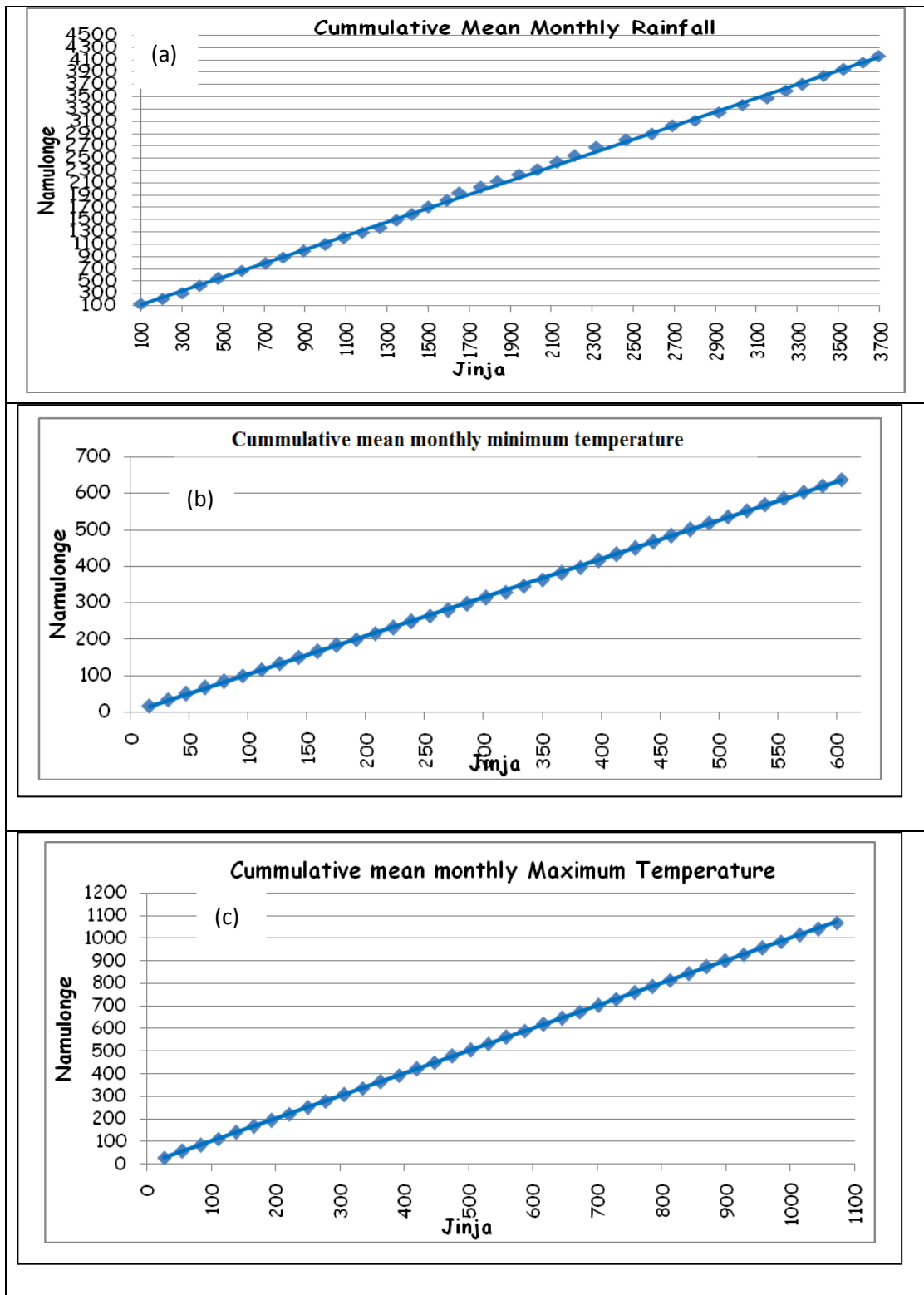


Figure 4.2: Rainfall (a), minimum temperature (b) and maximum temperature (c) mass curves for Namulonge and Jinja.

4.2.1 Ground Truthing of CRU Gridded Rainfall and Temperature Data over Uganda

The study has undertaken a comparison between the in-situ observed rainfall and temperature records and the CRU gridded data records over stations of Uganda. This was undertaken to provide the level of confidence that can be associated with the results of the study based on CRU rainfall and temperature data set. Seasonal rainfall totals, minimum and maximum temperature averages records for both actual observations and CRU data sets have been compared. The Correlation Coefficients (COR) and Root Mean Square Errors (RMSE) have been used as measures of agreements between the two data sets. Results based on June-July (JJA, dry) and October-December (OND, wet) seasons for rainfall, maximum and minimum temperatures have been presented for selected stations.

Table 4.1a presents values of Root Mean Square Error (RMSE) and Correlation Coefficient (CORR) for seasonal rainfall. Figures 4.3 (a-d) - 4.4 (a-d) show the degree of agreement between in-situ observed and CRU semi-observed seasonal rainfall totals (mm) for Gulu, Kasese, Namulonge and Tororo stations during a relatively dry JJA (Figure 4.3, a-d) and wet OND (Figure 4.4, a-d) seasons. The study observed a high agreement between the two data sets at most stations. This is evidenced from the values observed COR and RMSE computed across the different observational station over Uganda. Significant and very high correlation coefficients between 0.62 at Namulonge (central region) to 0.91 at Kasese (western region) were obtained for seasonal rainfall (Table 4.1a). The correlations are generally higher for OND than for JJA season. The results (Table 4.1a) further showed that the root mean square errors in CRU seasonal rainfall estimates range between 53-79 mm of seasonal rainfall.

The high correlations and low values of the root mean square errors point observations in some areas and CRU rainfall estimates can be attributed to the network of rainfall observation stations in a particular region. For example, the area around Lake Victoria is observed to perform poorly compared with other areas that can partly be explained by the sparse station network around the lake region. It was also notable from the results (Figure 4.3 and 4.4) that the agreement between CRU estimates and station observations is better for previous years than for recent years. This may be attributable to the reduction in the number of stations used in gridding the CRU and the errors from the introduction of Automated Weather Stations (AWS) that have not be fully calibrated. The results in this part of the study were important in understanding and providing an indication of the level of uncertainty of using CRU gridded observations in the subsequent analysis of this thesis.

Table 4.1: Values of Root Mean Square Error (RMSE) and Correlation Coefficient (CORR) for seasonal rainfall (a), minimum temperature (b) and maximum temperature (c).

SEASONAL RAINFALL (a)				
STATION/SEASON/ MEASURE	JJA		OND	
	RMSE (mm)	CORR	RMSE (mm)	CORR
GULU	79.52	0.88	50.0	0.90
KASESE	61.1	0.63	82.0	0.71
NAMULONGE	70.3	0.62	102.8	0.79
TORORO	60.7	0.87	52.5	0.91
MINIMUM TEMPERATURE (b)				
STATION/SEASON/ MEASURE	MAM		OND	
	RMSE	CORR	RMSE	CORR
KASESE	1.24	0.69	0.93	0.62
TORORO	1.45	0.55	1.27	0.56
MAXIMUM TEMPERATURE (c)				
KASESE	2.12	0.55	1.8	0.43
TORORO	0.71	0.60	0.87	0.45

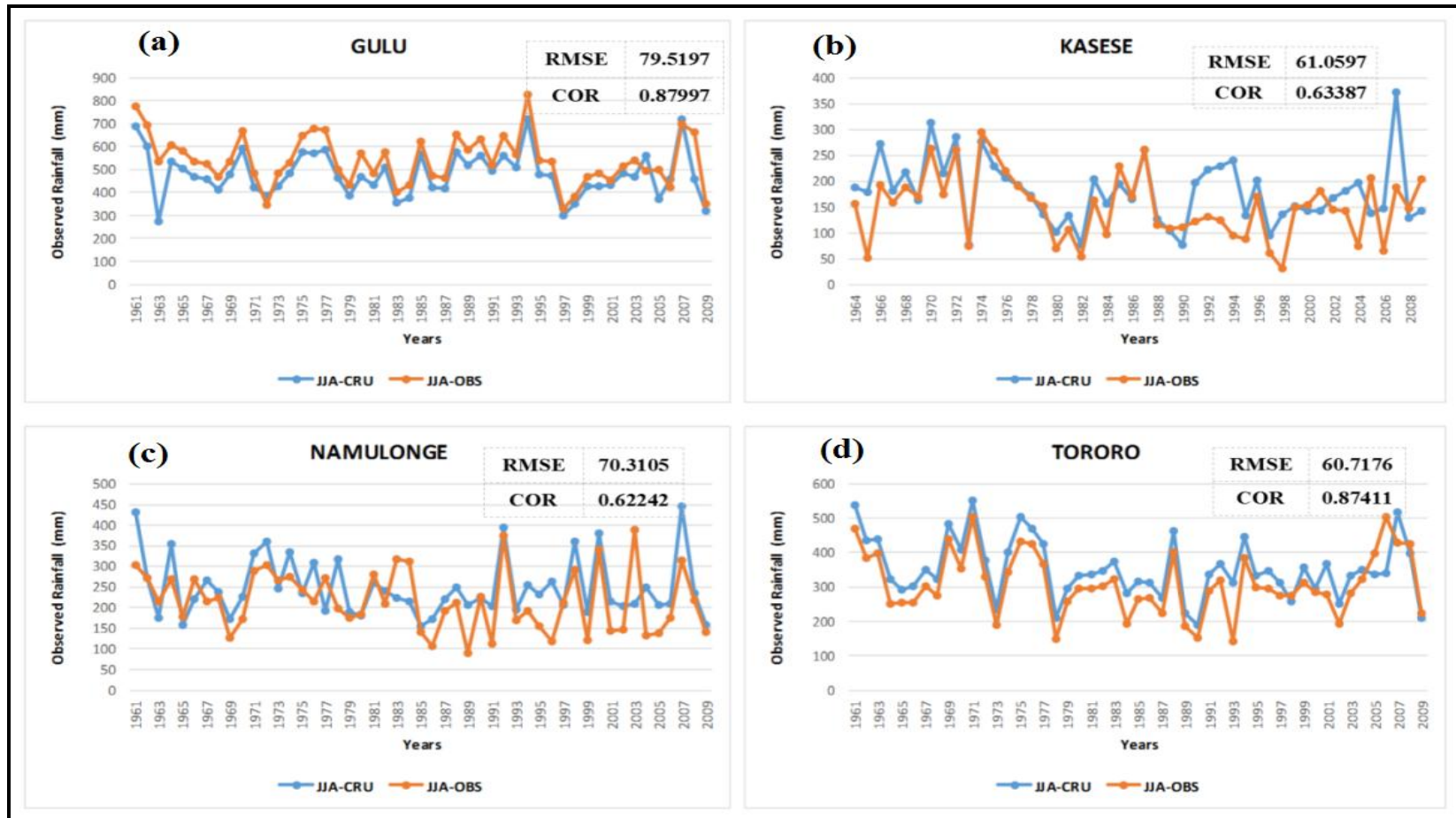


Figure 4.3 (a-d): Comparison between insitu station observed rainfall (mm, orange) and CRU rainfall (mm, blue) during the June-August (JJA) season for Gulu, Kasese, Namulonge and Tororo stations for the period 1961-2009. Values for the root mean square errors (RMSE) and correlation coefficients (COR) have been indicated for each station.

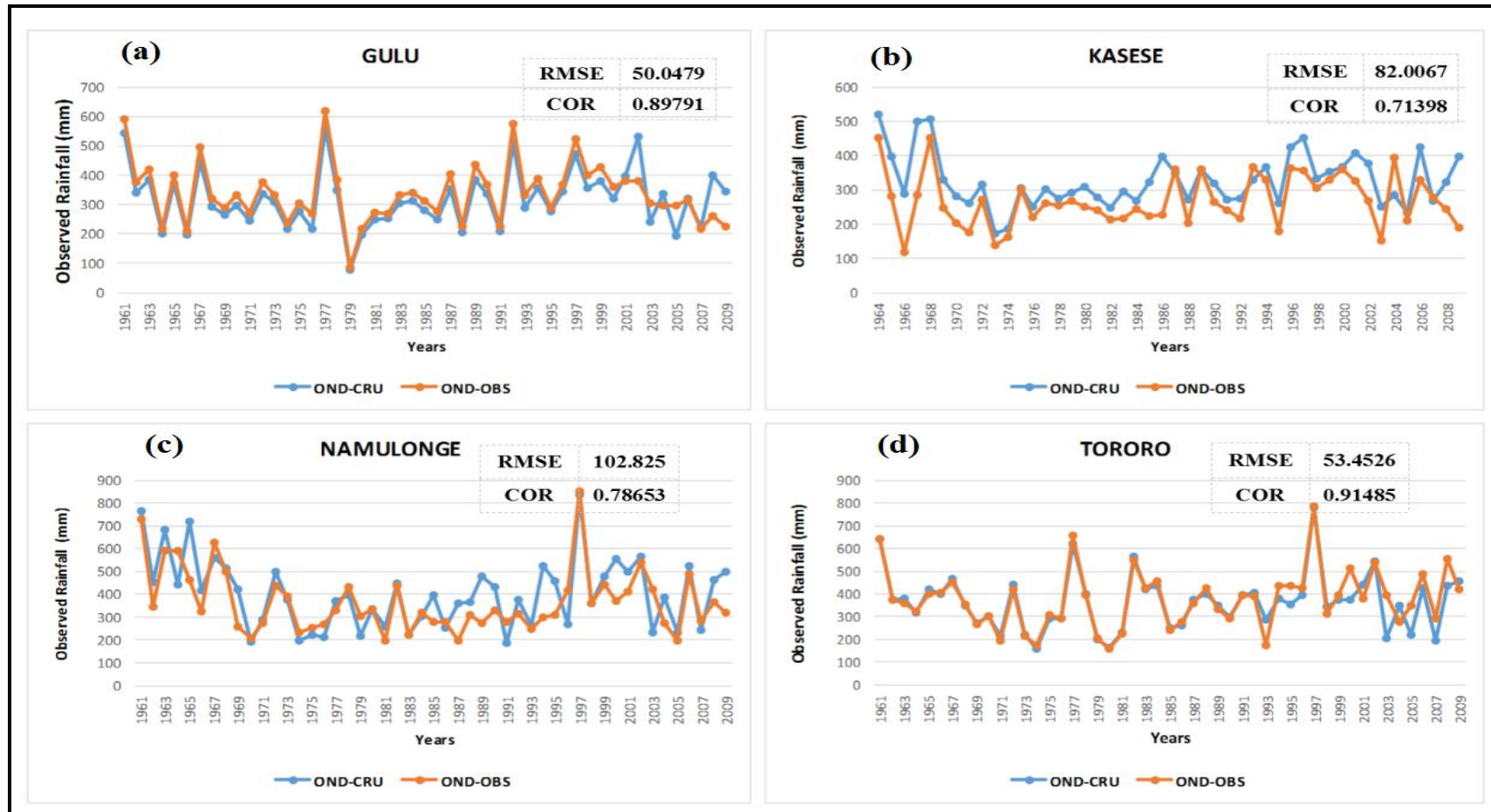


Figure 4.4 (a-d): Comparison between insitu station observed rainfall (mm, orange) and CRU rainfall (mm, blue) during the October-December (OND) season for Gulu, Kaseke, Namulonge and Tororo stations for the period 1961-2009. Values for the root mean square errors (RMSE) and correlation coefficients (COR) have been indicated for each station.

Table 4.1(b-c) presents values of Root Mean Square Error (RMSE) and Correlation Coefficient (CORR) for seasonal minimum temperature (b) and maximum temperature (c). The results in Figures 4.5(a-d)-4.6(a-d) indicate the agreement between in-situ and semi observed CRU minimum and maximum seasonal temperature for MAM and OND seasons. Scatter plots have been used to display the degree of the relationship. Both the correlation and root mean square errors have been computed for the different stations as statistical measures of the strength of the relationship (Table 4.1, b-c). There is reasonable discrepancy in the two data sets that can be partly attributed to the existence of significant gaps in temperature station observations used in the interpolation of CRU gridded data.

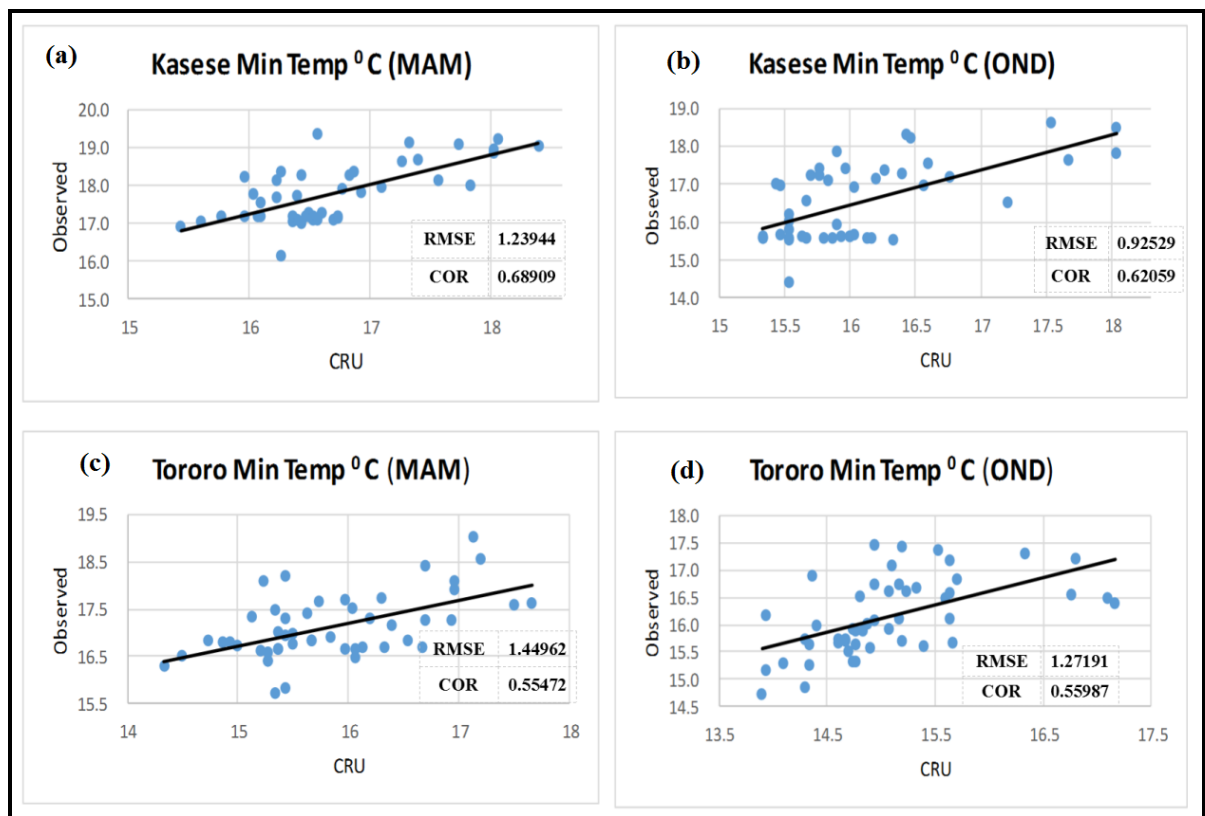


Figure 4.5 (a-d): Agreement between insitu station observed minimum surface temperature (°C) and CRU minimum surface temperature (°C) during the March-May (MAM, a, c) and the October-December (OND, b, d) seasons for Kasese (a, c) and Tororo (c, d) stations for the period 1961-2009. Values for the root mean square errors (RMSE) and correlation coefficients (COR) have been indicated for each station.

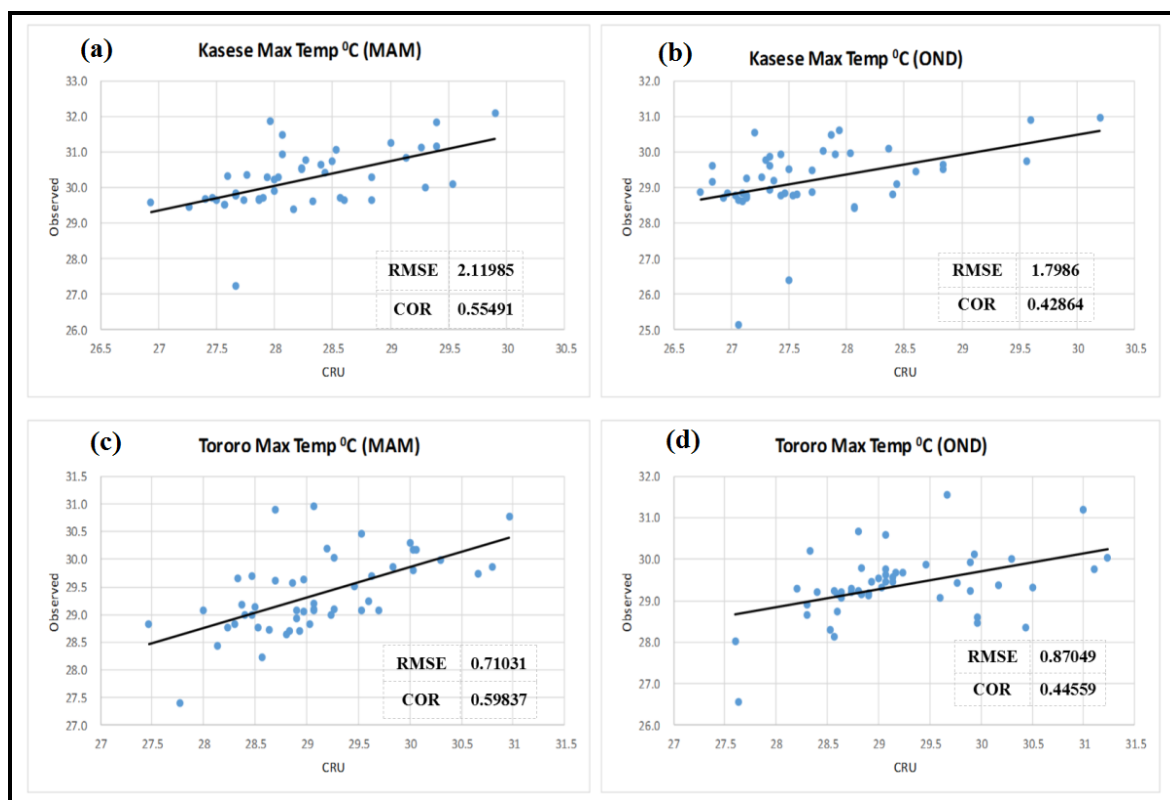


Figure 4.6 (a-d): Agreement between insitu station observed maximum surface temperature ($^{\circ}\text{C}$) and CRU maximum surface temperature ($^{\circ}\text{C}$) during the March-May (MAM, a, c) and the October-December (OND, b, d) seasons for Kasese (a, b) and Tororo (c, d) stations for the period 1961-2009. Values for the root mean square errors (RMSE) and correlation coefficients (COR) have been indicated for each station.

In general the results from the study observed that the extremely large and low observed values were well discernible from CRU data but they were sometimes underestimated or overestimated. CRU climate estimates may suffer from uncertainties in some areas particularly in east Africa partly due to inadequate station coverage (New *et al.*, 2000; Mitchell and Jones, 2005 and Nandozi *et al.*, 2012). The results from this part of the study provide great insights towards the reliability of CRU gridded rainfall and temperature observations that are used in the subsequent analysis of this thesis. The results of this study agree in part with those observed by Otieno *et al.* (2014).

4.2 Results on the Linkages between Current Banana Yields and Observed Climate Variability

This section presents results on the linkages between current banana yields and variations in observed rainfall, minimum and maximum surface temperature with specific reference to the central and western regions of Uganda. The results based on various methods are presented in

this section. The methods employed included empirical approaches based on changes in the mean, variance, skewness and kurtosis coefficients; trend analysis; use of correlation and regression analyses; and use of the FAO Crop Water Assessment Tool (CROPWAT) to estimate yield response to variations in rainfall and evapotranspiration (Smith, 1992 and Clarke *et al.*, 2001).

4.2.1 Empirical Approaches

Results on the empirical approaches are presented in this section. The results on the contribution of seasonal rainfall to the annual total rainfall (Figure 4.7, a-i) and the spatial patterns of long-term seasonal mean rainfall (Figure 4.8, a-l) and variability (Figure 4.9, a-f) are presented.

These results in Figures (4.7, 4.8 and 4.9) are based on the first timeseries moment (mean). Figure 4.7 (a-i) shows the spatial patterns in the contribution of each seasonal on the annual total rainfall during the periods 1931-1960, 1961-1990 and 1991-2013 over Uganda. In Figure 4.9 (a-f), seasonal rainfall mean for the periods 1931-1960 (a, c, e) and 1961-1990 (b, d, f) have been compared against that of the recent period 1991-2013.

The study observed that March-May (MAM) remains the major rainfall season for most parts of southern, western, central and eastern Uganda with the northern parts of the Country receiving most of their rainfall during the JJA season (Figures 4.7 and 4.8). In addition, the study observed that during the MAM (a-c) and OND (g-i) seasons, the rainfall is concentrated around Lake Victoria and the eastern parts of Uganda. On the other hand, during JJA (d-f) season, the rainfall is concentrated in the northern part of Uganda. It was further observed that the wet seasons over the various parts accounted for more than 40% of the annual total rainfall (Figure 4.7 a-i).

The results from Figures 4.7 (a-i) and 4.8 (a-l) observed that there has been significant changes in the contribution of the individual seasons to the annual total rainfall over few areas. Most of the country, experienced little or no change over the years (Figures 4.7a-i). The contribution of the season to annual total rainfall for individual year, however, varies significantly in some years, especially due to extreme rainfall during the ENSO and IOD years.

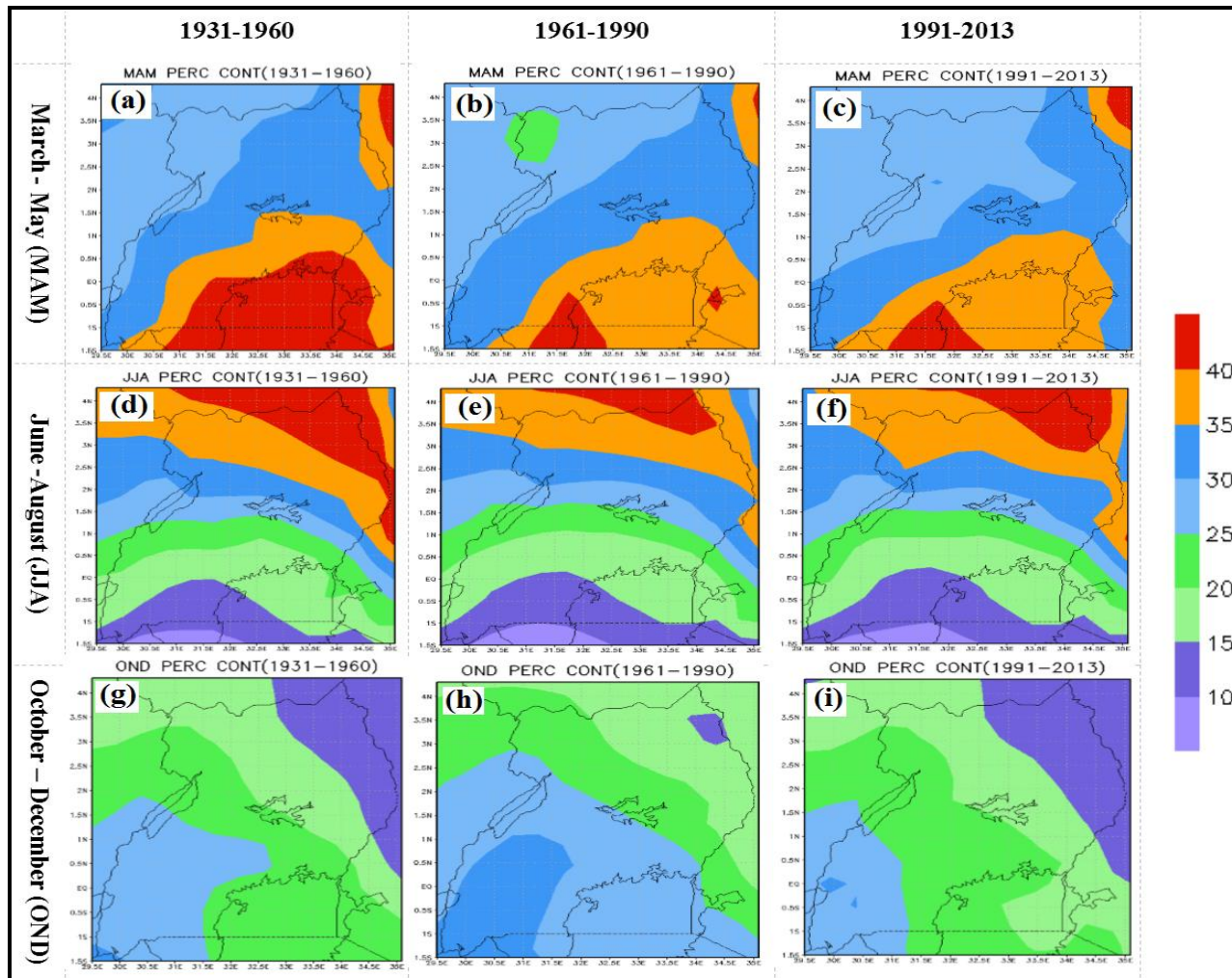


Figure 4.7 (a-i): Contribution of seasonal rainfall (%) to the total annual rainfall during March-May (MAM, a-c), June-August (JJA, d-f) and October-December (OND, g-i) for climatological periods 1931-1960 (a, d, g), 1961-1990 (b, e, h) and 1991-2013 (c, f, i) over Uganda.

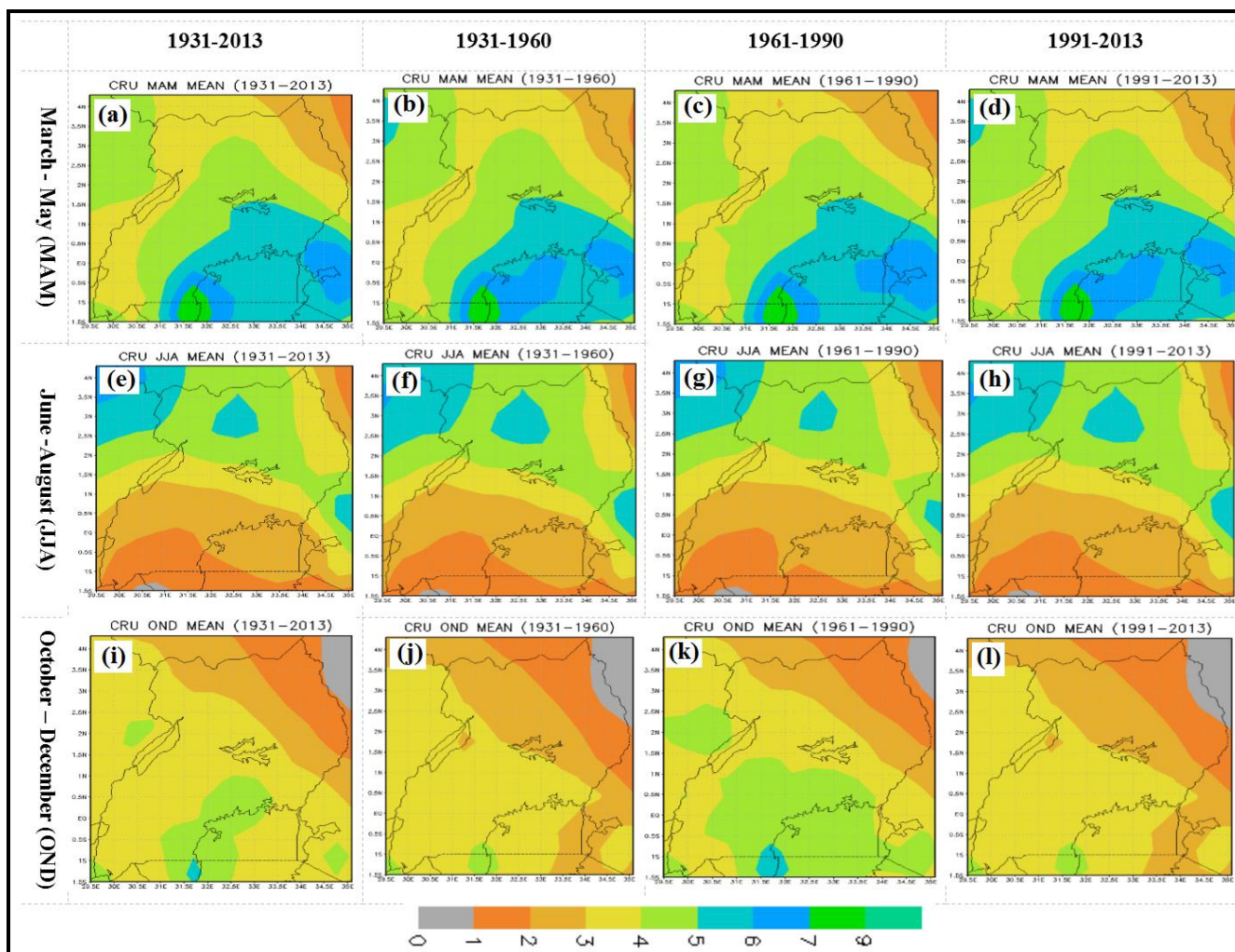


Figure 4.8 (a-l): Spatial patterns of CRU seasonal rainfall mean (mm/day) for the periods 1931-2013 (a, e, i), 1931-1961 (b, f, g), 1961-1990 (c, g, k) and 1991-2013 (d, h, l) during March-May (MAM, a-d), June-August (JJA, e-h) and October-December (OND, i-l) over Uganda.

Results in Figure 4.9a-f, observed that when the means for the periods 1931-1960 and 1961-1990 were compared with the means for the recent period 1991-2013, a tendency for previous two 30-year periods being wetter than the current period was evident for many areas in Uganda during MAM and JJA seasons. For OND season, relative dryness of the two periods compared to the period 1991-2013 was quite evident over most of Uganda (Figure 4.9a-f).

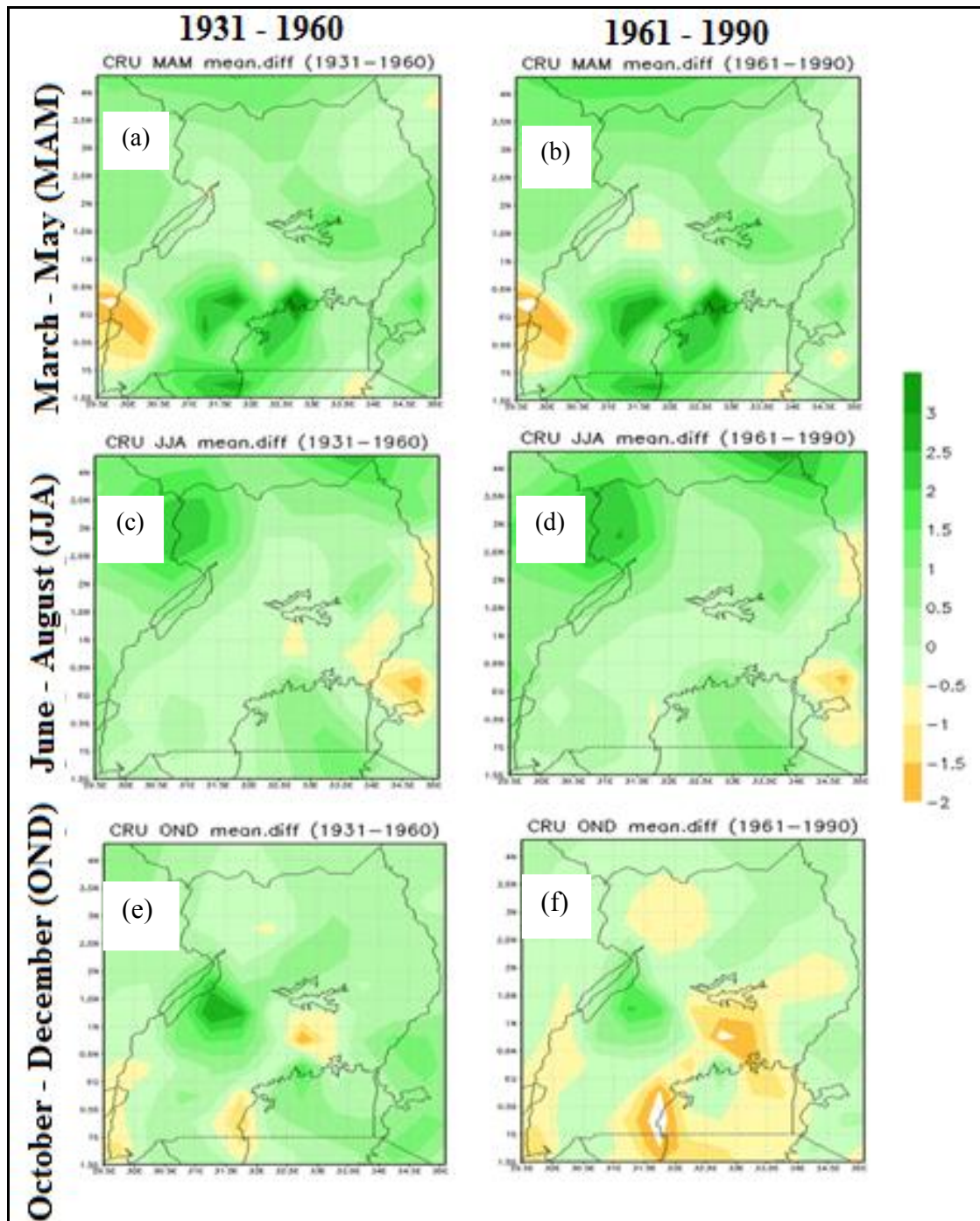


Figure 4.9 (a-f): Observed changes in CRU mean seasonal rainfall (mm/day) for the historical periods 1931-1960 (a, c, e) and 1961-1990 (b, d, f) for March-May (MAM, a-b), June-August (JJA, c-d) and October-December (OND, e-f) relative to the current period 1991-2013.

The results in Figures (4.10, and 4.11) were based on the second moment (variability) of seasonal rainfall spatial patterns. In Figure 4.10 (a-l), results for the spatial patterns of rainfall variability are presented while Figure 4.11 (a-f) shows the changes in the standard deviations at specific locations for the historical periods 1931-1960 (a, c, e) and 1961-1990 (b, d, f) relative to the current period 1991-2013.

The study observed that during MAM (a-b) season, significant rainfall variability is being experienced over the Lake Victoria region and eastern parts of Uganda. October-December (OND, i-l) season seem to have the highest rainfall variability compared to the other seasons. Rainfall variability was also high during JJA season (e-h) over northern Uganda that receives peak rainfall during this season. High rainfall variability is often associated with recurrences of too much/ too little rainfall in some years.

Over all, at most locations, variability was highest during OND and MAM, where study observed significant rainfall extremes. Several other studies (Ogallo and Nassib, 1984; Mwangi *et al.*, 2014; Ngaina *et al.*, 2014 and Otieno *et al.*, 2015) have observed drought as one of major climate extreme events that is common over the eastern Africa region. Climate extremes over Eastern Africa particularly Uganda have been associated with different phases of the ENSO, IOD and MJO patterns (Mutai and Ward, 2000; Camberlin and Philippon, 2002; Black *et al.* 2003; Omeny *et al.*, 2008; Ogallo, 2009; Omondi, 2010; Lyon and DeWitt, 2012 and Otieno *et al.*, 2015).

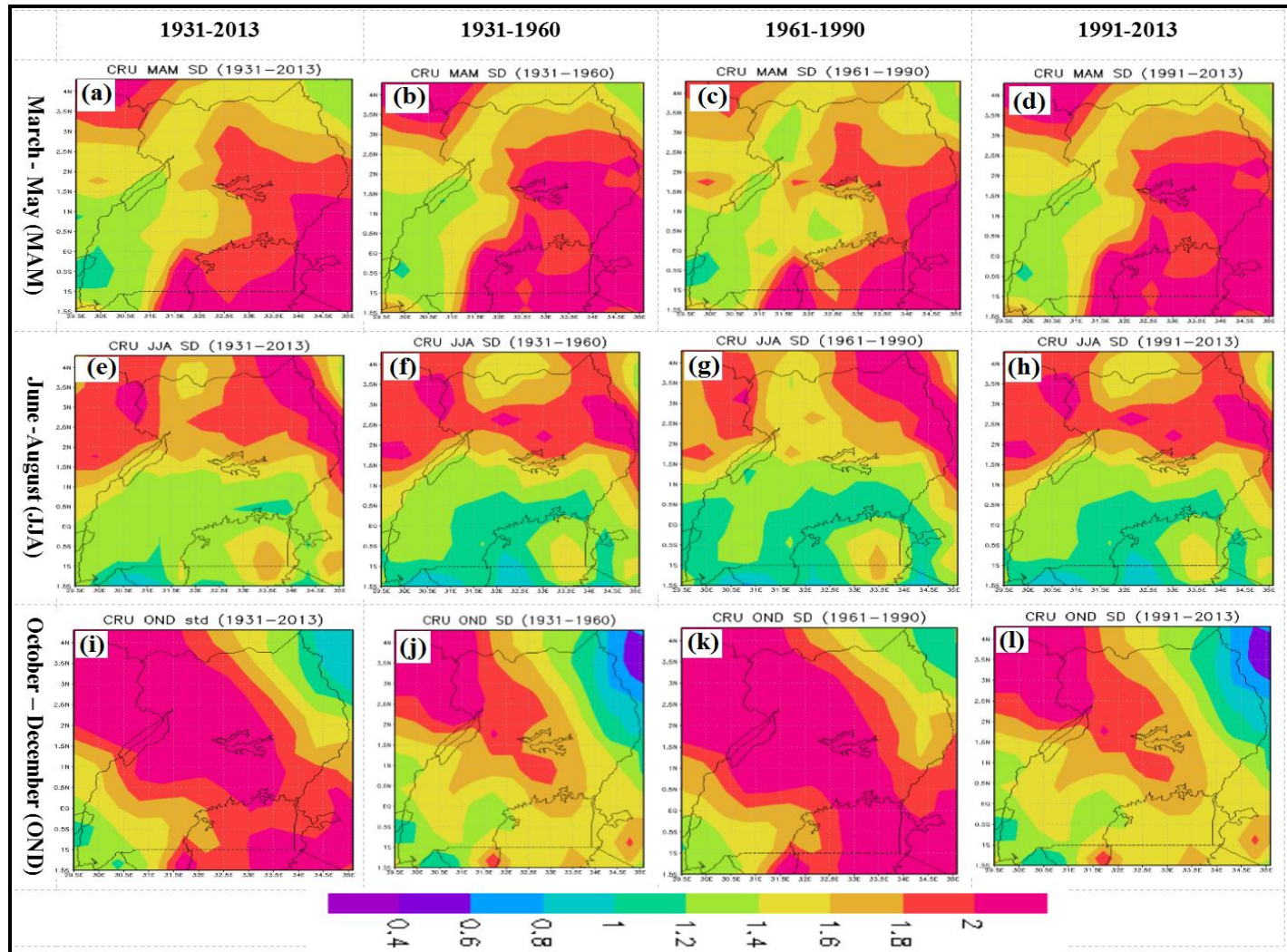


Figure 4.10 (a-l): Spatial patterns of CRU seasonal rainfall variability (mm/day) for the periods 1931-2013 (a, e, i), 1931-1961 (b, f, j), 1961-1990 (c, g, k) and 1991-2013 (d, h, l) during March-May (MAM, a-d), June-August (JJA, e-h) and October-December (OND, i-l) over Uganda.

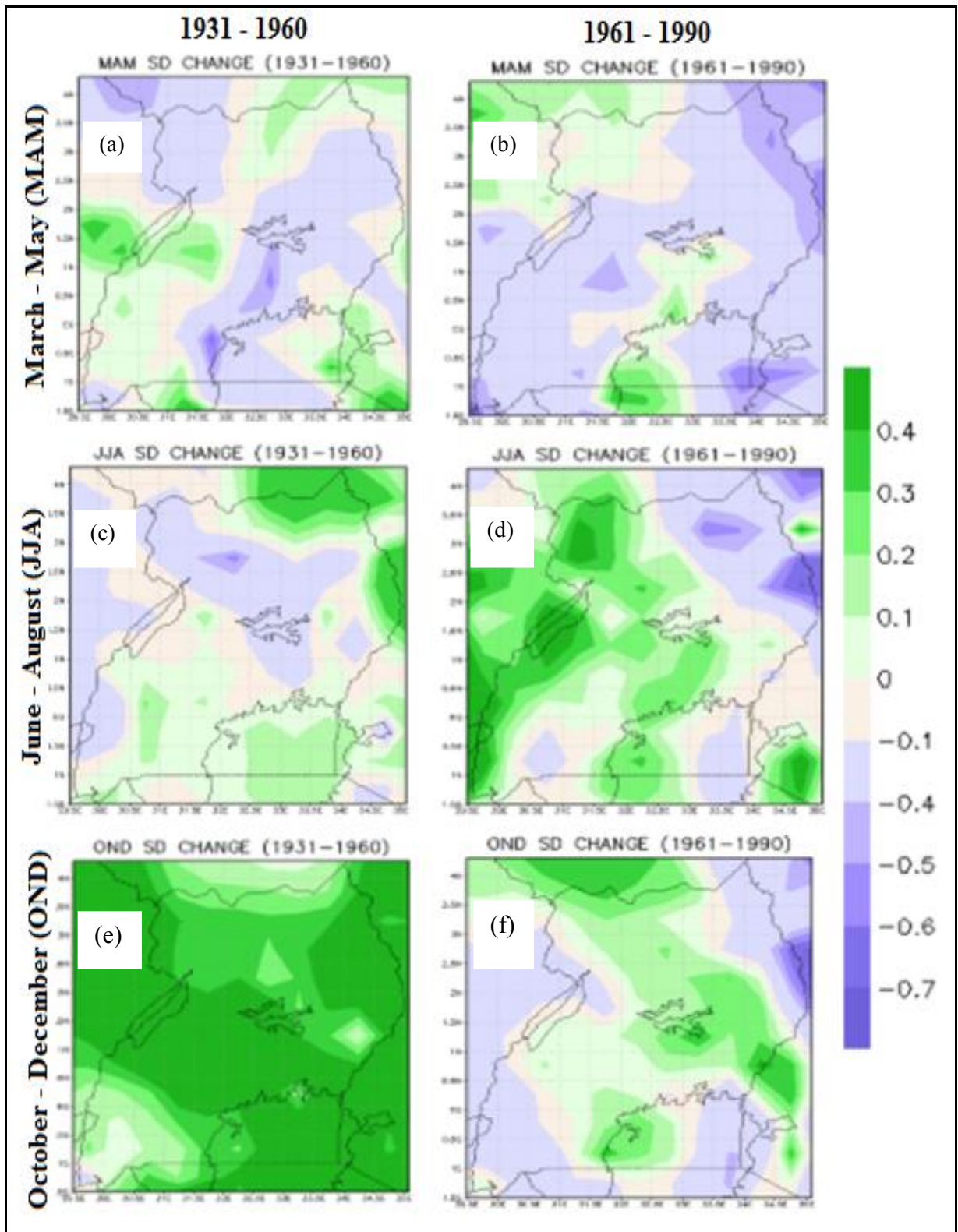


Figure 4.11 (a-f): Observed changes in seasonal rainfall variability (standard deviation) (mm/day) during current period 1991-2013 relative to two historical periods; 1931-1960 (a, c, e) and 1961-1990 (b, d, f) for March-May (MAM, a-b), June-August (JJA, c-d) and October-December (OND, e-f) over Uganda.

4.2.1.1 Drought Characteristics over Uganda

It was observed under methodology that the Standard Precipitation Indices (SPI) were used to examine extreme rainfall characteristics (drought and floods) in Uganda. SPI patterns for the period 1963-2013 over different regions of Uganda are presented in Figures 4.12 (a-c)-4.14 (a-c). Results in Figure 4.12a observed that over Namulonge, longest and worst drought occurred during the period 1982-1990 while recent years have very few dry episodes. In Tororo (Figure 4.12b), the results show that 1973-1974, 1979-1981, 1994-1995 experienced severe droughts while the recent years (2006-2013) recorded normal to enhanced rainfall events.

In general, the study observed year to year variations in rainfall in Uganda. It is also observed from the results that there has been a reduction in drought occurrences in the recent years over Namulonge (Figure 4.12a), Soroti (Figure 4.12b), Jinja (Figure 4.13a), Kabale (Figure 4.13b) and Arua (Figure 4.14a) areas. Despite the observed reduction in the frequency of droughts in some areas of Uganda, inadequate soil moisture is still one of the most important factors affecting banana productivity in many regions due to high dependence on rain-fed agriculture, poor water management and poor soil moisture conservation mechanisms in Uganda (Nyombi, 2013 and Umesh *et al.*, 2015). Van Asten (2011) also observed the frequency and intensity of droughts as one most important climatic factor affecting banana productivity in Uganda.

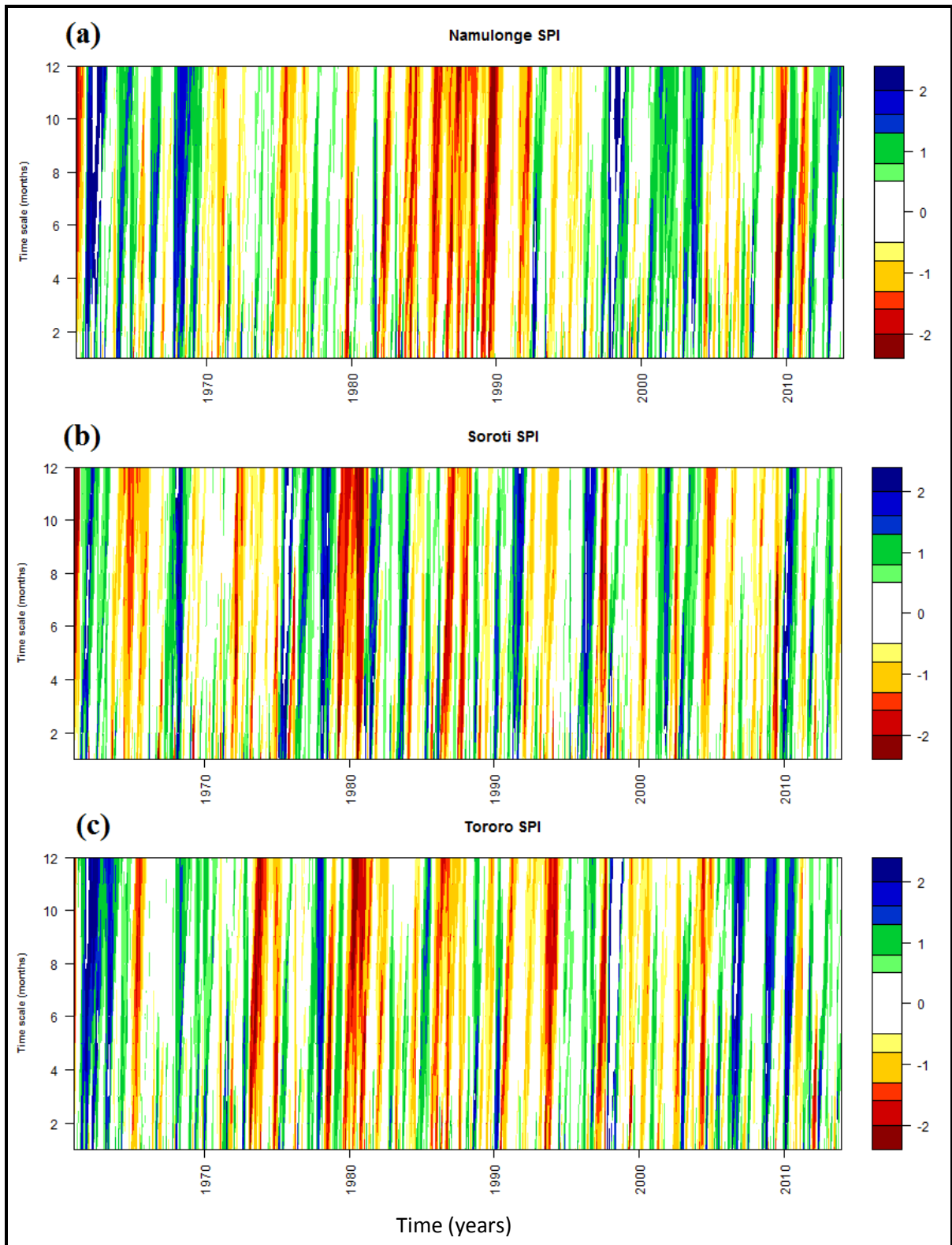


Figure 4.12 (a-c): Standardized precipitation indices (SPI) over Namulonge (a), Soroti (b) and Tororo (c). Blue indicated extremely wet periods while red indicated extremely dry (drought) periods during 1961-2013.

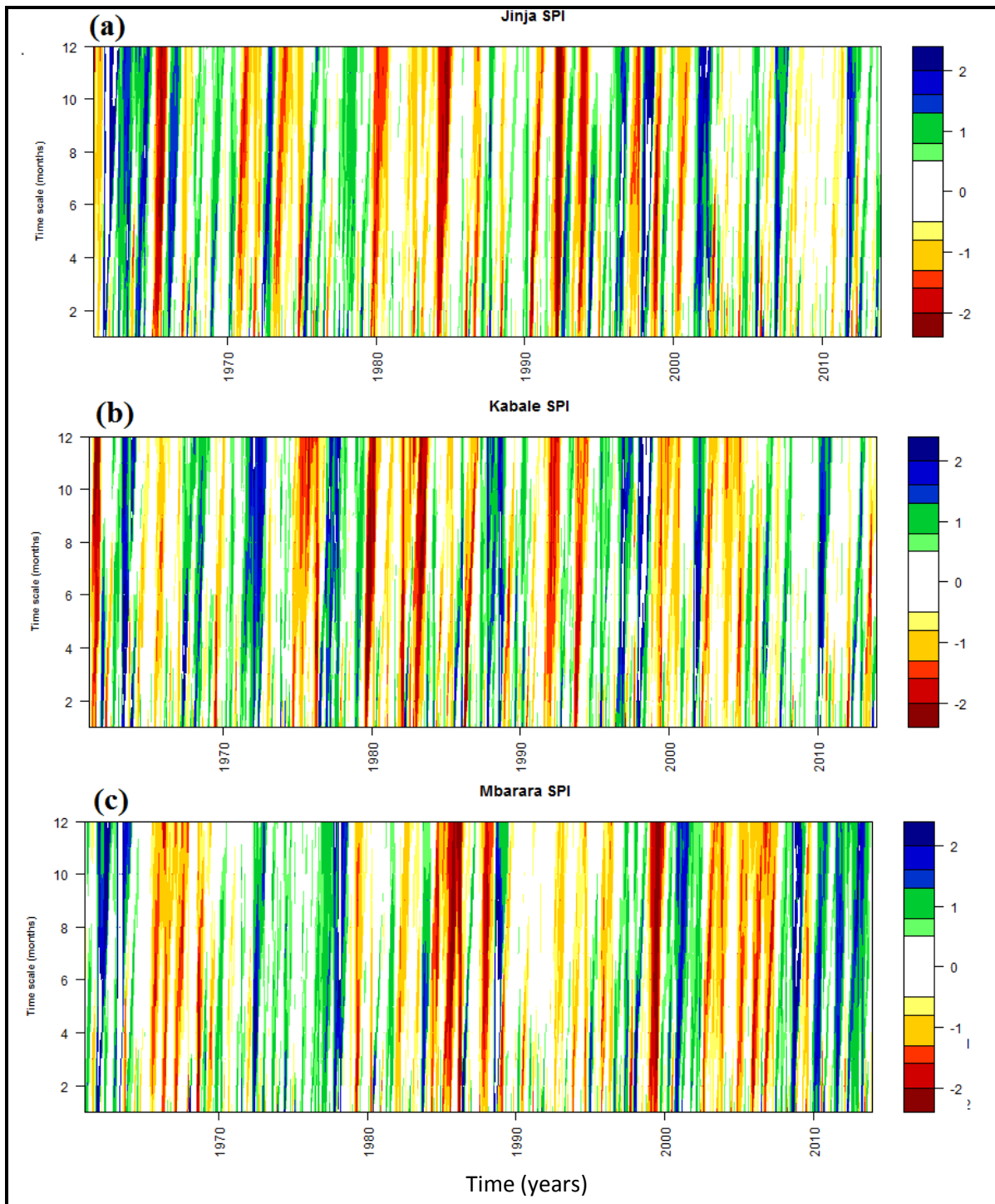


Figure 4.13 (a-c): Standardized precipitation indices (SPI) for Jinja (a), Kabale (b) and Mbarara (c). Blue indicated extremely wet periods while red indicated extremely dry (drought) periods during 1961-2013.

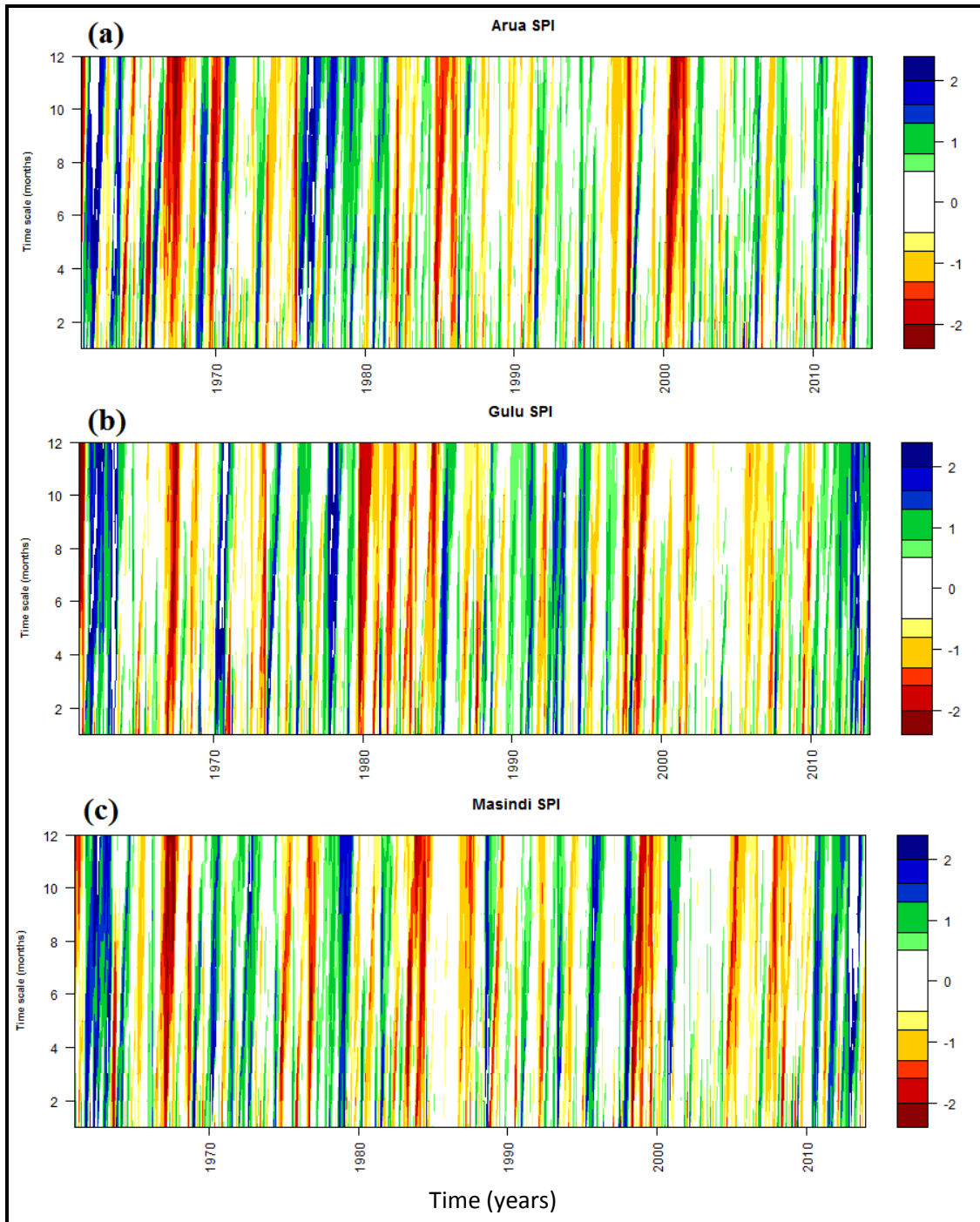


Figure 4.14 (a-c): Standardized precipitation indices (SPI) for Gulu (a), Arua (b) and Masindi (c). Blue indicated extremely wet periods while red indicated extremely dry (drought) periods during 1961-2013.

4.2.2 Observed Rainfall Trends

Graphical results from rainfall time series observed that there are notable trends in the annual and seasonal rainfall series particularly during March-May (MAM) and October-December (OND) seasons.

The results have been presented for Namulonge (Figure 4.15-4.16, a-d), Soroti (Figure 4.17-4.18, a-d), Tororo (Figure 4.19-4.20, a-d), and Mbarara (Figure 4.21-4.22, a-d). Over Namulonge, a decreasing trend in both annual (Figure 15) and seasonal rainfall (Figure 16, a-d) is evident during all four seasons of the year from the graphical plots. The study also observed increasing and decreasing trends during different seasons of the year at same location sometimes contributing to decreasing or increasing trends in the cumulative annual rainfall totals as is demonstrated by in Figures 4.15-4.22 (a-d). Over western parts of Uganda, the results show increasing trends in the June-August (JJA, c) season and no discernable trend in other seasons. An increasing rainfall trend is also observed in the annual rainfall series for stations over this part of the Country. There were, however, significant spatial differences in the observed trends of the rainfall series and no particular uniform trend was discernible in the observed rainfall trends over the whole of Uganda during any particular season.

Several past studies in East Africa and other parts of the world have also observed trends in seasonal rainfall pattern (Ogallo, 1982; Ogallo, 1984; Mahe *et al.*, 2001; Sabiiti, 2008; Rai *et al.*, 2010; Ngaina and Mutai, 2013; Nimusiima *et al.*, 2013; Yang *et al.*, 2013 and Nsubuga *et al.*, 2014).

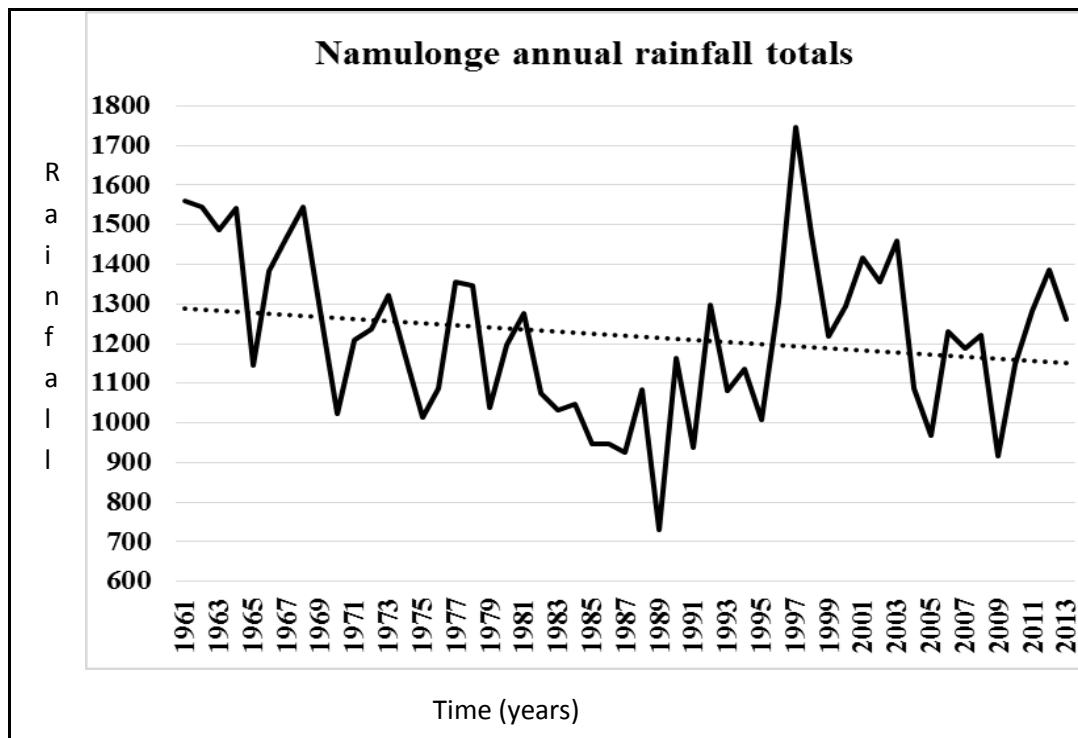


Figure 4.15: Inter-annual variability in annual rainfall totals (January-December) (mm) over Namulonge station during the period 1961-2013.

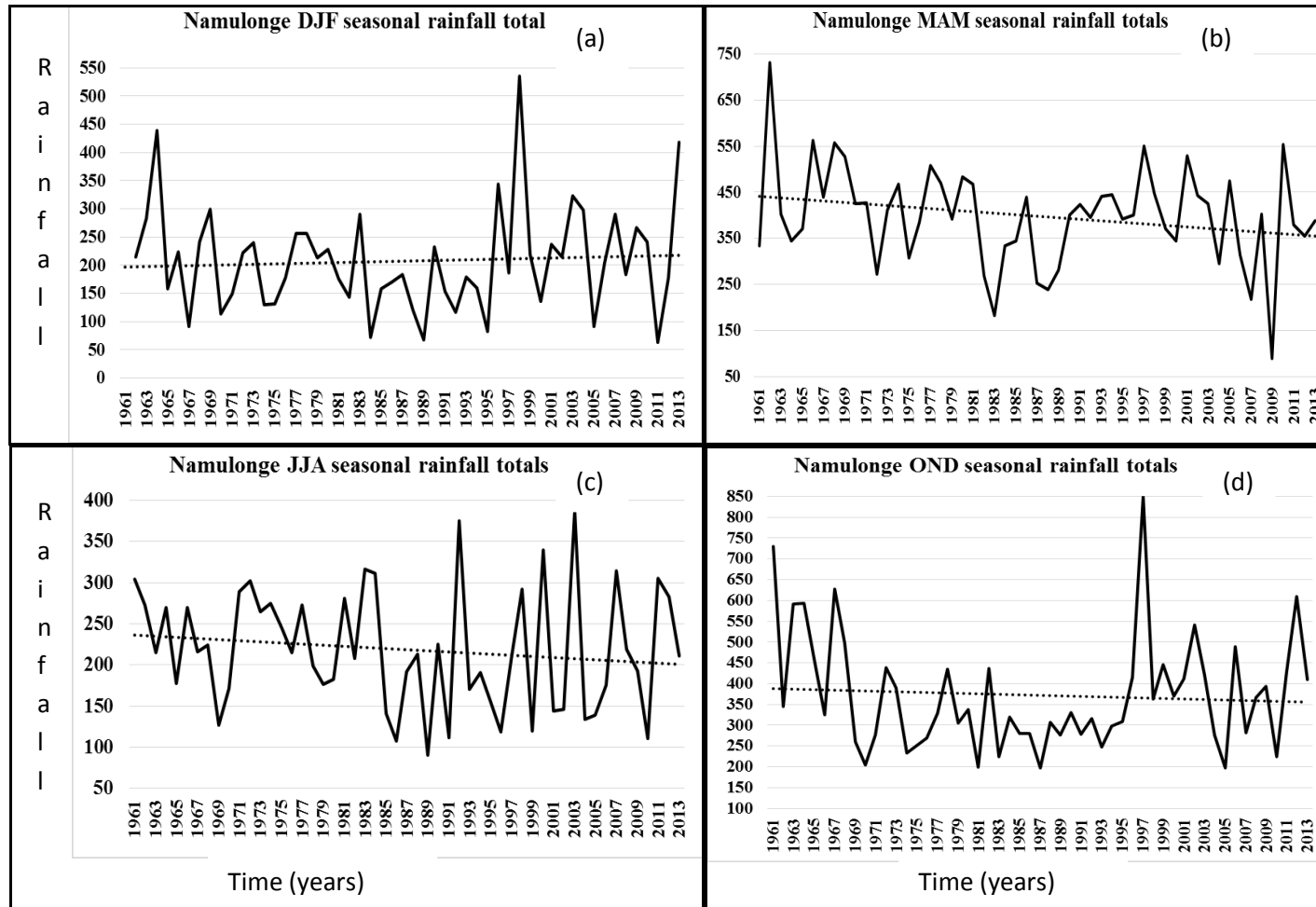


Figure 4.16 (a-d): Inter-annual variability in seasonal rainfall totals (mm) during December-February (DJF, a), March-May (MAM, b), June-July (JJA, c) and October-December (OND, d) over Namulonge station during the period 1961-2013.

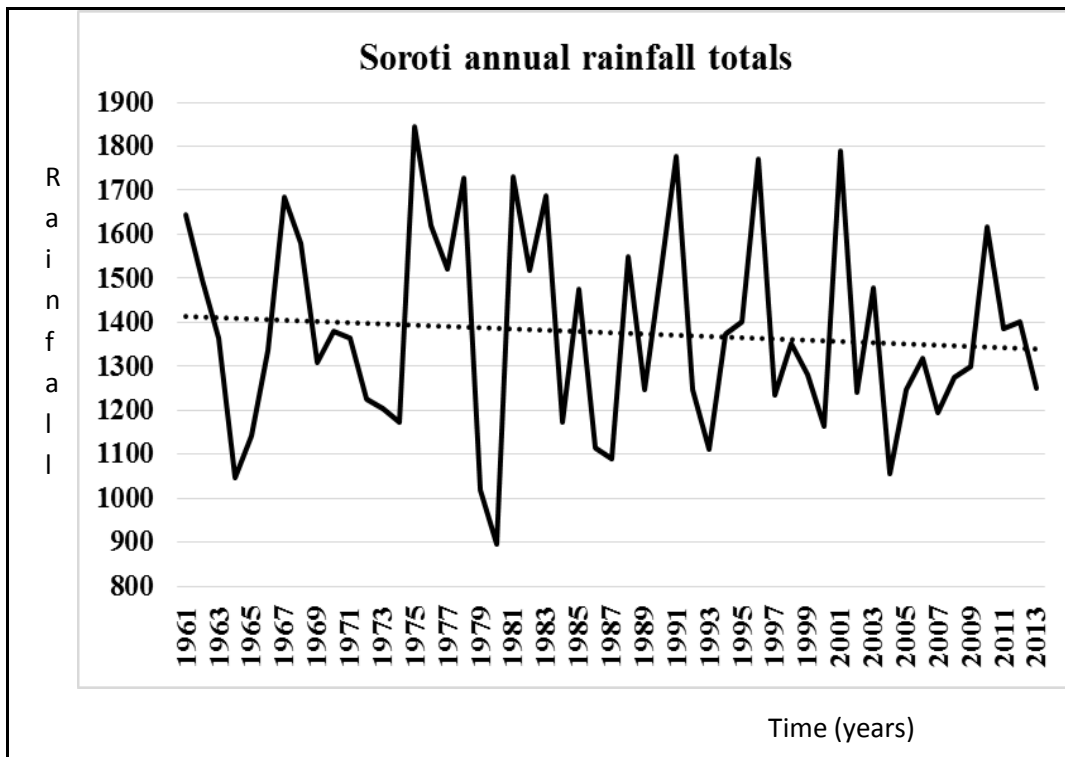


Figure 4.17: Inter-annual variability in annual rainfall totals (January-December) (mm) over Soroti station during the period 1961-2013.

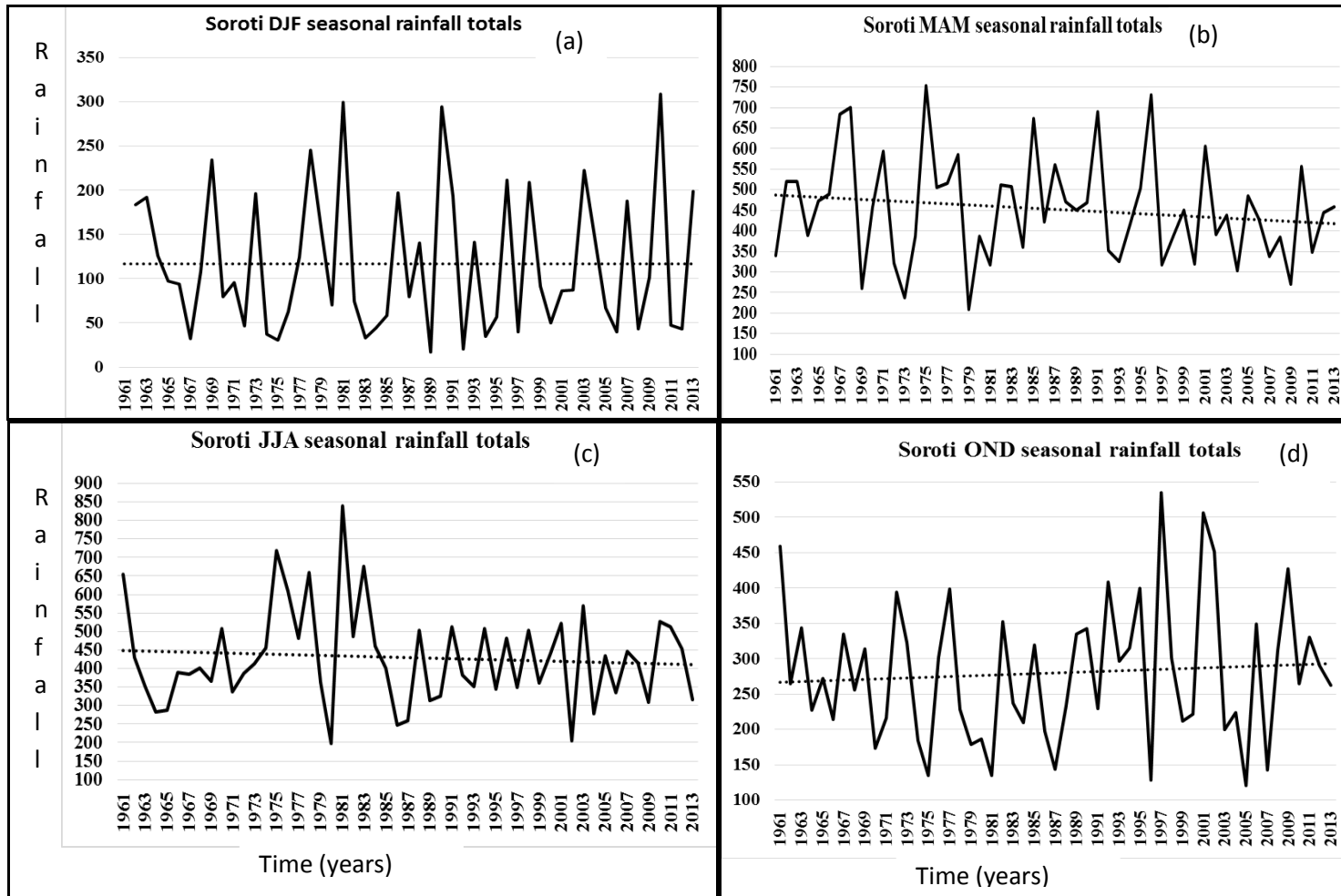


Figure 4.18 (a-d): Inter-annual variability in seasonal rainfall totals (mm) during December-February (DJF, a), March-May (MAM, b), June-July (JJA, c) and October-December (OND, d) over Soroti station during the period 1961-2013.

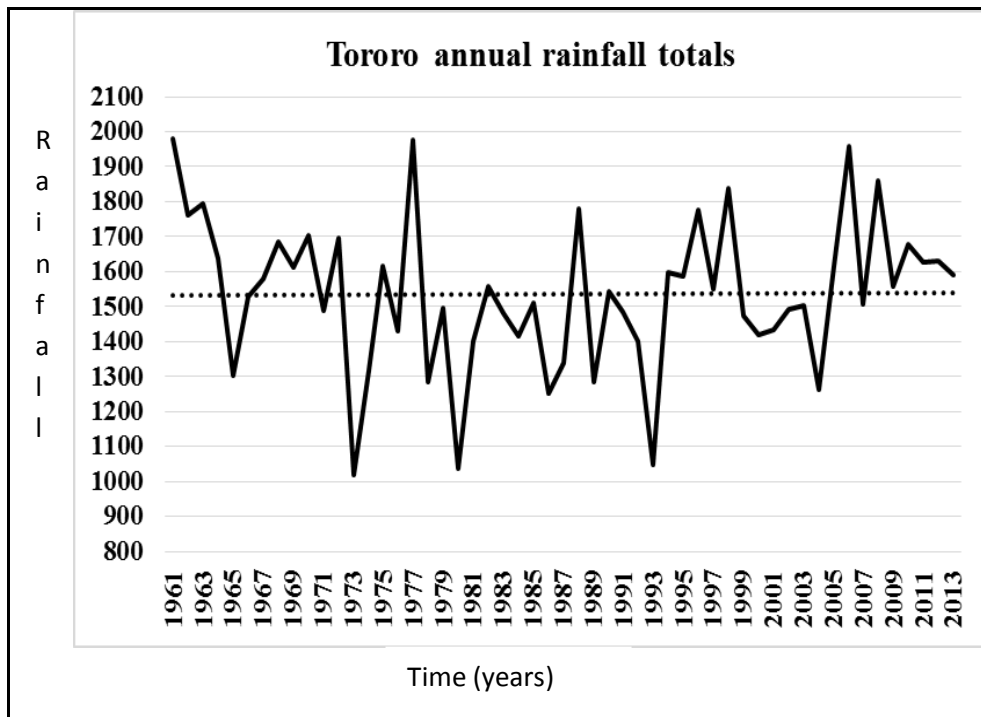


Figure 4.19: Inter-annual variability in annual rainfall totals (January-December, mm) over Tororo station during the period 1961-2013.

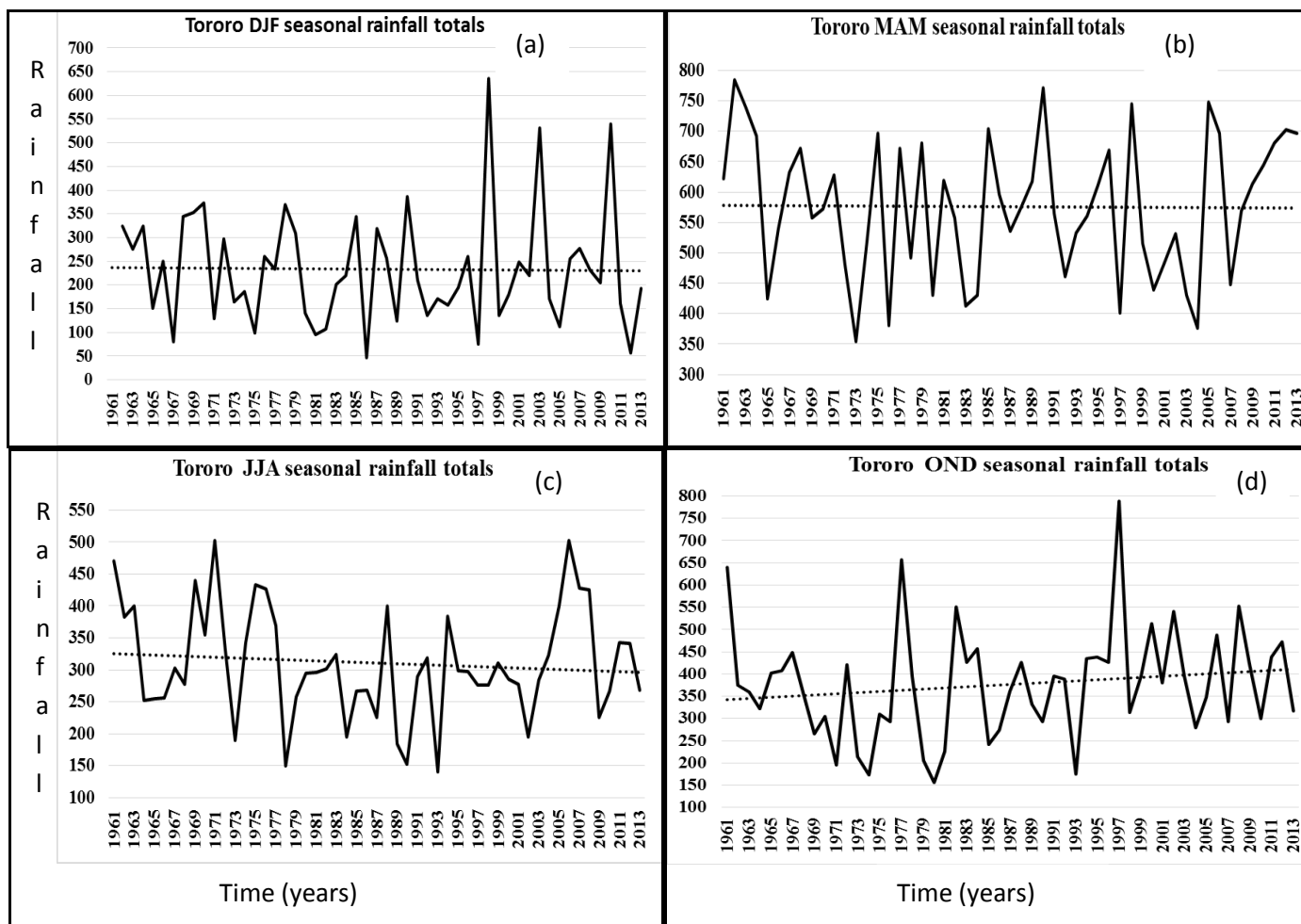


Figure 4.20 (a-d): Inter-annual variability in seasonal rainfall totals (mm) during December-February (DJF, a), March-May (MAM, b), June-July (JJA, c) and October-December (OND, d) over Tororo station during the period 1961-2013.

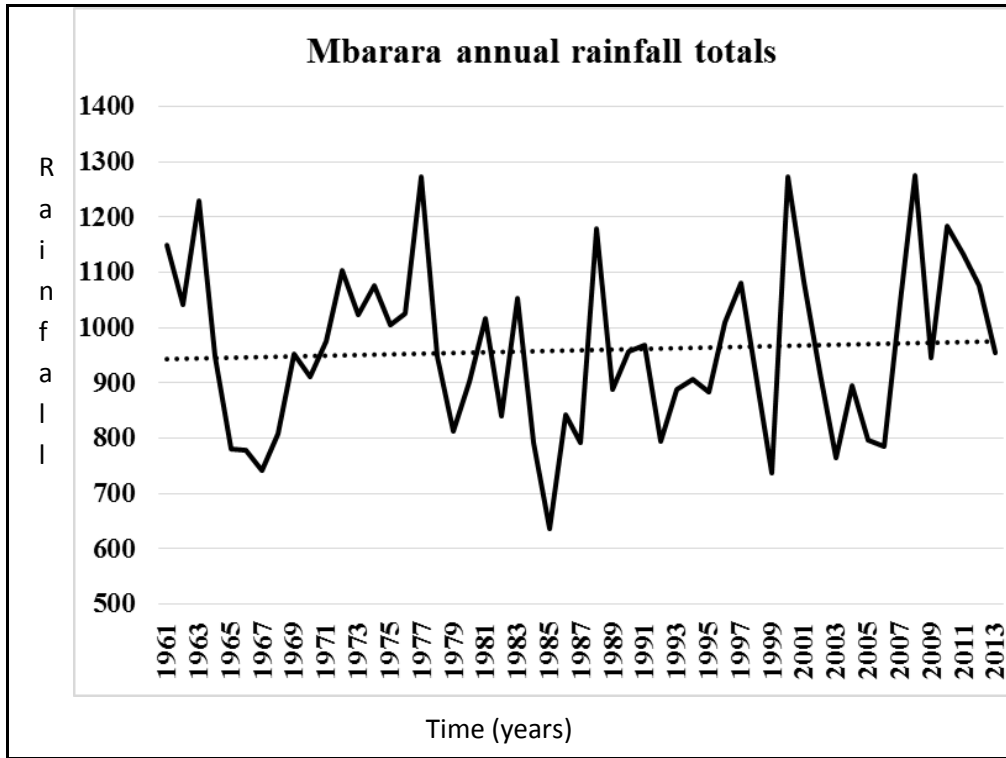


Figure 4.21: Inter-annual variability in annual rainfall totals (January-December, mm) over Mbarara station during the period 1961-2013.

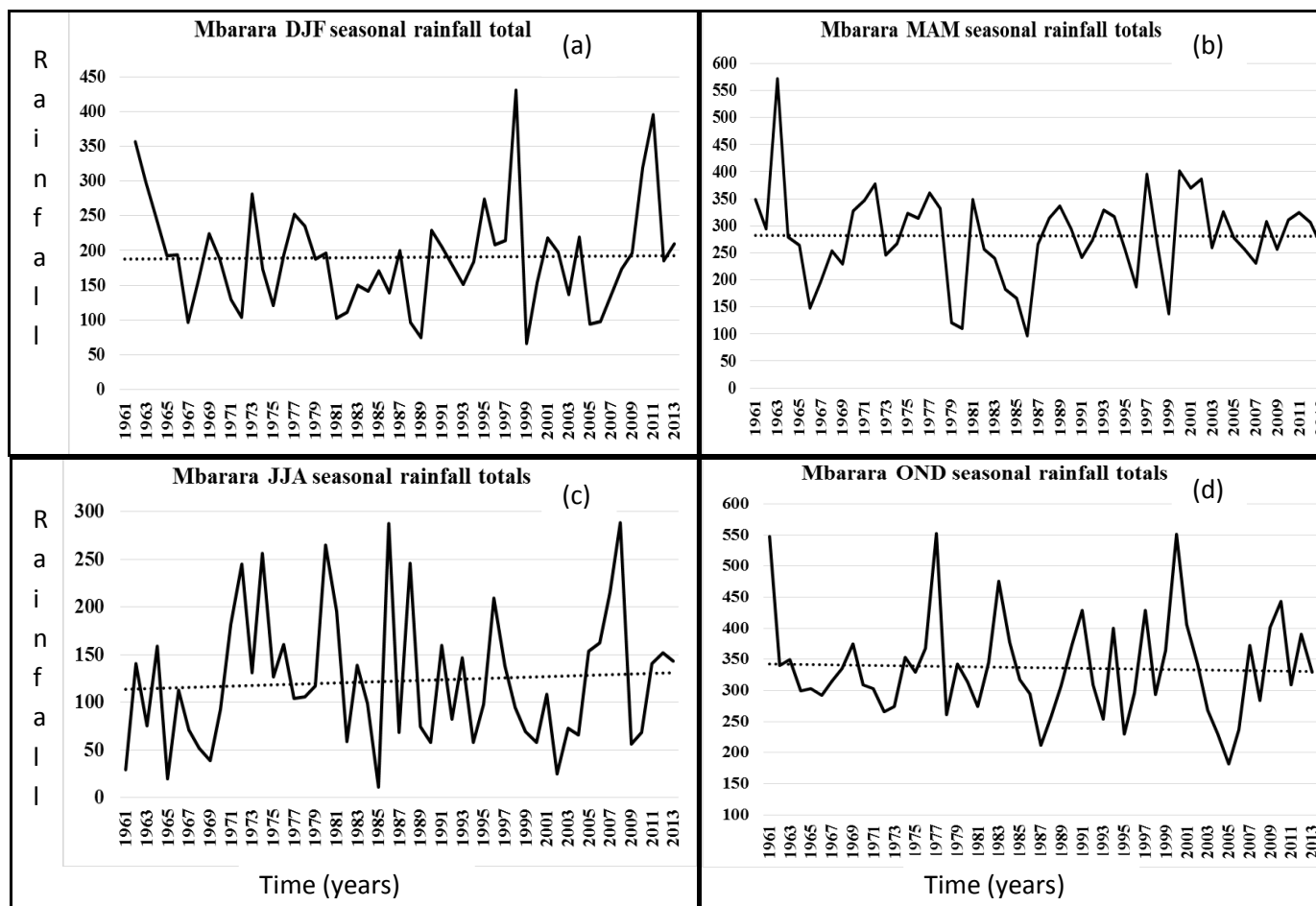


Figure 4.22 (a-d): Inter-annual variability in seasonal rainfall totals (mm) during December-February (DJF, a), March-May (MAM, b), June-July (JJA, c) and October-December (OND, d) over Mbarara station during the period 1961-2013.

4.2.2.1 Rainfall Trend Results from Mann Kendall Statistics

It was observed that graphical methods are very subjective and largely depend on individual's sight judgement. It was therefore critical that the statistical significance of the trends observed in the time series graphs be tested.

This section presents results from Mann Kendall statistics on the trends of seasonal rainfall over selected stations of Uganda. Table 4.2 presents results for March-May (MAM), June-August (JJA) and October-December (OND). The results showed a generally decreasing trend in observed MAM seasonal rainfall patterns over most stations. In some stations, the trends were, however, not statistically significant at 95% confidence level. The JJA and OND seasonal trends observed similar results as for the MAM season except that during OND season at few locations, where the trends observed from the graphical methods in the previous sections were observed statistically significant based on statistical method. A good example is Kampala station (Table 4.2). Several studies have documented evidences of rainfall trends and changes over parts of East Africa including Uganda (Ogallo, 1993; Basalirwa, 1995; Nicholson, 1996; King'uyu *et al.*, 2000; Mahe *et al.*, 2001; Kruger and Shongwe, 2004; Schreck and Semazzi, 2004; New *et al.*, 2006; Kizza *et al.*, 2009; Mubiru *et al.*, 2009; Longobardi and Villani, 2010; Yang *et al.*, 2013 and Nsubuga *et al.*, 2014).

Table 4.2: Trend test statistics for MAM, JJA and OND seasonal rainfall

Stations	MAM		JJA		OND	
	Tau	Significant at 0.025?	Tau	Significant at 0.025?	Tau	Significant at 0.025?
Arua	-0.01	No	-0.02	No	0.05	No
Entebbe	0.01	No	0.07	No	-0.04	No
Gulu	-0.17	No	-0.16	No	-0.04	No
Kabale	-0.06	No	-0.03	No	-0.02	No
Kampala	0.00	No	0.14	No	0.26	Yes
Kasese	-0.13	No	-0.15	No	0.08	No
Lira	-0.18	No	0.09	No	0.12	No
Masindi	-0.14	No	-0.01	No	-0.03	No
Mbarara	-0.03	No	0.02	No	-0.06	No
Namulonge	-0.12	No	-0.17	Yes	-0.05	No
Soroti	-0.16	No	-0.03	No	0.02	No
Tororo	-0.11	No	-0.05	No	0.13	No

4.2.3 Results from Changes in Skewness and Kurtosis Coefficients for Seasonal Rainfall Series

The changes in the mean and variance of climate series are always used to understand patterns in climate parameters. This study investigated how other statistics, namely skewness and kurtosis coefficients can represent changes in the climate data series during two recent periods. These higher order statistics were used to investigate shifts/changes in the frequencies and magnitudes of the extreme seasonal rainfall events.

Changes in the patterns of skewness and kurtosis coefficients at the specific locations are shown in Tables 4.3 and 4.4 respectively. The results show that although some large changes in the values of the coefficients were witnessed at some locations, there were no clear evidences of significant changes in the shifts in the frequencies and magnitudes of the extreme rainfall events for the specific seasons.

Table 4.3: Changes in the skewness coefficient of seasonal rainfall series between the periods 1961-1990 and 1991-2013 over Uganda

Stations/Seasons	MAM	JJA	OND
Arua	-0.3	-0.2	-0.7
Entebbe	-0.2	-0.2	1.1
Gulu	-1.3	0.5	-0.2
Kabale	0.5	0.4	-0.2
Kampala	0.4	-0.2	-1.6
Kasese	-0.6	1.0	-1.9
Lira	-1.2	0.5	-0.1
Masindi	-0.3	-0.5	0.5
Mbarara	-0.7	0.2	-1.2
Namulonge	-1.7	1.2	0.5
Soroti	1.0	-1.2	0.0
Tororo	0.2	0.2	0.3
Jinja	0.4	0.1	-1.0

Table 4.4: Changes in the kurtosis coefficients of seasonal rainfall series between the periods 1961-1990 and 1991-2013 over Uganda

Stations/Seasons	MAM	JJA	OND
Arua	0.1	0.7	-1.4
Entebbe	-0.9	0.1	-3.1
Gulu	-2.1	0.9	-1.5
Kabale	-1.5	1.2	0.3
Kampala	1.1	-1.6	-4.3
Kasese	-0.6	3.2	-4.6
Lira	-1.2	-0.6	0.0
Masindi	-0.7	0.6	1.2
Mbarara	-1.7	1.3	-3.0
Namulonge	1.6	-0.2	3.4
Soroti	1.1	-1.0	0.2
Tororo	-0.4	1.6	2.7
Jinja	-1.2	-1.0	-4.6

4.2.4 Trends of Surface Temperatures

Results from graphs of the plotted minimum and maximum surface temperature time series showed that there are observed increasing trends in the annual and seasonal surface temperature time series at most locations. Results have been presented for Tororo station in Eastern Uganda

Examples of the observed temperature trends are shown in Figures 4.23-4.26. Figures 4.23-4.24 (a-d) show trends in annual and seasonal minimum temperatures anomalies, while Figures 4.25-4.26 (a-d) observed annual and seasonal maximum temperature trends for Tororo station in eastern Uganda.

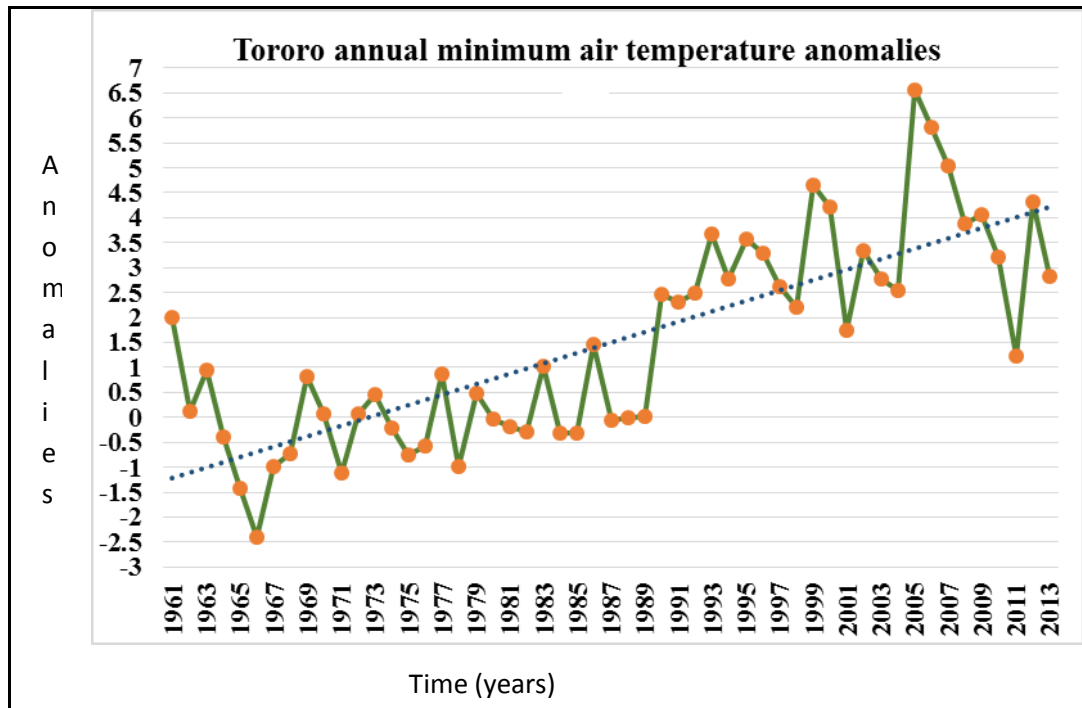


Figure 4.23: Inter-annual variability of annual minimum surface temperature anomalies over Tororo station during 1961-2013.

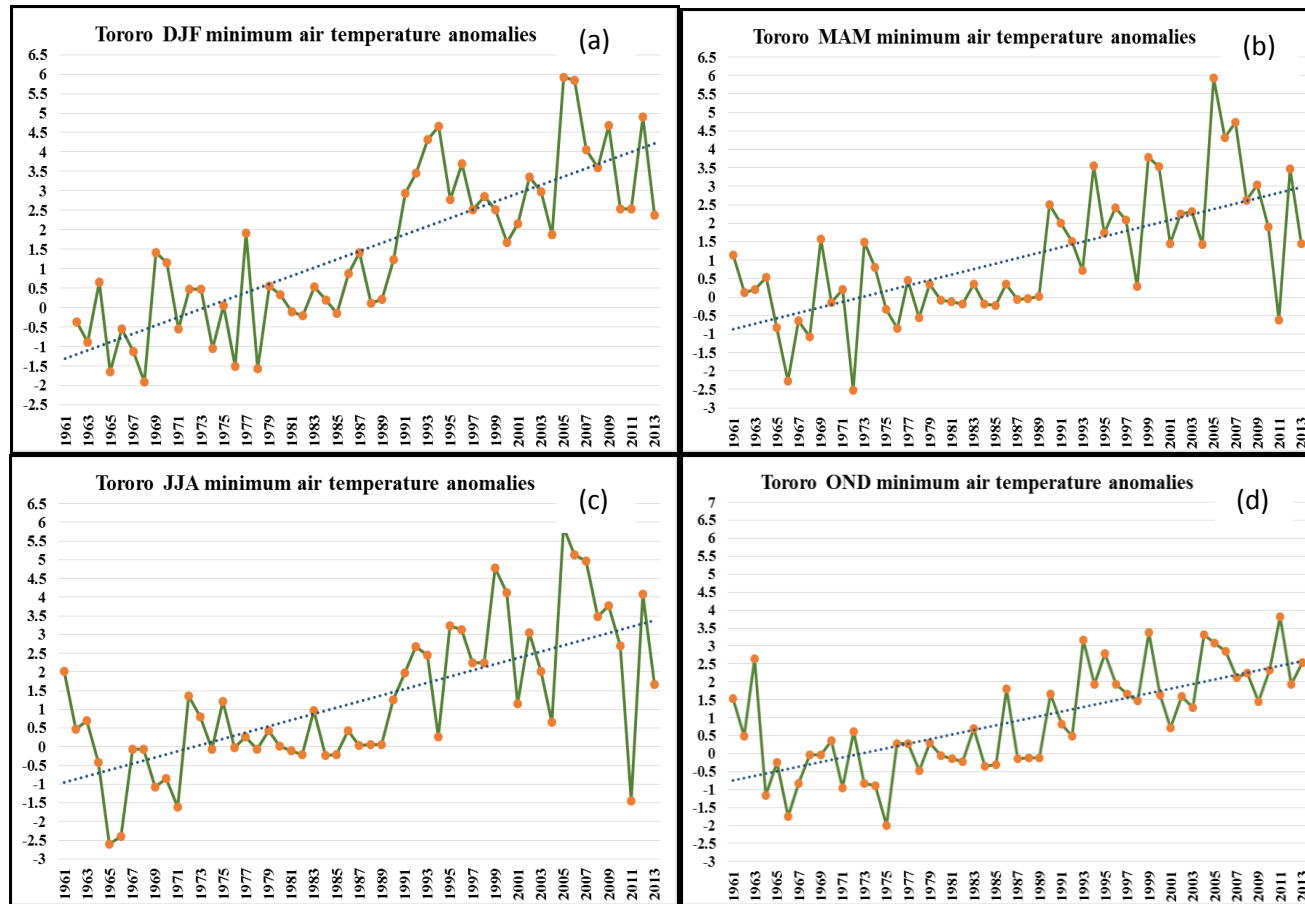


Figure 4.24 (a-d): Inter-annual variability of seasonal minimum surface temperature anomalies for December-February (DJF, a), March-May (MAM, b), July-August (JJA, c) and October-December (OND, d) over Tororo station during 1961-2013.

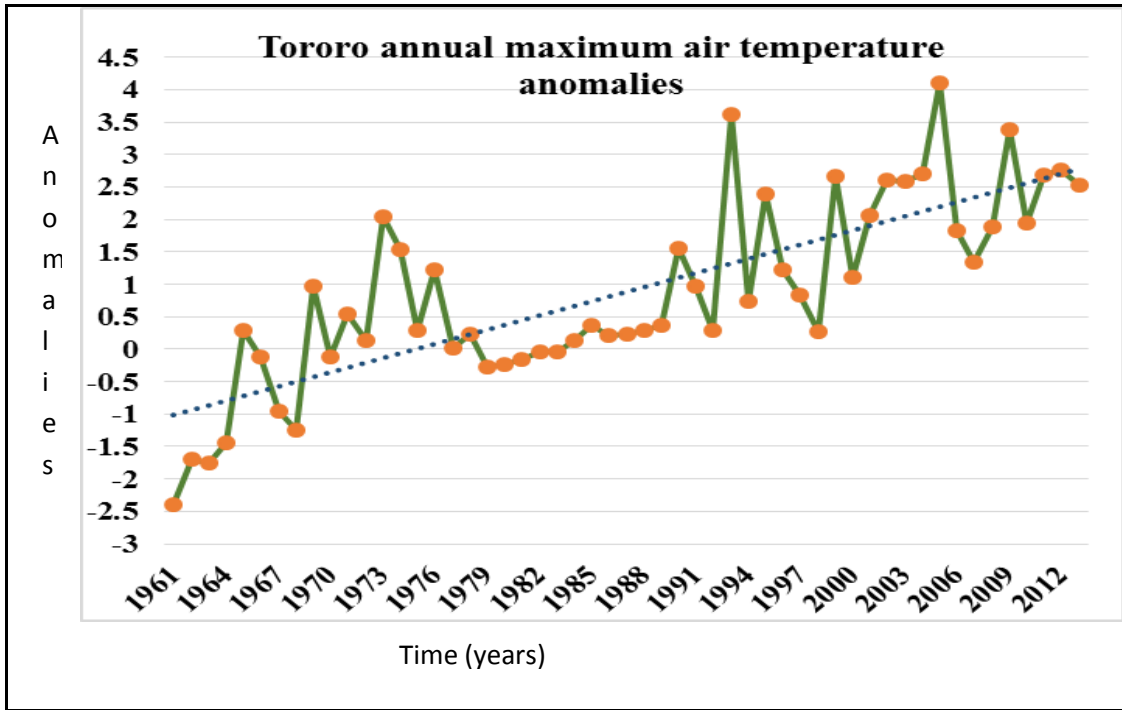


Figure 4.25: Inter-annual variability of annual maximum surface temperature anomalies over Tororo station during 1961-2013.

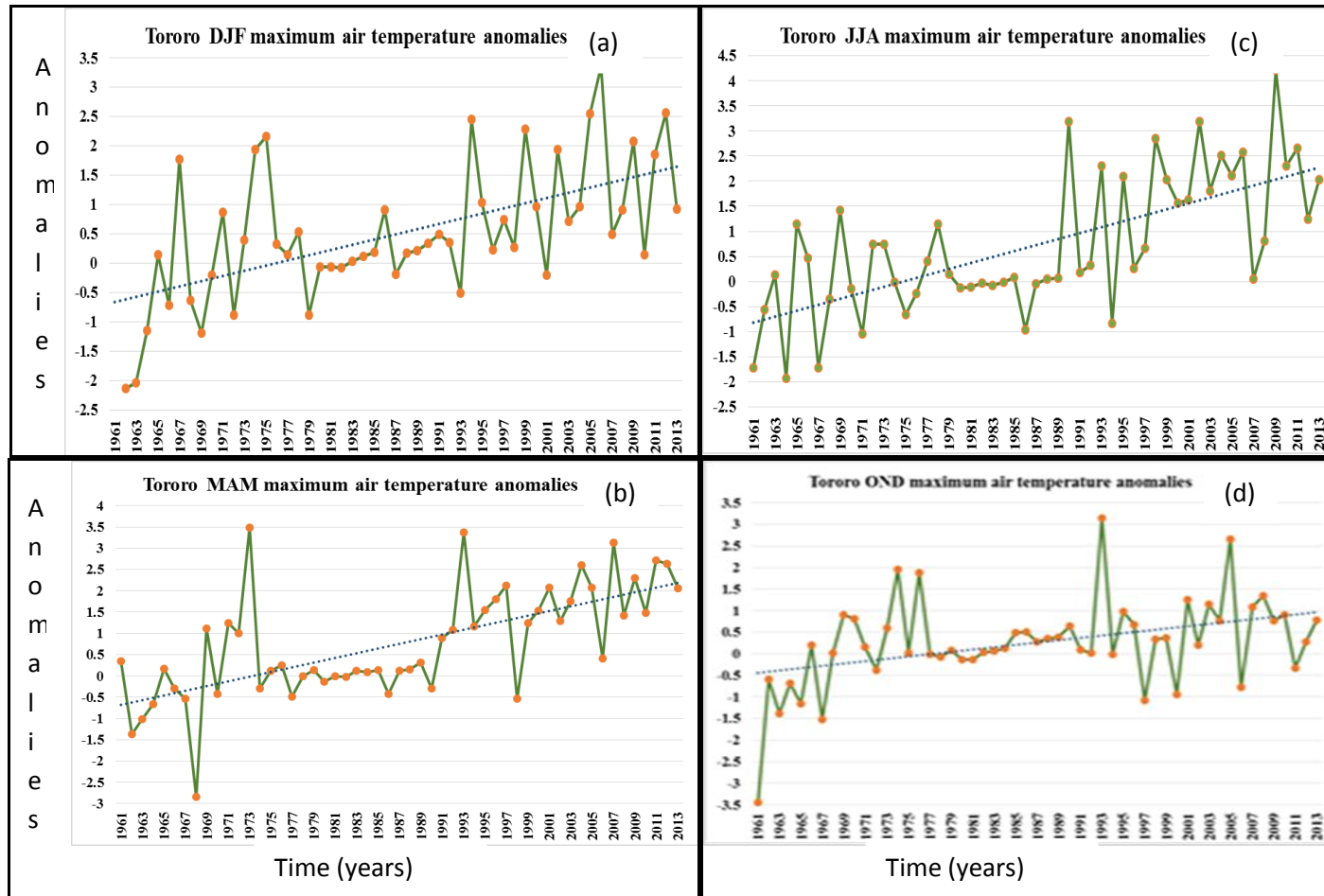


Figure 4.26 (a-d): Inter-annual variability of seasonal maximum surface temperature anomalies for December-February (DJF, a), March-May (MAM, b), July-August (JJA, c) and October-December (OND, d) over Tororo station during 1961-2013.

As indicated in the previous section, graphical representation of trends in surface temperature time series presented in previous section may be subjective. The study considered statistical methods to determine the statistical measure of trends in surface temperature time series. The analysis in this part of the study focused on MAM, JJA and OND seasons. Although temperatures anomalies during January and February could affect the bananas through time lagged responses, this specific study focused on relationships within the seasons that coincide with main rainfall seasons.

Tables 4.5-4.6 show results for the Mann Kendall trend statistics for both minimum and maximum surface temperature during the various seasons. The results showed that all the observed surface temperature trends were significantly increasing with variations in the rate of increase across the seasons and location. This has also been observed in many past studies in the region and worldwide as a reflection of global and regional warming trends (King'uyu *et al.*, 2000; Mahe *et al.*, 2001; Kruger and Shongwe, 2004; New *et al.*, 2006; IPCC, 2012; IPCC, 2014 and Nsubuga *et al.*, 2014).

Table 4.5: Mann Kendall trend test statistics for seasonal surface minimum temperature

Station	MAM		JJA		OND	
	Tau	Significant at 0.025?	Tau	Significant at 0.025?	Tau	Significant at 0.025?
Arua	0.50	Yes	0.66	Yes	0.61	Yes
Entebbe	0.35	Yes	0.28	Yes	0.30	Yes
Gulu	0.49	Yes	0.61	Yes	0.61	Yes
Kabale	0.48	Yes	0.52	Yes	0.52	Yes
Kampala	0.37	Yes	0.47	Yes	0.47	Yes
Kasese	0.63	Yes	0.68	Yes	0.56	Yes
Lira	0.47	Yes	0.57	Yes	0.60	Yes
Masindi	0.47	Yes	0.61	Yes	0.56	Yes
Mbarara	0.55	Yes	0.38	Yes	0.42	Yes
Namulonge	0.40	Yes	0.52	Yes	0.50	Yes
Soroti	0.41	Yes	0.29	Yes	0.51	Yes
Tororo	0.51	Yes	0.55	Yes	0.48	Yes

Table 4.6: Mann Kendall trend test statistics for seasonal surface maximum temperature

Stations	MAM		JJA		OND	
	Tau	Significant at 0.025?	Tau	Significant at 0.025?	Tau	Significant at 0.025?
Arua	0.47	Yes	0.58	Yes	0.55	Yes
Entebbe	0.27	Yes	0.30	Yes	0.44	Yes
Gulu	0.48	Yes	0.59	Yes	0.54	Yes
Kabale	0.39	Yes	0.42	Yes	0.43	Yes
Kampala	0.41	Yes	0.49	Yes	0.51	Yes
Kasese	0.42	Yes	0.37	Yes	0.27	Yes
Lira	0.49	Yes	0.57	Yes	0.55	Yes
Masindi	0.35	Yes	0.34	Yes	0.19	Yes
Mbarara	0.18	Yes	0.29	Yes	0.01	Yes
Namulonge	0.32	Yes	0.45	Yes	0.33	Yes
Soroti	0.05	Yes	0.12	Yes	0.29	Yes
Tororo	0.51	Yes	0.44	Yes	0.35	Yes

Tables 4.7-4.10 indicate changes (observed difference between the two specific sub periods used) in the mean, variability, skewness and kurtosis coefficients of seasonal maximum temperature between the periods 1961-1990 and 1991-2013. The study observed that the degree of variability of extreme temperature events (lowest and highest temperatures), as well as changes in the mean and frequencies were season and region specific. The study results based on the Mann-Kendall trend test (Table 4.5 and Table 4.6) observed that increasing trends in seasonal surface minimum and maximum temperature were statistically significant at 95% confidence level during the three seasons for all the stations.

It was also evident from the results (Tables 4.7-4.10) that there have been observed changes in four moments of minimum surface temperature during MAM, JJA and OND for different station of Uganda. The variability in maximum surface temperature has increased in some areas but results (Table 4.8) also observed cases of decreasing variability especially during October to December (OND) season.

As was indicated earlier, changes in the mean and variance are often used but there is need to investigate how other statistics, namely skewness and kurtosis also change in the climate data series. The results of this study have observed that there are observed changes in the skewness (Table 4.9) and kurtosis coefficients (Table 4.10). The direction of the change in the skewness and kurtosis coefficients varies with the location and season. In some cases, the observed changes vary slightly while in other cases the changes are uniform across different seasons and stations. Close patterns were also observed in seasonal minimum surface temperature trends

over station of Uganda. Results similar to the findings of this study have been observed in some previous studies (Mahe *et al.*, 2001; Kruger and Shongwe, 2004; IPCC, 2012; IPCC, 2014 and Nsubuga *et al.*, 2014) have observed similar results in many parts of Africa including Uganda.

Table 4.7: Changes in the mean ($^{\circ}\text{C}$) of seasonal maximum surface temperature series between the periods 1961-1990 and 1991-2013 over Uganda

Stations/Seasons	MAM	JJA	OND
Arua	1.1	1.0	1.2
Entebbe	1.0	1.0	1.1
Gulu	1.2	1.1	1.2
Kabale	0.8	0.9	1.0
Kampala	1.0	1.1	0.9
Kasese	1.1	1.0	1.0
Lira	1.1	1.0	1.2
Masindi	1.1	1.0	1.1
Mbarara	0.9	1.0	1.0
Namulonge	0.7	1.1	0.6
Soroti	1.0	0.8	0.8
Tororo	1.0	0.8	0.5
Jinja	1.0	1.0	1.1

Table 4.8: Changes in the variability (standard deviation, $^{\circ}\text{C}$) of seasonal maximum surface temperature series between the periods 1961-1990 and 1991-2013 over Uganda

Stations/Seasons	MAM	JJA	OND
Arua	0.2	0.1	0.2
Entebbe	0.3	0.3	0.4
Gulu	0.2	0.1	0.2
Kabale	0.2	0.3	0.4
Kampala	0.2	0.2	0.2
Kasese	0.2	0.2	0.2
Lira	0.2	0.2	0.2
Masindi	0.3	0.2	0.3
Mbarara	0.2	0.3	0.4
Namulonge	-0.1	0.0	0.1
Soroti	-0.3	-0.2	-0.3
Tororo	-0.1	0.1	0.0
Jinja	0.3	0.3	0.3

Table 4.9: Changes in the skewness coefficient of seasonal maximum surface temperature series between the periods 1961-1990 and 1991-2013 over Uganda

Stations/Seasons	MAM	JJA	OND
Arua	0.0	-0.5	1.5
Entebbe	-0.4	-1.1	-0.2
Gulu	0.0	-0.9	1.3
Kabale	0.0	-0.5	-0.5
Kampala	-1.1	-1.2	-0.6
Kasese	-1.2	-0.8	-1.5
Lira	0.0	-1.1	1.2
Masindi	-0.2	-1.0	1.1
Mbarara	-0.2	-0.5	-0.7
Namulonge	0.0	0.1	1.6
Soroti	0.4	1.7	0.7
Tororo	-1.2	-0.9	1.9
Jinja	0.2	-1.0	0.1

Table 4.10: Changes in the kurtosis coefficients of seasonal maximum surface temperature series between the periods 1961-1990 and 1991-2013 over Uganda

Stations/Seasons	MAM	JJA	OND
Arua	-1.2	-2.0	-1.9
Entebbe	-1.3	-1.0	-2.5
Gulu	-1.1	-1.8	-1.9
Kabale	-0.8	-0.3	-3.1
Kampala	-2.1	-2.7	-1.6
Kasese	-2.7	-1.6	-3.4
Lira	-1.2	-1.5	-1.9
Masindi	-0.8	-1.9	-1.5
Mbarara	-1.2	0.2	-3.1
Namulonge	0.8	-1.0	-1.6
Soroti	0.2	1.6	-0.5
Tororo	-5.2	-3.0	-3.0
Jinja	-1.1	0.0	-2.3

The results from analyses of moments of rainfall and surface temperature as reflected by changes in mean, variance, skewness and kurtosis coefficients have revealed that;

- (i) Between the periods 1961 - 2013, there have been little or no changes in the contribution of the individual seasons to the annual total rainfall over the years except over few areas. The contribution of the season to annual total rainfall for individual

years, however, varies significantly in some years, especially due to extreme rainfall during the ENSO and IOD years.

- (ii) There is a general decreasing trend in MAM seasonal rainfall patterns over most stations that were, however, not statistically significant at 95% confidence level. The JJA and OND seasonal trends observed similar patterns as for the MAM season trends at few locations.
- (iii) Significant trends in seasonal rainfall were observed graphically at many locations over Uganda especially during MAM and OND seasons. Most of the trends of the observed seasonal rainfall for MAM and OND seasons were decreasing and increasing respectively. Many of these trends were found not to be statistically significant when subjected to statistical tests.
- (iv) The second moment (variability) of seasonal rainfall observed that during MAM significant variability is being observed over the Lake Victoria region and eastern parts of Uganda. Rainfall variability was also high during JJA season over northern Uganda that receives peak rainfall during this season. October-December (OND) season observed the highest variability compared to the other seasons due to the strong association of the season with variations in the ENSO and IOD events. High rainfall variability is often associated with recurrences of extreme events with too much/ too little rainfall in some years in most areas.
- (v) Standard Precipitation Indices (SPI) analysis of drought observed year to year recurrences of severe droughts in Uganda but the highest number and intensity of drought occurrences were experienced in the period 1982-1990. It is also observed that there was a reduction in drought occurrences in the recent years over many parts of Uganda.
- (vi) Variability analysis showed significant year to year recurrences of seasonal rainfall extremes associated with floods and droughts in all seasons. Past studies have associated these to recurrences on the anomalies of SSTs in major basins of Pacific and Indian oceans and other global and regional climate systems. Recurrent floods and droughts have far reaching implications on life, livelihoods, and many other socio-economic activities.
- (vii) The results show that there were no clear evidences of significant shifts in the frequencies and magnitudes of the extreme rainfall events at most locations during the various seasons.

- (viii) Both minimum and maximum surface temperature showed significantly increasing trends with variations in the rate of increase across the seasons and locations. This has also been observed in many past studies in the region and worldwide as a reflection of global and regional warming trends.
- (ix) There were changes in the patterns of skewness and kurtosis coefficients at some locations. There were, however, no clear evidences of significant changes in the frequencies and magnitudes of the extreme rainfall events for the specific seasons across the Country.

4.2.5 Results on Banana Varieties and Production Patterns

Figure 4.27 shows the actual values and percentages of area planted (a), production (b) and yields of different banana varieties mainly grown in Uganda. The study observed that banana for food is the main variety grown. For example, the results further showed that the annual production of about 4,017,986 MT (93%, Figure 4.27a) and area planted of about 806,627 Ha (88%, Figure 4.27b) in parts of central, western and eastern Uganda. Both the banana varieties for beer (juice) and dessert are on relatively low production, area harvested and yield compared to banana for food in most parts of Uganda. The subsequent presentation of results and discussions in this thesis therefore refers to banana food which has the highest impact on the agricultural livelihoods and food security of banana farming communities in Uganda.

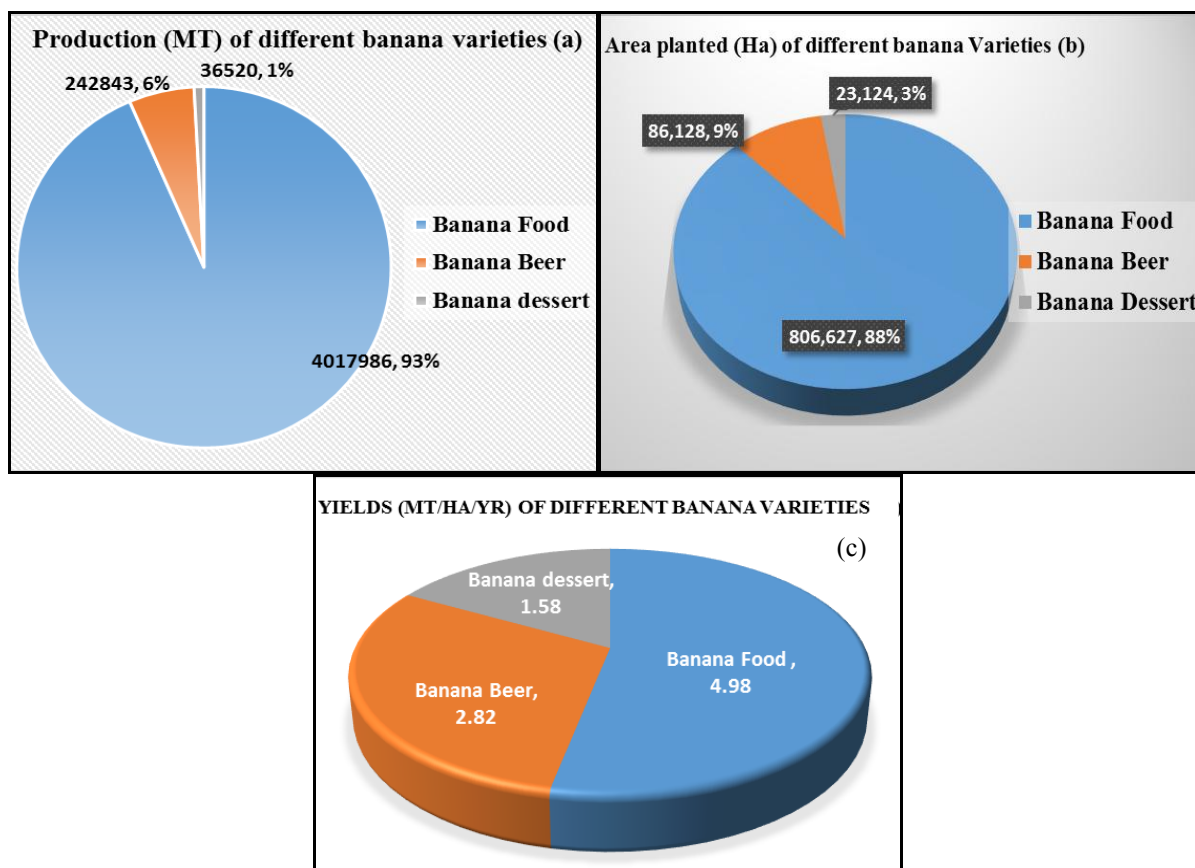


Figure 4.27 (a-c): Production (MT, a), area planted (Ha, b) and Yields (MT/Ha/yr, c) of different banana varieties in Uganda.

Figure 4.28 depicts the inter-annual anomalies of area harvested (blue), production (orange) and banana yield (black) for the period 1971-2009. The mean of the data series was analysed from the period 1971-2000. The results (Figure 4.28) shows that Uganda experienced a decline in the productivity of bananas in 1973, with the productivity improving to its maximum in 1995. The productivity, however, reduced (1995-2005/06) and shows a tendency to increase again thereafter. Major causes of this variability in banana yield figures have been attributed by many researchers to banana pests and disease out breaks (Tushemereirwe *et al.*, 2004), a shift from banana production to other crops by farmers, and variations in weather and climate including extremes that lead to droughts (Van Asten *et al.*, 2011) in banana growing regions of Uganda. Declining trends in crop productivity in this region have been observed in several previous studies (Van Asten *et al.*, 2011; Van den Bergh *et al.*, 2012; Surendran *et al.*, 2014 and Umesh *et al.*, 2015).

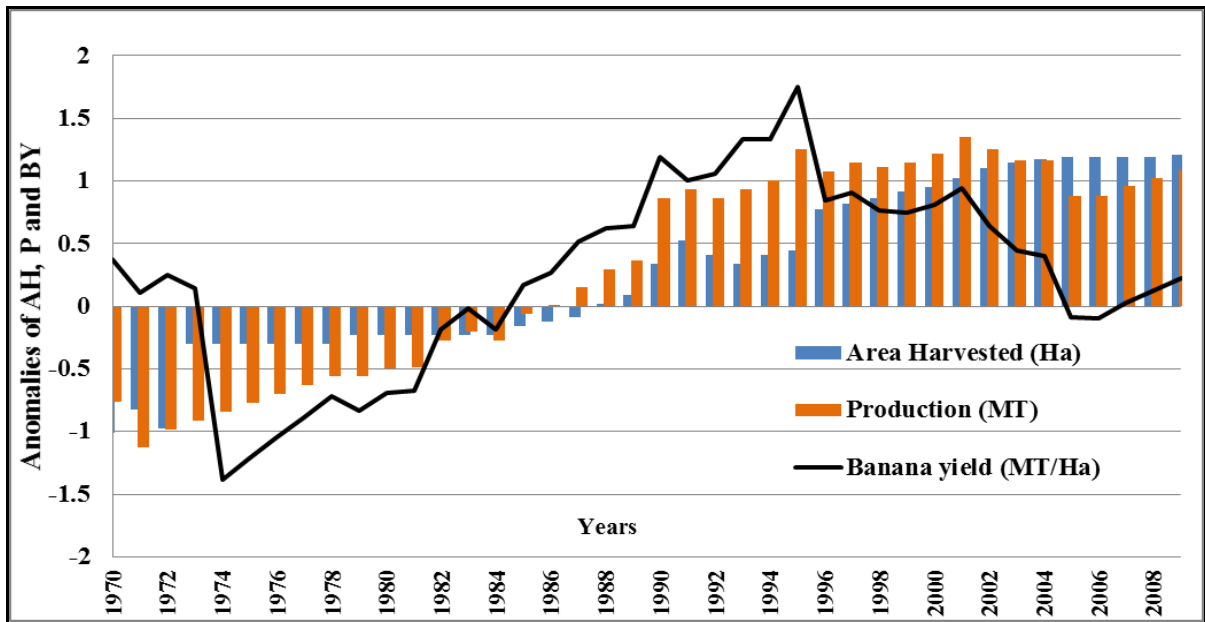


Figure 4.28: FAO estimated trends in Uganda’s standardized Banana Area Harvested (AH, blue bars), Production (P, orange bars), and Banana Yields (BY, black line) during the period 1971-2009.

Figure 4.29 shows the percentages of production (blue) and area harvested (orange) from the different sub regions of Uganda for the period 2008/09 following the Uganda Census of Agriculture (UCA, 2008/09). The study observed that the central region contributed about 20% of total production with 41% of total area harvested; the eastern region contributed about 3% of total production with less than 3% of the total area harvested; the western and southwestern regions combined contributed over 60% of total production with about 50% of the total area harvested; while northern Uganda had the lowest production and area harvested of the banana crop. The western (including southwestern) and central Uganda, therefore, are the major banana production zones with the highest banana productivity observed in southwestern Uganda followed by central parts of the Country (Figure 4.29). These regions were the main focus of this study because of their significant contribution in production of the banana crop. Similar similar patterns in banana production have been observed in Van Asten *et al.*, 2011 and Nyombi, 2013.

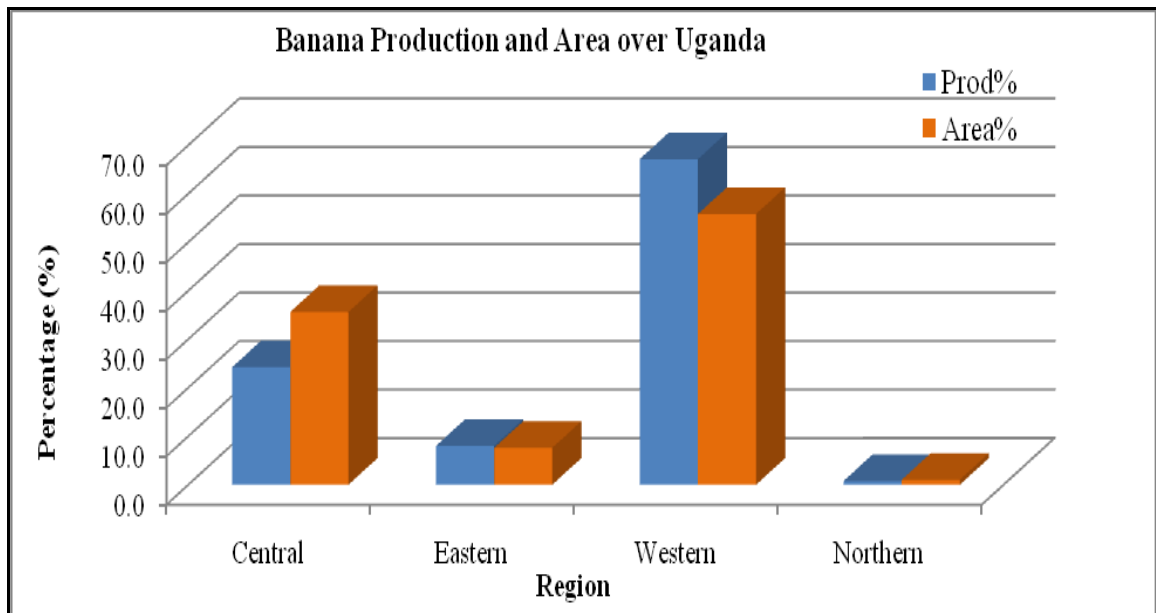


Figure 4.29: Annual banana production (% , blue) and area harvested (% , orange) for Central, Eastern, Western and Northern regions of Uganda.

Figures 4.30 show the production levels (a) and yields (b) for selected districts respectively. Although the production levels of banana in Mbale and Bududa districts is still low (Figure 4.30 a) due to a small area planted of bananas, this region shows the highest level of yield values (Figure 4.30 b). The low production levels of banana can be attributed to the cultural values of communities in these districts who prefer other alternative crops as food and cash crops (maize) and limited market for bananas in the region. On the other hand, the high productivity (Figure 4.30 b) of bananas in Mbale and Bududa areas can be associated with high rainfall on the windward side of Mt. Elgon that is evenly distributed throughout the year in addition to fertile soils down slope of the mountain.

The results further observed that western districts (Bushenyi, Mbarara, Kabarole and Ntungamo) of Uganda recorded higher production figures than central districts (Masaka, Mubende, Mpigi and Rakai) (Figure 4.30 a). Figure 4.30 (b) on the other hand, observed relatively high banana yields over the western districts than for both the central and eastern districts. The high productivity of bananas in the western region has been attributed to the relatively lower average temperatures, good crop management practices and readily available cattle manure to replenish soil fertility in banana crop fields. Similar results have been observed by Van asten *et al.* (2011); Wairegi *et al.* (2010), Van asten *et al.* (2011) and Nyombi (2013).

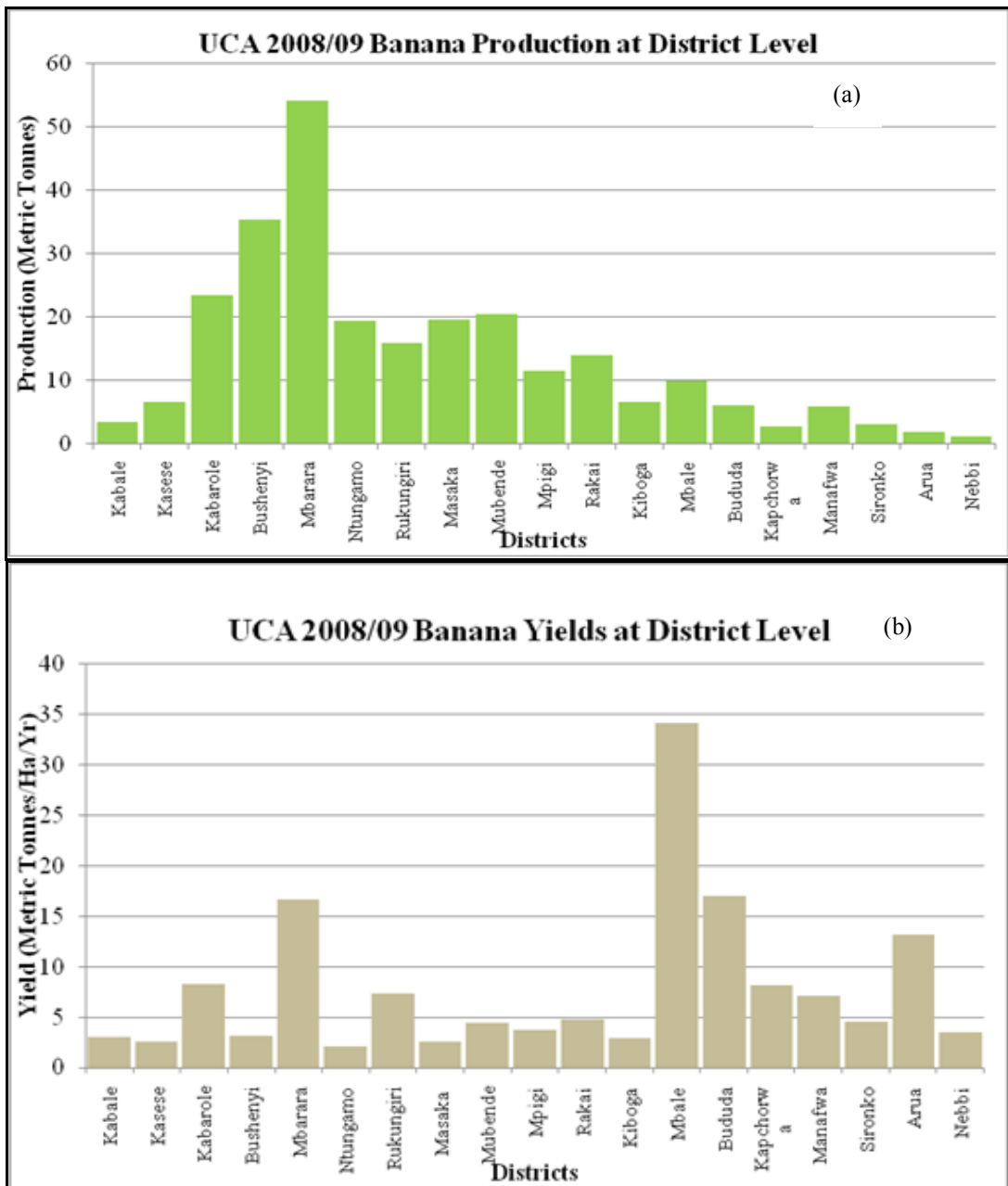


Figure 4.30 (a-b): Banana production (metric tonnes, a) and Banana yields (metric tonnes per Hactare per year, b) per district for 2008/2009 Uganda Census of Agriculture in Uganda (UBOS, 2010).

Figures 4.31 (a-b) shows the spatial patterns of current banana area harvested (Ha, a), production (metric tonnes, b) and banana yields (Metric tonnes per hectare) for the year 2008/2009. The results in Figure 4.31 (a) indicated the spatial patterns of area harvested (hectares) with the southwestern region showing banana plantations extending to as much as 46,953 hectares, with the central regions reporting plantation sizes between 1,529-23,627 hectares. Figure 4.30 (b) shows that the production of banana is highest in the southwestern

and estimated at 290,891-552,075 metric tonnes, that reduces towards central, eastern regions with very little or no banana production in the northern districts. On the other hand, Figure 4.31 (c) depicts the productivity (metric tonnes per hectare) for the year 2008/09 over Uganda. The results in Figure 4.31 (c) observed that highest banana productivity is currently observable over southwestern parts of the Country especially Bushenyi, Mbarara and Ntungamo districts. High to moderate productivity levels were observed in the Central (around L. Victoria), Eastern (areas around Mbale and Mt. Elgon), and northwestern parts of Uganda particularly Arua district. It is observed, however, that the production levels in the eastern and northwestern regions are still much lower compared to western and central districts. There is limited banana production activity in the northern part of the Country with moderate productivity levels over northwestern parts of the Country. Despite high annual rainfall totals, the dry spells longer than three months (October-May) and high surface temperatures in the northern parts of the country have been a major limitation to banana production in the region.

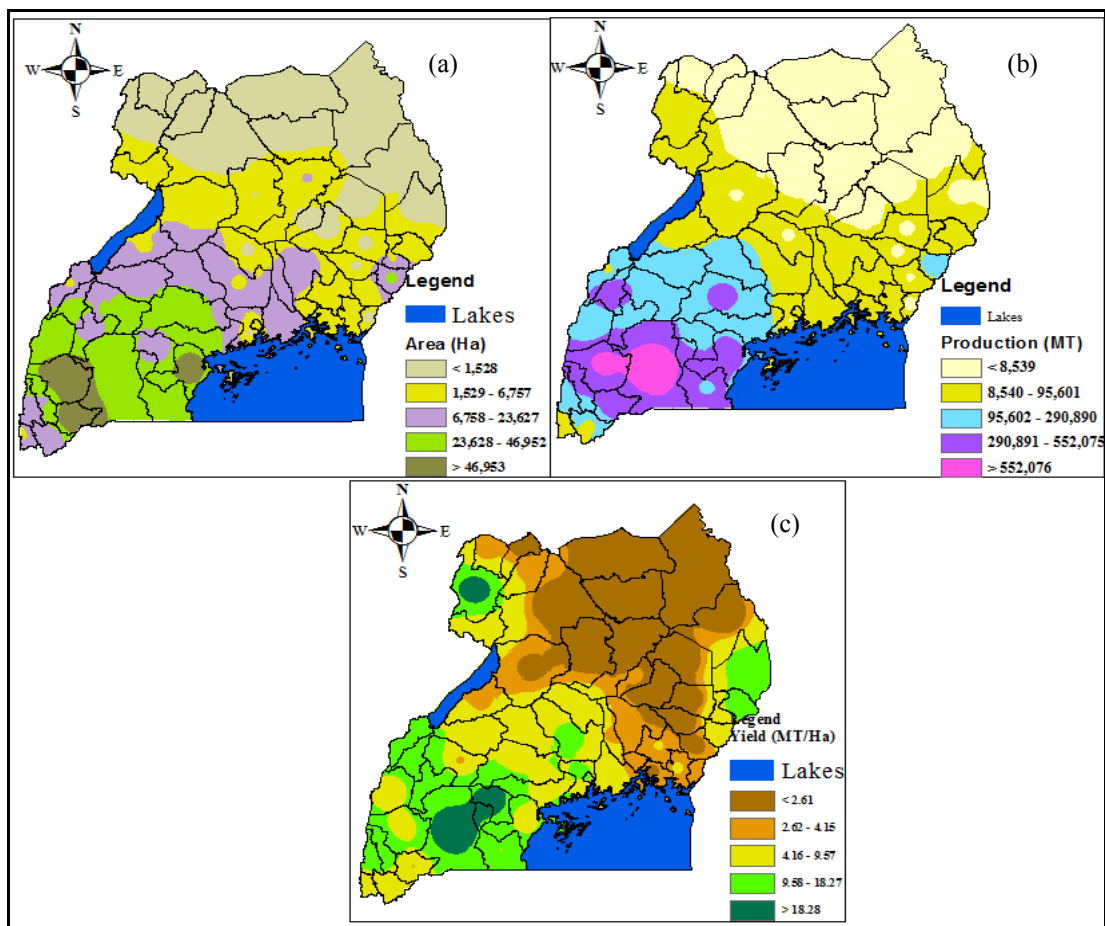


Figure 4.31 (a-c): Spatial patterns of banana area harvested (Ha, a), production (MT, b) and yields (MT/Ha, c) for 2008/2009 over Uganda.

4.2.6 Linkages between Observed Banana Productivity and Climate Variability based on Moments of Climate and Banana Series.

It has been highlighted under methodology section that linkages between banana yield and climate are very complex and require detailed long period data and specific field experiments that were out of the scope for this study. The study adopted empirical methods to compare interannual variability of climate and banana productivity based on various moments of the individual time series (Section 3.2.2). The interannual patterns of the first, second, third and fourth moments of the climate series as reflected from the mean, variance (standard deviation), skewness and kurtosis coefficients were presented in sections 4.2.1 to 4.2.4. This section presents results from the computed banana mean, standard deviation, skewness and kurtosis coefficients. It was observed under data section that only annual banana yields data were available for the study. The annual banana and climate records were first standardized to allow comparisons to be made for the two regions considered in detail.

Table 4.11 and 4.12 show results of time series moments for standardized climatic variables and banana yields over western and central parts of Uganda respectively. The results show that there were some cases when the moment values for both climate and bananas were comparable as highlighted in Tables 4.11 and 4.12 reflecting some close linkages between variations in banana yields and variability in climate parameters. Significant differences were, however, observed in the values of the climate and bananas moment values. This may partly be attributed to other non-climatic factors that affect banana productivity including variations in soil fertility, pests, diseases, management practices (Van asten *et al.*, 2005) among others . Complexity in the effects of rainfall and temperature on banana productivity have also been discussed in previous studies including Van Asten *et al.* (2011); Van den Bergh *et al.* (2012) and Washington and Pearce (2012) among other studies.

It may be concluded from the comparison of the moments of interannual banana yield and climate variability that;

- (i) When all the four moments of time series are considered, the cumulative effect of rainfall and surface temperature variations seems to be discernible at both locations, reflected by significant changes in the values of some coefficients of the moments.

- (ii) There were cases when the moment values for both climate and bananas were comparable reflecting some close linkages between banana yields and climate variability parameters. Significant differences were, however, observed in the values of the climate and bananas moment values.

Table 4.11: Comparison of time series moments of normalized rainfall, maximum, minimum surface temperatures and banana yields (highlighted values indicate agreement on the direction) over western Uganda

Variables/moments/ periods		Rainfall	Maximum Temperature	Minimum Temperature	Banana Yields
Mean	1971-2009	0.00	0.00	0.00	0.00
	1971-1990	-0.63	-0.06	-0.60	-0.76
	1991-2009	0.60	0.06	0.56	0.72
Standard deviation	1971-2009	1.00	1.00	1.00	1.00
	1971-1990	0.56	1.07	0.78	0.67
	1991-2009	0.55	0.95	0.86	0.68
Skewness coefficient	1971-2009	-0.42	0.23	0.35	0.06
	1971-1990	0.06	0.46	0.53	-1.42
	1991-2009	-0.04	-0.01	0.45	1.77
Kurtosis coefficient	1971-2009	-0.31	0.15	-0.43	1.46
	1971-1990	-0.99	1.34	-0.60	1.08
	1991-2009	-0.77	0.92	-0.82	1.05

Table 4.12: Comparison of time series moments of normalized rainfall, maximum, minimum surface temperatures and banana yields (highlighted values indicate strong linkages) over central Uganda

Variables/moments/ periods		Rainfall	Maximum Temperature	Minimum Temperature	Banana Yields
Mean	1971-2009	0.00	0.00	0.00	0.00
	1971-1990	-0.83	-0.27	-0.79	-0.70
	1991-2009	0.60	0.26	0.75	0.66
Standard deviation	1971-2009	1.00	1.00	1.00	1.00
	1971-1990	0.98	0.97	0.66	0.45
	1991-2009	0.55	0.98	0.60	0.93
Skewness coefficient	1971-2009	-0.62	0.46	-0.04	0.95
	1971-1990	0.06	0.54	0.08	-0.18
	1991-2009	-0.17	0.52	0.62	0.76
Kurtosis coefficient	1971-2009	-0.41	0.27	-0.54	1.02
	1971-1990	-0.87	0.92	-0.70	-1.09
	1991-2009	-0.57	0.20	0.72	1.09

4.2.7 Results from Correlation and Regression Analysis

Further investigations of the linkages between variations in climate variations and banana yields have been undertaken using other methods and tools. These include computation of correlation coefficients, use of polynomial regressions (to determine optimal values of climate parameters that correspond to maximum banana yield) and the FAO CROPWAT model that is a more robust tool (Smith, 1992; Clarke *et al.*, 2001 and FAO, 2003b) due to its ability to estimate the response of banana yields to variations in climatic parameters with the consideration of the intraannual climate characteristics. The results are presented in the subsequent sections.

Table 4.13 shows results of correlation coefficients between banana yields and climatic variables. The study observed close linkages between banana yields and surface temperature variability with lower correlation values between banana yields and rainfall anomalies for the two regions. The western region showed a stronger response of variation in banana yields for both minimum and maximum surface temperature than the central region.

Table 4.13: Correlation coefficients (coefficient of determination, R^2) between climatic variables and banana yields for western and central regions of Uganda.

Region	Minimum Temperature	Maximum Temperature	Rainfall
Western	0.72 ($R^2=52\%$)	0.78 ($R^2=61\%$)	0.34 ($R^2=12\%$)
Central	0.41 ($R^2=17\%$)	0.53 ($R^2=28\%$)	0.51 ($R^2=26\%$)

Figures 4.32-4.34 show the relationships between variations in banana yields and climatic parameters including minimum temperature (Figure 4.32), maximum temperature (Figure 4.33) and rainfall (Figure 4.34), over western region. The western region comprises of Kabale, Mbarara, Ntungamo, Rukungiri, Hoima and Kasese districts are the highest producers of bananas in Uganda. Figures 4.32-4.33 show that increase in minimum and maximum temperatures leads to an increase in banana yields up to an optimal value of temperature beyond which any further increase in temperatures would result into a drop in yields. The results (Figure 4.34) also suggest that an increase in rainfall progressively increases banana yields up to the optimal level beyond which the additional rainfall would negatively affect yields. The optimal levels for different locations vary and depend on the environmental and soil characteristics for the location.

The results also showed that in western region, variations in minimum temperature explain about 52% (Table 4.12) of the variations in banana yields, variations in maximum temperature explain about 61% variations in banana yield and variations in annual rainfall explain about 12% of the variation in banana yields (Table 4.12).

The F-test based on the Analysis of Variance (ANOVA) was used to test for the significance of the coefficients of the polynomial regressions. The tests revealed that the regression coefficients were significant upto degree two for the temperature. For the case of rainfall, the coefficients were significant only for degree one. The results were therefore able to determine optimal temperature that would support maximum banana productivity in the region (Figure 4.32-4.33).

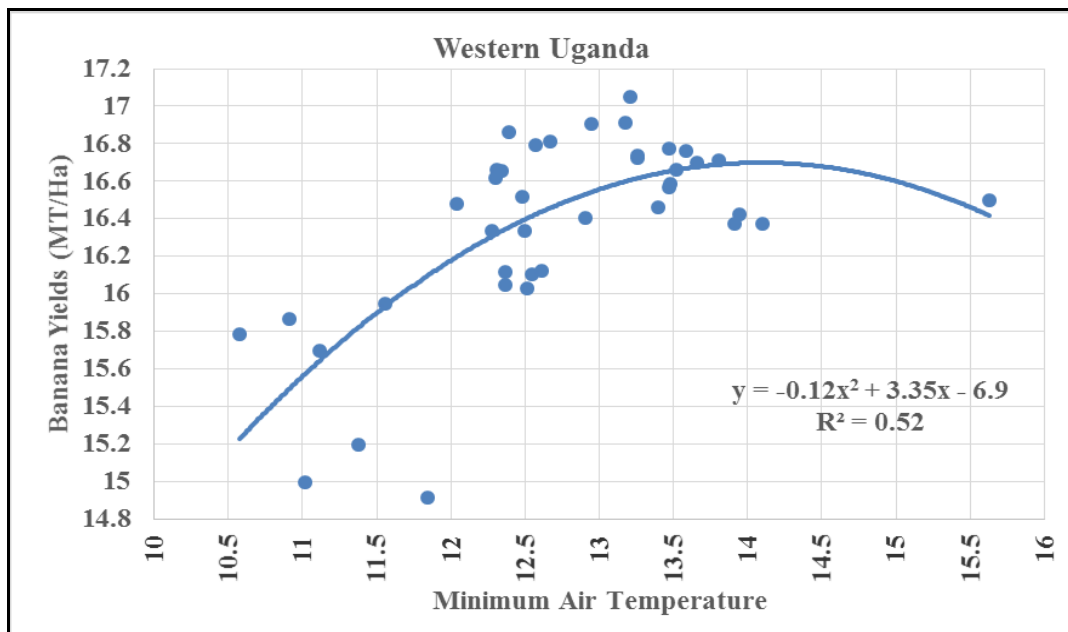


Figure 4.32: Relationship between banana yields (MT/Ha) and minimum surface temperature (°C) for the western region of Uganda.

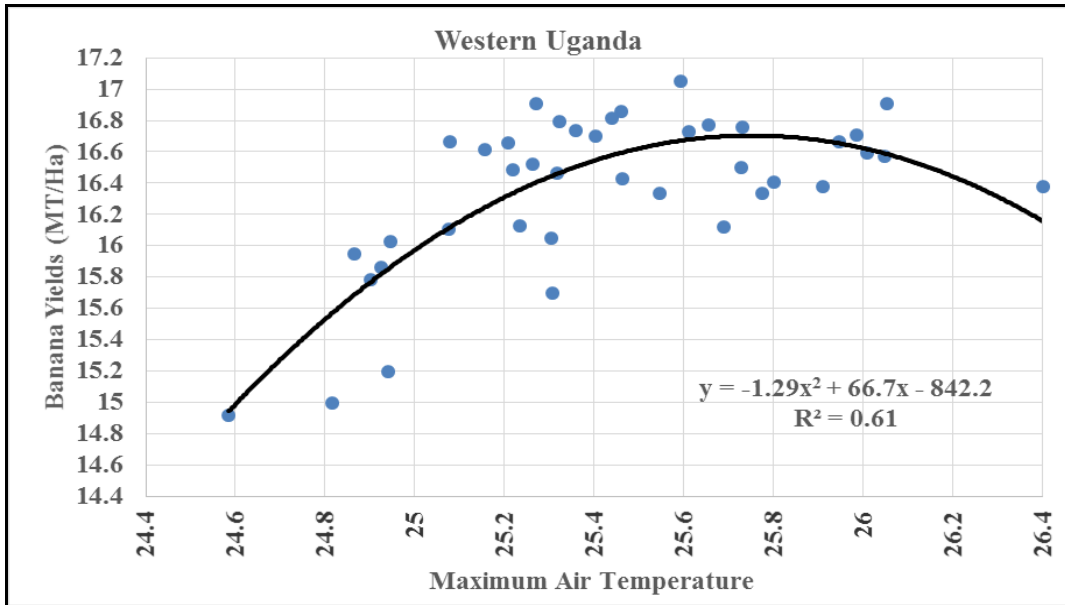


Figure 4.33: Relationship between banana yields (MT/Ha) and maximum surface temperature (°C) for western region of Uganda.

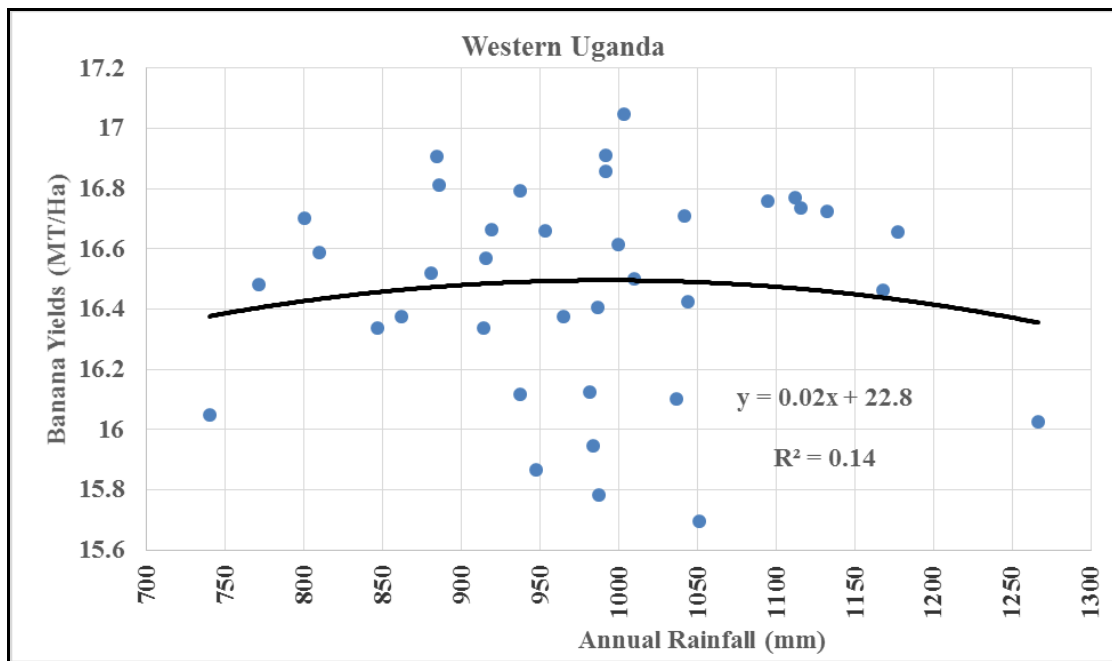


Figure 4.34: Relationship between banana yields (MT/Ha) and rainfall (mm) for western region.

Results on the relationship between banana yields and climatic variables for the central region are presented in Figures 4.35-4.37. In the central region, the study observed that variations in minimum temperature explained about 17% of the variations in banana yields, variations in maximum temperature explain about 28% variations in banana yields and variations in annual rainfall explain about 26% of the variation in banana yields. The responsiveness of banana

productivity to variations in climate over the western region is higher than that observable over the central region.

The Country's current minimum and maximum temperature levels in western and central Uganda still support favorable growth of bananas. Any further increases in temperatures beyond the optimal values will adversely/negatively affect banana production in many parts of Uganda. It has also been observed in several other studies, however, that warm temperatures are associated with the high population densities of banana nematodes and weevils (Speijer *et al.*, 1993; Speijer and Kajumba, 1996 and Talwana *et al.*, 2000) especially in the central region that tend to affect banana productivity.

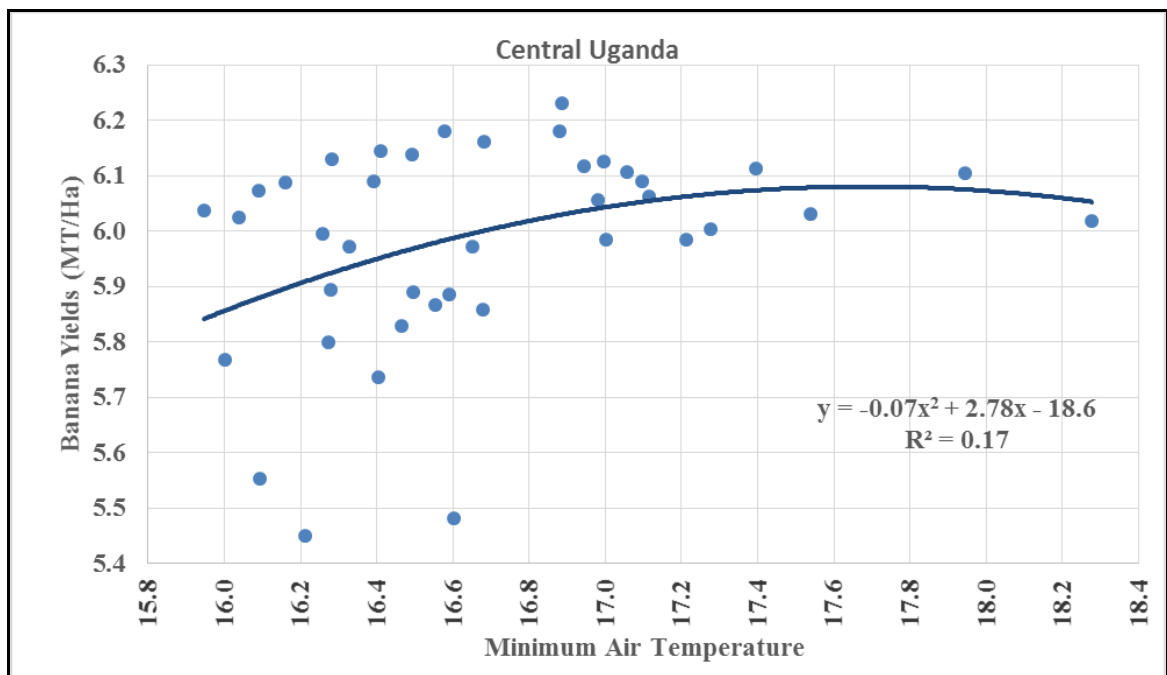


Figure 4.35: Relationship between banana yields (MT/Ha) and minimum surface temperature (°C) for central region of Uganda.

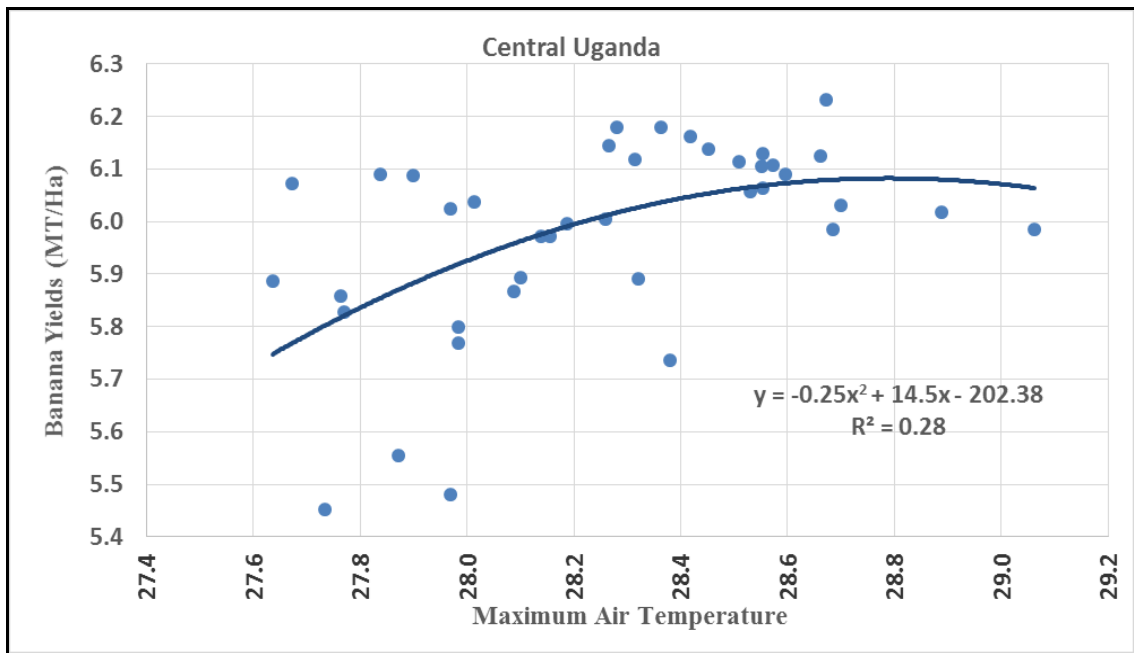


Figure 4.36: Relationship between banana yields (MT) and maximum temperature for central region.

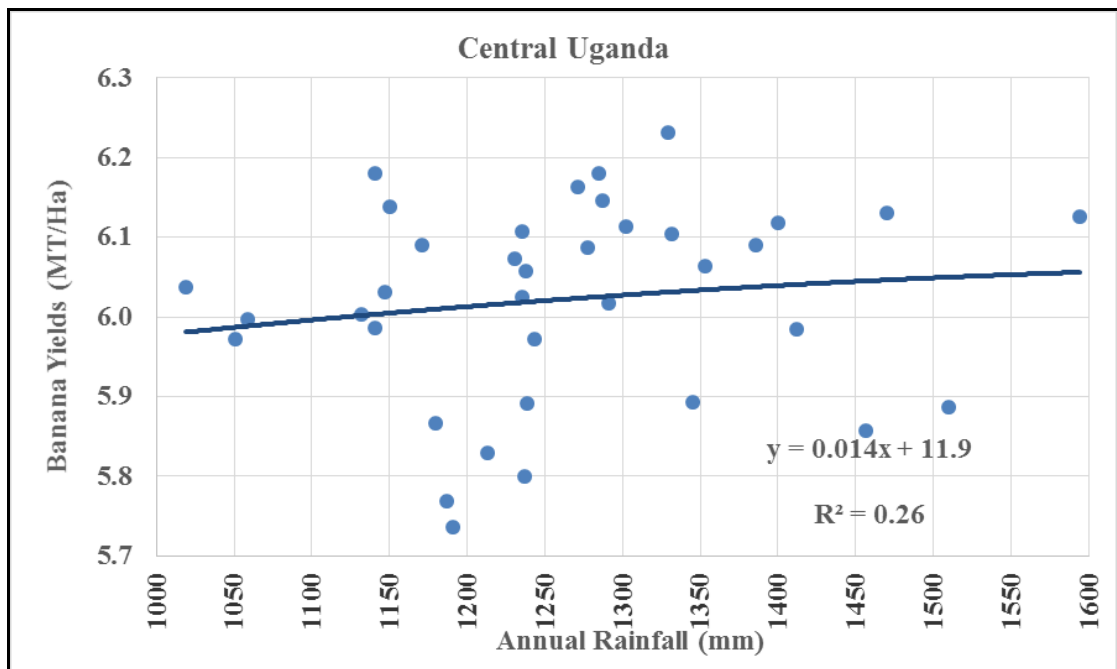


Figure 4.37: Relationship between banana yields (MT/Ha) and rainfall (mm) for central region of Uganda.

The study results in the previous section have observed clear linkages between surface temperature and banana yields variations. The study observed that there are both direct (evapotranspiration and photosynthesis rates) and indirect (crop pest and diseases) effects of temperature on banana yields which make temperature variations strongly linked to variations

in banana yields. The linkages between rainfall and banana yields would not be well captured based on analysis of interannual data time series using statistical methods. This is because, unlike temperature that has low inter and intra seasonal variations, rainfall exhibits stronger inter and intra seasonal variations that are important to understand effects of rainfall variations on banana yields. In addition, the effect of rainfall on yields may be lagged. The limitations in the use of correlation that relates normalized climate and banana yields for the same period were highlighted under Section 3.2.2.

To further understand these complex interactions, the study employed the FAO CROPWAT (Smith, 1992; FAO, 2003b and Karanja, 2006) to investigate the effects of rainfall variations (water stress) on rain-fed banana yields over different parts of Uganda. The tool was used to determine banana crop water requirements, moisture deficits and yield reductions among other parameters for a number of locations over Uganda.

4.2.8 Results on Multiple Regression Analysis

The combined effects of both rainfall and temperature on banana yields were investigated using the multiple linear regression models. Table 4.14 and Figures 4.38-4.39 show the results of the regression models for two regions of Uganda. As noted earlier, both banana and climate data was standardized to enable comparisons to be done. The values of the regression coefficients represented (Table 4.14) indicate the change in the banana yield (in standard deviations) associated with a change of one standard deviation in a particular climatic variable holding the value (s) of the other independent variable(s) constant. The coefficients were tested using the standard error method and found significant.

For example, the study noted that the responsiveness of banana yields was higher for changes in temperature compared with rainfall in the two regions. In addition, seasonal rainfall (temperature) variations were more important than total annual rainfall (average annual rainfall). The regression models revealed that climate variables influence yields and explained 46% (western, Figure 4.38) and 36.4% (central, Figure 4.39) of the variations in yields. The study noted that other non climatic factors such as soil fertility, banana varieties, pests and diseases and cultural values are important constraints for banana production.

Table 4.14: Multiple regression statistics between banana yields and climate variables

Variables / Regions	Regression Constant	Total annual rainfall	Rainfall of driest quarter	Average annual temperature	Temperature of coldest quarter	Adjusted R ²
western	-0.14	0.07	0.42	0.17	0.35	46 %
Central	-0.08	0.11	0.43	0.27	0.18	36.4%

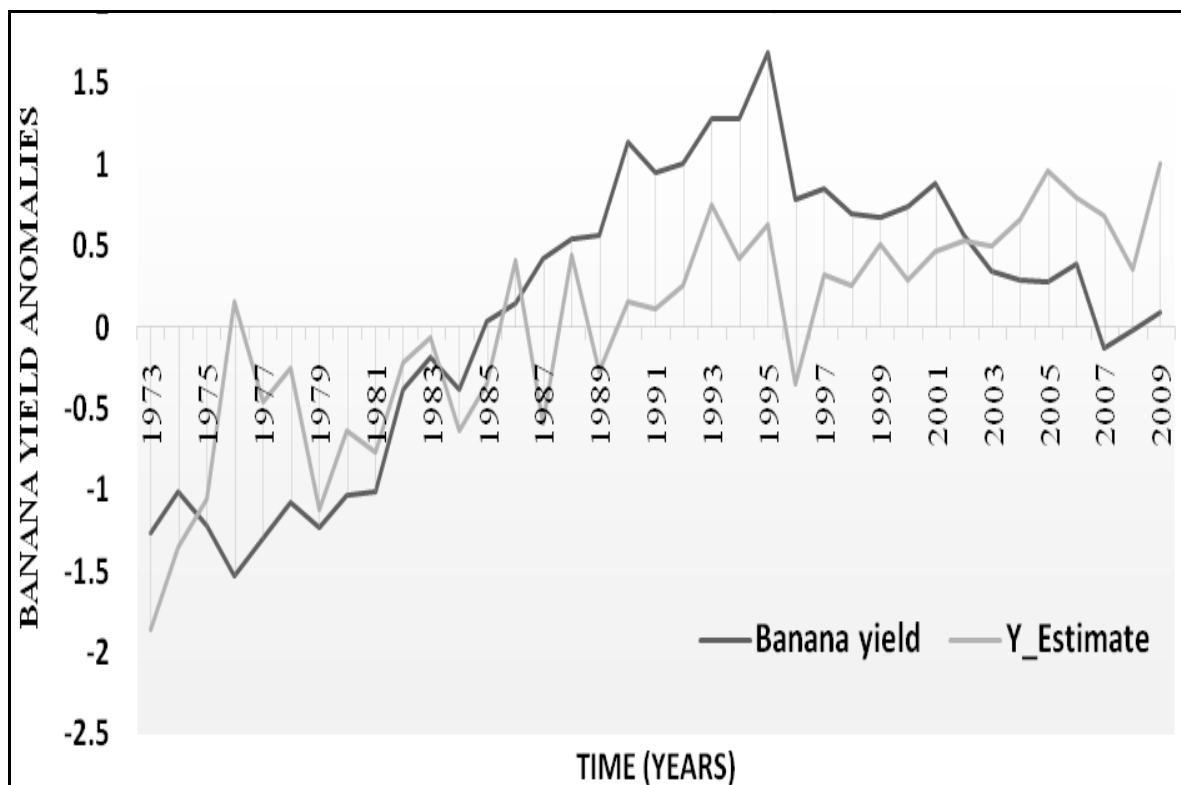


Figure 4.38: Regression model for banana yields over Western Uganda.

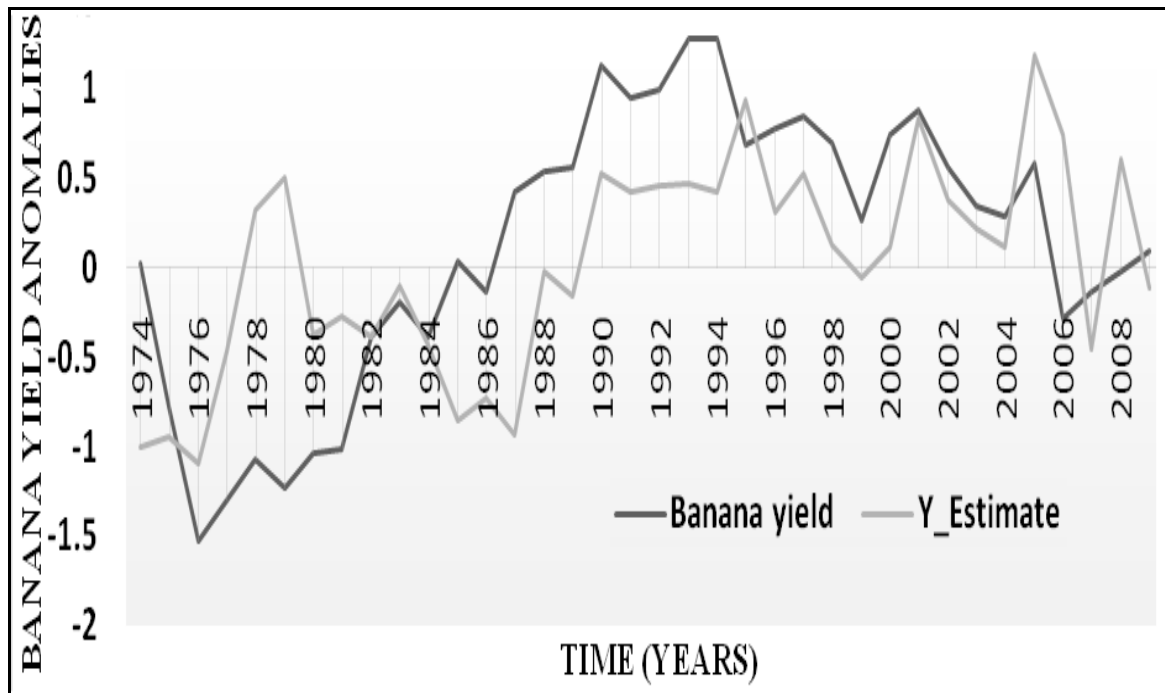


Figure 4.39: Regression model for banana yields over Central Uganda.

4.2.9 Results on FAO CROPWAT Simulation of Banana Crop Water Requirements

The effects of climate variations on banana yields have further been investigated using the FAO CROPWAT that is a more robust tool (Smith, 1992 and FAO, 2003b) and provides more information than statistical methods used in the previous sections. The tool was used to estimate banana crop water requirements, moisture deficits and yield reductions among other crop and water related parameters for different locations. This tool has been used in previous similar study by Karanja (2006) to assessing crop water requirements for different crops and regions. The results based on the FAO CROPWAT model are presented in the subsequent sections.

This section presents results on the analysis of banana crop water requirements under rain-fed banana production over Uganda. A comparison of monthly actual and effective rainfall for different regions is, however, presented first. Figures 4.40 (a-c)-4.42 (a-c) show actual and effective mean monthly rainfall distribution in the year for different regions of Uganda. These results compare both effective and actual monthly rainfall for a given year and also observed the persistence and length of the dry seasons.

Figure 4.40 (a-c) shows rainfall distribution for Kabale (a) and Mbarara (b) in the southwestern region and Kasese (c) to the western region of the Country. The study observed that Kabale (a)

receives 1028 mm of rainfall annually while the effective rainfall for banana is estimated at 861 mm annually. The difference between actual and effective rainfall (rainfall loss) is estimated to be about 167 mm. Mbarara area (b) receives 946 mm of rainfall annual with effective rainfall estimated at about 798 mm which gives rainfall loss of about 148 mm per year. Kasese area (c) on the other hand receives 883 mm of rainfall annually and effective rainfall of 763 mm giving a loss in rainfall of 120 mm annually. The results (Figure 4.38, a-c) further observed that June with mean rainfall of 26 mm and July with mean rainfall of 22 mm are the driest months in Kabale area. April with mean rainfall of 150 mm is the wettest month with the rest of the months receiving between 60-125 mm of rainfall. Over Mbarara (b), June with mean rainfall of 20 mm and July with mean rainfall of 25 mm record the lowest rainfall while November with mean rainfall of 140 mm and April with mean rainfall of 130 mm records the highest rainfall with most months recording rainfall between 50-122 mm. Areas around Kasese (c) receive the lowest rainfall in January with mean rainfall of 22 mm with the highest rainfall recorded in April with mean rainfall of 118 mm.

Figure 4.41 (a-c) presents results on the monthly distribution of annual actual and effective rainfall over central regions including Jinja (a), Namulonge (b) and Mubende (c). The study observed that regions in the central part of the Country receive higher rainfall than western and southwestern regions (Figure 4.41, a-c). It is observed that both the driest months and the wettest months in the central regions receive higher rainfall than the western regions.

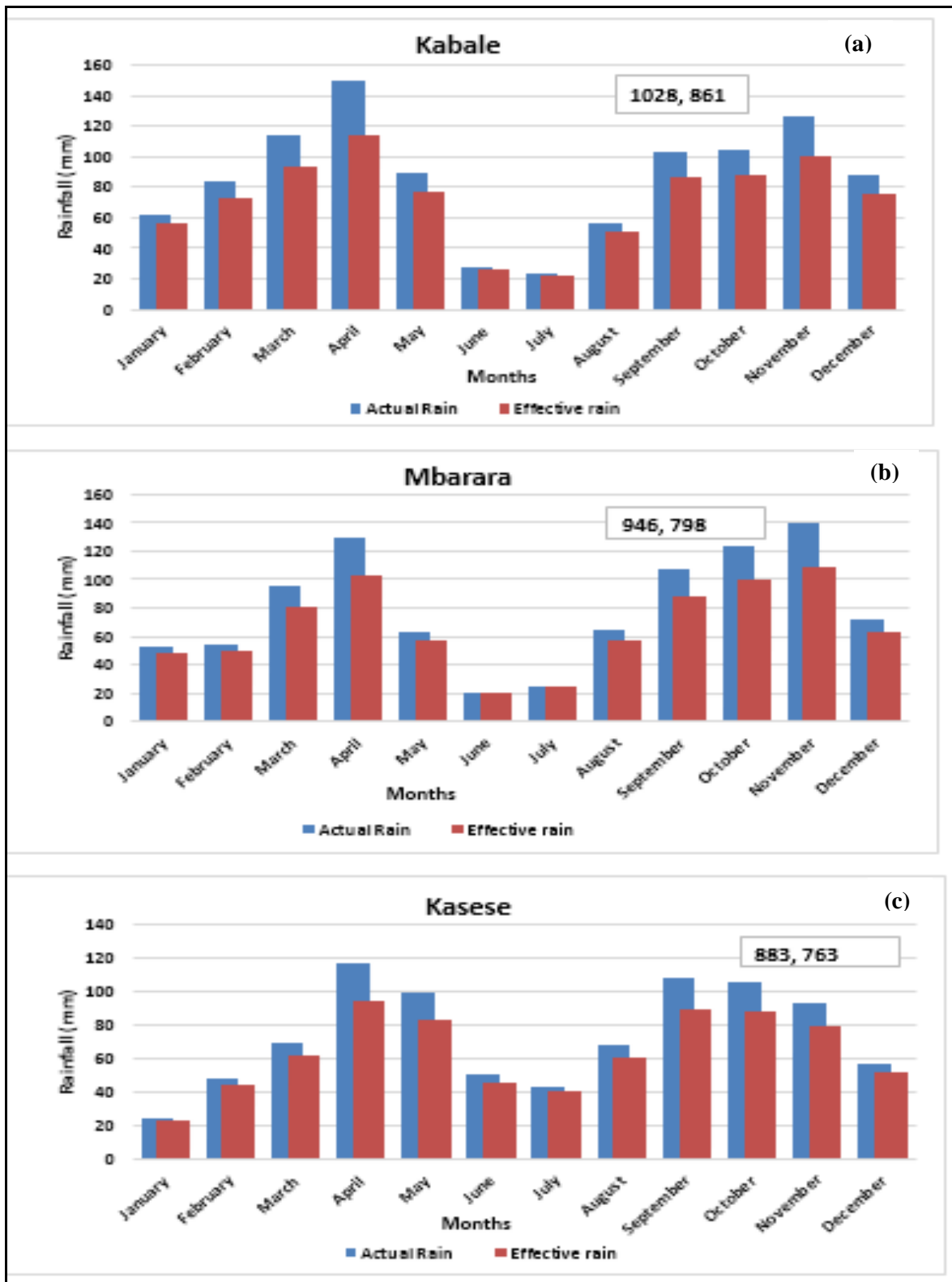


Figure 4.40 (a-c): Variation of monthly actual and effective mean rainfall for Kabale (a), Mbarara (b) and Kasese (c) stations. Numbers in the boxes indicate annual totals of actual and effective rainfall respectively.

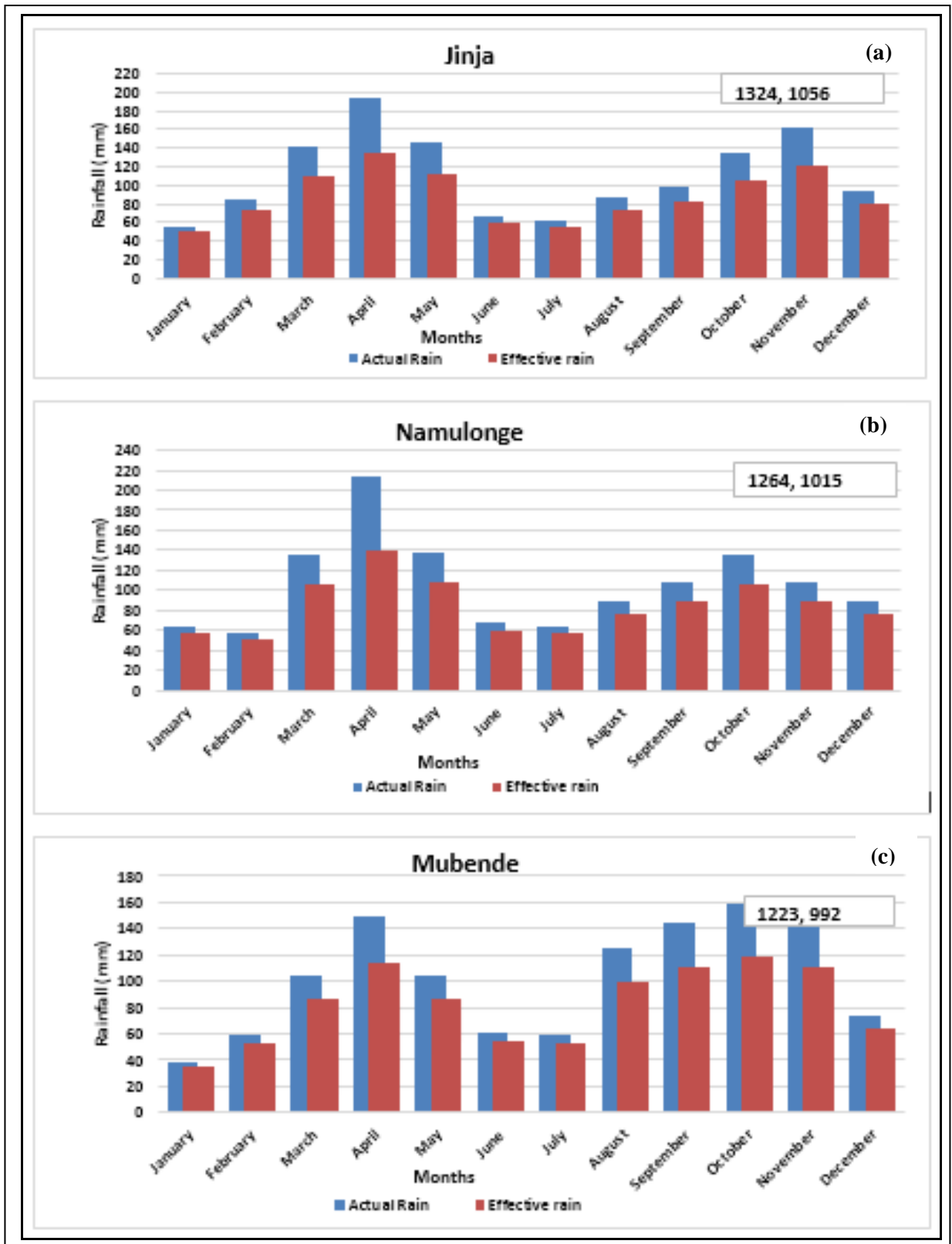


Figure 4.41 (a-c): Variation of monthly actual and effective mean rainfall for Jinja (a), Namulonge (b) and Mubende (c) stations. Numbers in the boxes indicate annual totals of actual and effective rainfall respectively.

Over the eastern part of the Country results show in Figure 4.42 a-c that Soroti (a), Tororo (b) and Mbale (c) recorded annual actual (effective) rainfall of 1383 (1063) mm, 1494 (1154) mm and 1147 (941) mm respectively. The study observed that highest rainfall is recorded over Tororo (b) that receives evenly distributed rainfall throughout the year with January (58 mm) as the driest month while April (212 mm) and May (220 mm) are the wettest months in the year.

This part of the study observed that most of the banana growing regions in Uganda receive between 1000 and 1300 mm of rainfall per year, with dry season not exceeding three consecutive months, observed from June to July and from December to February. This study further observed that although some regions in northern Uganda receive higher annual rainfall than central and western regions, occurrence of long dry spells does not favor banana production in northern Uganda. Similar findings have been observed in some studies (Van Asten *et al.*, 2011). Similar studies (Mubiru *et al.*, 2009; Osbahr *et al.*, 2011 and Claessens *et al.*, 2012) have observed that supporting agricultural innovations such as water harvesting and soil moisture conservation, improving crop varieties and value addition on agricultural outputs can greatly reduce climate risks to agricultural productivity in Uganda.

Table 4.14 shows banana crop water assessment statistics from the FAO CROPWAT during the first year from planting and the second year for crop maturity and harvest. The table presents results on Actual Water Use (AWU), Potential Water Use (PWU), soil Moisture Deficit at Harvest (MDH), Efficiency of Rainfall (ER) and Yield Reduction (YR).

The study (Table 4.15) observed differences in the water requirement and actual water use by banana crop exist across the Country while variations in related parameters are also evident. For example, in all banana growing regions, potential water use by the crop is still higher than actual water use implying that there is a moisture deficit and hence yield reduction in most areas is inevitable. Moisture deficits can either be reduced through irrigation or mulching, the latter is commonly practiced in the southwestern region to improve crop yields at farm level.

The study further observed that the first cycle of banana harvest is associated with higher yield reductions (YR) and lower rain efficiency (ER) than the second cycle of crop harvest. This may be attributable to the differences in Leaf Area Index (LAI) and crop density between the two crop cycles. In addition the seasonal rainfall variations are important. Regions that experience more than three months of rainfall shortages including Kitgum, Lira, Moroto and

Gulu areas can hardly sustain rain-fed banana production and have yield reductions greater than 35% of optimal yields. Intensive mulching is necessary in the plantations to promote moisture conservation and minimize on the water shortages and hence promote yields.

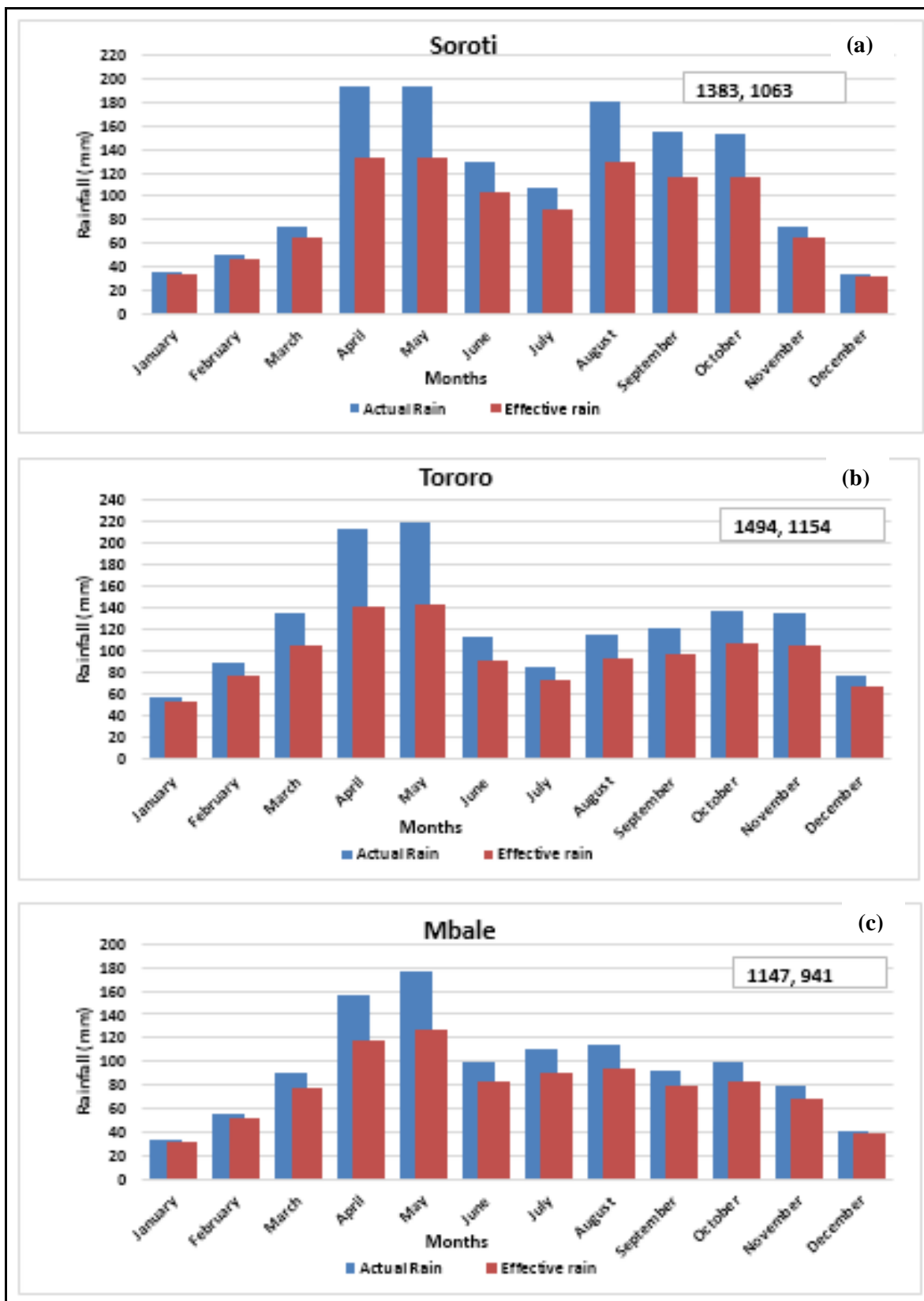


Figure 4.42 (a-c): Variation of monthly actual and effective mean rainfall for Soroti (a), Tororo (b) and Mbale (c) stations. Numbers in the boxes indicate annual totals of actual and effective rainfall respectively.

Table 4.15: Banana crop water statistics and yield reductions (YR) from the CROPWAT model for two crop cycles (highlighted values indicate cases of high yield losses).

Location	First crop cycle					Second crop cycle				
	AWU (mm)	PWU (mm)	MD (mm)	ER (%)	YR (%)	AWU (mm)	PWU (mm)	MDH (mm)	ER (%)	YR (%)
Kabale	898.6	945.9	8.5	88.1	5	654.2	872	78	97.3	25
Mbarara	885.2	1065.8	50.2	89.6	16	678.7	995.4	88.6	98.9	31.8
Kasese	888.5	1243.7	71	94.5	28.6	685.5	1099.2	106.9	97.6	24.6
Kitgum	888.5	1650.8	65.2	64.9	46.2	960.2	1348.4	121.8	85.5	28.8
Lira	950.2	1502.8	50.2	64.6	36.8	1021.5	1206.4	117	86.7	15.3
Mbale	915.3	1374.8	43.9	78	33.4	811.9	1152.1	113.6	92.3	29.5
Hoima	1000.7	1124.8	39.7	67	11	918	1061.9	74.2	81.5	22.9
Moroto	699.2	1281	62.2	73.8	45.4	683.3	1093.7	118.6	93.3	37.5
Mubende	1016.3	1316.1	60.3	79.5	22.8	925.5	1139.4	102.3	98.2	18.8
Namulonge	1020.3	1190.3	11.3	83.9	14.3	816.7	1031.9	91.3	96.2	20.9
Soroti	931.1	1451.7	40.9	67.6	35.9	993.2	1230.7	115.6	90.8	19.3
Tororo	1090.7	1309.2	17.8	76.4	16.7	944.4	1107.5	99.9	90.5	14.7
Jinja	1050.9	1163.9	11.1	81.2	9.7	855.5	1027	87.8	95.5	16.7
Arua	888.4	1385.9	71.7	58.1	35.9	1014.9	1122	114.5	81.5	9.5
Gulu	901	1417.6	40.8	56.5	36.4	990.6	1149.9	118.6	74.2	13.9

It may be concluded from analyses of changes in the moments of banana production as reflected by mean, variance, skewness, and kurtosis, as well as other analyses that;

- (i) Bananas for food are the most popularly grown variety in Uganda. However, despite high production levels and area planted of bananas for food, the yields of different varieties are comparable.
- (ii) Cumulative effects of rainfall and temperature variations on banana yields seem to be discernible in both regions, reflected by significant changes in the values of some coefficients of the four moments.
- (iii) There were cases when the moment values for both climate and bananas were comparable reflecting some close linkages between banana yields and climate variability parameters. Significant differences were, however, observed in the values of the climate and bananas moment.
- (iv) Correlation analysis observed clear linkages between surface temperature and banana yields variations. Linkages with temperature variations and yields were more pronounced when compared to linkages between rainfall and banana yields.

It can be further be concluded from the analysis based on simulation of the response of banana yields to variations in climate using the FAO-CROPWAT over different locations of Uganda that;

- (i) There are significant banana yields reductions attributable to climate variations (moisture deficits) across various banana growing regions of Uganda.
- (ii) The first cycle of banana harvests is associated with higher yield reductions (YR) and lower rain efficiency (ER) than the second cycle of crop harvest. In addition, it was observed that the intra annual rainfall variations are important and affect banana production over Uganda.
- (iii) Regions that experience more than three months of rainfall shortages including Kitgum, Lira, Moroto and Gulu areas can hardly sustain rain-fed banana production and have yield reductions greater than 35% of optimal yields.

4.3 Results on the Performance of Regional Climate Models Outputs

This section presents the results on the evaluation/validation of regional climate model performance in simulating observed climate patterns over Uganda. The spatial patterns of RCMs outputs are validated against gridded rainfall observations of CRU, UDEL and GPCP on seasonal time scales using methods described in Section 3.2.3. The temporal patterns were restricted to use of only CRU rainfall time series. The results for the three seasons; March-May (MAM), June-August (JJA) and October-December (OND) are presented.

A 5-member ensemble (“RCM_ENSEMBLE 5”) based on equal weights has been developed from the five RCMs including PRECIS-M1, PRECIS-M2, PRECIS-M2EA, HadGEM3-ra (50km) and HadGEM3-ra (25km). The results presented include the spatial and temporal patterns of simulated and gridded rainfall observations, the biases and errors between the RCMs and observations for different parts of Uganda. The results are presented and discussed in the following Sections.

4.3.1 Spatial Patterns of Observed and Simulated Mean Rainfall

This section focuses on the results on the evaluation of the ability of RCMs to represent the observed spatial patterns of mean seasonal rainfall for three rainfall seasons. Figures 4.43-4.45 show spatial patterns in time averaged (1991-2008) seasonal rainfall. Figure 4.43 depicts the patterns in MAM seasonal mean rainfall (mm/day) over Uganda. The gridded rainfall observations of CRU and UDEL observed a very good agreement although the GPCP slightly

deviates from these two over the L. Victoria basin and the western and southwestern districts but shows good agreement in parts of central and northeastern Uganda.

During March-May (MAM) season, CRU and UDEL rainfall observations observed that all western districts and parts of northern Uganda receive 3-4 mm/day, the central districts receive 4-5 mm/day with the districts around L. Victoria receive the highest rainfall of about 5-7 mm/day (Figure 4.43). The northeastern districts receive the lowest rainfall of about 1-3 mm/day. PRECIS RCMs simulate rainfall patterns similar to those observed with slight enhancement in the amounts.

The study results further observed that during MAM, most western, central and northern districts receive about 3-6 mm/day, the eastern districts especially areas around Mt. Elgon experience enhanced rainfall (5-7 mm/day) while the southern districts bordering L. Victoria to the west receive depressed rainfall (1-4 mm/day). The rainfall produced by the PRECIS RCMs over the eastern Africa domain is slightly enhanced compared to the rainfall from the RCMs runs based on the CORDEX domain.

The results from the HadGEM3-ra for two different resolutions (50 km and 25 km) are also showed in the bottom panel. The rainfall for these two RCM configurations (model physics) is enhanced over the L. Victoria region. The ensemble for the five RCMs shows an improvement in the RCM performance over most of the regions (Figure 4.43). Several other studies (Indeje *et al.*, 2000; Mutemi, 2003; Omondi, 2010; Moufouma-Okia and Jones, 2014 and Otieno *et al.*, 2014) have observed biases inherent in climate model outputs partly due to the complex interaction in the drivers of long rainy season mainly over the equatorial region. The long rains occur during the transition from Northern Hemisphere winter to summer when the large scale circulation patterns are not well organized and therefore not well captured by most climate models.

During June-August (JJA, Northern Hemisphere summer) season, the northern part of the Country receives more rainfall than central and southern districts (Figure 4.44). The mean rainfall pattern is well captured by all models. During this season, the global system are nearly well established that enables most models to adequately represent them during climate simulation.

During October-December (OND) season (Figure 4.45), the results from the RCMs get closer to the observations and show improvement in the ability of regional climate models in representing rainfall patterns except over Mt. Elgon region. Relative to the long rains (MAM), the short rains (OND) tend to have stronger spatial coherence of rainfall anomalies across a large part of the East Africa region, and a substantial association with ENSO and IOD (Ogallo 1988; Nicholson and Kim 1997; Saji *et al.*, 1999; Indeje *et al.*, 2000; Mutemi 2003; Riddle and Cook, 2008; Nyakwada, 2009 and Williams and Funk, 2010). This mainly explains improvement in the ability of climate models to represent observed rainfall patterns during short rains over most regions of East Africa particularly Uganda. The large scale systems which are dominant drivers of rainfall during the short rainfall season in the region are quite accurately represented in most models used.

In general, the results from the study observed the ability of the PRECIS and other RCMs to represent the observed spatial patterns of mean seasonal rainfall for the three different rainfall seasons over Uganda. There were, however, inter-model variation in the representation of seasonal rainfall patterns owing to the different model aspects and capacities. There is also observed disagreement among the gridded observations sets in many regions that makes their comparison with regional climate model outputs a challenge.

The results in this study agree with those of Sabiiti (2008); Omondi (2010); Nandozi *et al.* (2012); Endris *et al.* (2013); Otieno *et al.* (2014) and Otieno *et al.* (2015). This study, in addition to providing alternative regional climate model output choices, has developed a multi-model ensemble to provide an alternative that would improve the representation of rainfall over Uganda. This approach also been used in Endris *et al.*, 2013 and Otieno *et al.* (2014) over East Africa.

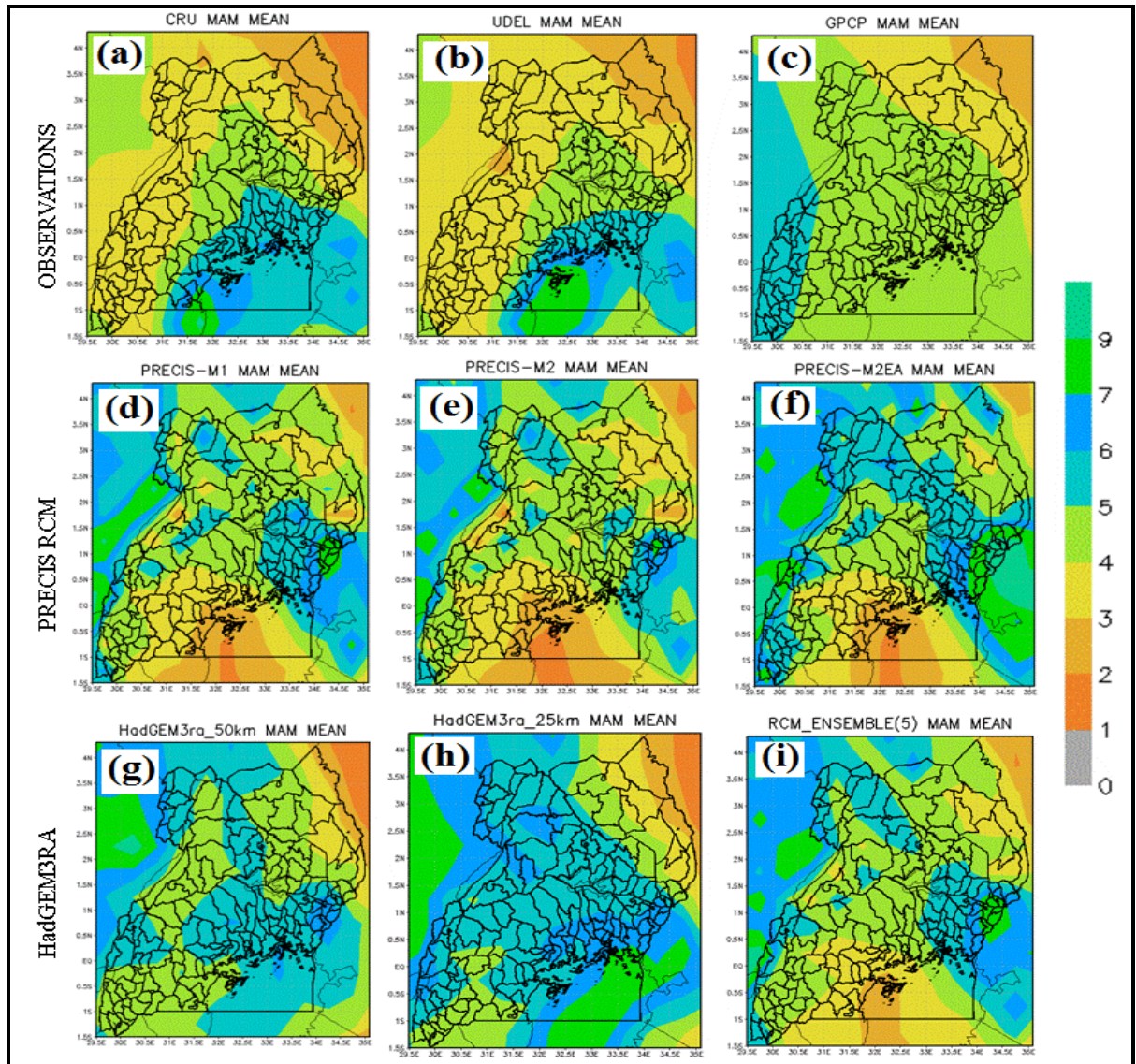


Figure 4.43 (a-i): Spatial patterns of gridded observed (a-c) and regional climate model (PRECIS configurations, d-f and HadGEM3ra, g-h) simulated March-May (MAM) season mean (1991-2008) rainfall (mm/day) over Uganda. Multi-model ensemble (MME, i) shows the mean of five model configurations (d-h).

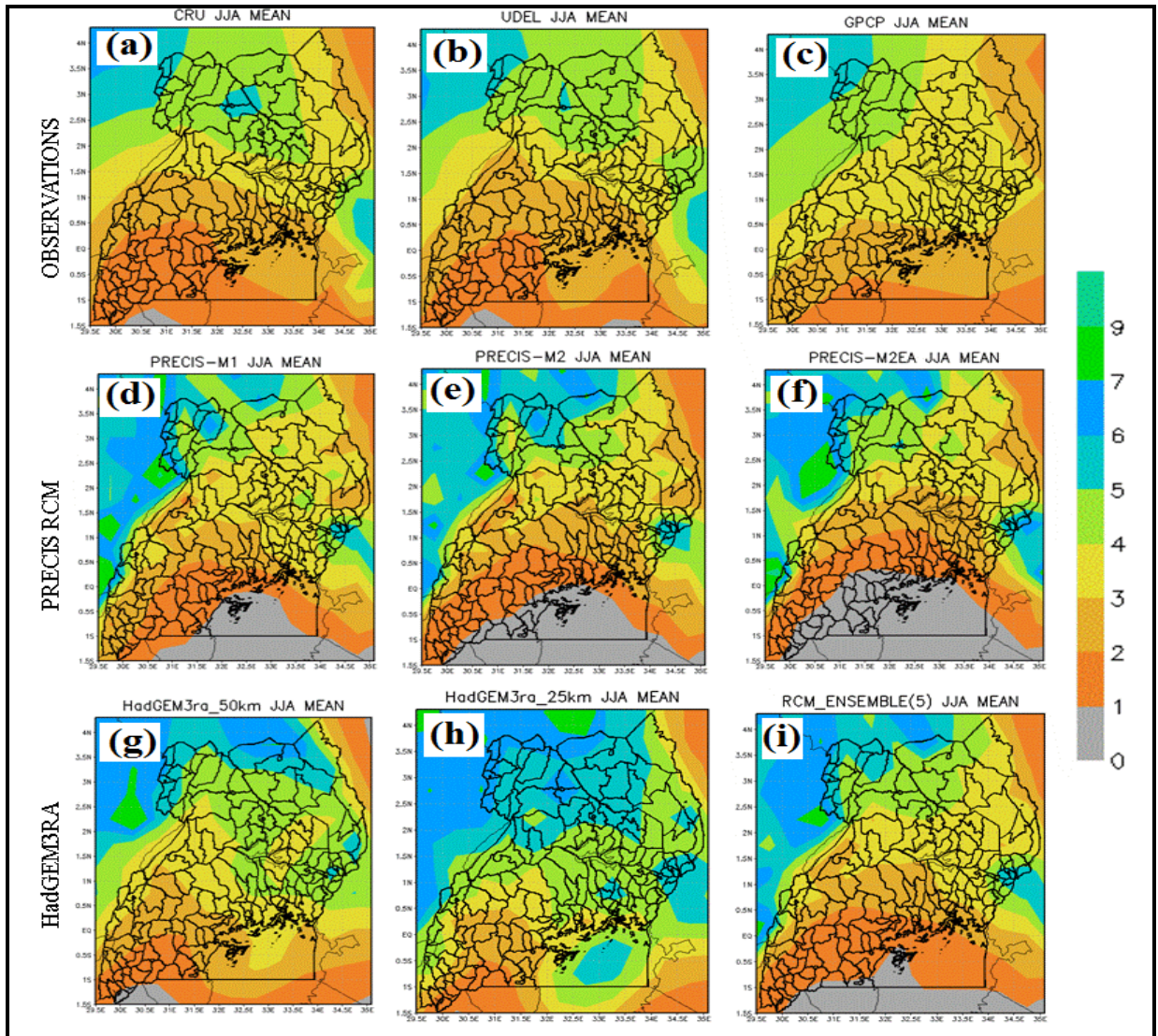


Figure 4.44 (a-i): Spatial patterns of gridded observed (a-c) and regional climate model (PRECIS configurations, d-f and HadGEM3ra, g-h) simulated June-August (JJA) season mean (1991-2008) rainfall (mm/day) over Uganda. Multi-model ensemble (MME, i) shows the mean of five models configurations (d-h).

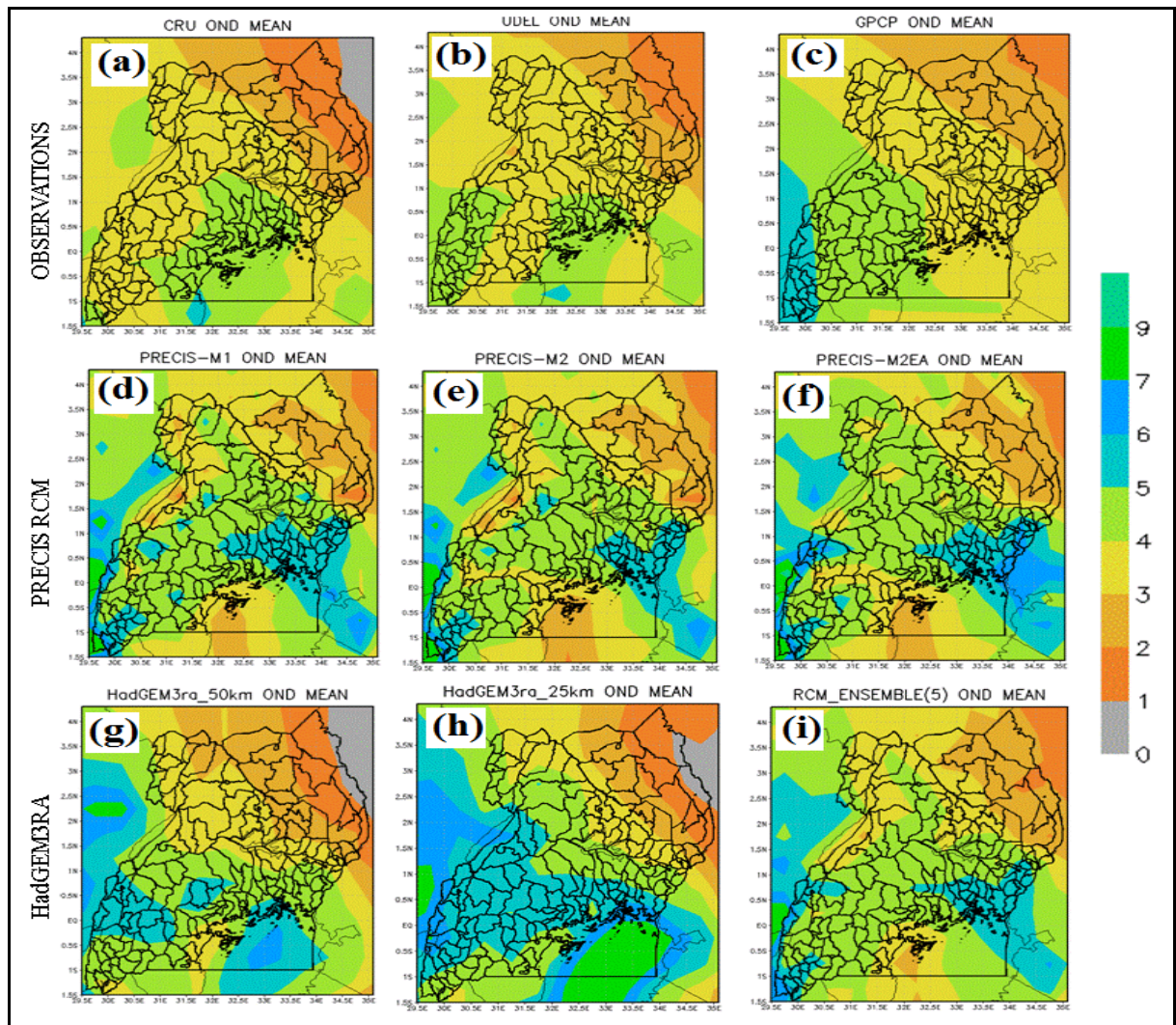


Figure 4.45 (a-i): Spatial patterns of gridded observed (a-c) and regional climate model (PRECIS configurations, d-f and HadGEM3ra, g-h) simulated October-December (OND) season mean (1991-2008) rainfall (mm/day) over Uganda. Multi-model ensemble (MME, i) shows the mean of five model configurations (d-h).

4.3.2 Simulated and Observed Coefficient of Variation of Seasonal Rainfall

This sub-section presents the spatial patterns of the coefficient of variation (the ratio of rainfall standard deviation to mean rainfall) of rainfall observations and regional climate model simulated rainfall. Figures 4.46 (a-i)-4.48 (a-i) show the results of the observed and simulated spatial patterns of seasonal rainfall coefficient of variation. The coefficient of variation has the advantage of comparing rainfall variability patterns regardless rainfall intensities across the regions.

Figure 4.46 (a-i) observed that during March to May, the variability of rainfall is stronger over the eastern part of the Country and Lake Victoria region in some cases. Over the western and

most of central parts of the Country, the variability in rainfall during this season is low partly due to the persistent influence of westerly flows that supply moisture to the western and central regions during the season. There is good agreement in the patterns of the variability, although most models are not able to adequately reproduce the correct magnitudes of variability in some areas.

During June to August season (Figure 4.47 a-i), the patterns are oriented in the northwest direction for all models with quite good agreement with the GPCP patterns of rainfall variability. Low rainfall variability is shown in the north and central region while the southern, southwestern and Lake Victoria regions experience high rainfall variability during this season.

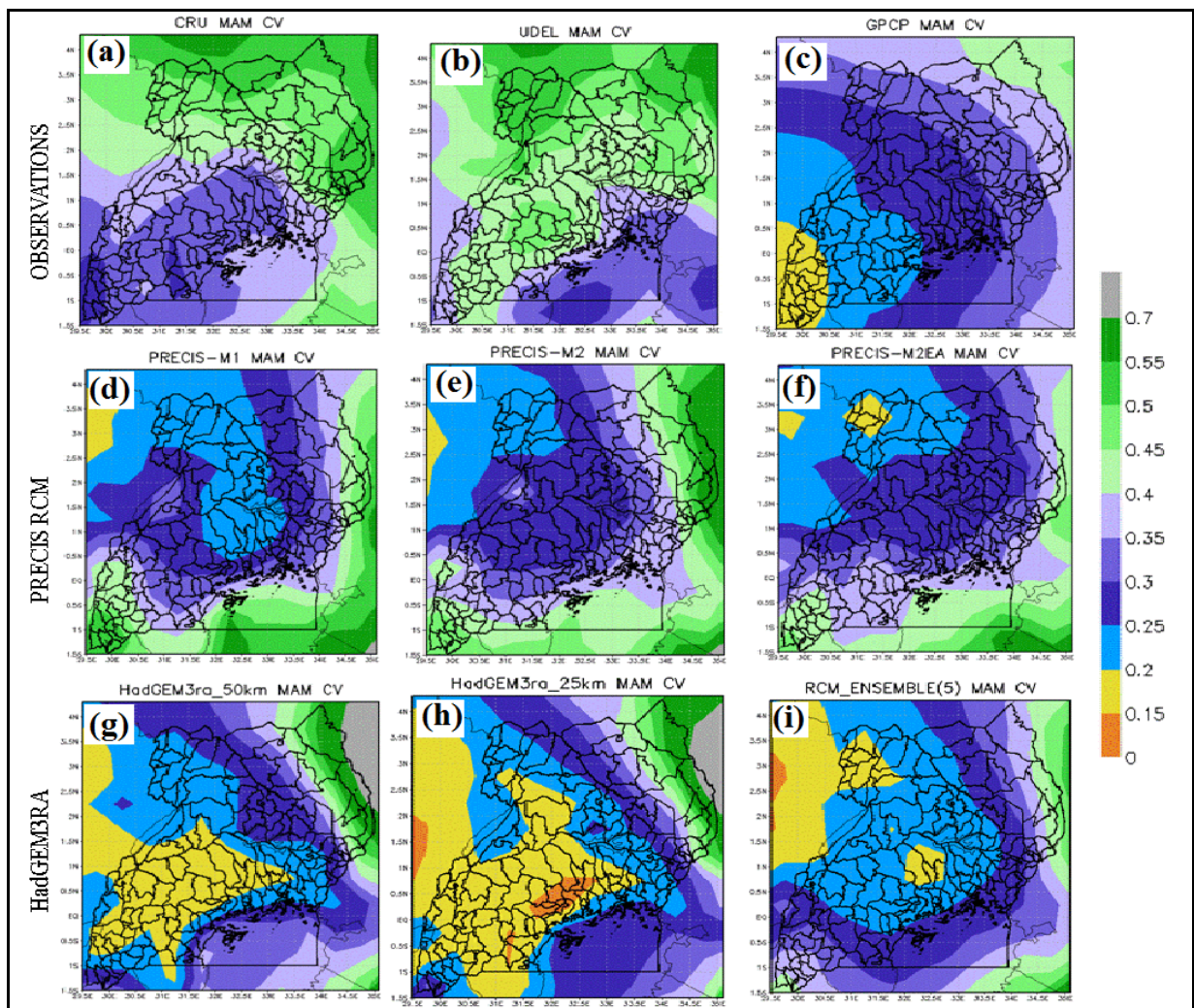


Figure 4.46 (a-i): Spatial patterns of gridded observed (a-c) and regional climate model (PRECIS configurations, d-f and HadGEM3ra, g-h) simulated March-May (MAM) season rainfall coefficient of variation (CV, x100%, 1991-2008) over Uganda. Multi-model ensemble (MME, i) shows the mean of five models configurations (d-h).

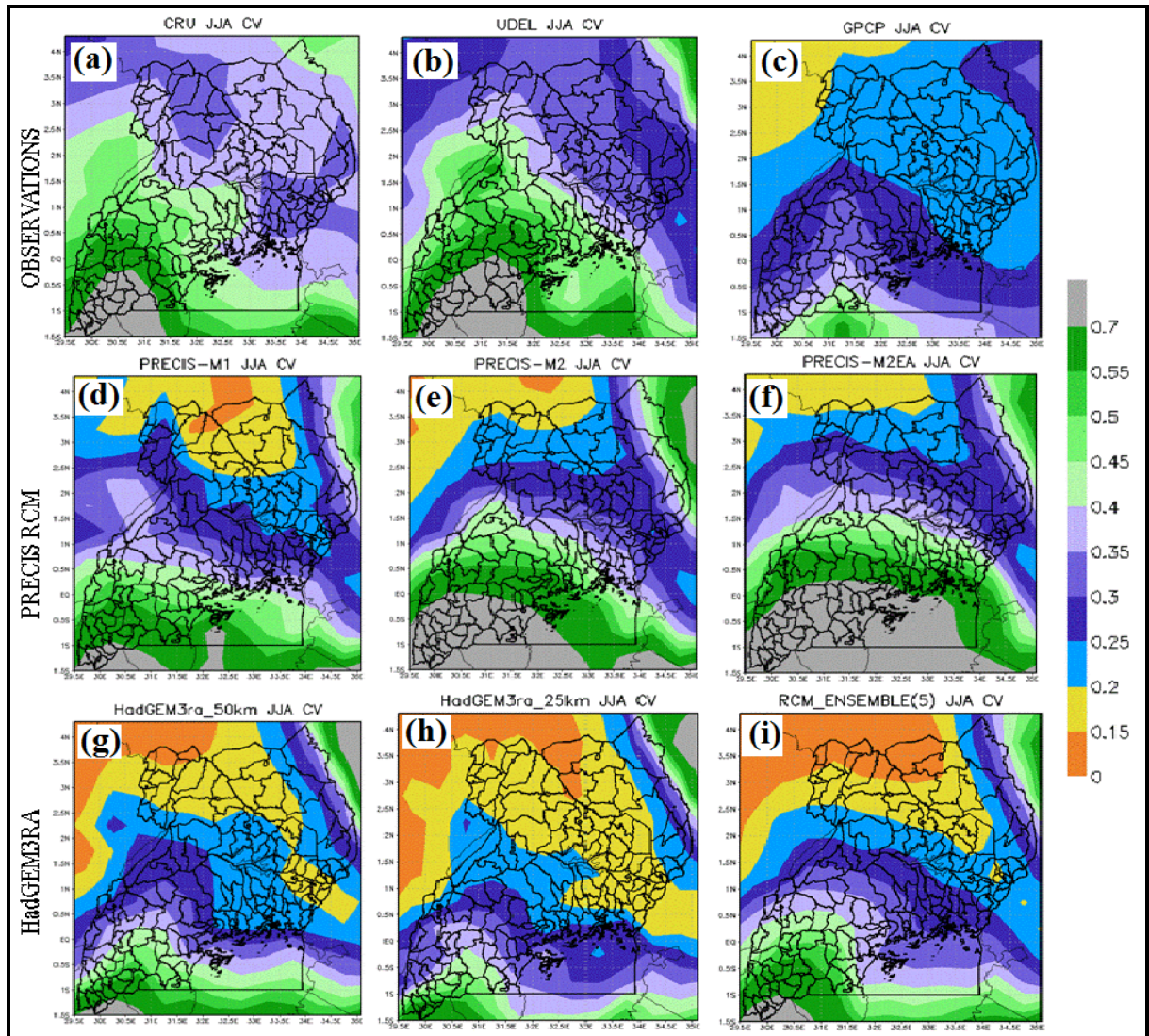


Figure 4.47 (a-i): Spatial patterns of gridded observed (a-c) and regional climate model (PRECIS configurations, d-f and HadGEM3ra, g-h) simulated June-August (JJA) season rainfall coefficient of variation (CV, x100%, 1991-2008) over Uganda. Multi-model ensemble (MME, i) shows the mean of five model configurations (d-h).

During October to December season (Figure 4.48 a-i), the study observed good agreement in the spatial patterns of rainfall variability over the Country. In the figure, it is observed that models produce rainfall with lower variability compared with the observed rainfall. The study results also observed that there are is higher rainfall variability in the northern regions than the southern regions of the Country.

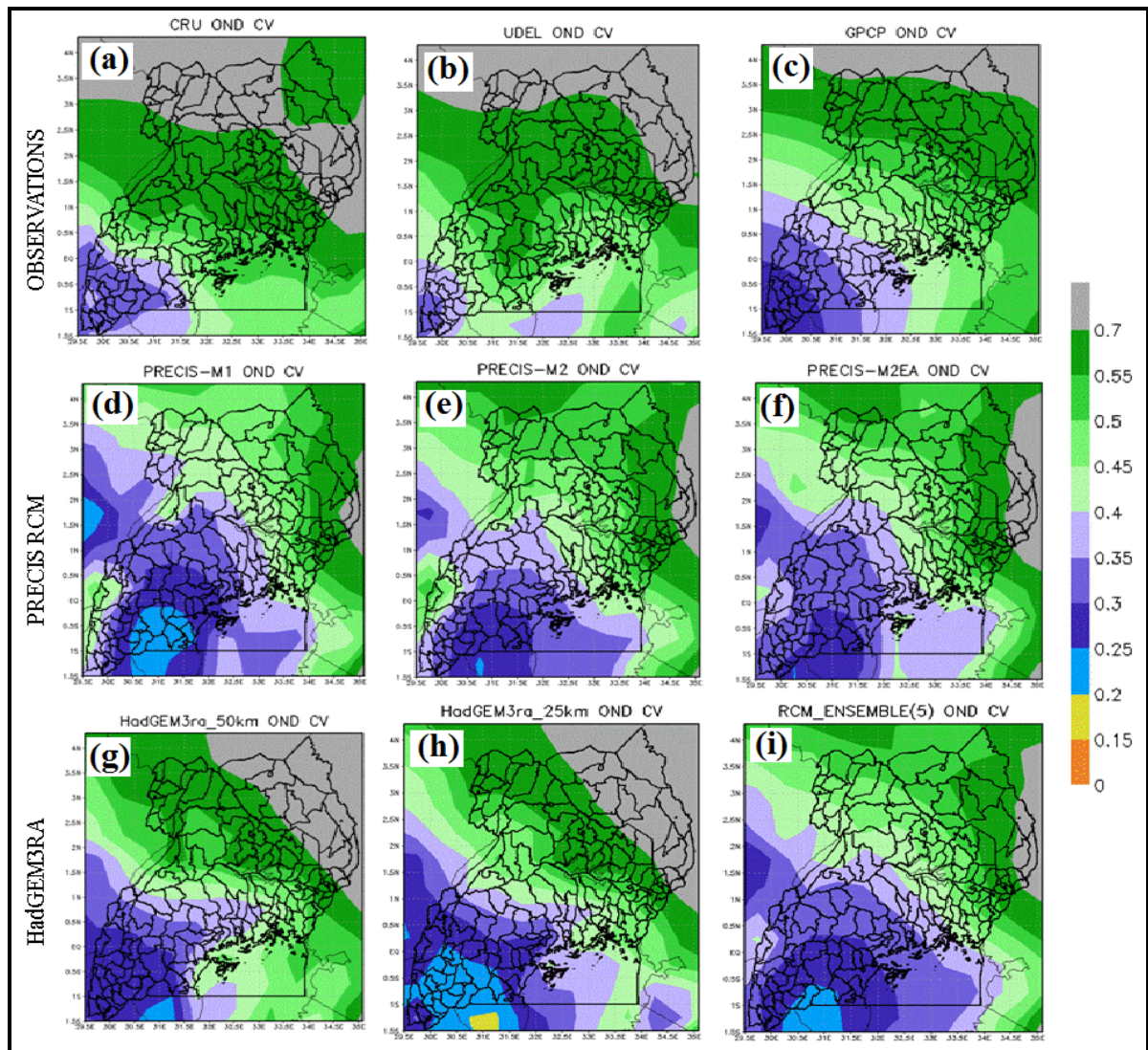


Figure 4.48 (a-i): Spatial patterns of gridded observed (a-c) and regional climate model (PRECIS configurations, d-f and HadGEM3ra, g-h) simulated October-December (OND) season rainfall coefficient of variation (CV, x100%, 1991-2008) over Uganda. Multi-model ensemble (MME, i) shows the mean of five model configurations (d-h).

In general, this section of the study observed the ability of the PRECIS and other RCMs to provide realistic simulation of the historical patterns of coefficient of variation (CV) observed rainfall for the three different rainfall seasons over Uganda.

4.3.3 Results based on Empirical Orthogonal Functions

Figure 4.49 (a-d)-4.50(a-d) show results based on Empirical Orthogonal Functions (EOFs) during March to May rainfall season. Figure 4.49 shows the spatial patterns of the first two dominant modes of rainfall variability. The patterns in PRECIS model simulated seasonal rainfall are compared against CRU observational rainfall. The study observed that the signs of the first mode of rainfall variability are opposite between CRU rainfall (positive) and PRECIS

model rainfall (negative). In CRU rainfall, the first mode explains 39.5% of rainfall variability in the region while in the PRECIS model rainfall, the first mode of variability explains 58.8% of rainfall variability. The second mode explains 16.8% (CRU) and 18.1% (PRECIS) of rainfall variability during March to May season and the spatial patterns become quite close in the two data sets.

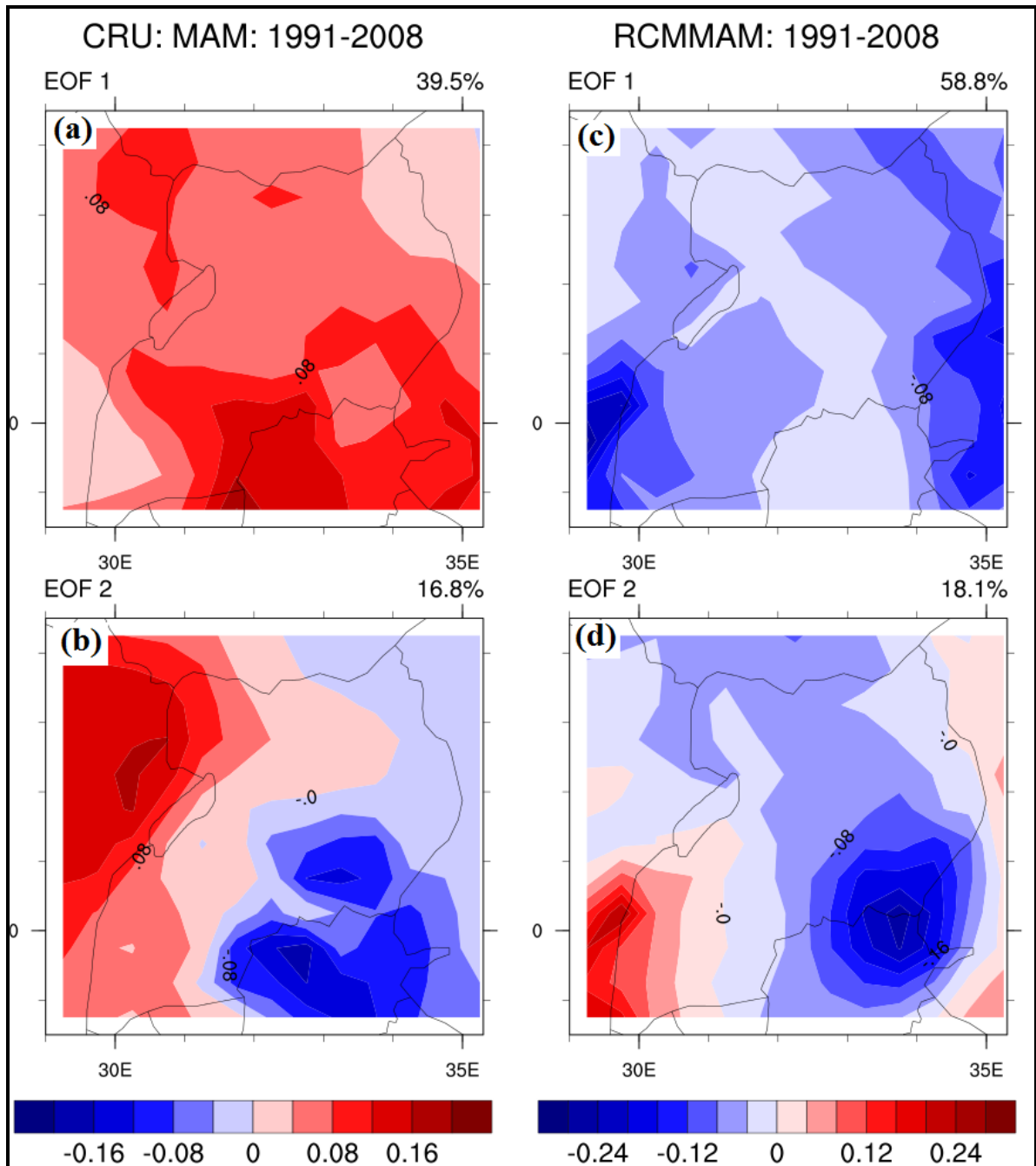


Figure 4.49 (a-d): Observed (a-b) and PRECIS RCM (c-d) spatial patterns of the first (a, c) and second (b, d) dominant modes of rainfall variability from Empirical Orthogonal Functions (EOFs) during March-May (MAM, 1991-2008) over Uganda.

Figure 4.50 (a-d) presents results similar to Figure 4.49 (a-d) but for temporal patterns of rainfall variability during March to May season.

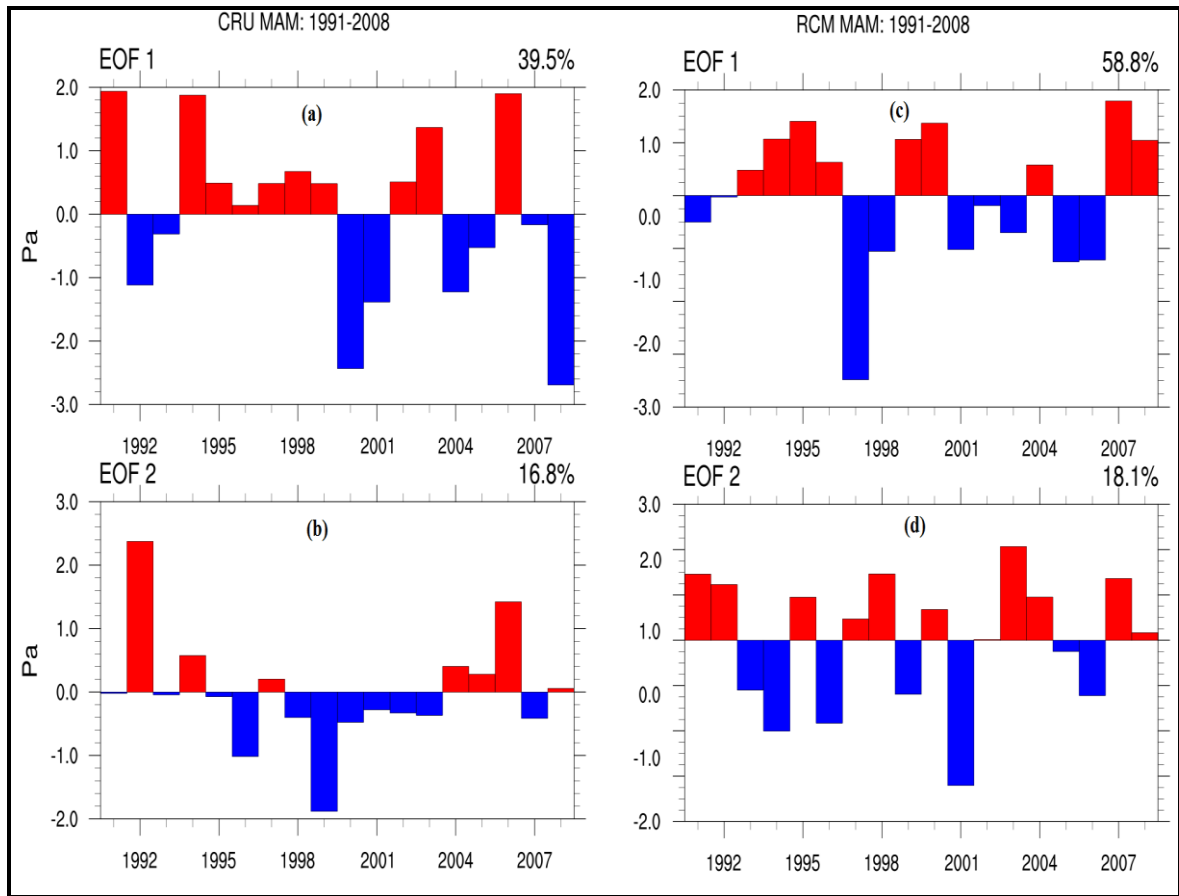


Figure 4.50 (a-d): Observed (a-b) and PRECIS RCM (c-d) temporal patterns of the first (a, c) and second (b, d) dominant modes of rainfall variability from Empirical Orthogonal Functions (EOFs) during March-May (MAM, 1991-2008) over Uganda.

Figure 4.51 (a-d)-4.52 (a-d) show results based on Empirical Orthogonal Functions (EOFs) during October to December rainfall season. Figure 4.51 (a-d) shows the spatial patterns of the first two dominant modes of rainfall variability. The patterns in PRECIS model simulated seasonal rainfall are compared against CRU observational rainfall. The study observed that the patterns of the first mode of rainfall variability between semi-observed CRU (a) and PRECIS model rainfall (c) are quite similar over most of the Country although the eigen values are high for CRU rainfall than for model rainfall. In CRU rainfall, the first mode explains 74.6% (a) of rainfall variability in the region while in the PRECIS model rainfall, the first mode of variability explains 76.8% (c) of rainfall variability. The second mode explains 8.4% (CRU, b) and 6.6% (PRECIS, d) of rainfall variability during October to December season and the spatial patterns become quite close in the two data sets.

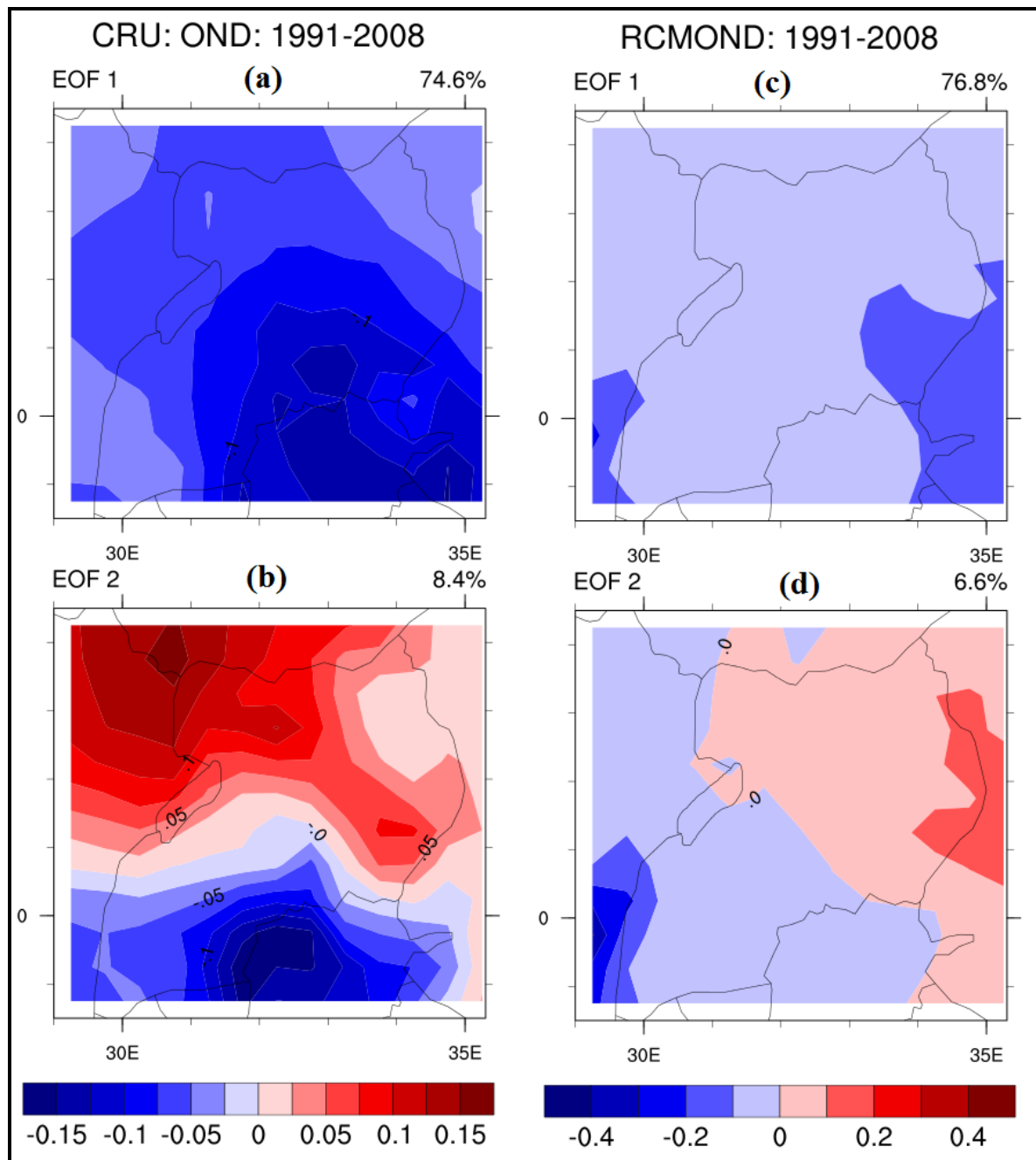


Figure 4.51 (a-d): Observed (a-b) and PRECIS RCM (c-d) spatial patterns of the first (a, c) and second (b, d) dominant modes of rainfall variability from Empirical Orthogonal Functions (EOFs) during October-December (OND, 1991-2008) over Uganda.

Figure 4.52 (a-d) presents results similar to Figure 4.51 (a-d) but for temporal patterns of rainfall variability during October to December season. The results show that the two series are fairly comparable with few cases of extreme values not adequately captured

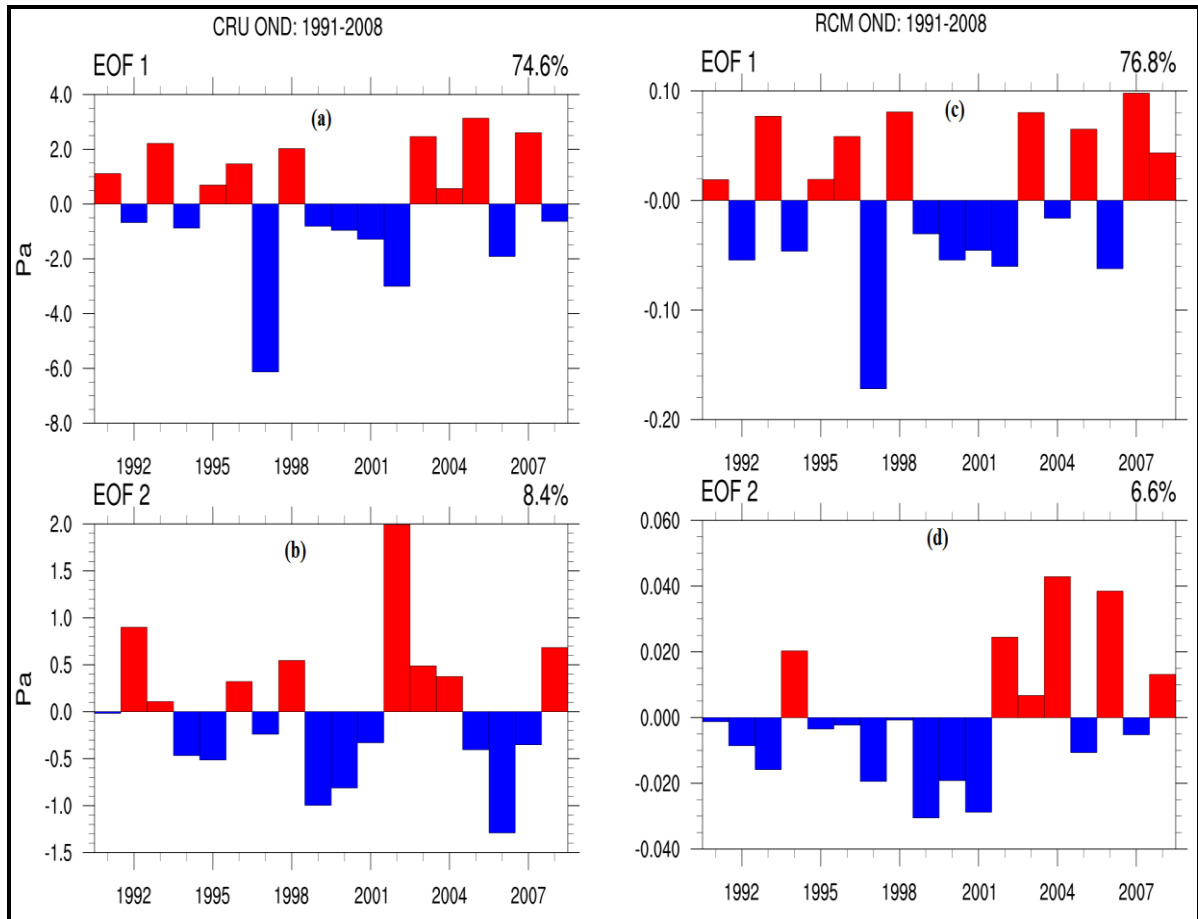


Figure 4.52 (a-d): Observed (a-b) and PRECIS RCM (c-d) temporal patterns of the first (a, c) and second (b, d) dominant modes of rainfall variability from Empirical Orthogonal Functions (EOFs) during October-December (OND, 1991-2008) over Uganda.

4.3.4 Seasonal 850 mb Wind Circulation Patterns

This part of the study analysed variations in seasonal patterns of wind fields that influence climate over the region. The results show the wind circulation patterns from the ERA-Interim reanalysis of the wind vectors at 850 mb.

Figure 4.53 (a-c) shows the mean ERA-Interim wind (ms^{-1}) patterns (1991-2008) at 850 mb for MAM (a), JJA (b) and OND (c). Winds were considered for analysis due to their role in transport of moisture predominantly from the adjacent Oceans and Congo River basin into the region and also redistribution of heat in the atmosphere. These wind patterns also show areas of convergence and upward motions that quite often lead to cloud formation that results in the rainfall. During MAM (Figure 4.53 a), for example, low wind speeds are dominant and observable (expected) over most parts of Uganda.

The flow of winds is mainly from the southwestern Indian Ocean inland along the East Africa coast through Kenya and Tanzania regions. Due to modulation of the winds by both the influence from complex topography (Oettli and Camberlin, 2005 and Otieno *et al.*, 2015) and inland water bodies particularly Lake Victoria and existence of the ITCZ within the area, convective activities and lifting of moist results into cloud formation and rainfall during the season. This situation gives rise to high chances rainfall condition over Uganda, Kenya and some parts of Tanzania.

Figure 4.53 (b) shows that during the JJA season, there is a high tendency of most winds from the Indian Ocean re-curve and accelerate northeast ward with relatively high speed with little influence on rainfall formation mechanisms over most parts of Equatorial East Africa particularly Uganda. Despite existence of low wind speeds over most of Uganda, low moisture content in the does not permit rainfall occurrence over most of southern, western and central Uganda during this season. The situation however, worsens due to absence of the ITCZ in the equatorial region with some influence of the ITCZ rainfall causing mechanism felt in the northern part of the Country. During this season the Turkana jet is more pronounced and tends to affect rainfall over most of the North eastern region. Generally, the wind speed over Uganda is relatively low due to its position along the equator and the complex topography (Oettli and Camberlin, 2005).

Figure 4.53(c), shows convergence of south easterlies and north easterlies in the region during the OND season. Both winds are moist and this promotes rainfall formation. The rainfall over the region is strongly link to the Indian Ocean Dipole with the positive IOD favoring high rainfall while the negative IOD depresses rainfall over most of East Africa particularly Uganda. The wind flow patterns in Era-Interim reanalysis data adequately explains the behavior of observed seasonal rainfall over Uganda and East Africa at large.

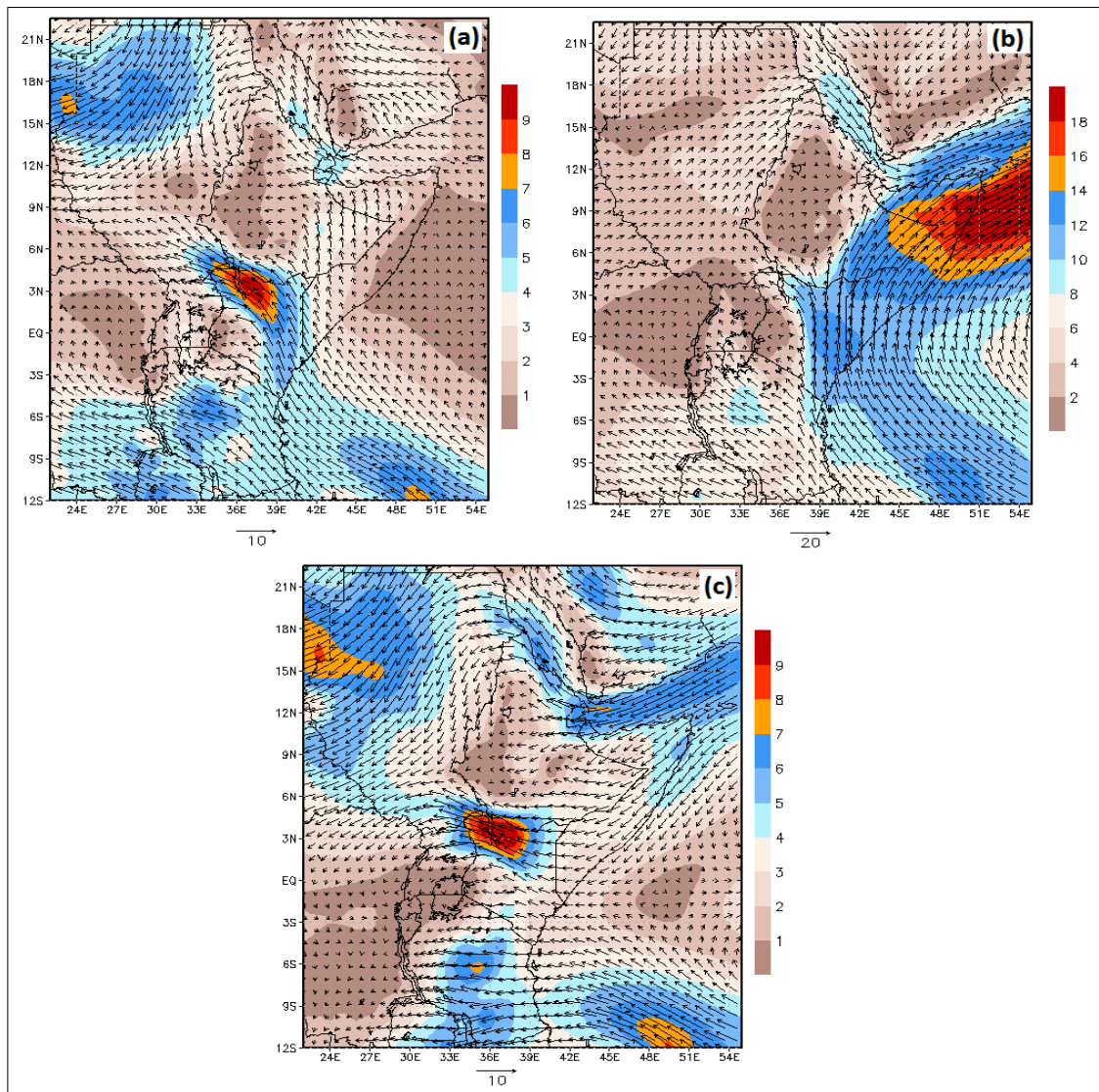


Figure 4.53 (a-c): ERA-Interim mean wind (ms^{-1}) patterns (1991-2008) at 850 mb for March-May (MAM, a), June-August (JJA, b) and October-December (OND, c) over Eastern Africa region. Shade colours represent wind speeds (m/s) while arrows represent direction.

Figure 4.54 (a-c) shows results for model simulated wind patterns over eastern Uganda during the three seasons. There is strong agreement between seasonal wind patterns in ERA-Interim and the PRECIS model despite the higher wind speeds observed in the PRECIS RCM wind patterns especially during June to August season. This partly explains why ERA-Interim forced climate simulations are quite close with the observed patterns particularly rainfall over East Africa including Uganda.

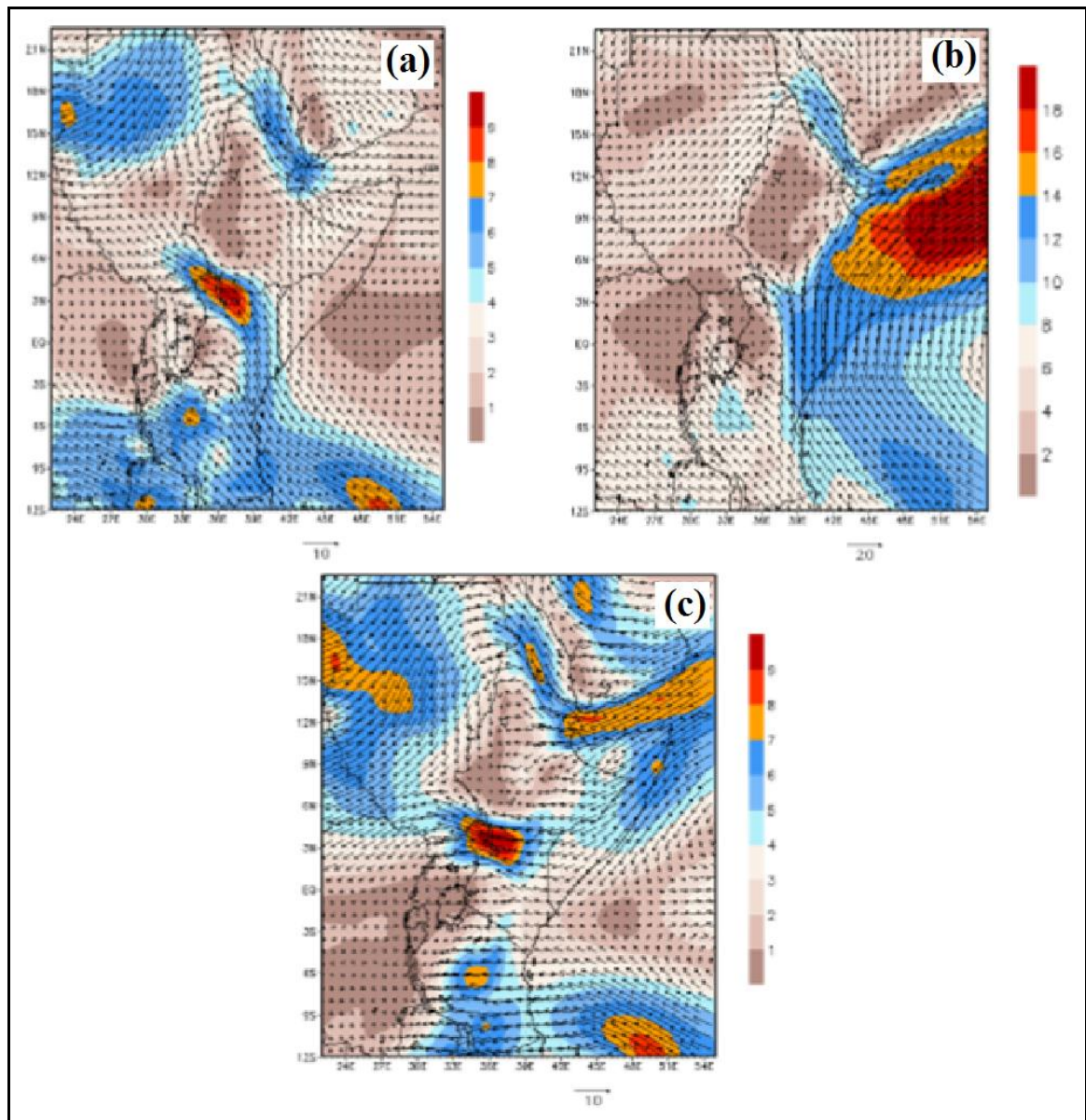


Figure 4.54 (a-c): PRECIS Simulated mean wind (ms^{-1}) patterns (1991-2008) at 850 mb for March-May (MAM, a), June-August (JJA, b) and October-December (OND, c) over Eastern Africa region. Shade colours represent wind speeds (m/s) while arrows represent direction.

4.3.5 Results of Simulated and Observed Rainfall Seasonality

This sub-section presents results on the simulated and observed rainfall seasonality (annual cycles). The results are presented and discussed for the different sub regions of Uganda. Figure 4.55 (a-d) shows the relationship between the observed and regional climate model simulated rainfall seasonality for different parts of Uganda including western (a), northwestern (b), central (c), northeastern (d) regions. Figure 4.56 (a-b), on the other hand, shows results for eastern (a) and southwestern (b) regions. The study observed that most regional climate models

were able to capture the observed seasonality in the different regions and also captured the rainfall maximum and minimum peaks.

It is observed that the UKMO Hadley Centre group of climate models (PRECIS-M1, PRECIS-M2, PRECIS-M2EA, and Hadgem3-ra) showed a better representation of rainfall over most parts of Uganda. In most cases, however, the CORDEX based RCMs (CCLM, RegCM, WRF) either over estimated or under estimated the observed rainfall over the different regions. The failure of CORDEX group of models to capture the observed rainfall patterns over Uganda can be attributed to the large model domain size used in the Africa-CORDEX experiments that cause the lateral boundary conditions to be less efficient for such a large domain.

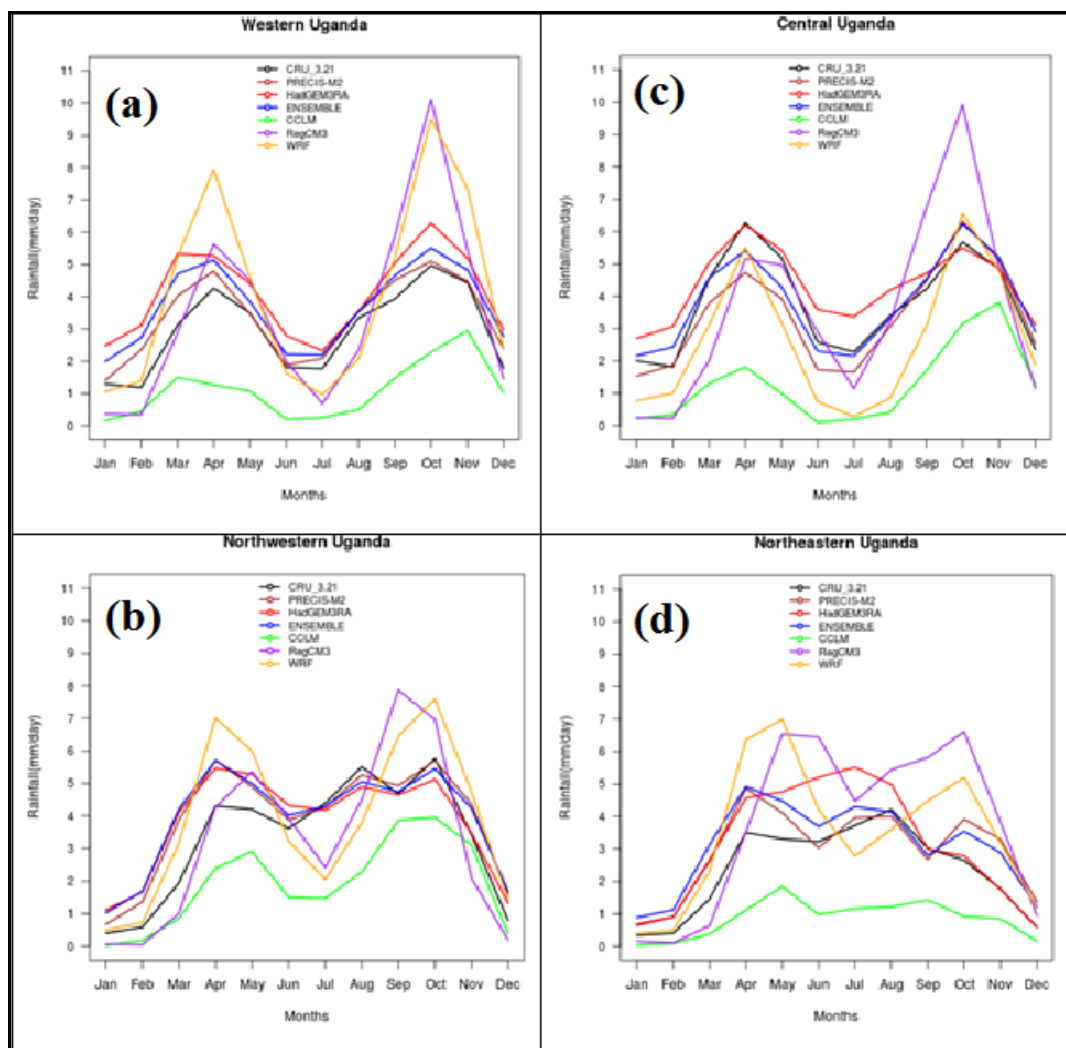


Figure 4.55 (a-d): Observed and simulated averaged (1991-2008) rainfall seasonality (annual cycles) over western (a), northwestern (b), central (c) and northeastern (d) regions of Uganda.

Figure 4.56 (a-b) shows results similar to those presented and discussed in Figure 4.55 but for eastern and southwestern Uganda.

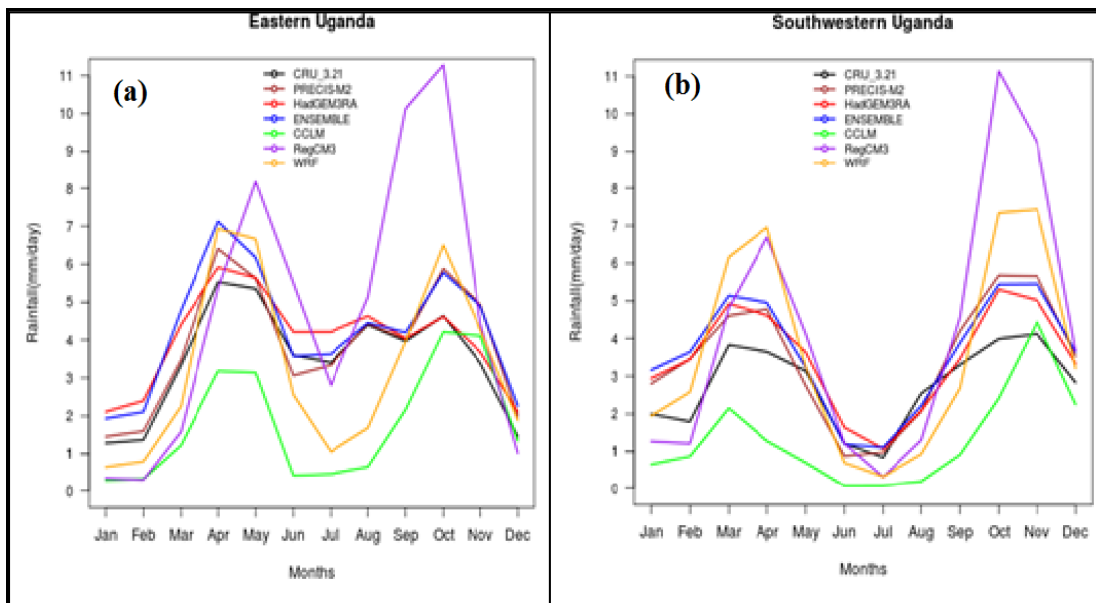


Figure 4.56 (a-b): Observed and simulated averaged (1991-2008) rainfall seasonality over eastern (a) and southwestern (b) regions of Uganda.

In general, the results from this section of the study observed the ability of the RCMs to provide realistic simulation of the observed seasonal rainfall for the three different rainfall seasons. Some of the peak values were however underestimated or overestimated by some regional climate models especially the ones from the Africa-CORDEX simulations.

4.3.6 Interannual Rainfall Variability

This section focuses on the inter-annual variability of seasonal observed and regional model simulated rainfall. Figure 4.57 (a-d) shows the inter-annual rainfall patterns for both the RCM and observed rainfall for MAM and OND seasons over western and central Uganda. The results show that most of the RCMs, reproduced the inter-annual rainfall patterns more accurately during OND than during MAM season both regions, several studies have found similar trends in RCM performance. This has been attributed by many studies to the dominance of large scale system in OND season as opposed to MAM season when the large scale flow is not well organized and therefore not well represented in most RCMs. This is due to the relatively coarse resolution of the RCMs that fails to adequately resolve these processes but also the limited understanding of the dynamics and nature of the small scale and meso-scale processes associated regions with complex topography. It is however, observed that models reproduce well the direction of rainfall patterns during MAM over the two regions and

UK-Met Office based models still reproduce the observed patterns better than the CORDEX group of regional models used in this study. The results in this part of the study are comparable to the findings of Sabiiti, 2008, Omondi, 2010, Nandozi *et al.*, 2012, Endris *et al.*, 2013 and Diallo, 2014 and Moufouma-Okia and Jones, 2014.

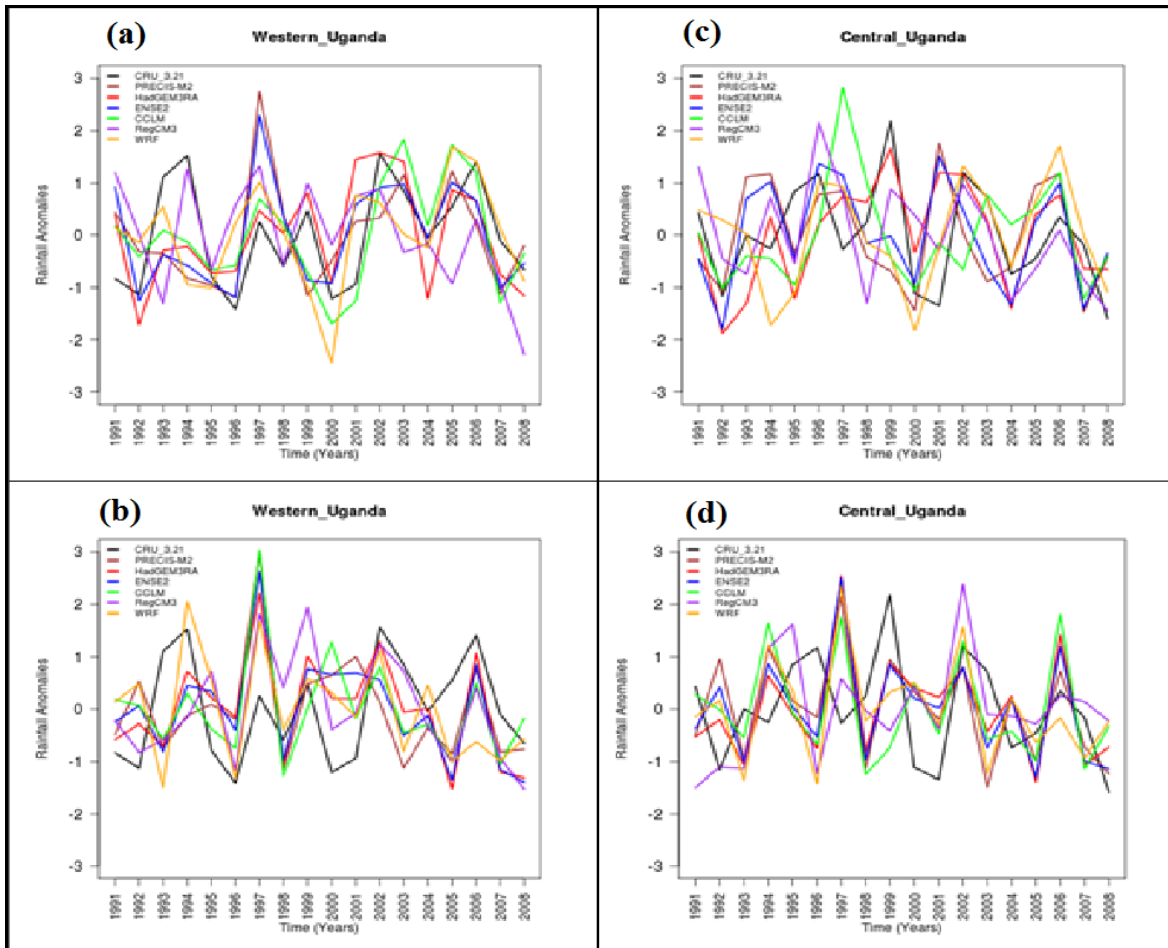


Figure 4.57: Observed and simulated interannual rainfall anomalies for MAM (a, c) and OND (b, d) over western (a-b) and central (c-d) regions of Uganda.

Several studies have shown that the interannual rainfall variability is strongly associated with perturbation in global SSTs, especially over the equatorial pacific and Indian Ocean basins (Nicholson and Kim 1997; Saji *et al.*, 1999; Indeje *et al.*, 2000; Black *et al.*, 2003; Clark *et al.*, 2003; Nyakwada, 2009; Kizza *et al.*, 2009; Omondi *et al.*, 2013; Lyon *et al.*, 2014 and Otieno *et al.*, 2015). The influence of rainfall depends on season and location. Changes in rainfall patterns associated with the SST patterns particularly the Indian Ocean threatens food security in many parts of East Africa particularly Uganda (Funk *et al.*, 2008).

Mutai and Ward, 2000 and Washington and Pearce, 2012 also observed that inter-annual rainfall variability over the East Africa arises from a complex interaction between sea surface temperature (SST) anomalies, large scale atmospheric patterns, synoptic scale weather disturbances, tropical cyclones and subtropical anticyclones, extratropical weather systems, wave perturbations and free atmosphere variations. Relative to the long rains, the short rains tend to have stronger inter-annual variability, greater spatial coherence across a large area and more significant associations with El Niño Southern Oscillation (ENSO); warm El Niño events are associated with increased rainfall with negative anomalies occurring during La Niño events (Mutai and Ward, 2000). The link to ENSO can be further connected to outbreaks of moist South Atlantic westerly flows, which are linked to anomalous rainfall over the region and tend to increase/decrease during El Niño/La Niño episodes respectively (McHugh, 2006). This also applies to Uganda's rainfall variability (Schreck and Semazzi, 2004).

The results from graphical methods observed the ability of the RCMs to provide realistic inter-annual rainfall for the three different rainfall seasons in Uganda. Some of the inter-annual rainfall peaks were however underestimated while others overestimated. The next section presents and discusses results based on computation of model skill scores.

4.3.7 Results based on Statistical Tests of Model Performance.

The results presented above are based on the graphical representation of model performance. The results based on graphical method are largely subject to human judgment and predominantly give a qualitative interpretation. This section presents results based on quantitative measure of model skill and therefore performance. The study uses three indices of model performance (correlation coefficient, root mean square errors and the refined Wilmott indices) computed between multiple regional model outputs and CRU3.21 gridded seasonal rainfall observations. These indices have also been computed between CRU and UDel gridded rainfall observations and ERA-Interim reanalysis data sets and also between CRU and seasonal rainfall outputs from CORDEX group of regional climate models. The regional climate models considered in this part of analysis and whose results have been presented include both the UK-Met Office regional climate models with different configurations (based on parameterization schemes and resolution) and RCMs used in the CORDEX initiative to provide users with coherent climate model outputs. This study observed that Sylla *et al.* (2013) argue that over

Africa, GPCP is more consistent with gauge observations than other gridded observational rainfall datasets.

Table 4.16 presents a summary of the correlation coefficients between CRU gridded observations of seasonal rainfall extracted for seven sub-regions over Uganda. The highlighted values in the table are statistically significant at 95% confidence level. It is evident from the table that the correlation coefficients are generally higher for the OND season compared to MAM and JJA seasons. Best model performance based on correlation coefficients is achieved over regions 3 and 4. The performance is well comparable though lower than that achievable over region seven (a region representative of the entire Country). These results have demonstrated that PRECIS RCM run with MOSES 2.2 performs better than that of similar experiments run with MOSES1. The study observed that HadGEM3-ra RCM (the newly developed UK-Met Office RCM) rainfall outputs generally observed a stronger relationship with the observations than those based on the PRECIS RCM that is currently used. The former was formulated and is being developed to replace the PRECIS RCM that is currently in use. This study is the first to evaluate the performance of this new RCM over Uganda. The results demonstrate that increasing model resolution from 50 km to 25 km improves the correlations (and hence model performance) values for the MAM season at the expense of lowering the performance during the OND season over most some regions.

Table 4.17 presents the results of model performance based on the computed Root Mean Square Errors (RMSE) between CRU observational seasonal rainfall and other observational data sets and regional climate model outputs for different regions and seasons. Values of very low root mean squares errors less than 1.5 mm/day in rainfall simulation are highlighted. These show cases where the performance of regional climate model exhibit relatively smaller biases in seasonal rainfall simulation. The errors in rainfall simulations vary across seasons and locations. Errors were found to be proportional to rainfall intensities. The results show lower errors during June-August season that is relatively dry compared with March-May and October-December seasons over most of Uganda. The UK-Met office RCMs have low values of RMSE with their ensemble showing even lower values over most of the region. For example, the lowest computed RMSE for the ensemble is 0.56 mm/day (JJA, region 1) and the highest value is 1.71 mm/day (MAM, region 4). The CORDEX based regional climate models show larger error margins compared with the UKMO based models. For example, RegCM3 rainfall shows an error margin of 4.57 mm/day over region 1, MPIREMO (the RCM version of

ECHAM6) shows relatively large errors (4.38 mm/day during MAM over region). In addition, the CCLM shows errors of about 4.14 mm/day during MAM over region 3.

Table 4.18 shows a summary of the computed refined wilmott indices between CRU and other gridded observational seasonal rainfall and the regional climate model simulated rainfall for the different regions during MAM, JJA and OND. The results show that the GPCP seasonal rainfall observations do not represent the observed rainfall variability over most of the regions (1, 2 and 4) for the three seasons. UDel seasonal observations, on the other hand, show good agreement with the CRU rainfall observation despite some discrepancy over some regions. The PRECIS and Hadgem3-ra RCMs rainfall simulation generally observed positive and high values (> 0.5) of the refined wilmott indices showing good agreement with the CRU observations. This shows that these RCM are able to represent the observed variability over most of the regions. Favorable values are highlighted. The CORDEX based RCMs observed both low and negative refined wilmott indices (Table 4.18) and thus do not well represent the observed variability with respect to CRU.

The multi-model ensemble mean outperforms the results of individual models, and even ERA-Interim, in most of the areas and seasons as assessed by all three criteria. This is likely because of the cancellation of opposite signed biases across the models. Similar results have been shown by Paeth *et al.* (2011) and Endris *et al.* (2013) and in the CORDEX context by Nikulin *et al.* (2012).

The study has observed that PRECIS and HadGEM3-ra regional climate models perform better than all individual models considered during the analysis. There were observed inter model variations across the sub regions of Uganda during the three seasons. The ensemble developed based five UKMO regional climate model configurations also show very good performance across different regions. In general, although RCMs show some weaknesses (wet and dry biases) and strength in replicating the spatial distribution of rainfall in most areas of Uganda and the analyses show that the UKMO regional climate models can be relied on to simulate of past and future climate patterns over Uganda.

Table 4.16: The Pearson’s product-moment correlations coefficient for different model configurations with respect to CRU rainfall observations over different regions of Uganda. Values in green are significant at 95% confidence level.

Correlation Coefficient		Region 1	Region 2	Region 3	Region 4	Region 5	Region 6	Region 7
UDEL	MAM	0.62	0.44	0.75	0.77	0.82	0.73	0.78
	JJA	0.38	0.46	0.61	0.64	0.79	0.78	0.65
	OND	0.73	0.68	0.89	0.73	0.57	0.51	0.83
GPCP	MAM	0.31	0.44	0.07	0.16	0.30	0.36	0.31
	JJA	0.10	0.05	0.32	0.51	0.53	0.52	0.54
	OND	0.41	0.17	0.40	0.61	0.36	0.66	0.60
ERAINT	MAM	0.60	0.44	0.66	0.62	0.60	0.61	0.78
	JJA	0.17	0.18	0.37	0.59	0.59	0.51	0.57
	OND	0.81	0.62	0.85	0.85	0.65	0.81	0.90
PRECISM1	MAM	0.14	0.16	0.01	-0.18	0.10	0.17	0.08
	JJA	-0.02	-0.17	0.09	-0.01	0.23	0.22	0.27
	OND	0.68	0.46	0.78	0.80	0.47	0.67	0.81
PRECISM2	MAM	0.20	0.22	-0.03	0.06	0.13	0.33	0.21
	JJA	0.19	-0.05	0.28	0.08	0.02	0.24	0.20
	OND	0.75	0.52	0.83	0.86	0.63	0.74	0.88
PRECISM2EA	MAM	0.31	0.44	0.29	0.16	0.23	0.34	0.36
	JJA	0.46	0.11	0.41	0.47	0.09	0.42	0.39
	OND	0.84	0.47	0.80	0.84	0.42	0.70	0.84
HADGEM50	MAM	0.40	0.51	0.44	0.39	0.22	0.42	0.48
	JJA	0.47	0.24	0.26	0.52	0.22	0.47	0.45
	OND	0.75	0.48	0.86	0.79	0.53	0.75	0.86
HADGEM25	MAM	0.36	0.39	0.49	0.35	0.13	0.36	0.43
	JJA	0.56	0.02	0.38	0.61	0.06	0.49	0.41
	OND	0.42	0.43	0.85	0.77	0.45	0.54	0.82
RCM ENSEMBLE (5)	MAM	0.44	0.36	0.37	0.22	0.47	0.44	0.48
	JJA	0.28	0.01	0.29	0.32	0.18	0.39	0.39
	OND	0.82	0.51	0.84	0.85	0.53	0.75	0.86
WRF	MAM	0.26	0.38	0.21	0.12	0.21	0.42	0.34
	JJA	0.16	0.11	0.25	0.25	0.40	0.46	0.45
	OND	0.49	0.49	0.84	0.80	0.61	0.71	0.86
REGCM3	MAM	-0.07	0.15	0.55	0.44	-0.19	0.01	0.36
	JJA	0.33	0.07	0.14	-0.05	0.23	0.32	0.25
	OND	0.18	0.37	0.41	0.16	0.39	0.24	0.53
CCLM	MAM	0.51	0.62	0.07	0.29	0.11	0.35	0.41
	JJA	0.15	0.30	0.24	0.11	0.29	0.23	0.33
	OND	0.83	0.62	0.65	0.74	0.59	0.51	0.82

Table 4.17: The computed Root Mean Square Errors for different model configurations with respect to CRU rainfall observations over different regions of Uganda. Values in green show cases of low errors.

Root Mean Square Errors		Region 1	Region 2	Region 3	Region 4	Region 5	Region 6	Region 7
UDEL	MAM	0.61	0.84	0.88	0.58	0.44	0.45	0.48
	JJA	0.63	0.77	0.66	0.60	0.70	0.60	0.50
	OND	0.82	0.86	0.69	0.76	0.82	0.81	0.54
GPCP	MAM	2.19	1.95	1.73	2.74	1.29	1.28	1.42
	JJA	0.92	1.13	1.06	1.87	0.81	1.65	0.78
	OND	2.20	2.04	2.14	1.86	1.19	0.86	1.36
ERAINT	MAM	1.60	1.51	0.94	0.75	0.95	0.67	0.44
	JJA	1.06	1.23	0.74	0.85	0.65	0.96	0.40
	OND	1.41	1.09	0.79	0.65	0.66	0.91	0.46
PRECISM1	MAM	1.25	1.13	1.35	1.76	1.47	1.52	0.80
	JJA	0.94	1.04	0.68	0.85	0.84	0.84	0.52
	OND	1.41	1.01	1.16	1.59	0.88	1.33	0.84
PRECISM2	MAM	1.03	0.91	1.69	1.29	1.53	1.30	0.74
	JJA	0.77	0.81	0.83	0.83	0.95	0.88	0.61
	OND	1.39	0.81	0.86	1.29	0.84	1.30	0.65
PRECISM2EA	MAM	1.82	1.35	1.24	3.37	1.98	2.04	1.07
	JJA	0.64	0.59	1.11	0.64	0.88	0.77	0.56
	OND	1.35	0.99	1.01	2.26	1.17	1.25	0.87
HADGEM50	MAM	1.04	1.51	0.95	1.09	1.65	1.53	0.99
	JJA	0.47	0.80	1.12	0.82	0.81	1.72	0.72
	OND	1.02	1.37	0.71	0.84	0.77	0.46	0.65
HADGEM25	MAM	1.69	1.82	1.13	1.41	2.49	1.12	1.35
	JJA	1.11	1.46	1.64	1.22	1.41	1.45	1.33
	OND	0.78	1.82	1.12	1.14	1.32	0.65	1.19
RCM ENSEMBLE (5)	MAM	1.22	1.16	1.19	1.71	1.64	1.53	0.80
	JJA	0.56	0.71	0.56	0.69	0.81	0.84	0.44
	OND	1.26	1.00	0.88	1.40	0.85	1.01	0.73
WRF	MAM	2.04	2.45	1.70	1.20	2.01	2.60	0.87
	JJA	1.03	0.97	2.19	2.17	1.69	1.00	1.33
	OND	2.56	2.87	0.76	1.32	1.53	1.67	1.07
REGCM3	MAM	2.07	1.20	1.64	1.19	0.96	1.33	0.89
	JJA	0.78	0.98	0.89	1.25	1.29	2.01	0.64
	OND	4.57	2.19	1.61	2.76	0.80	2.41	1.45
CCLM	MAM	2.24	2.41	4.14	2.54	1.67	1.84	2.68
	JJA	1.50	2.04	2.57	3.36	2.87	2.73	2.41
	OND	1.04	1.85	1.93	1.24	1.21	1.17	1.19

Table 4.18: The computed refined wilmott indices for different model configurations with respect to CRU rainfall observations over different regions of Uganda. Values in green show significant agreement.

Refined Wilmott Index		Region 1	Region 2	Region 3	Region 4	Region 5	Region 6	Region 7
UDEL	MAM	0.73	0.53	0.76	0.75	0.78	0.77	0.76
	JJA	0.83	0.70	0.84	0.68	0.74	0.81	0.70
	OND	0.70	0.61	0.79	0.78	0.70	0.80	0.76
GPCP	MAM	-0.02	-0.13	0.55	-0.15	0.31	0.37	0.34
	JJA	0.72	0.54	0.74	0.00	0.63	0.54	0.51
	OND	0.11	0.08	0.31	0.37	0.50	0.74	0.31
ERAINT	MAM	0.18	0.11	0.74	0.71	0.51	0.66	0.78
	JJA	0.69	0.48	0.80	0.55	0.72	0.68	0.79
	OND	0.41	0.51	0.77	0.78	0.72	0.71	0.78
PRECISM1	MAM	0.45	0.36	0.64	0.21	0.21	0.17	0.61
	JJA	0.74	0.57	0.85	0.57	0.63	0.74	0.71
	OND	0.42	0.60	0.61	0.35	0.58	0.51	0.49
PRECISM2	MAM	0.54	0.47	0.54	0.42	0.18	0.33	0.63
	JJA	0.78	0.68	0.80	0.60	0.60	0.71	0.68
	OND	0.41	0.68	0.69	0.47	0.58	0.52	0.62
PRECISM2EA	MAM	0.16	0.21	0.65	-0.36	-0.10	-0.13	0.48
	JJA	0.82	0.76	0.70	0.67	0.62	0.75	0.65
	OND	0.42	0.61	0.65	0.15	0.42	0.56	0.49
HADGEM50	MAM	0.52	0.10	0.74	0.54	0.10	0.22	0.53
	JJA	0.86	0.68	0.70	0.55	0.64	0.38	0.53
	OND	0.59	0.39	0.79	0.70	0.64	0.86	0.66
HADGEM25	MAM	0.18	-0.09	0.71	0.39	-0.31	0.43	0.29
	JJA	0.66	0.38	0.54	0.30	0.37	0.47	0.07
	OND	0.54	0.16	0.62	0.57	0.40	0.83	0.29
RCM ENSEMBLE (5)	MAM	0.45	0.35	0.68	0.25	0.09	0.15	0.64
	JJA	0.83	0.71	0.87	0.65	0.66	0.70	0.76
	OND	0.46	0.60	0.70	0.45	0.58	0.64	0.57
WRF	MAM	-0.03	-0.33	0.52	0.49	-0.14	-0.32	0.55
	JJA	0.70	0.62	0.36	-0.23	0.21	0.64	0.06
	OND	-0.05	-0.30	0.74	0.51	0.27	0.39	0.40
REGCM3	MAM	0.08	0.36	0.55	0.51	0.54	0.37	0.53
	JJA	0.78	0.61	0.78	0.32	0.40	0.29	0.60
	OND	-0.49	-0.03	0.48	-0.13	0.64	0.12	0.14
CCLM	MAM	-0.14	-0.35	-0.26	-0.16	0.11	0.02	-0.36
	JJA	0.52	0.07	0.25	-0.52	-0.32	-0.06	-0.44
	OND	0.65	0.13	0.37	0.53	0.41	0.56	0.33

4.3.8 Inter-comparison of RCMs Performance

This section presents the results on the inter-comparison of the performance of the regional climate models using the Taylor diagram described in Section 3.2.3.5. Figures 4.58-4.60 summarize the performance indices including standard deviation (mm/day), correlation coefficient and the root mean square difference (RMSD) (mm/day) based on CRU against other rainfall data sets including the regional climate models of regional climate models during MAM, JJA and OND over Uganda. Figure 4.58 indicated the results for MAM, Figure 4.59 indicated the results for JJA whereas Figure 4.60 depicts the results for OND season of Uganda that was observed as region 7 (Figure 3.1b). The results show reasonable disagreement between the gridded observational rainfall patterns over Uganda.

The results show variability in model performance and agreement across the three seasons over Uganda. For example, Figure 4.58 shows a large spread in the agreement that for during the MAM season that for the OND season (Figure 4.60). The study findings are in agreement with previous studies (Diro *et al.*, 2011 and Moufouma-Okia and Jones, 2014).

This study has compared improvements in the model's ability in rainfall simulation due to increasing (half) model resolution. Increasing model resolution is necessarily not sufficient in improving model performance as there are many other interacting factors. Giorgi and Marinucci (1996), however, showed that simulations of rainfall may be sensitive to model resolution regardless of the topographic forcing in the model experiment they showed that rainfall tends to increase at finer resolution. The outputs of most RCMs are very much affected by its topographic configurations (Sun *et al.*, 1999a; 1999b; Song *et al.*, 2004 and Anyah *et al.*, 2006).

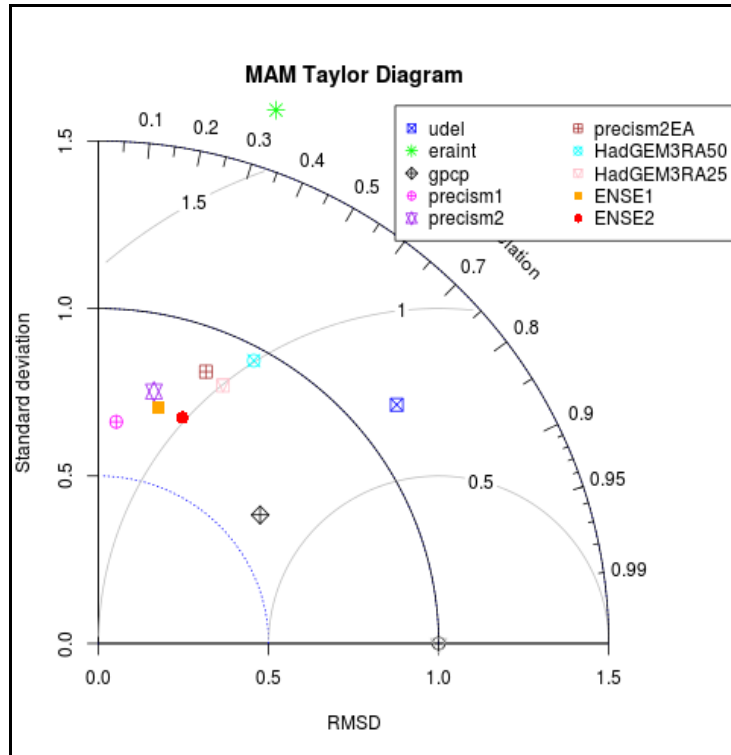


Figure 4.58: Inter model comparisons based on Taylor diagrams (summary of three model performance indices) for March-May (MAM) seasonal rainfall simulation during the period 1991-2008 over Uganda.

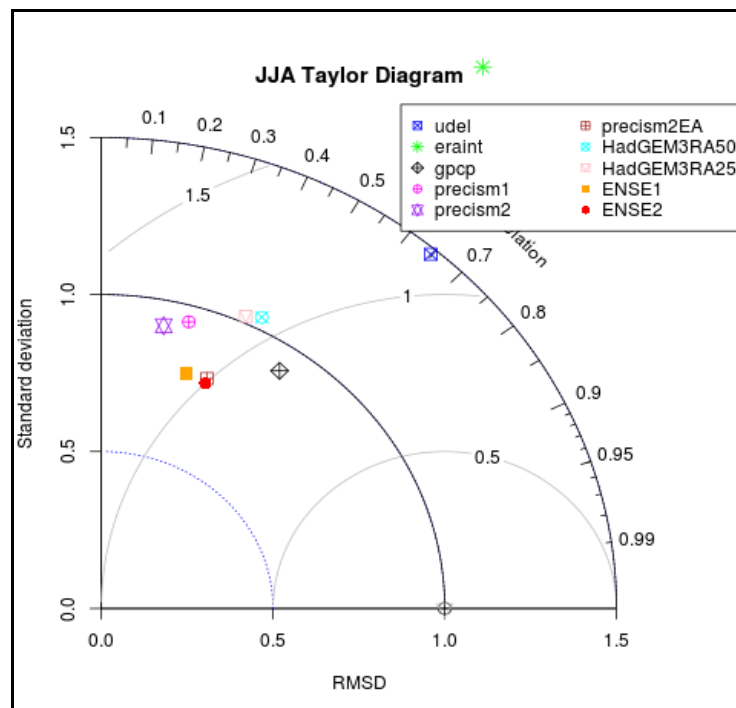


Figure 4.59: Inter model comparisons based on Taylor diagrams (summary of three model performance indices) for June-August (JJA) seasonal rainfall simulation during the period 1991-2008 over Uganda.

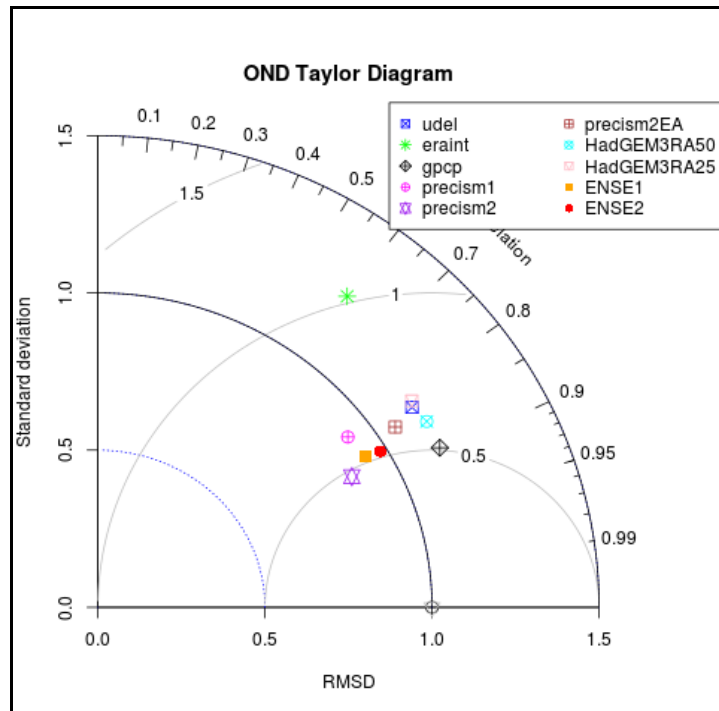


Figure 4.60: Inter model comparisons based on Taylor diagrams (summary of three model performance indices) for October-December (OND) seasonal rainfall simulation during the period 1991-2008 over Uganda.

This part of the study has examined the performance of a number of different regional climate models across the sub-regions of Uganda on seasonal time scales. The UK-Met Office regional climate model PRECIS was the main focus of the study but other models aided inter-model comparison and developing of an ensemble of the best group of models for Uganda. The study also examined the effect of resolution and domain size on performance score of the PRECIS RCM over Uganda.

Globally, there has been increase in RCMs simulation with very few RCM studies performed over the East Africa region (Sun *et al.*, 1999a; Indeje *et al.*, 2000; Anyah 2005; Anyah *et al.*, 2006; Anyah and Semazi, 2007 and Diro *et al.*, 2012). This part of the study, therefore, contributes to the effort to understand climate variability and change largely based on multiple regional climate models simulations over Uganda. By and large, evidently the results of model validation discussed here confirm the complexity of rainfall variability over most parts of Uganda especially during the MAM rainfall season. It is worth noting, however, that models were able to still display reasonable spatial and temporal patterns. Similar results showing the complexity of rainfall in regional climate models were evident in several previous studies over Lake Victoria Basin (Sabiiti, 2008), Eastern Africa (Kaspar and Cubasch, 2008; Omondi,

2010; Otieno and Anyah, 2012; Endris *et al.*, 2013; Moufouma-Okia and Jones, 2014; Opijah *et al.*, 2014; Otieno *et al.*, 2014 and Otieno *et al.*, 2015), South Africa (Engelbrecht *et al.*, 2011a; Engelbrecht *et al.*, 2011b and Moufouma-Okia and Jones, 2014) and West Africa (Diallo *et al.*, 2014 and Moufouma-Okia and Jones, 2014). The results have further observed that doubling the resolution of RCM does not significantly improve model performance over most of the region. This, however, increases rainfall intensities due to increased interaction between large scale and small scale systems.

On the other hand, unlike during short rains, meso-scale and small- (micro-) scale factors that dominate during the long rains are still not well understood in addition to failure of climate models to resolve them explicitly due to spatial resolution challenges and can only be approximated through parametrization schemes. This leaves challenges in rainfall simulation during this season.

In conclusion, the study has observed increased skill of PRECIS RCMs in the simulation of the spatial and temporal climate patterns over Uganda, especially during OND season. Key challenges were, however, still evident in the simulations of some of the low and high climate extremes. There were, inter-model variations in the representation of seasonal rainfall patterns, especially the extremes.

The study further concluded that PRECIS downscaled climate simulations provide realistic patterns of the current climate variability and can be adopted in the simulation of future climate changes effects assessments provided an optimal domain size is used.

4.4 Results on Simulated Climate Projections

This third specific objective of the study examined future climate change projections for both SRES (AR4) and RCPs (AR5) scenarios over Uganda. The results obtained from various methods of data analysis are presented in the subsequent sections.

4.4.1 IPCC SRES A1B and A2 Climate Change Projections

This section presents the results on future projections of rainfall (mm/day), average temperature (°C) and soil moisture content (SMC) (mm/day). The results were obtained from the analysis of PRECIS RCM downscaled outputs based on SRES A1B (ECHAM5) and SRES A2 (ECHAM4.5) over Uganda. The study analysis was based on the period 2011-2040 (near

future time slice) to represent the near future climate change conditions and the period 2061-2090 (far future time slice) to represent the longer term climate change conditions.

The analysis results on seasonal time scales indicating the patterns of the three climate parameters for the two SRES scenarios (A1B and A2) are presented. The study considers the mean, the variability (SD), the Coefficient of Variability (CV) [standard deviation/mean] and the projected changes in the mean and standard deviation relative to the present day gridded observations (rainfall and average temperature) [1971-2008]. The changes in soil moisture content are considered only as the difference in the projected values between the far future and the near future. This is, because, there are currently no observations on SMC over the study region.

4.4.1.1 Spatial Patterns of Projected Rainfall

Figures 4.61 (a-f) and 4.62 (a-f) show the projected spatial patterns of near term and longer term (30-year) mean seasonal rainfall (mm/day) for MAM (a, d), JJA (b, e) and OND (c, f) for two IPCC SRES A1B (Figure 4.61 a-f) and A2 (Figure 4.61 a-f) respectively over Uganda. Under the SRES A1B (Figure 4.61 a-f), the projected mean seasonal rainfall patterns for both near future and the far future periods are nearly similar for each of the three seasons with a slight increase in rainfall projected in the central and northeastern Uganda. The study observed that the L. Victoria region is likely to receive the highest amount of rainfall during MAM (a, d) and OND (c, f) with depressed rainfall during JJA season.

On the other hand, Figure 4.62 (a-f) indicated depressed seasonal mean rainfall projections under the SRES A2, compared to the SRES A1B scenarios especially around L. Victoria with more depressed rainfall more pronounced during the OND (c, f) season. The results for the OND (Figure 4.62 c, f) seasonal mean rainfall under SRES A2 show a slight increase between the near future and far future around central Uganda region.

The study results are consistent with those of previous studies. For example, Bowden *et al.* (2005) observed an increasing rainfall trend over the northern parts of the greater horn of Africa. In addition, projections by Shongwe *et al.* (2011) observed a potential increase in rainfall by a value greater than 10% at 95% confidence level.

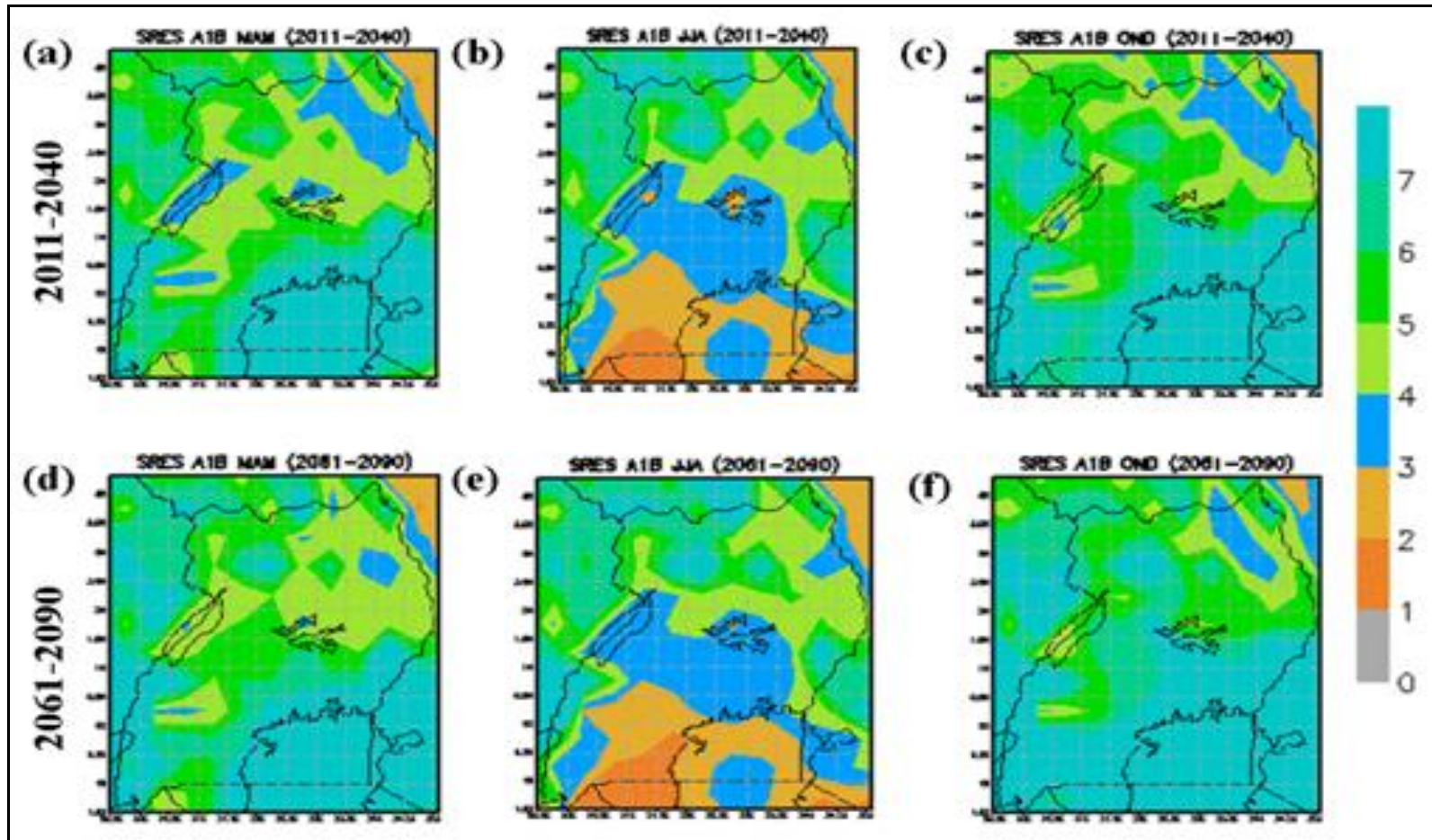


Figure 4.61 (a-f): PRECIS simulated seasonal mean rainfall (mm/day) projections for the periods 2011-2040 (a-c) and 2061-2090 (d-f) during March-May (MAM a, d), June-August (JJA b, e) and October-December (OND c, f) seasons for SRES A1B scenario over Uganda.

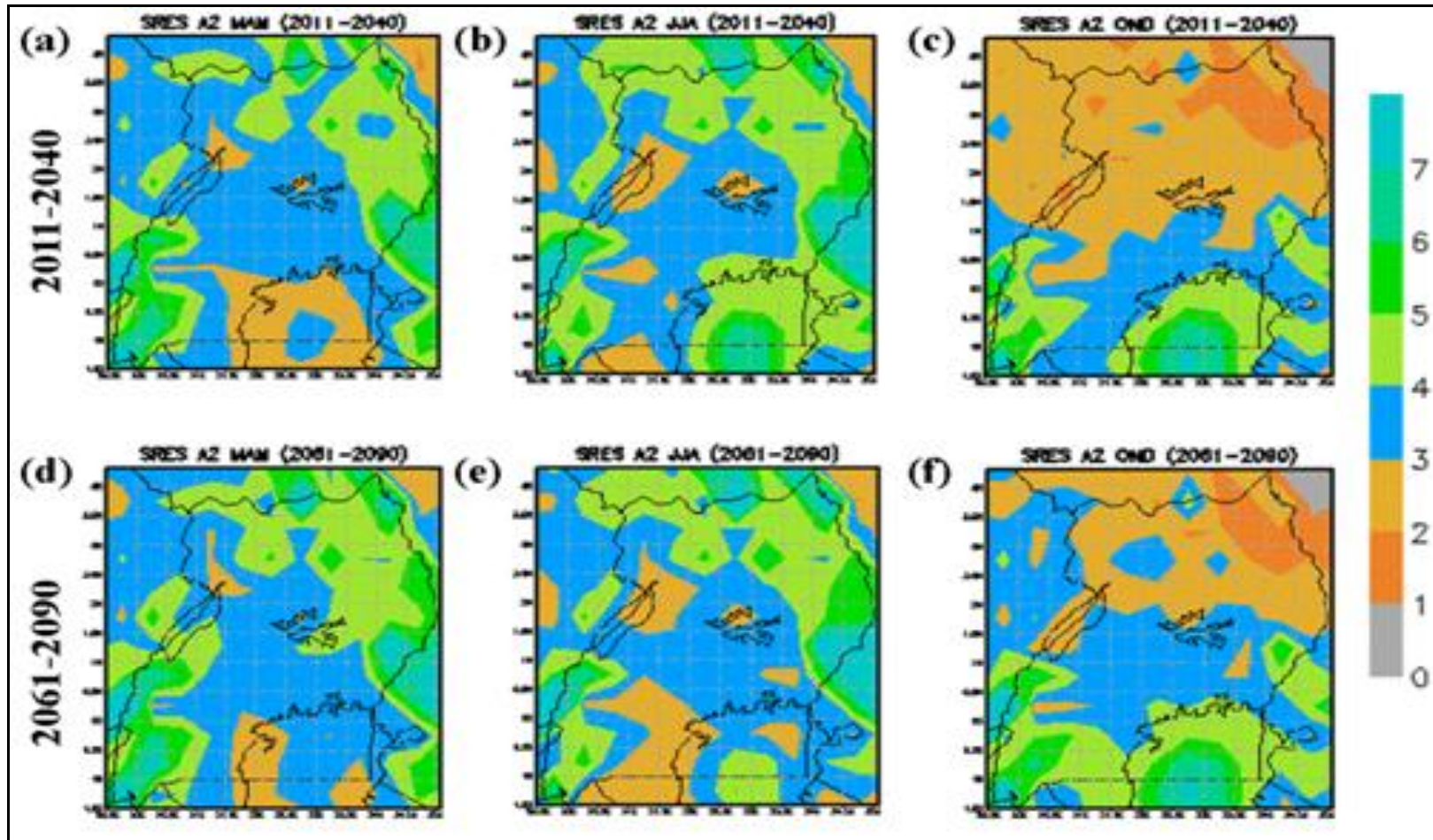


Figure 4.62 (a-f): PRECIS simulated seasonal mean rainfall (mm/day) projections for the periods 2011-2040 (a-c) and 2061-2090 (d-f) during March-May (MAM a, d), June-August (JJA b, e) and October-December (OND c, f) seasons for SRES A2 scenario over Uganda.

Figures 4.63(a-f) and 4.64 (a-f) show spatial patterns of projected seasonal rainfall variability based on computation of the standard deviation during MAM, JJA and OND rainfall seasons. The patterns in seasonal rainfall variability are presented for two SRES scenarios (A1B and A2) and the patterns have been compared in the two periods of future climate. During MAM (a, d) and OND (c, f), the results of the SRES A1B (Figure 4.63 a-f), project a likelihood of the central and the northern regions to experience the lowest variability of rainfall while the L. Victoria and southwestern regions likely to experience high rainfall variability.

The study generally observed likely increase in the variability of rainfall in future over most of the Country. Although the JJA (b, e) projected seasonal rainfall shows low rainfall variability for the period 2011-2040, the result show that there is an expected increase in rainfall variability during this season especially on the eastern border of the Country. Generally, the study observed that there might be stronger (high) variability associated with A2 than that associated with A1B SRES for the three seasons. Variability of rainfall is stronger during OND season than during MAM and JJA season with MAM variability stronger than that of JJA season. Under A1B SRES scenario, rainfall variability is likely to reduce in the far future period (2061-2090) compared with the near future period (2011-2040). Under A2 SRES scenario, the increase in rainfall variability for all seasons is likely to be quite significant between the two periods over most parts of Uganda (Figures 4.63 a-f).

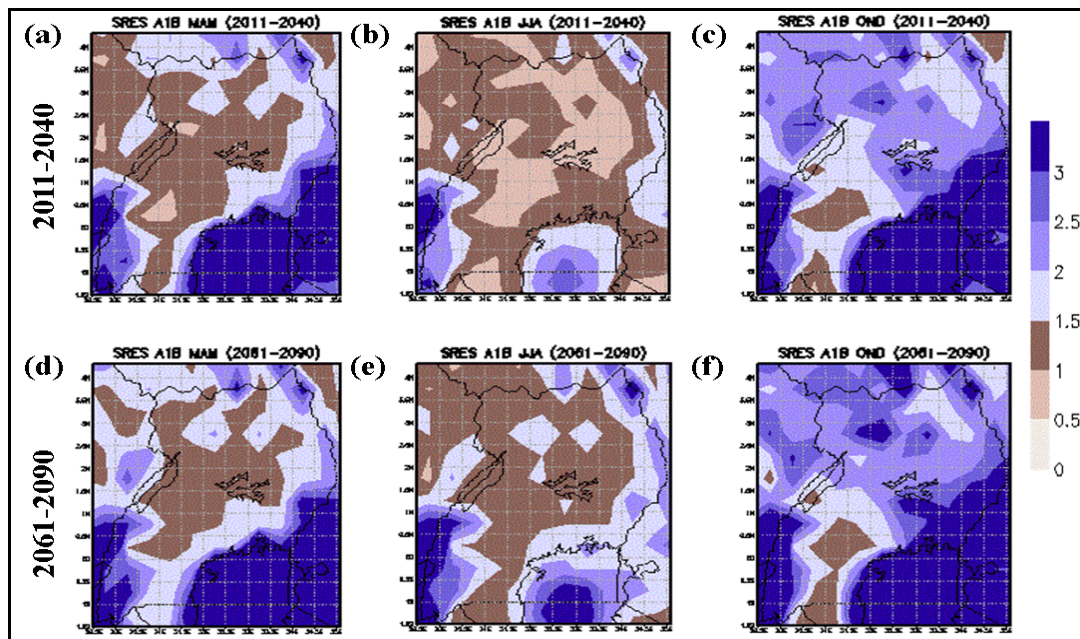


Figure 4.63 (a-f): PRECIS simulated seasonal rainfall (mm/day) variability projections for the periods 2011-2040 (a-c) and 2061-2090 (d-f) during March-May (MAM a, d), June-August (JJA b, e) and October-December (OND c, f) seasons for SRES A1B scenario over Uganda.

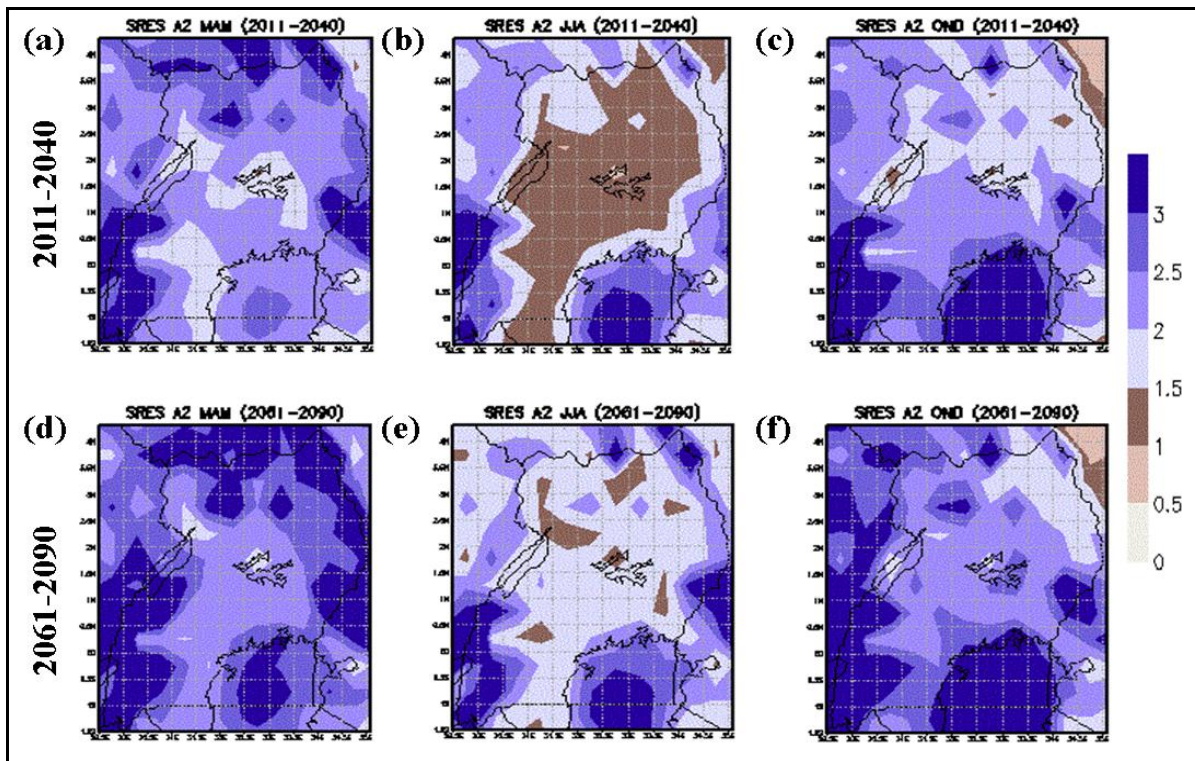


Figure 4.64 (a-f): PRECIS simulated seasonal rainfall (mm/day) variability projections for the periods 2011-2040 (a-c) and 2061-2090 (d-f) during March-May (MAM a, d), June-August (JJA b, e) and October-December (OND c, f) seasons for SRES A2 scenario over Uganda.

Figures 4.65(a-f)-4.64(a-f) present the spatial patterns of averaged Coefficient of Variation under both SRES A1B and A2 for two periods. The Coefficient of Variability (CV, %) has been used in this study as a measure of the percentage ratio of the standard deviation to the mean of seasonal rainfall. This index helps to compare the patterns of the mean and variability fairly in both wet and dry regions and seasons. The results (Figures 4.65 a-f) for SRES A1B scenario show lower coefficient of variability over most of Uganda. Figure 4.66 (a-f), on the other hand shows pronounced (quite high) coefficient of variability for A2 scenario and a significant increase between the two periods (2011-2040 and 2061-2090).

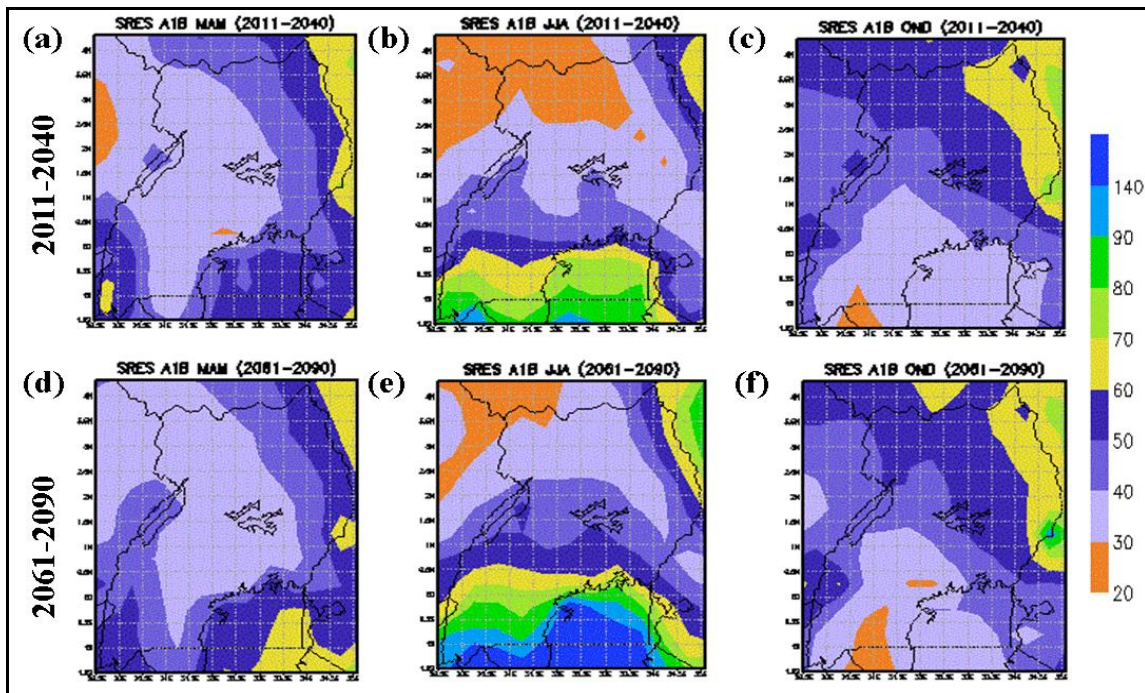


Figure 4.65 (a-f): PRECIS simulated seasonal rainfall coefficient of variation (CV, %) projections for the periods 2011-2040 (a-c) and 2061-2090 (d-f) during March-May (MAM a, d), June-August (JJA b, e) and October-December (OND c, f) seasons for SRES A1B scenario over Uganda.

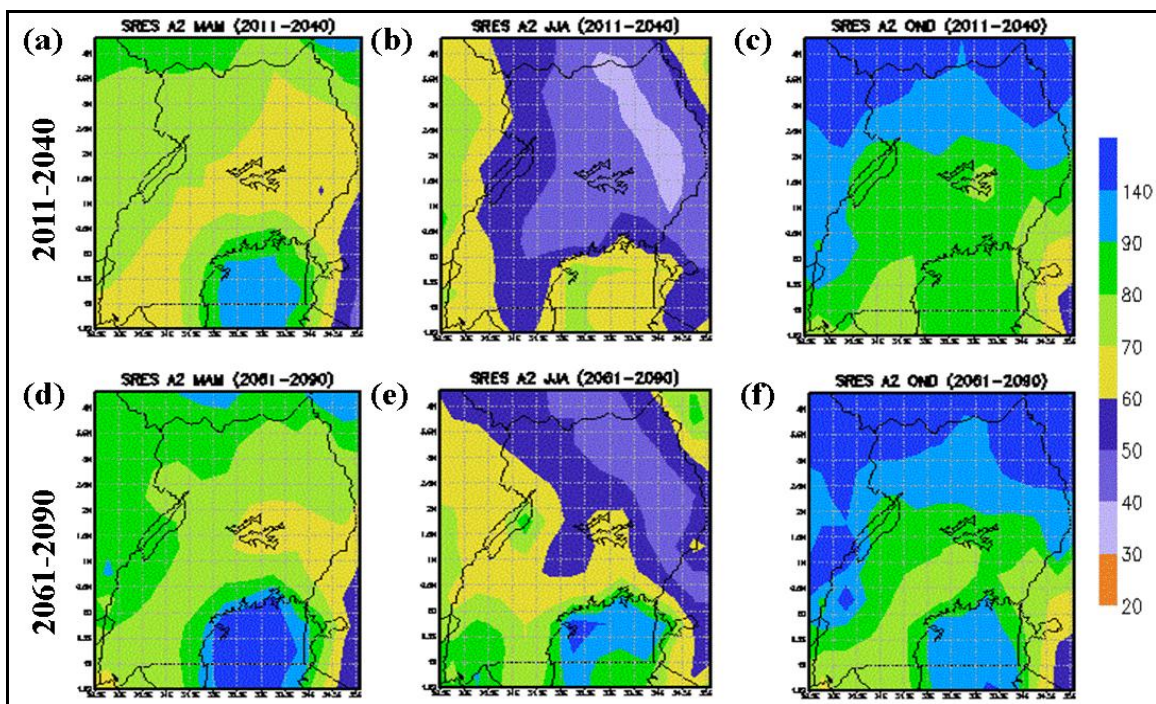


Figure 4.66 (a-f): PRECIS simulated seasonal rainfall coefficient of variation (CV, %) projections for the periods 2011-2040 (a-c) and 2061-2090 (d-f) during March-May (MAM a, d), June-August (JJA b, e) and October-December (OND c, f) seasons for SRES A2 scenario over Uganda.

Figures 4.67 (a-f) and 4.68 (a-f) show the change in the projected mean seasonal rainfall during the two periods for the two SRES scenarios relative to the present CRU observations during the climatological period (1971-2008) over the Country. Figure 4.67 indicated likelihood of enhanced mean rainfall change during MAM (a, d) and OND (c, f) of at least 1-2 mm/day over most of the regions of Uganda. During JJA (b, e), on the other hand, rainfall will be slightly depressed in few regions under A1B scenario.

Generally seasonal rainfall is projected to slightly increase between 2011-2040 (a-c) and 2061-2090 (d-f). During OND (c, f), areas around L. Victoria are likely to receive enhance rainfall that has potential to cause floods over some regions. Some parts of southwestern Uganda also observed enhanced rainfall under the A1B scenarios. This part of the study (Figure 4.68 a-f) also observed a likelihood of strong reduction in rainfall during all the three seasons that is more pronounced during all the three seasons. The direction of change in rainfall is evident over northwestern region during JJA (b, e) for both periods under A2 SRES scenarios.

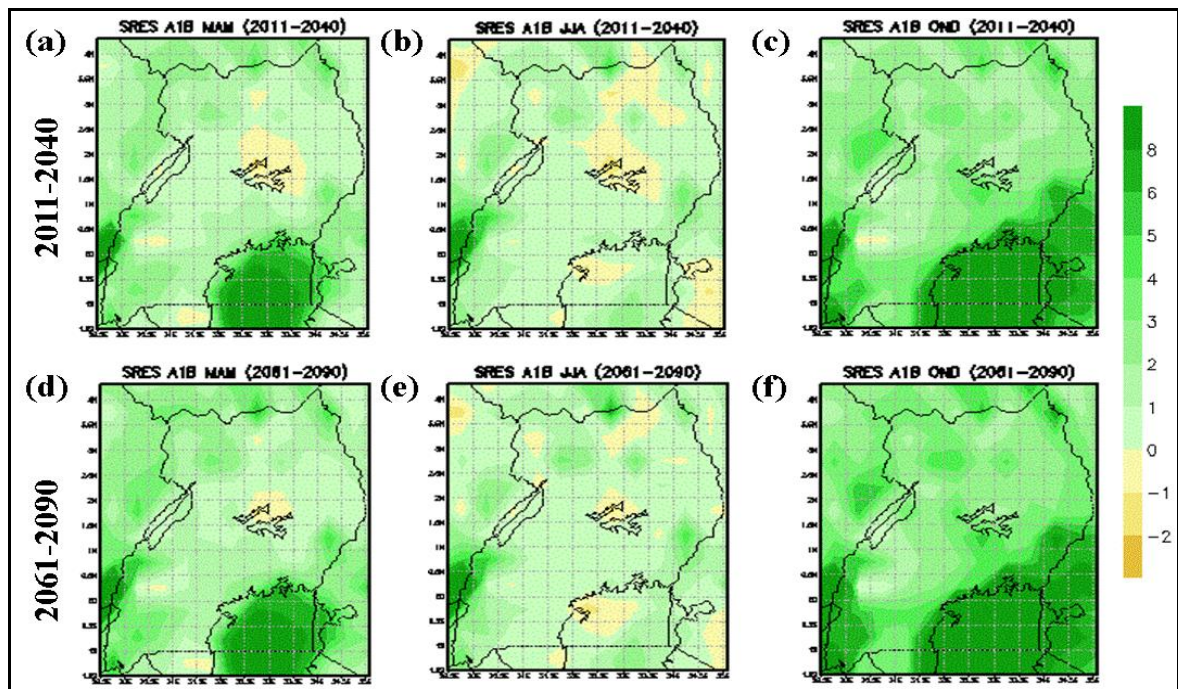


Figure 4.67 (a-f): PRECIS simulated seasonal rainfall (mm/day) changes for the periods 2011-2040 (a-c) and 2061-2090 (d-f) during March-May (MAM a, d), June-August (JJA b, e) and October-December (OND c, f) seasons for SRES A1B scenario over Uganda.

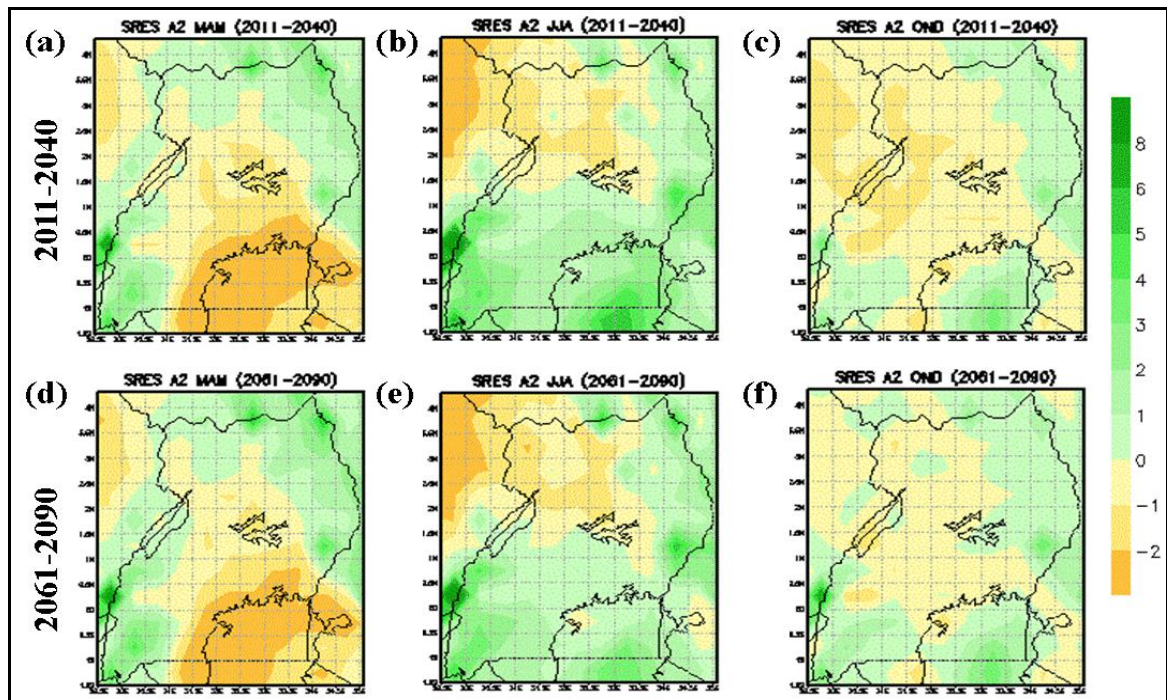


Figure 4.68 (a-f): PRECIS simulated seasonal rainfall (mm/day) changes for the periods 2011-2040 (a-c) and 2061-2090 (d-f) during March-May (MAM a, d), June-August (JJA b, e) and October-December (OND c, f) seasons for SRES A2 scenario over Uganda.

Tables 4.19 and 4.20 show the computed values for the seasonal mean rainfall, standard deviation and changes (in the mean and standard deviation) for the two SRES scenarios for the periods (2011-2040 and 2061-2090). The projections of seasonal rainfall change mean and variability changes were computed for the future period with reference to the CRU observations (1971-2008) over different sub-regions. In contrast, there is likely to be higher seasonal rainfall under A1B (Table 4.19) than under A2 (Table 4.20) SRES scenarios, higher seasonal rainfall variability under A2 (Table 4.20) than A1B (Table 4.19) SRES scenarios, rainfall is expected to increase under A1B while it is expected to decrease under A2. In addition, the study observed a decrease in rainfall variability under A1B while the rainfall variability will increase under A2 SRES scenario. These results have revealed changes in rainfall seasonality that are consistent with earlier findings observed in previous research (Shongwe *et al.*, 2009; Omondi, 2010; Van den Bergh *et al.*, 2012; Washington and Pearce, 2012; Anyah and Qui, 2012 and Rowell, 2012).

Table 4.19: IPCC SRES A1B scenario projected mean rainfall, standard deviation (SD) and change (mm/day) over different regions of Uganda.

		MAM		JJA		OND	
		2011-2040	2061-2090	2011-2040	2061-2090	2011-2040	2061-2090
Mean	Southwestern	6.04	6.80	2.93	3.35	8.66	10.22
	Western	4.78	5.34	3.71	3.76	5.05	5.78
	Central	6.82	7.23	3.39	3.41	8.61	9.59
	Eastern	6.67	7.19	5.20	5.34	8.22	9.31
	Northwestern	4.86	5.38	5.44	5.58	5.41	6.14
	Northeastern	4.27	4.65	4.67	5.01	4.04	4.65
	Uganda	6.72	7.20	4.13	4.24	9.05	10.14
SD	Southwest	2.40	2.76	1.77	2.54	2.36	2.76
	Western	1.28	1.63	1.26	1.71	1.66	1.83
	Central	1.85	2.10	1.10	1.58	2.70	3.10
	Eastern	2.63	2.70	1.38	1.79	3.48	4.47
	Northwestern	1.30	1.41	1.05	1.38	2.27	2.53
	Northeastern	1.80	1.82	1.27	1.79	2.02	2.30
	Uganda	2.35	2.72	1.29	1.72	2.94	3.40
Change (Mean)	Southwest	2.50	3.26	1.47	1.89	4.56	6.13
	Western	0.90	1.46	1.11	1.16	1.06	1.79
	Central	1.60	2.01	0.66	0.67	4.68	5.67
	Eastern	1.48	2.00	1.13	1.26	5.22	6.32
	Northwestern	1.14	1.66	0.78	0.92	2.15	2.89
	Northeastern	1.28	1.67	0.46	0.80	2.47	3.09
	Uganda	2.14	2.62	0.75	0.85	5.69	6.78
Change (SD)	Southwest	0.92	1.44	0.68	1.45	0.92	1.32
	Western	-0.37	0.12	-0.04	0.41	-0.37	-0.20
	Central	0.86	0.20	-0.13	0.35	0.86	1.26
	Eastern	1.78	0.60	-0.08	0.33	1.78	2.78
	Northwestern	0.03	-0.27	-0.66	-0.33	0.03	0.29
	Northeastern	0.80	0.31	-0.20	0.32	0.80	1.08
	Uganda	1.11	0.91	-0.11	0.33	1.11	1.58

Table 4.20: IPCC SRES A2 scenario projected mean rainfall, standard deviation (SD) and change (mm/day) over different regions of Uganda.

		MAM		JJA		OND	
		2011-2040	2061-2090	2011-2040	2061-2090	2011-2040	2061-2090
Mean	Southwest	5.34	5.50	4.47	4.02	4.57	5.05
	Western	3.82	4.17	3.66	3.55	2.84	3.41
	Central	3.40	3.54	3.86	3.41	3.34	3.69
	Eastern	4.89	5.23	5.57	5.37	3.31	3.67
	Northwestern	3.56	3.61	3.63	3.49	2.33	2.82
	Northeastern	4.47	4.92	4.80	5.14	2.00	2.13
	Uganda	3.87	4.11	4.23	3.97	3.15	3.51
SD	Southwest	3.10	3.51	2.40	2.84	3.33	3.48
	Western	2.36	3.03	1.68	2.01	2.21	2.78
	Central	2.12	2.45	1.52	1.91	2.45	2.63
	Eastern	2.57	3.01	1.83	2.26	2.32	2.60
	Northwestern	2.34	2.53	1.43	1.61	2.00	2.41
	Northeastern	2.68	3.28	1.57	2.06	1.83	1.97
	Uganda	2.39	2.83	1.81	2.10	2.41	2.76
Change (Mean)	Southwest	1.80	1.96	3.01	2.56	0.47	0.96
	Western	-0.06	0.29	1.05	0.95	-1.15	-0.57
	Central	-1.82	-1.68	1.13	0.67	-0.58	-0.23
	Eastern	-0.30	0.04	1.49	1.30	0.32	0.67
	Northwestern	-0.16	-0.11	-1.03	-1.17	-0.92	-0.44
	Northeastern	1.49	1.94	0.59	0.92	0.44	0.56
	Uganda	-0.70	-0.47	0.84	0.58	-0.20	0.16
Change (SD)	Southwest	1.78	2.18	1.31	1.75	1.89	2.04
	Western	0.85	1.51	0.38	0.72	0.18	0.75
	Central	0.21	0.54	0.29	0.68	0.61	0.79
	Eastern	0.48	0.92	0.36	0.79	0.62	0.90
	Northwestern	0.67	0.85	-0.28	-0.10	-0.24	0.17
	Northeastern	1.16	1.76	0.10	0.59	0.61	0.75
	Uganda	0.58	1.02	0.42	0.70	0.59	0.93

4.4.2 Spatial Patterns of Projected Average Temperature

The PRECIS downscaled projection of seasonal average temperature over Uganda is presented in this section. Spatial patterns in the mean average temperature for the two SRES scenarios and two periods are showed in Figures 4.69 (a-f, SRES A1B) and 4.70 (a-f, SRES A2). Figure 4.69 indicated warmer temperature for the period 2061-2090 (d-f) than for 2011-2040 (a-c) over all the Country. Temperatures are projected to be warm in northern Uganda during MAM (a, d) than during JJA (b, e) and OND (c, f) seasons for both periods. During OND season, the rise in temperatures between 2011-2040 and 2061-2090 is quite high (Figure 4.69 c, f). The temperature under A2 SRES is quite warmer than that for A1B in all season during both

periods (Figure 4.70). The MAM and OND seasonal temperature patterns are quite similar with JJA indicating warmer temperatures.

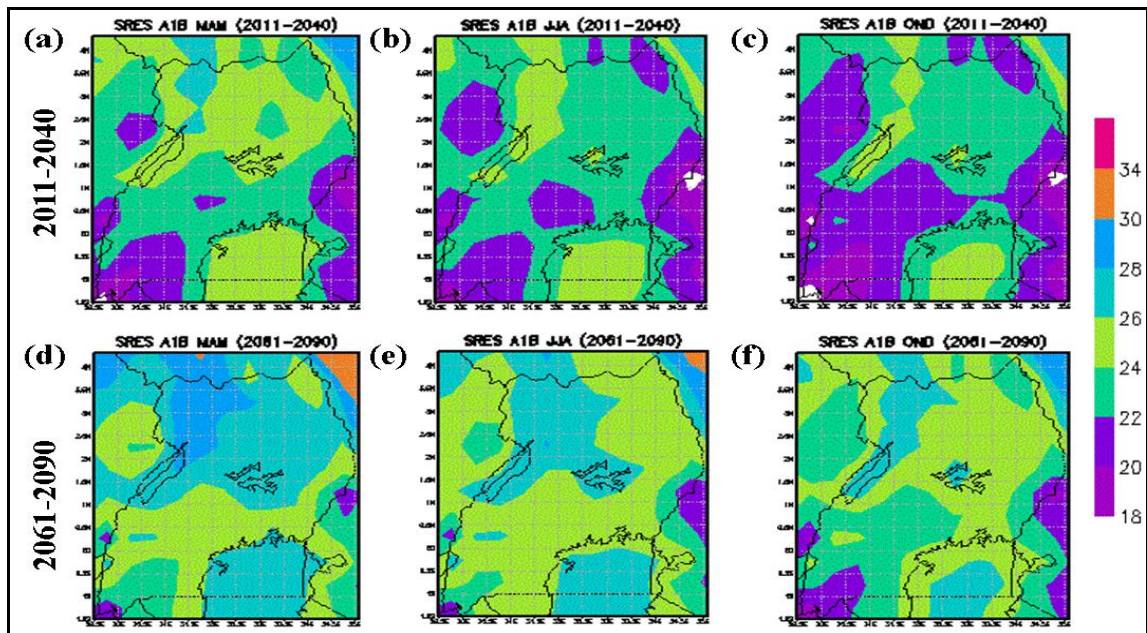


Figure 4.69 (a-f): PRECIS simulated seasonal mean surface temperature ($^{\circ}\text{C}$) projections for the periods 2011-2040 (a-c) and 2061-2090 (d-f) during March-May (MAM a, d), June-August (JJA b, e) and October-December (OND c, f) seasons for SRES A1B scenario over Uganda.

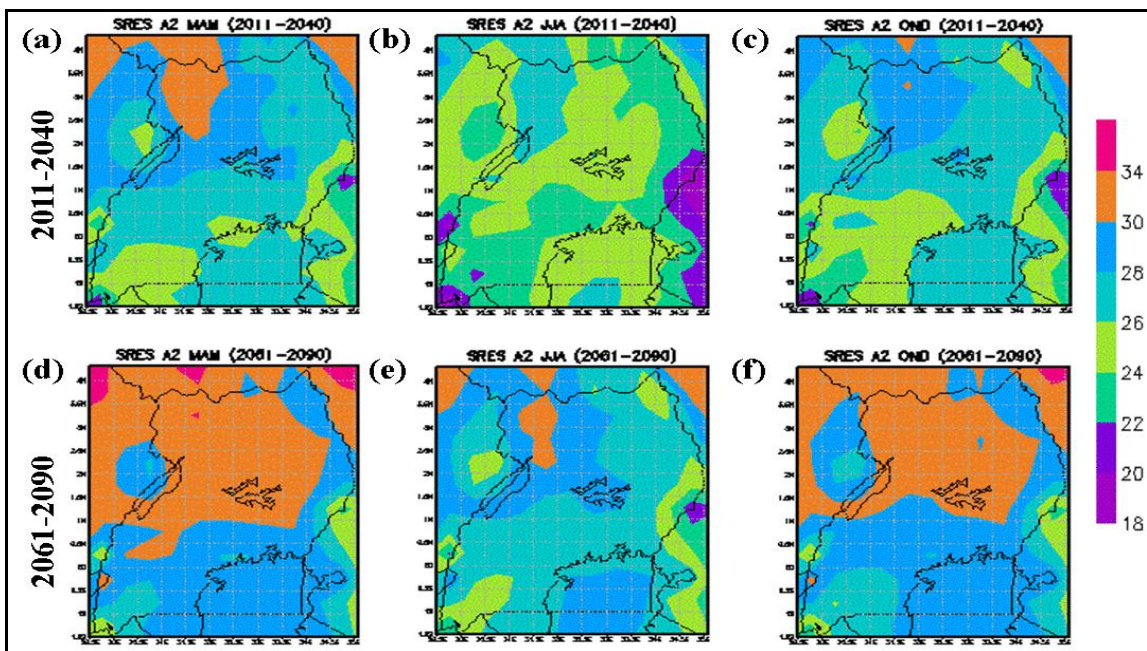


Figure 4.70 (a-f): PRECIS simulated seasonal mean surface temperature ($^{\circ}\text{C}$) projections for the periods 2011-2040 (a-c) and 2061-2090 (d-f) during March-May (MAM a, d), June-August (JJA b, e) and October-December (OND c, f) seasons for SRES A2 scenario over Uganda.

The projected variability (SD) in temperature is shown in Figure 4.71 (a-f, SRES A1B) and Figure 4.72 (a-f, SRES A2). Figure 4.71 indicated that temperatures variability is higher over northern parts of Uganda especially during MAM (a, d) and JJA (b, e) seasons under the A1B scenario. Under the A2 scenario on the other hand, the variability in temperature is higher for MAM and OND scenarios over the northern parts of the Country (Figure 4.72). MAM shows the higher variability during the A2 SRES while JJA season is projected to experience low temperature variability. The period 2061-2090 has higher variability than 2011-2040 under both climate scenarios.

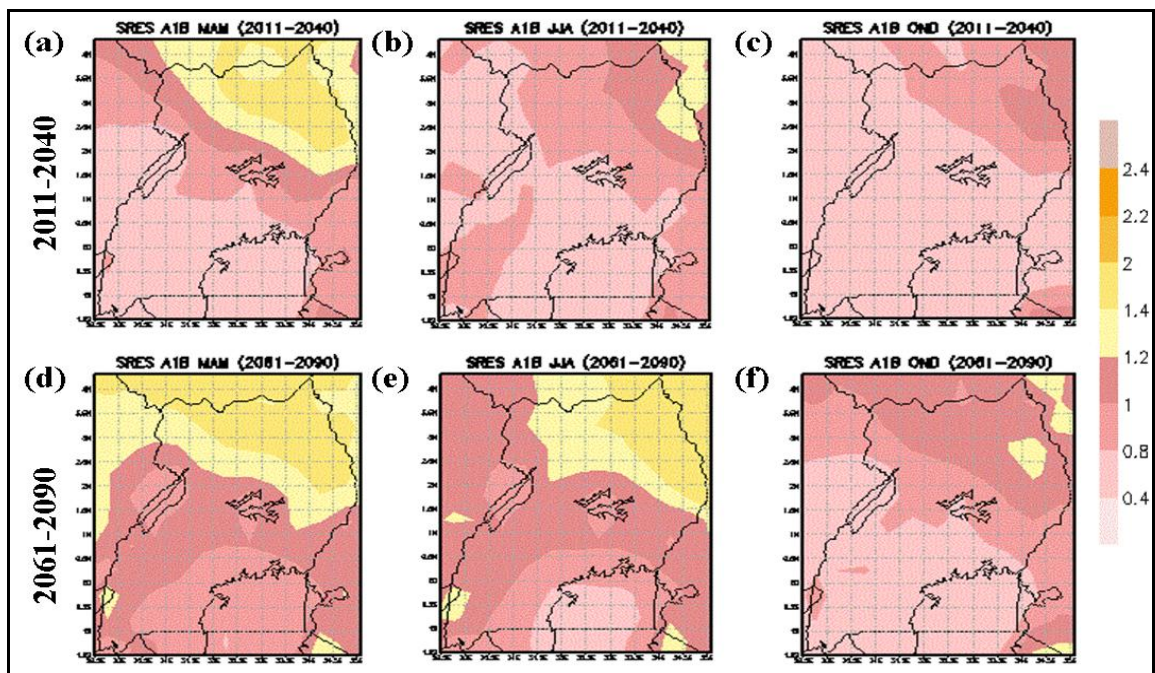


Figure 4.71 (a-f): PRECIS simulated seasonal surface temperature ($^{\circ}\text{C}$) variability (standard deviation) projections for the periods 2011-2040 (a-c) and 2061-2090 (d-f) during March-May (MAM a, d), June-August (JJA b, e) and October-December (OND c, f) seasons for SRES A1B scenario over Uganda.

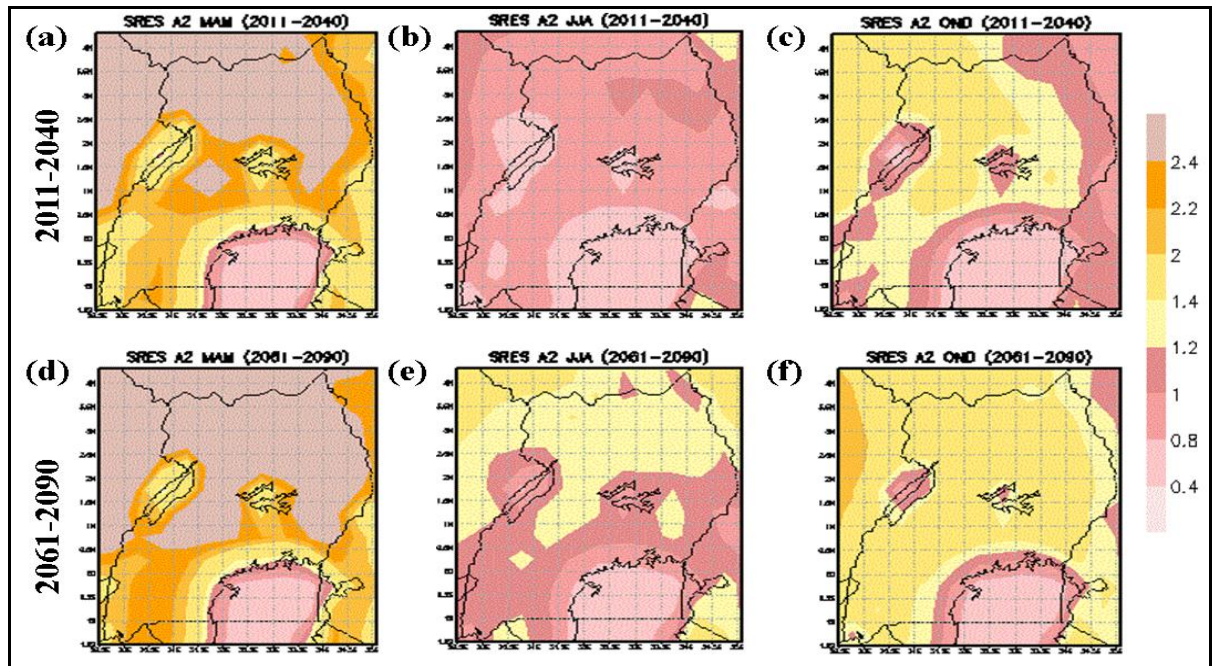


Figure 4.72 (a-f): PRECIS simulated seasonal surface temperature ($^{\circ}\text{C}$) variability (standard deviation) projections for the periods 2011-2040 (a-c) and 2061-2090 (d-f) during March-May (MAM a, d), June-August (JJA b, e) and October-December (OND c, f) seasons for SRES A2 scenario over Uganda.

The associated coefficient of variation is presented in Figure 4.73 (SRES A1B) and 4.74 (SRES A2). Figure 4.73 and 4.74 shows the spatial patterns of Coefficient of Variability for temperature. Figure 4.73 shows patterns for A1B scenario while Figure 4.74 presents results for A2 scenario. The study observed that A2 scenario is more likely to experience higher CV than A1B scenarios. The MAM season is likely to experience higher CV than both JJA and OND seasons. The study observed that CV values are expected to be higher for the period 2061-2090 than for 2011-2040 for both scenarios over most regions.

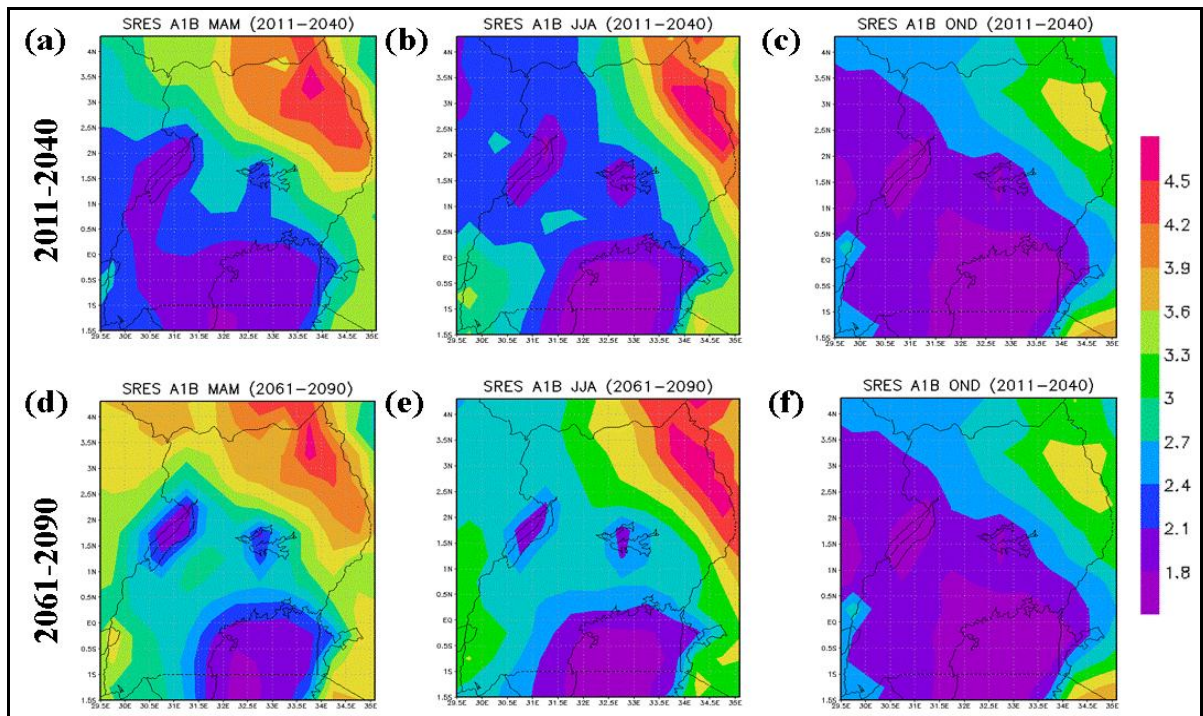


Figure 4.73 (a-f): PRECIS simulated seasonal surface temperature coefficient of variation (CV, %) projections for the periods 2011-2040 (a-c) and 2061-2090 (d-f) during March-May (MAM a, d), June-August (JJA b, e) and October-December (OND c, f) seasons for SRES A1B scenario over Uganda.

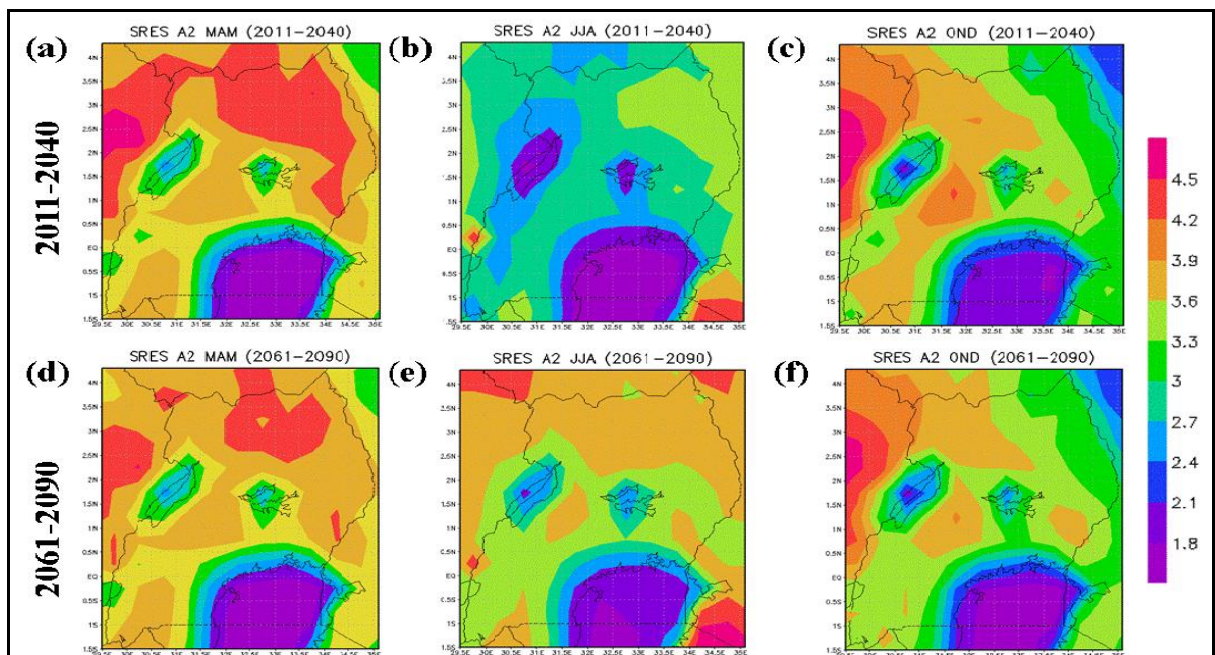


Figure 4.74 (a-f): PRECIS simulated seasonal surface temperature coefficient of variation (CV, %) projections for the periods 2011-2040 (a-c) and 2061-2090 (d-f) during March-May (MAM a, d), June-August (JJA b, e) and October-December (OND c, f) seasons for SRES A2 scenario over Uganda.

The projected changes in average temperature between the model for the two periods (2011-2040 and 2061-2090) and the CRU gridded observational are presented in Figure 4.75 (a-f,

SRES A1B) and 4.76 (a-f, SRES A2). Figure 4.75 indicated that season temperature is expected to be higher for A2 than for A1B relative to the current CRU observed for the period 1971-2008. Stronger spatial variability in temperature will be experienced during JJA (c, e). This is also observed during the OND season for the period 2061-2090 both in A1B (Figure 4.75f) and A2 (Figure 4.76f).

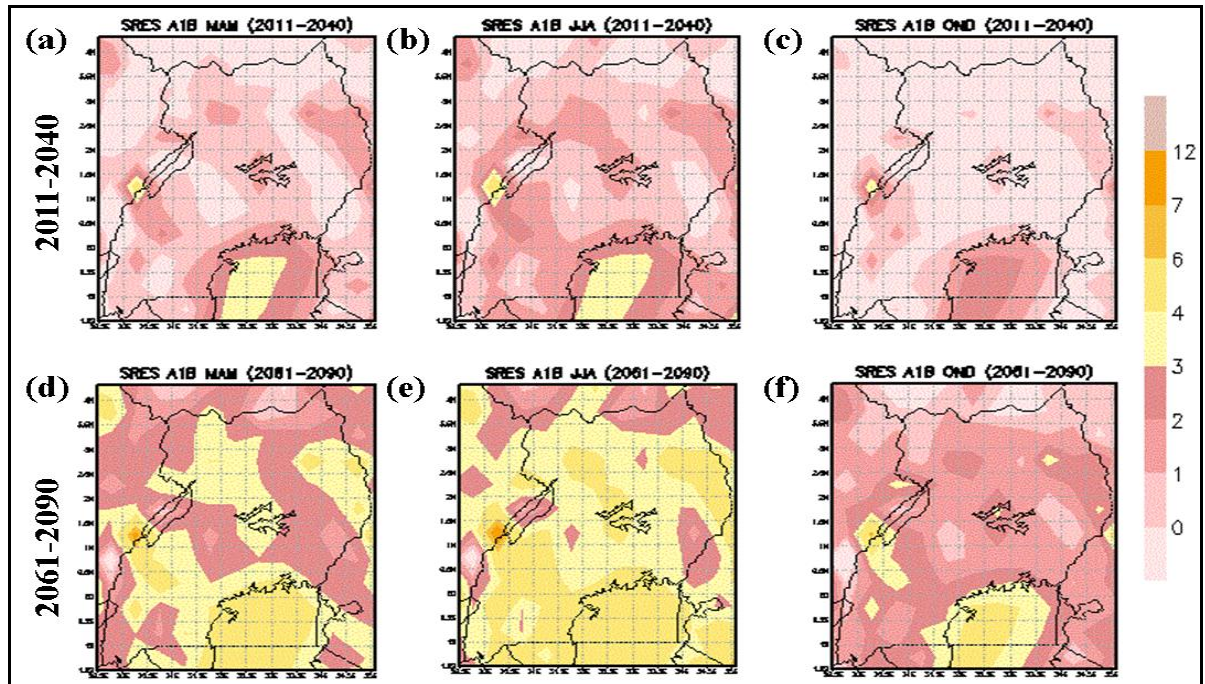


Figure 4.75 (a-f): PRECIS simulated seasonal surface temperature changes (°C) for the periods 2011-2040 (a-c) and 2061-2090 (d-f) during March-May (MAM a, d), June-August (JJA b, e) and October-December (OND c, f) seasons for SRES A1B scenario over Uganda.

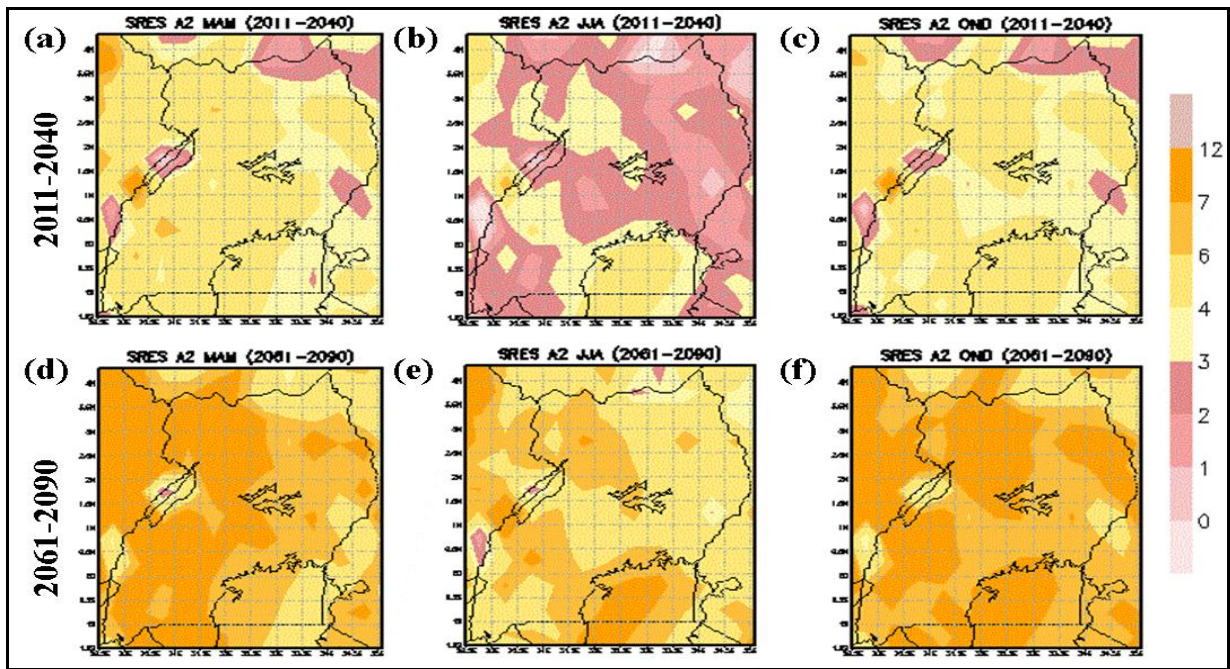


Figure 4.76 (a-f): PRECIS simulated seasonal surface temperature changes ($^{\circ}\text{C}$) for the periods 2011-2040 (a-c) and 2061-2090 (d-f) during March-May (MAM a, d), June-August (JJA b, e) and October-December (OND c, f) seasons for SRES A2 scenario over Uganda.

Tables 4.21 and 4.22 present the summary of the mean, standard deviation, change in the mean and change in the standard deviation for SRES A1B and A2 respectively during MAM, JJA and OND over the sub-regions of Uganda. Table 4.21 shows small changes in temperature for A1B scenario of about 2-3 $^{\circ}\text{C}$ between 2011-2040 and 2061-2090. Temperature variability is projected to be between 0.5 and 1.5 $^{\circ}\text{C}$ with a change in variability of about 0.2-0.5 $^{\circ}\text{C}$ between the period 2011-2040 and 2061-2090 over most sub-regions in Uganda. The changes in average temperature mean relative to current observation under SRES A1B scenario is small and in some cases negative especially for the period 2011-2040 with the changes getting higher in future period (2061-2090). It is also observed that variability changes of projected average temperature under SRES A1B scenario relative to current CRU observations range between 0.02-1.04 $^{\circ}\text{C}$.

Table 4.22 shows results for projected average temperature under SRES A2 over sub regions of Uganda. The study observed that future average temperatures are likely to range between 22-31 $^{\circ}\text{C}$ with a temperature increase of about 3 $^{\circ}\text{C}$ between the period 2011-2040 and 2061-2090. The variability under SRES A2 is projected to range between 0.7-2 $^{\circ}\text{C}$ (Table 4.22). The variability is also expected to be low during JJA season and high during MAM and OND season over most sub-regions. Under A2 scenario the change in temperature for the two future

periods relative to the current observations range between 1.62-7.4 °C while the changes in variability in temperature relative to the current temperature observation are projected to range between 0.2-1.7 °C.

Unlike rainfall, the inter-annual variability of average annual temperature is very small. Models agree on the continuation of the already observed increasing trends in temperatures by 2030 with low average projected temperatures increase for lower emission scenario and slightly higher in the high emission scenario. Several models project an increase higher than 2 °C (Omondi, 2010; Washington and Pearce, 2012; IPCC, 2014 and James *et al.*, 2014).

Table 4.21: IPCC SRES A1B projected average temperature (2011-2040 & 2061-2090) mean, standard deviation and change.

		MAM		JJA		OND	
		2011-2040	2061-2090	2011-2040	2061-2090	2011-2040	2061-2090
Mean	Southwest	20.74	23.49	21.25	24.25	19.68	21.97
	Western	23.39	26.13	23.06	25.95	22.02	24.36
	Central	23.21	25.79	22.36	25.27	22.08	24.31
	Eastern	22.00	24.49	20.79	23.65	20.88	23.00
	Northwestern	25.77	28.47	24.38	27.21	23.85	26.19
	Northeastern	23.74	26.34	22.20	25.13	22.09	24.29
	Uganda	23.51	26.07	22.60	25.39	22.15	24.36
SD	Southwest	0.65	1.05	0.84	1.06	0.57	0.73
	Western	0.71	1.05	0.80	1.08	0.57	0.76
	Central	0.78	0.98	0.75	0.97	0.56	0.74
	Eastern	1.02	1.15	0.84	1.12	0.69	0.91
	Northwestern	1.13	1.26	0.82	1.19	0.74	0.97
	Northeastern	1.45	1.48	1.11	1.54	0.95	1.12
	Uganda	0.95	1.13	0.84	1.10	0.68	0.86
Change (Mean)	Southwest	1.44	4.17	2.03	4.92	0.78	3.12
	Western	0.70	3.28	0.99	3.90	-0.33	1.90
	Central	-0.02	2.47	0.24	3.11	-0.74	1.39
	Eastern	0.60	3.29	0.92	3.75	-0.69	1.65
	Northwestern	-0.14	2.46	0.30	3.23	-1.02	1.19
	Northeastern	0.59	3.16	1.01	3.80	-0.29	1.92
	Uganda	-0.02	0.38	0.04	0.26	-0.10	0.06
Change (SD)	Southwest	-0.02	0.38	0.04	0.26	-0.10	0.06
	Western	0.03	0.37	0.25	0.53	0.01	0.20
	Central	-0.04	0.15	0.30	0.52	0.04	0.22
	Eastern	0.11	0.24	0.40	0.67	0.14	0.36
	Northwestern	0.06	0.19	0.19	0.55	0.08	0.31
	Northeastern	0.37	0.40	0.61	1.04	0.39	0.56
	Uganda	0.07	0.25	0.29	0.56	0.09	0.28

Table 4.22: IPCC SRES A2 projected average temperature (2011-2040 & 2061-2090) mean, standard deviation and change over sub-regions of Uganda.

		MAM		JJA		OND	
		2011-2040	2061-2090	2011-2040	2061-2090	2011-2040	2061-2090
Mean	Southwest	25.26	27.87	22.70	25.96	24.06	26.97
	Western	27.715	30.362	24.70	27.83	26.54	29.46
	Central	26.864	29.403	24.13	27.27	26.41	29.20
	Eastern	25.462	28.021	22.24	25.33	25.05	27.88
	Northwestern	30.25	32.894	26.62	29.78	29.18	32.06
	Northeastern	27.223	29.848	23.52	26.59	26.68	29.61
	Uganda	27.154	29.696	24.28	27.33	26.54	29.33
SD	Southwest	2.04	1.14	0.84	2.22	1.22	1.45
	Western	2.09	2.32	0.85	1.17	1.27	1.52
	Central	1.85	1.93	0.76	1.01	1.10	1.33
	Eastern	2.13	2.28	0.86	1.11	1.13	1.43
	Northwestern	2.54	2.70	0.91	1.32	1.50	1.76
	Northeastern	2.53	2.68	0.97	1.24	1.15	1.45
	Uganda	2.03	2.17	0.85	1.13	1.15	1.40
Change (Mean)	Southwest	4.54	5.51	2.24	7.15	3.90	6.81
	Western	5.76	8.41	3.67	6.79	5.30	8.22
	Central	4.36	6.90	2.76	5.89	4.00	6.79
	Eastern	3.44	6.00	1.69	4.78	3.44	6.26
	Northwestern	5.08	7.72	3.16	6.32	4.64	7.52
	Northeastern	3.34	5.96	1.62	4.69	3.57	6.50
	Uganda	4.24	6.78	2.69	5.73	4.10	6.89
Change (SD)	Southwest	1.37	0.34	0.04	1.55	0.56	0.79
	Western	1.41	0.62	0.30	1.64	0.71	0.97
	Central	1.02	0.56	0.31	1.11	0.58	0.81
	Eastern	1.22	0.67	0.41	1.36	0.57	0.88
	Northwestern	1.47	0.69	0.28	1.63	0.83	1.10
	Northeastern	1.45	0.74	0.47	1.60	0.59	0.88
	Uganda	1.15	0.59	0.30	1.28	0.56	0.81

4.4.3 Spatial Patterns of Projected Soil Moisture Content at root zone

The results on the PRECIS downscaled projections of seasonal soil moisture content at root zone (here after referred to as soil moisture content) over Uganda are presented in this section. Spatial patterns in the mean soil moisture content for the two SRES scenarios and two periods are showed in Figures 4.77 (a-f, SRES A1B) and 4.78 (a-f, SRES A2). Figure 4.77 indicated future seasonal soil moisture content under A1B scenario to range between 0.4-7 mm/day with considerably high spatial variability for all the three seasons. During MAM season (a, d), the patterns in soil moisture are likely to remain close during the two periods. The JJA season (b, e) is likely to have low soil moisture content compared to MAM (a-d) and JJA season while OND season (c, f) is projected to have higher soil moisture content in both periods under the A1B scenario (Figure 4.77 c, f). Under the A2 scenario, the projected seasonal soil moisture content is lower than the compared with A1B scenario. There is still high spatial variability in all the seasons. A slight reduction in the soil moisture content is observed in both JJA (Figure 4.78 b, e) and OND (Figure 4.78 c, g) seasons while a slight enhancement in soil moisture is expected for the MAM season (Figure 4.78 a, d).

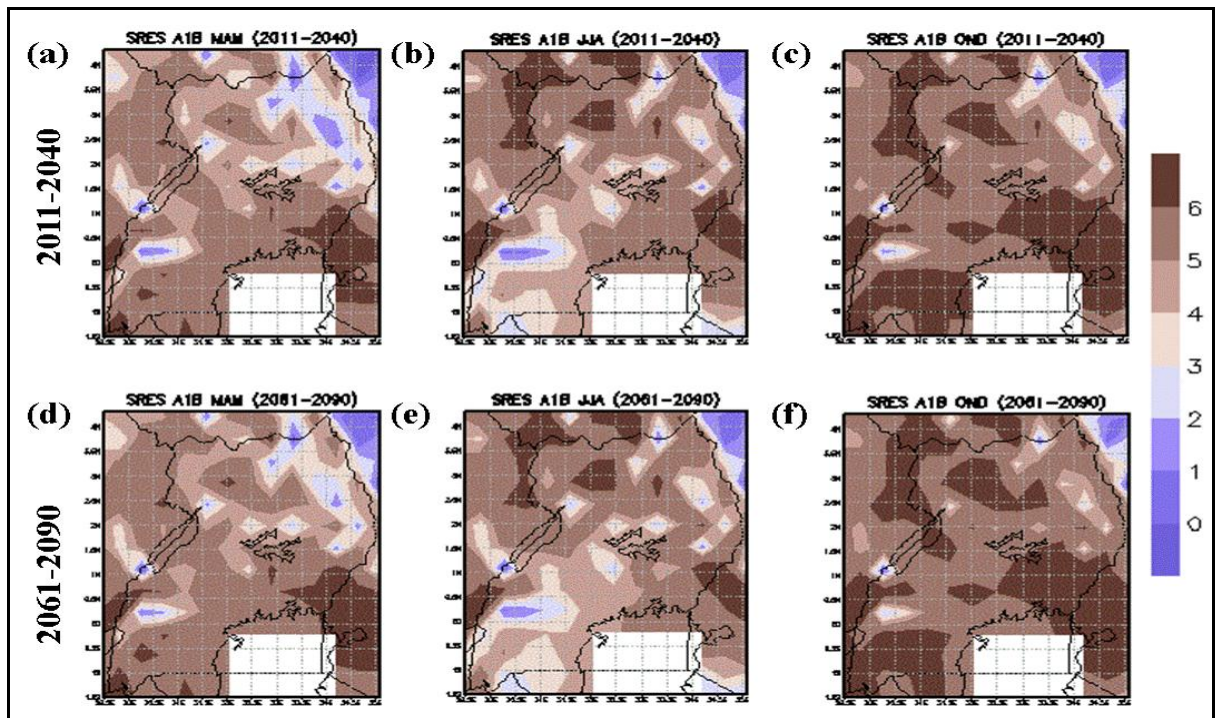


Figure 4.77 (a-f): PRECIS simulated seasonal mean soil moisture content (mm/day) projections for the periods 2011-2040 (a-c) and 2061-2090 (d-f) during March-May (MAM a, d), June-August (JJA b, e) and October-December (OND c, f) seasons for SRES A1B scenario over Uganda.

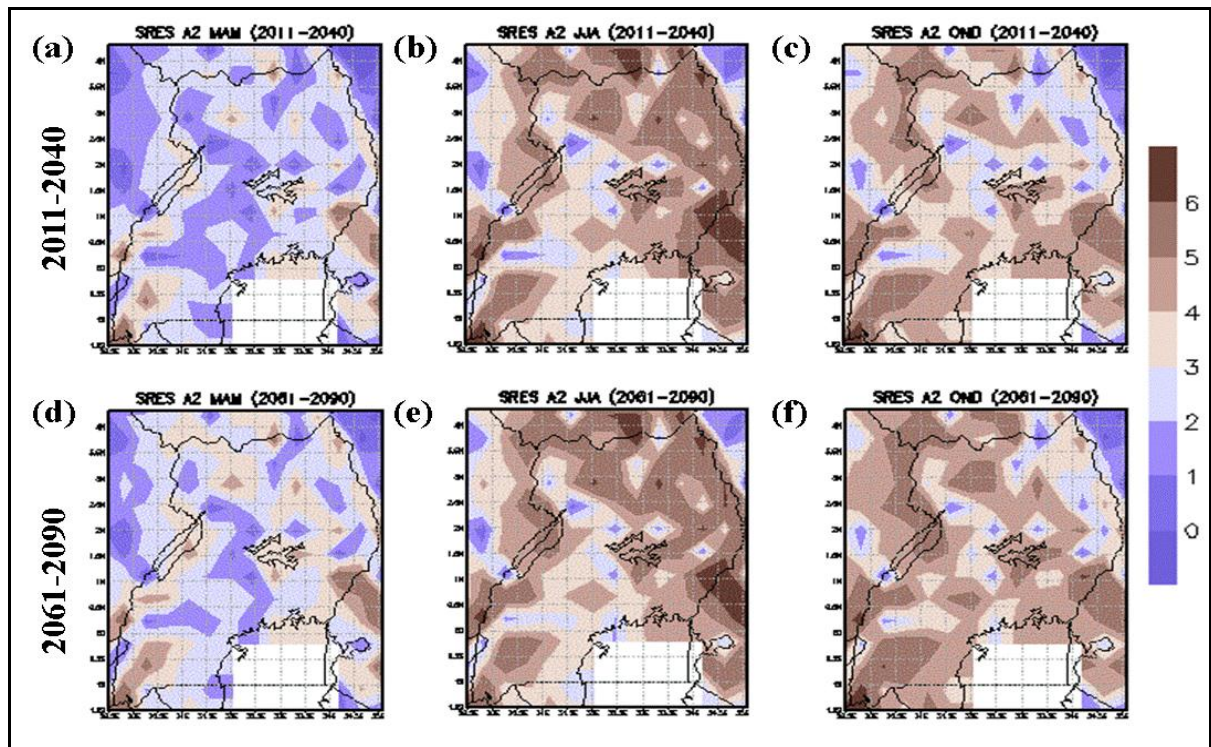


Figure 4.78 (a-f): PRECIS simulated seasonal mean soil moisture content (mm/day) projections for the periods 2011-2040 (a-c) and 2061-2090 (d-f) during March-May (MAM a, d), June-August (JJA b, e) and October-December (OND c, f) seasons for SRES A2 scenario over Uganda.

The projected variability (SD) in soil moisture content is shown in Figure 4.79 (a-f, SRES A1B) and 4.80 (a-f, SRES A2). Figure 4.77 (a-f) indicated that the seasonal moisture content will exhibit stronger variability especially during MAM (a) over northern eastern Uganda and low variability is expected in JJA (b, e) and OND (c, f) seasons under A1B scenario. Stronger variability is also expected over south western Uganda during JJA season. Figure 6.80 (a-f) shows that very strong variability in soil moisture is expected under A2 scenario during MAM and strong variability during OND over most region of the Country with relatively variability expected during JJA in both time periods. The study also observed that there will be higher variability projected under A2 scenario than under A1B scenario over most parts of Uganda.

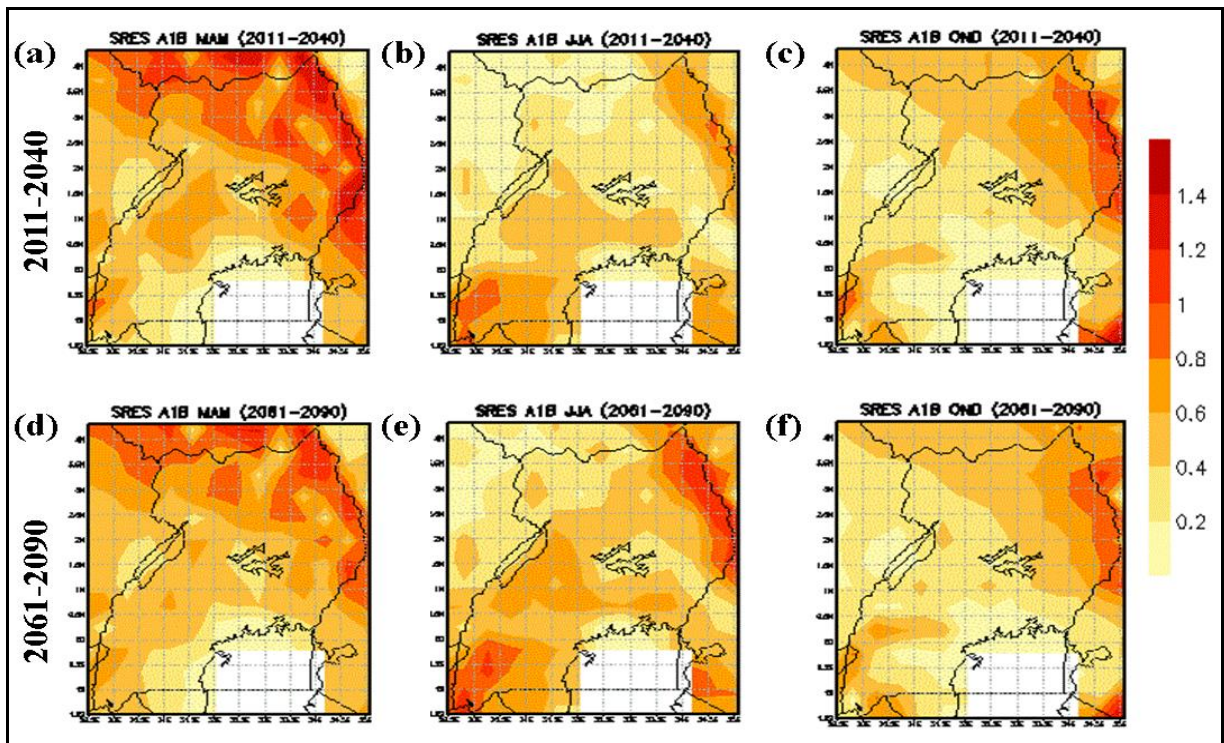


Figure 4.79 (a-f): PRECIS simulated seasonal variability (standard deviation) of soil moisture content (mm/day) projections for the periods 2011-2040 (a-c) and 2061-2090 (d-f) during March-May (MAM a, d), June-August (JJA b, e) and October-December (OND c, f) seasons for SRES A1B scenario over Uganda.

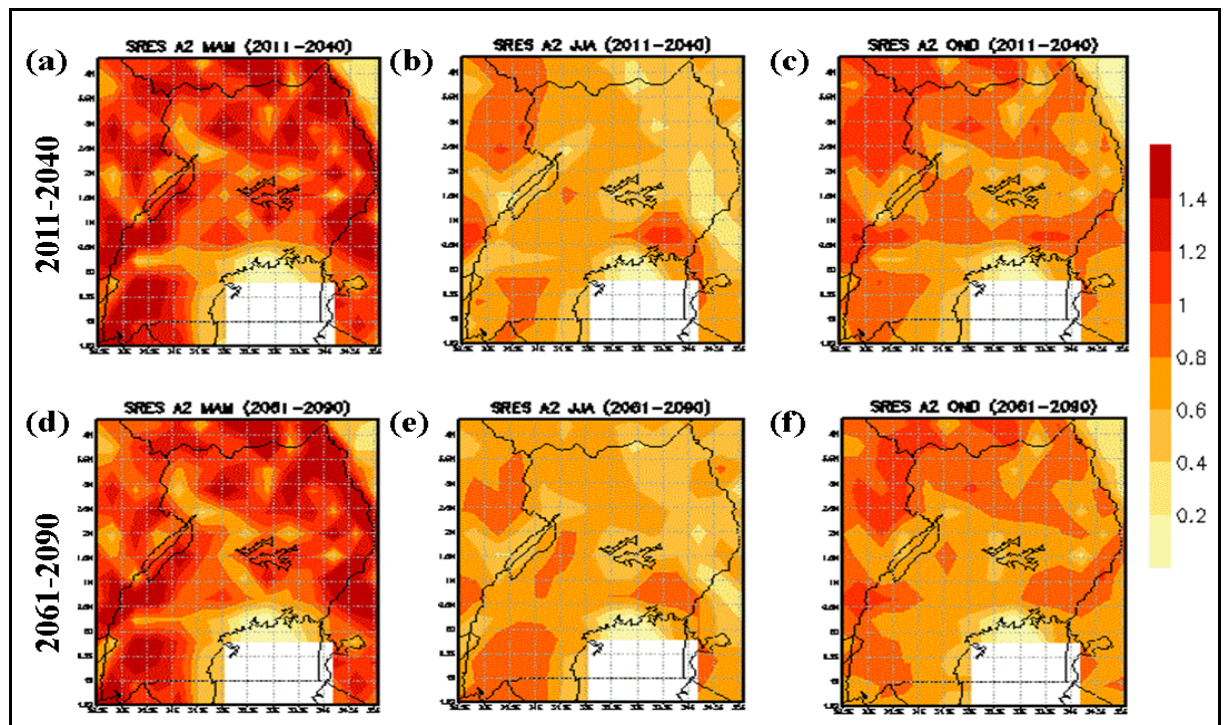


Figure 4.80 (a-f): PRECIS simulated seasonal variability (standard deviation) of soil moisture content (mm/day) projections for the periods 2011-2040 (a-c) and 2061-2090 (d-f) during March-May (MAM a, d), June-August (JJA b, e) and October-December (OND c, f) seasons for SRES A2 scenario over Uganda.

The associated coefficient of variation is presented in Figure 4.81 (a-f, SRES A1B) and 4.82 (a-f, SRES A2). Figure 4.81 (a-f) shows strong Coefficient of Variability (CV) over northeastern region during MAM (a, d) compared to other seasons during A1B scenario, relatively strong coefficient of variability is expected over southwestern to central Uganda during JJA (b, e) under A1B with low coefficient of variability expected for central and southern part of the Country during OND (c, f) season during the two periods. It is also observed that there may be a slight increase in the coefficient of variability values between the period 2011-2040 and 2061-2090 over a few parts of the Country.

Under A2 scenario, Figure 4.82 (a-f) shows very strong CV expected during MAM with strong spatial variability and relatively low values of CV during JJA and OND seasons. JJA (b, e) also shows low CV values for both periods compared with OND season over most parts of the Country.

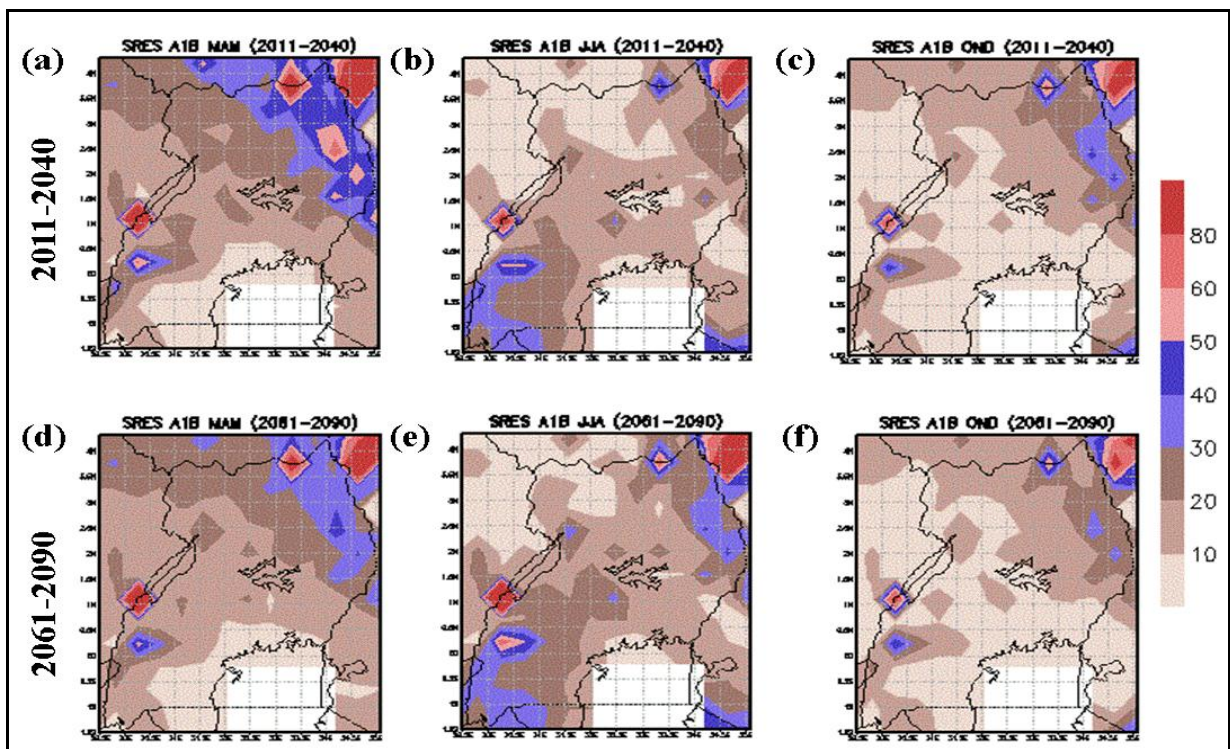


Figure 4.81 (a-f): PRECIS simulated seasonal coefficient of variation (CV, %) of soil moisture content projections for the periods 2011-2040 (a-c) and 2061-2090 (d-f) during March-May (MAM a, d), June-August (JJA b, e) and October-December (OND c, f) seasons for SRES A1B scenario over Uganda.

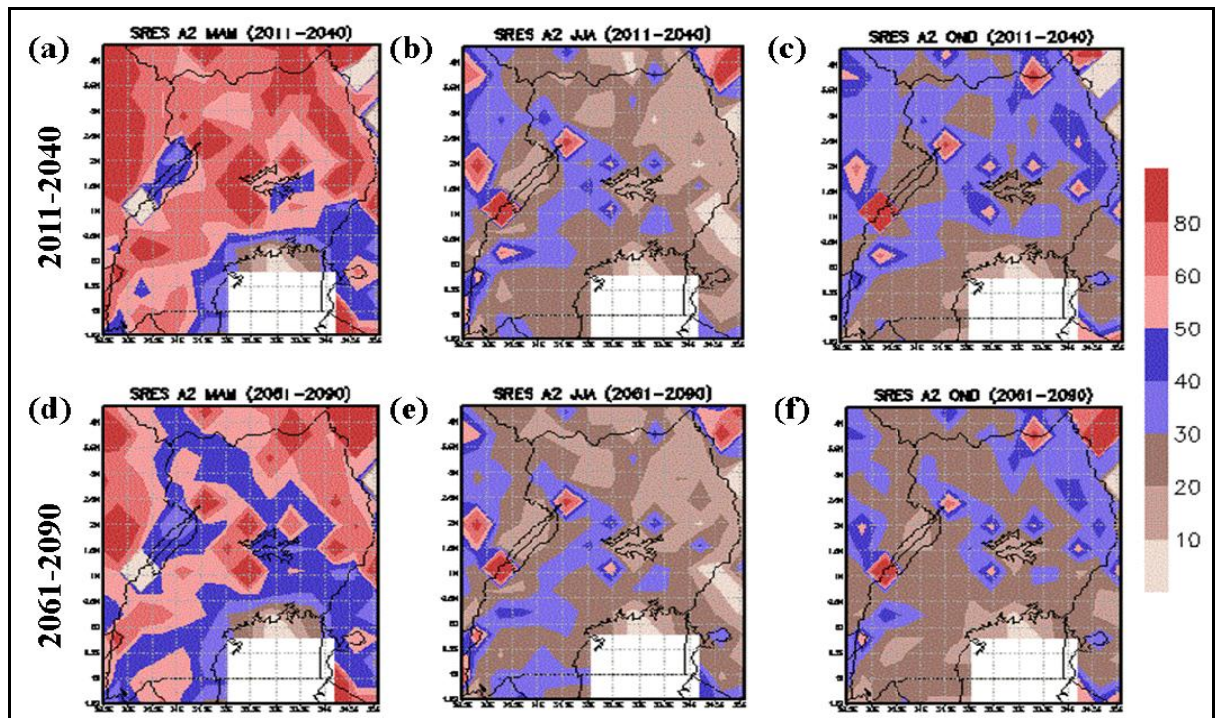


Figure 4.82 (a-f): PRECIS simulated seasonal coefficient of variation (CV, %) of soil moisture content projections for the periods 2011-2040 (a-c) and 2061-2090 (d-f) during March-May (MAM a, d), June-August (JJA b, e) and October-December (OND c, f) seasons for SRES A2 scenario over Uganda.

The projected changes in soil moisture content between the two periods (2011-2040 and 2061-2090) are presented in Figure 4.83 (a-f). The study observed that during MAM (a, d) season low changes are expected over central Uganda while high changes are expected over northern region under A1B scenario. Negative changes in soil moisture content are expected during JJA (b) over some parts of Country under A1B with A2 scenario (e) showing marketable changes over areas around Lake Victoria. During OND season, high changes are expected over northeastern part of the Country under A1B (c) with similar pattern expected for A2 scenario (f) but with higher changes over the central parts of Uganda.

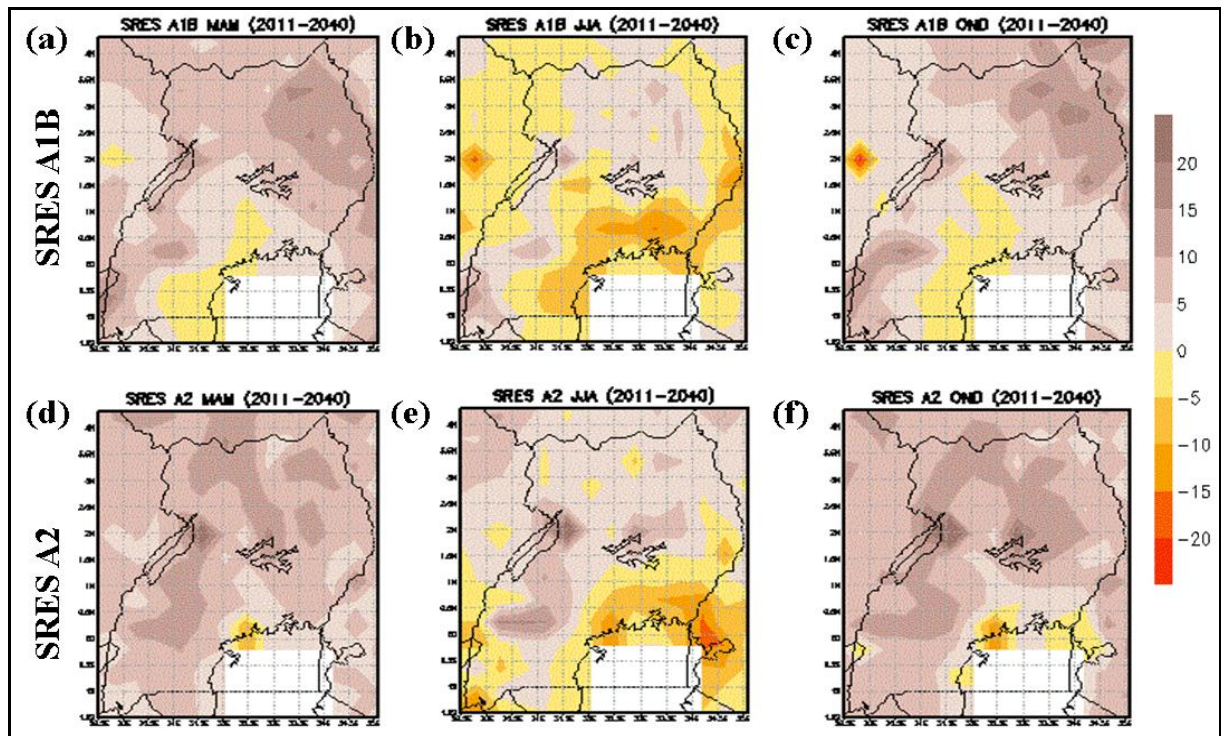


Figure 4.83 (a-f): Changes in PRECIS seasonal soil moisture content for SRES A1B (a-c) and A2 (d-f) scenarios during March-May (MAM a, d), June-August (JJA b, e) and October-December (OND c, f) seasons over Uganda.

Tables 4.23 and 4.24 present the summary of the mean, standard deviation, change in the mean and change in the standard deviation for SRES A1B and A2 respectively during MAM, JJA and OND over the sub-regions of Uganda. Table 4.23 shows that soil moisture content will range between 2-6 mm/day for most areas of Uganda. Under A1B scenario, the variability in soil moisture content will range between 0.13-1 mm/day with the change in the mean either indicating decrease in a few cases and an increase of above 0.5-11.64 mm/day. The change in variability is expected to decrease during MAM and OND season with increasing variability expected during JJA season.

Table 4.24 on the other hand, shows that mean soil moisture is likely to be lower in all seasons under A1B scenario, variability is expected to be relatively higher under A2 scenario than under A1B scenario, higher increase in soil moisture content are expected under A2 scenario than A1B scenario with higher variability expected to occur in soil moisture content compared with A1B SRES scenario.

Table 4.23: PRECIS projected soil moisture content [mm/day] (2011-2040 & 2061-2090) mean, standard deviation and changes for A1B scenario.

		MAM		JJA		OND	
		2011-2040	2061-2090	2011-2040	2061-2090	2011-2040	2061-2090
Mean	Southwestern	4.40	4.58	2.85	2.94	5.05	5.26
	Western	3.01	3.23	2.72	2.74	3.71	3.88
	Central	4.27	4.32	3.69	3.48	4.81	4.82
	Eastern	4.13	4.39	4.45	4.30	5.01	5.19
	Northwestern	3.38	3.62	4.18	4.20	4.67	4.82
	Northeastern	2.39	2.76	3.51	3.54	3.39	3.78
	Uganda	3.71	3.90	3.71	3.65	4.50	4.65
SD	Southwest	0.56	0.57	0.79	0.86	0.53	0.54
	Western	0.57	0.57	0.49	0.63	0.45	0.47
	Central	0.48	0.44	0.45	0.52	0.31	0.33
	Eastern	0.87	0.70	0.43	0.58	0.61	0.59
	Northwestern	0.73	0.70	0.39	0.50	0.50	0.48
	Northeastern	0.92	0.84	0.56	0.76	0.75	0.73
	Uganda	0.66	0.62	0.48	0.59	0.50	0.50
Change (Mean)	Southwest	-	5.37	-	2.61	-	6.04
	Western	-	6.58	-	0.69	-	5.14
	Central	-	1.33	-	-6.12	-	0.20
	Eastern	-	7.88	-	-4.66	-	5.50
	Northwestern	-	7.22	-	0.46	-	4.55
	Northeastern	-	11.21	-	1.01	-	11.64
	Uganda	-	5.55	-	-1.81	-	4.56
Change (SD)	Southwest	-	0.53	-	2.17	-	0.13
	Western	-	0.15	-	4.13	-	0.73
	Central	-	-1.33	-	1.90	-	0.76
	Eastern	-	-5.26	-	4.41	-	-0.55
	Northwestern	-	-0.68	-	3.33	-	-0.56
	Northeastern	-	-2.22	-	6.14	-	-0.52
	Uganda	-	-1.36	-	3.49	-	-0.06

Table 4.24: PRECIS projected soil moisture content [mm/day] (2011-2040 & 2061-2090) mean, standard deviation and changes for A2 scenario.

		MAM		JJA		OND	
		2011-2040	2061-2090	2011-2040	2061-2090	2011-2040	2061-2090
Mean	Southwestern	2.44	2.61	3.36	3.28	3.57	3.77
	Western	1.59	1.90	2.57	2.80	2.52	2.88
	Central	1.83	1.96	3.01	2.87	2.93	3.01
	Eastern	2.44	2.66	4.23	4.07	3.24	3.42
	Northwestern	1.69	2.03	2.97	3.09	2.75	3.14
	Northeastern	1.77	2.07	3.78	3.87	2.22	2.46
	Uganda	1.88	2.12	3.25	3.26	2.86	3.10
SD	Southwest	1.30	1.22	0.79	0.87	0.87	0.83
	Western	1.02	1.06	0.67	0.75	0.79	0.81
	Central	0.80	0.74	0.67	0.64	0.72	0.66
	Eastern	1.15	1.13	0.62	0.66	0.84	0.82
	Northwestern	1.02	0.97	0.70	0.69	0.85	0.83
	Northeastern	1.23	1.27	0.57	0.63	0.79	0.82
	Uganda	1.03	1.01	0.68	0.71	0.80	0.79
Change (Mean)	Southwest	-	5.23	-	-2.44	-	6.02
	Western	-	9.50	-	6.90	-	10.59
	Central	-	3.63	-	-4.22	-	2.41
	Eastern	-	6.42	-	-4.83	-	5.64
	Northwestern	-	10.43	-	3.82	-	11.79
	Northeastern	-	8.83	-	2.55	-	7.24
	Uganda	-	7.24	-	0.34	-	7.10
Change (SD)	Southwest	-	-2.30	-	2.44	-	-1.21
	Western	-	1.37	-	2.42	-	0.40
	Central	-	-1.88	-	-0.86	-	-1.77
	Eastern	-	-0.39	-	1.18	-	-0.70
	Northwestern	-	-1.36	-	-0.11	-	-0.39
	Northeastern	-	1.41	-	1.74	-	1.02
	Uganda	-	-0.51	-	0.71	-	-0.35

The study results have, for the first time revealed patterns in future projections of soil moisture content over Uganda. The results are important for planning future crop farming and development of crop varieties that are suitable for the projected soil moisture content across the two climate scenarios considered in this study. The results can further be used for developing water conservation and harvesting mechanisms to minimize soil moisture deficits and promote crop productivity in various area of the Country. The study results therefore are key pointers to adaptation mechanisms to expected climate change effects that are required in the agricultural sector.

4.4.4 Projected Seasonality of Rainfall, Average Temperature and Soil Moisture Content for Sub-regions

Figure 4.83 (a-i) shows the seasonality of rainfall, temperature and soil moisture for SRES A1B and SRES A2 scenarios over western Uganda. The study observed that higher rainfall is expected during January to May under A1B scenario than under A2 scenario. During June-October months, the rainfall is nearly equally for both scenarios while more rainfall is projected for A1B scenario during November and December under A1B scenario than under A2 scenario (Figure 4.84 a). Results also show that temperatures are expected to increase during the period 2011-2040 and 2061-2090 for all months in western region (Figure 4.84 d). The magnitude of change is relatively equal in both scenarios with A2 scenario exhibiting a warmer future climate and strong seasonality with May to July relatively colder than other months. On the other hand, A1B scenario predicts a slightly warmer climate during January-May with slight reduction in temperature in June-December months (Figure 4.84 d).

Soil moisture content exhibits seasonality over western Uganda with A1B predicted to exhibit higher moisture content than A2 scenario during January to May and November to December (Figure 4.84 g). During JJA results show relatively equal amount of soil moisture projected for the two periods over western Uganda under both scenarios. Figure 4.84 indicates variability in rainfall (b), temperature (e) and soil moisture (h). The study observed that there is variability of month to month levels of the three climatic parameters over western Uganda under the two climate scenarios.

Figure 4.84 (c, f, i) shows the seasonality in the CV for the two scenarios and two periods. The study observed that very high CV is projected for rainfall under A2 scenario during January to March and December months (Figure 4.84 c). During April to October and November, the coefficient of variability in both scenarios, relatively compare (Figure 4.84 c). The study also observed stronger month to month variability in projected for temperature with a tendency to show a reduction during the last months of the year (Figure 4.84 f). Results for soil moisture content indicated very strong coefficient of variation (CV) for A2 scenario for March and April with the result indicating similar patterns for the months May-December (Figure 4.84 i). July and August showed significantly higher changes in coefficient of variability in soil moisture during the two periods (Figure 4.84 i).

The results for central Uganda region are shown in Figure 4.85 (a-i). The results showed quite similar patterns for central region as in Figure 4.84 (a-i) although in some cases, there is a

tendency to project significantly high values under A2 scenario in some months than for A1B scenario.

Figure 4.86 (a-i) shows results for Eastern region with similar interpretation as Figure 4.84 (a-i) and 4.85(a-i) indicating noticeable deviations in the patterns of projected level of coefficient variation for both A1B and A2 scenarios. The study observed higher values for A2 scenario than for A1B scenarios over most part of Uganda for both periods being studied during all the seasons considered. Similar findings have been observed in Van den Bergh *et al.* (2012); USAID, 2013 and James *et al.* (2014) that observed an anticipated progression in temperature change with an increase in the margin of 0.7 to 1.5 °C in the short term and 1.5 to 4.3 °C by 2080s.

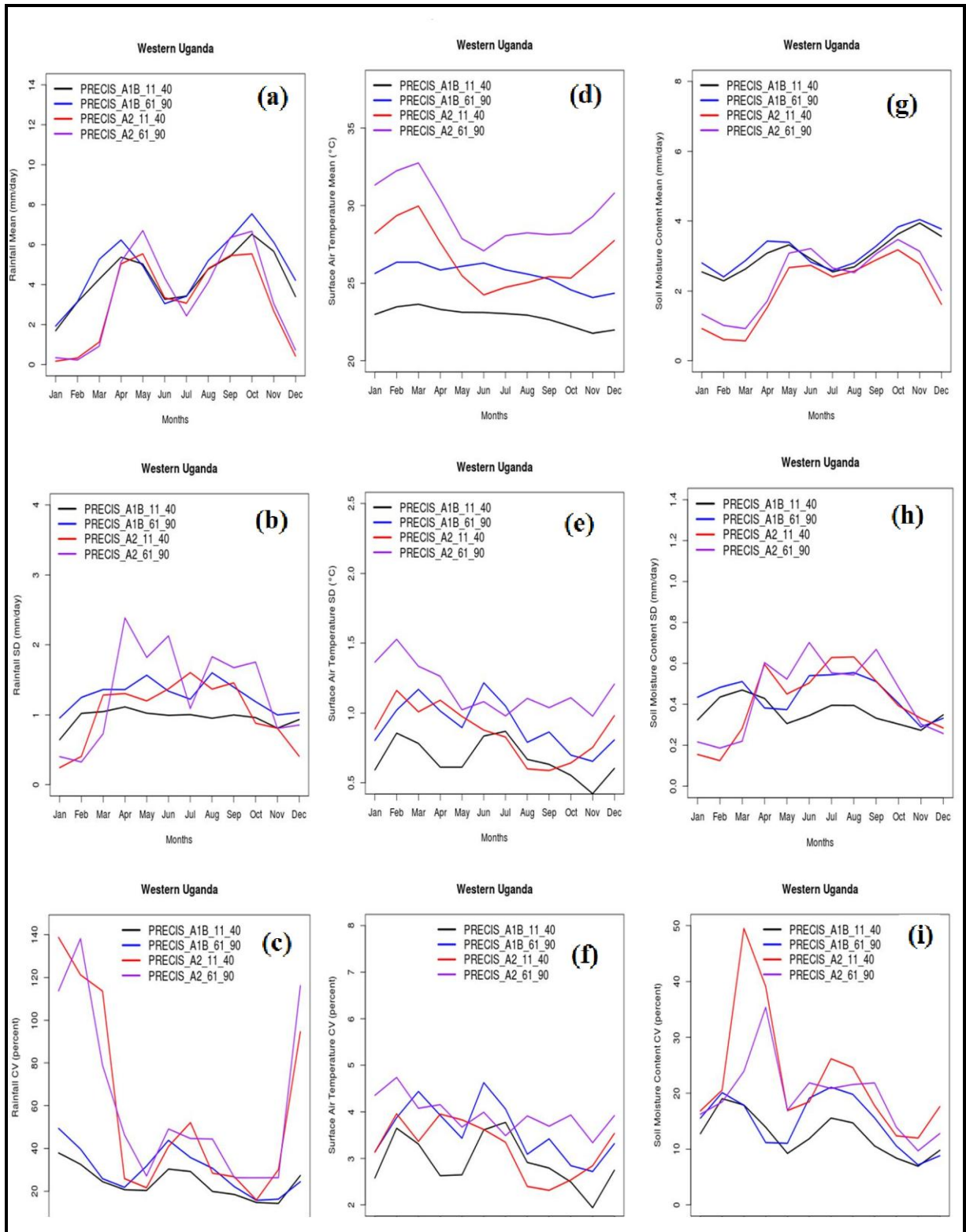


Figure 4.84 (a-i): PRECIS projected variations of rainfall (a-c), temperature (d-f) and soil moisture content (g-i) for mean (a, d, g), standard deviation (b, e, h) and coefficient of variation (c, f, i) for both SRES A1B and A2 (see legend) over Western region of Uganda.

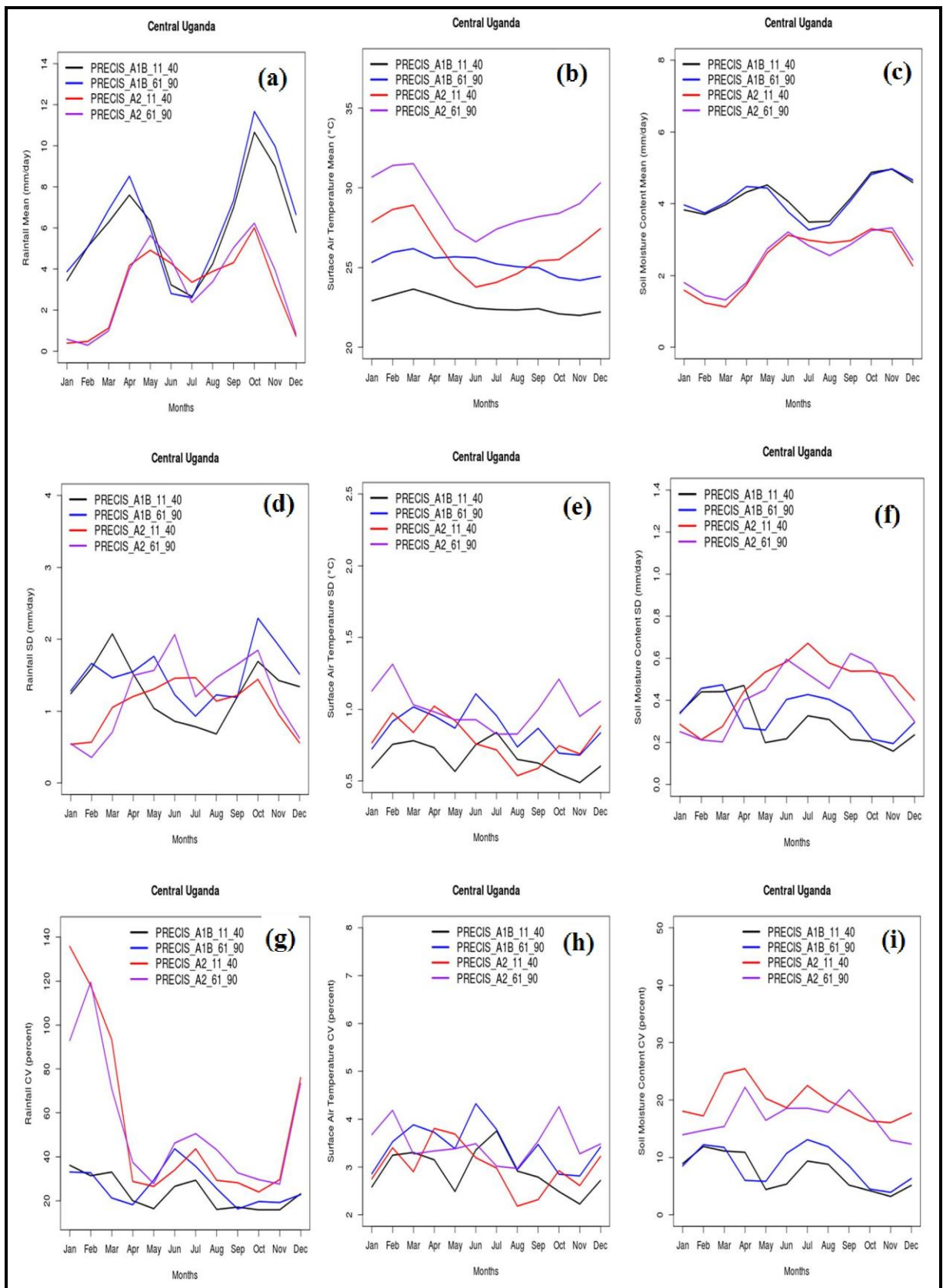


Figure 4.85 (a-i): PRECIS projected variations of rainfall (a-c), temperature (d-f) and soil moisture content (g-i) for mean (a, d, g), standard deviation (b, e, h) and coefficient of variation (c, f, i) for both SRES A1B and A2 (see legend) over Central region of Uganda.

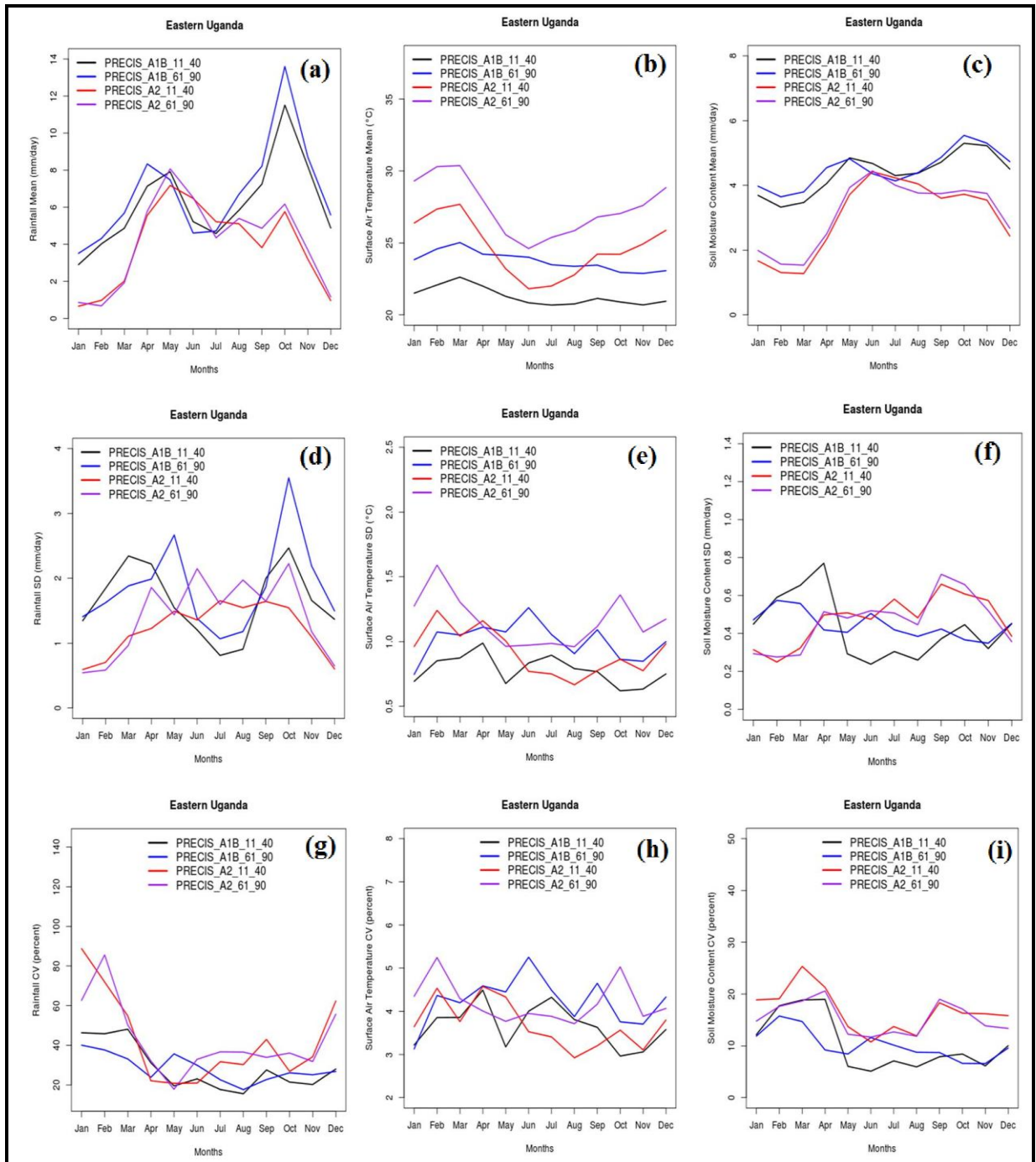


Figure 4.86 (a-i): PRECIS projected variations of rainfall (a-c), temperature (d-f) and soil moisture content (g-i) for mean (a, d, g), standard deviation (b, e, h) and coefficient of variation (c, f, i) for both SRES A1B and A2 (see legend) over Eastern region of Uganda.

The results on the coefficient of variation for the projected climate variables over different sub regions of Uganda are presented in Table 4.25. It is evident from the results that rainfall and soil moisture over most regions will be highly variable in future, while temperature will exhibit low variability. SRES A2 is likely to be associated with higher variability in rainfall compared with SRES A1B over most parts of Uganda.

Table 4.25: Coefficient of variation (%) of projected rainfall and average temperature and soil moisture content for different scenarios and region of Uganda.

		MAM		JJA		OND	
		2011-2040	2061-2090	2011-2040	2061-2090	2011-2040	2061-2090
Rainfall A1B	Southwest	39.02	40.28	63.71	80.01	25.86	25.96
	Western	26.84	30.90	35.33	47.18	33.29	32.09
	Central	26.32	27.37	32.61	46.66	31.42	31.73
	Eastern	39.95	37.78	26.87	34.57	44.24	49.10
	Northwestern	26.51	26.10	20.20	25.54	41.93	41.23
	Northeastern	41.99	38.97	27.28	35.81	50.68	49.84
	Uganda	33.78	35.28	36.29	48.28	37.11	37.17
Rainfall A2	Southwest	58.46	64.43	53.45	71.12	73.60	69.92
	Western	61.27	72.17	45.59	57.02	77.99	82.09
	Central	62.94	69.87	38.94	56.20	73.22	70.88
	Eastern	53.55	58.72	33.71	43.25	71.22	72.17
	Northwestern	65.61	69.57	40.27	47.20	85.57	85.90
	Northeastern	59.64	66.65	32.01	39.09	92.23	93.41
	Uganda	63.00	70.49	43.32	55.22	78.41	80.08
Temperature A1B	Southwest	3.13	4.46	3.95	4.38	2.90	3.31
	Western	3.05	4.02	3.49	4.15	2.60	3.12
	Central	3.37	3.78	3.36	3.86	2.53	3.06
	Eastern	4.65	4.72	4.08	4.74	3.33	3.99
	Northwestern	4.39	4.44	3.37	4.36	3.12	3.71
	Northeastern	6.11	5.61	5.02	6.13	4.32	4.62
	Uganda	4.02	4.35	3.73	4.36	3.07	3.56
Temperature A2	Southwest	8.11	7.99	3.68	4.40	5.08	5.38
	Western	7.55	7.65	3.43	4.22	4.81	5.19
	Central	6.84	6.52	3.17	3.71	4.17	4.55
	Eastern	8.35	8.12	3.86	4.39	4.48	5.13
	Northwestern	8.38	8.19	3.44	4.42	5.13	5.48
	Northeastern	9.29	8.97	4.14	4.68	4.32	4.88
	Uganda	7.43	7.25	3.51	4.15	4.34	4.76
SMC A1B	Southwest	12.61	12.51	27.53	29.19	10.54	10.22
	Western	18.90	17.79	18.13	23.00	12.08	12.17
	Central	11.24	10.10	12.25	14.79	6.35	6.88
	Eastern	21.18	15.91	9.72	13.49	12.07	11.29
	Northwestern	21.54	19.48	9.23	11.83	10.75	10.02
	Northeastern	38.43	30.55	15.92	21.53	22.01	19.29
	Uganda	17.84	15.82	12.81	16.20	11.13	10.72
SMC A2	Southwest	53.17	46.70	23.59	26.65	24.37	22.01
	Western	63.92	55.67	26.12	26.86	31.50	28.10
	Central	43.73	37.82	22.36	22.46	24.65	22.03
	Eastern	46.97	42.69	14.66	16.21	25.93	23.83
	Northwestern	60.34	47.78	23.45	22.37	30.79	26.52
	Northeastern	69.17	61.61	15.12	16.29	35.59	33.47
	Uganda	54.77	47.74	20.94	21.59	27.99	25.48

4.4.5 Projected Trends in Seasonal and Annual Rainfall

Figure 4.87 shows trends in seasonal and annual rainfall over western Uganda for both A1B and A2 scenarios for the period 2000-2100. The results indicate seasons that are projected to have increasing rainfall over the region. For example the study observed that under A1B scenario, DJF will have the highest increasing trend in rainfall with MAM, OND and annual rainfall also exhibiting increasing trends while JJA will have a decreasing trend. Figure 4.85(b) shows the case for A2 scenario which tend to observed that the projected rainfall under this scenario will increase during OND season while in other seasons and annual rainfall indicating either very slight increment or no trend. JJA season rainfall has been projected to have decreasing trend in this scenario but with the slope A1B higher than that of A2.

Figure 4.88(a) shows that DJF, OND, and annual rainfall are projected to exhibit increasing trends over the central region under A1B scenario with MAM and JJA showing no trend and reducing trend respectively. Figure 4.88(b) on the other hand indicated weak trends for MAM and DJF and annual rainfall with significantly increasing trends and decreasing trend for OND and JJA respectively under A2 scenario.

Over Eastern Uganda, results of seasonal rainfall trends are shown in Figure 4.89 (a) for A1B and Figure 4.89(b) for A2 scenario. The study observed increasing trends for DJF, OND and annual rainfall with MAM showing weak increasing trend while JJA is projected to decrease under A1B scenario. Figure 4.89(b) shows that increasing rainfall trend are predicted for OND season and annual rainfall with the other seasons either showing constant or no trend while JJA show decreasing trend.

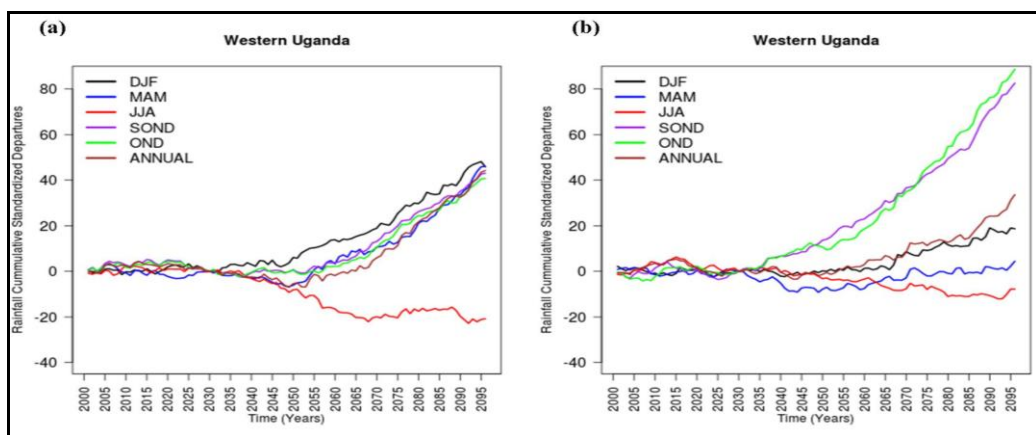


Figure 4.87 (a-b): A1B (a) and A2 (b) PRECIS projected seasonal and annual rainfall trends (2001-2095) over the Western region of Uganda.

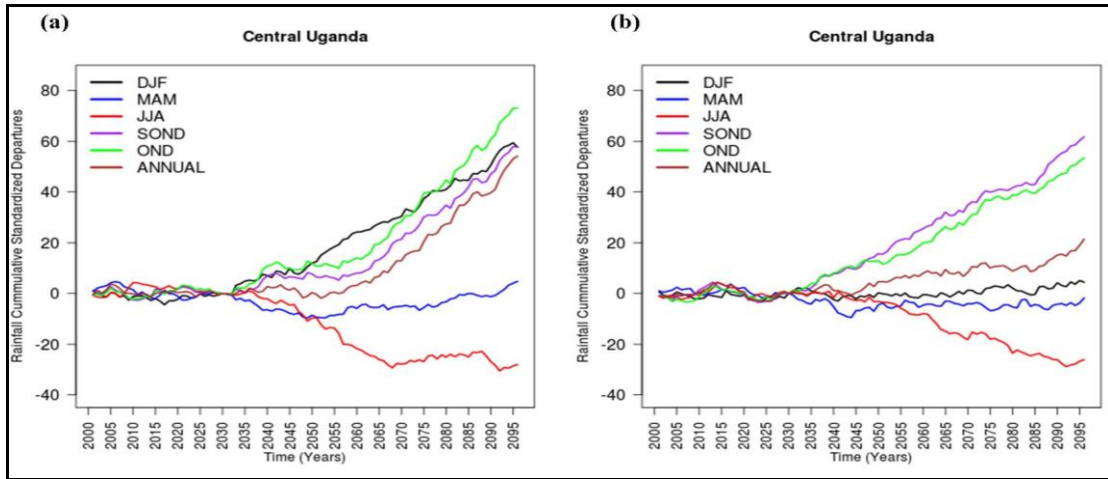


Figure 4.88 (a-b): A1B (a) and A2 (b) PRECIS projected seasonal and annual rainfall trends (2001-2095) over the Central region of Uganda.

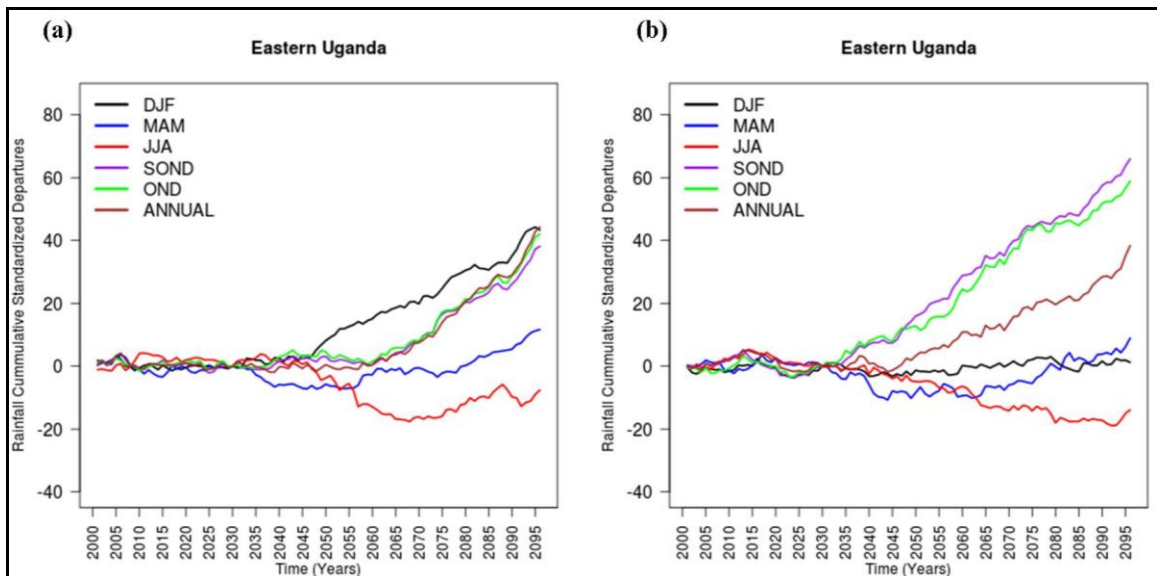


Figure 4.89 (a-b): A1B (a) and A2 (b) PRECIS projected seasonal and annual rainfall trends (2001-2095) over the Eastern region of Uganda.

4.4.6 Projected Trends in Seasonal and Annual Average Temperature

Figure 4.90 (a-b) shows results for temperature trends in western Uganda for seasonal and annual averages. The study observed increasing trends in all the seasons for both A1B (a) and A2 (b) scenarios. Trends are stronger for Annual and MAM seasons under A1B (a) while under A2 scenario (b), the trends are stronger for annual and JJA seasonal temperature over western Uganda. Similar results are presented for central (Figure 4.91 a-b) and eastern (Figure 4.92 a-b) region of Uganda. It should be noted that any anomalies in temperature of a given month may have far reaching implications of the bananas conditions months to come. Cumulative values often attempt to reflect accumulation of the specific variables.

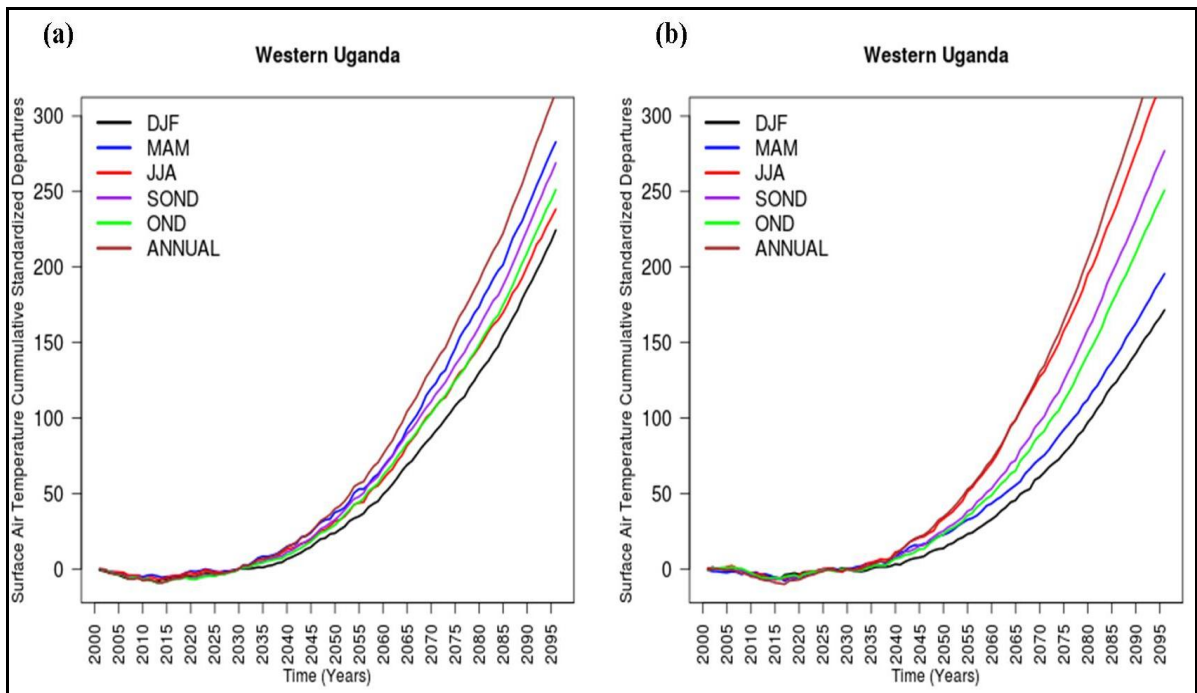


Figure 4.90 (a-b): A1B (a) and A2 (b) PRECIS projected seasonal and annual average temperature trends (2001-2095) over the Western region of Uganda.

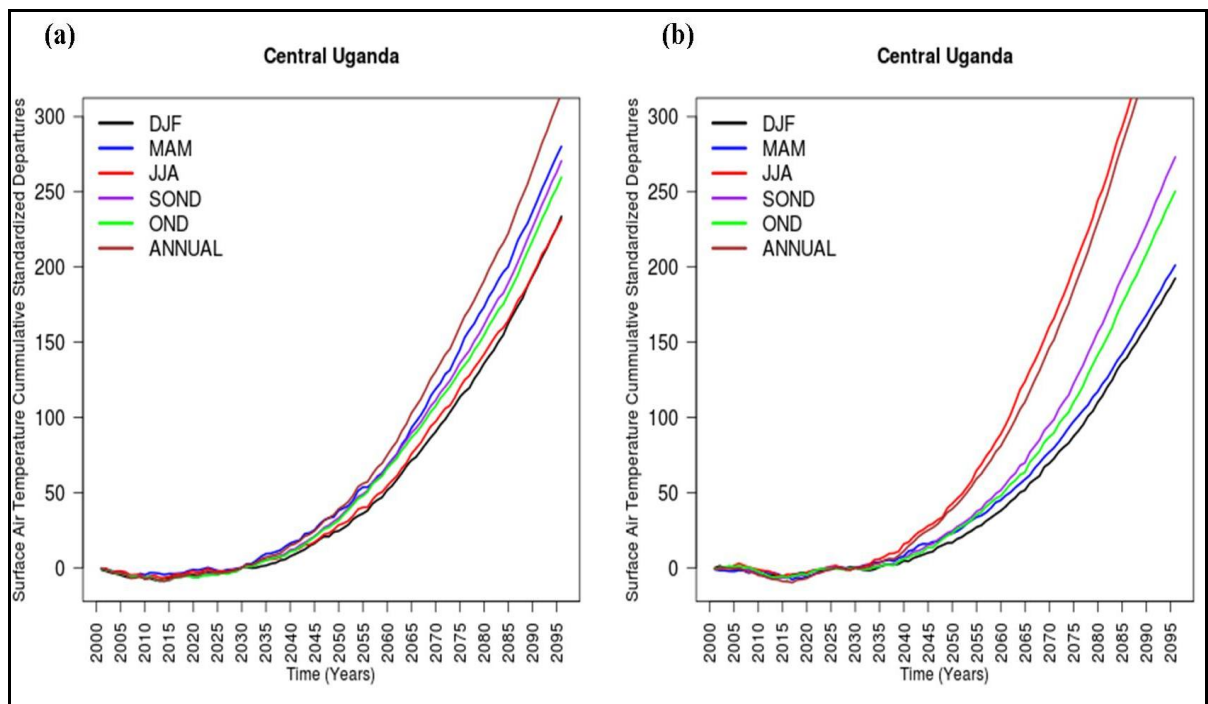


Figure 4.91 (a-b): A1B (a) and A2 (b) PRECIS projected seasonal and annual average temperature trends (2001-2095) over the Central region of Uganda.

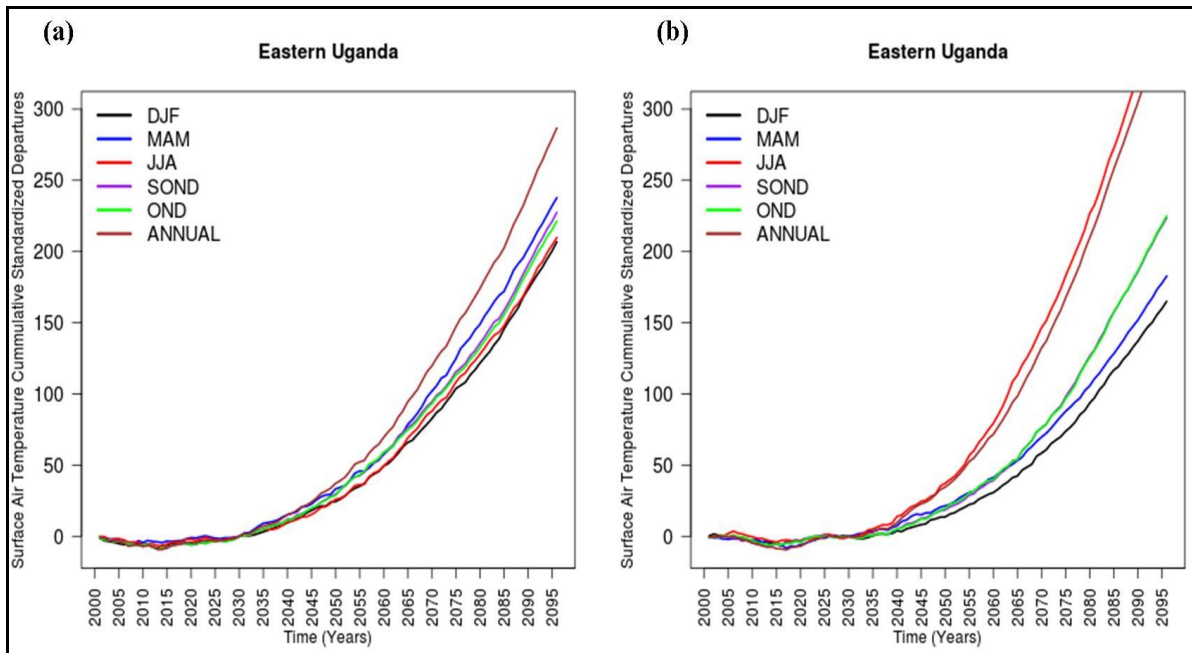


Figure 4.92 (a-b): A1B (a) and A2 (b) PRECIS projected seasonal and annual average temperature trends (2001-2095) over the Eastern region of Uganda.

4.4.7 Projected Trends in Seasonal and Annual Soil Moisture Content

The results for soil moisture content are shown in Figure 4.93 (western region), Figure 4.94 (central region) and Figure 4.95 (eastern region) for SRES A1B (a) and SRES A2 (b) scenario. The results show general decreasing trends in JJA soil moisture content with a general increase in DJF and OND in most of the cases considered. The decrease trend in JJA soil moisture content are stronger under A1B scenario while the increase in DJF and OND seasons, trends in soil moisture content are more pronounced under the A2 (b) scenario over the three regions of Uganda.

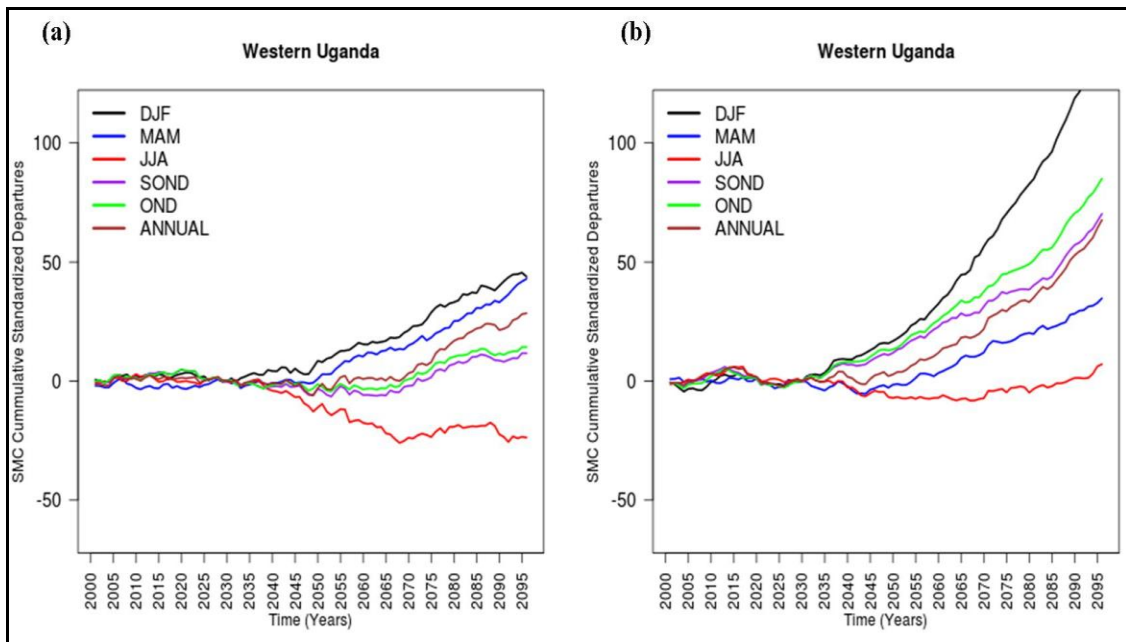


Figure 4.93 (a-b): A1B (a) and A2 (b) PRECIS projected seasonal and annual soil moisture content trends (2001-2095) over the Western region of Uganda.

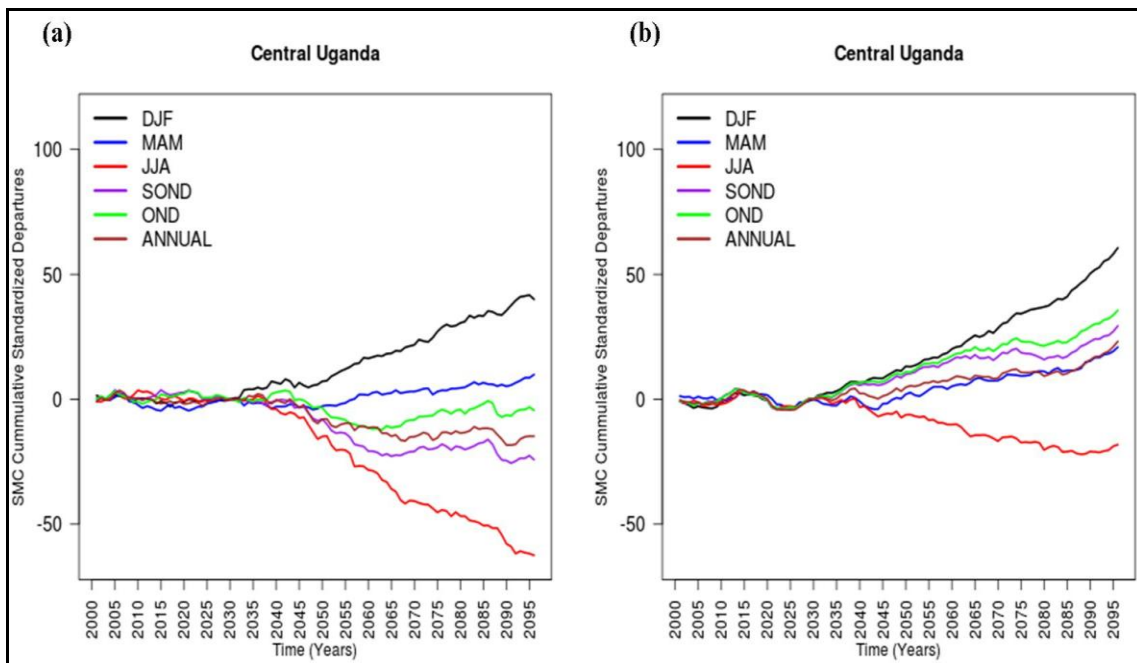


Figure 4.94 (a-b): A1B (a) and A2 (b) PRECIS projected seasonal and annual soil moisture content trends (2001-2095) over the Central region of Uganda.

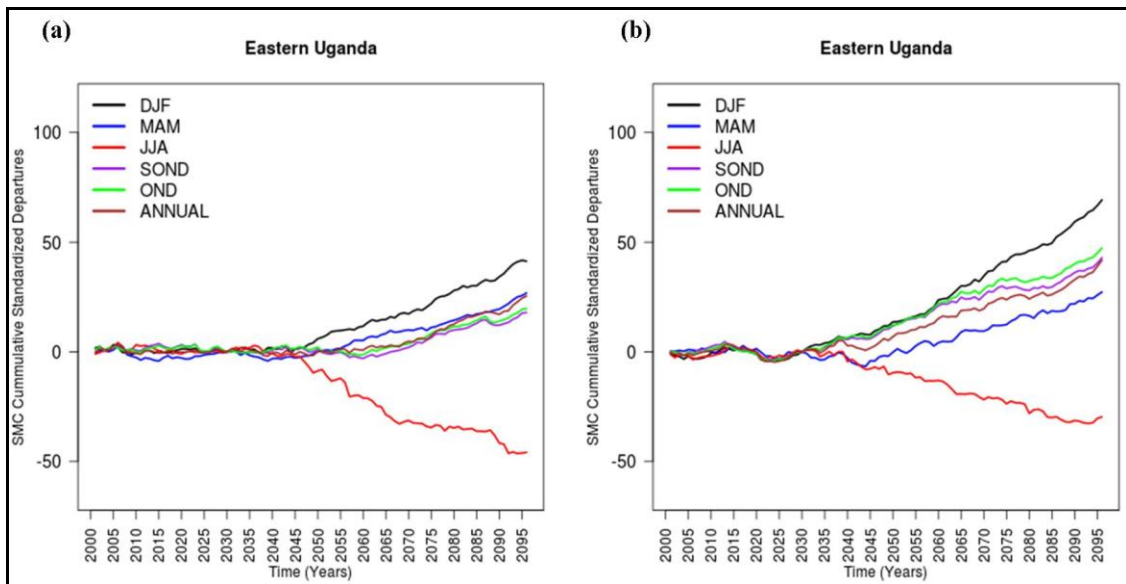


Figure 4.95 (a-b): A1B (a) and A2 (b) PRECIS projected seasonal and annual soil moisture content trends (2001-2095) over the Eastern region of Uganda.

4.4.8 Relationship between Projected Rainfall, Temperature and Soil Moisture Content

Figure 4.96 (a-f) and Figure 4.97 (a-f) show the relationship between simulated soil moisture content and the percentage of the ratio of rainfall and temperature for southwestern, western and central region under the two scenarios during 2011-2040 period (Figure 4.96) and 2061-2090 (Figure 4.97). The study observed steep slopes of the line of best fit for 2011-2040 period, over all the regions and two scenarios. This study further observed that projected variation in rainfall patterns accompanied by consistent increase in surface temperature. Some parts of Uganda are projected to experience a positive but not significant trend in rainfall coupled with a projected positive trend in surface temperature.

In some areas, the trends in rainfall, temperature and soil moisture content could mean that the rainfall patterns may not offset the potential effects of progressively rising temperature in terms of soil moisture content for the banana crop particularly under SRES A2 scenario. However, Neely *et al.* (2009) have observed that temperature increase of up to 3.0-3.5 °C should increase the productivity of crops, fodder and pastures in many regions. This implies that effective adaptation mechanisms such as water harvesting and conservation (plantation mulching) can greatly advance banana productivity in Uganda despite the projected temperature changes especially in the near future (up to 2040). Development of banana pests and disease risk management and control strategies are also required to reduce the effects of increasing temperature on banana production in Uganda.

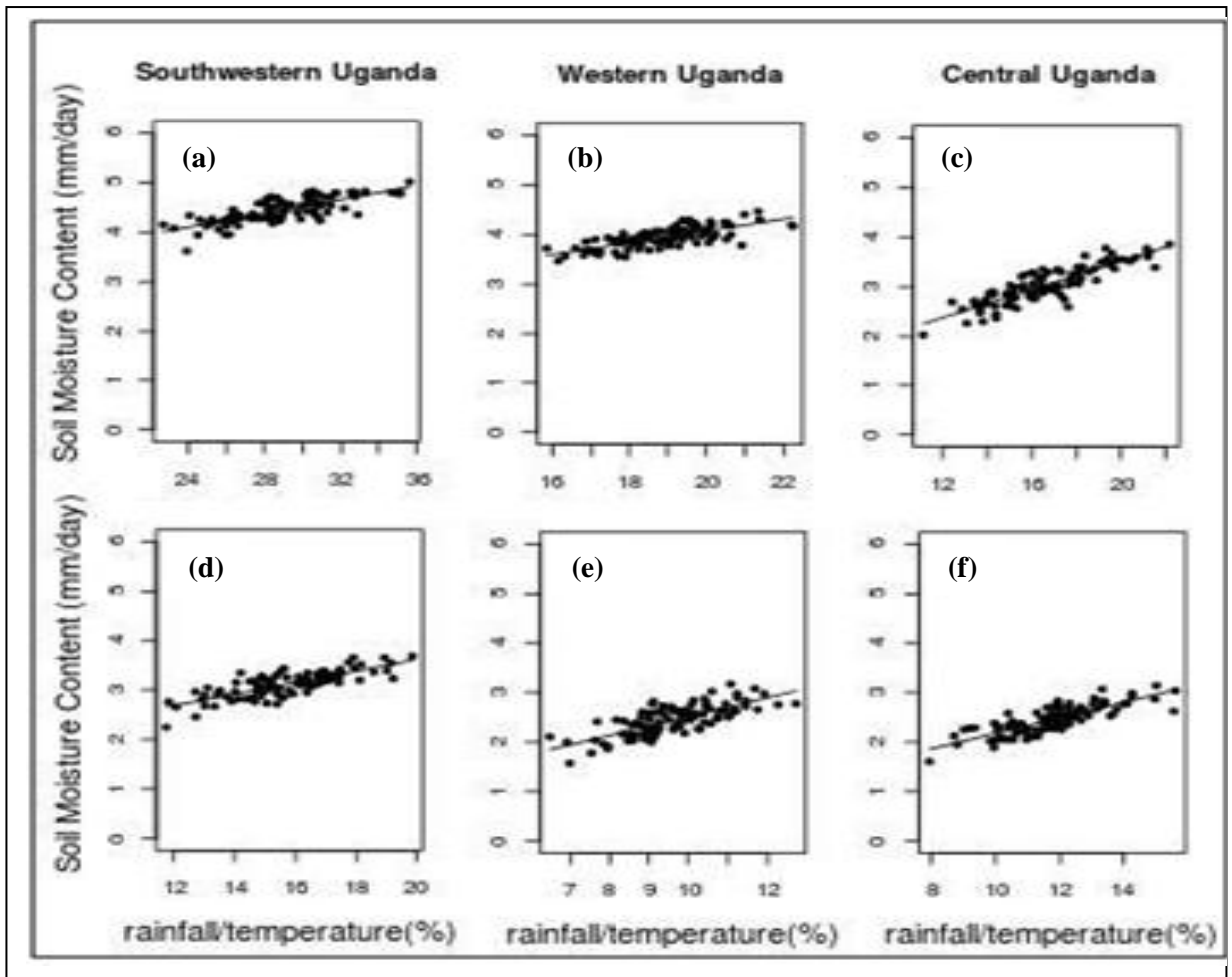


Figure 4.96 (a-f): PRECIS projected annual soil moisture content (mm/day) and rainfall-temperature ratio (%) for SRES A1B (a-c) and A2 (d-f) scenarios (2011-2040).

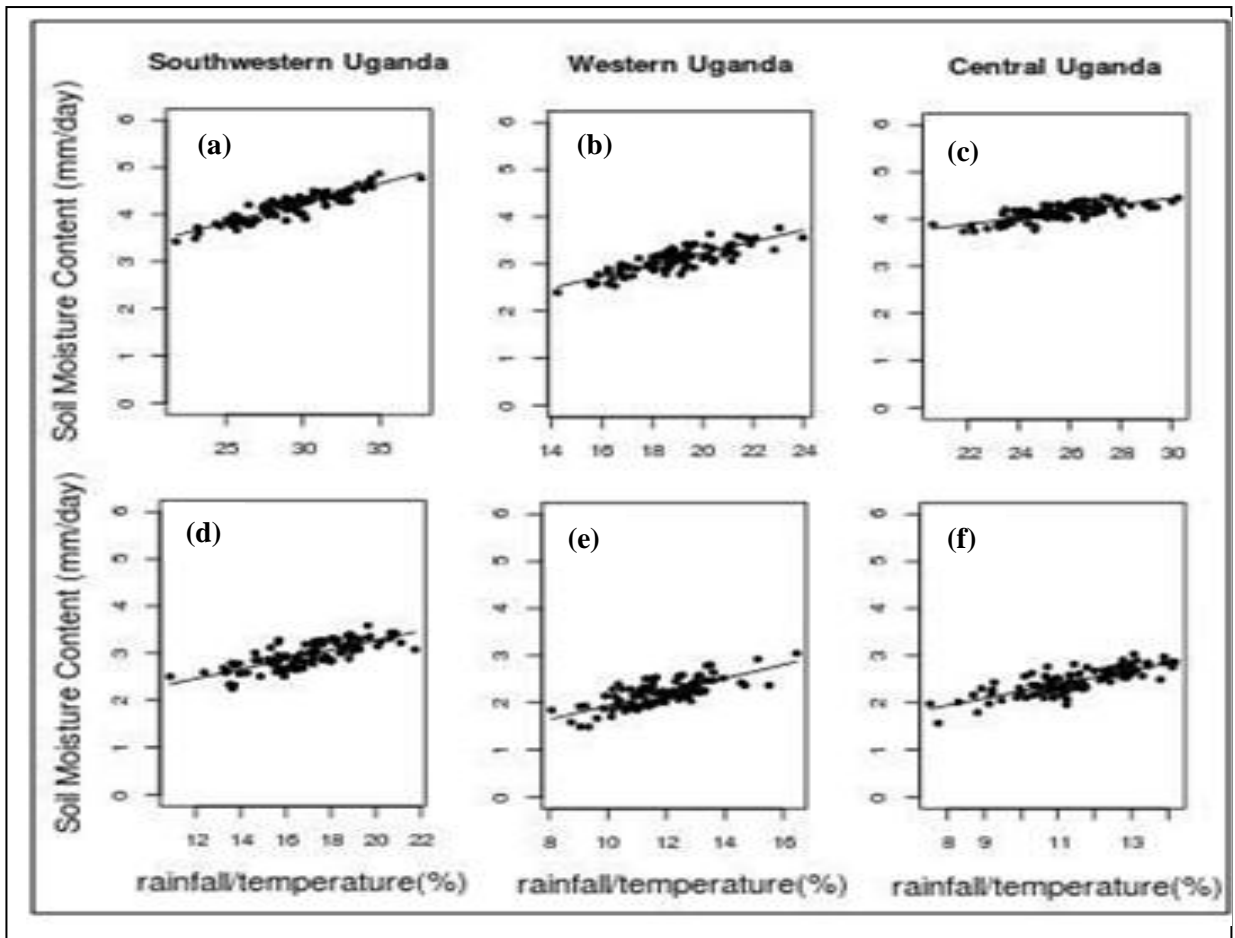


Figure 4.97 (a-f): PRECIS projected annual soil moisture content (mm/day) and rainfall-temperature ratio (%) for SRES A1B (a-c) and A2 (d-f) scenarios (2061-2090).

4.4.9 Climate Projections under IPCC RCPs 4.5 and 8.5

This section of the study presents the analysed climate projections under the AR5 Representative Concentration Pathways (RCPs) scenarios that are fully integrated socio-economic narratives or scenarios and pathways of corresponding radiative forcing. The detailed description of RCPs scenario development process can be found in Moss *et al.* (2010). RCP 4.5 corresponds to a medium emission pathway (some mitigation) while RCP 8.5 corresponds to a high emission pathway (no mitigation) and a radiative forcing that exceeds 8.5 W/m^2 by 2100. Results based on the downscaled Hadley Centre Global Environmental Model version 3 (HadGEM3) model are presented for both seasonal rainfall and temperature patterns considering RCP 4.5 and RCP 8.5 during MAM, JJA and OND seasons over Uganda.

4.4.9.1 Projected Spatial Patterns of IPCC RCPs Seasonal Rainfall and Temperature

Figure 4.98 (a-l) shows the patterns in seasonal mean rainfall under the new AR5 representative concentration pathways (RCPs). These results have been presented for

CORDEX projection of two scenarios RCP 4.5 and RCP 8.5. The results are presented for MAM (a-d). During MAM (a-d), the study observed low projected rainfall for over most of the Country with considerable spatial variability during JJA (e-h). The northern part of Uganda is projected to receive significantly high rainfall under both scenarios and for both periods with low rainfall over the southern part of Uganda. On the other hand, during OND (i-l) higher rainfall has been projected for southern part of the region with relatively low rainfall for the northern part of Uganda. There is a strong relationship in the patterns of rainfall across the scenarios, and the two periods, with clear distinction in the seasonal rainfall patterns. Generally OND is predicted to receive more rainfall than MAM under the two scenarios considered in this part of the study.

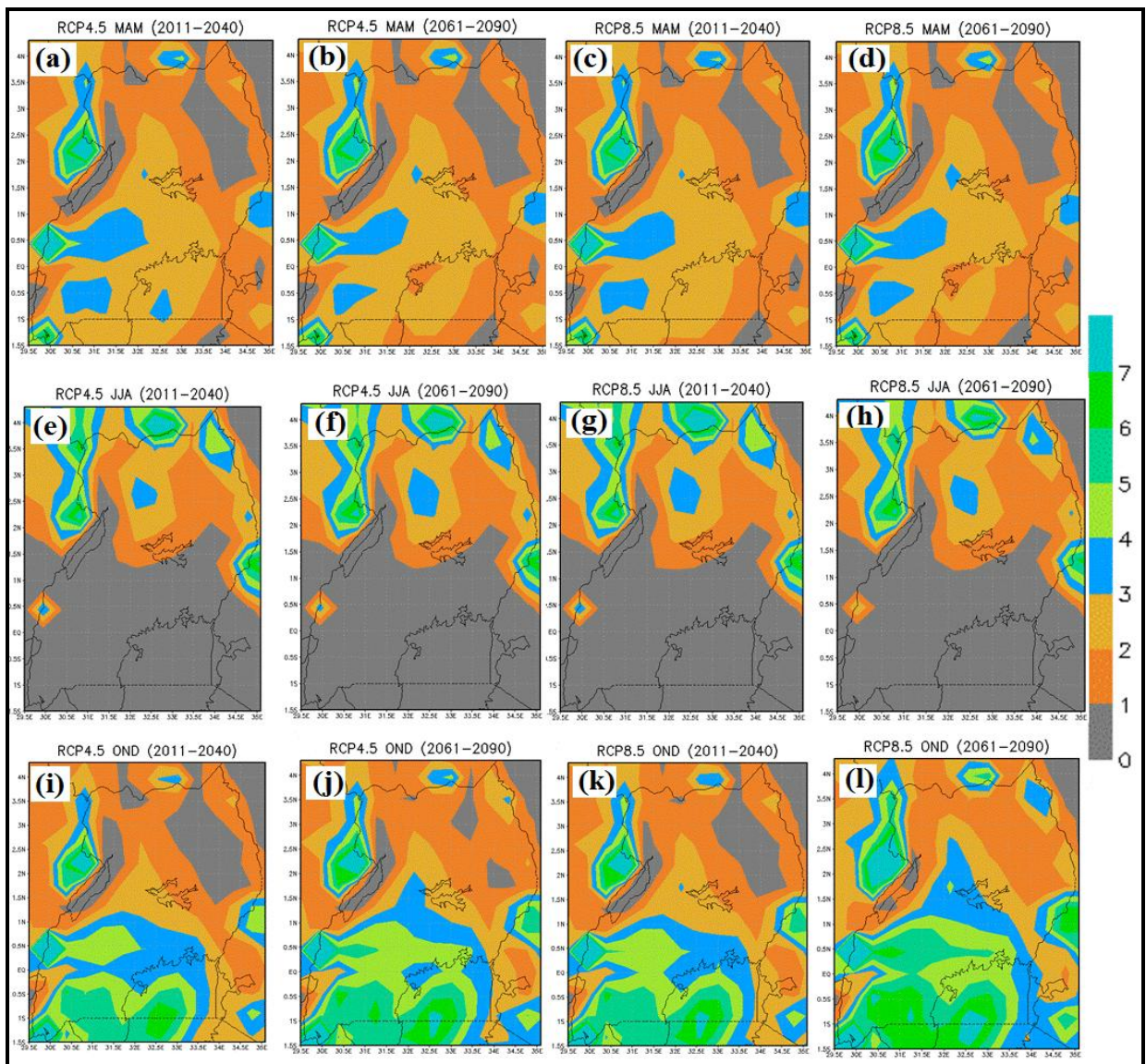


Figure 4.98 (a-l): The RCP 4.5 (a, b, e, f, i, j) and RCP 8.5 (c, d, g, h, k, l) projected mean rainfall (2011-2040 & 2061-2090) during MAM (a-d), JJA (e-h) and OND (i-l) over Uganda.

Figure 4.99 (a-l) shows the Coefficient of Variability of rainfall projected under the two scenarios. The study observed stronger variability during JJA (e-h) and relatively low variability during MAM (a-d) and OND (i-l). There is a strong tendency for the projected rainfall variability to be higher in all seasons over the southern with low variability projected for the central and northern part of the Country.

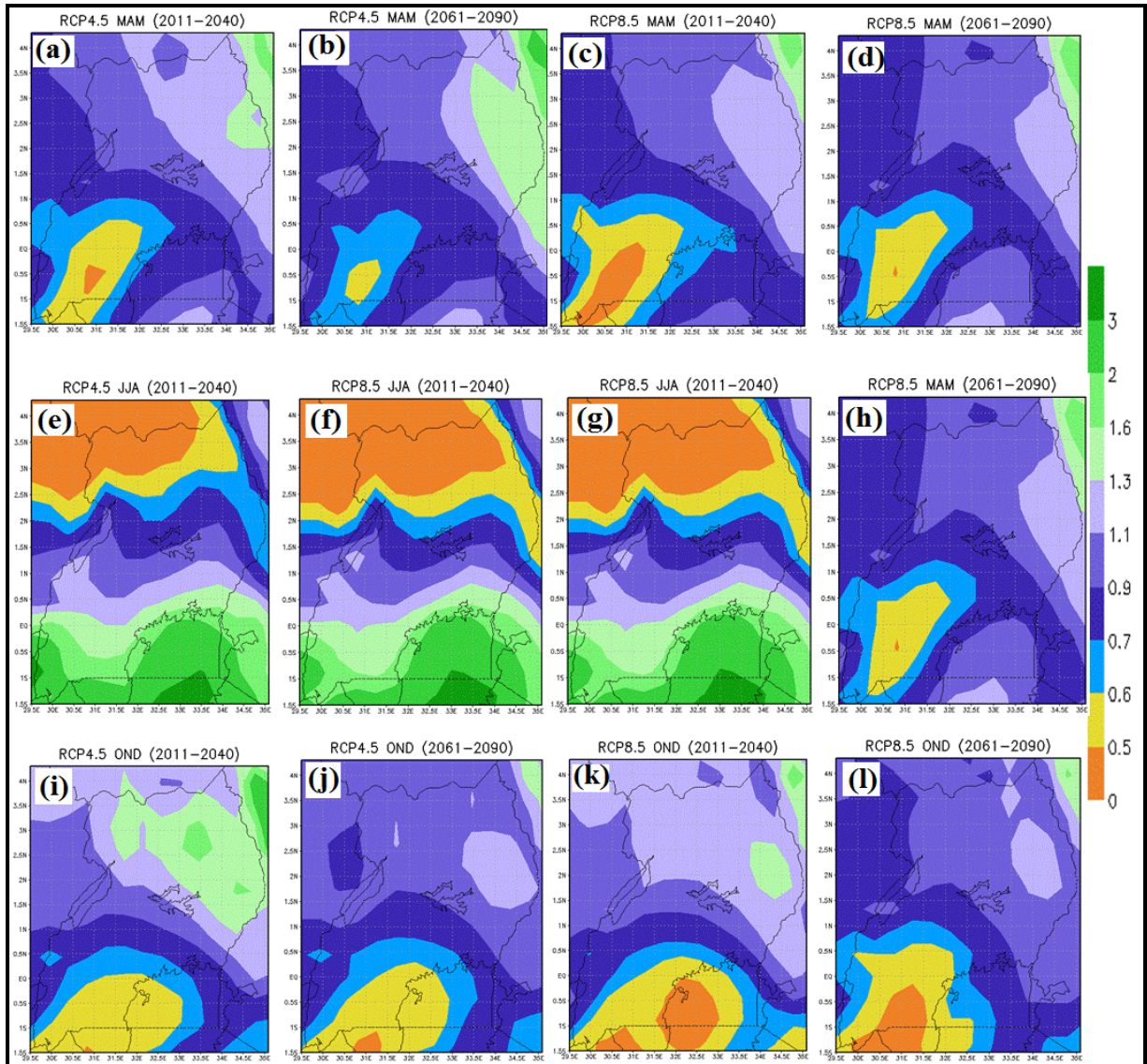


Figure 4.99 (a-l): The RCP 4.5 (a, b, e, f, i, j) and RCP 8.5 (c, d, g, h, k, l) projected coefficient of variability of rainfall (2011-2040 & 2061-2090) during MAM (a-d), JJA (e-h) and OND (i-l) over Uganda.

Figure 4.100 (a-l) shows the pattern in seasonal projected temperature over Uganda. Warm temperature is predicted during MAM and JJA while colder temperatures are predicted during OND. There is strong spatial variation of temperature over Uganda. In addition the northern region is projected to be warmer than the southern region of the Uganda.

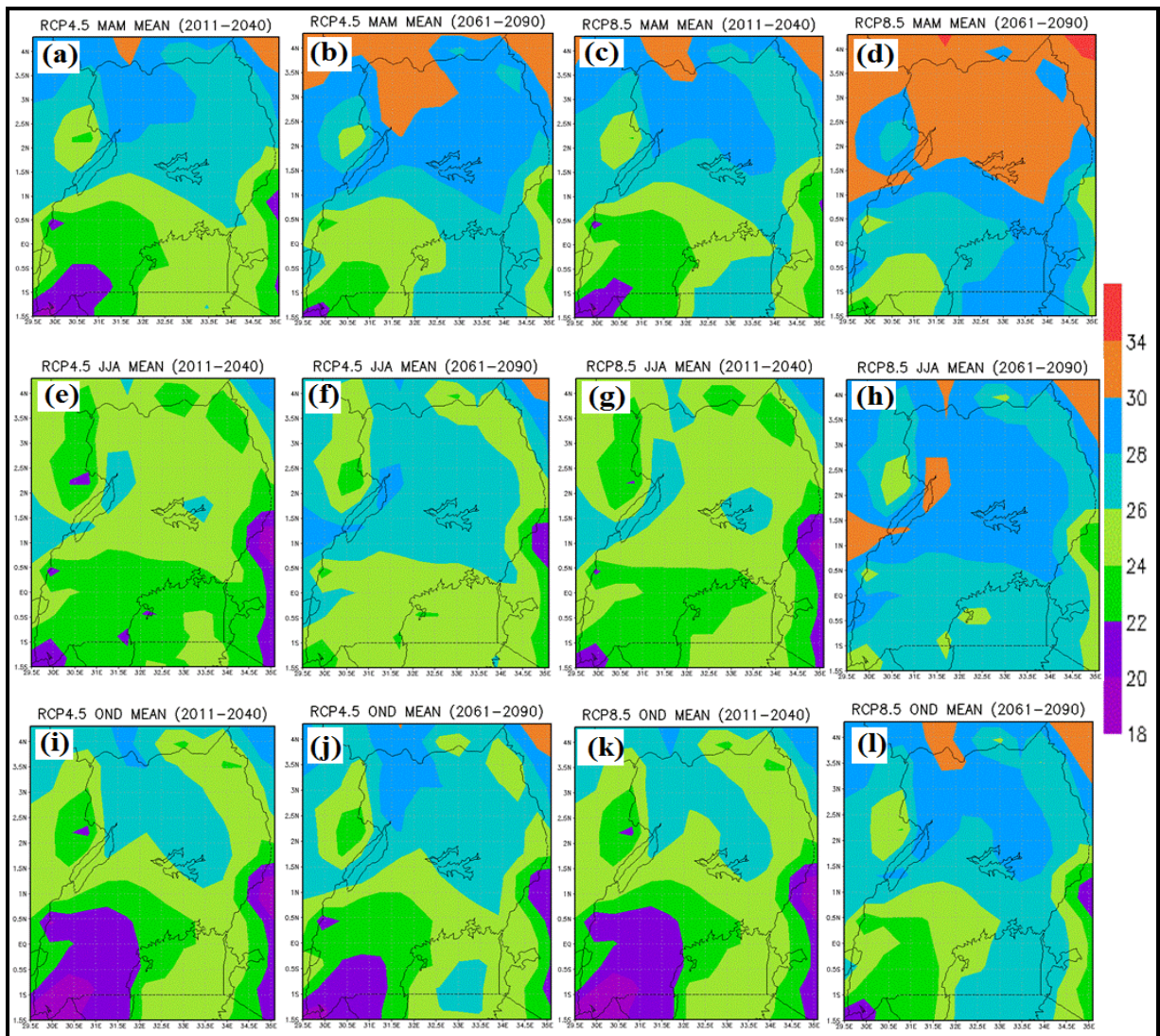


Figure 4.100 (a-l): The RCP 4.5 (a, b, e, f, i, j) and RCP 8.5 (c, d, g, h, k, l) projected seasonal mean surface temperature ($^{\circ}\text{C}$) (2011-2040 & 2061-2090) during MAM (a-d), JJA (e-h) and OND (i-l) over Uganda.

Figure 4.101 (a-f) shows results for the change in average temperature between the period 2011-2040 and 2061-2090. The study observed that under RCP 8.5 very low temperature change is expected to occur in all seasons. The study further observed that, during the OND (e-f) season under RCP 4.5 and RCP 8.5 is predicted to exhibit relatively low temperature changes especially for RCP 4.5 (e). The study generally observed that the southwestern part of the Country will experience relatively higher seasonal changes in temperature.

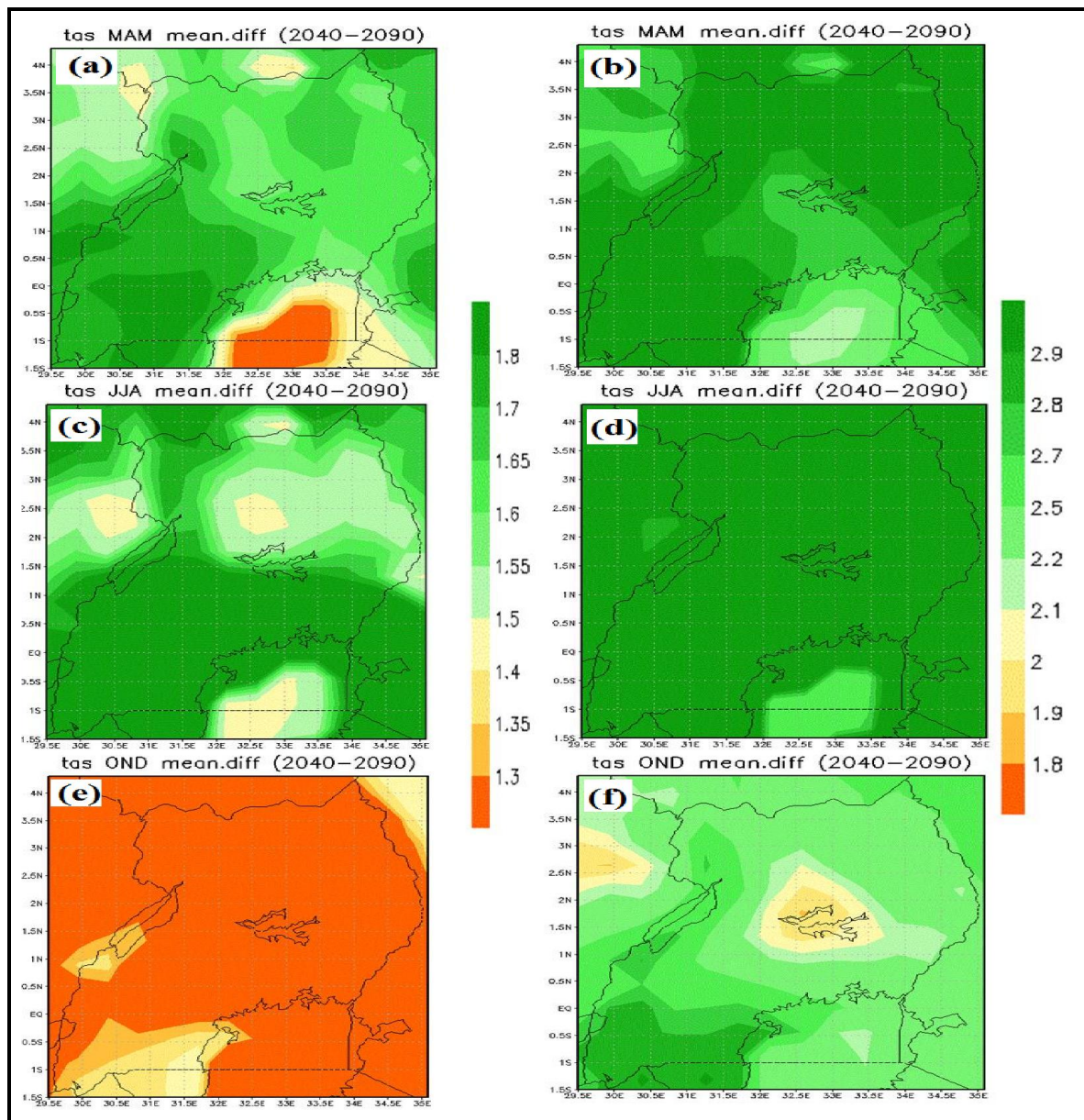


Figure 4.101 (a-f): Spatial patterns of projected changes in seasonal surface temperature ($^{\circ}$ C) for RCP 4.5 (a, c, e) and RCP 8.5 (b, d, f) between the periods 2061-2090 and 2011-2040 over Uganda.

4.4.9.2 Results on the Spatial Patterns of the Projected Bio-climatic Variables

In this section of the study, results on the analysis of the spatial patterns of four bioclimatic variables have been presented for the new RCP scenarios for two periods including 2041-2060 and 2061-2080. The bioclimatic variables presented here include the annual mean temperature, mean temperature of coldest quarter, annual mean rainfall, and mean rainfall of driest quarter. The spatial patterns of these bioclimatic variables have been analysed and results presented.

Figure 4.102 shows the representation of observed patterns of the four bioclimatic variables. The study observed that there is minimal spatial variation in annual mean temperature over

most of central, western and eastern Uganda. High temperatures are observable over northwestern parts of Uganda (Figure 4.102a). The results further show that central region and parts of the central north and eastern region receive the highest amount of rainfall with parts of south western and north western regions receiving low rainfall (Figure 4.102c). Mean temperature of the coldest quarter is lowest in the southern parts of the Country with the northern regions receiving relatively warmer conditions (Figure 4.102c). On the other hand, mean seasonal rainfall of the driest quarter is lowest over the northern region and increases south in the central and western parts of the Country (Figure 4.102d).

Figure 4.103 (a-d) shows the spatial patterns of the four bioclimatic variables for RCP 2.6 for the period 2041-2060. The study observed variability in the annual mean temperature that is highest over the northern part of Uganda and lowest in the southwestern region (Figure 4.103a). Annual mean rainfall is highest over mountainous areas including areas around mountain Elgon and mountain Rwenzori (Figure 4.103c). The same observations apply to the parts of central and northern Uganda, however, low rainfall is projected over northern and southwestern region. The mean temperature of the coldest quarter observed that this scenario exhibits relatively low temperatures over south western and the southern part of central Uganda with warmer temperatures anticipated over the northern part of the Country especially northwestern region (Figure 4.103b). The results further observed that the annual mean rainfall of the driest quarter is likely to fall between 121-220 mm in most of central Uganda where highest rainfall is expected during the driest quarter while the northern region is projected to experience low levels of rainfall that may fall less than 70 mm (Figure 4.103d).

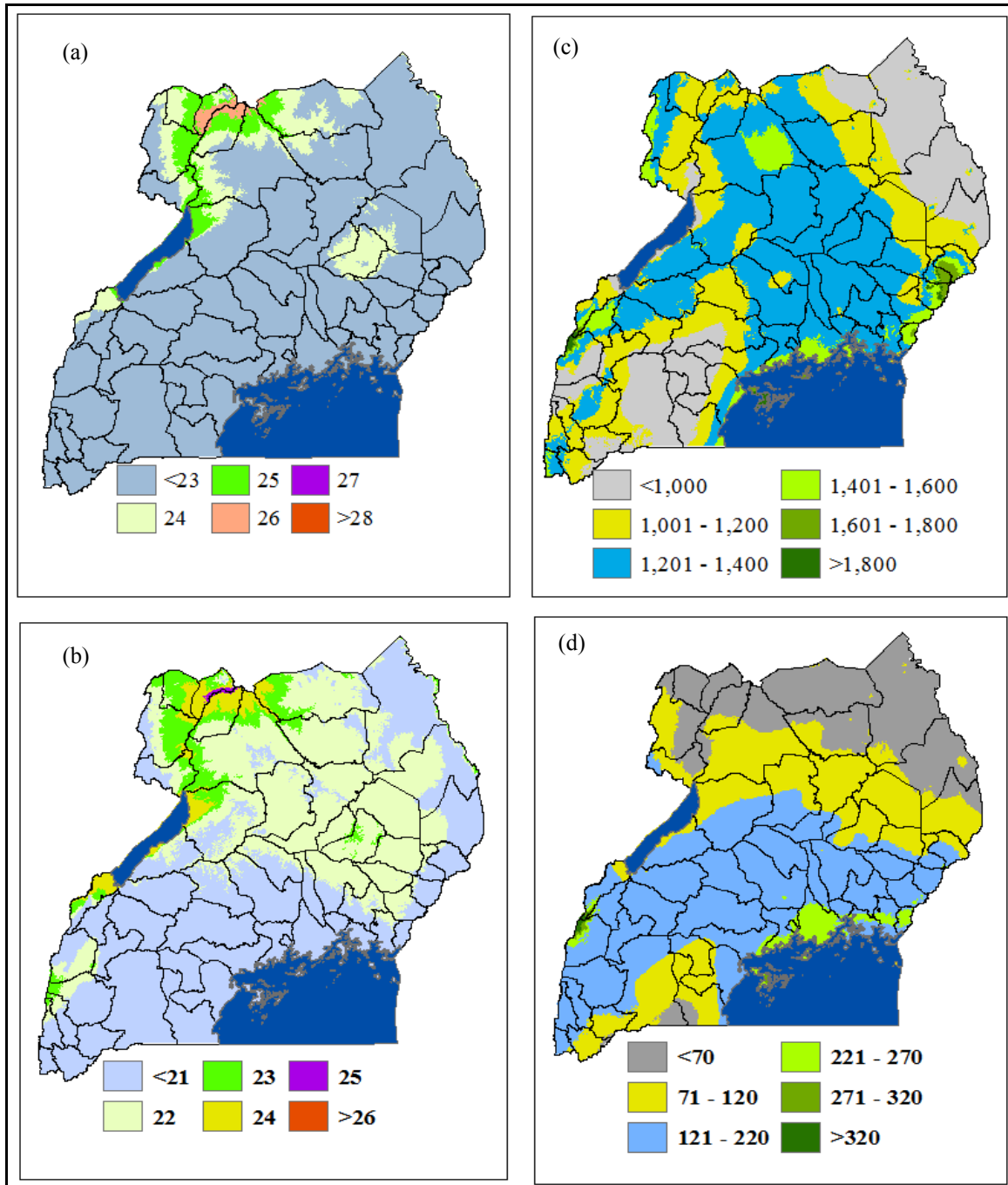


Figure 4.102 (a-d): Observed annual mean surface temperature (a), mean temperature of coldest quarter (b), annual mean rainfall (c) and mean rainfall of driest quarter (d) over Uganda.

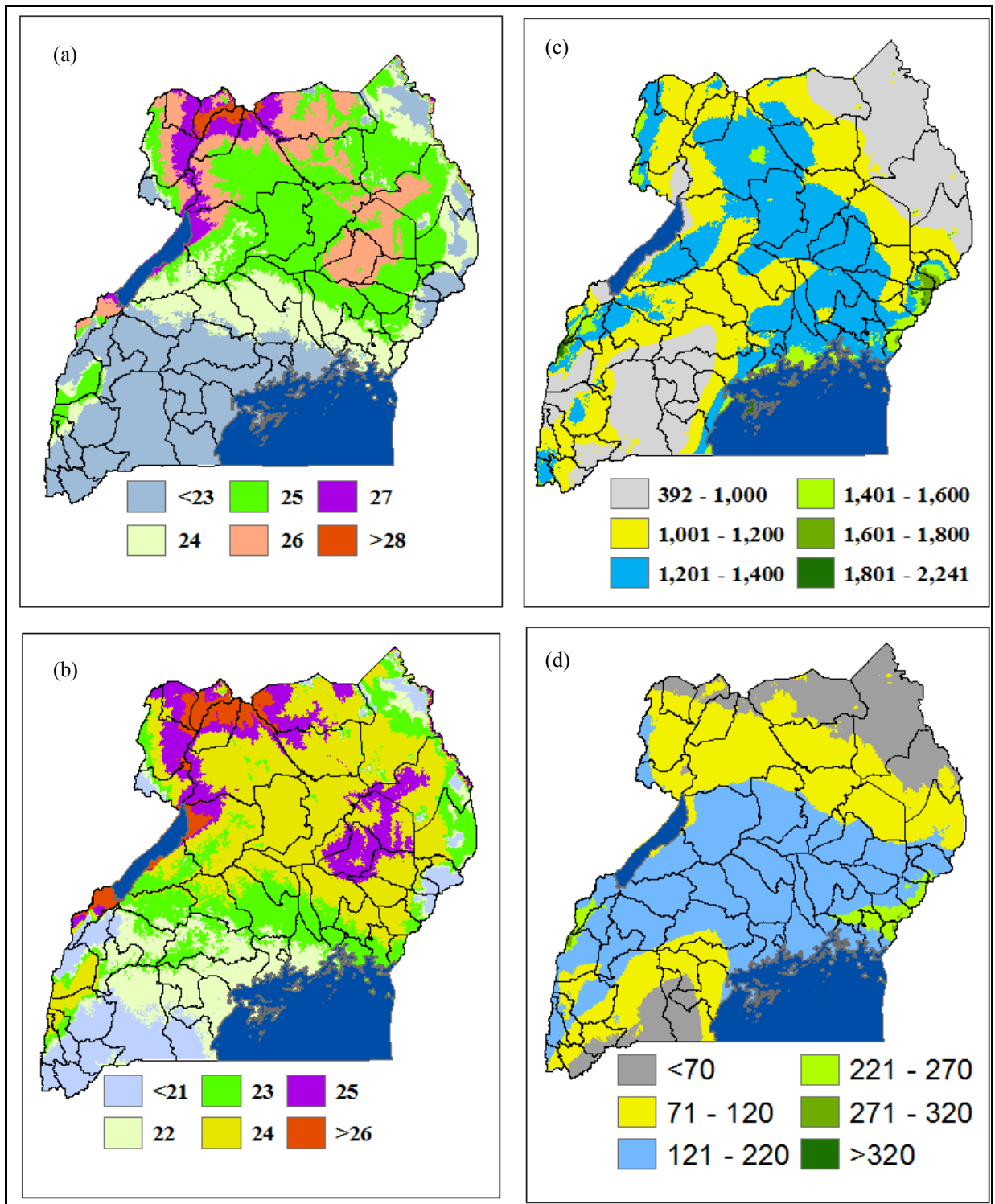


Figure 4.103 (a-d): Projected annual mean surface temperature (a), mean temperature of coldest quarter (b), annual mean rainfall (c) and mean rainfall of driest quarter (d) for RCP 2.6 (2041-2060) over Uganda.

Figure 4.104 (a-d) shows patterns for RCP 2.6 for the further period of 2061-2080. The results show a likelihood of decrease in both annual rainfall and rainfall of the driest quarter compared with the results of some scenario during the period 2041-2060, on the other hand, temperature is expected to increase by about 1.2 °C between these two periods.

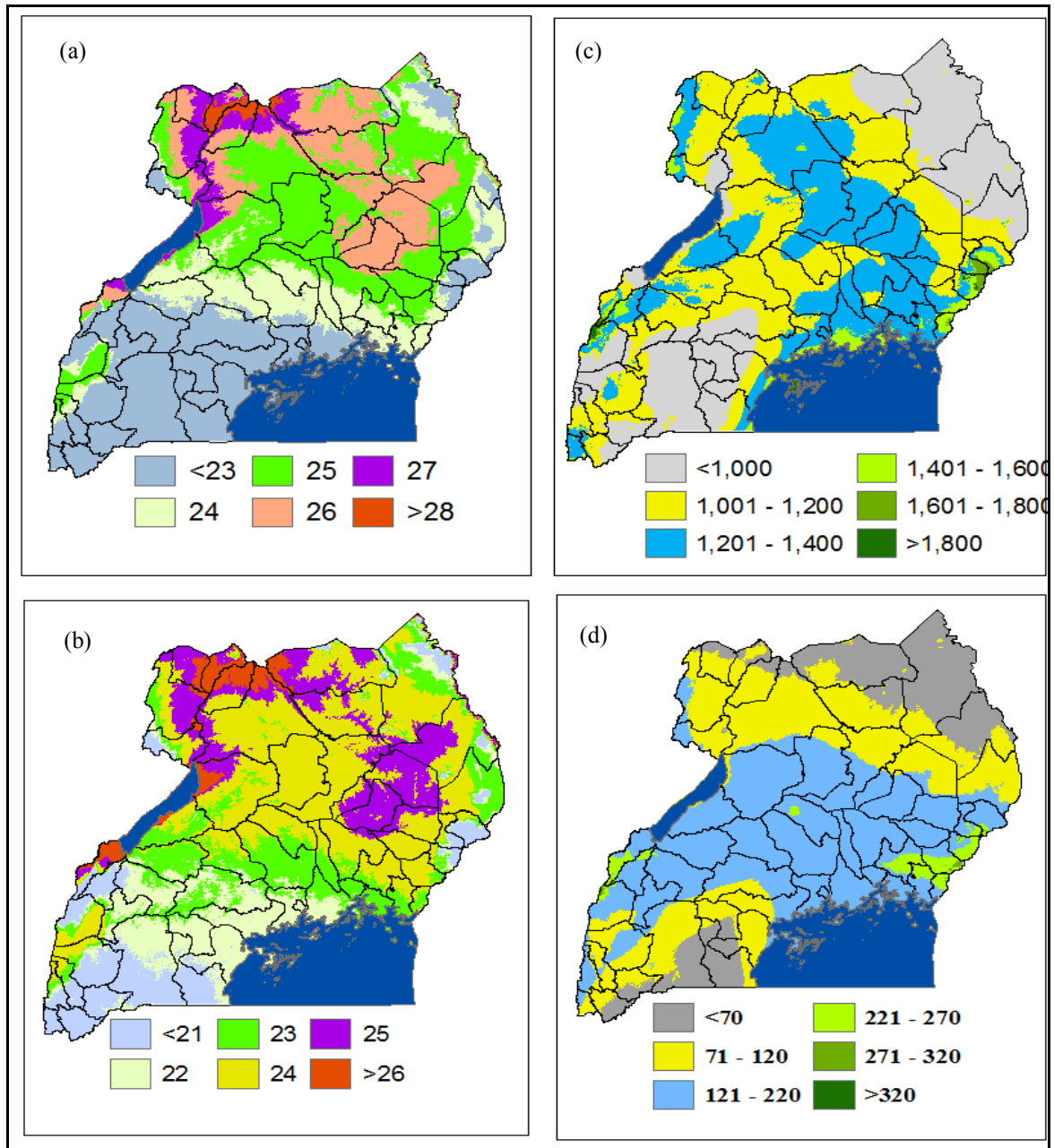


Figure 4.104 (a-d): Projected annual mean surface temperature (a), mean temperature of coldest quarter (b), annual mean rainfall (c) and mean rainfall of driest quarter (d) for RCP 2.6 (2061-2080) over Uganda.

Figure 4.105 (a-d) shows results of the four bioclimatic variables for the period 2041-2060 while Figure 4.106 (a-d) indicated the spatial patterns of the four variables for the period 2061-2080 for RCP 4.5. It is observed from the results that similar patterns of rainfall are expected

as those described under RCP 2.6 (Figure 4.105 a-d and Figure 4.106 a-d). It is however, observed that temperature projected under RCP 4.5 is slightly higher than that for RCP 2.6 during the corresponding periods. The results show slight increase in the rainfall between 2041-2060 and 2061-2080 under RCP 4.5.

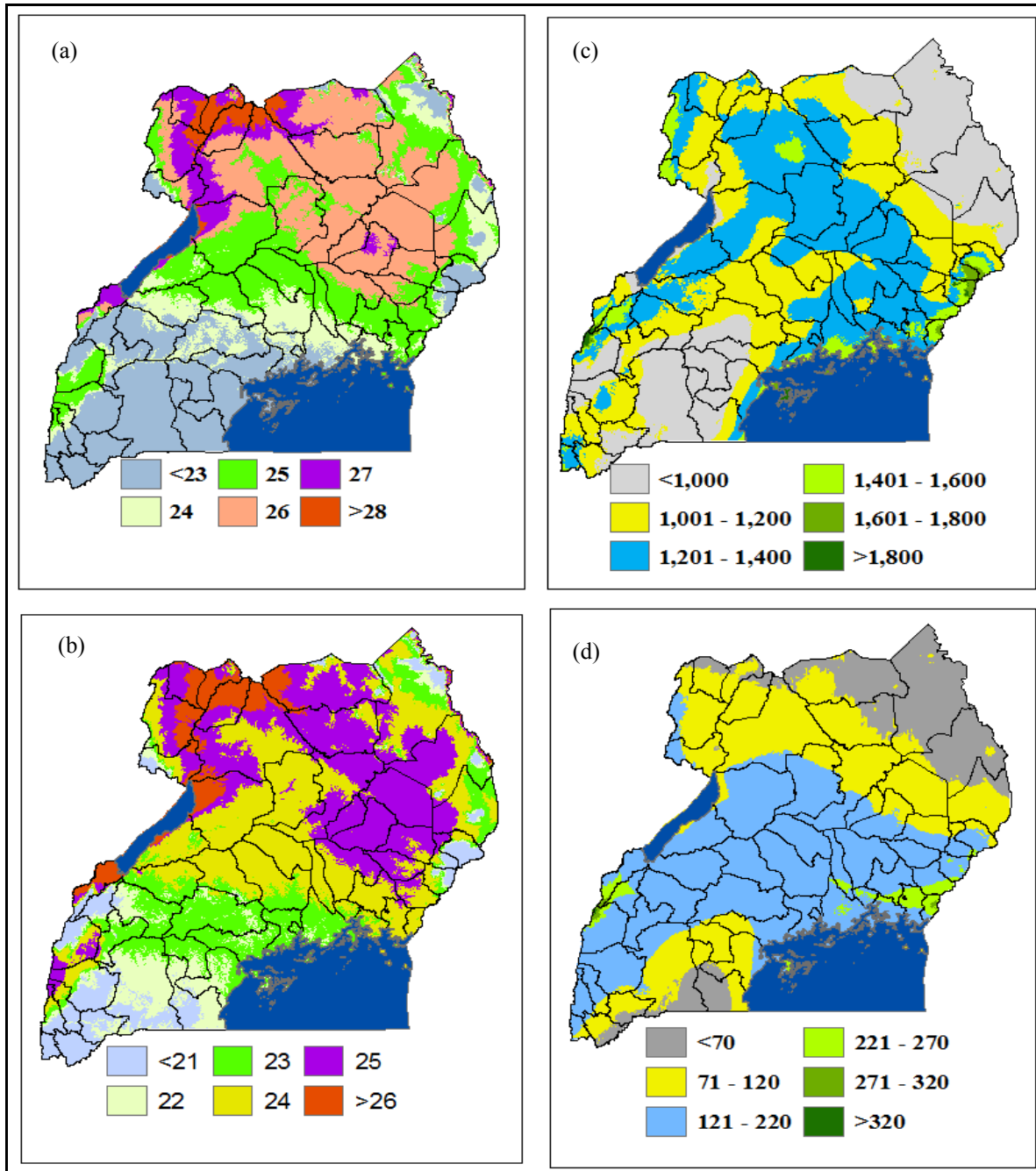


Figure 4.105 (a-d): Projected annual mean surface temperature (a), mean temperature of coldest quarter (b), annual mean rainfall (c) and mean rainfall of driest quarter (d) for RCP 4.5 (2041-2060) over Uganda.

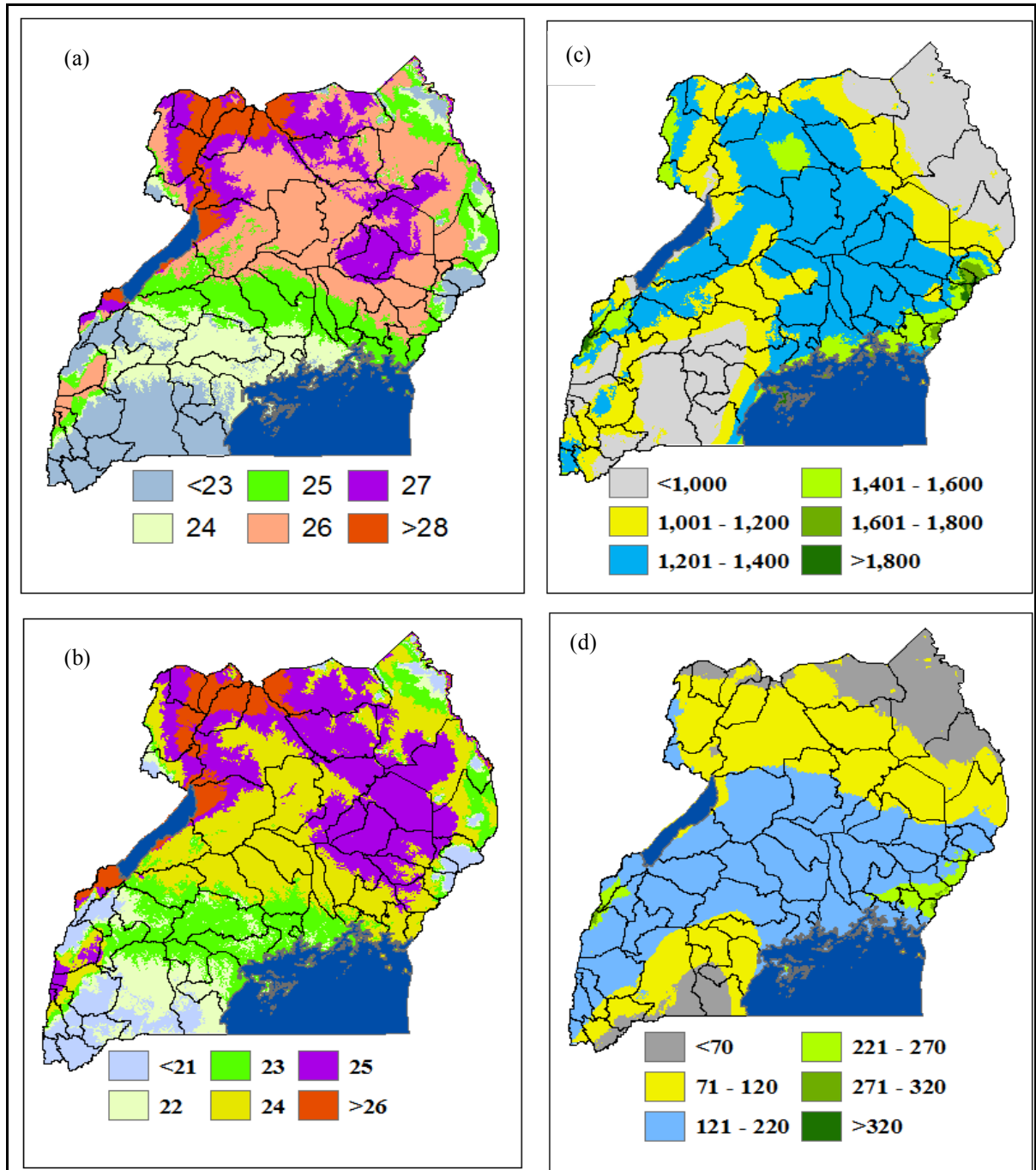


Figure 4.106 (a-d): Projected annual mean surface temperature (a), mean temperature of coldest quarter (b), annual mean rainfall (c) and mean rainfall of driest quarter (d) for RCP 4.5 (2061-2080) over Uganda.

Under the RCP 6.0, annual temperatures are low in south western region and highest in the northern region (Figures 4.107 c-d). The temperature in most parts of the Country is warmer than that projected under RCP 2.6 and RCP 4.5 (Figure 4.107 a, b). The annual mean rainfall increases under this scenario, with most parts of the central and northern region expected to receive between 1200-1400 mm per year (Figures 4.107 c). The rainfall during the driest quarter is slightly comparable to the one for RCP 2.6 and RCP 4.5 (Figure 4.107 d). Figure

4.107 (a-d) shows similar pattern as Figure 4.108 (a-d) but with slightly enhanced annual rainfall especially over western region bordering Lake Albert. On the other hand, warmer temperatures are expected under RCP 6.0 (2061-2080) over most parts of the region as compared to temperatures in during the period 2041-2060.

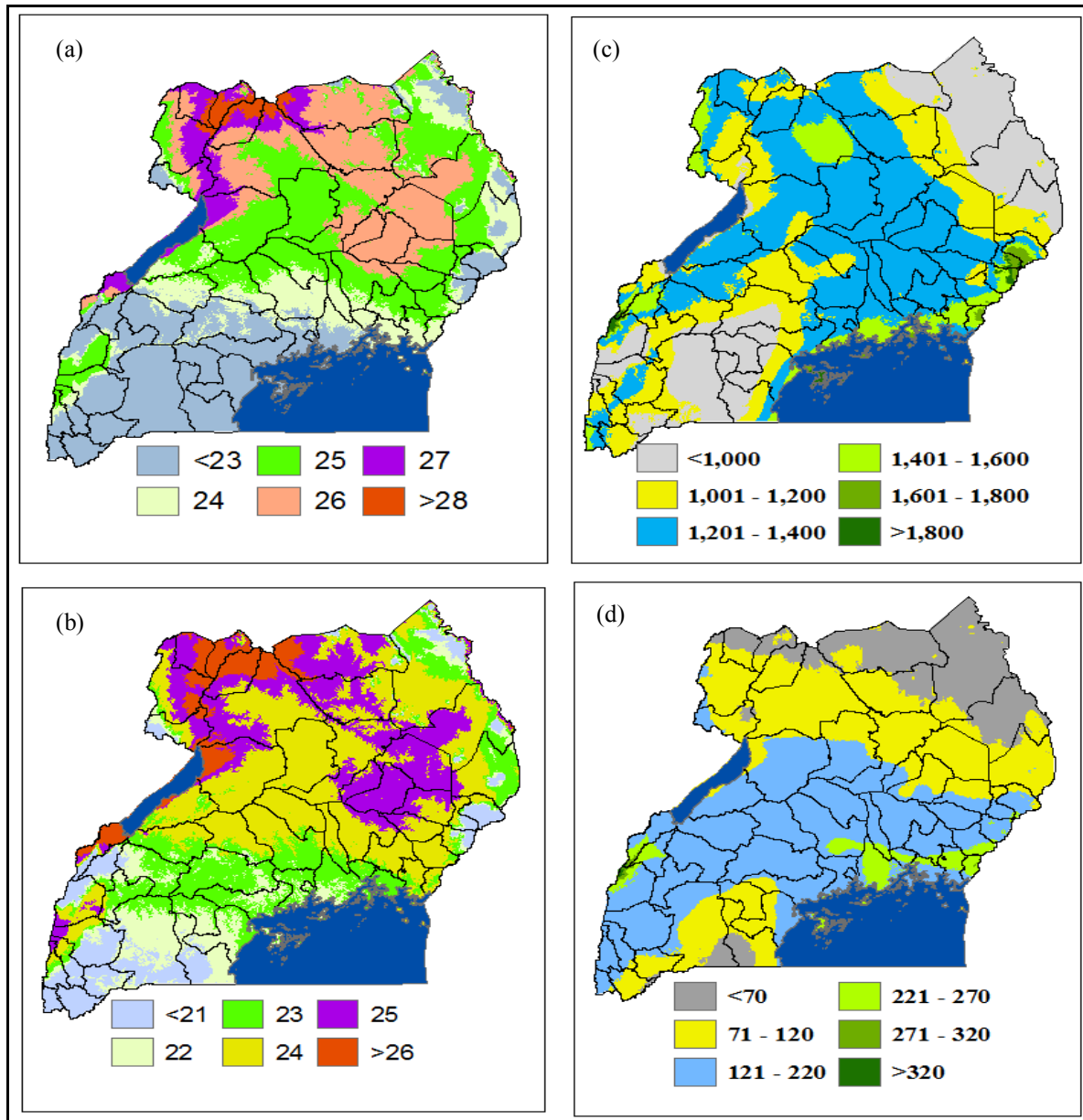


Figure 4.107 (a-d): Projected annual mean surface temperature (a), mean temperature of coldest quarter (b), annual mean rainfall (c) and mean rainfall of driest quarter (d) for RCP 6.0 (2041-2060) over Uganda.

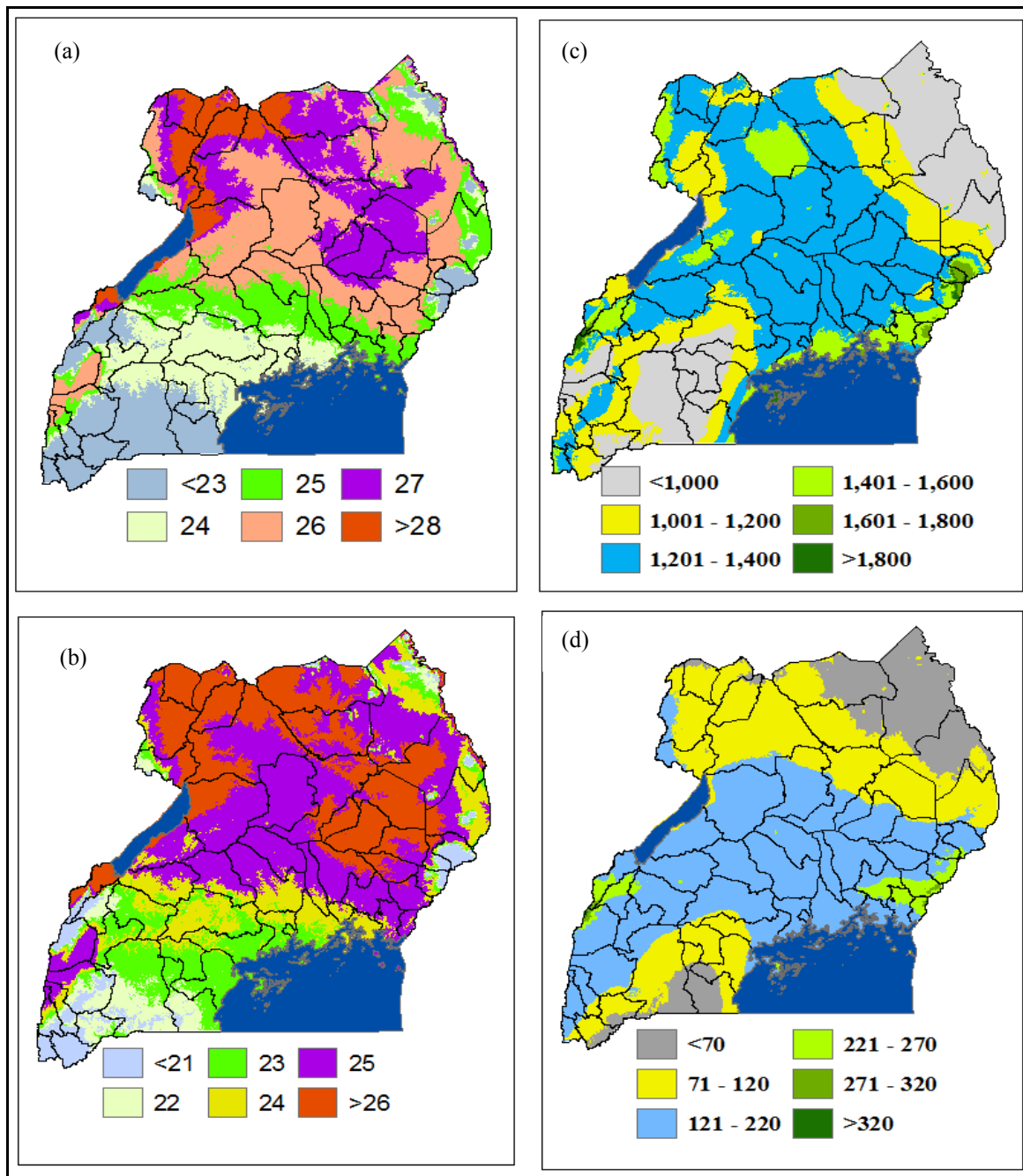


Figure 4.108 (a-d): Projected annual mean surface temperature (a), mean temperature of coldest quarter (b), annual mean rainfall (c) and mean rainfall of driest quarter (d) for RCP 6.0 (2061-2080) over Uganda.

Figure 4.109 (a-d) presents the results on the spatial patterns of the four bioclimatic variables under RCP 8.5 for the period of 2041-2060. The pattern in both rainfall and temperature are quite similar to those RCP 6.0 presented in Figure 4.108 for the period 2061-2080. It is however observed that temperatures under RCP 8.5 indicated a warmer future than the condition under RCP 6.0. Enhanced rainfall is expected in the same way as that expected under RCP 6.0 especially the annual rainfall over most of the Country. The southern region is expected to remain relatively dry under all scenarios with slight increase in rainfall between the

periods 2041-2060 and 2061-2080. The results show a consistent increase in temperature across the scenarios and time periods over Uganda.

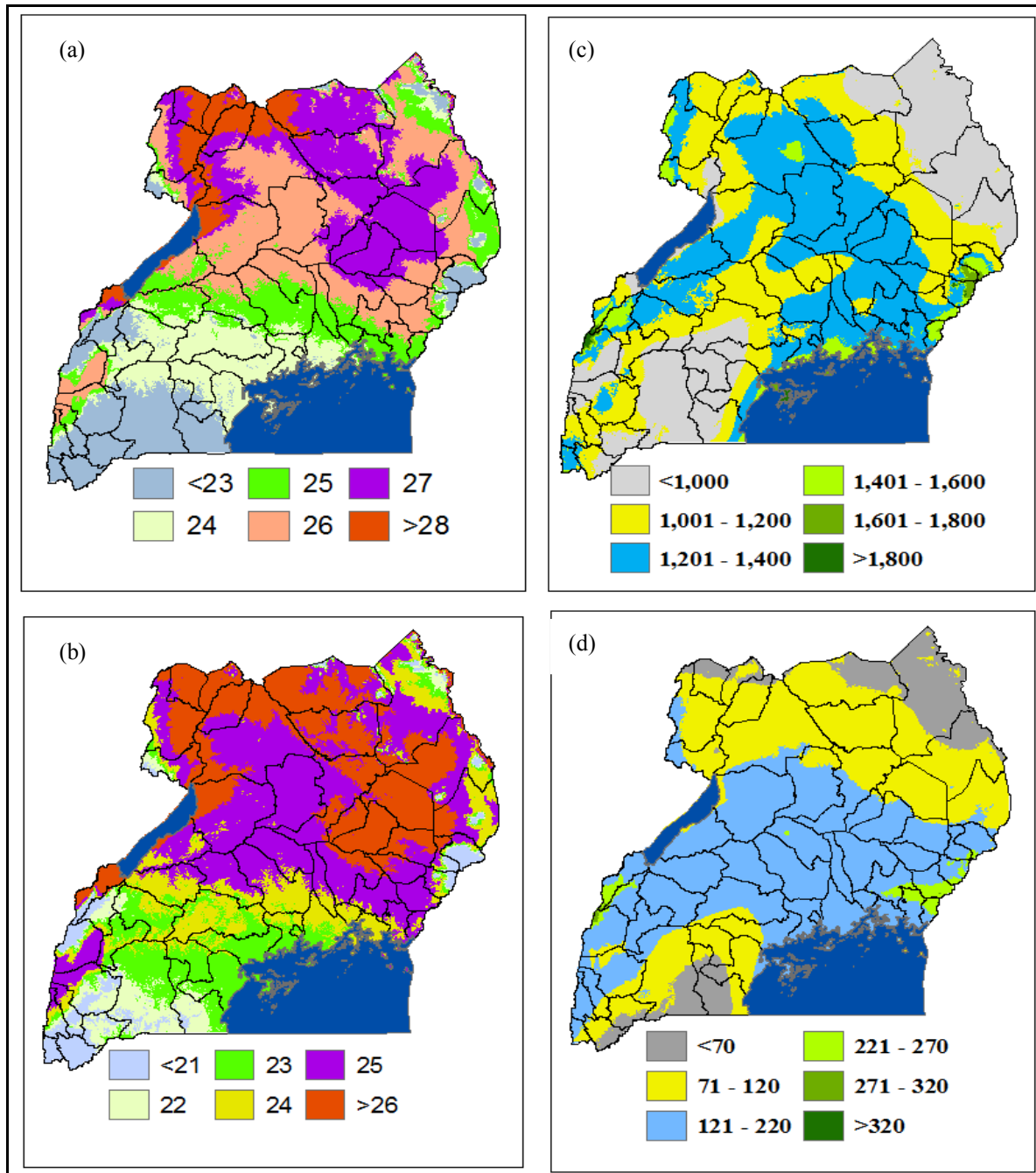


Figure 4.109 (a-d): Projected annual mean surface temperature (a), mean temperature of coldest quarter (b), annual mean rainfall (c) and mean rainfall of driest quarter (d) for RCP 8.5 (2041-2060) over Uganda.

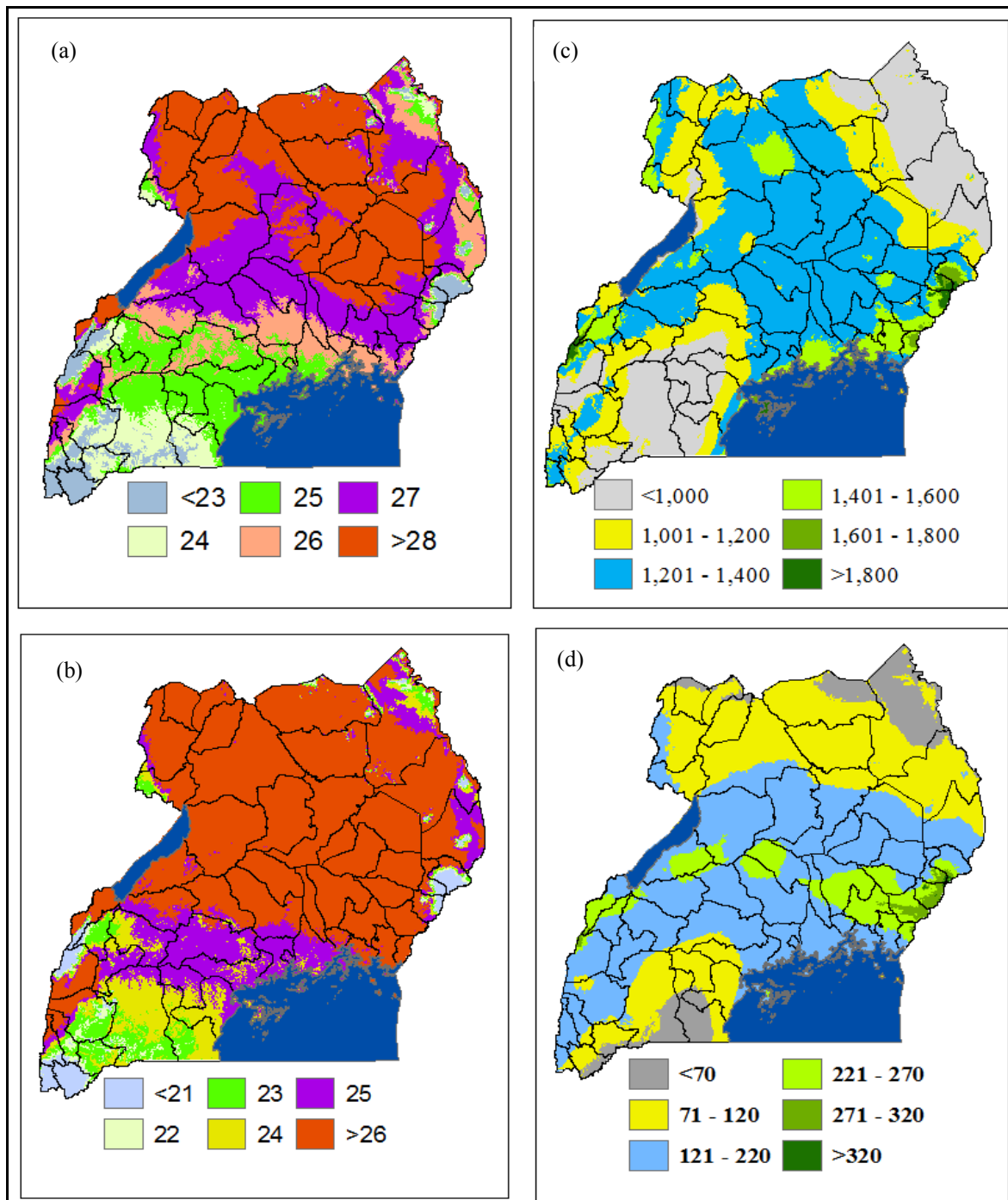


Figure 4.110 (a-d): Projected annual mean surface temperature (a), mean temperature of coldest quarter (b), annual mean rainfall (c) and mean rainfall of driest quarter (d) for RCP 8.5 (2061-2080) over Uganda.

It may be concluded from the results of climate projections under both SRES and RCPs scenarios that high spatio-temporal variations and changes in future rainfall are discernible across locations under all scenarios over Uganda. The results showed likelihood of decrease in future rainfall on the one hand and an increase in temperature on the other hand. There are also cases of increasing rainfall during some seasons in some locations. Temperature increases

were, however, common with all scenarios. For example, temperature increases as high as 4 °C was observed under SRES A2 with lower temperature changes under A1B by the year 2100.

Projections based on the bio-climatic variables presented by annual mean temperature, mean temperature of coldest quarter, annual mean rainfall, and mean rainfall of driest quarter observed significant changes that would have far reaching implication on the current bananas varieties in Uganda.

Under the RCP scenarios, lowest temperatures are like to be associated with RCP 2.6 and RCP 4.5 while high temperatures are expected under RCP 6.0 and RCP 8.5. The results showed a likelihood of decrease in both total annual rainfall and rainfall of the driest quarter compared with the results of some scenario during the period 2041-2060. On the other hand, temperature is expected to increase by about 1.2 °C between these two periods under the RCP scenarios.

Effective adaptation strategies are required to maximize and optimize on the opportunities and threats respectively from projected climate change over Uganda.

4.5 Results on the Effects of the Future Climate Change on Bananas Production

This study further examined the effects of climate change on banana production based on suitability indices that were developed using the suitability mapping ARC GIS spatial analyst tools for the four bioclimatic variables already presented. The results are presented in Figures 4.111 (a-b) - 4.114 (a-b) for the suitability scores under the four RCP scenarios for the two time periods. As already discussed under Section 3.2.5, the suitability mapping delineated regions of varying future banana growth conditions as (1) excellent (86-100%), (2) very suitable (71-85%), (3) suitable (56-70%), (4) marginal (41-55%), (5) very marginal (26-40%) and (6) unsuited (less than 25%). This Section presents results on the suitability of banana production over Uganda under the different RCP scenarios during the periods 2041-2060 and 2061-2080 based on the suitability mapping over Uganda.

In addition, the study also used results obtained from the temperature-banana growth regression model to analyse the impact of temperature change on banana growth for both a wet (MAM) and dry (JJA) seasons. The results are presented in Figures 4.115 (a-d) - 4.120 (a-d).

4.5.1 Projected Suitable Areas for Banana Production under the RCP Climate Scenario on rainfall and temperature changes

Figure 4.111 (a) observed that under RCP 2.6, most of central and western Uganda is likely to remain suitable with banana growth rates of about 56-70% during the 2040-2061 period. The central region north of Lake Victoria is projected to be excellent (growth rate above 86%) banana producing area with the eastern and southwestern Uganda projected to be very suitable (growth rate above 71-85%) for production of bananas. The northern and particularly north eastern region is likely to experience very marginal (26-40%) to not suitable (less than 25%) condition for banana production (Figure 4.111a). Similar conditions are expected for the period 2061-2080 under RCP 2.6 (Figure 4.111b) with slight reduction in the areas suitable for banana production. This may be attributed to increase in temperature that will be accompanied by slight reductions in annual rainfall over some parts of the Country under the RCP 2.6 between the two periods considered in this study.

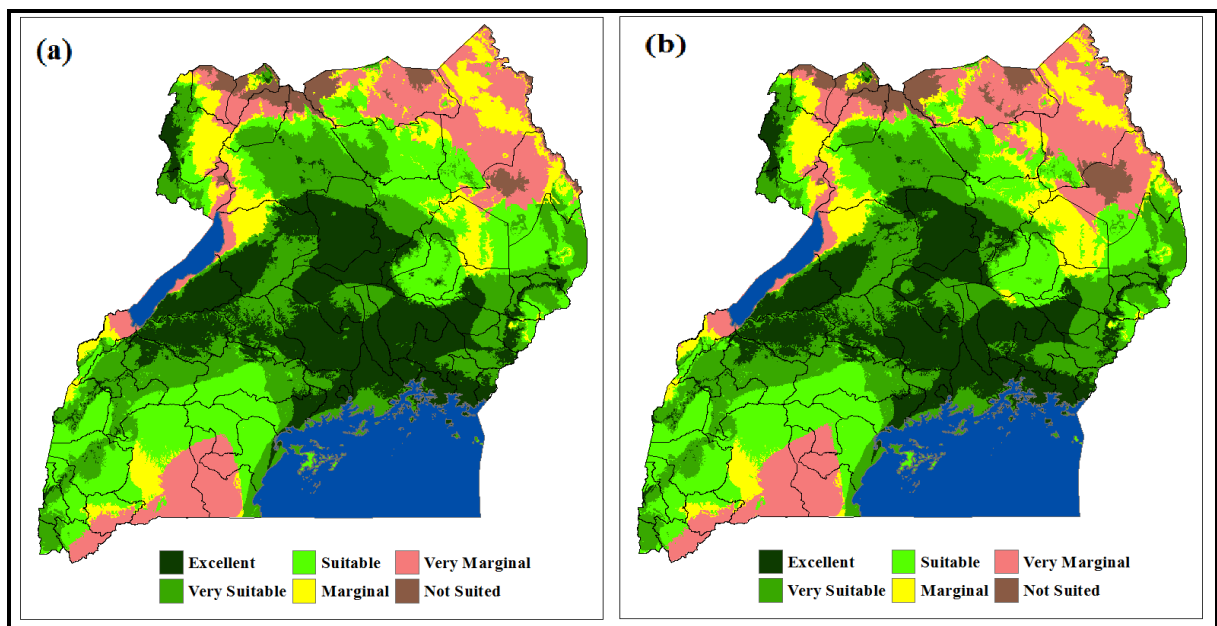


Figure 4.111 (a-b): Projected future suitability of banana growth under RCP 2.6 for the period 2041-2060 (a) and 2061-2080 (b) over Uganda.

Figure 4.112 (a) presents results of suitability conditions (86-100%, 71-85%, 56-70%, 41-55%, 26-40% and 0-25%) for growth of bananas under RCP 4.5 during 2041-2060. There is an observed reduction in the area suitable for production of bananas as compared to the conditions depicted in Figure 4.111 (a) for RCP 2.6 during 2041- 2060 period. The climatic conditions have been predicted to become less conducive for production of the banana crop under RCP 4.5 relative to RCP 2.6 during the period 2041-2060. The climatic conditions for the future

(2061-2080) worsen under RCP 4.5 scenario and become slightly less favorable, the leaving only area around Lake Victoria showing excellent conditions while the northern and northwestern and northeastern remain marginal (26-40%) to not suitable (less than 25%) for production of bananas (Figure 4.112b).

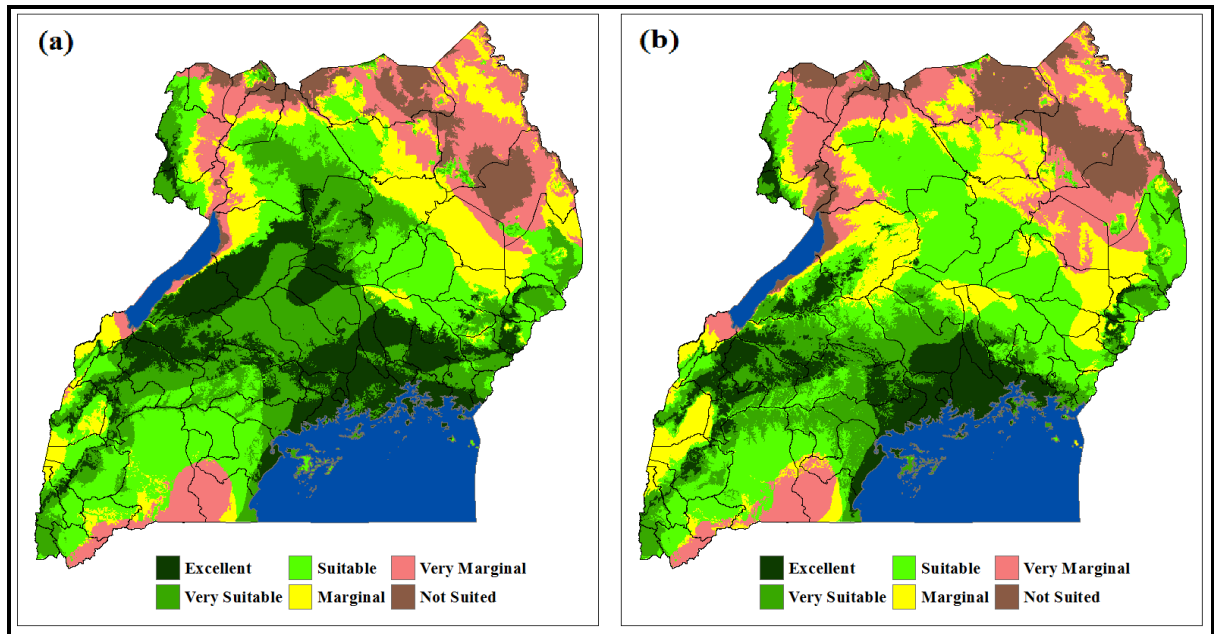


Figure 4.112 (a-b): Projected future suitability of banana growth under RCP 4.5 for the period 2041-2060 (a) and 2061-2080 (b) over Uganda.

The study observed that, under the RCP 6.0 scenario (Figure 4.113a) there is high potential for production of bananas (suitable to excellent, 56-100%) during the period 2041-2060 compared to all other scenarios over most of the country. It was further observed that banana production during this period is likely to remain highest compared with all scenarios and periods. There is an expected significant decrease in banana production during 2061-2080 despite significantly large area Uganda still remain suitable to very suitable (56-85%, Figure 4.113b) under RCP 6.0.

Figure 4.114 (a) shows the suitability of banana production based on projected climatic conditions under RCP 8.5 during 2041-2060 while Figure 4.114 (b) shows conditions for production of banana during the period 2061-2080. The results showed during 2041-2060 (Figure 4.114a), projected rainfall and temperature conditions will favor higher production of bananas only over most central western and south western Uganda under this scenario. On the other hand, the period 2061-2080 is likely to experience climatic conditions that marginally (less than 40%) favor or don't favor banana production over most parts of Uganda (Figure 4.114 b). The results showed that most parts of Uganda including central will be marginal to not suitable for production of bananas under this scenario. Generally, the results have observed

the worse anticipated condition for banana production in the future under RCP 8.5 due to very high temperatures associated with the scenario.

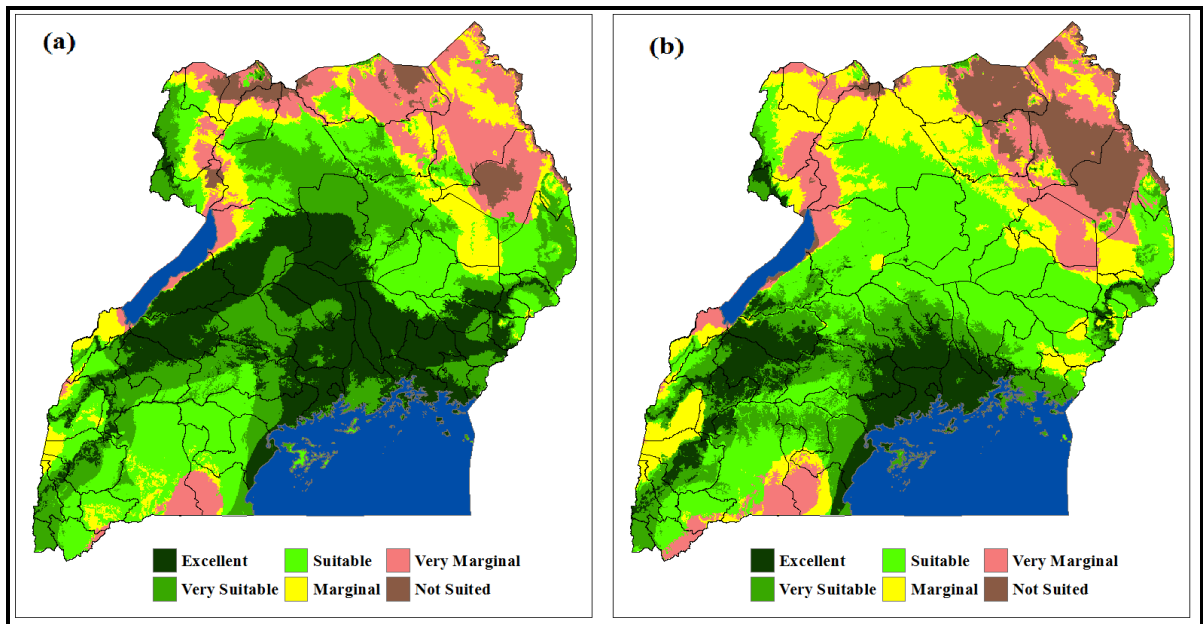


Figure 4.113 (a-b): Projected future suitability of banana growth under RCP 6.0 for the period 2041-2060 (a) and 2061-2080 (b) over Uganda.

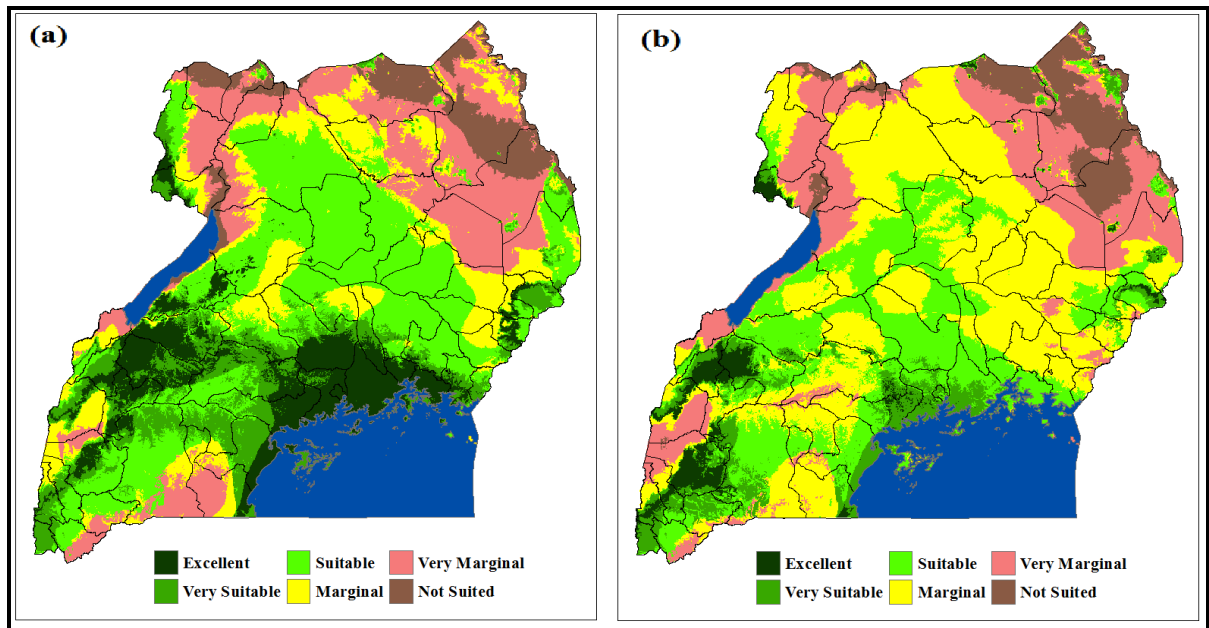


Figure 4.114 (a-b): Projected future suitability of banana growth under RCP 8.5 for the period 2041-2060 (a) and 2061-2080 (b) over Uganda.

The best case scenario for production of bananas includes RCP 2.6 and RCP 6.0. The change in production of banana is sudden and high under RCP 6.0 between the two periods while that under RCP 2.6 is small between the two periods. RCP 4.5 projects climatic conditions that favor banana production better than the RCP 8.5 over most of Uganda. A similar approach has

been employed to investigate climate change patterns and its impacts on the growing conditions of bananas in the tropics (Ramirez-Villegas *et al.*, 2011) and to investigate the impact of climate change on banana productivity (Van den Bergh *et al.*, 2012) in the tropics.

In general, the study results have revealed for the first time that future projected pattern of rainfall, temperature and the resultant soil moisture content will have varying potential effects on the growth patterns and production of bananas in Uganda. For example, the results have observed that a larger (smaller) area suitable for banana production under RCP 2.6 and RCP 6.0 (RCP 4.5 and RCP 8.5) for the intermediate period 2041-2060 over Uganda. Due to projected temperature increases across all scenarios, the areas suitable for banana production will reduce under all the four RCP scenarios in the far future period 2061-2080 compared to the intermediate period 2041-2060. The northern parts of Uganda will most likely remain unsuitable for banana production across all climate change scenarios.

4.6.2 Likely Effects of IPCC SRES A1B & A2 Projected Temperatures on Banana Growth

The effects of increasing minimum, average and maximum temperature on banana growth is presented in Figures 4.115-4.120 (a-d) for different sub-region of Uganda. The results are presented for rainy MAM (Figure 4.115 – 4.117) and dry JJA (Figure 4.116 – 4.118) seasons. Results for both SRES A1B and A2 SRES climate scenarios have been presented and contrasted across the periods 2011-2040 and 2061-2090.

Figure 4.115 (a-d) shows the effects of increasing minimum, average and maximum temperature on banana growth of over northwestern and eastern region for the periods during MAM for SRES A1B and A2 climate scenarios over Uganda. The period 2011-2040 (near future) is therefore being contrasted with 2061-2090 (far future). The study observed that the temperatures (21 – 22° C) projected under A1B SRES are still lower than the optimal temperature (26.7° C) for banana production and increasing temperatures would favor high growth (Figure 4.115a-b). This is likely to promote high banana growth from lower than 50% to over 60% in these regions under SRES A1B scenario given favorable rainfall and other conditions. In contrast, under SRES A2 scenario, temperatures are close to optimal temperature for banana growth results show that any further increases in projected temperatures would retard banana growth from over 60% to about 45% or lower in these areas (Figure 4.115a-b).

Over eastern region, both SRES A1B and A2 scenarios predicted temperatures slightly lower than the optimal conditions for maximum banana growth. Foreexample, the further increases in

projected temperatures under A1B for the period 2061-2090 indicate that there is a likelihood of mid century temperatures to favor high banana growth from less than 45% to over 65% in the eastern region (Figure 4.115c-d).

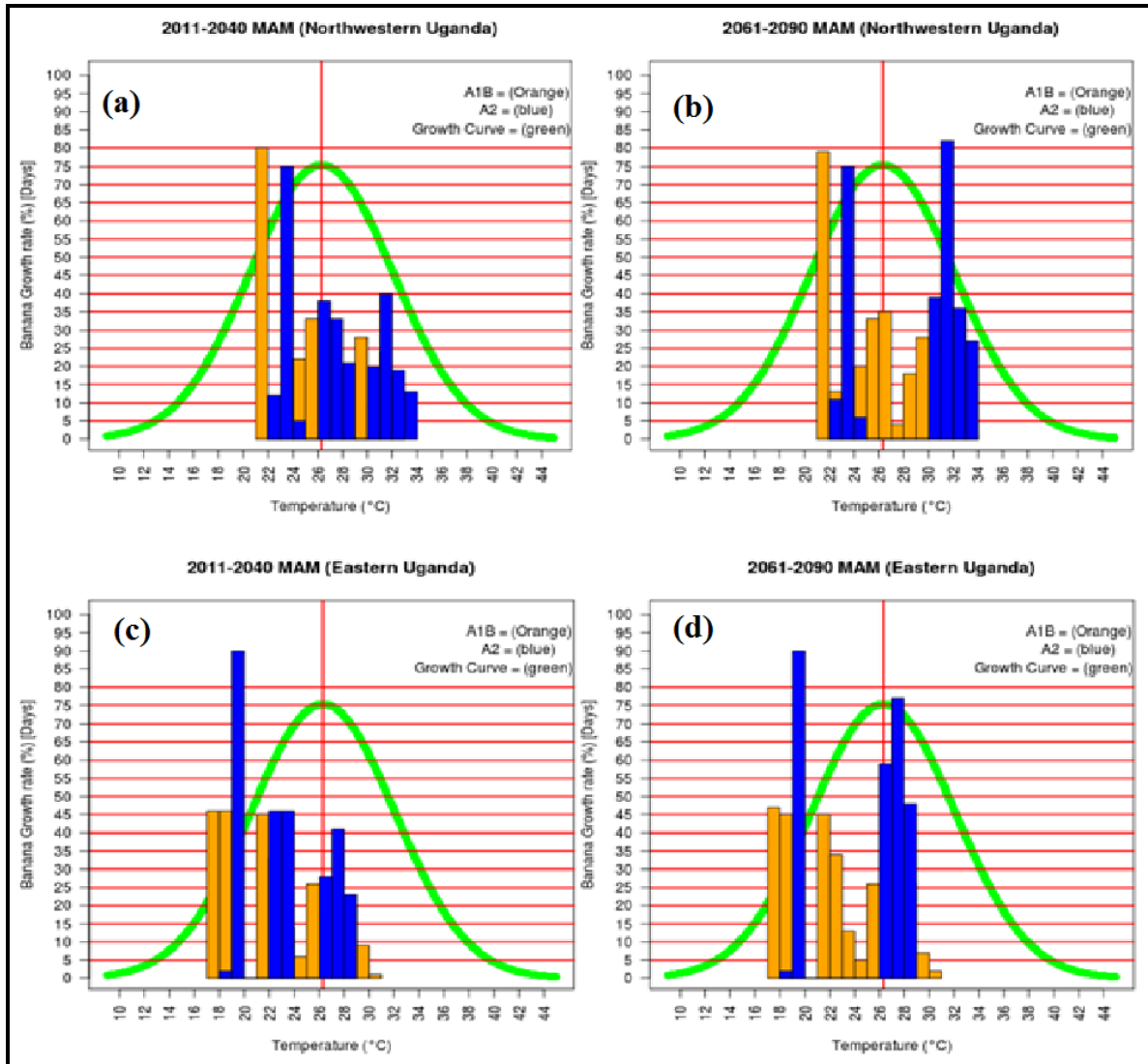


Figure 4.115 (a-d): Projected effects of MAM surface temperature changes on banana growth under A1B and A2 scenarios for northwestern (a-b) and eastern (c-d) regions. Orange bars indicate frequency of SRES A1B temperature, blue bars indicate frequency of SRES A2 temperature, green curve indicate temperature-banana growth.

Figure 4.116 (a-b) and Figure 4.116 (c-d) show results for central and western Uganda respectively. Over central region, the projected increase in temperature are expected to promote banana growth from about 45% to over 55% under SRES A1B scenario while the projected increase in temperature under A2 scenario will most likely retard banana growth (Figure 4.116a-b). Banana growth will, however, retard towards the end of the century under both scenarios. There is therefore a need to promote climate smart agricultural policies

(Ampaire *et al.*, 2015) in the country in addition to mitigation of climate change through the reduction of GHGs emission and adaptation to the impacts of climate change.

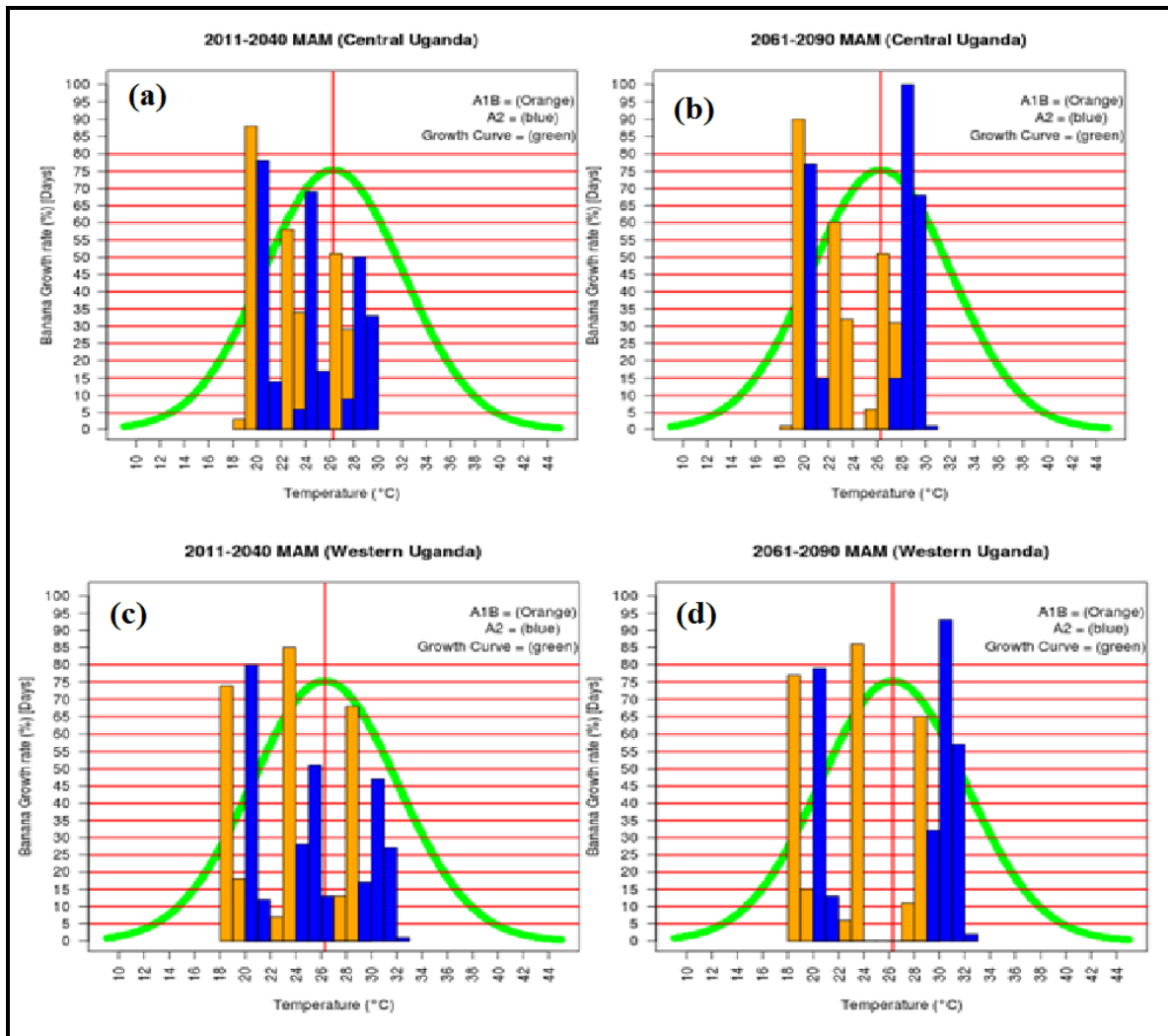


Figure 4.116 (a-d): Projected effects of MAM surface temperature changes on banana growth under A1B & A2 scenarios for central (a-b) and western (c-d) regions. Orange bars indicate frequency of SRES A1B temperature, blue bars indicate frequency of SRES A2 temperature, green curve indicate temperature-banana growth.

Figure 4.117 (a-d) presents results for southwestern Uganda and the Country as a whole. Over the southwestern parts of Uganda, temperature changes projected under both SRES A2 and A1B scenario will favor growth and productivity of bananas. Due to low temperature projected for southwestern Uganda under SRES A1B an increase in temperatures (20 - 22° C) will favor high banana growth of about 65% in the near future (2011-2040) under this scenario. During the period 2011-2040, projected temperatures in SRES A2 may favor banana growth and negatively affect banana growth in the longrun (2061-2090) over the southwestern region (Figure 4.117 a-b). Over Uganda, temperature increases projected under SRES A1B scenarios favor banana growth with increase from 45% to over 53% while the projected temperatures

under SRES A2 will negatively affect banana growth most area (Figure 4.117 c-d) especially by end of the century.

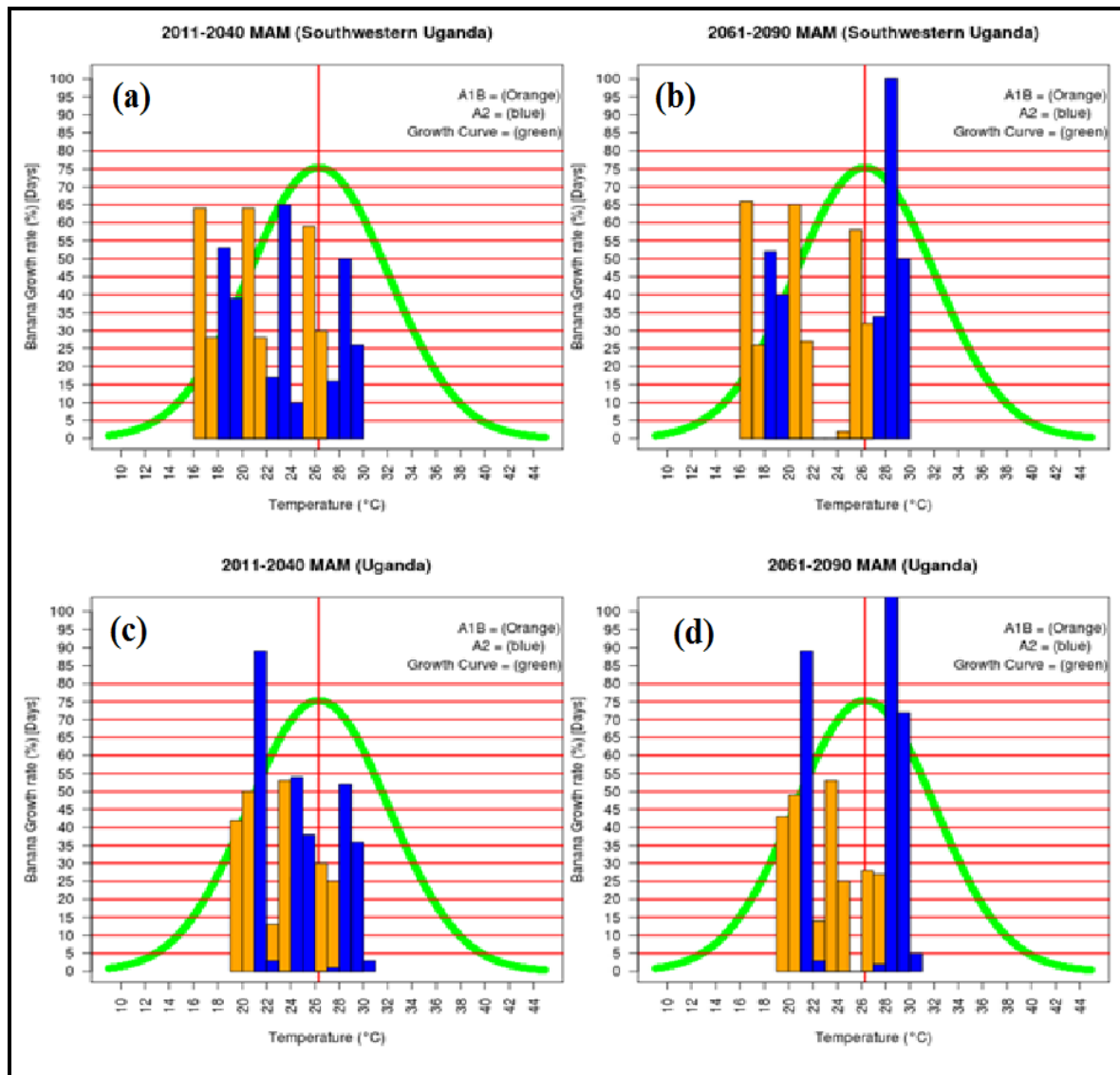


Figure 4.117 (a-d): Projected effects of MAM surface temperature changes on banana growth under A1B & A2 scenarios for southwestern (a-b) and Uganda (c-d) regions. Orange bars indicate frequency of SRES A1B temperature, blue bars indicate frequency of SRES A2 temperature, green curve indicate temperature-banana growth.

Results on the effects of increasing temperature on banana growth during JJA are presented in Figure 4.118 (a-d, northwestern and eastern Uganda), Figure 4.119 (a-d, central and western Uganda), and Figure 4.120 (a-d, southwestern Uganda and Uganda). In general, it is evident from the results that projected increases in temperature affect the growth of bananas in most regions while those projected for A1B are likely to promote banana growth and productivity. In addition, the results reveal that projected increasing temperature during JJA might negatively affect banana growth due to the dry conditions that prevail during the season.

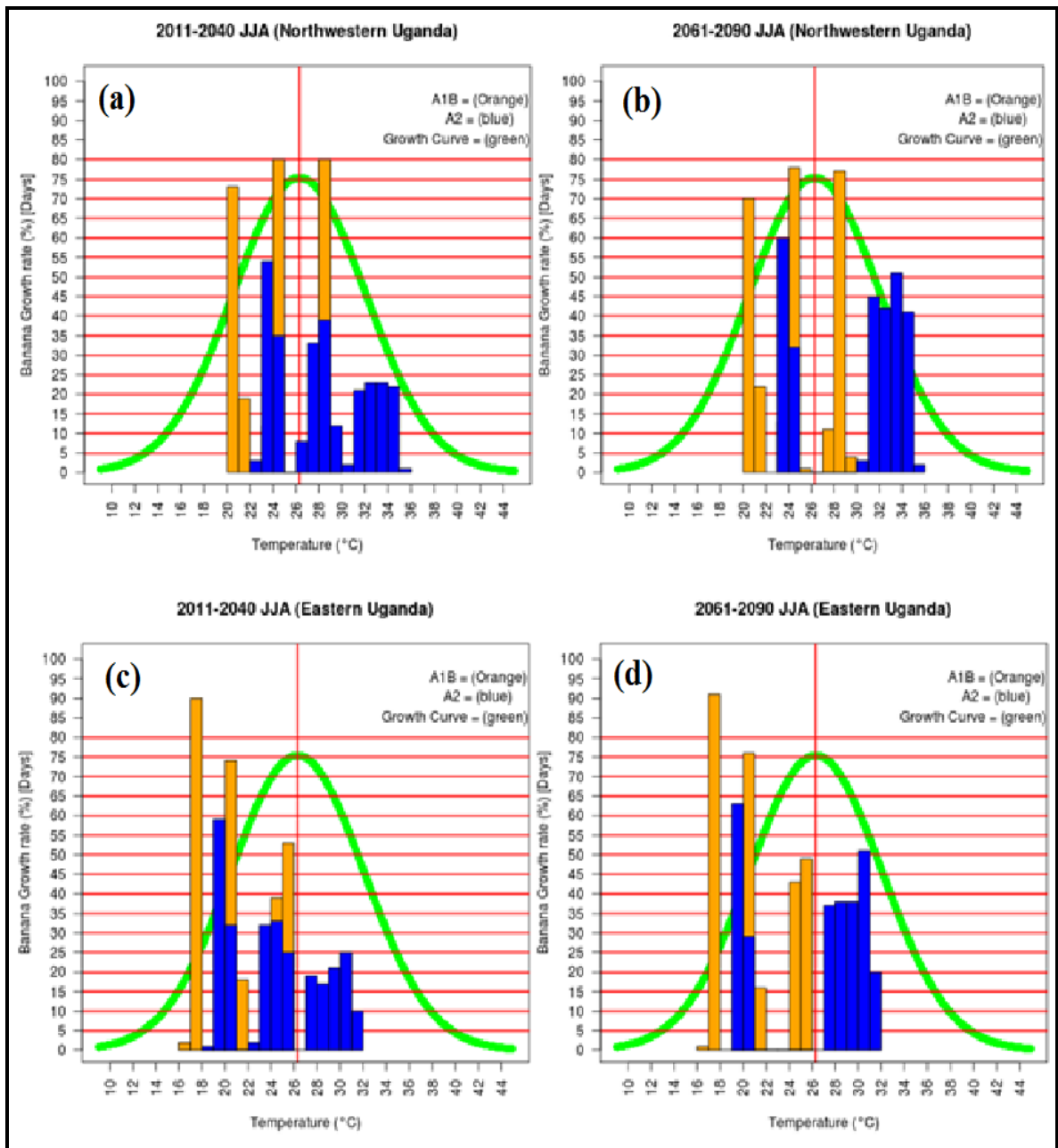


Figure 4.118 (a-d): Projected effects of JJA surface temperature changes on banana growth under A1B & A2 scenarios for northwestern (a-b) and eastern (c-d) regions. Orange bars indicate frequency of SRES A1B temperature, blue bars indicate frequency of SRES A2 temperature, green curve indicate temperature-banana growth.

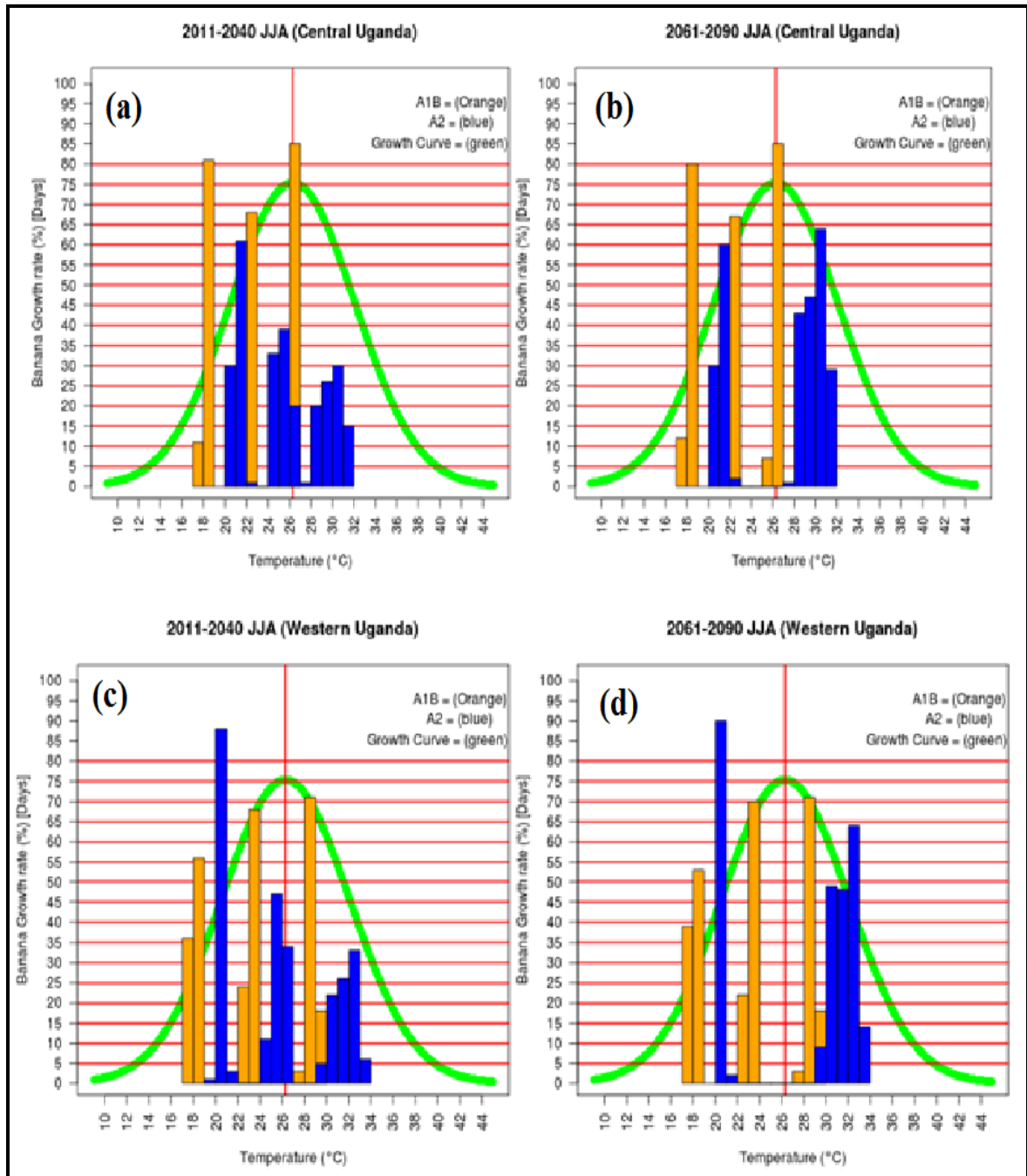


Figure 4.119 (a-d): Projected effects of JJA surface temperature changes on banana growth under A1B & A2 scenarios for central (top-panel) and western (c-d) regions. Orange bars indicate frequency of SRES A1B temperature, blue bars indicate frequency of SRES A2 temperature, green curve indicate temperature-banana growth.

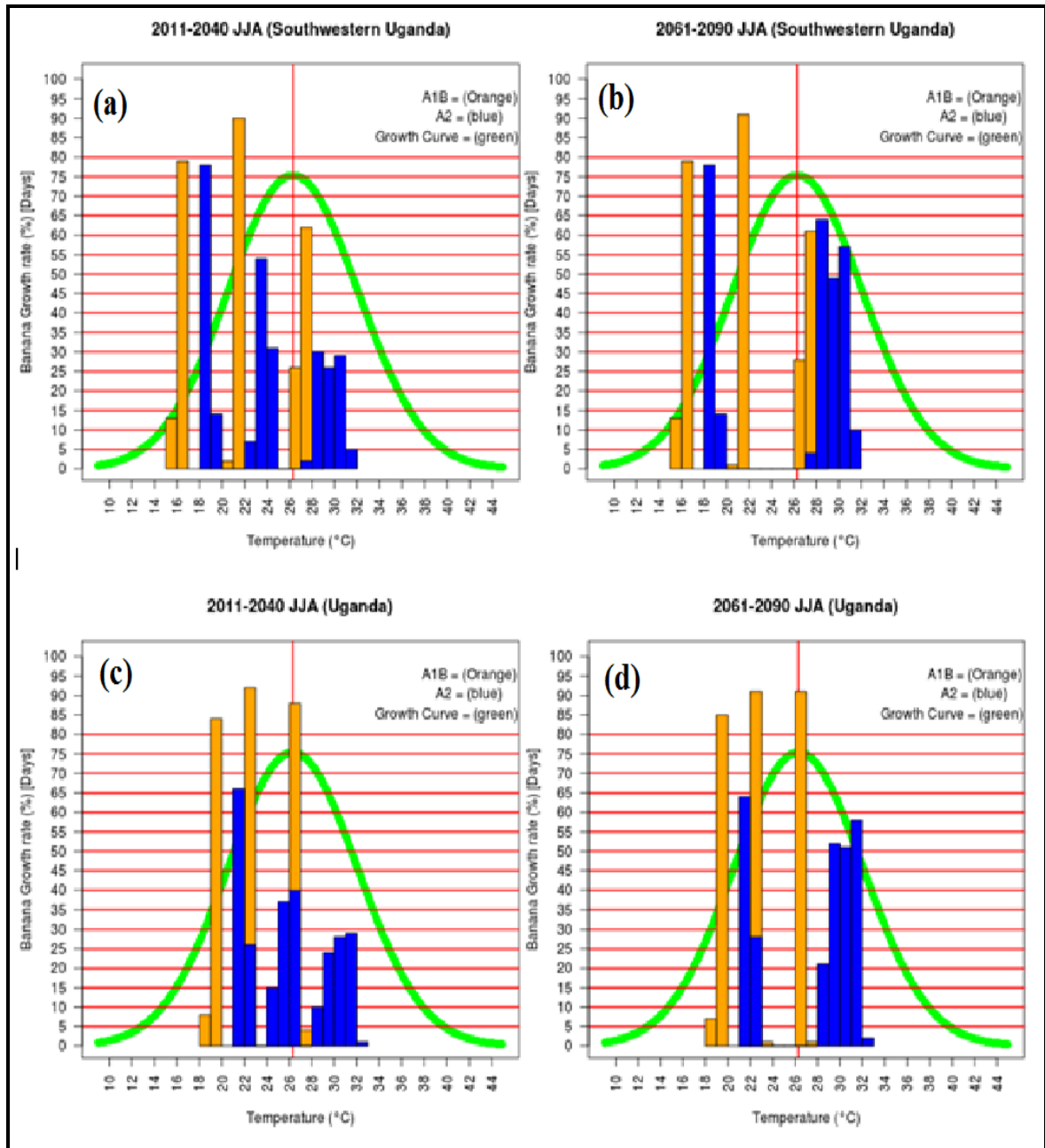


Figure 4.120 (a-d): Projected effects of JJA surface temperature changes on banana growth under A1B & A2 scenarios for southwestern (a-b) and Uganda (c-d) regions. Orange bars indicate frequency of SRES A1B temperature, blue bars indicate frequency of SRES A2 temperature, green curve indicate temperature-banana growth.

The results of this part of the study have for the first time shown that the projected temperature increases under SRES A1B will enhance banana growth from about 45% to over 60% while further increases in projected temperatures are likely to retard banana growth under SRES A2 from 55% to lower than 40% in most areas due to the already warmer temperatures and depressed rainfall projected under the SRES A2 scenario. In conclusion, the results of the study observed that favorable conditions for production of banana over Uganda are expected under SRES A1B scenario due to enhanced rainfall and relatively low temperature while A2 scenario

may have low rainfall and relatively high temperature that will limit production of banana to only isolated areas such as those around Lake Victoria basin by end the century. This part of the study has observed that suitability levels of banana production will significantly reduce in the far future period across all the RCPs scenarios. The effects of future climate change on banana production are, however, region specific and vary across climate scenarios. The results have further observed that;

- (i) The northern part of the country remains unsuitable for banana production under all scenarios.
- (ii) SRES A1B with enhanced rainfall and relatively low temperature increase is likely to favor high future banana production while A2 with decrease in rainfall and high temperature increase will stress banana production over most parts of Uganda.

CHAPTER FIVE

SUMMARY, CONCLUSIONS AND RECOMMENDATIONS

This chapter provides a summary of the study, key results and major conclusions drawn from the results of the study. It also provides some recommendations for applications of the study findings and suggestions for future studies.

5.1 Summary

The main objective of this study was achieved through the determination of linkages between banana productivity and current climate variability; examination of the performance of the PRECIS RCM in simulating observed climate patterns; determining the extent of expected future climate changes under different scenarios over Uganda, and finally the potential effects of future climate change on banana production based on suitability mapping over Uganda.

The study used climate data that consisted of both observed climatological and regional climate model simulated data for rainfall, temperature and soil moisture content for both historical and future periods over Uganda. The historical climate data was obtained from Uganda National Meteorological Authority (UNMA) and IGAD Climate Prediction and Applications Centre (ICPAC). Gridded observations used in the study were obtained from the archives of the UKMO and the ECMWF. The banana data analyzed consisted of historical records of banana production, area of banana harvested and banana yields over Uganda. Both climate and banana yields data were standardized to enable comparisons to be made during the analysis. The study also employed the Standardized Precipitation Index (SPI) based on rainfall anomalies to characterize variations in observed historical rainfall into three categories namely extremely dry, normal and extremely wet events over different locations of Uganda.

The linkages between inter annual climate and banana production changes were determined through empirical approaches. The empirical approaches examined and compared changes in the year to year variability of banana productivity and climate anomalies independently, based on the first, second, third, and fourth moments of the specific time series representing the mean, variance, skewness (extremes distributions), and kurtosis (shape or peakedness). For the first moment, the interannual trends of the individual banana yields and climate series were examined. Parameters examined under the second moment also included patterns of the recurrences of large positive/ negative extremes. Apart from using these empirical methods to compare linkages between interannual changes in climate and banana yields, the FAO Crop

Water Assessment Tool (FAO-CROPWAT) was also used to evaluate the response of banana yields to variations in rainfall and water stress (moisture deficits) under rain-fed conditions.

The second objective determined the performance of regional climate model to identify the best model configuration (or group of regional models) that would provide a more realistic simulation of observed climate patterns over sub regions of Uganda. The study emphasis was on the UKMO PRECIS regional climate model and selected regional climate models from the CORDEX-Africa runs. The focus on UKMO PRECIS RCM was based on the results from some past studies. The third objective used UKMO PRECIS regional climate model to downscale future climate change projections over Uganda based on AR4 SRES scenarios (A1B and A2) and also analyzed AR5 RCPs scenarios (RCP 2.6, RCP 4.5, RCP 6.0 and RCP 8.5) over Uganda. The future climate projections were extended up to 2100. The fourth objective determined the potential effects of projected future climate on banana production in Uganda.

5.2 Conclusions

The first objective sought to establish the linkages between banana productivity and current climate variability over Uganda. Under this objective, the study observed changes in the contribution of the individual rainfall seasons namely DJF, MAM, JJA and OND to the annual total rainfall over the years across a few areas. The contribution of the individual seasons total rainfall for individual year, varied significantly in some years, especially due to extreme rainfall during the (ENSO) and (IOD) years. Trend analysis showed that the observed seasonal rainfall for MAM and OND seasons were decreasing and increasing respectively. Many of these trends were found not to be statistically significant at 95% confidence level.

Further analysis of the second moment (variability) of seasonal rainfall observed that during MAM, significant variability was observed over the Lake Victoria region and eastern parts of Uganda. October-December (OND) season observed the highest variability compared to the other seasons. Results from Standard Precipitation Indices (SPI) analysis of extreme rainfall events observed year to year recurrences of severe droughts in Uganda with the highest number and intensity of drought occurrences were experienced in the period 1982-1990. It can be concluded that that there was a reduction in drought occurrences in the recent years over many parts of Uganda while some years showed recurrence of extremely wet conditions leading to floods. The results from skewness and kurtosis coefficients showed that there were evidences

of changes in the distribution of extreme rainfall events at some locations during the various seasons. These included frequencies and magnitudes of the seasonal floods and droughts.

Both minimum and maximum surface temperatures showed significantly increasing trends during all seasons and at all locations. This has also been observed in many past studies in the region and worldwide as a reflection of global and regional warming trends associated with climate change. Changes were also observed in the patterns of surface temperature skewness and kurtosis coefficients at some locations.

In conclusion, several cases of the moment values for both climate and banana yields were comparable with close patterns in the central and western regions. This indicated that there are observable cumulative effects (linkages) of rainfall and surface temperature variations on banana crop yields. There were also significant banana yields reductions attributable to climate factors across banana growing regions of Uganda. Regions that experience more than three months of rainfall deficits can hardly sustain rain-fed banana production and have banana yield reductions greater than 35% of optimal yield levels for the different regions. In addition, due to non-linearity in the response of banana production to change in climate elements, small changes in climate variables could have stonger effects on banana crop yields and vice-versa.

In the second objective, the performance of the PRECIS RCM in simulating observed climate patterns was determined over Uganda. It may be concluded based on study results that PRECIS RCM has better skill compared with other regional models in the simulating spatial and temporal climate patterns over Uganda, especially during OND season. Key challenges were, however, still evident in the simulations of some of the low and high climate extremes. There were also some significant inter-model variations in the representation of seasonal rainfall patterns, especially the extremes. Doubling the resolution of the RCM does not significantly improve model performance over most parts of Uganda. The high resolution climate information of the regional climate models particularly the PRECIS RCM is highly valuable for national and sub-national climate impacts and vulnerability assessments.

The third objective aimed to establish the extent of expected future climate change over Uganda. From the study results, it may be concluded that future rainfall is likely to exhibit high spatio-temporal variations and changes in future rainfall across locations and under various scenarios over Uganda. The results showed likelihood of decrease in future rainfall in some scenarios and regions on one hand and an increase in surface temperature over most parts of Uganda. On the other hand, there were also cases of increasing rainfall during some seasons at

some locations. Projected surface temperature increases were common with all scenarios with significant variations in the rate of temperature increases across scenarios and sub-regions over Uganda. Under the IPCC AR5 RCP scenarios, the results showed a likelihood of decrease in both total annual rainfall and rainfall of the driest quarter between the periods 2041-2060 and 2061-2080. For the temperatures, the lowest temperatures increases are likely to be associated with RCP 2.6 and RCP 4.5 while high temperatures are expected under RCP 6.0 and RCP 8.5.

With respect to surface soil moisture patterns, the projections have observed a likelihood of high potential of soil moisture stresses under all scenarios over Uganda. These changes in climate conditions would have far reaching implications on banana productivity in different parts of Uganda in future.

Projections based on the bio-climatic variables have also been analysed based on annual mean temperature, mean temperature of coldest quarter, annual mean rainfall, and mean rainfall of driest quarter. The study observed significant changes in the spatial patterns of the bio-climatic variables that would have far reaching implication on the overall growth and production patterns of banana crop in Uganda.

Under this objective, the study determined potential effects of future climate change on banana production over Uganda. It may be concluded based on the results that future climate change will have varying potential effects on banana production that are region specific and vary across climate scenarios. The growth rate of the banana crop is likely to decrease due to increasing temperatures while the areas suitable for banana growth might significantly reduce depending on the levels of future climate change associated with a particular scenario. The northern part of the Country remains unsuitable for banana production under all scenarios. This is partly due to existence of three consecutive months of dry conditions in addition to other non-climatic factors.

Over all, the study concludes that there are observable and projected changes in rainfall and temperature which affect banana yields in addition to other crops. The most important effects are associated with increasing temperature and extreme rainfall events that have become more frequent and severe in some regions of Uganda. Sustainable future banana farming, will therefore require farmers to adapt to climate changes using various adaptation options that may include introduction of new banana varieties that could cope with the current climate variability including extremes and expected future climate changes as well as other emerging challenges.

The next section provides some recommendations to application areas and future studies.

5.3 Recommendations

This study has provided critical findings and knowledge and presented recommendations for various stakeholders. These include National Meteorological and Hydrological Services (NMHS), training institutions, Government of Uganda, researchers, the agricultural sector, banana farmers and other users of climate information.

5.3.1 National Meteorological and Hydrological Services, Training Institutions, and Government of Uganda

The study recommends that National Meteorological Services should develop area-specific climate information from climate observations and high resolution regional climate models. This information will greatly help users from a number of socio-economic sectors assess climate variability and change impacts for their areas and enhance their decision making process for high productivity that will promote national and regional development.

National Meteorological Services and training institutions should offer skills to their staff and students on use and application of regional climate models as tools for providing valuable information to understand climate variability and change patterns for different regions and assessing of climate related impacts.

There is need to build the capacity of the Uganda National Meteorological Authority (UNMA), Climate Change Unit (CCU) and Ministry of Agriculture, Animal, Industry and Fisheries (MAAIF) to improve production, distribution and use of climate information that respond to the needs of decision makers, as well as those of farmers and other stakeholders.

There is need to provide necessary technical and financial support to the Uganda National Meteorological Authority (UNMA) and Climate Change Unit (CCU) for development of the national climate dataset and generation of user relevant products and information to help farmers and other stakeholders cope with climate risks. In addition, there is need to build capacity and promote training of Uganda institutions to develop and routinely use downscaled climate projections for future climate change impacts and vulnerability for various sectors of the economy.

The government needs to develop a platform/mechanism for results (current trends and projections) to be shared at regional, national, district, and local levels. This will promote mainstream of climate change perspective in the programming and planning of agricultural and

natural resource management services. There is therefore a need to improve mechanisms for climate observations and climate change projections archives and sharing in the region. This will improve the performance of socio-economic sectors and go a long way to create avenues for proper planning within the short-term but also the long term.

5.3.2 The Agricultural Sector and Banana Farmers

There is need to mainstream weather and climate information in planning farming activities and also provide feedback to weather and climate information providers to help improve the quality of information provided for early warning in the country.

Farmers need to harvest water during periods of excessive rainfall and use it for irrigation during dry periods for sustainable agricultural yields. They should also undertake effective crop management (mulching, pest control, timely weeding and pruning) to optimize banana productivity amidst climate extremes.

Banana farmers in the high temperature and low rainfall areas of Uganda should devise adaptive/coping agricultural methods and strategies that modulate micro climate and conserve moisture through strategies such as mulching and shade systems from selected trees. Diversification of farming activities such as inter-cropping of coffee in banana plantations has also been found useful to most farmers. Farmers should also do animal rearing which will provide manure to the banana plantation and also enable them to acquire extra income for food and other financial requirements.

There is need to increase implementation of climate change adaptation pilot projects, resilience and capacity building linked to farmers and also addresses gender issues (women and children) for sustainable development of Uganda.

5.3.3 Other Users of Climate Information

The study recommends that other climate users should take advantage of the available current and future climate information generated by this study to assess the impact and vulnerability in their respective socio-economic sectors. These socio-economic sectors include; water resources, health, energy, settlement and transport. This will aid informed decisions to be made and responsible choices and actions be taken to reduce the risks of climate, promote productivity and enhance the socio-economic welfare of various communities and promote overall national and regional growth and development.

5.3.4 Further Research

Research on the different crop water requirements is necessary to provide baseline information in assessing the vulnerability of different crops to climate impacts under specific environments. Experimental studies on the sensitivity of crop growth and yields to variations in rainfall on intra-seasonal time scales are still necessary to understand the impacts of current climate variability on yields. This would inform appropriate technologies and coping mechanisms for climate risks in the agriculture sector.

Regional climate modelling over most regions in Africa including GHA region is still at its infancy. Further research is needed to increase understanding of regional climate model strength and weaknesses, and reduce uncertainty in model simulations and future climate projections over a region of high physiographic complexity of Eastern Africa.

More research is still required on the physical formulation and parameterization schemes used in the current regional climate models and customization of regional climate models to reproduce more realistic climate simulations and minimize the errors inherent in climate outputs from such models in many regions of Eastern Africa.

Attribution of climate variability and change at any location is still one of the major challenges in all climate change studies. Investigating attribution factors to regional and local climate variability and change is one of the key issues that should be addressed by future research to help demystify some of the observed and projected complex patterns in this study. In addition, there is need to generate farm level resolution climate information of future climate to assess impacts of climate extremes on Agriculture.

New training approaches, for-example; interdisciplinary approaches for Disaster Risk Management (DRM) to support new, used and improvement of technology, crop varieties for the changing local environment due to increased climate variability and change patterns in the current period and near future.

References

- Abera, A. M., Gold, C. S., Kyamanywa, S., and Karamura, E. B. (2000). Banana weevil, *Cosmopolites sordidus* (Germar), ovipositional preferences, timing of attack and larval survivorship in a mixed cultivar trial in Uganda. In: Craenen, K., Ortiz, R., Karamura, E.B., & Vuylsteke (Eds.) Proceedings of the International Conference on Banana and Plantain for Africa. *ActaHorticulturae* **540**, 487-495, International Society for Horticultural Science (ISHS), Leuven, Belgium.
- Aguilar, E., Auer, I., Brunet, M., Peterson, T. C. and Wieringa, J. (2003). Guidelines on Climate Meta data and Homogenization. WCDMP-No. 53, WMO-TD No. 1186. World Meteorological Organisation, Geneva.
- Ampaire, E. L., Happy, P., Van Asten, P. and Radeny, M. (2015). The role of policy in facilitating adoption of climate-smart agriculture in Uganda. CGIAR Research Program on Climate Change, Agriculture and Food Security (CCAFS). Copenhagen, Denmark. Available online at: www.ccafs.cgiar.org
- Antle, J. (2010). Adaptation of Agriculture and the Food System to Climate Change: Policy Issues, Issue Brief 10-03. Washington, DC: Resources for the Future.
- Anyah, R. O., Semazzi, F. H. M. and Xie, L. (2006). Simulated physical mechanisms associated with multi-scale climate variability over Lake Victoria Basin in East Africa. *Mon. Wea. Rev.*, **134**, 3588-3609.
- Anyah, R. O., and Semazzi, F. H. M. (2007). Variability of East African rainfall based on multiyear RegCM3 simulations. *Int. J. Climatol.*, **27**, 357-371.
- Anyah, R. O., and Qiu, W. (2012). Characteristic 20th and 21st century rainfall and temperature patterns and changes over the Greater Horn of Africa. *Int. J. Climatol.*, **32**, 347-363.
- Anyah, R. O. (2005). Modeling the variability of the climate system over Lake Victoria Basin. Ph.D. dissertation, North Carolina State University, 287 pp.
- Arnell, N., Warren R., Nicholls R., Levy P., and Price, J. (2002). Understanding the regional impacts of climate change; Research report prepared for the Stern Review, Tyndall Centre Working Paper 90, Norwich: Tyndall Centre
- Asnani, G. C. (1993). *Tropical Meteorology*, Published by Pashan, Pune: Indian Institute of Tropical Meteorology, 1993.
- Bagamba, F. (2007). Market access and agricultural production: the case of banana production in Uganda. *Ph.D. Thesis. Wageningen University, The Netherlands.*

- Baijukya, F. P., and Piters, B. S. (1998). Nutrient balances and their consequences in the banana-based land use systems of Bukoba district, northwest Tanzania. *Agric Ecosyst Environ*, **71**, 147-158.
- Barasa, B., Kakembo, V., Mugagga, F., and Egeru, A. (2013). Comparison of extreme weather events and streamflow from drought indices and a hydrological model in River Malaba, Eastern Uganda. *Int. J. of Environmental Studies*, **70(6)**, 940-951.
- Barekye, A. (2009). Breeding investigations for black Sigatoka resistance and associated traits in diploids, tetraploids and the triploid progenies of bananas in Uganda. *PhD Thesis, Faculty of Science and Agriculture, University of KwaZulu-Natal, Republic of South Africa*.
- Barekye, A., Tongoona, P., Derera, J., Laing, M. D. and Tushemereirwe, W. K. (2013). Analysis of Farmer-preferred Traits as Improvement of East African Highland Bananas in Uganda. *Banana Systems in the Humid Highlands of Sub-Saharan Africa: enhancing resilience and productivity*, 30-36.
- Basalirwa, C. (1991). Rain gauge network designs for Uganda. *PhD. Thesis, Department of Meteorology, University of Nairobi, Kenya*.
- Basalirwa, C. (1995). Delineation of Uganda into climatological rainfall zones using the method of principal component analysis. *Int. J. Climatol.***15**: 1161-1177.
- Bashaasha, B., Thomas, T. S., Waithaka, M. and Kyotalimye, M. (2013). East African agriculture and climate change. (Chapter 12). doi:<http://dx.doi.org/10.2499/9780896292055>.
- Behera, S. K., Luo, J. J., Masson, S., Delecluse, P., Gualdi, S., Navarra, A., and Yamagata, T. (2005). Paramount impact of the Indian Ocean dipole on the East African short rains: A CGCM study. *J. Climate*, **18(21)**, 4514-4530.
- Bekunda, M., and Woome, P. L. (1996). Organic resource management in banana based cropping systems of the Lake Victoria basin, Uganda. *Agric. Ecosyst. Environ*, **59**, 171-180.
- Bekunda, M. A., Nkonya, E., Mugendi, D., and Msaky, J. J. (2002). Soil fertility Status, Management, and research in East Africa. *IFPRI Uganda research paper*, 1-8.
- Benin, S., Thurlow, J., Diao, X., Kebba, A., and Ofwono, N. (2007). Agricultural Growth and Investment Options for Poverty Reduction in Uganda. IFPRI Discussion Paper no. 790. Washington, DC: International Food Policy Research Institute.

- Berrisford, P., Dee, D. P., Fielding, K., Fuentes, M., Kallberg, P., Kobayashi, S., and Uppala, S. M. (2009). 'The ERA-Interim Archive'. ERA Report Series, No.1. ECMWF: Reading, UK.
- Best, M. J. (2005). Representing urban areas within operational numerical weather prediction models, *Boundary Layer Meteorol.*, **114**, 91-109.
- Black, E., Slingo, J., and Sperber, K. R. (2003). An observational study of the relationship between excessively strong short rains in the coastal East Africa and Indian Ocean SST. *Mon. Wea. Rev.*, **131**, 74-94.
- Boko, M., Niang, I., Vogel, C., Githeko, A., Medany, M., Osman-Elasha, B., Tabo, R., and Yanda, P. (2007). Africa, in: Parry, M.L., Canziani, O.F., Palutikof, J., Linden, P.J., Hanson, C.E. (eds.). *Climate Change 2007: Impacts, Adaptation and Vulnerability. Contribution of Working Group II to the Fourth Assessment Report of the Intergovernmental Panel on Climate Change*, Cambridge (UK), 433-467.
- Bouwmeester, H., Van Asten, P., and Ouma, E. (2009). Mapping Key Variables of Banana Based Cropping Systems in the Great Lakes Region, Partial Outcomes of the Baseline and Diagnostic Surveys. CIALCA Technical Report 11. <http://www.cialca.org/IITA>, Ibadan www.cialca.org.
- Bowden, J. H. and Semazzi, F. H. M. (2007). Empirical Analysis of Intra-seasonal Climate Variability over the Greater Horn of Africa. *J. Climate*, **20**, 5715-5731.
- Bowden, J. H., Semazzi, F. H. M., Anyah, R. O., and Schreck, C. (2005). Decadal temperature, rainfall and hydrological trends over the Greater Horn of Africa. 85th AMS Annual Meeting, San-Diego, California, 9-13 Jan 2005.
- Box, G. E. P., Jenkins, G. M., and Reinsel, G. C. (1994). *Time Series Analysis: Forecasting and Control*. Third Edition. Prentice Hall.
- Bridge, J. (1988). Plant parasitic nematode pests of banana in East Africa with particular reference to Tanzania. 35-39 in *Nematodes and Borer Weevil in Bananas: Present Status of Research and Outlook*, Proceedings of a Workshop. Bujumbura, Burundi 7-11 December, 1987. INIBAP, Montpellier, France.
- Camberlin, P. and Philippon, N. (2002). The East African March-May rainy season: Associated atmospheric dynamics and predictability over the 1968-97 period. *J. Climate*, **9**, 1002-1019.
- Caminade C. and Terray, L. (2006). Influence of increased greenhouse gases and sulphate aerosols concentration upon diurnal temperature range over Africa at the end of the 20 century. *Geophysical Research Letters*, **33** (15): L15703.

- Christy, J. R., Norris, W. B., and McNider, R. T. (2009). Surface temperature variations in East Africa and possible causes. *J. Climate*, **22**(12), 3342-3356.
- Claessens, L., Antle, J. M., Stoorvogel, J. J., Valdivia, R. O., and Herrero, M. (2012). A method for evaluating climate change adaptation strategies for small-scale farmers using survey, experimental and modelled data. *Agricultural Systems*, **111**, 85-95.
- Clarke, T. (2003). Banana lab opens in Uganda: Genetic modification of clonal crop could soon follow. Nature News, August 22. (Accessed 12.9.2010).
- Clark, C. O., Webster, P. J., and Cole, J. E. (2003). Inter decadal variability of the relationship between the Indian Ocean zonal mode and East African coastal rainfall anomalies. *J. Climate*, **16**, 548-554.
- Clarke, D., Smith, M., and El-Askari, K. (2001). CropWAT for Windows: user guide. IHE.
- Conrad, V., and Pollak, L. W. (1950). *Methods in Climatology*. Harvard University Press, Cambridge.
- Conway, D. (2005). From headwater tributaries to international river: Observing and adapting to climate variability and change in the Nile Basin, *Global Environmental Change*, **15**, 99-114.
- Cook, K. H., and Vizy, E. K. (2013). Projected changes in East African rainy seasons. *J. Climate*, **26**(16), 5931-5948.
- Cooper, P. J. M., Coe, R., and Stern, R. D. (2011). Assessing and addressing climate-induced risk in Sub-Saharan rain-fed Agriculture: foreword to a special issue of *Experimental Agriculture*. *Experimental Agriculture*, **47** (2), 179-184
- Cox, P. M., Betts, R. A., Bunton, C. B., Essery, R. L. H., Rowntree, P. R., and Smith, J. (1999). The impact of new land surface physics on the GCM simulation of climate and climate sensitivity. *J. Clim Dyn*, **15**(3), 183-203.
- Davidson, O., Halsnaes, K., Huq, S., Kok, M., Metz, B., Sokona, Y., and Verhagen, J. (2003). The development and climate nexus: the case of sub-Saharan Africa. *Climate Policy*, **3**, 97-113.
- Davies, T. (2013). Lateral boundary conditions for limited area models. *Q. J. R. Meteorol Soc*, doi:10.1002/qj.2127.
- Davis, N., Bowden, J., Semazzi, F. H. M., Xie, L., and Onol, B. (2009). Customization of RegCM3 Regional Climate Model for Eastern Africa and a Tropical Indian Ocean Domain. *J. Climate*, **22**, 3595-3616.
- Dee, D. P., Uppala, S. M., Simmons, A. J., Berrisford, P., Poli, P., Andrae, U., Balmaseda, M.A., Balsamo, G., Bauer, P., Bechtold, P., Kobayashi, S., Beljaars A.C.M., van de

- Berg, L., Bidlot, J., Bormann, N., Delsol, C., Dragani, R., Fuentes, M., Haimberger, L., Healy, S.B., Hersbach, H., Holm, E.V.H., Isaksen, L., Kohler, M.K., Matricardi, M., McNally, A.P., Monge-Sanz, B.M., Geer, A.J., Kallberg, P.K., Morcrette, J.-J., Peubey, C., deRosnay, P., Tavolato, C., Thepaut, J.-N., and Vitart, F., and Park, B. K. (2011). The ERA-Interim reanalysis: configuration and performance of the data assimilation system. *Q. J. R. Meteorol Soc*, **137**, 553-597.
- Denis, B., Laprise, R., and Cote, J. (2002). Downscaling ability of one-way nested regional climate models: The big-brother experiment. *Mon Wea Rev*, **128**, 71-94.
- Desanker, P. V. (2002). Impacts of Climate Change on Life in Africa, WWF Climate Change Brief, Washington D.C., USA.
- Desanker, P. V., Justice, C. O., Masamvu, K., and Munthali, G. (2001). Requirements for integrated assessment modelling at the sub regional and national levels in Africa to address climate change. In: Lo PS (ed) Climate change for Africa: science, technology, policy and capacity building. Kluwer Academic Publishers, Dordrecht.
- Department for International Development, DfID (2004). Key sheet 7 Adaptation to climate change: The right information can help the poor to cope; Global and Local Environment Team, Policy Division.
- Diallo, I., Bain, C. L., Gaye, A. T., Moufouma-Okia, W., Niang, C., Dieng, M. D. B., and Graham, R. J. (2014). Simulation of the West African monsoon onset using the HadGEM3-RA regional climate model. *J. Clim Dyn*, **43(3)**, 575-594.
- Dickinson, R. E., Ericco, R. M., Giorgi, F., and Bates, G. T. (1989). A regional climate model for the Western United States. *Climatic Change*, **15**, 383-422.
- Diro, G. T., Grimes, D., and Black, E. (2011). Teleconnections between Ethiopian summer rainfall and sea surface temperature: Part I-Observation and modelling. *J. Clim. Dyn.*, **37**, 103-119.
- Diro, G. T., Tompkins, A. M. and Bi, X. (2012). Dynamical downscaling of ECMWF ensemble seasonal forecasts over East Africa with RegCM3. *J. Geophys. Res.*, **117**, 103.
- Easterling, D. R. and Peterson, T. C. (1992). Techniques for detecting and adjusting for artificial discontinuities in climatological time series: a review. *5th International Meeting on Stat. Climatology*, June 22-26, 1992, Toronto.
- Easterling, D. R., and Peterson, T. C. (1995). A new method for detecting undocumented discontinuities in climatological time series. *Int. J. Climatol.*, **15**, 369-377.

- Easterling, D. R., Meehl, G. A., Parmesan, C., Changnon, S. A., Karl, T. R., and Mearns, L. O. (2000). Climate extremes: Observations, modeling, and impacts. *Science* **289** (5487), 2068-2074.
- Egeru, A. (2012). Water Productivity in Agriculture: Challenges and Opportunities for Smallholder Farmers in the Drylands of Eastern and Southern Africa, University of Nairobi.
- Egeru, A., Osaliya, R., MacOpiyo, L., Mburu, J., Wasonga, O., Barasa, B., Said, M., Aleper, D., and Majaliwa, G. J. M. (2014). Assessing the spatio-temporal climate variability in semi-arid Karamoja sub-region in north-eastern Uganda. *International Journal of Environmental Studies*.
- Elsen, A., Speijer, P. R., Swennen, R., and Waele, D. D. E. (1998). Effect of cultivar and altitude on nematode densities and species composition, root damage and yield of *Musa* in Uganda. *Nematologica*, **44**, 490-491.
- External Monitoring Unit, EMU (2007). External Monitoring Unit of the Agricultural Sector Programme Support Reports on the Agricultural Modules. Kampala: Danida.
- Endris, H. S., Omondi, P., Jain, S., Lennard, C., Hewitson, B., Chang'a, L., Awange, J. L., and Tazalika, L. (2013). Assessment of the performance of CORDEX regional climate models in simulating East African rainfall. *J. Clim*, **26**(21), 8453-8475
- Endris, H. S., Lennard, C., Hewitson, B., Dosio, A., Nikulin, G., and Panitz, H. J. (2015). Teleconnection responses in multi-GCM driven CORDEX RCMs over Eastern Africa. *J. Clim Dyn*. Online publication date: 8-Jul-2015.
- Engelbrecht, C. J., Engelbrecht, F. A., and Dyson, L. L. (2011a). High-resolution model-projected changes in mid-tropospheric closed-lows and extreme rainfall events over southern Africa. *Int. J. Climatol*. doi: 10/1002/joc.3420.
- Engelbrecht, F. A. (2000). Nested climate modeling over southern Africa with a semi-Lagrangian limited area model, *MSc. Dissertation, University of Pretoria, Pretoria*.
- Engelbrecht, F. A., Landman, W. A., Engelbrecht, C. J., Landman, S., Roux, B., Bopape, M.M., McGregor, J. L., and Thatcher, M. (2011b). Multi-scale climate modelling over southern Africa using a variable-resolution global model. *Water SA*, **37**, 647-658.
- Eriksen, S., O'Brien, K., and Losentrater, L. (2008). 'Climate Change in Eastern and Southern Africa: Impacts, Vulnerability and Adaptation' in *Global Environmental Change and Human Security*, Report 2008.
- Essery, R. L. H., Best, M. J., Betts, R. A. and Cox, P. M. (2003). Explicit representation of subgrid heterogeneity in a GCM land surface scheme. *J. Hydrometeor.*, **4**, 530-543.

- Food and Agriculture Organization, FAO (2003a). World Agriculture towards 2015/2030: An FAO Perspective. Rome: Food and Agriculture Organisation of the United Nations.
- Food and Agriculture Organization, FAO (2003b). Water Resources, Development and Management Service. CLIMWAT: A climatic database for CROPWAT. (Food and Agriculture Organisation), FAO Land and Water Development Division. <http://www.fao.org/ag/AGL/AGLW/climwat.stm>. Accessed 27 August 2012.
- Food and Agriculture Organization, FAO (2004). The state of food security in the world. FAO Perspective'. Rome: Food and Agriculture Organisation of the United Nations. Accessed 14 July 2013.
- Food and Agriculture Organization, FAO (2008). Soaring food prices: Facts, perspectives, impacts and action required. HLC/08/INF/1. High Level Conference on World Food Security: The Challenges of Climate Change and Bioenergy, Rome, 3-5 June 2008.
- Famine Early Warning System Network, FEWS NET (2011). Past year one of the driest on record in the eastern Horn. Famine Early Warning System Network Report, 14 June 2011, U.S. Agency for International Development. Accessed on 21st July 2012 from: <http://reliefweb.int/report/ethiopia/east-africa-past-year-one-driest-record-eastern-horn>.
- Fischer, G, Mahendra, S., and Velthuizen, H. V. (2002). 'Climate Change and Agricultural Vulnerability. A special report prepared by the International Institute for Applied Systems Analysis as a contribution to the World Summit on Sustainable Development, Johannesburg 2002.
- Fischer, G., Shah, M., Tubiello, F. N., and Velhuizen, H. (2005). 'Socio-economic and climate change impacts on agriculture', *Philosophical Transactions of the Royal Society B* 360: 2067-2083.
- Foster, H. L. (1981). The basic factors which determine inherent soil fertility in Uganda. *J. Soil Sci.* **32**, 149–160.
- Frison, E. A., and Sharrock, S. L. (1998). Banana streak virus: a unique virus-*Musa* interaction? Proceedings of a workshop of the PROMUSA Virology working group held in Montpellier, France, January 19-21, 1998. International Plant Genetic Resources Institute, Rome, Italy; International Network for the Improvement of Banana and Plantain, Montpellier, France.
- Fujino, J., Nair, R., Kainuma, M., Masui, T., and Matsuoka, Y. (2006). Multi-gas mitigation analysis on stabilization scenarios using aim global model. *Energy Journal*, **0**, 343-353.
- Funk, C., Dettinger, M. D., Michaelsen, J. C., Verdin, J. P., Brown, M. E., Barlow, M., and Hoell, A. (2008). Warming of the Indian Ocean threatens eastern and southern African

- food security but could be mitigated by agricultural development. *Proceedings of the National Academy of Sciences of the United States of America*, **105(32)**, 11081-11086.
- German, C. G., Staver, C., and Siles, P. (2015). An assessment of global banana production and suitability under climate change scenarios, In: *Climate change and food systems: global assessments and implications for food security and trade*, Aziz Elbehri (editor). Food Agriculture Organization of the United Nations (FAO), Rome, 2015.
- Giorgi, F., and Bates, T. (1989). The climatological skill of a regional climate model over complex terrain. *Mon. Wea. Rev.*, **117**, 2325-2347.
- Giorgi, F., and Marinucci, M. R. (1996). An investigation of the sensitivity of simulated precipitation to model resolution and its implications of climate studies, *Mon. Weather Rev.*, **124**, 148-166.
- Giorgi, F., Jones, C., and Asrar, G. R. (2009). Addressing climate information needs at the regional level: the CORDEX framework. *WMO Bulletin*, **58(3)**, 175-183.
- Gitau, W. (2005). Characteristics of the wet and dry spells during the wet seasons over Kenya: *MSc. Thesis, Department of Meteorology, University of Nairobi, Kenya.*
- Gitau, W. (2011). Diagnosis and Predictability of Intra-seasonal characteristics of wet and dry spells over Equatorial East Africa. *PhD. Thesis, Department of Meteorology, University of Nairobi, Kenya.*
- Gold, C.S., Karamura, E. B., Kiggundu, A., Bagamba, F., and Abera, A. M. K. (1999a). Monograph on geographic shifts in highland cooking banana (*Musa*, group AAA-EA) production in Uganda. *J. Africa Crop Science*. **7**, 223-298.
- Gold, C. S., Karamura, E. B., Kiggundu, A., Bagamba, F., and Abera, A. M. K. (1999b). Geographic shifts in highland cooking banana (*Musa* spp., group AAA-EA) production in Uganda. *International Journal of Sustainable Agriculture and World Ecology* 6:45-59. National Council for Science and Technology (UNCST) in Collaboration with Program for Biosafety Systems (PBS), July 2007.
- Gold, C. S., Rukazambuga, N. D. T. M., Karamura, E. B., Nemeye, P., and Night, G. (1999). Recent advances in banana weevil biology, population dynamics and pest status with emphasis on East Africa. Proceedings of a workshop on banana IPM held in Nelspruit, South Africa, 23-28 November 1998. In: E. A. Frison, C.S. Gold, E. B Karamura and R. A. Sikora (eds.) 35-50. **59**, 171-180.
- Gowen, S. and Queneherve, P. (1990). Nematode parasites of bananas, plantains and abaca. 431-460 in M. Luc, R. A. Sikora, and J. Bridge eds. *Plant Parasitic Nematodes in Subtropical and Tropical Agriculture*, C.A.B. International, UK.

- Gregory, P. J., and Ingram, J. S. I. (2000). Global change and food and forest production: future scientific challenges. *Agriculture Ecosystems and Environment*, **82**, 3-14.
- Hansen, J. W., Mason, S., Sun, L., and Tall, A. (2011). Review of seasonal climate forecasting for agriculture in sub-Saharan Africa. *Experimental Agriculture*, **47**, 205-240.
- Harper, G., Hart, D., Moulton, S., and Hull, R. (2004). Banana streak virus is very diverse in Uganda. *Virus Research*, **100**, 51-56
- Hastenrath, S. and Polzin, D. (2004). Dynamics of the surface wind field over the equatorial Indian Ocean, *Q. J. R. Meteor. Soc.*, **130**, 503-517.
- Hedge, D. M., and Srinivas, K. (1989). Effect of soil matric potential and nitrogen on growth, yield, nutrient uptake and water use of banana. *Agric. Water Manage.* **16**, 109-117.
- Hein, D. (2008). The representation of Extreme Precipitation in HadRM3P Regional Climate Model. *MSc. Dissertation, University of Reading, UK.*
- Henderson-Sellers, A., and McGuffie, K. (1987). *A Climate Modelling Primer*. Wiley, Chichester.
- Henderson-Sellers, A., and Robinson, P. J. (1986). *Contemporary Climatology*. Longman Group UK Ltd., Harlow, England. 439.
- Hewitson, B., Lennard, C., Nikulin, G., and Jones, C. (2012). CORDEX-Africa: a unique opportunity for science and capacity building. *CLIVAR Exchanges*, **17(3)**, 6-7.
- Hijmans, R.J., Guarino, L., Cruz, M., and Rojas, E. (2001). Computer tools for spatial analysis of plant genetic resources data. 1. DIVA-GIS. *Plant Genetic Resources Newsletter*, **127**, 15-19.
- Hijmans, R. J., Cameron, S. E., Parra, J. L., Jones, P. G., and Jarvis, A. (2005). Very high resolution interpolated climate surfaces for global land areas. *Int. J. Climatol.*, **25**, 1965-1978.
- Holton, J. R. (2004). *An introduction to dynamic meteorology*. Elsevier Academic Press. **4**, 535.
- Hudson, D., Wilson, S. S., Jenkins, G. J., and Mitchell, J. F. B. (2004). *Generating high resolution climate change scenarios using PRECIS*, Met Office Hadley Centre, Exeter, UK.
- Hulme, M., Doherty, R., Ngara, T., and New, M. (2005). Global warming and African climate change. In: Low PS, ed. *Climate Change and Africa*. Cambridge: Cambridge University Press; pp 29-40.
- Hulme, M., Doherty, R., Ngara, T., New, M., and Lister, D. (2001). African climate change: 1900-2100. *Climate Research*, **17**, 145-168.

- ICRA (Integrated Climate Risk Assessment) (2009). Workshop manual on integrated climate risk assessment. Nairobi, Kenya.
- Indeje, M., Semazzi, F. H. M., and Ogallo L. J. (2000). ENSO signals in East African rainfall seasons. *Int. J. Climatol.*, **20**, 19-46.
- Ingram, J. C., and Dawson, T. P. (2005). Climate change impacts and vegetation response on the island of Madagascar. *Philosophical Transactions of the Royal Society of London, Series A, Mathematical Physical and Engineering Sciences*, **363(1862)**, 55-59.
- Ininda, J. M. (1994). Numerical Simulation of the Influence of SST anomalies on the East Africa Seasonal Rainfall. *PhD. Thesis, Department of Meteorology, University of Nairobi, Kenya*.
- Ininda, J. M. (1995). Simulation of the impact of sea surface temperature anomalies on the short rains over East Africa. *J. African Meteor. Soc.*, **3(1)**, 127-140.
- IPCC TAR (2001). Climate Change (2001). The Scientific Basis. IPCC. IPCC Third Assessment Report, Cambridge University Press, UK.
- IPCC (2007). Climate Change (2007). Impacts, Adaptation and Vulnerability: Contribution of Working Group II to the Fourth Assessment Report of the Intergovernmental Panel on Climate Change, M.L. Parry, O.F. Canziani, J.P. Palutikof, P.J. van der Linden and C.E. Hanson, Eds., Cambridge University Press, Cambridge UK, 433-467.
- IPCC (2012). Managing the Risks of Extreme Events and Disasters to Advance Climate Change Adaptation. A Special Report of Working Groups I and II of the Intergovernmental Panel on Climate Change [Field, C.B., V. Barros, T.F. Stocker, D. Qin, D.J. Dokken, K.L. Ebi, M.D. Mastrandrea, K.J. Mach, G.-K. Plattner, S.K. Allen, M. Tignor, and P.M. Midgley (eds.)]. Cambridge University Press, Cambridge, UK, and New York, NY, USA, 582.
- IPCC (2014). Climate Change (2014). The Physical Science Basis. Contribution of Working Group I to the Fifth Assessment Report of the Intergovernmental Panel on Climate Change [Stocker, T.F., D. Qin, G-K. Plattner, M. Tignor, S.K. Allen, J. Boschung, A. Nauels, Y. Xia, V. Bex and P.M. Midgley (eds.)]. Cambridge University Press, Cambridge, United Kingdom and New York, NY, USA, 1535
- James, R., Washington, R., and Rowell, D. P. (2014). African Climate Change uncertainty in Perturbed Physics Ensembles: implications of warming to 4°C and beyond. *J. Climate*, **27**, 4677-4692.
- Jassogne, L., Nibasumba, A., Wairegi, L., Baret, P. V., Deraeck, J., Mukasa, D., Wanyama, I., Bongers, G., and Van Asten, P. J. A. (2013). Coffee/Banana Intercropping as an

- Opportunity for Smallholder Coffee Farmers in Uganda, Rwanda and Burundi. *Banana Systems in the Humid Highlands of Sub-Saharan Africa: enhancing resilience and productivity*, 144-149.
- Jassogne, L., Van Asten, P., Wanyama, I., and Baret, P. V. (2012). Perceptions and outlook on intercropping coffee with banana as an opportunity for smallholder coffee farmers in Uganda, *Int. J. of Agric, Sustainability*, doi: 10.1080/ 14735903 .2012.714576.
- Jones, C., Giorgi, F., and Asrar, G. (2011). The Coordinated Regional Downscaling Experiment: CORDEX-An international downscaling link to CMIP5. *CLIVAR Exchanges*, **16(2)**, 34-40.
- Kabanda, T. A., and Jury, M. R (1999). Inter-annual variability of short rains over northern Tanzania. *Climate Research*, **13**, 231-241.
- Kabubo, M. J., and Karanja, F. (2006). The economic impact of climate change on Kenyan crop agriculture: a Ricardian approach. CEEPA Discussion Paper No. 12, Centre for Environmental Economics and Policy in Africa, University of Pretoria.
- Kaiser, H. F. (1960). The application of electronic computers to factor analysis. *Educational and Psychological Measurement*, **20**, 141-151.
- Kampata, J. M., Parida, B.P., and Moalafhi, D. B (2008). Trend analysis of rainfall in the headstreams of the Zambezi River Basin in Zambia. *Physics and Chemistry of the Earth*. **33**: 621-625.
- Karanja, F. K. K. (2006). CROPWAT model analysis of crop water use in six districts in Kenya, *CEEPA Discussion Paper No. 35, CEEPA, University of Pretoria*.
- Kashaija, I. N., McIntyre, B. D., Ssali, H., and Kizito, F. (2004). Spatial distribution of roots, nematode populations and root necrosis in highland banana in Uganda. *Nem.* **6**: 7–12
- Robinson, J.C., 1996. Bananas and Plantains. CAB International, UK.
- Kaspar, F. and Cubasch, U. (2008). Simulation of East African precipitation patterns with the regional climate model CLM. *Meteorologische Zeitschrift*, **17(4)**, 511-517.
- Kizza, M., Rodhe, A., Xu, C. Y., Ntale, H. K., and Halldin, S. (2009). Temporal rainfall variability in the Lake Victoria Basin in East Africa during the twentieth century. *J. Theoretical and Applied Climatology*, **98(1-2)**, 119-135.
- King'uyu, S. M, Ogallo, L. A., and Anyamba, E. K. (2000). Recent Trends of Minimum and Maximum surface temperature over Eastern Africa, *Journal of climate* **13**: 2876-2886.
- Komutunga, T. E. (2006). Optimum cropping calendars derived for rain-fed agriculture of Uganda from rainfall data. *PhD Thesis, Department of Meteorology, University of Nairobi, Kenya*.

- Kumar, K. and Parikh, J. (1998). Climate change impacts on Indian agriculture: The Ricardian approach. In Dinar *et al.* (eds), 1998. Measuring the Impact of Climate Change on Indian Agriculture. World Bank Technical paper 402. Washington, DC.
- Kumar, M. N., Murthy, C. S., Sessa-Sai, M. V. R. and Roy P. S. (2009). On the use of Standardized Precipitation Index (SPI) for drought intensity assessment, *J. Appl. Meteorol.* **16**: 381-389.
- Kumar, N. S., Aggarwal, P. K., Swaroopa, R. J. S., Saxena, R., and Chauhan, N. (2011). Impact of climate change on crop productivity in Western Ghats, coastal and northeastern regions of India. *Current Science.* **101 (3)**, 332-341.
- Kurukulasuriya, P., and Rosenthal, S. (2003). Climate change and agriculture: A review of impacts and adaptations. Paper No. 91 in Climate Change Series, Agriculture and Rural Development Department and Environment Department, World Bank, Washington, DC.
- Kurukulasuriya, P., Mendelsohn, R., Hassan, R., Benhin, J., Diop, M., Eid, H. M., Fosu, K. Y., Gbetibouo, G., Jain, S., Mahamadou, A., El-Marsafawy, S., Ouda, S., Ouedraogo, M., Sène, I., Maddison, D., Seo, N., and Dinar, A. (2006). Will African agriculture survive climate change? *World Bank Economic Review* **20 (3)**, 367-388.
- Kruger, A. C., and Shongwe, S. (2004). Temperature trends in South Africa: 1960- 2003. *Int. J. Climatol.* **24**: 1929-1945.
- Laderach, P., and Van Asten, P. (2012). Coffee and climate change, coffee suitability in East Africa. 9th African Fine Coffee Conference and Exhibition, Addis Ababa, Ethiopia.
- Laderach, P., Lundy, M. A., Jarvis, A., Ramirez, J., Prez-Portilla, E., Schepp, K., and Eitzinger, A. (2011). Predicted impact of climate change on coffee supply chains. The economic, social and political elements of climate change. Part 4, 703-723.
- Lockhart, B. E. L., and Olszewski, N. E. (1993). Serological and genomic heterogeneity of banana streak virus: implications for virus detection in *Musa* germ plasm. 105-114 in *Breeding Bananas and Plantain for Resistance to Diseases and Pests* (J. Ganry, ed.). CIRAD/INIBAP, Montpellier, France.
- Longobardi, A., and Villani, P. (2010). Trend analysis of annual and seasonal rainfall time series in the Mediterranean area. *Int. J. Climatol.* **30**: 1538-1546.
- Lucinda, M. (2008). Impact of climate change on the terrestrial hydrology of a humid equatorial catchment in Uganda: *PhD. Thesis, Department of Geography, University College London, UK.*

- Lynch, S. D., and Schulze, R. E. (1995). Techniques for estimating areal daily rainfall. ESRI User conference proceedings, California, USA.
- Lyon, B., and DeWitt, D. G. (2012). A recent and abrupt decline in the East African long rains. *Geophysical Research Letters*, **39** (2), 401-435.
- Lyon, B., Barnston, A. G., and DeWitt, D. G. (2014). Tropical pacific forcing of a 1998-1999 climate shift: observational analysis and climate model results for the boreal spring season. *J. Climate Dyn*, **43**, 893-909.
- MAAIF (Ministry of Agriculture Animal Industry and Fisheries) (2008). MAAIF Development Strategy and Investment Plan, Uganda (2004/05-2006/07).
- Mahe, G., L'hote, Y., Olivry, J. C., and Wotling, G. (2001). Trends and discontinuities in regional rainfall of West and Central Africa: 1951-1989. *Hydrological Sciences Journal*, **46**(2), 211-226.
- Masefield, G. B. (1949). *The Uganda Farmer*. Longman, London.
- Masui, T., Matsumoto, K., Hijioka, Y., Kinoshita, T., Nozawa, T., Ishiwatari, S., Kato, E., Shukla, P.R., Yamagata, Y., and Kainuma, M. (2011). An emission pathway for stabilization at 6 Wm^{-2} radiative forcing. *Climatic Change*, **109**, 59-76.
- Matsuura, K., and Willmott, C. J. (2009). Terrestrial Temperature and Precipitation: 1900-2008 Gridded Monthly Time series, version 2.1. University of Delaware.
- McGregor, J. L. (1993). Economic determination of departure points for semi-Lagrangian models, *Mon Wea Rev.* **119**, 1057-1074.
- McHugh, M. J. (2006). Impact of South Pacific circulation variability on east African rainfall. *Int. J. of Clim*, **26**(4), 505-521.
- McMaster, D. N. (1962). *A Subsistence Crop Geography of Uganda*. The world land use survey. Occasional papers no. 2. Geographical Publications Limited. Bude, Cornwall, England, 111.
- Mearns, L. O., Hulme, M., Carter, T. R., Leemans, R., Lal, M., and Whetton, P. (2001). 'Climate Scenario Development', Chapter 13 in Houghton *et al.* (eds.), IPCC Third Assessment Report. The Science of Climate Change, Cambridge University Press, 739-768.
- Mendelsohn, R., and Dinar, A. (2003). Climate, water, and agriculture. *J. Land Economics*, **79**, 328-341.
- Mendelsohn, R., Dinar, A., and Dalfelt, A. (2000). Climate change impacts on African Agriculture:http://www.ceepa.co.za/Climate_Change/pdf/afrbckgrnd-impact.pdf.

- Mendelsohn, R., Nordhau, W., and Shaw, D. (1994). The impact of global warming on agriculture: A Ricardian analysis. *American Economic Review*: **84**, 753-771.
- Mitchel, G. A. (1980). *Banana Entomology in the Windward Islands: Final report, 1974-1978*. London, Centre for Overseas Pest Research, 216.
- Mitchell, T. D., and Jones, P. D. (2005). An improved method of constructing a database of monthly climate observations and associated high-resolution grids. *Int. J. Climatol.*, **25**, 693-712.
- Moise, A. F., and Hudson, D. A. (2008). Probabilistic predictions of climate change for Australia and southern Africa using the reliability ensemble average of IPCC CMIP3 model simulations. *J. of Geophysical Research D: Atmospheres*, **113(15)**, 247-389.
- Molg, T., Cullen, N. J., Hardy, D. R., Winkler, M., and Kaser, G. (2009). Quantifying Climate Change in the Tropical Mid troposphere over East Africa from Glacier Shrinkage on Kilimanjaro. *J. Climate*, **22(15)**, 4162-4181.
- Molua, E. L. (2002). Climate variability, vulnerability and effectiveness of farm-level adaptation options: The challenges and implications for food security in southwestern Cameroon. *Environment and Development Economics* **7**, 529-545.
- Morita, T., and Robinson, J. (2001). Greenhouse Gas Emission Mitigation Scenarios and Implications. In *Climate Change (2001). Mitigation*, Cambridge University Press, 115-166.
- Moss, R. H., Edmonds, J. A., Hibbard, K. A., Manning, M. R., Rose, S. K., Van Vuuren, D. P., Carter, T. R., Emori, S., Kainuma, M., Kram, T., Meehl, G. A., Mitchell, J. F. B., Nakicenovic, N., Riahi, K., Smith, S. J., Stouffer, R. J., Thomson A. M., Weyant J. P., and Wilbanks, T. J. (2010). The next generation of scenarios for climate change research and assessment. *Nature*, **463**, 747-756.
- Moufouma-Okia, W., and Jones R. (2014). Resolution dependence in simulating the African hydroclimate with the HadGEM3RA regional climate model, doi: 10.1007/s00382-014-2322-2.
- Mubiru, D. N., Agona, A., and Komutunga, E. (2009). Micro-level analysis of seasonal trends, farmers' perception of climate change and adaptation strategies in eastern Uganda. Paper presented at: International Conference on Seasonality; 2009 Jul 08-10; Brighton, UK. Brighton: Institute of Development Studies, University of Sussex; 2009. Available from: <http://www.event.future-agricultures.org>.

- Mubiru, D. N., Komutunga, E., Agona, A., Apok, A., and Ngar, T. (2012). Characterising agrometeorological climate risks and uncertainties: Crop production in Uganda. *South African J. of Science*, **108(3/4)**, 1-11.
- Mutai, C. C., and Ward M. M (2000). East African rainfall and the tropical circulation/convection on intra-seasonal to inter-annual timescales. *J. Climate*, **13(22)**, 3915-3939.
- Mutemi, J. N. (2003). Climate anomalies over East Africa associated with various ENSO evolution phases. *PhD. Thesis, Department of Meteorology, University of Nairobi, Kenya*.
- Mwangi, E., Wetterhall, F., Dutra, E., Di Giuseppe, F., and Pappenberge, F. (2014). Forecasting droughts in East Africa. *Syst. Sci. Discuss.*, **10**, 10209-10230.
- Mwebaze, S. M. N. (1999). Uganda Pasture forage resource profile; Grassland and Pasture crops, FAO.
- Nakaegawa, T., Wachana, C., and KAKUSHIN Team-3 Modeling Group. (2012). First impact assessment of hydrological cycle in the Tana River Basin, Kenya, under a changing climate in the late 21st Century. *Hydrological Research Letters*, **6**, 29-34.
- Nakicenovic, N., and Swart, R. (2000). Special report on emissions scenarios. *Special Report on Emissions Scenarios, IPCC, Nebojsa Nakicenovic and Robert Swart, (Eds.)*. Cambridge, UK: Cambridge University Press.
- Nalumansi, O., Bbosa, G. S., Lubega, A., and Onegi, B. (2014). Fresh and decayed stem juice of *Musa acuminata* x *balbisiana* (*Musa paradisiaca*) reduce the force and rate of contractility of an isolated perfused rabbit heart. *British Journal of Pharmaceutical Research*, **4(9)**, 1105-1115.
- Nandozi, C. S., Majaliwa, J. G. M., Omondi, P., Komutunga, E., Aribo, L., Isubikalu, P., Tenywa, M. M., and Massa-Makuma, H. (2012). Regional climate model performance and prediction of seasonal rainfall and surface temperature of Uganda. *J. Africa Crop Science*, **20**, 213-225.
- National Adaptation Plan for Action, NAPA (2007). National Adaptation Plan for Action, Uganda.
- Neely, C., Bunning, S., and Wilkes, A. (2009). Review of Evidence on Drylands Pastoral Systems and Climate Change. Land and Water Discussion Paper No. 8, pp. 1–50.
- New, M., Hulme, M., and Jones. P. (2000). Representing twentieth-century space-time climate variability: Part II. Development of 1901-96 monthly grids of terrestrial surface climate. *J. Climate*, **13**: 2217-2238.

- New, M., Bruce Hewitson, B., Stephenson, D. B., Tsiga, A., Kruger, A., Manhique, A., Gomez, B., Coelho, C. A. S., Masisi, D. N., Kululanga, E., Mbambalala, E., Adesina, F., Saleh, H., Kanyanga, J., Adosi, J., Bulane, L., Lubega, F., Mdoka, M. L. and Lajoie R. (2006). Evidence of trends in daily climate extremes over southern and West Africa. *J. Geophys. Res.*, **111**, D14102, doi: 10.1029/2005JD006289.
- Ngaina, J., and Mutai, B. (2013). Observational evidence of climate change on extreme events over East Africa. *J. Global Met*, **2(2)**, doi:10.4081/gm.2013.e2
- Ngaina, J. N., Mutua, F.M., Muthama, N.J., Kirui, J.W., Sabiiti. G., Mukhala, E., Maingi, N.W., and Mutai, B.K. (2014). Drought monitoring in Kenya: A case of Tana River County. *International Journal of Agricultural Science Research*, **3(7)**, 126-135.
- Ngongondo, C., Xu, C.Y., Gottschalk, L., and Alemaw, B. (2011). Evaluation of spatial and temporal characteristics of rainfall in Malawi: a case of data scarce region. *Theor Appl Climatol*. doi: 10.1007/s00704011-0413-0.
- Nicholson S. E. (1996). 'A Review of Climate Dynamics and Climate Variability in Eastern Africa', in Johnson, T. C. and Odada, E. (eds.), *The Limnology, Climatology and Paleoclimatology of the East African Lakes*, Gordon and Breach, Amsterdam, pp. 25-56.
- Nicholson, S. E., and Kim, J. (1997). The relationship of the El Niño Southern Oscillation to African rainfall, *Int. J. Climatol.*, **17**, 117-135.
- Nicholson, S. E. (2000). The nature of rainfall variability over Africa on time scales of decades to millennia. *Global Planet. Change Lett.* **26**, 137-158.
- Nicholson, E. S. (2014). The Predictability of Rainfall over the Greater Horn of Africa. Part I: Prediction of Seasonal Rainfall. *J. Hydrometeor*, **15**, 1011-1027.
- Nikulin, G., Jones, C., Giorgi, F., Asrar, G., Buchner, M., Cerezo-Mota, R., Christensen, O. B., Deque', M., Fernandez, J., Hansler, A., Van Meijgaard, E., Samuelsson, P., Sylla, M. B., and Sushama, L. (2012). Precipitation climatology in an ensemble of CORDEX-Africa regional climate simulations. *J. Climate*, doi:10.1175/JCLI-D11-00375.1.
- Nimusiima, A., Basalirwa, C. P. K., Majaliwa, J. G. M., Otim-Nape, W., Okello-Onen, J., Rubaire-Akiiki, C., Konde-Lule, J., and Ogwal-Byenek, S. (2013): Nature and dynamics of climate variability in the Uganda cattle corridor. *African Journal of Environmental Science and Technology*, **7(8)**, 770-782.
- Nsubuga F. W. N., Olwoch, J. M., and Rautenbach, C. J. (2011). Climatic trends at Namulonge in Uganda: 1947-2009. *J. Geogr Geol.*, **3**:119-131.

- Nsubuga, F. W. N., Botai, O. J., Olwoch, J. M., Rautenbach, C. J., Yvette, B., and Adebayo, O. A. (2014). The nature of rainfall in the main drainage sub-basins of Uganda. *J. Hydrol. Sci.*, **59** (2), 278-299.
- Nyakwada, W. (2009). Predictability of East African seasonal rainfall with sea surface temperature gradient modes. *Ph.D. dissertation, University of Nairobi, Kenya*
- Nyombi, K., Van Asten, P. J. A., Leffelaar, P. A., Corbeels, M., Kaizzi, C. K., and Giller, K. E. (2009). Allometric growth relationships of East Africa highland bananas (*Musa* spp., AAAEAHB) cv. Kisansa and Mbwarzirume. *Annals of Applied Biology* **155**, 403–418.
- Nyombi, K. (2010). Understanding growth of East Africa highland banana: experiments and simulation. *PhD Thesis, Wageningen University, Netherlands*.
- Nyombi, K. (2013). Towards sustainable highland banana production in Uganda: opportunities and challenges. *African Journal for Food, Agriculture, Nutrition and Development*, **13**, 7544-61.
- Oettli, P., and Camberlin, P. (2005). Influence of topography on monthly rainfall distribution over East Africa. *Climate Research*, **28**(3), 199-212.
- Ogalo, L. A. (1979). Rainfall variability in Africa. *Mon. Wea. Rev.* **107**, 1113-1139.
- Ogalo, L. A. (1980). Time series analysis of rainfall in East Africa: *PhD. Thesis, Department of Meteorology, University of Nairobi, Kenya*.
- Ogalo, L. A. (1982). Quasi-periodic patterns in the East African rainfall records, *J. Science and Techn.*, **A3**, 43-54.
- Ogalo, L. A., and Nassib I. R. (1984). Drought patterns and famines in East Africa during 1922-1983: The second WMO symposium on meteorological aspects of Tropical droughts. *Fu. 1984*, 41-44.
- Ogalo L. A. (1993). Dynamics of East African Climate. Proceedings Indian Academy of Sciences. *Earth and Planetary sciences*. **102**(1): 203-217.
- Ogalo, L. A., Boulahya, M. S., and Keane, T. (2002). Applications of seasonal to inter-annual climate prediction in agricultural planning and operations. *Int J. Agric For Met.*, **103**, 159-166.
- Ogalo, L. A. (2009). Relationships between seasonal rainfall in East Africa and the Southern Oscillation, *J. Climate*, **8** (1), 31-43, doi: 10.1002/joc.3370080104
- Okech, S. H., Asten, P. J. A., Gold, C. S., and Ssali, H. (2004). Effects of potassium deficiency, drought and weevils on banana yield and economic performance in Mbarara, Uganda. *J. Agric. Sci.* **9**, 511-519.

- Okoola, R. E. (1996). Space-Time Characteristics of the ITCZ over Equatorial Eastern Africa during Anomalous Rainfall Years, *Ph.D. thesis, Department of Meteorology, University of Nairobi, Kenya.*
- Okoola, R. E., and Camberlin, P. (2003). The onset and cessation of the "Long Rains" in Eastern Africa and their inter-annual variability. *J. Theoretical and Applied Climatology*, **75**, 43-54.
- Omondi, A. P. (2010). The Teleconnections between decadal rainfall variability and global sea surface temperatures and simulation of future climate scenarios over East Africa. *PhD Thesis, University of Nairobi.*
- Omondi, P., Ogallo, L. A., Anyah, R., Muthama, J. M., and Ininda, J. (2013). Linkages between global sea surface temperatures and decadal rainfall variability over Eastern Africa region. *Int. J. Climatol.*, **33 (8)**, 2082-2104.
- Omeny, P., Ogallo, L., and Okoola, R. (2008). East Africa rainfall variability associated with the MJO, *J. Meteorol. Rel. Sci.*, **2**, 105–114.
- Opijah, F. J. (2000). Numerical simulation of the impact of urbanization on the microclimate over Nairobi area. *PhD. Thesis, Department of Meteorology, University of Nairobi, Kenya.*
- Opijah, F. J., Mutemi, J. N., and Ogallo, L. A. (2014). Application of the Ems-Wrf Model in Dekadal Rainfall Prediction over the GHA region. *Africa Journal of Physical Sciences* **1**, 1.
- Osbaahr, H., Dorward, P., Sterns, R. and Cooper. S. (2011). Supporting agricultural innovation in Uganda to respond to climate risk: Linking climate change and variability with farmer perceptions. *Experimental Agriculture* **47**, 293-316.
- Otieno, G. L., Opijah, F. J., Mutemi, J. N., Ogallo, L. A., Anyah, R. O., Ongoma, V. O., and Sabiiti, G. (2014). Seasonal rainfall forecasting using multimodel ensemble technique over Greater Horn of Africa, *Int. J. Phys. Sci*, **2(6)**, 096-104.
- Otieno, G., Opijah, F., Mutemi, J., Artan, G., Sabiiti, G., Ouma, J., Ogallo, L., Wabwire, E., and Onyango, A. (2015). Extreme Rainfall Assessment using Global Climate Model over the Greater Horn of Africa, *Ethiopian e-Journal for Research and Innovation Foresight*, **7(1)**, 55-65.
- Otieno, V., and Anyah, R. O. (2012). CMIP5 Simulated Climate conditions of the Greater Horn of Africa (GHA). Part I: Contemporary Climate. *J. Climate Dyn*, **41**, 2081-2097.
- Otieno, V., and Anyah, R. O. (2013). CMIP5 Simulated Climate Conditions of the Greater Horn of Africa (GHA). Part II: Contemporary Climate. *J. Climate Dyn*, **41**, 2099-2113.

- Ouma, G. O. (2000). Use of satellite data in the monitoring and prediction of rainfall over Kenya. *Ph.D. Thesis, Department of Meteorology, University of Nairobi, Kenya.*
- Paeth, H., Hall, N. M. J., Gaertner, M. A., Alonso, M. D., Moumouni, S., Polcher, J., Ruti, P. M., Fink, A. H., Gosset, M., Lebel, T., Gaye, A. T., Rowell, D. P., Moufouma-Okia, W., Jacob, D., Rockel, B., Giorgi, F., and Rummukainen M. (2011). Progress in regional downscaling of West African precipitation. *J. Atmos. Sci. Lett.*, **12**, 75-82, doi:10.1002/asl.306.
- Pandey, D. N., Gupta, A. K., and Anderson, D. M. (2003). Rainwater harvesting as an adaptation to climate change. *Curr. Sci. India*, **85**, 46-59.
- Parry, M. L, Rosenzweig, C., and Iglesias, A. (2004). 'Effects of climate change on global food production under SRES emissions and socio-economic scenarios', *Global Environmental Change* **14**, 53-67.
- Parry, M., Rosenzweig, C., Iglesias, A., Fischer, G., and Livermore, M. (1999). Climate change and world food security: A new assessment. *Global Environ. Change*, **9**, 51-67.
- Patricola, C. M., and Cook, K. H. (2011). Sub-Saharan Northern African climate at the end of the twenty-first century: forcing factors and climate change processes. *J. Climate Dyn.*, **37(5-6)**, 1165-1188.
- Purseglove, J. W. (1988). *Tropical Crops: Monocotyledones*, 5th ed. Longman, London.
- Rai, R. K., Upadhyay, A., and Ojha, C. S. P. (2010). Temporal variability of climatic parameters of Yamuna River basin: spatial analysis of persistence, trend and periodicity. *Open Hydrol. J.*, **4**:184-210.
- Ramirez-Villegas, J., Jarvis, A., Van den Bergh, I., Staver, C., and Turner, D. (2011). Changing climates: Effects on growing conditions for banana and plantain (*Musa* spp.) and possible responses, in: Yadav, S.S., Redden, R., Lotze-Campen, H., and Hall, A. (Eds.), *Crop Adaptation to Climate Change*, Wiley-Blackwell, Oxford, United Kingdom, 426-438pp.
- Ramirez-Villegas, J., Jarvis, A. and Laderach, P. (2011b). Empirical approaches for assessing impacts of climate change on agriculture: The EcoCrop model and a case study with grain sorghum. *J. Agricultural and Forest Meteorology*, **170 (2013)**, 67–78
- Reeves, J., Chena, J., Wang, X. L., Lund, R., and Lu, Q. (2007). A review and comparison of change point detection techniques for climate data. *J. Appl. Meteorol. Clim.* **46**, 900-915.
- Rhodes, P. L. (1964). A new banana disease in Fiji. *Common Wealth Phytopathological News*, **10**:38-41.

- Riahi, K., Grübler, A., and Nakicenovic, N. (2007). Scenarios of long-term socio-economic and environmental development under climate stabilization. *Technological Forecasting and Social Change*, **74**, 887-935.
- Riahi, K., Krey, V., Rao, S., Chirkov, V., Fischer, G, Kolp, P., Kindermann, G., Nakicenovic, N., and Rafai, P. (2011). RCP 8.5: A scenario of comparatively high greenhouse gas emissions. *Climatic Change*, **109**, 33-57.
- Riddle, E. E., and Cook, K. H. (2008). Abrupt rainfall transitions over the Greater Horn of Africa: Observations and regional model simulations. *J. of Geophysical Research Atmospheres*, 113(D15):D15109.
- Robinson, J. C. (1996). Bananas and Plantains. CAB International, UK.
- Robinson, J. C., and Alberts, A. J. (1989). Seasonal variations in crop water use coefficient of banana in the sub-tropics. *Scientia Horticulturae*, **40**, 215–225.
- Roeckner, E., Bauml, G., Bonaventura, L., Brokopf, R., Esch, M., Giorgetta, M., Hagemann, S., Kirchner, I., Kornblueh, L., Manzini, E., Rhodin, A., Schlese, U., Schulzweida, U., and Tompkins, A. (2003). The atmospheric general circulation model ECHAM5, Part I: Model description, Tech. Rep. 349, Max-Planck-Institute for Meteorology, Hamburg, Germany.
- Roeckner, E., Brokopf, R., Esch, M., Giorgetta, M., Hagemann, S., Kornblueh, L., Manzini, E., Schlese, U., and Schulzweida, U. (2006). Sensitivity of simulated climate to horizontal and vertical resolution in the ECHAM5 atmosphere model. *J. Climate*, **19(16)**, 3771-3791.
- Roeckner, E., Oberhuber, J. M., Bacher, A., Christoph, M., and Kirchner, I. (1996). ENSO variability and atmospheric response in a global coupled atmosphere- ocean GCM. *J. Climate Dyn*, **12**, 737-754.
- Rowell, D. P. (2012). Sources of Uncertainty in Future Changes in Local Precipitation. *J. Climate Dyn*, **39**, 1929-1950.
- Rubaihayo, P. R. (1991). Banana-based cropping systems research: A report on rapid appraisal survey of banana production in Uganda. Research Bulletin 1. Department of Crop Science, Makerere University, Kampala, Uganda.
- Rubaihayo, P. R., and Gold, C. (1993). Banana-based cropping systems research: A report on rapid appraisal survey of banana production in Uganda. Research Bulletin 2. Department of Crop Science, Makerere University, Kampala, Uganda.

- Rutherford, M., and Gowen, S. (2003). Crop Protection Programme: Integrated Management of Banana Diseases in Uganda, R7567(ZA0372). Final Technical Report, 1 January 2000–30 June 2003. CABI Bioscience/University of Reading, UK.
- Sabiiti, G. (2008). Simulation of climate scenarios using the PRECIS Regional Climate Model over the Lake Victoria basin: *MSc. Dissertation, Department of Meteorology, University of Nairobi, Kenya.*
- Sachs, J., Panatayou, T., and Peterson, A. (1999). Developing Countries and the Control of Climate Change: A theoretical Perspective and Policy Implications. CAER II Discussion Paper, no. 44. Cambridge, MA, USA: Harvard Institute for International Development (HIID).
- Saji, N. H., Goswami, B. N., Vinayachandran, P. N., and Yamagata, T. (1999). A dipole mode in the tropical Indian Ocean. *J. Nature*, **401(6751)**, 360-363.
- Samson J. A. (1980). Tropical fruits Longmans, London. pp. 119-161.
- Sastry, P. S. N. (1988). Agrometeorology of the banana crop. Geneva: World Meteorological Organization.
- Schafer, N. W. (1991). Modelling the areal distribution of daily rainfall. *MSc. Eng. Thesis, Department of Agricultural Engineering, University of Natal, Pietermaritzburg, South Africa.*
- Schneider, S. H. (1992). Introduction to climate modelling. In: Climate System Modeling, Trenberth, K.E. (ed.). Cambridge University Press, Cambridge, 3-26.
- Schreck, C. J., and Semazzi, F. H. M. (2004). Variability of the recent climate of eastern Africa. *Int. J. Climatol.*, **24(6)**: 681-701.
- Sengooba, T. (1986). Survey of banana pest problem complex in Rakai and Masaka districts: preliminary trip report. Uganda Ministry of Agriculture, Kawanda Research Station, 10pp.
- Seo, S. N., Mendelsohn, R., and Munasinghe, M. (2005). Climate change impacts SIVAKUMAR MVK, 1992. Climate change and implications for agriculture in Niger. *Climate Change*, **20**, 297-312.
- Shepard, D. (1968). A two-dimensional interpolation function for irregularly-spaced data. In *Proceedings, 1968 ACM National Conference*, ed. R. B. Blue and A. M. Rosenberg, 517-23. New York: Association for Computing Machinery.
- Shongwe, M. E., Van Oldenborgh, G. J., Van Den Hurk, B. J. J., De Boer, M. B., Coelho, C. A. S., and Van Aalst, M. K. (2009). Projected changes in mean and extreme

- precipitation in Africa under global warming. Part I: Southern Africa. *J. Climate*, **22**, 3819-3837.
- Shongwe, M. E., Van Oldenborgh, G. J., Van den Hurk, B., and Van Aalst, M. (2011). Projected changes in mean and extreme precipitation in Africa under global warming. Part II: East Africa. *J. Climate*, **24(14)**, 3718-3733.
- Shukla, J., and Paolino, D. A. (1983). The Southern Oscillation and the long-range Forecasting of the Summer Monsoon Rainfall over India. *Mon. Wea. Rev.*, **111**, 1830-1837.
- Simmonds, N. W., and Shepherd, K. (1955). The taxonomy and origins of the cultivated bananas, *J. of the Linnean Society of London, Botany*, **55(359)**, 302-312.
- Simon, W., Hassell, D., Hein, D., Eagle, C., Tucker, S., Jones, R., and Taylor, R. (2012). Installing and using the Hadley Centre regional climate modelling system, PRECIS, Version 1.9.4. Met Office Hadley Centre; Exeter. www.metoffice.gov.uk/precis.
- Sivakumar, M. V. K., Das, H. P., and Brunini, O. (2005). Impacts of present and future climate variability and change on agriculture and forestry in the arid and semi-arid tropics. *Climatic Change*, **70**, 31-72.
- Smith, R. N. B., Blyth, E. M., Finch, J. W., Goodchild, S., Hall, R. L., and Madry, S. (2006): Soil state and surface hydrology diagnosis based on MOSES in the Met Office Nimrod nowcasting system. *J. Meteor. Appl.*, **13**, 89–109.
- Smith, M. (1992). CROPWAT: A computer program for irrigation planning and management. FAO Irrigation and Drainage Paper 46, FAO. Rome, 1992.
- Smithson, P. C., McIntyre, B. D., Gold, C. S., Ssali, H., Kashaija, I. N. (2001). Nitrogen and potassium fertilizer vs. nematode and weevil effects on yield and foliar nutrient status of banana in Uganda. *Nutr. Cycl. Agroecosyst.* **59**, 239-250.
- Song, Q., Vecchi, G. A., and Rosati, A. J. (2007). Indian Ocean Variability in the GFDL Coupled Climate Model. *J. Climate*, **20**, 2895-2916.
- Song, Y., Semazzi, F. H. M., Xie, L., and Ogallo L. A. (2004). A coupled regional climate model for Lake Victoria basin of East Africa. *Int. J. Climatol.* **24**, 57-75.
- Speijer, P. R., and Kajumba, C. (2000). Yield loss from plant parasitic nematodes in East African highland banana (*Musa* spp. AAA) in Proceedings of the First International Conference on Banana and Plantain for Africa. (K. Craenen, K., R. Ortiz, B.E. Karamura, D.R. Vuylsteke, eds.). 14-18 October, 1996. Kampala, Uganda. *ActaHorticulturae*, **540**, 453-459.

- Speijer, P. R., Buchenberg, W. J., and Sikora, R.A. (1993). Relationship between nematodes, weevils, bananas and plantains cultivars and damage. *Annals of Applied Biology*, **123**, 517-525.
- Speijer, P. R., Gold, C. S., Karamura, E. B., and Kashaija, I. N. (1994). Banana weevil and nematode distribution patterns in highland banana systems in Uganda: Preliminary results from a diagnostic survey. In: First International Crop Science Conference for Eastern and Southern Africa, held in Kampala, 14-18 June 199, Volume 1. Adipala, E., M.W. Ogenga-Latigo, M. Bekunda, J.O., Mugah and J.S. Tenywa (Eds.), 285-289. African Crop Science Society, Makerere University, Kampala, Uganda.
- Speijer P.R., and Kajumba C. (1996). Yield loss from plant parasitic nematodes in East Africa Highland banana (*Musa AAA*). *MusAfrica* 10:26.
- Speijer, P. R., Boonen, E., Vuylsteke, D., Swennen, R. L., and Waele, D. D. E. (1999a). Nematode reproduction and damage to *Musa* sword suckers and sword sucker derived plants. *Nematropica*, **29**, 197-207.
- Speijer, P. R., Kajumba, C., and Sango, F. (1999b). East African Highland banana production as influenced by nematodes and crop management in Uganda. *Int. J. Pest Manage.* **45**, 41-49.
- Ssali, H. (2002). Soil organic matter and its relationship to soil fertility changes in Uganda. In: Policies for Improved Land Management in Uganda: second national workshop. EPTD workshop summary paper no. 12. Nkonya, E., Sserunkuuma, D., Pender J. (eds). International Food Policy Research Institute (IFPRI), Kampala, Uganda, 99–107.
- Ssali, H., McIntyre, B. D., Gold, C. S., Kashaija, I. N., and Kizito, F. (2003). Effects of mulch and mineral fertilizer on crop, weevil and soil quality parameters in highland banana. *Nutr. Cycl. Agroecosyst.* **65**, 141–150.
- Sseguya, H., Semana, A. R., and Bekunda, M. A. (1999). Soil fertility management in the banana-based agriculture of central Uganda: farmers' constraints and opinions. *African Crop Science Journal*, **7**, 559-567.
- Ssenyonga, J. W., Bagamba, F., Gold, C. S., Tushemereirwe, W. K., Ssendege, R., and Katungi, E. (1999). Understanding Current Banana Production with Special Reference to Integrated Pest Management in Southwestern Uganda. NARO, Kampala.
- Stern, N. (1996). Growth theories, old and new and the role of agriculture in economic development. FAO, Economic and Development Paper, 136.
- Stern, N., Peters, S., Bakhshi, V., Bowen, A., Cameron, C., Catovsky, S., Crane, D., Cruickshank, S., Dietz, S., Edmonson, N., Garbett, S. L., Hamid, L., Hoffman, G.,

- Ingram, D., Jones, B., Patmore, N., Radcliffe, H., Sathiyarajah, R., Stock, M., Taylor, C., Vernon, T., Wanjie, H., and Zenghelis, D. (2006). *Stern Review: The Economics of Climate Change*, HM Treasury, London.
- Stover, R. H. (1978). Distribution and probable origin of *Mycosphaerella fijiensis* in South East Asia. *Tropical Agriculture, Trinidad* **55(1)**, 65-68.
- Stover, R. H., and Simmonds, N. W. (1987). *Bananas*. 3rd Edition., Longman Scientific and Technical, New York, USA., 512.
- Strzepek, K., Yates, D. N., Yohe, G., Tol, R. J. S., and Mader, N. (2001). Constructing ‘not implausible’ climate and economic scenarios for Egypt. *Integrated Assessment* **2**, 139-157. In Conway, D. 2003. *From headwater tributaries to international river: observing and adapting to climate variability and change in the Nile basin/Global Environmental Change*, 16.
- Sun, L., Semazzi, F. H. M., Giorgi, F., and Ogallo, L. A. (1999a). Application of the NCAR Regional Climate model to Eastern Africa. Part 1: Simulation of the short rains of 1988. *J. Geophys Res.*, **104**, 6529-6548.
- Sun, L., Semazzi, F. H. M., Giorgi, F., and Ogallo, L. A. (1999b). Application of the NCAR Regional Climate model to Eastern Africa. Part II: Simulation of inter-annual variability of short rains. *J Geophys. Res.*, **104**, 6549-6562.
- Sun, L., Moncunill, D. F., Li, H., Moura, A. D., Filho, F. D. A. D. S., and Zebiak, S. E. (2006). An operational dynamical downscaling prediction system for Nordeste Brazil and the 2002–04 real-time forecast evaluation. *J. Climate*, *19*, 1990–2007.
- Surendran, A., Ashok, K. R., Kulshreshtha, S. N., Vellangany, I., and Govindasamy, R. (2014). Does Climate Variability Influence Crop Yield? - A Case Study of Major Crops in Tamil Nadu. *Agricultural Economics Research Review*. **27(1)**:61-71.
- Sylla, M. B., Giorgi, F., Coppola, E., and Mariotti, L. (2013). Uncertainties in daily rainfall over Africa: Assessment of gridded observation products and evaluation of a regional climate model simulation. *Int. J. Climatol.*, *33*, 1805-1817, doi:10.1002/joc.3551.
- Talwana, H. A. L., Speijer, P. R., and DeWaele, D. (2000). Spatial distribution of nematode population densities and nematode damage in roots of three banana cultivars in Uganda. *Nematropica*, **30(1)**, 19-32.
- Taylor, K. E. (2012). Summarizing multiple aspects of model performance in a single diagram. *J. Geophys Res: Atmos* **106**, 7183-7192.
- Thomson, A. M., Calvin, K. V., Smith, S. J., Kyle, G. P., Volke, A., Patel, P., Delgado-Arias, S., Bond-Lamberty, B., Wise, M. A., Clarke, L. E., and Edmonds, J. A. (2011). RCP

- 4.5: A pathway for stabilization of radiative forcing by 2100. *Climatic Change*, **109**, 7-94.
- Thornton, P. K., Jones, P. G., Alagarwamy, G., and Andresen, J. (2009). Spatial variation of crop yield response to climate change in East Africa. *Global Environmental Change*, **19(1)**, 54-65.
- Turner, D.W., and Lahav, E. (1983). The growth of banana plants in relation to temperature. *Australian. J. of Plant Physiology*, **10**, 43-54.
- Tushemereirwe, K. W., and Ploetz, R. C. (1993). First report of Fusarium wilt on East African highland cultivars of banana. *Plant Disease*, **77**, 1063.
- Tushemereirwe, K. W., and Waller, J. M. (1993). Black streak (*Mycosphaerella fijiensis*) and associated diseases of bananas in Uganda. *Plant Pathology*, **42**, 471-472.
- Tushemereirwe, W. K. (1996). Factors influencing the expression of leaf spot diseases of highland bananas in Uganda. *PhD. Thesis. University of Reading, UK*.
- Tushemereirwe, W. K. (2006). Experiences with banana bacterial wilts: the national strategy for the management of BXW in Uganda. In: Karamura, E.B., Osiru, M., Blomme, G., Lusty, C., Picq, C. (Eds.), *Proceedings of the Banana Xanthomonas Wilt Regional Preparedness and Strategy Development Workshop*. Kampala, Uganda, 14-18 February 2005. International Plant Genetic Resources Institute, Montpellier, 13-16.
- Tushemereirwe, W. K., Kangire, A., Kubiriba, J., Nakyanzi, M., and Gold, C. S. (2004). Diseases threatening banana biodiversity in Uganda, *African Crop Science Journal*, **12(1)**, 19-26.
- Tushemereirwe, W. K., Kashaija, I., Tinzaara, W., Nankinga, C., and New, S. (2001). A guide to successful banana production in Uganda. *Banana Production Manual*, first ed. NARO, Kampala.
- Uganda Bureau of Statistics, UBOS (2010). *Uganda Bureau of Statistics; Statistical Abstract*. Kampala.
- Uganda Bureau of Statistics, UBOS (2011). *Uganda Bureau of Statistics; Statistical Abstract*. Kampala.
- Uganda Bureau of Statistics, UBOS (2013). *Uganda Bureau of Statistics; Statistical Abstract*. Kampala.
- Uganda Bureau of Statistics, UBOS (2015). *Uganda Bureau of Statistics; Statistical Abstract*. Kampala.
- UK Climate Impacts Programme, UKCIP (2003). *Climate Adaptation. Risk, uncertainty and decision-making*. http://www.ukcip.org.uk/images/stories/Pub_pdfs/Risk.pdf.

- Umesh, A., Nejadhashemi, A. P., and Woznicki, S. A. (2015). Climate change and Eastern Africa: A review of impact on major crops. *Food and Ener. Sec.* **4(2)**:110-132.
- United States Agency for International Development, USAID (2013). Uganda Climate Change Vulnerability Assessment Report. A report of the African and Latin American resilience to climate change project, pp. 1-78. Available online at: <http://www.community.eldis.org>.
- Van Asten, P. J., Gold, C. S., Wendt, J., De Waele, D., Okech, S. H. O., Ssali, H., and Tushemereirwe, W. K. (2005). The contribution of soil quality to yield and its relation with other banana yield loss factors in Uganda. In: Blomme, G., Gold, C.S., Karamura, E. (Eds.), Proceedings of a Workshop held on Farmer Participatory Testing of IPM Options for Sustainable Banana Production in Eastern Africa. Seeta, Uganda, 8-9 December 2003. International Plant Genetic Resources Institute, Montpellier, 100-115.
- Van Asten, P. J., Fermont, A. M., and Taulya, G. (2011). Drought is a major yield loss factor for rain-fed East African highland banana. *Agricultural Water Management*, **98**, 541-552.
- Van den Bergh, I., Ramirez, J., Staver, C., Turner, D., Jarvis, A. and Brown, D. (2012). Climate change in the subtropics: The impacts of projected averages and variability on banana productivity. *Acta Hort.* **928**, 89-99.
- Van Vuuren, D. P., Edmonds, J., Kainuma, M., Riahi, K., Thomson, A., Hibbard, K., and Rose, S. K. (2011). The representative concentration pathways: an overview. *Climatic Change*, **109**, 5-31.
- Van Vuuren, D., den Elzen, M., Lucas, P., Eickhout, B., Strengers, B., Van Ruijven, B., Wonink, S., and Van Houdt, R. (2007). Stabilizing greenhouse gas concentrations at low levels: an assessment of reduction strategies and costs. *Climatic Change*, **81**, 119-159.
- Venema, V. K. C., Mestre, O., Aguilar, E., Auer, I., Guijarro, J. A, Domonkos, P., Vertacnik, G., Szentimrey, T., Stepanek, P., and Zahradnicek, P. (2012). Benchmarking homogenization algorithms for monthly data. *J. Clim.*, **8**, 89-115.
- Vicente-Serrano, S., Beguería, S., Lopez-Moreno, J. I., García-Verac, M. A., and Stepanek, P. (2010). A complete daily precipitation database for northeast Spain: reconstruction, quality control, and homogeneity. *Int. J. Climatol.* **30**, 1146-1163.
- Vizy, E. K., and Cook, K. H. (2012). Mid-twenty-first-century changes in extreme events over northern and tropical Africa. *J. Climate*, **25 (17)**, 5748-5767.

- Wairegi, L. W. I., Van Asten, P. J., Tenywa, A., and Bekunda, M. (2010). Abiotic constraints override biotic constraints in East African highland banana systems. *Field Crops Res.* **117**, 146-153.
- Wang, Y., Leung, L. R., McGregor, J. L., Lee, D. K., Wang, W. C., Ding, Y., and Kimura, F. (2004). Regional climate modeling: Progress, Challenges and Prospects. Submitted to *J. Meteorol. Soc. Japan*.
- Wara, M. W., Ravelo, A. C., and Delaney, M. L. (2005). Permanent El Niño-like conditions during the Pliocene Warm Period. *Science*, **309**, 758-761.
- Washington, R., and Pearce, H. (2012). Climate Change in East African Agriculture: Recent Trends, Current Projections, Crop-climate Suitability, and Prospects for Improved Climate Model Information. CGIAR Research Program on Climate Change, Agriculture and Food Security (CCAFS). Copenhagen, Denmark. Available online at: www.ccafs.cgiar.org.
- Williams, A. P., and Funk, C. (2011). A westward extension of the warm pool leads to a westward extension of the Walker circulation, drying eastern Africa. *J. Climate Dyn.*, **37(11-12)**, 2417-2435.
- Williams, A. P., and Funk, C. (2010). A Westward Extension of the Tropical Pacific warm pool leads to March through June drying in Kenya and Ethiopia. U.S Geological Survey Open-File Report 2010-1199.
- Willmott, C. J., and Robeson, S. M. (1995). Climatologically aided interpolation (CAI) of terrestrial temperature. *Int. J. Climatol.*, **15** (2). 221-229.
- Willmott, C. J., Robeson, S. M., and Matsuura, K. (2012). Short Communication: A refined index of model performance. *Int. J. Climatol.*, **32**, 2088-2094.
- Willmott, C. J., Rowe, C. M., and Philpot, W. D. (1985). Small-scale climate maps: A sensitivity analysis of some common assumptions associated with grid-point interpolation and contouring. *The American cartographer*, **12**, 5-16.
- Wise, M., Calvin, K., Thomson, A., Clarke, L., Sands, R., Smith, S. J., Janetos, A., and Edmonds, J. (2009). Implications of Limiting CO₂ Concentrations for Land Use and Energy. *Science*, **324**, 1183-1186.
- World Meteorological Organization, WMO (2012): Standardized Precipitation Index User Guide (M. Svoboda, M. Hayes and D. Wood). (WMO-No. 1090), Geneva.
- Woomer, P. L., Bekunda, M. A., Karanja, N. K, Moorehouse, T., and Okalebo, J. R. (1998). Agricultural resource management by smallholder farmers in East Africa. *Nature and Resources*, **34**, 22-33.

- Xue, Y., Vasic, R., Janjic, Z., Mesinger, F., and Mitchell, K.E. (2007). Assessment of dynamical downscaling of the continental U.S. regional climate using the Eta/ SSI B regional climate model, *J. Clim.*, **20**, 4172-4193.
- Yang, W., Seager, R., and Cane, M. A. (2013). The East African Long Rains in Observations and Models. *Columbia University, Palisades, New York. USA International Research Institute for Climate and Society.*
- Zake, Y. K., Bwamiki, D. P., and Nkwiine, C. (2000). Soil management requirements for banana production on the heavy soils around Lake Victoria in Uganda. *Acta Hort.* **540**, 285–292.